INVESTIGATING GDF5-INDUCED TENOGENESIS IN MESENCHYMAL STEM CELLS FOR THE POTENTIAL IMPROVEMENT OF TENDON REPAIR

TAN SIK LOO

THESIS SUBMITTED IN FULFILMENT OF THE REQUIREMENTS FOR THE DEGREE OF DOCTOR OF PHILOSOPHY

FACULTY OF MEDICINE

UNIVERSITY OF MALAYA

KUALA LUMPUR

2013

UNIVERSITI MALAYA

ORIGINAL LITERARY WORK DECLARATION

Name of Candidate: **TAN SIK LOO** (I.C/Passport No: **791229-01-5854**)

Registration/Matric No: **MHA 080017**

Name of Degree: **DOCTOR OF PHILOSOPHY**

Title of Project Paper/Research Report/Dissertation/Thesis ("this Work"):

Investigating GDF5-induced Tenogenesis in Mesenchymal stem cells for the potential improvement of tendon repair

Field of Study: **MEDICAL BIOTECHNOLOGY AND STEM CELLS**

I do solemnly and sincerely declare that:

(1) I am the sole author/writer of this Work;
(2) This Work is original;
(3) Any use of any work in which copyright exists was done by way of fair dealing and for permitted purposes and any excerpt or extract from, or reference to or reproduction of any copyright work has been disclosed expressly and sufficiently and the title of the Work and its authorship have been acknowledged in this Work;
(4) I do not have any actual knowledge nor do I ought reasonably to know that the making of this work constitutes an infringement of any copyright work;
(5) I hereby assign all and every rights in the copyright to this Work to the University of Malaya ("UM"), who henceforth shall be owner of the copyright in this Work and that any reproduction or use in any form or by any means whatsoever is prohibited without the written consent of UM having been first had and obtained;
(6) I am fully aware that if in the course of making this Work I have infringed any copyright whether intentionally or otherwise, I may be subject to legal action or any other action as may be determined by UM.

Candidate's Signature Date 21/8/2013

Subscribed and solemnly declared before,

Witness's Signature Date 21.8.2013

Name: Prof. Dr. Tunku Kamarul Zaman
Designation: No. Pendaftaran Penuh 35591
Pakar Perunding
Jab. Surgeri Ortopedik
Pusat Perubatan Universiti Malaya

ABSTRACT

Mesenchymal stem cell (MSC) has an immense potential for use in clinical applications, however, there is still paucity in the fundamental knowledge in the techniques and processes involved in MSCs differentiation, especially tenogenic differentiation. Growth and differentiation factor 5 (GDF5) is a potential inducer which may induce tenogenic differentiation response in MSC. The aims of this current study were: (1) to investigate the tenogenic differentiation in human and rabbit MSCs (hMSCs and rbMSCs respectively) in response to GDF5 treatment; (2) to investigate the potential of GDF5-induced rbMSCs in tendon repair in *in vivo* rabbit model; and (3) to investigate the differentially expressed genes between GDF5-induced hMSCs and the untreated hMSCs compared to the native tenocytes (hTeno). In this study, both hMSCs and rbMSCs were isolated and characterized following the ISCT guidelines. Upon GDF5 (0, 5, 25, 50, 100 and 500 ng/ml) treatment, the results demonstrated that there was (i) no significant differences in the proliferation rate between the hMSCs cultured at different concentrations of GDF5; (ii) a significant increase in total collagen levels comparable to that of hTeno culture ($p<0.05$) when hMSCs were cultured at 100 ng/mL of GDF5, (iii) a significant increase in total collagen levels in 500 ng/ml GDF5-induced rbMSCs to a level comparable to rbTeno (rabbit tenocyte) cultures, however there were no significant difference in total collagen levels between rbMSCs treated with 100 ng/ml and 500 ng/ml of GDF5; (iv) a significant ($p<0.05$) up-regulation in the expression of candidate tenogenic marker genes (Scleraxis (*Scx*), tenascin-C and type-I collagen (*Col-I*)) whilst a significant ($p<0.05$) down-regulation of the non-tenogenic marker genes (runt-related transcription factor 2 and sex determining region Y (SRY)-box 9) at day 7 upon 100 ng/mL GDF5 treatment in hMSCs; (v) a significant increase in *Scx* and *Col-I* gene expression levels were also detected in 100 ng/ml GDF5-induced rbMSC; (vi) increase in COL-I expression at protein level in rbMSCs cultures treated

with 100 ng/ml GDF5. In the *in vivo* study to investigate the potential use of tenogenic rbMSCs (TMSC, 100 ng/mL of GDF5-induced rbMSCs), the quality of the infraspinatus tendon repair in New Zealand white rabbits using TMSCs and other methods were evaluated, which showed significant improvement in the cell based treated groups compared to the non-cell-based treated groups. A significant up-regulation in expression of tenogenic marker genes (*Scx* and *Col-I*) in TMSCs group as compared to other treatment groups were also observed. Furthermore, microarray analysis showed: (i) significant differences in 954 genes in GDF5-induced hMSC and tenocytes compared to control hMSCs; (ii) the differentially expressed genes were involved in specific pathways (i.e. cytoskeleton remodeling, cell adhesion, and extracellular matrix related genes) that are closely related to the native behavior of hTeno *in vivo*. The findings of this study demonstrate that concentration of GDF5, ≥100 ng/mL is able to induce tenogenic differentiation in both hMSCs and rbMSCs. These data suggest that tenogenic MSCs may potentially provide similar function to that of native tenocytes e.g. during tendon repair. These findings provide evidence of potential use of GDF5-induced MSCs in the clinical applications in future.

ABSTRAK

Sel stem mesenkima (MSC) merupakan sel yang berpotensi tinggi untuk aplikasi klinikal. Namun, pengetahuan asas dalam teknik dan proses pembezaan MSC masih amat kekurangan, khususnya pembezaan tenogenik. Dalam pembezaan tenogenik pada sel MSC, faktor pertumbuhan dan pembezaan 5 (GDF5) berpotensi tinggi untuk merangsangkan gerak balas ini. Objektif kajian ini ialah untuk: (1) mengkaji kesan pembezaan tenogenik sel MSC manusia dan arnab (hMSCs dan rbMSCs) akibat cetusan GDF5; (2) mengkaji potensi sel tenogenik rbMSC (sel rbMSC yang dicetus GDF5) dalam pembaik pulihan tendon terkoyak dengan menggunakan model *in vivo* arnab; dan (3) mengkaji gen terungkap pada aras yang berbeza pada sel hMSC cetusan GDF5 berbanding dengan sel hMSC tanpa rawatan dan sel tenosit asli (sel tendon daripada tisu tendon; hTeno). Dalam kajian ini, kedua-dua hMSC dan rbMSC diasingkan dan dicirikan mengikuti garis panduan ISCT. Dalam eksperimen cetusan GDF5 (pada kepekatan 0, 5, 25, 50, 100 dan 500 ng/ml) didapati: (i) tiada perbezaan yang signifikan dalam kadar pembahagian sel antara sel hMSC yang dikultur pada kepekatan GDF5yang berbeza; (ii) peningkatan aras jumlah kolagen yang signifikan dan setanding dengan aras sel hTeno (p<0.05) pada hMSC yang dikultur pada 100 ng/mL GDF5, (iii) peningkatan yang signifikan dalam aras gen calon penanda tenogenik (seperti scleraxis, tenascin-C dan kolagen jenis-I (*Col-I*)) dan pengurangan yang signifikan (p<0.05) dalam aras gen penanda bukan tenogenik (seperti *runt-related transcription factor 2* and *sex determining region Y (SRY)-box 9*; pada hari ke-7 sel hMSC yang dicetus oleh 100 ng/mL GDF5; (iv) perbezaan yang signifikan dalam 954 gen yang dikenal pasti melalui analisis mikroatur pada sel hMSC yang dicetus olah GDF5; (v) gen-gen terungkap pada aras yang berbeza didapati terlibat dalam tapak jalan tertentu (iaitu pembentukan semula *cytoskeleton*, perlekatan sel, dan gen yang berkaitan dengan matriks extraselular) yang berkait rapat dengan kelakuan sel tenosit asli dalam keadaan

in vivo. Dalam eksperimen *in vitro* rbMSC, didapati: (i) peningkatan yang signifikan (p<0.05) dan setanding dengan sel rbTeno (sel tenosit arnab) dalam aras jumlah kolagen pada sel rbMSC cetusan dengan 100 ng/ml GDF5; (ii) peningkatan yang signifikan dalam aras ungkapan gen scleraxis dan *Col-I* (p<0.05); (iii) peningkatan dalam aras pengekspresan protein COL-I pada sel rbMSC yang dirawat dengan 100 ng/ml GDF5 berbanding sel MSC tanpa rawatan, melalui pewarnaan berpendafluor. Kajian *in vivo* untuk mengkaji potensi sel tenogenik rbMSCs (sel rbMSC yang dicetus oleh 100 ng/mL GDF5) dalam meningkatkan kualiti pembaik pulihan tendon infraspinatus terkoyak dalam arnab menunjukkan peningkatan kualiti pemulihan tendon dalam kumpulan arnab dengan rawatan yang berasaskan sel berbanding kumpulan yang dirawat tanpa sel. Selain itu, juga didapati peningkatan yang signifikan dalam aras gen penanda tenogenik (scleraxis dan *Col-I*) dalam kumpulan arnab yang dirawat dengan sel tenogenik rbMSCs berbanding kumpulan rawatan lain. Keputusan kajian ini menunjukkan bahawa ≥100 ng/mL GDF5 dapat mencetuskan pembezaan tenogenik pada sel hMSC dan rbMSC. Pemerhatian kajian ini mencadangkan bahawa sel tenogenik MSC berpotensi untuk memainkan peranan yang sama seperti yang sel tenosit asli, contohnya semasa pembaik pulihan tendon. Penemuan ini memberikan bukti bahawa sel MSC yang dicetus oleh GDF5 berpotensi tinggi untuk digunakan dalam aplikasi klinikal pada masa hadapan.

ACKNOWLEDGEMENTS

With thanks to

Prof. Dr. Tunku Kamarul Zaman:

For allowing me to do research inquisitively, independently, creatively and giving me the freedom to take my project where I wanted it to go. For trusting my judgement while remaining always generously available to offer advice and help. Last but not least, for his enormous patience and encouragement ever since I joined the TEG.

Prof. Dato' Dr. Tunku Sara:

For her patience, compassion and generous advice over the years and for continually building my self-confidence; not forgetting her unfailingly kind words of encouragement and enthusiasm.

Assoc. Prof. Dr Lakshmi Selvaratnam:

For her endless advice, for her profound and comprehensive knowledge of anatomy/cell biology; for her generous scientific advice.

Prof. John Fairclough:

For reviewing this dissertation and for his philosophical advice; for his willingness to hold discussions via Skype despite his busy professional commitments in the UK.

Assoc. Prof. Dr. Azlina AA, Assoc. Prof. Dr. Ng WM and Prof. Dr. Azhar Mahmood:

For their patience and generous assistance in getting samples.

Prof. Simon Frostick, Prof. Dr. Margaret Roebuck and Prof. Dr. Dan Bader

For their profound and comprehensive knowledge in the basic medical sciences; for sharing their insightful advice and expertise as visiting professors.

Dr Raja Elina:

For her thoughtful, insightful and generous advice over the years, especially in extensively reviewing my manuscript.

Dr. Chan CK:

For his kind assistance in animal surgery and for his enthusiasm in research.

Dr Chong BK and Dr Lim FT:

For their kind assistance in imaging, especially AFM and CLSM imaging.

Sandra Wee AS:

For being my early morning buddy, even after the darkest nights. For her persistent optimism, unwavering perseverance and focus.

Savatey H:

For her optimism and excitement about science; and always assuring me of a great laugh whenever we met in the lab.

All other members of the TEG, NOCERAL, past and present, not specifically mentioned here but whose paths crossed mine with friendship and advice.

See YK:

For love and support. For accepting my unacceptable work schedule and making sure I didn't come home too late during these years, helping me keep my priorities straight, and embarking with me on our journey through life.

My late mother:

For limitless encouragement and care, and making sure I remember what really matters.

My dad, parents-in-law and daughter:

For their endless support and patience, especially these past ten years. For their encouragement of the love for learning and knowledge throughout my life, as a student. For reminding me what I have accomplished - when I forget - and providing me endless courage and strength to keep moving on.

IPS, University of Malaya

For accepting me as a PhD student in the University of Malaya and providing my scholarship for the PhD degree.

CONTENT

LIST OF TABLES

LIST OF FIGURES

LIST OF SYMBOLS AND ABBREVIATIONS

α	Alpha
A	Adenine
A_{260}	Absorbance of ultraviolet at 260 nm
A_{280}	Absorbance of ultraviolet at 280 nm
Alpl	Alkaline phosphatase liver
β	Beta
b	Base
bFGF	Basic fibroblast growth factor
Bglap	Bone gamma-carboxyglutamate protein
BLAST	Basic Local Alignment Search Tool
BMP	Bone morphogenetic protein
b.w.	Body weight
C	Cytosine
^{o}C	Degree Celsius
cDNA	Complimentary DNA
Col-I	Type-I collagen
Col-III	Type-III collagen
Comp	Cartilage oligomeric matrix protein
DEPC	Diethylpyrocarbonate
DMSO	Dimethyl sulfoxide
Dcn	Decorin
DNA	Deoxyribonucleic acid
DMEM	Dulbecco's Modified Eagle Medium
ECM	Extracellular matrix

EDTA	Ethylenediaminetetraacetic acid
FACS	Fluorescence-activated cell sorting
FBS	Fetal bovine serum
Figf	c-fos induced growth factor (or *Vegf-d*)
γ	Gamma
G	Guanine
GDF5	Growth and Differentiation Factor-5
Gapdh	Glyceraldehyde-3-phosphate dehydrogenase
hMSC	Human mesenchymal stem cell
Hprt1	hypoxanthine phophoribosyltransferase 1
∞	Infinity
ISCT	International Society for Cellular Therapy
LOD	limit of detection
mAb	Monoclonal antibody
Mkx	Mohawk homeobox
ml	Milliliter
μm	Micrometer
mm	Millimeter
Mmp3	Matrix metallopeptidase 3
mRNA	Messenger ribonucleic acid
NCBI	National Center for Biotechnology Information
Nst	Nucleostemin
PBS	Phosphate buffered saline
pAb	Polyclonal antibody
PCR	Polymerase chain reaction
Pgk1	Phosphoglycerate kinase 1

PMT	photomultiplier tube
Ppar γ	Peroxisome proliferator-activated receptor-gamma
PRP	Platelet rich plasma
*q*RT-PCR	Quantitative reverse transcription-polymerase chain reaction
rnMSC	Rabbit mesenchymal stem cell
RIN	RNA Integrity Number
RNA	Ribonucleic acid
rpm	Revolutions per minute
RT-PCR	Reverse transcription- polymerase chain reaction
Runx2	Runt-related transcription factor 2
Scx	Scleraxis
S.D.	Standard deviation
Sox9	SRY (sex determining region Y)-box 9
T	Thymine
Tbp	TATA box binding protein
TGF	Transforming Growth Factor
Thbs4	Thrombospondin 4
Tnc	Tenascin C
Tnmd	Tenomodulin
TPC	Tendon progenitor cells
TSC	Tendon stem cells
v/v	Volume in volume
w/v	Weight in volume

LIST OF APPENDICES

CHAPTER 1

GENERAL INTRODUCTION

1.0 GENERAL INTRODUCTION

1.1 Structure and Function of Normal Tendon

1.1.1 Tendon, Tenocyte and Tendon Extracellular Matrix

Tendon is dense connective tissue which connects muscle to bone and allows transmission of forces generated by muscle to bone, resulting in joint movement. It is a living tissue with mechanical adaptation ability that allows it to respond to mechanical forces (eg. high tensional loading). This is achieved through changes in the metabolism as well as its structural and mechanical properties (Kjaer, 2004; Provenzano & Vanderby, 2006; Wang, 2006). These critical biological and biomechanical roles of tendon are played through a reciprocal relationship between its two main components, i.e. cells and extracellular matrix (ECM) (Table 1.1).

Table 1.1 Structural compositions of tendon (Sharma & Maffulli, 2005; Wang, 2006).

Component	**Total (%)**
Cellular materials	**20**
Tenocytes and tenoblasts	90-95
Others (chondrocytes, synovial cells and vascular cells)	5-10
Extracellular matrix(ECM)	**80**
Water	60-80
Dry mass	20-40
Collagen	**75-85**
Type I	95-99
Type III and V	1-5
Others (Type II, VI, IX, X and XI)	Trace amount
Ground substance (Proteoglycan, glycoproteins and etc.)	**15-25**

The overall cell content in tendon tissue is low (20%). Tenocytes and tenoblasts are the two main cell types which coexist in tendon. Both of these cells are of mesenchymal origin and they constitute about 90-95% of the cellular component of

tendons (Amiel et al., 1984). Tenoblasts are immature tendon cells. They are spindle-shaped and have numerous cytoplasmic organelles. They have a high organelle content which reflects their high metabolic activity. As they mature, tenoblasts become elongated and transformed into tenocytes. Tenocytes have lower nucleus-to-cytoplasm ratio than tenoblasts. These cells lie between the collagen fibers along the long axis of the tendon (Kirkendall & Garrett, 1997). The remaining 5-10% of the cellular elements of tendon consists of chondrocytes at the bone attachment and insertion sites (Fukuta et al., 1998), synovial cells of the tendon sheath, and vascular cells, including capillary endothelial cells and smooth muscle cells of arterioles (Sharma & Maffulli, 2005). Recently, several studies have shown that multipotent tendon stem cells/tendon progenitor cells (TSC/TPC) also exist in human and animal tendon tissues (Bi et al., 2007; Rui et al., 2010; Yin et al., 2010). Nevertheless, it remains unclear whether the TSC/TPC are the same population of cells as the tenoblast. It is also unclear as to whether tenoblast is in fact committed tenogenic progenitor cells and that these cells are different from TSC/TPC. Cell markers to differentiate between the tenocyte, tenoblast and TSC/TPC are at this point remains unknown.

In normal tendon, tenocyte synthesizes a wide range of ECM proteins in a well-ordered structure. Among the most abundant of these proteins is the type-I collagen. This protein is organized in a parallel arrangement providing a distinct hierarchal structure, which ultimately forms the tendon (Figure 1.1). The tenocyte secretes soluble trihelical tropocollagen that is assembled and cross-linked in parallel fibrillar arrays. Higher-order organization of these arrays is provided by the endotenon, which appears as a loose connective tissues layer that envelopes collagen fibrils to form tendon fascicles. Fascicles in turn are bundled together by the epitenon, a layer contiguous with the endotenon through which the microvasculature traverses and provides nutrients (Boyer et al., 2005; Fenwick et al., 2002). This multi-unit hierarchical structure aligns

fiber bundles parallel with the long axis of the tendon and affords the tendon high tensile strength (Wang, 2006).

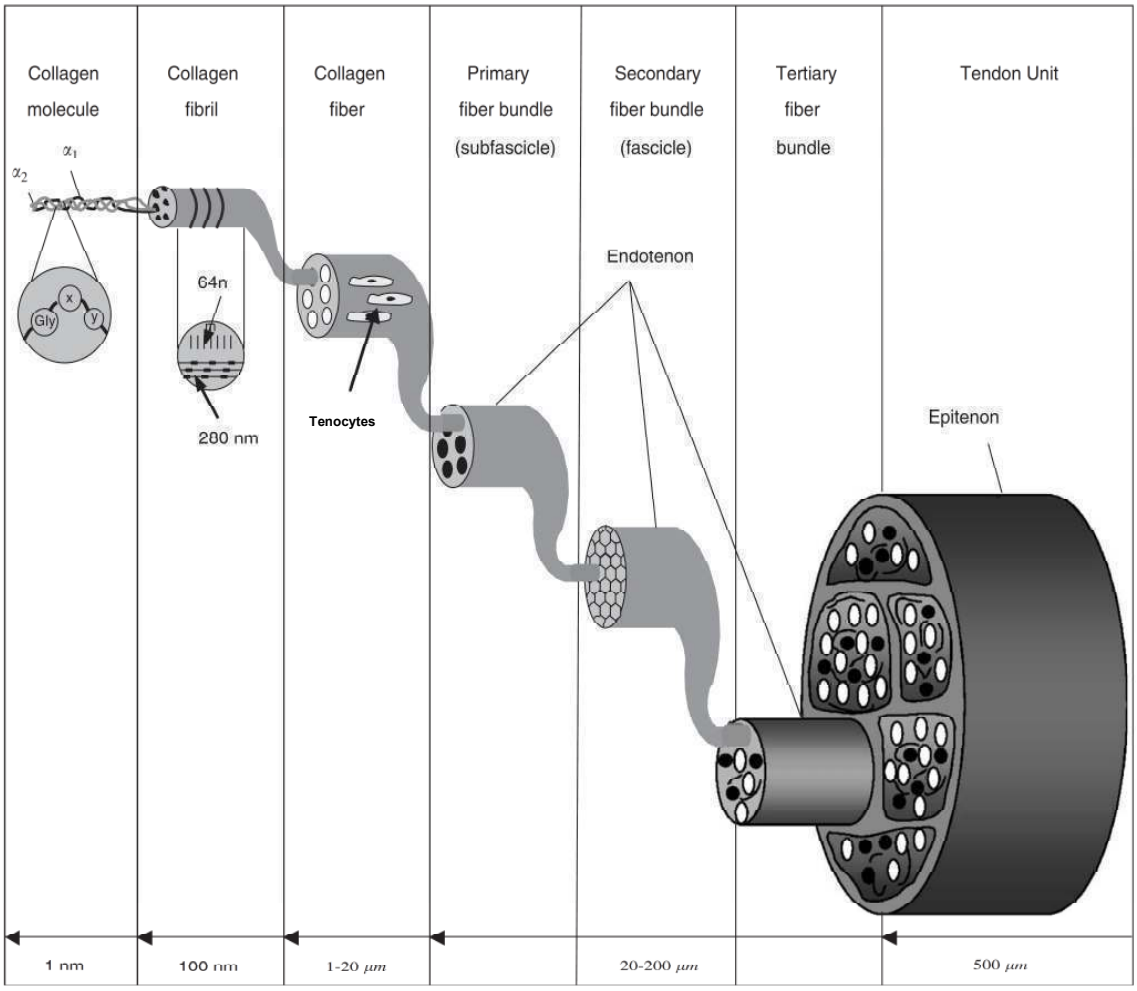

Figure 1.1 Schematic diagram of hierarchical structure of tendon (Silver et al., 2003). The fibril is the smallest tendon structural unit; it consists largely of rod-like collagen molecules aligned end-to-end in a quarter staggered arrays. Fibers form the next level of tendon structure. Fibers are composed of collagen fibrils and are bound by endotenons. Fiber bundles form fascicles, and bundles of fascicles are enclosed by the epitenon. Tendons are also surrounded by a third layer of connective tissue called paratenon (not shown in this figure).

Normal tendon ECM is composed largely of collagen (predominantly type-I collagen, COL-I [1]), which provides structural integrity and mechanical strength (Benjamin et al., 2008). A small amount of ground substances (Table 1.1) is not only important in fibrillogenesis but also provides tendon its high resistance behaviour to

[1] Please note that the abbreviation for the gene is given in italics and the abbreviation for the protein expressed by the gene is given in capital letters.

compressive and tensile forces (Yoon & Halper, 2005). COL-I constitutes about 60% of the dry mass of the tendon and about 95% of the total collagen in tendon (Evans & Barbenel, 1975). The remaining 5% consists of type III and V collagens. In a normal tendon, type III collagen (COL-III) is mainly located in the endotenon and epitenon (Becker et al., 1976; Duance et al., 1977). The ratio of COL-I to COL-III has been previously used as indicators of the tenogenic characteristics in tendon tissues and tenocyte cultures (Maffulli et al., 2000; Yao et al., 2006). Other collagens (type II, VI, IX, X and XI) are present in trace amount in tendons (Fukuta, et al., 1998). The ground substances of the tendon ECM network surrounding the collagens and tenocytes are composed of proteoglycans and several other small molecules (Sharma & Maffulli, 2005). The proteoglycan content in a tendon (dry mass) is relatively lower (~6% in compression region and ~0.2% in tensional region) as compared to other musculoskeletal tissue (Yoon & Halper, 2005). The content varies at different sites of the tendon and is dependant on the mechanical loading conditions, eg. tension vs. compression (Berenson et al., 1996; Riley et al., 1994b; Waggett et al., 1998). A summary of the abundant proteoglycans in tendon is presented in Table 1.2. Although normal mechanical function of tendon depends on the precise alignment of collagen fibrils, it is proteoglycans that regulate collagen fibrillogenesis. This is achieved via the interactions between the positively-charged groups of collagen fibers and the negatively-charged groups of the glycosaminoglycans (GAGs) in a proteoglycan molecule (Yoon & Halper, 2005). This, indirectly affects a tendon's functionality. Members of the small-leucine-rich proteoglycans (SLRP) family (eg. decorin, biglycan, fibromodulin and lumican) bind to collagen fibrils and actively participate in fibrillogenesis (Vogel & Heinegard, 1985). Depletion of biglycan and fibromodulin affects the TSP/TPC differentiation and impairs tendon formation *in vivo* (Bi, et al., 2007). Other proteins, such as adhesive glycoproteins (eg. fibronectin and

thrombospondin) are involved in binding the tenocytes to the collagen fibers (O'Brien, 1992). These, are important in the repair and regeneration process in tendon (Jozsa et al., 1991; Lawler, 1986; Miller & McDevitt, 1991). Apart from these ECM proteins, several polypeptide factors are important in regulating the expression of specific genes that are commonly found in tendons and the expression of these genes influences the ECM metabolism and subsequently modulates the composition and organization of the tendon ECM (Table 1.3).

Table 1.2 Summary of most abundant tendon proteoglycans.

Designation	**Class**	**Role in Tendon**
Decorin	SLRP	Binds to fibrillar collagen, inhibits collagen fibrillogenesis, binds TGF, and EGF (Zhang et al., 2006).
Biglycan	SLRP	Binds to fibrillar collagen, absent in avian species (Vogel & Heinegard, 1985).
Fibromodulin	SLRP	Binds to type I collagen, facilitates formation of mature large collagen fibrils, modulation of tendon strength (Iozzo & Murdoch, 1996).
Lumican	SLRP	Binds to type I collagen, inhibits size of collagen fibrils, modulation of tendon strength (Iozzo & Murdoch, 1996).
Aggrecan	Modular (lectican)	Linked to hyaluronan, provides resiliency, low levels in tensional parts of tendon, high levels in compressed regions, particularly in fibrocartilage (Rees et al., 2000).
Versican	Modular (lectican)	Linked to hyaluronan, low levels in tensional parts of tendon, somewhat higher levels in compressed regions, increases viscoelasticity, maintains cell shape (Scott et al., 2008).

Table 1.3 Genes involved in tendon development and repair (Adapted from (James et al., 2008).

Gene	Function in Development, Repair and Tissue Regeneration
Scleraxis (*Scx*)	Transcription factor specifically detected in tendon cell precursor populations and selectively expressed in later stages (Schweitzer et al., 2001; Shukunami et al., 2006; Wang et al., 2005).
Tenomodulin (*Tnmd*)	A type II transmembrane glycoprotein that been reported predominantly expressed in tendons and ligaments (Shukunami, et al., 2006). A regulator of cell proliferation, differentiation and collagen fibril maturation (Docheva et al., 2005).
Tenascin C (*Tnc*)	A mechano-responsive modulator of matrix formation expressed in high tensional loading tissue such as tendons and ligaments (Mehr et al., 2000). An ECM protein that is evident during embryonic and tendon development (Chiquet-Ehrismann & Tucker, 2004).
Collagen I (*Col-I*)	Mature and highly organized collagen fibrils (Lejard et al., 2007).
Collagen III (*Col-III*)	Early ECM collagen in wound repair (Maffulli, et al., 2000; Williams et al., 1984).
Decorin (*Dcn*) and aggrecan (*Acan*)	Proteoglycan interactions modulating collagen fibril orientation and alignment (Sini et al., 1997).
Smad8	Tenocyte differentiation, phenotype modulation and intracellular signaling (Towler & Gelberman, 2006).

1.1.2 Early Tendon Development

The formation of musculoskeletal system from the somatic mesoderm requires the coordinated development of muscle, cartilage and tendon lineages. In the early somite development, muscle and cartilage emerge from two distinct compartments, the myotome and the sclerotome. This is in response to signals secreted from the surrounding tissues. As the somite matures, the tendon lineage is established within the dorsolateral sclerotome (or syndetome, the fourth somitic compartment (Brent et al., 2003)), which is adjacent to and beneath the myotome. The formation of a scleraxis

(*Scx*)-expressing tendon progenitor (TP) population in the sclerotome is induced by a fibroblast growth factor (FGF) signal secreted from the myotome (Figure 1.2).

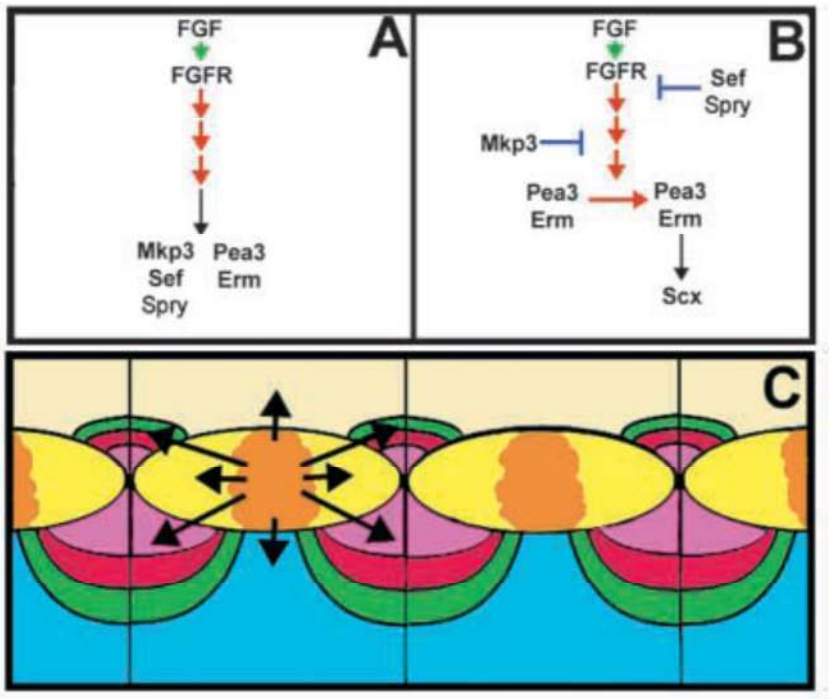

Figure 1.2 Model of FGF-dependent activation of *Pea3* and *Erm*, and subsequent induction of *Scx* in the Somite (Adapted from Brent et al. 2004).

(A) FGF signaling leads to expression of *Ets* transcription factors *Pea3* and *Erm* and inhibits *Mkp3*, *Sef* and *Spry* in the anterior and posterior sclerotome and dermomyotome. FGF secreted by myotome bind to and activate an FGFR (green arrow). Receptor activations results in series of phosphorylation events (red arrows), culminating in direct or indirect transcriptional activations (black arrow) of target genes such as *Pea3*, *Erm*, *Mkp3*, *Sef* and *Spry*.

(B) Once *Pea3* and *Erm* expression domains have been established, further FGF signaling triggers phosphorylation and subsequent activation of *Pea3* and *Erm*, which, in turn, activate transcription of target genes resulting in *Scx* expression.

(C) Schematic of four somites, frontal view: dermomyotomes are beige; myotomes are yellow; sclerotomes are aqua. FGF expressed in center of myotome (orange) can diffuse to surrounding dermomyotome, myotome and dorsal sclerotome (arrows). FGF signaling here results in expression of *Pea3* (red) and *Erm* (green), in a nested pattern, within anterior and posterior dermomyotome and dorsal sclerotome. *Scx* expression (purple) is induced when myotomal FGFs signal to the *Pea3*- and *Erm*- expressing dermomyotome and sclerotome.

The FGF transcription effectors (*Pea3* and *Erm*) are necessary for TP marker *Scx* expression in the somite to be expressed (Brent et al., 2005; Brent & Tabin, 2004). The domain of *Scx* expression, or the location of the syndetome, is dependent on the

combined conditions of the restricted expression pattern of *Pea3* and *Erm* within the anterior and posterior sclerotome, and the distances that FGFs secreted from the center of the myotome are able to travel. Brent and colleagues (2005) also suggested that the early myotome regulatory factors, *Myf5* and *Myod1* (previously known as *MyoD*) expressions are required for FGF protein expression in the myotome, which in turn is required for the induction of TP markers. In addition, they suggested that tendon and cartilage lineages arising from the sclerotome appear to be an alternative and mutually exclusive, where the loss of chondrocyte differentiation results in an expanded somitic TP population. This causes the *Sox9*-expressing mesenchymal condensations to begin expressing tendon markers. It worth noting that when the differentiation of one cell fate is blocked, the other is adopted. (Brent, et al., 2005).

In contrast to the differentiation of axial tendons, that of the cartilages or tendons of the appendicular skeleton arises *in situ*. The initiation of tendons differentiation in the appendicular skeleton does not seem to require the presence of muscle (Kardon, 1998). Nevertheless, the maintenance of distal tendons does require interaction with muscle because in the absence of muscle these tendons gradually degenerate (Kardon, 1998). Based on the observation of *Scx* expression in the subectodermal location of the appendicular skeleton, it has been postulated that ectodermal signals might play a role in the occurrence of *Scx*-expressing TPs (Liu et al., 2011). However, the signals that initiate the expression of *Scx* in the appendicular skeleton remain unknown.

In addition to FGF signaling for inducing sclerotomal cells to become tendon progenitor cells (TPC), transforming growth factor - β (TGFβ) signaling is also a potent inducer of *Scx* both in organ culture and in cultured cells (Pryce et al., 2009). This is said to be essential for the maintenance of the early TPC and has been suggested to mediate the recruitment of additional tendon cells by the adjacent muscles and cartilage condensations. This recruitment is to establish the connections of tendon primordial

with these tissues, and it is an essential event for the subsequent differentiation and growth of mature tendons (Pryce, et al., 2009). In coordinating the cartilage and tendon differentiation in the developing limb mesenchyme, TGF-interacting factor, *Tgif1*, has been identified as one of the potential candidates which modulates the TGFβ signaling from chondrogenesis to fibrogenesis, and its expression pattern in the limb marks the developing tendons (Lorda-Diez et al., 2009). This reprogramming of TGFβ signaling provokes down-regulation of *Sox9* and aggrecan and up-regulation of *Scx* and tenomodulin through the Smad pathway (Lorda-Diez, et al., 2009). A recent review on the musculoskeletal assembly in the vertebrate embryo postulated that the induction and differentiation of TPCs occur in three distinct stages (Figure 1.3): induction, organization as well as aggregation and differentiation (Schweitzer et al., 2010). In brief, the differentiation of tendon in the somite depends upon a combination of both activating and repressing signals from the other compartments of the somite.

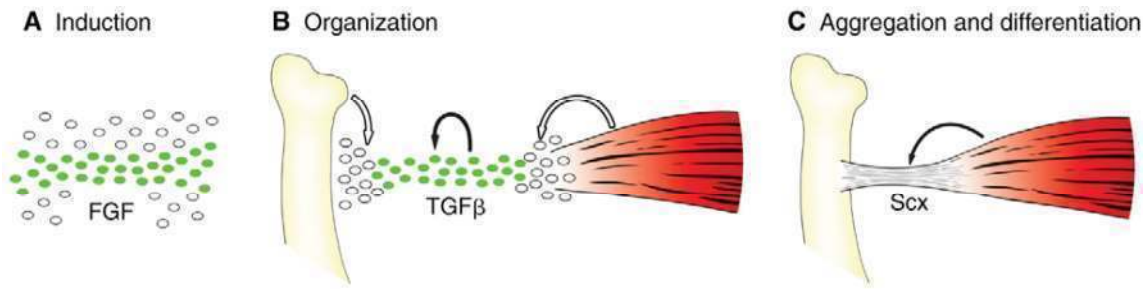

Figure 1.3 The three main stages and regulators of tendon induction and differentiation in vertebrate embryos (Adapted from Schweitzer et al. 2010).
The *Scx*-expressing tendon progenitors (TPs) are represented in green and mesenchymal cells in white to show the different stages of tendon induction and differentiation.
(A) Induction. The initial induction of *Scx*-expressing TPs is associated with FGF signaling, but the myotome in somites is the only identified source to date. In somites and digits, the progenitors are induced at or near their functional position between the myogenic and skeletogenic cells, but in the early limb bud and branchial arches the site of progenitor induction is not related to their final destination.

Figure 1.3, continued

(B) Organization. In an E12.5 mouse embryo, TPs throughout the embryonic body organize as loose cellular aggregations between the differentiating muscle and skeletal tissues. This transition depends on TGFβ signaling, which mediates the recruitment of additional TPs by the muscle and cartilage tissue to position and integrate the TPs with their interacting musculoskeletal tissues (white arrows). In addition, TGFβ ligands expressed by the TPs are likely to contribute to the maintenance of the tenoblastic identity of the TPs (black arrow).

(C) Aggregation and differentiation. By E13.5, the TPs condense and organize into structurally distinct tendons that connect to the muscle and cartilage. In some, but not all tendons, tenocyte differentiation depends on *Scx* function. In most tissue, tendon differentiation depends on the presence of muscle (arrow), but the extensor and flexor tendons that extend into the autopod differentiate as structurally distinct tendons even in the absence of muscles.

However, little is known about other TGF-β family members, in particular the bone morphogenetic protein (BMP) family members in the musculoskeletal development. BMP5 is expressed in precise domains in the developing muscle masses and in the autopodial tendons. In the limb mesoderm, Smad and MAPK pathways act synergistically in the BMP pathway controlling limb development (Zuzarte-Luis et al., 2004). Other BMP family members include growth and differentiation factor (GDF) isomers such as GDF5, -6 and -7 (also known as BMP 14, 13 and 12) have also been implicated in tendon development and healing (Mikic et al., 2009; Mikic et al., 2001; Settle et al., 2003). Mice deficient GDF5, -6 or -7 exhibit tendon ultrastructural, biological and/or biochemical abnormalities (Mikic, et al., 2009; Mikic, et al., 2001), whereas exogenous delivery of these factors causes ectopic tendon formation (Wolfman et al., 1997). In addition, as one of the earliest known markers of joint formation (Settle, et al., 2003; Storm & Kingsley, 1999), GDF5 dysregulation is strongly linked to various musculoskeletal malformations. GDF5 expression/activity is important in controlling different stages of skeletogenesis, in particular chondrogenesis in a GDF5 dose-dependent manner (Francis-West et al., 1999). In cartilage development, GDF5 signaling has a characteristic development pattern in pre-cartilage condensations and in

the developing cartilaginous joints (Settle, et al., 2003). Mutations in either GDF5 or its receptor BMP receptor 1B (BMPR1B) lead to similar skeletal malformation phenotypes, indicating that in chondrogenesis, GDF5 signaling seem to be exclusively mediated through BMPR-1B (Kotzsch et al., 2009). Many developmental processes, including limb skeletogenesis, also require the segregation of signaling molecules into gradient or the functional compartmentalization of one cell type from another to generate information for differentiation and morphogenesis. Although GDF5 has functional roles in both tendon and cartilage development, it remains unclear whether GDF5 plays a role similar to that of FGF. It may be the case that tendon and cartilage lineages develop in an alternative and mutually exclusive manner through the functional compartmentalization processes.

1.2 Tendon Damage and Repair Mechanism

1.2.1 Tendon Injury

Tendon injuries, specifically at the shoulder, are a common cause of morbidity and contribute a significant health burden to the society. It is defined as a loss of cells or ECM caused by trauma (Leadbetter, 1992). Injury represents a failure of cell and matrix adaptation to a mechanical loading, in excess of the tolerance level, which can be repetitive or prolonged. In these circumstances, there is an inadequate response from the cells or tissues to the mechanical loading applied. In other words, tendon is injured when it is exposed to forces that damage it. Tendon injury at the shoulder can be as the result from forces that cause elongation of the tendon tissue extending into the micro- and macro-failure region. Under physiological circumstances, tendons function in the toe and linear region of the stress-strain curve. Repeated and prolonged load application has been shown to alter the stress-strain curve of the tendon tissue, where tendon injury may result from repeated loading into what would normally be the higher linear region

of that curve (Wang, 2006). Rapid unloading has also been associated with tendon injury. Sudden force release is suggested to break interfibrillar adhesion because of shearing force within the tendon (Sharma & Maffulli, 2005). In lieu of forces that are too big for the tissue to withstand, tendon can also be injured when "normal" forces are applied. This occurrence can be seen in genetic disorders, aging, vascular changes, endocrine influences, nutritional deficiencies, inactivity, immobilization and exercise (Hess et al., 1989).

The cellular events in ruptured tendon (i.e. rotator cuff tendon) are closely related to the composition and integrity of ECM structure (Riley et al., 1994a; Riley, et al., 1994b; Wu et al., 2010). Tendon ECM transmits mechanical loads, stores and dissipates loading-induced elastic energy. Mechanical deformation in the ECM can transmit forces through tendon cell actin cytoskeleton and cause the remodeling of the actin cytoskeleton (Wang, 2000; Wang et al., 2001). The cytoskeleton remodeling in turn controls the cell shape, affects cell motility and mediates various cellular functions including DNA and protein synthesis (Janmey, 1991). Tendon cells sense mechanical force and convert them into biochemical signals via mechanotransduction mechanisms that ultimately lead to the physiological adaptiveness of tissue or conversely result in pathological changes.

1.2.2 Normal Repair Mechanism

Tendon injury will initiate attempts of tissue repair, which has been defined as replacement of damaged or lost cells and ECM by new cells or new matrices (Leadbetter, 1992). In the natural healing process, tendon repair can be divided into different phases (Figure 1.4). Generally, they consist of an inflammatory phase, proliferation phase, differentiation phase and remodelling phase. In brief, the healing process starts with a hematoma, platelet activation and invasion of cells that form a

granuloma. Inflammation after injury protects the body by eliminating and diluting harmful agents, preventing further injury, supplying large quantities of oxygen and nutrients needed for repair, and allowing the entry of clotting agents. Inflammation is triggered by several chemical mediators such as histamines, kinins, prostaglandins, complement, and lymphokines (Frank et al., 1999).

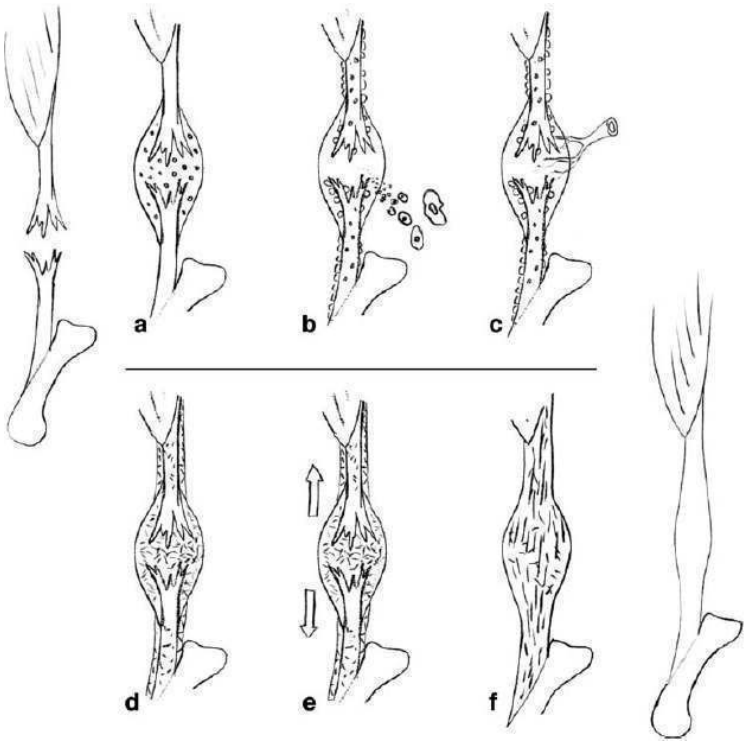

Figure 1.4 Schematic diagram of tendon repair (Aspenberg, 2007).
(a) Haematoma with platelet activation (inflammatory phase).
(b) Invasion of cells and proliferation of paratenon (proliferation phase).
(c) Vascular and neuronal ingrowth.
(d) Loose collageneous callus formation (differentiation phase).
(e) Mechanical stimulation.
(f) Maturation and remodeling (remodelling phase).

During the repair process, the clot formed during inflammation is transformed into a granulation tissue. The circulating monocytes then differentiate into macrophages after entering the extravascular space. These macrophages are capable of digesting and removing the clot while providing a continuing source of growth factors, chemoattractants, and proteolytic enzymes as needed for tenocyte activation (Leadbetter, 1992). The macrophage-derived growth factor and TGFβ cause the proliferation of

tenoblasts originated in the epitenon (Fyfe & Stanish, 1992). As tenoblasts infiltrate the wound, blood vessels are formed and facilitate RBC to carry oxygen and nutrients to the developing tissue. Tenoblasts rapidly produce COL-III, which is characterized by smaller fibrils lacking cross-links, which means that the tissue will be lacking tensile strength. At the later stage of this phase, the tenoblasts shift to produce COL-I. Initially, no cross-link occurs between the tropocollagen molecules. This facilitates the enzymatic breakdown and reorganization in the repaired tendon. Cross-links start to develop at 6-14 days post injury increasing tensile strength to the area of injury. At approximately 48 hours to 8 weeks post-injury, the disorganized collagen fibril deposition lies parallel to tensile forces within the tissue.

In the maturation and remodelling phase, cellularity and synthetic activity decreases in the tendon. However, the collagen production has been shown to be 15 times of normal tendon. The granulation tissue is supplanted by new collagen synthesis and deposition, as well as by remodelling myofibroblasts (which derived from the tenoblast that migrated from the edge of wound) that contract the matrix along the axis of the tendon. The ECM becomes more organized at this stage. Wound healing cells and their matrix exist in a dynamic reciprocity whereby cells deposit new matrix and that the matrix modulates gene expression and cell-matrix receptors (Gurtner et al., 2008). Through cell-cell and cell-matrix interactions, collagen fibrils align with tenocytes and join end-to-end with other fibrils in the wound and at the margin via covalent crosslinks (Kjaer, 2004). Most cells (endothelial cells, macrophages and myofibroblasts) then enter apoptosis (programmed cell death), the ECM thereby undergoes a transition from a highly cellular granulation tissue to a less densely populated scar tissue (Gurtner, et al., 2008). Consequently, tendons usually heal with fibrosis and scar tissue, which may regain only 70-80% of their original structural and biomechanical integrity for as long as one-year-post injury. The healed tendon (with suboptimal tensile strength) is prone to

reinjury, resulting in lifestyle changes with activity restriction. Poor vascularization (Hegedus et al., 2010) and histopathological changes (Maffulli et al., 2011) have been suggested as factors contributing to the resulting tendon thickening, fibrosis and being less resistant to tensile stress compared to its preinjured state. The origin of the cells responsible for repairing an injured tendon is controversial. Two mechanisms have been postulated: intrinsic and extrinsic. The former postulates that fibroblast populations come from the endotenon and epitenon, whereas the latter postulates that inflammatory cells and fibroblasts migrate in from surrounding tissues (Boyer, 2005). However, a recent report suggested that intrinsic repair may require a progenitor class with predominant tendon marker expression, while extrinsic repair may involve a progenitor class recruited from perivascular cells of the peritenon (Mienaltowski et al., 2013). Tendon TSC/TPC decreases with age and alludes to its association with the age-related reduction in tendon repair as seen in rotator cuff tears (Gulotta et al., 2012). Molecular mechanisms controlling these events, either via tenocytes, tenoblast or/and TSC/TPC, and whether a fully differentiated replacement tendon forms at these sites remains largely unclear. The understanding of molecular mechanism in tendon development could assist us in better understanding of tendon etiology and repair.

1.2.3 Surgical Repair and Cell Based Therapy in Tendon Healing

Clinically, tendons are repaired or reconstructed using a variety of traditional and innovative methods or surgical techniques that vary with tendon location. These techniques demonstrate various degrees of success. Tendon grafts are also used (Table 1.4). In the light of current shortcomings of tendon repair, the current focus in tissue engineering research is to investigate a repair method which can restore the tissue defects with living cells, or a cell based therapy. A number of cell sources have been suggested (Table 1.5).

Table 1.4 The advantages and disadvantages of various type of tendon augmentation grafts.

Graft Type	Source	Advantages	Disadvantages
Autograft	Human	1. No disease transmission risk. 2. No storage required. 3. No preservation problem.	1. Donor site complication (Aune et al., 2001; Comley & Krishnan, 1999). 2. Limited availability.
Allograft	Human	1. No donor site complications. 2. Availability.	1. Immunogenicity problem (Minami et al., 1982; Nellas et al., 1996; Nutton et al., 1999). 2. High risk of disease transmission (Nutton, et al., 1999). 3. Required proper storage or preservation (Vangsness et al., 2003).
Xenograft	Animal	1. As with allograft above.	1. As with allograft above. 2. Ethical issue, i.e. inappropriate animal source such as porcine derived tissue graft.
Prosthesis	Human or animal	1. As with allograft above.	1. Low mechanical properties (often result in failure of surgery). 2. Non-specific new tissue induction ability. 3. Induce inflammatory response and rejection (Chen et al., 2009).
Synthetic	Chemical compounds	1. Stronger mechanical strength and consistency in quality (Chen, et al., 2009).	1. Low biocompatibility. 2. Induce inflammatory response and rejection (Chen, et al., 2009).

Table 1.5 A summary of cell therapy of different cell origins.

Cell Type	Source	Advantages	Disadvantages	Study model (Reference)
Mesenchymal stem cells (MSCs)	Bone marrow-derived	1. Multilineage potential. 2. Hypoimmunogenecity. 3. Increase rate of tendon healing and maturation. 4. Improve biomechanical and histologic properties of the tendon.	1. Cannot control differentiation into undesired tissue lineage such as bone, cartilage and muscle. 2. Cell population diminished with age.	Rabbit (Awad et al., 1999; Chong et al., 2007; Djouad et al., 2003; Harris et al., 2004) and Mice (Djouad *et al.* 2003)
	Adipose tissue-derived	1. Widely available. 2. Simple to obtain. 3. No morbidity to donor site.	1. As with bone marrow derived MSCs above. 2. Limited application in tendon therapy.	Equine (de Malttos Carvalho et al., 2011; Del Bue et al., 2008)
	Synovium-derived	1. May promote bone-tendon regeneration.	1. As with bone marrow derived MSCs above.	Nil (Chen et al., 2011)
	Muscle-derived	1. As with bone marrow derived MSCs above.	1. As with bone marrow derived MSCs above. 2. Limited evidence in tendon therapy.	Nil (Rosenbaum et al., 2008)
Fibroblasts	Skin	1. Great potential in tendon engineering and tendon repair. 2. Widely available. 3. Relatively noninvasive method for cell harvesting. 4. No significant effect to the donor site. 5. Potential source of cells for storage.	1. Differentiated cells. 2. Uncertainty about behavior in tendon environment. 3. Unsubstantiated repair process. 4. Qualitative repair.	Human (Connell et al., 2009)
Tendon progenitor/ stem cells	Tendon	1. Can develop into tendon like tissue.	1. Morbidity to donor site. 2. No tenocyte markers. 3. No human studies.	Rat (Gurkan et al., 2010)

Cell based therapy seeks to enhance tissue repair by providing a cell and/or biological scaffold to a repair site in an attempt to elicit a healing response. In order to achieve this, investigators have seeded differentiated cells (mature cells or tenocytes) and undifferentiated cells (mesenchymal stem cells) on scaffolds to develop tissue engineered constructs. Various stimulations, either chemical (using growth factors and cytokines) or mechanical (by stretching), which can mimic the nature of normal tendon *in vivo* environment have been used to enhance the properties of the constructs. Advances in tendon tissue engineering approaches potentially yield a cell-based product that can markedly advance the repair of this soft tissue.

Nevertheless, would tendon development events re-occur and regenerate tendon tissue, should the TP cells be transplanted to the defect site? In the course of cell-based therapy, would the TP, tenoblast and tenocytes together orchestrate cellular events of tendon regeneration? A better understanding in the cellular events involved in tendon development, differentiation and repair is needed in order to lead us to better outcomes for treating tendon injury.

1.3 Mesenchymal Stem Cells and Their Potential Role in Tenogenesis

1.3.1 Mesenchymal Stem Cells and Its Potential

Mesenchymal stem cells (MSCs, bone marrow stromal cells or multipotent progenitor stromal cells) are multipotent adult stem cells that are capable of differentiating into various cells of mesodermal lineage (Huang et al., 2012; Platt et al., 2009). According to International Society for Cellular Therapy (ISCT), the three criteria used to define MSC are: (i) they adhere to plastic when maintained in standard culture conditions using culture flasks, (ii) there is a specific surface antigen (Ag) expression and (iii) presence of multipotent differentiation potential (Dominici et al., 2006). Firstly, MSCs must be plastic-adherent, as described by Friedenstein et al. in the 1970s

(Friedenstein et al., 1974). Secondly, more than or at least 95% of MSC population must express CD105, CD73 and CD90, as measured by flow cytometry. In addition, these cells must lack expression (not more than 2% positive) of CD45, CD34, CD14 or CD11b, CD79α or CD19 and HLA class II. Third, the cells must able to differentiate into trilineages (i.e. osteoblasts, adipocytes and chondrocytes) under standard *in vitro* differentiating condition.

Although the traditional source of MSCs has been the bone marrow, there are other potential sources of MSCs (Beitzel et al., 2012; Pierini et al., 2012). These have included peripheral blood (Kassis et al., 2006; Roufosse et al., 2004), adipose tissue (Boquest & Collas, 2012; Choi et al., 2012; Nishiwaki et al., 2012) and cord blood (Joyce et al., 2012; Kim et al., 2012). The roles of these cells in an organism are to maintain and repair the tissue in which they are found. In recent years, the interest in MSCs have been growing immensely due to speculation that these cells, having both the ability for multipotency and self-renewal, have the potential to bring about tissue regeneration and repair. As such, in several conditions requiring tissue repair, MSCs have been shown to enhance the healing potential when these cells are placed directly into the defective site (Awad, et al., 1999; Lee et al., 2011; Schnabel et al., 2009). However, these findings have been received with some reservations. Many researchers have expressed their concern as to the validity of such findings mainly because the exact etiology as to why tissue regeneration occurs is still poorly understood. Furthermore, the existence of a mixed population in MSCs has been shown to lose its viability after being transplanted into tissues (Toma et al., 2002). It is speculated that such repair outcomes may be attributed to other factors such as the release of cytokines, interaction with the extracellular matrix (loss of attachment to ECM which cause anoikis), ischemia and other causes (Rodrigues et al., 2010). In addition, transplantation outcome has been worsened by conditions such as *in situ* ectopic bone formation which has been reported

in transplantation of undifferentiated MSCs (Harris, et al., 2004), although the opposite result has also been reported (Pacini et al., 2007). To overcome such issues, a number of tissue engineering approaches are presently being developed to induce differentiation in a specific lineage, i.e. tenogenic differentiation, prior to transplantation.

1.3.1.1 Tenogenic Differentiation of MSC

One of the unique biological properties of MSC is the ability to differentiate into cells of multi-mesenchymal lineages (Caplan & Bruder, 2001). The tenogenic MSC lineage is one of the MSC lineages that have been of great interest to orthopaedic surgeons, especially for cell-based therapy in tendon disorders. In the case of tenogenesis (tendogenesis, ligamentagenesis), MSCs undergo lineage commitment into tenogenic MSCs and ultimately mature into tenocytes (Figure 1.5). *In vitro* differentiation of MSCs towards tenogenic lineage before transplantation has been postulated to be a good strategy to promote tendon healing apart from minimizing the chances of ectopic bone formation or tumour formation in tendons. Thus, a new enlightened era of stem cell research has been initiated with human and non-human MSCs, *in vitro* and *in vivo*, in relation to MSC tenogenic differentiation as well as its use in tendon repair. However, to date, neither tenogenic lineage transition sequence nor differentiation has been comprehensively discussed or widely reported, neither has it been compared to other lineage transition sequences such as osteogenesis, chondrogenesis or myogenesis.

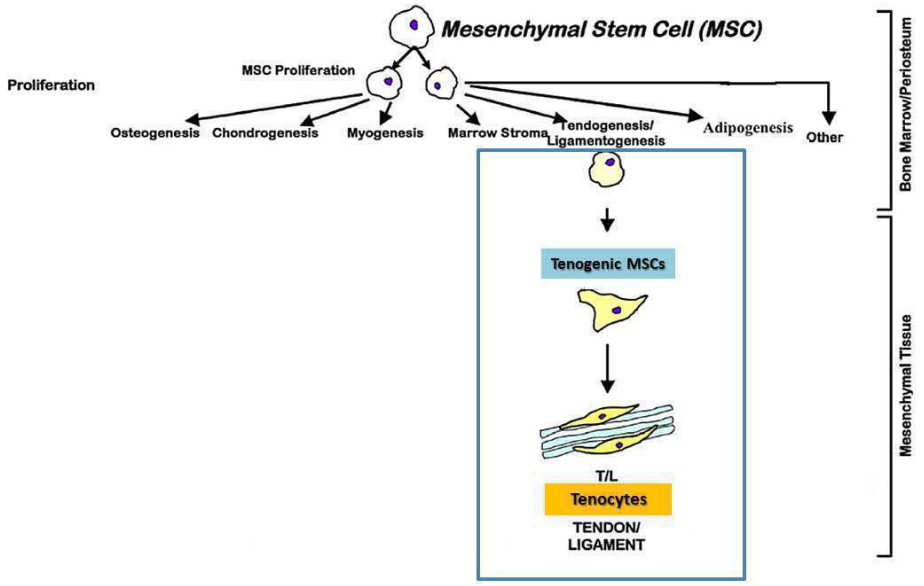

Figure 1.5 Mesenchymal stem cells and tenogenic differentiation. Modified from Caplan & Bruder (2001).

The current focus of tendon tissue engineering is to develop an optimal method for MSC tenogenic differentiation, potentially to be used for tendon repair. To achieve this goal, various tissue engineering approaches have been applied to MSCs of various tissue sources in order to elucidate their effects in tenogenesis induction. Among the techniques that have been reported are; mechano-transduction (Farng et al., 2008; Kuo & Tuan, 2008; Lee et al., 2007), gene transfer (Wang, et al., 2005), co-culture systems (Lee, et al., 2007; Luo et al., 2009) and making use of biomaterials (Kishore et al., 2012) as well as growth factors, either in the purified form (Lee, et al., 2011; Tan et al., 2012) or the crude extract such as platelet-rich–plasma releasate (Zhang & Wang, 2010). Nevertheless, the optimal method to induce tenogenic differentiation for maximal phenotypic expression has yet to be proven. Table 1.6 summarizes all the tenogenic differentiation studies that been reported thus far.

Table 1.6 Summary of methods for tenogenic differentiation in MSCs from various tissue origin sources.

No	Differentiation method (Reference)	Cell type	Tissue source	Principle Findings
(A)	**Gene transfer**			
1	Transfection of BMP-12 gene by electroporation into rhesus MSCs (Wang, et al., 2005)	i. Rhesus primary MSCs	i. Adult rhesus bone marrow aspirates	i. Transfected cells became more slender and their processes became thinner and were interwoven into a network. ii. More organelles were observed in transfected cells. iii. Transfected cells expressed *BMP-12*, *Col-I* and *Scx*, but not *Col-III* mRNA.
2	Transfection of active Smad8 variant into an MSC line that coexpressed BMP2 (Hoffmann et al., 2006)	i. Multipotent mouse C3H10T1/2 cell ii. C3H10T1/2 constitutively expressing BMP2	i. Transfection with pSV2pac followed by selection with puromycin (5μg/ml) (Moutsatsos et al., 2001)	i. Smad8 inhibits the osteogenic pathway in MSCs, while promoting tendon differentiation. ii. Expression of BMP2 and Smad8 linker plus MH2 domain leads to tenocytic cell differentiation in C3H10T1/2 cells. iii. Smad8 plays a pivotal role in the signaling cascade that leads to tenocytic differentiation of MSCs, however, this cascade is not directly activated by BMP2 but by another factor, which is still unknown.
3	hMSC cell line lentivirally transduced with FLAG-*Scx* cDNA (Alberton et al., 2012)	i. Immortalized Bone marrow derived-hMSC cell line (SCP-1)	i. HMSCs were purchased from Cambrex Corporation (East Rutherford, NJ, USA) and transduced with hTERT lentivirus (Boker et al., 2008)	i. Increased cell area. ii. Reduced self-renewal and restricted multipotentiality. iii. Gene expression of *Col-I*, decorin and tenomodulin were significantly increased. iv. *Sox-9* gene expression was significantly decreased.
(B)	**Mechanical stimulation**			
4	MSCs stretched at 10% strain, 1 Hz for 48 hours or MSCs stretched after co-culture in 1/1 ratio of anterior cruciate ligament (ACL) cells and MSCs (Lee, et al., 2007)	i. Human MSC primary culture ii. Human ACL primary culture	i. Human bone marrow ii. Human ACL	i. ACL typical markers (*Col-I*, *Col-III* and tenascin C) were significantly increased in cell exposed to mechanical stress, either with or without co-culture with ACL cells prior to stretching. ii. Specific regulatory signals released from ACL cells appear to be responsible for supporting the selective differentiation toward ligament cells.

Table 1.6, continued

5	Mechanical stimulation with cyclic uniaxial 10% strain at 0.33 Hz for 48 hours applied to the scaffold administered with 1600ng of GDF5 (per scaffold) to the collagen coating (Farng, et al., 2008)	i. Immortalized mouse bone marrow derived-MSC cell line (D1 ORL UVA)	i. From ATCC (Manassas, VA)	i. After 48 hours, both mechanical stimulation and GDF5 increased mRNA production of *Col-I*, *Col-II* and *Scx*. ii. Tenascin C mRNA expression did not increase. iii. Combined stimuli did not change mRNA gene expression.
6	Mechanotransduction in 3D dynamic model at 1%, 1 Hz for 30 min/day for 7 days (Kuo & Tuan, 2008)	i. MSC primary culture	i. Human bone marrow	i. 3D MSC tenogenesis culture system upregulate scleraxis, but cyclic stretching was required to maintain expression of scleraxis. ii. Neo-tendon formation due to matrix deposition and remodeling activity (increased gene expression levels in scleraxis, Col-I, Col-III, elastin, MMP1, MMP3 and MMP13) under dynamic loading conditions. iii. Similar role for Wnt4 and Wnt5a in tenogenesis with cyclic stimulation.
7	Substrate with mechanical property gradients and various extracellular matrix ligand (Sharma & Snedeker, 2010)	i. Human bone marrow MSCs	i. Human bone marrow MSCs from Dr Simon Hoerstrup's lab (University of Zurich)	i. Higher level of attachment on collagen substrate after 1 h and increase spreading and organization trends after 24 h. ii. Differentiation studies showed an increase in osteoblast differentiation on fibronectin substrates than collagen substrates. iii. Osteogenic differentiation decreased on substrates of lower stiffness and lower ligand density. iv. Tenoblast markers were detected on collagen substrates within a narrow range of stiffness.
8	Mechanical stretching at 10%, 1 Hz for 48 hours (Xu et al., 2011; Xu et al., 2012)	i. Immortalized bone marrow derived-hMSC cell line (UE6E7T-3)	i. hMSC infected with recombinant retroviruses expressing the E6, E7 and hTERT; acquired from Health Science Research Resource Bank (Osaka, Japan)	i. Stretched cells showed increased in *Col-I*, *Col-III*, tenascin C and *Scx* mRNA expression. ii. FAK signaling molecule plays an important role in regulating hMSCs cell realignment and mechanical stretch induced tenogenic differentiation.

Table 1.6, continued

				iii. RhoA/ROCK and cytoskeletal organization were essential to mechanical stretch-activated FAK phosphorylation at Tyr397. iv. RhoA/ROCK, cytoskeletal organization and FAK compose a "signaling" network" that sense mechanical stretching and induced hMSCs tenogenic differentiation.
(C) Co-culture system				
9	In 1:1 ratio co-cultured system with adult primary tenocytes cultured in transwell chambers and MSC plated onto the plate wells (Luo, et al., 2009)	i. Rat primary MSC culture ii. Rat primary tenocyte culture	i. Adult Sprague-Dawley (SD) rat bone marrow ii. Adult AD rat Achilles tendons	i. MTT assay showed no significant growth difference between control and co-culture group at the first two days of co-culture, but after day 3, MSC in co-culture group grew significantly faster than control. ii. The mRNA expression level of *c-fos* gene was significantly up-regulated on day 4 and day 7 in co-culture group. iii. On day 7, the co-culture group also showed significant up-regulation in tenascin C and *Scx* mRNA gene expression levels but no changes for *Col-I* and *Col-III*. iv. On day 14 and 21, up-regulation in *Scx*, tenascin C, *Col-I* and *Col-III* were also detected in the co-cultured group.
10	In 50/50 ratio co-cultured of anterior cruciate ligament (ACL) cells and MSCs (Canseco et al., 2012)	i. Porcine MSCs primary culture ii. Porcine ACL primary culture	i. Bone marrow from Yorkshire pig ii. ACL from 4-8 month Yorkshire pig legs	i. Significant increase in *Col-I* and tenascin-C mRNA/protein expression levels. ii. Ratio of *Col-I* to *Col-III* is similar to native ligament levels.
11	In 1:1 ratio co-cultured system with adult primary tenocytes cultured in transwell chambers and amnion epithelial cells (AEC) plated onto the plate wells (Barboni et al., 2012)	i. AEC primary culture ii. Fetal tenocytes primary culture iii. Adult tenocytes primary culture	i. Sheep Amnions ii. Sheep fetal calcaneal tendons iii. Sheep adult calcaneal tendons	i. AEC exposed to fetal derived tenocytes/explants developed *in vitro* tendon-like three dimensional structures with expression of Col-I and Thsb4. ii. Significant increase in tendon related mRNA genes expression levels (*Col-I*, *Scx* and tenomodulin). iii. Increased COL-I, OCN and connexins (Cx32and Cx34).

Table 1.6, continued

(D)	**Growth factor or other culture supplements**			
12	With 50 ng/mL BMP-12 (GDF-7) supplement for 14 days (Violini et al., 2009)	i. Equine primary MSCs	i. Adult Dutch Warm blood mare bone marrow	i. Equine MSCs expressed tenomodulin and decorin mRNA at day 14 of BMP-12 induction. ii. Upon tenogenic differentiation in BMP-12, equine MSCs exhibited heterogeneous morphology with most cells fibroblast-like and elongated.
13	Treatment with GDF5 in monolayer (Park et al., 2010)	i. Rat primary MSCs culture	i. Fisher 344 rat adipose tissue	i. GDF5 increased MSCs proliferation in a dose- and time-dependent manner. ii. The mRNA expression level of ECM (*Col-I*, decorin and aggrecan) and tenogenic marker (*Scx*, tenomodulin and tenascin C) in MSCs treated with 100 ng/mL of GDF5 were significantly up-regulated. iii. Western blot analysis confirmed dose- and time-dependent increases in protein expression of tenomodulin, tenascin C, Smad-8 and matrix metalloproteinase-13. iv. GDF5 treatment induced cellular events leading to tenogenic differentiation in rat adipose tissue-derived MSCs.
14	Spatial control of multiple differentiation fate with growth factors (BMP-2, FGF-4 and GDF-7) printed onto fibrin coated glass coverslips and growth factors as a supplement in culture medium (Ker et al., 2011)	i. Multipotent mouse C3H10T1/2 cells ii. Mouse C2C12 cells iii. Multipotent muscle derived stem cells (MDSC)	i. From ATCC (Manassas, VA, USA) ii. From ATCC (Manassas, VA, USA) iii. Primary mouse gastrocnemius muscle biopsies	i. Fibroblast growth factor-2 (FGF-2) up-regulated *Scx* mRNA expression levels in C3H10T1/2 cells, mouse C2C12 cells and primary MDSC in dose dependant manner. ii. FGF-2 may direct stem cells toward a tendon fate via the *Ets* family members of transcription factors such as *pea3* and *erm*.

Table 1.6, continued

15	Treatment with a single physiological dose of insulin (10^{-10} mol/L) (Mazzocca et al., 2011)	i. MSC primary culture	i. Human bone marrow	i. 10^{-10}-mol/L insulin was determined as the optimal single dose for one time treatment to differentiate MSCs into tendon. ii. 1-time treatment with a physiologic dose of 10^{-10} mol/L insulin exhibit significantly higher transcript levels of *Col-I*, *Col-III*, *Scx* and tenascin C compared with untreated cells. iii. MSCs treated with 10^{-10} mol/L insulin also showed a significant increase in the protein levels of COL-I, COL-III and tenascin C compared with the untreated cells and cells treated with the 10^{-9}, 10^{-12}, 10^{-13} mol/L insulin.
16	Growth factor induction (10 ng/mL IGF-1, 10 ng/mL TGFβ1, IGF-1/ TGFβ1 (5 ng/mL each), 10 ng/mL PDGF-BB, 10 ng/mL BMP-12), high density co-culture of primary MSCs and tenocyte cultures, with spent media obtained from primary tenocytes (Schneider et al., 2011)	i. Canine primary MSCs culture ii. Canine primary tenocyte culture	i. Canine adipose tissue biopsies ii. Canine tendon biopsies	i. Tenogenesis was induced in MSCs through a combination of treatment with IGF-I and TGFβ1, in high density co-cultures and through cultivation with the spent media from primary tenocytes. ii. Electron microscopy and immunoblotting demonstrate up-regulation of COL-I, COL-III, decorin, tenomodulin, β1-integrin, MAPKinase pathway (Shc, Erk1/2) and SCX in the co-cultures, and provide simultaneous evidence for the inhibition of apoptosis. iii. Cells actively exchanged vesicles suggesting the uptake and interchange of soluble factors produced by the MSCs and/or tenocytes.
17	Use of recombinant human bone morphogenetic protein 12 and bone morphogenetic protein 13 (rhBMP12 and rhBMP12) to induce the formation of tendon-like tissue or tendon-specific gene expression (Berasi et al., 2011)	i. Murine MSC cell line C3H10T1/2 (clone 8)	i. From ATCC (Manassas, VA, USA)	i. Ectopic expression of rhBMP12 and rhBMP13 induces the formation of tendon-like tissue. ii. Treatment of C3H10T1/2 cells with rhBMP12 or rhBMP13 resulted in a dose-dependent induction of a tendon-specific gene (Thrombospondin, *Thbs4*) expression with no detectable activation of SMAD 1/5/8. iii. Differential regulation of *Thbs4* and osteocalcin has potential utility as an *in vitro* biomarker for induction of tenogenic signaling.

Table 1.6, continued

(E)	**Scaffold/substrate with or without growth factor**			
18	MSCs seeded on basic fibroblast growth factor (bFGF) releasing nanofibrous scaffolds (Sahoo et al., 2010)	i. Rabbit MSCs	i. New Zealand white rabbits bone marrow	i. bFGF incorporated in nanofibrous scaffolds released in bioactive form over 1 week. ii. The released bFGF activated tyrosine phosphorylation signaling within seeded MSCs. iii. bFGF releasing nanafibrous scaffold facilitated MSC proliferation, up-regulated mRNA gene expression levels of tendon/ligament-specific ECM proteins (*Col-I*, *Col-III*, biglycan and fibronectin) and induced tendon/ligament-like fibroblastic differentiation.
19	Human tendon stem/progenitor cells (hTSPCs) culture on aligned nanofibers (Yin, et al., 2010)	i. Human tendon stem/progenitor cells	i. Human foetal Achilles tendon from an aborted embryo (5months)	i. The hTSPCs were spindle-shaped and well orientated on the aligned nanofibers. ii. The mRNA expression of tendon-specific genes (*Eya2*, *Scx*, *Col-14* and *Col-I*) was significantly higher in hTSPCs growing on aligned nanofibers than those on randomly-oriented fibrous nanofibers in both normal and osteogenic media. iii. Aligned cells expressed significantly higher mRNA levels of integrin $\alpha 1$, $\alpha 5$ and $\beta 1$ subunits, myosin IIB. iv. *In vivo* experiments, the aligned nanofibers induced the formation of spindle-shaped cells and tendon-like tissue.
20	Collagen substrates with moderate rigidity (~30-50 kPa) (Sharma & Snedeker, 2012)	i. Human primary MSCs	i. Human bone marrow (Hoerstrup et al., 2002)	i. *Scx* and tenomodulin mRNA expression observed only in cells cultured on the collagen substrate with moderate rigidity (~30-50kPa). ii. *Smad8* and *BMP-2* mRNA expression levels were increased on collagen substrate with moderate rigidity (~30-50kPa). BMP-2 secretion was confirmed by colorimetric assay. iii. BMP-2 supplementation was sufficient to arrest osteoblastic differentiation on substrate sections that were otherwise osteogenic.

1.3.2 Growth and Differentiation Factor 5 (GDF5) and Tenogenesis

1.3.2.1 Growth and Differentiation Factor 5 (GDF5)

Growth and differentiation factor 5 (GDF5) is also known as Cartilage-derived morphogenetic protein 1 (CDMP1) or BMP 14 (Chang et al., 1994). It is a growth factor of the BMP family, a subgroup of TGFβ superfamily secreted at the stage of pre-cartilageneous mesenchymal condensations in the perichondrium around the cartilaginous cores, especially in the joint inter-zones, and be observed clearly during the embryonic development (Chang, et al., 1994; Luyten, 1997). It is also expressed by fibroblast (You et al., 1999), articular chondrocytes (Erlacher et al., 1998) and odontoblasts (Morotome et al., 1998). It is initially synthesized as a large precursor protein (proGDF5) consisting of 501 amino acids including an N-terminal signal peptide of 27 amino acid length (Hotten et al., 1994). Inferring from studies reporting on other BMPs (Cui et al., 2001; Cui et al., 1998), the proGDF5 undergoes proteolytic cleavage at a cluster of basic residues [RX(K/R)R] at position 381. Consequently, a C-terminal mature protein is released from the N-terminal prodomain. The bioactivity and signaling range of this secreted mature protein is regulated by proteolytic cleavage (Herpin et al., 2004). The mature GDF5 protein consists of 120 amino acids, which form homo- or hetero- dimers with other BMPs that are linked via a disulfide-bridge. The importance of GDF5 is underlined by a number of clinical syndromes associated with mutations in GDF5 or BMPR1B (Kornak & Mundlos, 2003; Schwabe & Mundlos, 2004).

1.3.2.2 Tenogenesis Effects of GDF5

The first published work which produced evidence of ectopic tendon formation by administration of GDF5, -6 and -7 (Wolfman, et al., 1997) has made it possible for GDF5, -6, and -7 to be used to augment tendon and ligament repair in a manner similar to the use of more traditional BMPs for fracture healing and bone fusion. Since then,

various studies have reported the use of GDF5 in tendon formation or functional repair (Table 1.7). These studies consistently demonstrated as well as evidenced the pivotal role of GDF5 in synovial joint formation, especially tendon formation, and in modulating tendon repair (Table 1.7). GDF5 is therefore being suggested as a viable candidate for eventual therapeutic use to augment tendon repair in human.

1.3.2.3 Other Effects of GDF5

The findings of tenogenicity using GDF5 induction are not without controversy. Several researchers have found that GDF5 is capable of inducing osteogenic (Shimaoka et al., 2004; Zeng et al., 2007) and chondrogenic (Coleman & Tuan, 2003; Hotten et al., 1996; Nakamura et al., 1999). Such discrepancies may be explained by many factors. These have included different recombinant protein production processes, different delivery mechanisms as well as different culture conditions (monolayer, 3D culture, micromass culture, medium used etc.). Further, during early development, the progenitor cells differentiated into various types of mature cells, e.g. osteocytes, chondrocytes and tenocytes, in response to the amount of signal molecules received. Thus, different differentiation effects from different concentrations of GDF5 could be expected considering that gradient effect is an important mechanism in early development which compartmentalizes one cell type from another. As such, fine-tuning the factor amount or form of delivery may play an important role in achieving controlled healing of tendon tissue.

Table 1.7 A summary of tendon and GDF5 related studies.

No	Model Used	Finding
(A) ***In vivo*** **study**		
1	Rodent Achilles tendon	The tensile strength of the tendon repair with GDF5 increased in a dose-dependent manner (Aspenberg & Forslund, 1999).
2	GDF5 deficient murine model	GDF5 deficient Achilles tendons were structurally weaker than controls and structural strength differences appeared to be caused by compromised material properties. Mutant Achilles tendon contained 40% less collagen per microgram of DNA when compared to control (Mikic, et al., 2001).
3	GDF5 deficient murine model	Mutant tail showed 17% increase in the proportion of medium diameter (100-225 nm) collagen fibrils in tail tendon (at the expense of larger fibrils) when compared to controls ($p<0.05$). Mutants also exhibited a trend toward an increase in irregular-shaped polymorphic fibrils (33% more, $P>0.05$). In stress-relaxation test, mutant fascicle relaxed 11% more slowly ($p<0.05$) than control tendons (Clark et al., 2001).
4	GDF5 deficient murine model	Achilles tendon of GDF5 deficient mice contained significantly more fat within the repair tissue and was significantly weaker than control tissue after surgery. GDF5 may play an important role in modulating tendon repair (cell recruitment, migration/adhesion, differentiation, proliferation, and angiogenesis) (Chhabra et al., 2003).
5	Rodent medial collateral ligament (MCL) laceration model	Administration of GDF5 once at the time of surgery significantly improve ligament repair as observed in increased the ultimate tensile strength and stiffness of the femur-ligament-tibia complex. Quantitative PCR and in situ hybridization revealed enhanced type-I procollagen expression by GDF5. PCR analysis also revealed that the GDF5 treatment reduced the expression of type III procollagen relative to type I procollagen (Tashiro et al., 2006).

Table 1.7, continued

6	Rodent Achilles laceration tendon	Tendon transduced with BMP-14 exhibit less visible gapping, a greater number of neotenocytes at the site of healing and greater tensile strength than did either those transduced with GFP or the sham controls at two weeks after repair. No inflammatory response and ectopic bone formed in the tendon transduced with BMP-14 or GFP (Bolt et al., 2007).
7	Rodent Achilles tendon	Histological grading at 3 weeks showed improved healing (significantly higher ultimate tensile load and stiffness) in tendons repaired with GDF5 coated suture versus control (Dines et al., 2007).
8	Murine distal flexor digitorum longus (FDL) tendon; recombinant adeno associated (rAAV)-*Gdf5* vector & freeze-dried mouse FDL tendon allografts with rAAV-*Gdf5*	Recombinant adeno-associated vector (rAAV)-*Gdf5* vector significantly accelerates wound healing in an *in vitro* fibroblast (Mouse embryonic fibroblast (NIH3T3)) scratch model, and when loaded onto freeze-dried FDL tendon allografts significantly improves the metatarsophalangeal joint flexion compared to rAAV-*lacZ* controls (Basile et al., 2008).

(B) *In vitro* study

9	Immortalized murine bone marrow stromal cell lines (from ATCC, Manassas, VA)	GDF5 increased mRNA production of *Col- I, II*, and *Scx* compared to control; no additive synergism effect with mechanical stimulation (Farng, et al., 2008).
10	Rodent adipose tissue-derived MSCs	GDF5 treatment can induce cellular events leading to the tendonogenic differentiation of adipose-derived mesenchymal stem cells (Park, et al., 2010).
11	Lagomorpha anterior cruciate ligament (ACL) and medial collateral ligament (MCL).	ACL cells proliferation to GDF5 treatment was similar to that of MCL cells. GDF5 enhanced *Col-1a1* expression in ACL and MCL fibroblasts. MCL fibroblasts showed stronger migration activities in response to GDF5, depended on the integrin α2-mediated adhesion on *Col-I* (Date et al., 2010).

Table 1.7, continued

12	Lagomorpha MCL fibroblast	bFGF/GDF5 treatment additively enhanced cell proliferation and migration *in vitro*. MCL repaired with bFGF/GDF5 hydrogel stimulated *Col-IaI* expression and deposition and organization of fiber alignment, induced better morphology of fibroblasts in healing MCL (Saiga et al., 2010).
13	Primary rat adipose-derived stromal cells (ADSCs)	Gene expression of *Scx* was upregulated at one week with GDF5 treatment when cultured on 3D electrospun scaffold compared to 2D films with or without GDF5 treatment. Expression of *Col-I* was increased at 1 week on treatment of 100 ng/ml GDF5 compared to 2D film (James et al., 2011).

Initial studies suggest that murine GDF5 play a role in osteogenesis via the process of endochondral ossification, i.e., bone formation. This process starts with mesenchymal cell condensations which forms a cartilage matrix that later calcifies to form mature bone (Chang, et al., 1994; Storm et al., 1994). The osteogenic effect of GDF5 in the *in vivo* model utilizing the hydroxyapatite (HA) implants has been reported in MSC/HA composites supplemented with GDF5 (Shimaoka, et al., 2004). Besides the *in vivo* studies, an *in vitro* study with rat adipose tissue derived stromal cells has also been reported. Based on the *in vitro* study, GDF5 not only promotes osteogenic differentiation, but also angiogenic activity of stromal cells. These findings suggest that several distinct regulatory mechanisms may exist in association with osteogenic differentiation, particularly in GDF5 induced differentiation processes (Zeng, et al., 2007).

Several studies have also demonstrated that the TGFβ superfamily of proteins induces chondrogenesis in cultured MSCs. In ATDC5 (the cell line which has differentiated to chondrocytes) culture, GDF5 has been shown to promote chondrocyte differentiation and activate p38 MAPK to promote chondrogenesis (Nakamura, et al., 1999). In an *in vitro* high-density micromass culture of chick embryonic limb mesenchymal cells, GDF5 has been demonstrated to increase cellular condensation, which resulted in chondrocyte maturation. This is achieved via gap junction mediated cellular communication. However, it does not increase the cellular viability, biosynthetic activity, or function through enhanced N-cadherin mediated cellular adhesion (Coleman & Tuan, 2003). This finding is in contrary to previous study that demonstrated GDF5 causes the increase in cell adhesiveness. It has been postulated that through the cell adhesiveness mechanism, the GDF5 initiates condensation formation (Buxton et al., 2001). Recently, *Trps1* (a novel transcription factor of GATA family) was demonstrated to act downstream of the GDF5 signaling pathway and promote the

differentiation and apoptosis of ATDC5 cells (Itoh et al., 2008). It has a synergistic dedifferentiating effect in expanded human and bovine chondrocyte primary culture when combined with 2.5 μg/ml insulin (Appel et al., 2009).

1.3.2.4 Tenogenesis Signaling Pathways

In the Transforming Growth Factor β (TGFβ) signaling pathway, GDF5 has been shown to bind specifically to three different cell-surface transmembrane receptors: serine/threonine kinase receptor type 1 (BMPR-IB) or serine/threonine kinase receptor type 2 which could be either BMPR-II or ActR-IIA (Nishitoh et al., 1996). Generally, upon ligand (GDF5) binding, the type II receptor forms heterodimer with type I receptor. This then activates the type I receptor. The intracellular substrates of the activated type I receptors are Smads. Smads 1, 5 and 8 are phosphorylated and then translocate to the nucleus, where they participate in the transcriptional regulation of genes involved in tendon formation (Figure 1.6) (Prime et al., 2004; Roelen & Dijke, 2003). The TGFβ signaling pathway is of key importance in the control of embryogenesis and tissue homeostasis. It plays an important role during the specification of early tendon progenitor cells as described in the earlier section (Section 1.1.2, page 10). Besides, TGFβ1 has been demonstrated to mediate the production of COL-I in human tendon fibroblasts under *in vitro* cyclic uniaxial stretching conditions (Yang et al., 2004). However, the exact cellular and molecular downstream mechanistic pathway of GDF5 remains to be completely understood.

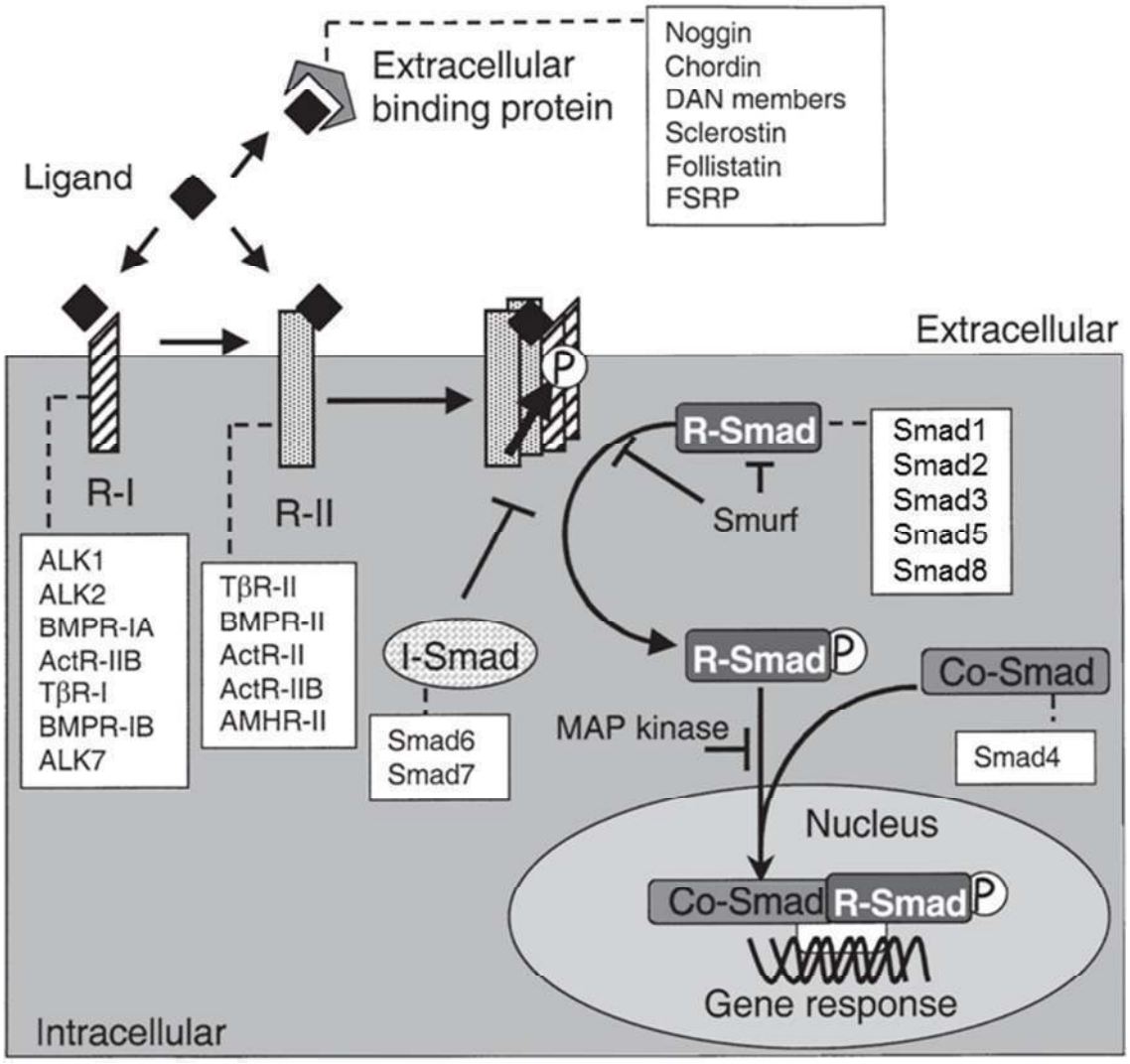

Figure 1.6 Transforming growth factor β (TGFβ) signaling pathway (Modified from Roelen & Dijke 2003).
Ligand (GDF5) binding-induced heterodimerization of type II and type I receptors leads to type I receptor phosphorylation by type II receptor followed by receptor-regulated Smad (R-Smad: Smad 1, Smad 5 and Smad 8 are substrate of BMP type I receptor; Smad 2, Smad 3 and Smad 7 are activated primarily in response to TGFβ1) phosphorylation by type I receptors. A complex is formed of phosphorylated R-Smad with the Co-Smad, and this complex translocates to the nucleus where it regulates transcription.

1.4 Aim and Objectives

1.4.1 Aim of This Study

Tenogenesis is a tightly controlled process in which several factors regulate discrete stages of the differentiation programme. Understanding the mechanism of cell commitment and further differentiation into particular lineage is of importance in the

development of therapeutic treatments of tendon lesions based on MSC transplantation techniques. This research aims to understand the GDF5 effect in tenogenic differentiation and function in the regulation of adult stem cells, particularly in MSC.

The overall objective is to identify regulatory mechanisms in GDF5-induced tenogenic MSC. This would lead to a better understanding in the molecular and cellular events in early tenogenic differentiation processes induced by GDF5 in MSC, in particular, human MSC. This ultimately have a potential for future development of molecular therapeutic approaches to repair tendon lesions.

1.4.2 Hypothesis

The hypotheses are:

I. GDF5 is involves in tenogenesis of MSCs;

II. GDF5-induced MSCs is superior for tendon healing compared to the undifferentiated MSCs;

III. Gene expression profile studies could reveal putative molecular pathways involved in tenogenesis of MSC.

1.4.3 Specific Objectives

The effects of GDF5 induced tenogenesis in adult MSC at cellular and transcriptional (mRNA) levels as well as in *in vivo* transplantation model were studied. To evaluate the hypothesis, the following objectives were established:

I. To isolate human and rabbit mesenchymal stem cells (hMSCs and rbMSCs) from human and rabbit bone marrow respectively.

II. To differentiate the hMSCs into tenogenic lineage using GDF5.

    i. To determine the effect of different concentration of GDF5 on MSC proliferation;

ii. To determine the optimal concentration of GDF5 for tenogenic induction in hMSCs (with comparison to native tenocytes from tendon);

iii. To determine tenogenic lineage commitment in hMSCs using gene expression analysis.

III. To differentiate rbMSCs into tenogenic lineage using GDF5, in view of possible animal transplantation models being used in our later experiments.

i. To optimize the best concentration of GDF5 for tenogenic induction in rbMSCs (in comparison to native tenocytes from tendon);

ii. To confirm tenogenic lineage using gene expression analysis in tenogenic rbMSCs.

IV. To determine the potential of GDF5 induced tenogenic MSCs in a rabbit tendon repair model.

i. To create a defect on a rotator cuff tendon (infraspinatus tendon) in the New Zealand white rabbit model;

ii. To determine the suitability of tenogenic MSCs in rabbit tendon repair.

V. To compare the gene expression profile in GDF5 induced hMSC compared to untreated MSC control and native tenocyte from tendon.

i. To generate the gene expression profiles of untreated MSCs, GDF5 induced MSC and native tenocytes;

ii. To compare the differentially expressed genes in untreated hMSC control, GDF5 induced MSCs and native tenocytes;

iii. To determine the putative pathways potentially involved in the events of tenogenesis which could potentially contribute to the tendon repair mechanism.

CHAPTER 2

METHODS

Part of this chapter has been published in:

Tan S.L., Ahmad T.S., Selvaratnam L. & Kamarul T. (2013) Isolation, characterization and the multi-lineage differentiation potential of rabbit bone marrow-derived mesenchymal stem cells. *Journal of Anatomy* 222: 437-450.

2.0 METHODS

2.1 Materials

2.1.1 General Chemicals

All the chemicals used were either cell culture grade, analytical grade or molecular biology grade as stated in Table 2.1.

Table 2.1 General chemicals used in this study.

No.	Chemical Name	Grade	Manufacturer, Country
1	Absolute ethanol	Molecular Biology grade Catalogue No: 1.08543.0250	Merck, Damstadt, Germany.
2	Acetic acid (glacial)	ACS grade Catalogue No: 1410-58	R & M Marketing, Essex, UK.
3	Agarose	Molecular Biology grade Catalogue No: 75510-019	Invitrogen, Carlsbad, California, USA.
4	Ascorbic acid	Not specify. Catalogue No: A5706-100G	Sigma-Aldrich, Germany.
5	BD CompBead	Anti-mouse Ig kappa Cat No: 552843	BD Pharmingen™, USA.
6	β-mercaptoethanol,	Molecular biology grade (Catalogue No: 1.12006)	Merck, Damstadt, Germany.
7	Collagenase Type 1A-S	Cell culture grade. Catalogue No: C9722-50mg)	Sigma-Aldrich, Germany.
8	Copper (II) sulphate	ACS grade Catalogue No: 171-500G	Univar Analytical Reagent, Australia.
9	DEPC treated water	Molecular Biology grade Catalogue No: 750023	Invitrogen, Carlsbad, California, USA.
10	Dimethyl sulfoxide	Cell culture grade Catalogue No: 196055	MP Biomedical, Santa Ana, CA, USA.
11	Eosin Y	Histology grade. Catalogue No: E-6003	Sigma-Aldrich, Germany.
12	Fast Green	Histology grade. Catalogue No: F-7252	Sigma-Aldrich, Germany.

Table 2.1 continued

13	Formaldehyde	Not specify. Catalogue No: FO 129-20	System®, Italy.
14	Formic acid	Not specify. Cat No: FO 264-70	System®, Italy.
15	Glutaraldehyde	Histology grade. Cat No: G6257- 1L	Sigma-Aldrich, Germany.
16	Haematoxylin	Histology grade. Cat No: 1798-25G	Laboratory Chemical, Australia.
17	Isopropanol	ACS grade Catalogue No: 4778-50	R & D Chemical, UK.
18	L-proline	Not specify. Cat No: P5607-25G	Sigma-Aldrich, Germany.
19	Mayers Haematoxylin	Histology grade. Catalogue No: S330930	Dako, Denmark.
20	Methanol	ACS grade Catalogue No: ME313-50	System®, Italy.
21	Ficoll-Paque Premium	Density: 1.077 g/mL Catalogue No: 17-5442-02	GE Healthcare, Sweden.
22	Oil-red-O	Histology grade. Catalogue No: O0625-25G	Sigma-Aldrich, Germany.
23	RNase away	Molecular Biology grade Catalogue No: 75510-019	Molecular BioProducts, San Diego, CA.
24	Safranin O	Histology grade. Catalogue No: 3260-25G	Laboratory Chemical, Australia.
25	Sodium acetate anhydrous	Not specify. Catalogue No: A679-500G	Analytical Chemical, New Zealand.
26	Sodium chloride	Not specify. Catalogue No: 31434	Sigma-Aldrich, Germany.
27	Stabilizing fixative	For immuno staining. Catalogue No: 338036	BD Pharmingen™, USA.
28	Stain buffer (FBS)	For immuno staining. Catalogue No: 554656	BD Pharmingen™, USA.
29	50X TAE	Molecular Biology grade Catalogue No: 129237	Qiagen, USA

2.1.2 Cell Culture Consumables

For cell culture procedures, sterile disposable plastic pipettes (Orange Scientific, Belgium), Pasteur pipettes (Copan, Italy), cell scrappers (TPP, Switzerland) and centrifuge tubes (Orange Scientific, Belgium) were used. Cell culture consumables such as petri dishes (Orange Scientific, Belgium), cell culture flasks (Nunc^{TM}, USA), six-well- and 96-well- plates (TPP, Switzerland) and chamber slide with cover (Lab-Tek II, Nunc, Japan) were used for *in vitro* experiment. All the general cell culture components were obtained from Gibco, Invitrogen, Carlsbad, California, USA, unless stated otherwise (Table 2.2). Due to the inavailability of recombinant rabbit GDF5 at time when the experiments were conducted, the recombinant mouse GDF5 was used for rbMSCs; whereas the recombinant human GDF5 was used for hMSCs. Althought the signaling and mature domains of GDF5 is highly conserved among different species (Seemann et al., 2005), the recombinant human and mouse GDF5 were tested separately at diferent concentrations to determine their effective concentration towards the treated cells. The cell culture images were captured via digital camera (Xcam Alpha, 3M pixel) attached on the inverted phase contrast trinocular microscope (CKX41, Olympus, Tokyo, Japan).

Table 2.2 Cell culture components used in this study.

No.	Cell Culture Component	Manufacturer, Country
1	Dulbecco's Modified Eagle Medium (DMEM) 4.5 g/L D-glucose (Catalogue No: 11995-065)	Invitrogen, Carlsbad, California, USA.
2	Dulbecco's Modified Eagle Medium (DMEM) 1.0 g/L D-glucose (Catalogue No: 11885-065)	Invitrogen, Carlsbad, California, USA.
3	Dulbecco's Modified Eagle Medium (DMEM) 4.5 g/L D-glucose (without fenol red) (Catalogue No: 31053-036)	Invitrogen, Carlsbad, California, USA.

Table 2.2 continued

4	Dulbecco's Modified Eagle Medium (DMEM) 1.0 g/L D-glucose (without fenol red) (Catalogue No: 11054-020)	Invitrogen, Carlsbad, California, USA.
5	GlutaMAX^{TM}-I Supplement (Catalogue No: 35050-061)	Invitrogen, Carlsbad, California, USA.
6	Fetal Bovine Serum (Catalogue No: 10270-098)	Invitrogen, Carlsbad, California, USA.
7	Sodium pyruvate (Catalogue No: 11360)	Invitrogen, Carlsbad, California, USA.
8	Antibiotic-Antimycotic (100x) (Catalogue No: 15240-062)	Invitrogen, Carlsbad, California, USA.
9	Penicillin-Streptomycin (Catalogue No: 15140-122)	Invitrogen, Carlsbad, California, USA.
10	Recombinant fragment (Human) GDF5 protein (Catalogue No: AB55329)	Abcam, UK
11	Recombinant Mouse GDF5, Carrier free (Catalogue No: 853-G5-050/CF)	R&D Systems, UK
12	TrypLE (Catalogue No: 12604-013)	Invitrogen, Carlsbad, California, USA.
13	Accutase, cell detachment solution (Catalogue No: L03-AT104)	ICT,USA
14	Phosphate-Buffered Saline (PBS) 7.2 (1X) (Catalogue No: 20012-027)	Invitrogen, Carlsbad, California, USA.
15	Phosphate-Buffered Saline (PBS) 7.2 (10X) (Catalogue No: 70013-032)	Invitrogen, Carlsbad, California, USA.

2.1.3 Immunostaining Reagents

Both direct and indirect staining methods were used for immunofluorescence staining, in flow cytometry analysis as well as immunohisto- and immunocyto- staining. The reagents used for immune staining are listed in Table 2.3.

Table 2.3 Reagents used for immunofluorescence staining for flow cytometry analysis (A) and for fluorescence imaging (B).

(A)

Antigens	Clone No.	Fluorochrome conjugate	Catalogue No.	Manufacturer	Species specificity
Integrin beta 1 (CD29)	P4G11	Non-conjugated	Ab78502	Abcam, UK	Rabbit only
CD29	MAR4	APC	559883	BD Biosciences, US	Human only
H-CAM (CD44)	W4/86	Non-conjugated	MCA806G	SeroTec, US	Rabbit only
CD44	G44-26 (C26)	APC	559942	BD Biosciences, US	Human only
5'-nucleotidase cytosolic II (CD73)	eBioTY/11.8	PE-Cy™ 7	25-0731	eBioscience, US, California)	Rabbit only
CD73	AD2	PE-Cy™7	561258	BD Biosciences, US	Human only
CD73	AD2	FITC	561254	BD Biosciences, US	Human only
TAPA-1 (CD81)	JS-81	APC	555676	BD Biosciences, US	Rabbit and Human
Thy-1 membrane glycoprotein (CD90)	5E10	PE-Cy™ 7	561558	BD Biosciences, US	Rabbit and Human
Hematopoietic precursor antigen (CD34)	ICO115	PerCP-Cy5.5	Sc-7324 PCPC5	Santa Cruz Biotechnology, California	Rabbit only
CD34	My10	PE	348057	BD Biosciences, US	Human only
CD34	My10	PerCP-Cy5.5	347203	BD Biosciences, US	Human only
Leukocyte common antigen (CD45)	L12/201	Non-conjugated	MCA808GA	Gentaur Molecular Products, Belgium	Rabbit only
CD45	2D1	APC-H7	641399	BD Biosciences, US	Human only
c-kit (CD117)	YB5.B8	PE	555714	BD Biosciences, US	Rabbit and Human
HLA-DR	TU36	FITC	555560	BD Biosciences, US	Rabbit and Human

Table 2.3 continued

(B)

No	Antibody	Dilution	Catalogue No.	Manufacturer
1	Type-I collagen mouse mAb	1:200	GTX26308	GeneTex, Inc, Irvine, CA
2	Type-II collagen mouse mAb	1:200	CP18	Calbiochem, Darmstadt, Germany
3	Type-III collagen mouse mAb	1:200	CP19	Calbiochem, Darmstadt, Germany
4	Nucleostamin (9D5.3) mouse mAb	1:200	ab78129	Abcam, UK
5	Tenascin C (EB2) mouse mAb	1:200	ab88280	Abcam, UK
6	Scleraxis (D-14) goat polyclonal antibody	1:200	sc-87425	Santa Cruz Biotechnology, California
7	Tenomodulin (C-20) goat polyclonal antibody	1:200	sc-49324	Santa Cruz Biotechnology, California
8	Fluorescein isothiocyanate (FITC)-conjugated rat anti-mouse IgG (A85-1)	1:200	553443	BD Biosciences, US
9	Texas red-conjugated donkey anti-goat IgG	1:200	sc-2783	Santa Cruz Biotechnology, California
10	Alexa Fluor® 546 phalloidin	1:40	A22283	Invitrogen, Carlsbad, California, USA
11	Hoechst 33342, trihydrochloride, trihydrate (10 mg/ml)	5 μg/ml	H3570	Invitrogen, Carlsbad, California, USA
12	FluoroGel mounting medium	-	GTX28214	GeneTex, Inc, Irvine, CA

2.1.4 Surgical Procedures

The consumables used for surgical procedures and animal (rabbit) handling, i.e. surgical scrubbing for bone or tendon harvesting, aseptic and anesthetic procedure in

defect creation and tendon repair. The scrubbing solutions and anesthetics used are as listed in Table 2.4.

Table 2.4 Consumables and drugs for surgical procedure.

No.	Sterilize/Anesthetics Solutions	Manufacturer, Country
1	Povidon iodine topical solution USP (10% w/v) Catalogue No: MAL070101352x	Unidon Solution, Mumbai, India.
2	Ketamine (100 mg/ml; 300 mg/kg b.w.)	Ilium, Australia.
3	Xylazil-20 (20 mg/ml; 3 mg/kg b.w.)	Ilium, Australia.
4	Ophthalmologic ointment (Eye ointment) 10mg/g chloramphenicol, 5000 IU/g polymyxin B sulphate	Ilium opticin, Australia.
5	Lignocaine hydrochloride (20 mg/ml)	Ilium, Australia.
6	Premilene® 3-0 non-absorbable polypropylene monofilament suture	B. Braun, Germany.
7	Ethicon 4-0 coated Vicryl undyed braided absorbable suture	Johnson & Johnson International, Brussels, Belgium.
8	Meloxicam injection (5 mg/ml; 0.3 mg per kg b.w.)	Meloxicash, India.
9	Kombitrim 240 (sulfamethoxazole 200 mg/ml + trimethoprim 40 mg/ml; 30 mg per kg b.w.)	Kela, Belgium.
10	Pentobarbital sodium (Nebutal ® Sodium Solution; 50 mg/ml)	Boehringer, Ingelheim, Germany.

2.1.5 Gene Specific Primers

Primers used for RT-PCR and *q*RT-PCR in this study were synthesized by 1st Base, Malaysia as listed in Table 2.5. Gene specific primers for rabbit and human genes were designed with Primer Premier 5 (Premier Biosoft, Palo Alto CA) or adapted from previous study as listed in Table 2.5. The primers for CD29, CD166, CD34 and CD45 were only used for rabbit samples in reverse transcription-polymerase chain reaction

(RT-PCR) analysis, whereas, for Glyceraldehyde-3-phosphate dehydrogenase (*Gapdh*), type-I collagen (*Col-I*) and scleraxis (*Scx*), the primers were used in both human and rabbit samples in quantitative RT-PCR (*q*RT-PCR) analysis. The nucleostemin (*Nst*), type-III collagen (*Col-III*) and decorin (*Dcn*) were used for *q*RT-PCR in human samples only.

Table 2.5 Primers used for RT-PCR and *q*RT-PCR in this study.

No	Gene name/ Sample	Primer sequence	Amplicon size (bp)	GenBank Accession No	Primer design software or Reference source
1	CD29	Forward: 5'-CAA GAA GGA ATG CCT ACG TC -3' Reverse: 5'-CAA TGC CAC CAA GTT TCC CAT-3'	720	FCU27351	Primer Premier 5
2	CD166	Forward: 5'-GCT CCC CAG TAT TTA TTG CCT TC-3' Reverse: 5'-GTA GCA CCT TTC CAT TCC TGT A-3'	345	Y13243	Primer Premier 5
3	CD45	Forward: 5'-AGGTAGTAGATGTTTTCCAAG TAGTGA-3' Reverse: 5'-ACTTGTCCATTCTGGGCAGGG TAG-3'	130	XM_002717662	Primer Premier 5
4	CD34	Forward: 5'-AGAACTTTCCAGCATGTTCCA GTTTATG-3' Reverse: 5'-GGCTTGCCACATCTTGCTCGG TGA-3'	95	XM_002717543	Primer Premier 5
5	Glyceraldehyde-3-phosphate dehydrogenase (*Gapdh*)	Forward: 5'-AAC ATC ATC CCT GCC TC TAC TG -3' Reverse: 5'-CTC CGA CGC CTG CTT CAC -3'	196	NM_002046	Kuo and Tuan 2008
6	Type-I Collagen (*Col-I*)	Forward: 5'- CTG ACT GGA AGA GCG GAG AG -3' Reverse: 5'- TCT GGG CAA TGC TGG GCT GTG TGG G-3'	129	AY633663	Primer Premier 5
7	Scleraxis (*Scx*)	5'-CAG CGG CAC ACG GCG AAC -3' 5'-CGT TGC CCA GGT GCG AGA TG -3'	165	BK000280	Kuo and Tuan 2008

Table 2.5, continued

8	Nucleostemin (*Nst*)	5'-ATG ACC TGC CAT AAG CGG TAT-3' 5'-AAG GGA GCA CTG TTT GGA ACT-3'	131	AK315484	Primer Premier 5
9	Type-III Collagen (*Col-III*)	5'-CAG CGG TTC TCC AGG CAA GG-3' 5'-CTC CAG TGA TCC CAG CAA TCC C-3'	179	NM_000090	Kuo and Tuan 2008
10	Decorin (*Dcn*)	5'-CTC TGC TGT TGA CAA TGG CTC TCT-3' 5'-TGG ATG GCT GTA TCT CCC AGT ACT-3'	257	NM_133505, NM_133504, NM_001920, NM_133503	Kuo and Tuan 2008
11	Tenascin C (*Tnc*)	Forward: 5'-GGG TCC TCA AGA AAG TCA TCC G-3' Reverse: 5'-CTG ACT CCA GAT CCA CCG AAC-3'	62	NM 002160	Primer Premier 5
12	Peroxisome proliferator-activated receptor-gamma (*Ppar-γ*)	Forward: 5'-AGCAAAGAAGTCGCCATCC-3' Reverse: 5'-CGTTCAAGTCAAGGCTCACA-3'	118	NM_001082148	Primer Premier 5
13	Runt-related transcription factor 2 (*Runx2*)	Forward: 5'-TCAGGCATGTCCCTCGGTAT-3' Reverse: 5'-TGGCAGGTAGGTATGGTAGTGG-3'	54	AY598934	Primer Premier 5
14	SRY (sex determining region Y)-box 9 (*Sox9*)	Forward: 5'-AGAGCGAAGAGGACAAGTTCCCCGT-3' Reverse: 5'-ATGGGCACCAGCGTCCAGTCGTAGC-3'	85	XM_002719499	Primer Premier 5

2.1.6 Commercial Kits

2.1.6.1 Differentiation Assay

StemPro® Osteogenesis Differentiation Kit (Invitrogen, Carlsbad, California, USA) was used for osteogenic differentiation of mesenchymal stem cells in *in vitro* cell culture environment.

StemPro® Adipogenesis Differentiation Kit (Invitrogen, Carlsbad, California, USA) was used for adipogenic differentiation of mesenchymal stem cells in *in vitro* cell culture environment.

2.1.6.2 Colorimetric Assay

The Sircol™ Soluble Collagen Assay (Biocolor, Ireland) was used to determine the acid-soluble collagens released into culture medium by mammalian cells during *in vitro* culture.

2.1.6.3 Histology Staining

The Von Kossa special stain kit, method for calcium (Bio-Optica, Milano, Italy) was used for staining of calcium deposition in monolayer cultured cells in chamber slides.

The Van Gieson Trichrome staining kit (Bio-Optica, Milano, Italy) was used for connective tissue and collagen fibers staining in histological sections and monolayer cells seeded in chamber slides.

2.1.6.4 Total RNA Purification and Quality Assessment

The AllPrep DNA/RNA/Protein Mini Kit (Qiagen, USA) was used to purify total RNA. This kit allowed an enrichment for mRNA and most RNA <200 nucleotides are selectively excluded. The purified RNA samples were ready to use for RT-PCR, quantitative *q*RT-PCR and microarray.

The Qiagen® RNase-Free DNase Set (Qiagen, USA) was used with the AllPrep DNA/RNA/Protein Mini Kit for on-column digestion of DNA during RNA purification.

The Agilent RNA 6000 Nano kit (Agilent Technologies, Germany) was used to determine the total RNA integrity and quality with the Agilent 2100 expert bioanalyzer.

2.1.6.5 Polymerase Chain Reaction (PCR)

The Superscript^{TM} III One-Step RT-PCR System with Platinum^{R} Taq DNA Polymerase kit (Invitrogen, Carlsbad, California, USA) was used for one step reverse transcription-PCR.

The Transcriptor High Fidelity cDNA Synthesis kit (Roche Diagnostics GmbH, Mannheim, Germany) was used to synthesize cDNA of high accuracy which suitable for used in quantitative PCR (*q*RT-PCR).

The iQ™ Sybr® Green Supermix (Bio-Rad, Hercules, CA, USA) was used for dye-based *q*RT-PCR with Bio-Rad CFX96™ real-time PCR System.

2.1.6.6 Microarray Gene Expression Analysis

The Applaus™ WT-Amp ST System (NuGEN Technologies, Inc, San Carlos, CA, USA) was used to prepare amplified cDNA sample for global gene expression analysis on Affymetrix® Gene Chip® Gene 1.0 ST Arrays.

The GeneChip® Human Gene 1.0 ST Array (Affymetrix Inc, Santa Clara, CA, USA) was used for whole-genome gene level expression studies of known genes. This GeneChip array comprised more than 750,000 unique 25-mer oligonucleotide features constituting over 28,000 gene-level probe sets.

The MinElute Reaction Cleanup Kit was used for purified the cDNA samples amplified with Applaus™ WT-Amp ST System, prior to *in vitro* cDNA fragmentation and transcription with biotinylated nucleotide, in preparation for hybridization on Affymetrix GeneChip® Human Gene 1.0 ST Array.

The Encore™ Biotin Module (NuGEN Technologies, Inc, San Carlos, CA, USA) was used to fragmentize and label the purified cDNA samples in preparation of targets for hybridization on Affymetrix GeneChip® Human Gene 1.0 ST Array. The GeneChip® Hybridization Wash and Stain Kit was used for hybridization with

GeneChip® Hybridization Oven 640, automated washing and staining of GeneChip® Human Gene 1.0 ST Array with the Fluidics Staition 450 and scanning probe arrays using the Affymetrix GeneChip® Scanner 3000 7G.

2.1.6.7 Validation of Microarray Data

QuantiGene® Plex 2.0 Assay (Plex set 11904 Human) kit (Affymetrix, Santa Clara, CA) was used for confirmation of the microarray analysis. This assay was used to determine the gene expression levels in total RNA samples without RNA amplification step. Thus, it provided an independent method of measurement relative to the quantitative PCR and microarray platforms. It used three sets of pooled oligonucleotides that function to capture, provide binding sites for signal amplification molecules, and stabilize the mRNA of interest.

2.2 Biological Samples

2.2.1 Human Samples Procurement

Ethics approval to conduct this study was granted by the University of Malaya Medical Centre (UMMC) Ethics Committee (Reference number: 602.22; Appendix A1). Human bone marrow was harvested from adult donors (Appendix A2) undergoing intramedullary nailing in UMMC. The bone marrow samples were collected in the blood collection (EDTA) tubes and transported to tissue culture laboratory for isolation and culture.

Adult human hamstring tendons free of pathology were obtained from donors who underwent ligamentous reconstruction of the knees and arthroplasty of the knee(s) (Appendix A2). Written informed consent was obtained from each donor. The hamstring tendons that were obtained were kept in sample bottle with sterile normal saline before transported to laboratory for further processing.

2.2.2 Rabbit Samples Procurement

Ethics approval to conduct the *in vitro* and *in vivo* experiments in this study was granted by the Animal Care and Use Committee (ACUC), Faculty of Medicine, University of Malaya (Reference number: PM/24/06/2008/TKZ(b)(R); Appendix B).

2.2.2.1 *In vitro* Study

For primary culture purpose, the New Zealand white rabbits (at least 4 months old) were euthanized by an overdose of pentobarbital sodium (Nebutal® Sodium Solution) (Boehringer, Ingelheim, Germany). All the long bones (tibia, femur and humerus bones) were harvested from the rabbit under aseptic condition. All the harvested bones were kept in phosphate buffered saline (PBS, pH 7.2) supplemented with penicillin-streptomycin 1% (v/v Invitrogen-Gibco) before transferred to tissue culture laboratory for further processing. Figure 2.1 depicted the surgical tools used for rabbit bone and tendon harvesting.

Figure 2.1 Surgical tools used in aseptic rabbit bone and tendon procurement.

2.2.2.2 *In vivo* Transplantation Study

For *in vivo* transplantation study, eighteen healthy adult New Zealand white rabbits (2.87±0.53 kg and age of 6-12 months) were randomly assigned into 6 groups (n=3). The rabbits were anesthetized by intramuscular injection of ketamine (100 mg/ml; 300 mg/kg body weight; Ilium, Australia) and xylazil-20 (20 mg/ml; 3 mg/kg body weight; Ilium, Australia). The rabbit eyes were protected by application of ophthalmologic ointment (Ilium opticin, Australia) to prevent damage or dryness of the cornea during induction phase of anesthesia and the surgery. The surgical area was disinfected with povidon iodine topical solution 10% w/v (Unidon Solution, India) and 3 ml of 20 mg/ml lignocaine hydrochloride (Ilium, Australia) was injected subcutaneously for local anesthetic effect. Surgical defect creation and repair were conducted with assistance from a medical officer. Figure 2.2 depicted the surgical tools used for rabbit *in vivo* transplantation surgery.

Figure 2.2 **Surgical tools used for rabbit transplantation study.**
The microsurgery set was used for tendon defect creation.

2.3 General Laboratory Equipment

The laboratory equipment used for the experiments conducted in this study was as listed in Table 2.6.

Table 2.6 List of general and specialized equipment used for cell culture, molecular biology analysis and cell imaging analysis.

No	Equipment	Model	Brand
1	CO_2 incubator	CCL-170B-8	Esco, Singapore
2	CO_2 incubator	Galaxy 170R	New Brunswick, Enfield, CT, USA
3	Refrigerated centrifuge	5810R	Eppendorf, Hauppauge, NY, USA
4	Orbital mixing chilling/Heating dry bath	Echotherm™ SC20	Torrey Pines Scientific Inc, Carlsbad, CA.
5	Vortex mixer	VTX-3000L	Uzusio, Japan
6	Inverted phase contrast microscope	CKX41	Olympus, Tokyo, Japan
7	Water bath	Precisterm	Selecta®, Spain
8	Laser confocal microscope	TCS SP5 II	Leica Microsystems, Mannheim, Germany
9	Class II biosafety cabinet	Airstream (AB2-4S1)	Esco, Singapore
10	Automated microfluidic electrophoresis system	Experion™	Bio-Rad, Hercules, CA, USA
11	Bioanalyzer	Agilent 2100	Agilent Technologies, Germany
12	Nanodrop UV-Vis Spectrophotometer	NanoDrop™ 2000c	Thermo Scientific, Wilmington, DE
13	CFX96 Real time PCR system	C1000™	Bio-Rad, Hercules, CA, USA
14	Genechip® hybridization incubator	GeneChip® Hybridization Oven 640	Affymetrix Inc, UK

Table 2.6, continued

15	Genechip® automated fluidic system	Fluidics Station 450	Affymetrix Inc, UK
16	Genechip® scanner	GeneChip® Scanner 3000 7G	Affymetrix Inc, UK
17	Microtiter plate luminometer	Luminex	Bio-Rad, Hercules, CA, USA
18	Fume cabinet	DFH4000	Erla Technologies, Malaysia

2.4 Standard Methods

2.4.1 Tenocyte Primary Culture

2.4.1.1 Human Hamstring Tendon-Derived Tenocyte (hTeno) Primary Culture

Human hamstring tendon specimens were processed using the methods modified from Zhang and Wang (2010a). Briefly, the tendons were minced into approximately 1 mm^3 in size under a sterile condition. The explants were then transferred into a 15 mL falcon tube with 0.4 mg/mL type I collagenase (200 U/ml solution) in PBS (pH 7.2), and incubated at 37^oC in a humidified atmosphere of 5% CO_2 for 2 h to allow for the enzymatic digestion process to occur. The specimens were subsequently centrifuged at 1800 rpm at 15^oC for 5 mins. The supernatant was then removed and the pellet was washed twice with 10 mL PBS. Following that, the digested explants were cultured in T75 tissue culture flasks (Nunc^{TM}, USA) with DMEM-high glucose (4.5 g/L glucose) (Invitrogen-Gibco, USA), supplemented with 10% fetal bovine serum (FBS) (Invitrogen-Gibco, USA), 100 unit/mL penicillin-streptomycin and 200 mM GlutaMAX™-I (Invitrogen-Gibco, USA). Cultures were incubated at 37^oC in a humidified atmosphere of 5% CO_2 and supplemented with fresh culture medium at 3-day intervals. Forty eight hours after culturing, the digested tissues were discarded, and the outgrown cells were maintained at 80-90% of confluency for subculture using

trypsin digestion. These primary native human tenocyte (hTenos) cultures (P2 or P3) were used as positive controls in the subsequent total collagen and gene expression experiments. The cells isolated appeared to have fibroblastic morphology (Figure 2.3), similar to that reported by Zhang and Wang (2010a) in rabbit tenocyte culture.

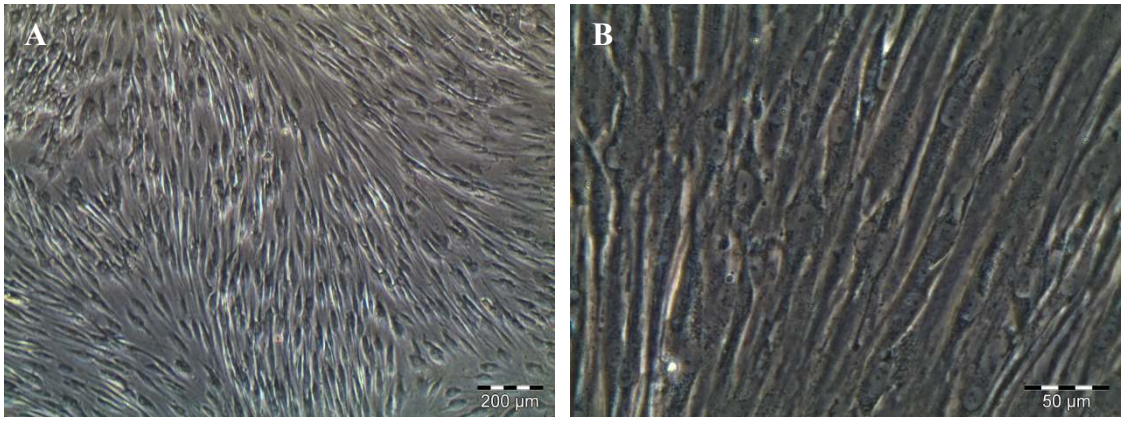

Figure 2.3 Human tenocyte primary culture.

A. Cells were appeared in fibroblastic spindle shape. Low magnification image (4x).
B. Cells appeared to be stretched with long and thin processes, these cells tended to group in close contact, parallel arrangement and grow in high-density colonies. High magnification image (20x).

2.4.1.2 Rabbit Achilles Tendon-Derived Tenocyte (rbTeno) Primary Culture

Rabbit Achilles tendons were processed with the same protocol used in human hamstring tendon-derived tenocyte (hTeno) isolation and culture (Section 2.4.1.1). Rabbit tenocytes isolated appeared to have fibroblastic morphology (Figure 2.4), similar to that reported by Zhang and Wang (2010a) in rabbit tenocyte culture.

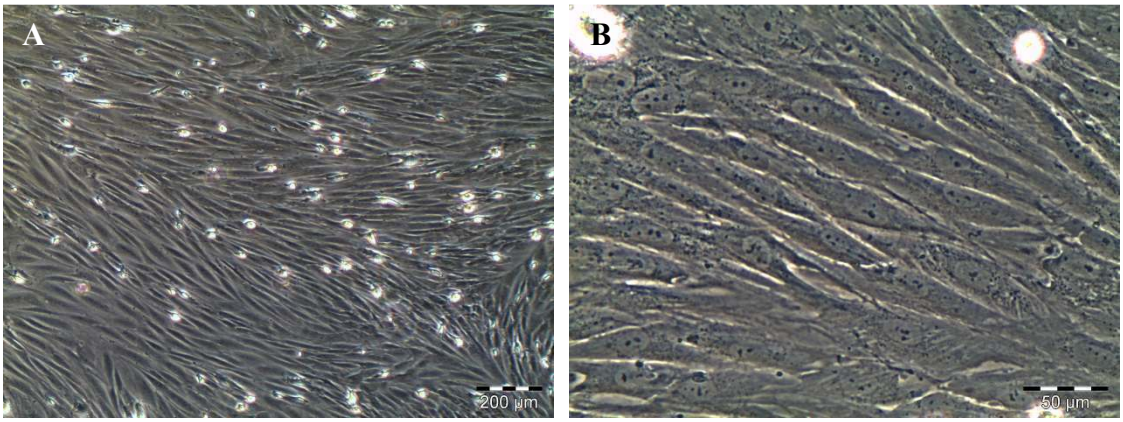

Figure 2.4 Rabbit tenocyte primary culture.

Figure 2.4, continued

A. Cells were appeared in fibroblastic spindle shape. Low magnification image (4x).
B. Cells appeared to have similar morphology compared to that of human tenocyte primary culture. High magnification image (20x).

2.4.2 Measurement of Cell Length and Width

Photographs were taken at representative areas of culture plates. The length and the maximum widths (cell body width) perpendicular to the long axes of individual cells were measured using ImageJ 1.46r software (National Institute of Mental Health, Maryland, USA). At least 8 representative cells were measured from each independent experiment. Data were presented as mean ± standard error of mean. The statistical analysis was performed using SPSS Statistic software (version 19). Student's t-test (2 sided, unpaired) was carried out to compare the differences in mean values and p-value < 0.05 was taken as significant.

2.4.3 Trilineages Differentiation Assay

MSC primary cultures (at P2, N=3) were seeded in the cell culture vessel at cell density of $5x10^3$ cells/cm^2. For histological staining, cells were seeded onto chamber slides, whereas for gene expression analysis, cells were seeded in T-25 culture flask. MSC cultures were incubated in MSC growth medium for three days at 37 ^oC in a humidified CO_2 incubator. The MSC growth medium was then replaced with pre-warmed StemPro® Osteogenesis Differentiation medium (Invitrogen, Carlsbad, California, USA) or StemPro® Adipogenesis Differentiation medium (Invitrogen, Carlsbad, California, USA) or chondrogenic medium (Appendix C) and refed at every 3 days interval. After 28 days, cells seeded in chamber slides were fixed with appropriete fixative and proceeded to specific histological staining (Section 2.4.9).

2.4.4 Cell Proliferation Assay

AlamarBlue® assay was conducted to determine the cell proliferation in MSCs based on the colorimetric quantitative analytical principle. Two days after the cells were supplemented with various concentration levels of GDF5, 25 µl of alamarBlue® reagent (Invitrogen-Gibco, USA) was added into the medium. Culture plates were protected from light with aluminium foil. Absorbance readings at 570 nm and 600 nm were obtained using a spectrophotometer (Epoch, Biotek, USA) at various time points i.e. 0, 2, 4, 6, 12 and 24, 36, 48 and 60 h. Untreated hMSCs cultured in MSC growth medium were used as controls. Three independent experiments were performed, each in octuplicates in the 96-well plates.

2.4.5 Total Soluble Collagen Assay

Total soluble collagen in the culture medium was quantified with colorimetric Sircol^{TM} soluble collagen assay (Biocolor, Ireland). Briefly, the cell culture medium was mixed with Sircol dye reagent with vigorous agitation in a 1.5 mL microcentrifuge tube for 30 mins. The mixture was then centrifuged for 10 mins at 10,000xg to collect the collagen-dye complex at the bottom of the centrifuge tubes. The unbound dye solutions were later removed by draining the tubes. Subsequently, 1 mL of the alkaline reagent was added to each microcentrifuge tube. As the unbound dye dissolved, the absorbance of the samples was measured at 540 nm. The collagen content in the medium was calculated based on the standard curve plot, with type-I collagen supplied with the kit as the reference sample. In both the dose and time response experiments, three independent experiments, each in triplicates were performed.

Statistical analysis was analyzed with SPSS (ver. 17) software. Comparisons of mean values between the different concentrations and various time points were conducted using one-way analysis of variance (ANOVA) statistical test. Least

significant differences (LSD) analysis with Bonferroni adjustment for multiple pairwise comparisons of the mean total collagen differences was conducted. Statistical significance was accepted when *p* value was less than 0.05 ($p<0.05$).

2.4.6 Sample Preparation for Transmission Electron Microscopy Imaging

For electron microscopy imaging, the medium was discarded from the culture flask containing rbMSC (or hMSC) at 70-80% confluence. The cells were rinsed twice with PBS (pH 7.2) (Invitrogen-Gibco, USA) before being trypsinized and scraped from flask with a cell scraper, centrifuged at 800 xg for 10 mins to form a cell pellet at the bottom of centrifuge tube. The cell pellet was then fixed in 4% glutaraldehyde (Sigma-Aldrich, Germany) overnight before being further processed. The pellet was washed three times in 0.1 M cacodylate buffer (pH7.4) (Merck AG, Darmstadt, Germany), prior to, and post-secondary fixation for 2 h at room temperature in a mixture of osmium tetraoxide : cacodylate buffer (1:1). The pellet was kept overnight in 0.1 M cacodylate buffer (pH7.4 (Merck AG, Darmstadt, Germany)). The next day, the pellet was washed with uranyl acetate for 10 mins, followed by three washes with double distilled water. Then, the pellet was dehydrated through a graded ethanol series (35, 50, 70 and 95%) for 10 mins each; 100% for 15 mins, three times; propylene oxide and epoxy resin mixture (1:0 for 15 mins twice; 1:1 for 1 h and 1:3 for 2 h) and in fresh epoxy resin, overnight, on the rotary mixer (Ted Pella, Redding, California, USA), at 1 rpm. The specimen was then embedded in epoxy resin for semithin and ultrathin sectioning with ultramicrotome (Reichert Ultracuts, Leica Microsystems, Vienna, Austria). Images were obtained with a transmission electron microscope (Leo Libra 120, Carl Zeiss SMT AG, Oberkochen, Germany). Electron micrographs were prepared by the Electron Microscope Unit in University of Malaya.

2.4.7 Gene Expression Analysis

2.4.7.1 Total RNA Isolation

Total RNA was extracted from $1X10^6$ cells of 70-80% confluent rbMSC primary culture (P1-P3) using AllPrep DNA/RNA/Protein Mini kit kit according to manufacturer's instructions and treated with RNase-free DNase I (Qiagen GmbH, Hilden, Germany). Briefly, the cell harvested for total RNA extraction were lysed with buffer RLT before loaded into the Allprep DNA spin column. The flow through collected in the collection tube was mixed with 100% ethanol before loaded into the RNeasy spin column. After one wash with buffer RW1, the sample was treated with on-column DNase I (Qiagen GmbH, Hilden, Germany) digestion. After washing steps with buffer RW1 (once) followed by buffer RPE (twice) the total RNA was eluted with 30 µl of nuclease-free water. Total RNA samples were stored at -80^{o}C until further analysed with RT-PCR, *q*RT-PCR or microarray. The concentration of total RNA was determined by NanoDrop™ 2000c UV-Vis Spectrophotometer (Thermo Scientific, Wilmington, DE). The integrity of total RNA samples used for microarray analysis was determined by Agilent 2100 bioanalyzer and Agilent RNA 6000 Nano kit (Agilent Technologies, Germany).

2.4.7.2 One Step RT-PCR Analysis

A. RT-PCR Analysis

The RT-PCR analysis was carried out using Superscript^{TM} III One-Step RT-PCR System with Platinum^R Taq DNA Polymerase kit (Invitrogen, Carlsbad, California, USA). The RT-PCR reactions were prepared according to the manufacturer's instructions (with some modifications) in a final volume of 25 µl with 12.5 µl 2X reaction mix, 1 µl (or 1 µg) of total RNA, 10 µM of each primers, 1 µl of Superscript^{TM} III RT/Platinum^R Taq Mix. The RT step involved incubation at 42^{o}C for 60 mins. The

amplification protocol was as follows: an initial denaturation of 94^{o}C for 2 mins followed by 35 cycles of 94^{o}C for 15 s, 58^{o}C for 30 s and 72^{o}C for 30 s. Negative control tubes for each gene that contained water instead of template RNA or cDNA were also run under the same conditions. *Gapdh* was used as internal control and RNA from mononuclear cells was used as positive control.

B. PCR Amplicon Analysis

To confirm the absence of primer-dimers and other spurious products, the PCR products were evaluated using an Experion^{TM} automated microfluidic electrophoresis system (BioRad) as described in the manufacturer's protocol. This provides high resolution banding patterns of the separated DNA molecules as well as the quantitative output of their relative abundance. Briefly, a small aliquot (~1 µl) of PCR product or DNA ladder was loaded into the sample well or ladder well on the DNA 1K chip (Bio-Rad, Hercules, CA) and analysed with the Experion^{TM} automated electrophoresis system (Bio-Rad, Hercules, CA, USA). An electropherogram and a virtual gel were generated by the Experion software analysis tool when the run was completed for each sample, and the sizing of the PCR product was performed automatically based on the DNA standard electropherogram.

2.4.7.3 Two Steps *q*RT-PCR

A. Reverse Transcription of Total RNA

In this study, 1 µg of total RNA was reverse-transcribed into cDNA with the transcriptor high fidelity cDNA synthesis kit (Roche Diagnostics GmbH; Mannheim, Germany). The reverse-transcription (RT) reaction was conducted based on the manufacturer's protocol with the oligo-dT primer. RT was performed with an initial denaturation of 11.4 µl primer-template mixture (which consist of 1µg of total RNA,

2.5 μM anchored-oligo$(dT)_{18}$ primer and PCR-grade water) at 65^{o}C for 10 min. Then, the reaction mixture was immediately chilled on ice, before the remaining RT mixture (consist of 4 μl of RT buffer, 0.5 μl of 20U protector RNase inhibitor, 2 μl of deoxynucleotide mix, 1 μl of DTT and 1.1 μl of high fidelity reverse transcriptase) was added into it. The RT reaction was completed by incubation for 30 min at 55^{o}C. The RT reaction was inactived by incubation at 85^{o}C for 5 min. The synthesized cDNA was stored at -20^{o}C until further analysed in *q*RT-PCR analysis.

B. *q*RT-PCR *Analysis*

*q*RT-PCR was performed with a Bio-Rad CFX96™ Real-time detection system (Bio-Rad Laboratories, Inc., Hercules, CA) and in a final volume of 20 μl of reaction mixture which consist 10 uL iQ^{TM} SYBR® Green Supermix (Bio-Rad Laboratories, Inc., Hercules, CA), 0.6 μL cDNA samples, and 0.2 μM of each primer (forward and reverse primers; Table 2.4). The optimum annealing temperature for each pair of primers was determined empirically (Appendix D). The amplification protocol was as follows: an initial denaturation and activation step at 95^{o}C for 30 s followed by 40 cycles of 95^{o}C for 15 s and 61^{o}C for 45 s. A melting curve program was carried out routinely to confirm the presence of a single product (55-95^{o}C with a heating rate of 0.5^{o}C per second and a continuous fluorescence measurement). The annealing temperature at 61^{o}C was derived empirically with temperature gradients. To estimate amplification efficiency, a standard curve was generated for each target molecule via 5-fold serial dilution of a cDNA pool containing the target gene sequences. Data was analysed with the CFX manager software. A relative quantification method (with corrected PCR efficiency (Pfaffl, 2001)) was performed. All the data was normalized to GAPDH, which was used as the reference gene, after correcting for differences in amplification efficiency (as recommended in the CFX manager package). Data was

presented as $\log_{10}$-fold (or $\log_2$-fold change (±S.D.) of relative quantification of target mRNA relative to control samples (untreated hMSCs). Student's t-tests were employed to determine the differences between the untreated and GDF5 treated samples. For all comparisons, the statistical significance was accepted at 95% confidence interval (p<0.05).

2.4.7.4 Microarray Sample Preparation and Analysis

A. Total RNA Integrity Assessment

Total RNA quality and integrity was assessed with Agilent 2100 bioanalyzer and Agilent RNA 6000 Nano kit (Agilent Technologies, Germany) according to protocols suggested by manufacture. Briefly, 9 μL gel-dye mix was loaded into the assigned well in the RNA Nano chip. The chip was subsequently pressurized for 30 sec. Then, another two assigned wells were filled with the gel-dye mix, while the remaining wells were loaded with 6 μL of each RNA Nano marker. 1 μL of denatured RNA ladder was loaded into the ladder well and 1 μL of denatured total RNA sample was loaded into each sample well. The chip was vortex at 2400 rpm for 60 s and inserted into the receptacle in the Agilent 2100 bioanalyzer. To prevent denaturation of RNA samples, the electrode was decontaminated with RNase away and RNase-free water prior to chip loading. RNA 6000 Nano assay was executed via Agilent 2100 expert software. During the run, a current was sequentially applied to each sample to separate the RNA samples sequentially. RNA is detected by fluorescence of the intercalating dye in the gel-dye mix. An electropherogram was generated at the end of each sample run. A successful run was observed with one marker peak, two ribosomal (18S, 28S) peaks, which denoted a successful sample preparation. The total RNA concentration, ratio of ribosomal subunit (28S/18S) and the RNA Integrity Number (RIN) was automatically

generated by the 2100 expert software based on the electropherogram. Only samples with RIN value ≥ 7.0 were proceeded for microarray analysis (Appendix E1).

B. Target Preparation

Sample preparation protocols were conducted as described in NuGEN Ovation manual and Affymetrix GeneChip Expression Analysis Technical Manual. Briefly, an aliquot of 200 ng of total RNA (in 5 μL of nuclease free water) was converted to first-strand cDNA using reverse transcriptase primed by a poly-(T) oligomer that incorporated a synthetic RNA sequence. Second-strand cDNA synthesis was followed by ribo-SPIA (Single Primer Isothermal Amplification, NuGEN Technologies Inc. San Cario, CA) for linear amplification of each transcript, and the resulting cDNA was purified. As assessed by Nanodrop UV-Vis spectrophotometer, the cDNA yields in this experiment ranged from 0.053 to 1.250 μg (Appendix E2). A total of 2.5 μg of purified cDNA (per sample in 12.5 μL) was fragmented and biotin labelled. Then, the biotinylated cDNA samples were added to Affymetrix hybridization cocktails and heated at 99^{o}C for 2 min and hybridized for 20 h at 60 rpm rotation and 45^{o}C to Human GeneChip (Affymetrix Inc, Santa Clara, CA) in GeneChip® Hybridization Oven 640 (Affymetrix Inc, Santa Clara, CA). Microarrays were washed at low (6X SSPE) and high (100 mM MES, 0.1 M NaCl) stringency and stained with streptavidin-phycoerythrin. Fluorescence was amplified by adding biotinylated anti-streptavidin and an additional aliquot of streptavidin-phycoerythrin stain. All the washing and staining steps were conducted with Fluidics Station 450 (Affymetrix Inc, Santa Clara, CA). Fluorescence signals were collected after excitation at 570 nm by the Affymetrix Gene Chip Scanner 3000 7G (Affymetrix Inc, Santa Clara, CA). The captured microarray image files were analysed via Affymetrix GeneChip® Command Console 3.2.3 (v.5, Affymetrix Inc., Santa Clara, CA) to get the CEL intensity files. The CEL files were

processed with data preprocessing bioinformatics software and gene expression was assessed after normalization.

C. Bioinformatics Analysis

Various bioinformatics analysis software/programs were used in microarray data analysis. The software/programs used in this study are as listed in Table 2.7.

Table 2.7 The software/programs used for bioinformatics analysis of microarray data.

No.	Software/Programe	Reference	Application
1.	Affymetrix GCOS	www.affymetrix.com	Preprocessing of microarray image files.
2.	Affymetrix Power Tools and DABG detection calls	www.affymetrix.com	Preprocessing and filtering.
3.	Linear Models for Microarray Data (Limma) software package for R programming	http://www.bioconductor.org	Differential expression analysis.
4.	GeneGo Metacore™ Pathway Analysis	http://www.genego.com/metacore.php	Signaling pathway analysis

2.4.7.5 QuantiGene® Plex 2.0 Assay

QuantiGene® Plex 2.0 Assay (Affymetrix, Santa Clara, CA) was used for confirmation of the microarray analysis. The assays of 15 genes (12 target and three housekeeping genes, detailed in Appendix F) were performed according to the manufacturer's protocol for (A) control hMSCs, (B) day 4 GDF5-induced hMSCs, (C) day 10 GDF5-induced hMSCs and (D) tenocytes. Briefly, 20 µL of starting total RNA (200 ng) from each sample was mixed with 33.3 µL of Lysis mixture, 1 µL of Capture Beads and 5 µL of target gene-specific probe set (2.0 probe set), and 2 µL of blocking reagent and 38.7 µL nuclease-free water. Each sample mixture was then dispensed into

an individual well of Capture plate (Affymetrix, Santa Clara, CA). The Capture Plate was sealed with a foil tape and incubated at 53 ^{o}C for 20 h. The hybridization plate was spin-down briefly to collect all the evaporated solution to the bottom of the hybridization plate. Then, the sample mixtures in the hybridization plate were completely transferred to the magnetic separation plate. The magnetic separation plate was then placed on a hand-held magnetic plate washer before the hybridization mixture was removed, and followed by three washing steps with 250 μL of wash buffer. After the last wash, the residual wash buffer was removed by blotting the magnetic separation plate on the folded tissue. Signals for the bound target mRNA were developed by successive incubation in three working solutions: 2.0 pre-amplifier, 2.0 amplifier and biotinylated label probes and SAPE. Two washes was performed between the incubations to remove unbound reagents. The plate was covered with aluminium foil during SAPE incubation to prevent photo bleaching. At the end of last washing step, 130 μL of SAPE buffer was added to each well and the plate was protected with foil plate seal and aluminium foil at each washing step.

Luminescence from each well was measured using a microtiter plate luminometer (Bio-Rad, Hercules, CA, USA). The signals were captured with the instrument after a calibration was performed. Prior to the measurement, each bead type was identified in the luminometer software in order to specify to which transcripts the beads corresponded.

For all samples, background signals were determined in the absence of RNA samples and subtracted from signals obtained in the presence of RNA samples. The presence and absence call was determined by limit of detection (LOD) of the assay, where LOD = background + 3 x standard deviation of background. The expression value of each sample was calculated by normalizing the average background-subtracted signal of each sample to the geomean of the selected housekeeping genes (which consist

of TATA box binding protein (*Tbp*), hypoxanthine phophoribosyltransferase 1 (*Hprt1*) and phosphoglycerate kinase 1 (*Pgk1*) that represented low, medium and high abundant housekeeping genes, respectively) prior to the calculation of gene expression fold change. The gene expression fold change value, for instance fold change in sample X versus sample Y, was calculated with formula $\log_2$ fold changes = $\log_2$(expression value of X/expression value of Y). A gene is considered for fold change analysis if the signal in both sample X and sample Y passes the LOD.

2.4.8 Immunofluorescence Staining

2.4.8.1 Flow Cytometry Immunophenotyping

A. Sample Preparation

The hMSCs or rbMSCs were harvested with accutase™ (Innovative Cell Technologies, Inc, California, USA) and resuspended in phosphate buffered saline (PBS, pH 7.2) at a final concentration of $1x10^7$/mL. An aliquote of 100 μL was distributed into each round-bottomed tubes for phenotypic characterization using fluorescence-activated cell sorting (FACS; BD FACS Cantor II, BD Biosciences, US). Cell suspension was incubated with the optimum dilution of fluorochrome-conjugated or unconjugated primary antibody (Table 2.3) at 4 ^oC for 30 min.

The MSC positive antigens included to the phenotyping profile were: CD29, CD44, CD73, CD81, and CD90.1. To discriminate MSCs from hematopoietic stem and progenitor cells, isolates were stained for CD34, CD45, CD117 and HLA-DR. All mAbs were immunoglobulin G_1 (IgG_1) isotype except for HLA-DR, which is immunoglobulin G_{2b} (IgG_{2b}). After 30-mins of incubation, cells were washed using 2 mL of PBS and resuspended in the stabilizing fixative (BD Pharmingen™, USA) to protect the tandem dyes such as PE-Cy7- or AP-Cy7. Non-specific fluorescence emission was detected by incubating cells with fluorescence conjugated isotype control.

At least 10,000 events were captured by the system. Flow cytometry data were analyzed using CELLQUEST software (Becton Dickinson). Gating was done to exclude cell debris and unwanted aggregates (FSC/SSC dotplot). Non-specific isotype-control (IgG_1 or IgG_{2a}) were used to determine the background fluorescence emission, if any.

B. Unlabeled Spectral Overlap Determination (Compensation Setup with BD CompBeads)

All PMT voltages were adjusted with the unstained control tube before recording the single-stained control tubes (with anti-mouse Ig Kappa CompBeads; BD Pharmingen™, USA; Appendix G1). Then the pre-set photomultiplier tube (PMT) voltages were used to record each of the single-stained BD CompBead Tube. All the voltages for colour detector were kept constant for the remaining compensation tubes, only scatter was adjusted when needed. The auto-compensation feature in the BD FACSDiva was used to calculate the overlapping spectral. Briefly, a region on the dot plot was adjusted to encompass the appropriate population for one of the single stained controls and the gate was copied and applied to all the other control tubes. Subsequently, a gate was created around each of the negative and positive populations on the histogram of each single-stained control (Appendix G2). The Auto-Interval tool was used to quickly create an Interval gate around each population. The gate on the negative population was adjusted to go past the left axis of the histogram to include all events, as recommended by the manufacturer, BD Biosciences. After all histogram have been gated, the spectral overlaps were calculated automatically and stored for future use as compensation setup. The spectral overlap values from this compensation setup were used for all the following experiments as the instrument setting. The compensation was automatically calculated for each tube in the experiments based on the corresponding single-stained control in the saved setup. Based on the predetermined unlabeled spectral

overlap setup, the Spectral overlap values were calculated from the single-stained controls (recorded earlier) and applied to the particular tubes in the linked experiment. This system description was used in all the downstream experiments for multicolour stained samples compensation.

2.4.8.2 Fluorescence Imaging

For fluorescence imaging, cells seeded on cover slips or tissue sections (8 μm thick) mounted on the silanized slides (Dako, Denmark) were fixed with ice cold acetone for five min. Then, the specimens were rinsed twice with stain buffer (BD Pharmingen™, USA) before hybridized with primary antibodies (unconjugated mouse monoclonal or goat polyclonal antibodies; Table 2.3) at 4 ^{o}C, overnight in a humid chamber. After overnight hybridization, the specimens were washed twice with stain buffer before proceed to staining with fluorescence-conjugated-secondary antibodies (fluorescein isothiocyanate (FITC)-conjugated anti-mouse IgG and Texas Red-conjugated anti-goat IgG) and counterstained with nucleus stain (either with or without phalloidin-Alexa Fluor® 546 stain), for 30 min at room temperature. Then, the specimens were washed twice with stain buffer before mounted with fluoroGel mounting medium (GeneTex, Inc, Irvine, CA). Fluorescence images were examined and captured either using Nikon-Eclipse-Ti-U microscope with NIS-Element AR software (Nikon, Japan) or laser confocal microscope (Leica TCS SPII confocal laser scanning system; Leica Microsystem, GmbH, Germany) with LAS AF Lite software (Leica Microsystems, Mannheim, Germany). For stained specimens observed under the confocal microscope, fluorescence images were captured with sequential scanning to avoid fluorescence signal cross-talk; and line averaging (8 lines) was used to enhance the quality of the image.

2.4.9 Histological Staining

2.4.9.1 Hematoxylin and Eosin Stain

Hematoxylin and eosin (H&E) staining method was used in this study for morphological evaluation. Tissue sections of 8 μm from cryosectioning were mounted on to the glass slides and fixed with 70% ethanol. For monolayer culture cells in chamber slides, cells were fixed with 4% formaldehyde (System®, Italy). The slides were stained with hematoxylin and eosin stain in a fume hood. After ethanol or formaldehyde fixation, the slides were stained with Mayer's hematoxylin (Dako, Denmark) for 5 min, and immediately washed in running tap water for 5 min or less, and continued to differentiate in 1% acid alcohol for 5 s. The slides were then washed again in tap water for 5 min or less, followed by counterstaining in 1% eosin (Appendix H) for 10 min. Then, the slides were washed again in tap water for 5 min before dehydrated through ascending ethanol (85%, 90%, 100%), cleared in xylene and mounted in DPX mounting medium (Fluka, Germany).

2.4.9.2 Van Gieson Trichrome Stain

Van Gieson trichrome staining kit (Bio-Optica, Milano, Italy) was used in this study to stain the connective tissue. This staining kit consist of Weigert's iron haematoxylin for nuclei, picric acid for cytoplasm and fuchsin for collagen. Similar to H&E staining, the slides were brought to distilled water after being fixed with ethanol. Then, five drops of reagent A and reagent B were put on the tissue section and incubated at room temperature for 10 min. Subsequently, the tissue section was blue in running tap water for 10 min, followed by adding 10 drops of reagent C on to the tissue section. The reagent C was left to react on the tissue section for 10 min. Then, the tissue sections were washed rapidly (3 second) in distilled water and dehydrated through ascending ethanols. The tissue sections were stopped for one minute in the final

absolute ethanol. The stained slides were then cleared in xylene and mounted with DPX mounting medium (Fluka, Germany). The collagen fibers appeared purplish red, while the nuclei appeared black, cytoplasm, smooth and striated muscle and erythrocytes appeared yellow.

2.4.9.3 Von Kossa Stain

Von Kossa special stain kit, method for calcium (Bio-Optica, Milano, Italy) was used to demonstrate calcium depositions in cell culture. Similar to H&E staining, the slides were brought to distilled water after being fixed with ethanol or formaldehyde. Then, 10 drops of reagent A were put on the tissue section and left to react at room temperature for 10 min. After that, the slides were rinsed well in distilled water before 10 drops of reagent B were put to the slides and left to react in dark for one hour. After that, the slides were rinsed well again in distilled water, followed by adding 5 drops of distilled water and 10 drops of reagent C, and left to react for 5 min (or until the silver salt turned black). Then, the slides were rinsed again in distilled water. Subsequently, 10 drops of reagent D were added to the slides and left to react for 5 min before rinsed in distilled water, followed by addition of 10 drops of reagent E to react for another 5 min. Lastly, the slides were rinsed again with distilled water, dehydrated through ascending ethanol, cleared in xylene and mounted with DPX mounting medium (Fluka, Germany). The deposited calcium appeared black and nuclei appeared red.

2.4.9.4 Oil-red-O Stain

Cells cultured in monolayer on the slides were fixed with 10% buffered formalin for 10 min. After fixation, the slides were gently rinsed with distilled water. Then, 2 ml of 60% isopropanol was added to the slides and incubated at room temperature for 5 min. After that, the isopropanol was replaced with 2 ml of oil-red-O working solution

(Appendix H) and incubated for another 5 min at room temperature. Then, the oil-red-O solution was removed and the slides were rinsed with room temperature tap water until the water rinsed off was clear. Finally, 2 ml of tap water was added to each slides and the stained slides were viewed on a phase contrast microscope. The lipids appeared red and the nuclei are blue.

2.4.9.5 Safranin O Stain

Safranin O staining reagents/solutions were prepared as stated in Appendix H. Cells cultured in monolayer on the slides were fixed with 10% buffered formalin for 10 min and gently rinsed with distilled water. The slides were stained with modified Weigert's iron hematoxylin for 5 min followed by gentle wash in distilled water until the excess dye stop leaching out from the stained sample. Then, the slides were differentiated in 1% acid-alcohol for 2 s followed by three gentle rinses in distilled water. Subsequently, the slides were stained for 1 min in 0.02% fast green, 30 s in 1% acetic acid and 10 min in 1% safranin O. Then, the slides were rinsed briefly in 95% ethanol, dehydrated in ascending ethanol (95% 100% and 100%), cleared in 3 changes of xylene and lastly mounted with DPX mounting medium (Fluka, Germany). The proteoglycan appeared orange to red while the nuclei stained black and cytoplasm stained bluish green.

2.4.10 Atomic Force Microscopy Live Cell Imaging

2.4.10.1 Sample Preparation

Cells were seeded onto glass cover slip. To increase the stability of cell membrane and to prevent the lateral mobility of receptors, cells were incubated with mild concentration of glutaraldehyde (0.5% v/v) for 2 h at 37^{o}C prior to imaging. The

cover slip was attached to a closed cell incubation sample plate (Figure 2.5) for imaging in a fluidic environment.

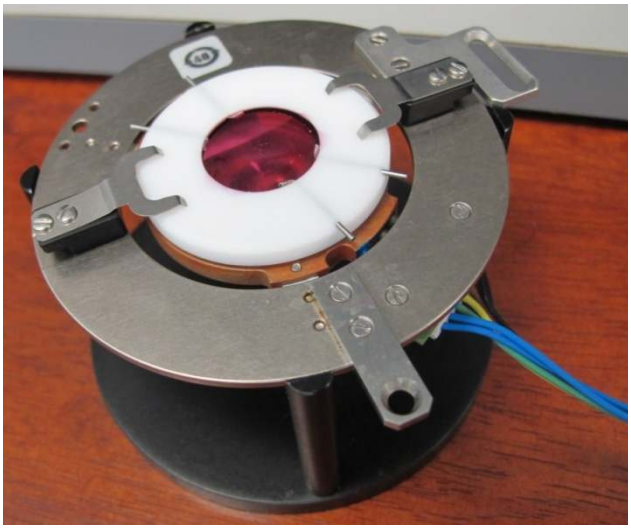

Figure 2.5 Closed cell incubation sample plate for atomic force microscopy imaging. The closed cell incubation sample plate was used to incubate the cells during the entire imaging process.

2.4.10.2 Image Acquisition

Atomic force microscopy imaging was conducted with an atomic force scanner (AFM5500, Agilent Technologies, Germany) mounted in an acoustic chamber (vibration free environment) to reduce the noise or turbulence from the surrounding environment. Cantilever used were sharpened microlever (Bruker, Italy) with silicon nitride probe (spring constant 0.0005 to 0.02; nominal value=0.01) for soft sample such as cells. Atomic force images were acquired in AC mode for liquid imaging with harmonic frequency (tip resonance frequency) at ~3-5 V amplitude. All images were taken in cell culture medium at 37 ^{o}C, with low scanning speed at ~0.3 Hz (or <0.5) and with at least 512X512 points/line resolution. Each sample was scanned for at least three times, and the best representative image was shown. During the entire experiment process, the cells were tightly adhered to the substrate (cover slip).

2.5 METHODS DEVELOPMENT

2.5.1 Isolation and Culturing of Primary Mesenchymal Stem Cells

2.5.1.1 Human Bone Marrow-Derived MSC (hMSC) Primary Culture

Human MSCs (hMSC) were isolated from bone marrow samples and expanded *in vitro* following methods that had been previously established (Tan et al., 2011). Briefly, a volume of 2 mL of bone marrow was diluted with 2 mL of phosphate buffered saline (PBS, pH 7.2) and layered onto 3 mL of Ficoll-Paque Premium (GE Healthcare, Sweden) before undergoing gradient centrifugation at 2200 rpm for 30 mins (Eppendorf 5810R).

The mononuclear layer (second from top layer) was then collected and washed twice with Dulbecco's modified Eagle's medium-low glucose (DMEM-LG; Invitrogen-Gibco, USA) supplemented with antibiotic/antimycotic 1% (v/v) (Invitrogen-Gibco, USA). The isolated mononuclear cells were cultured in growth medium (DMEM-LG supplemented with 10% fetal bovine serum (FBS), antibiotic/antimycotic 1% (v/v) and GlutaMAX™-I (Invitrogen-Gibco, USA), and transferred into T75 tissue culture flasks (Nunc™, USA). The medium was changed at day five to remove non-adherent cells, and the subsequent medium change was conducted at three-day intervals.

2.5.1.2 Rabbit Bone Marrow-Derived MSC (rbMSC) Primary Culture

Rabbit bone marrow was harvested from New Zealand white rabbits with the protocol approved by the Animal Care and Use Committee, Faculty of Medicine, University of Malaya. Three adult New Zealand white rabbits (at least 4 months old) were euthanized by an overdose of pentobarbital sodium (Nebutal® Sodium Solution) (Boehringer, Ingelheim, Germany). Rabbit bone marrow was isolated from the tibia and femur and resuspended in 2 mL of phosphate buffered saline (PBS, pH 7.2; Invitrogen-Gibco, USA). The bone marrow suspension was layered on 3 mL Ficoll-Paque™

Premium (density: 1.077 g/mL; GE Healthcare, Sweden) for gradient centrifugation at 2200 rpm for 30 min in a 15 mL centrifuge tube. The same protocols used in hMSCs isolation (Section 2.5.1.1) were applied in the subsequent isolation steps.

2.5.2 Determination and Comparison of hMSC and rbMSC Characteristics

2.5.2.1 Cell Morphology and Size

The isolated hMSC and rbMSC were observed under phase contrast microscope and the morphological appearances between these two cell types were compared. Both cell types appeared to have heterogeneous fibroblastic appearance and formed distinct colonies on flask surfaces (Figure 2.6). The cells demonstrated increased proliferation, gradually and uniformly maintaining a homogeneous fibroblastic morphology. Both hMSCs and rbMSCs were mainly of spindle-shaped appearance and elongated morphology with two processes that extended in opposite directions from a small cell body. In the subsequent passages i.e. P1 to P3, cultures with low proliferative (prolonged passage time), large polygonal and flattened cells with short or no processes (Figure 2.6 H and K) were discarded. These cells were discarded because these cellular morphology has been reported as (i) senescent MSC (Cheng et al., 2003; Fu et al., 2012; Schellenberg et al., 2011), and (ii) associated with low proliferative rate and were less potential or characterized as “mature” (Colter et al., 2000; Colter et al., 2001; Neuhuber et al., 2008; Sekiya et al., 2002) and (iii) associated with different stages of cell differentiation rather than the existence of distinct cell types or subtypes (Docheva et al., 2008; Sekiya, et al., 2002; Smith et al., 2004). This further alludes to the importance of culturing the subset of hMSCs or rbMSCs that is more homogeneous, proliferative and exhibit fibroblastic spindle-shaped for the downstream applications. Although similar in their morphological appearance, the rbMSCs cell length (202.66 ±8.40 μm)

and width (13.09±0.91 μm) were significantly longer and wider than hMSCs (152.04±43.35 μm in length; 9.82±0.66 μm in width) (p<0.01; Figure 2.6 M & 1N).

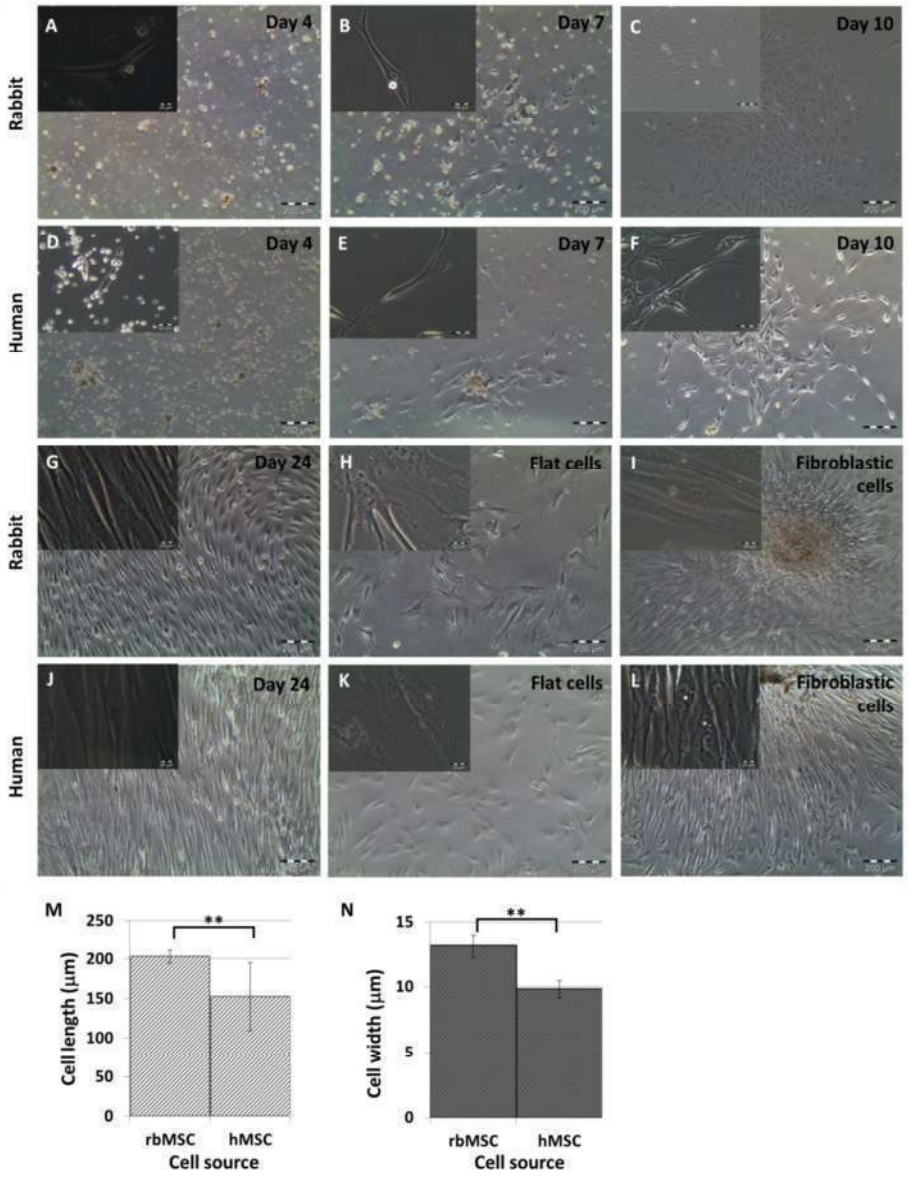

Figure 2.6 Morphology of primary culture of human and rabbit bone-marrow derived mesenchymal stem cells (hMSC and rbMSC respectively).
Representative images from three independently performed experiments were shown (A to L); images were captured under phase contrast microscope at 4x objective (images of 40 x objectives were shown on the left upper corner of each image). Cell lengths and widths of eight representative cells from each individual experiment (n=3) were measured and data are presented as mean ± standard error of the mean (M and N). Cells were in fibroblast-like spindle-shaped at day 4, 7, 10 and 24 in rbMSC cultures (A, B, C and G respectively) and in hMSCs cultures (D, E, F and J respectively). Some non-fibroblastic flat cells were observed in rbMSC (H) cultures and hMSC cultures (K) upon subculturing (P1 onwards). Majority of the cells remained fibroblastic spindle shaped in rbMSCs (I) and hMSCs (L) upon subculturing from P1 to P3. The rbMSCs possessed significantly higher cell length (M) and cell width (N) compared to hMSC (p<0.05).

2.5.2.2 Ultrastructural Characteristics

Both hMSCs and rbMSCs were harvested and processed for transmission electron microscopy imaging (Figure 2.7).

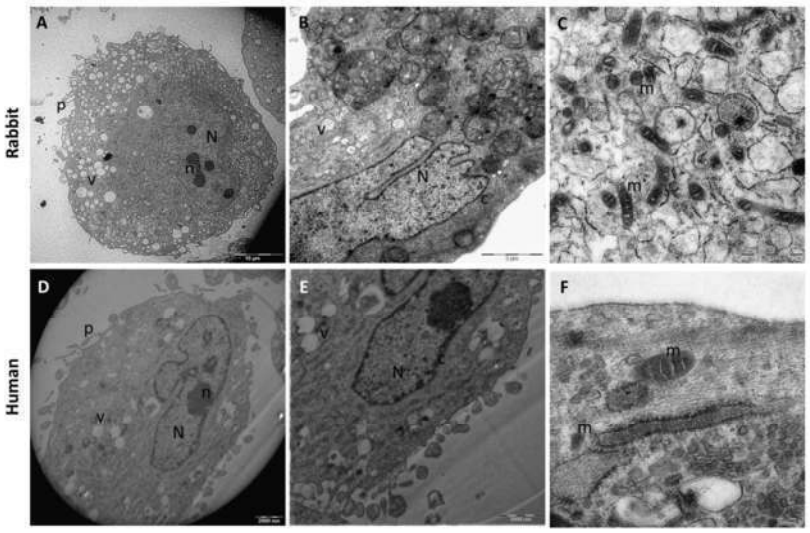

Figure 2.7 Transmission electron microscopy analysis of the ultrastructure of rbMSCs and hMSCs.
Representative images of rbMSCs and hMSCs ultrastructure were shown. Both rbMSCs and hMSCs showed similar ultrastructure features. An eccentric and irregular-shaped nucleus (N), usually with multiple nucleoli (n), with various mitochondrial profiles (m); and small vacuoles (v) in rbMSCs (A and B) and hMSC (D and E). Chromatin formed a thin and dense layer inside the perinuclear cisternae (c) and the plasma membrane formed many thin pseudopodia (p). Mitochondrial showed both rounded and elongated profile with thick cristae in both rbMSCs (C) and hMSCs (F).

The rbMSCs displayed phenotypic appearances that were indistinguishable to hMSCs (Figure 2.7). They were relatively uniform in their ultrastructural characteristics. Generally, both hMSCs and rbMSCs possessed a large, eccentric, irregular-shaped nucleus and a rich inner cytoplasmic zone (Figure 2.7 A, B, D and E). The nucleus showed multiple nucleoli and the chromatin formed a thin and dense layer inside the perinuclear cisternae. The periphery of the plasma membrane displayed many small pseudopodia in both hMSCs and rbMSCs (Figure 2.7 A and D). In addition, within the rich cytoplasm region (Figure 2.7 A and B), a small amount of Golgi rough endoplasmic reticulum as well as a modest number of mitochondrial with different profiles (rounded and elongated profile with thick cristae) were present. There was

neither fat globule in the cells nor ultrastuctural disruption, denoting that no cell was at the senescence stage of development.

2.5.2.3 Surface Markers Expression

A. rbMSC Surface Markers Expression

Due to the limited availability of mAb for rbMSC characterization, initially, rbMSC could only be analysed for CD44 (with immunofluorescence staining) as well as CD29, CD166, CD34 and CD45 (with RT-PCR analysis using our custom designed primers based on the available sequences obtained from other species). Immunofluorescence staining to detect CD44 surface markers was positive for rbMSCs (Figure 2.8 A). RT-PCR analysis demonstrated a positive expression for CD29 and CD166 in rbMSCs (Figure 2.8 B), but was negative for other surface markers (CD45 and CD34) (Figure 2.8 B). Glyceraldehyde-3-phosphate dehydrogenase (GAPDH) was used as the house-keeping gene.

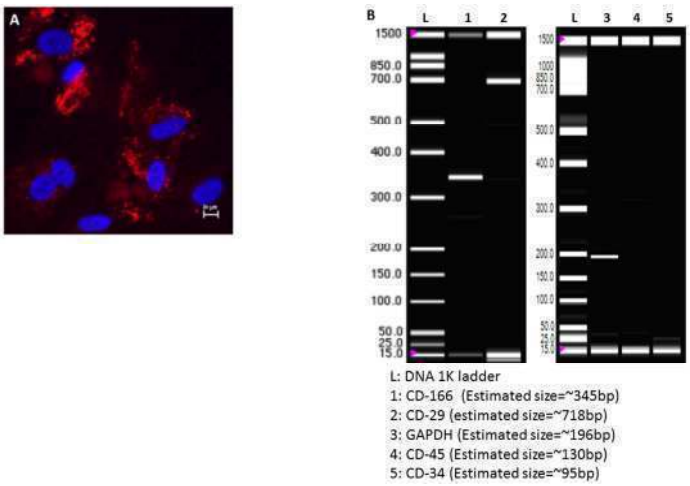

Figure 2.8 Surface marker analysis for rbMSCs.

(A) Immunofluorescence staining image for positive expression of CD44 (in red, anti-mouse IgG allophycocyanin conjugated Goat F $(ab')_2$) counterstained with nucleus stain (in blue) in both rbMSC and hMSC.

(B) RT-PCR analysis for CD166 (lane 1), CD29 (lane 2), CD45 (lane 4), CD34 (lane 5) and glyceraldehyde-3-phosphate dehydrogenase (GAPDH, in lane 3). Lane L indicates the DNA ladder. Presence of amplicon in lane 1, 2 and 3 indicated positive expression of the corresponding genes and absence of amplicon in lane 4 and 5 denoted that these genes were not expressed.

B. Flow Cytometry Immunophenotyping of hMSC and rbMSC

With the increase availability of the mAb for rbMSC, flow cytometry analysis was conducted for immunophenotyping of rbMSC for a better comparison with that of hMSCs. The cultured hMSC donor cells fulfilled all MSC criteria set by ISCT (Table 2.8; Appendix I1), including CD105, CD14 and CD19 (only tested in hMSCs due to mAb availability; Appendix I2). The cultured rbMSCs expressed multiple markers of MSCs. The cultured rbMSCs revealed positive for CD29, CD44, CD73, CD81 and CD90, but was negative (or dim positive) for CD34, CD45, CD117 and HLA-DR (Table 2.8 A; Appendix I1). In the multi-colour analysis, at least 70% of rbMSCs expressed double positive, double negative or co-expressed positive and negative markers as compared to 90% of that in hMSCs. The results of these analyses are summarized in Table 2.8 B.

Table 2.8 Summary of flow cytometry analysis for (A) single marker and (B) co-expression of two markers.

(A)

Cell type	$CD29^+$ (%)	$CD44^+$ (%)	$CD73^+$* (%)	$CD81^+$ (%)	$CD90^+$* (%)	$CD34^-$* (%)	$CD45^-$* (%)	$CD117^+$ (%)	$HLA\text{-}DR^-$* (%)
rbMSC	85.0	81.6	96.4	96.9	96.9	7.1	18.0	17.4	4.3
hMSC	100.0	99.6	98.6	99.9	100.0	0.2	0.1	1.4	0.2

(B)

Antigens	rbMSC (%)	hMSC (%)
$CD29^+$ and $CD34^-$*	78.4	99.8
$CD44^+$ and $CD73^+$*	70.9	93.7
$CD44^+$ and $CD34^-$*	82.1	98.4
$CD90^+$* and $CD73^+$*	70.1	96.4
$CD90^+$* and $CD81^+$	89.8	100.0
$CD90^+$* and $CD34^-$*	89.8	97.3
$CD90^+$* and $CD45^-$*	81.6	92.0
$CD90^+$* and $CD117^-$	79.6	99.0
$CD73^+$* and $CD81^+$	75.0	99.5
$CD73^+$* and *$CD34^-$*	83.2	97.7
$CD73^+$* and *$CD117^-$	71.2	98.6
$CD81^+$ and $CD34^-$*	91.8	98.0

Table 2.8 continued

$CD81^+$ and $CD117^-$	76.9	98.6
$CD81^+$ and $HLA\text{-}DR^-$*	76.3	99.4
$CD34^-$* and $CD45^-$*	76.2	91.0
$CD34^-$* and $CD117^-$	77.3	97.0
$CD45^-$* and $HLA\text{-}DR^-$*	72.0	97.7

*CD markers that are prerequisite by ISCT criteria.

2.5.2.4 Cell Proliferation

AlamarBlue® assay was used to determine the cell proliferation rate of hMSC and rbMSC. Both hMSC and rbMSC showed typical "S shaped curve" as seen in many cell cultures (Figure 2.9). No significant differences were observed in the alamarBlue® reduction in both hMSCs and rbMSCs during the "lag phase" of cell proliferation. As the cells enter into their exponential "log phase", although rbMSCs showed a lower cell proliferation than hMSCs, both rbMSCs and hMSCs reached a plateau phase at 72 h. The population doubling time of rbMSCs and hMSCs were 6.4±1.3 and 7.6±1.7 hours respectively. However, there were no significant differences between the two (p>0.05).

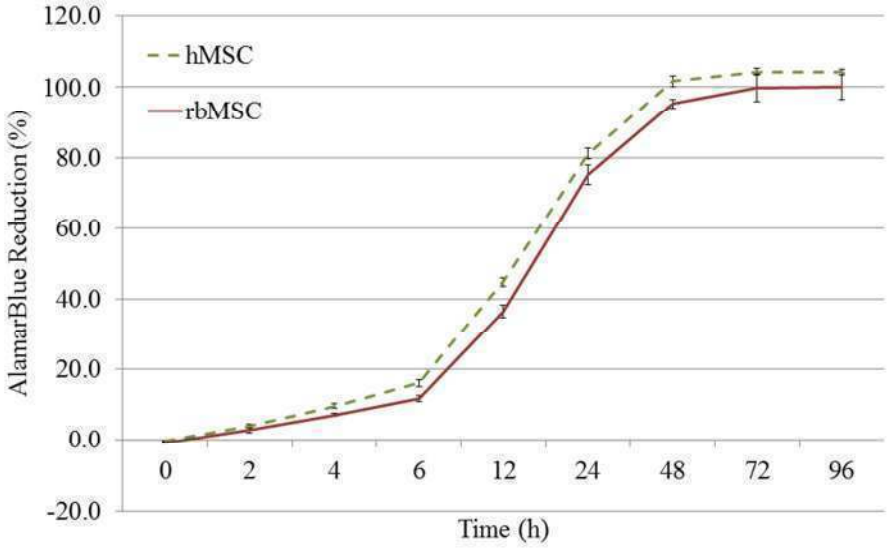

Figure 2.9 AlamarBlue® cell proliferation assay of hMSC and rbMSC cultures.
No significant difference in cell proliferation rates at the lag phase and plateau phase between hMSC and rbMSC.

2.5.2.5 Trilineage Differentiation Analysis

Trilineage differentiation assay was conducted in both hMSC and rbMSC to determine their multilineage differentiation (osteogenic, adipogenic and chondrogenic differentiation) capability. The differentiation potential was determined with histological staining and gene expression quantification analysis.

A. Histological Staining

In the osteogenic differentiation assay, the presence of calcium oxalates was clearly observed from the Von Kossa staining on the differentiated rbMSCs, which was not present in the undifferentiated cells (Figure 2.10 A). Adipogenesis of rbMSCs was detected by staining intracellular lipid droplets using oil-red-O (Figure 2.10 B) in the adipogenic-induced rbMSCs cultures. The use of safranin-O aided the detection of proteoglycan deposition in chondrogenic-induced rbMSCs, however, this was negative in the control group (Figure 2.10 C). These observations suggest that rbMSCs have the potential to undergo the tri-lineage i.e. osteogenic, chondrogenic and adipogenic, differentiation required to fulfil the characteristics of MSCs.

As compared to cultured hMSCs, hMSCs demonstrated a greater propensity to differentiate into the osteogenic and adipogenic lineages than rbMSCs based on the qualitative (histological staining) results where more prominent deposition of calcium oxalate crystals and more mature adipocytes (more lipid vacuoles present) were observed in induced hMSCs compared to that of rbMSCs under the same culture conditions.

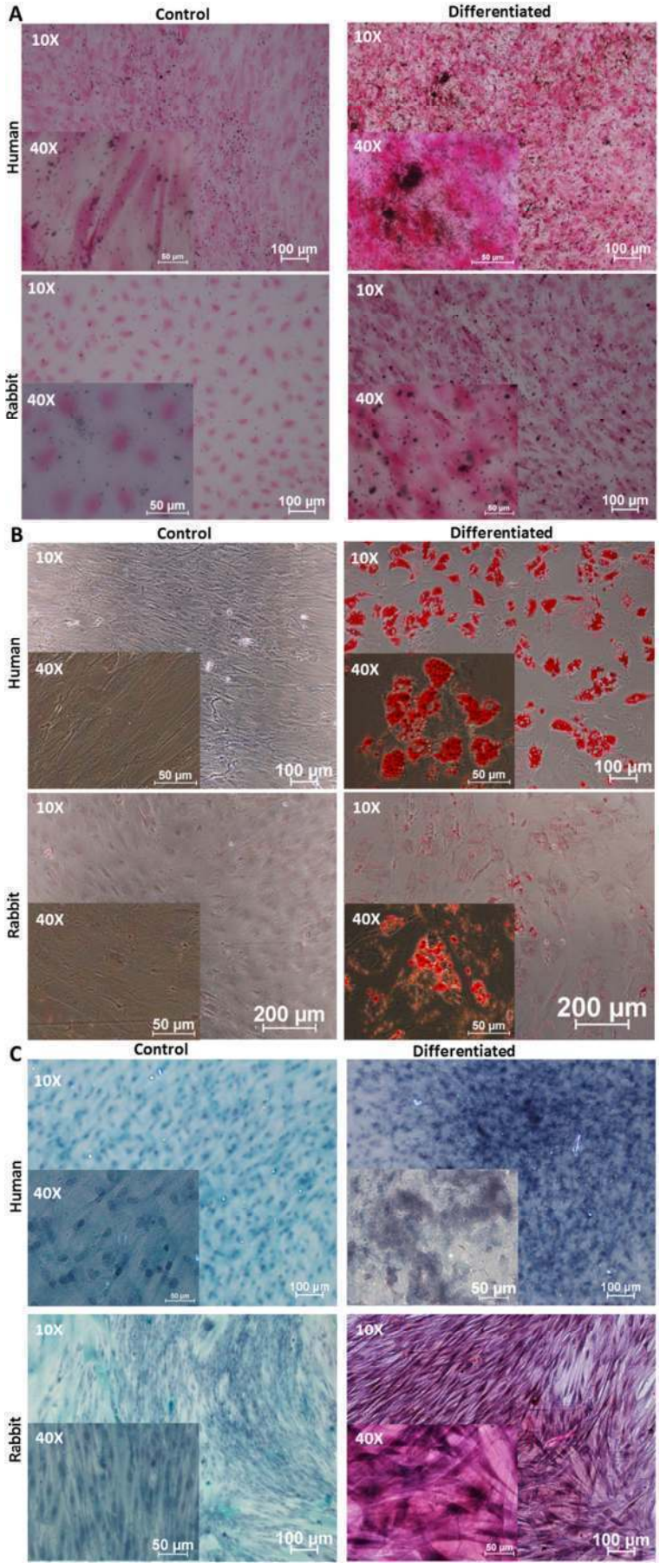

Figure 2.10 Tri-lineage differentiations of primary hMSCs and rbMSCs.

Figure 2.10 continued

(A) Osteogenic differentiation of rbMSC and hMSC (as positive control) for 28 days. rbMSC and hMSC were cultured in standard MSC growth medium (control cultures) or osteogenic induction medium. Lower images: Intracellular deposition of calcium oxalate crystals (black colour signifies) in osteogenic-rbMSCs as revealed by Von Kossa staining (right). No accumulation of calcium oxalate crystals was observed in uninduced control rbMSC culture stained with Von Kossa staining for comparison (left). Upper images: Positive control of adipogenic differentiation in hMSCs (right) and non-induced control hMSC (left) stained with oil-red-O staining. Magnifications were denoted at the upper left corner of the images.

(B) Adipogenic differentiation assay of rbMSC and hMSC (as positive control) for 28 days. rbMSC and hMSC were cultured in standard MSC growth medium (control cultures) or adipogenic induction medium. Lower images: Presence of intracellular accumulated lipid droplets (red colour in the image) in adipogenic-rbMSCs as revealed by oil-red-O staining (right). No accumulation of lipid droplets was observed in non-induced control rbMSC culture stained with oil-red-O staining for comparison (left). Upper images: Positive control of adipogenic differentiation in hMSCs (right) and uninduced control hMSC (left) stained with oil-red-O staining. Magnifications were denoted at the upper left corner of the images.

(C) Chondrogenic differentiation assay of rbMSC and hMSC (as positive control) for 28 days. rbMSC and hMSC were cultured in standard MSC growth medium (control cultures) or chondrogenic induction medium. Lower images: Presence of glycosaminoglycans or highly sulfated proteoglycans (pinkish colour in the image) in chondrogenic-rbMSCs as revealed by safranin-O staining (right). No accumulation of glycosaminoglycans was observed in non-induced rbMSC culture stained with safranin-O for comparison (left). Upper images: Positive control of chondrogenic differentiation in hMSCs (right) and non-induced control hMSC (left) stained with safranin-O. Magnifications were denoted at the upper left corner of the images.

B. Gene Expression Quantification Analysis

rbMSCs expressed significantly higher *Runx2* (osteogenic marker) and *Sox9* (chondrogenic marker) expression on both day 7 and day 28 as compared to that of hMSC ($p<0.05$) (Figure 2.11). In adipogenic medium, both rbMSCs and hMSCs showed similarly elevated *PPARγ* (adipogenic marker) gene expression levels on day 28 ($p>0.05$). An overall summary of comparison between hMSC and rbMSC chrateristics is showed in Table 2.9.

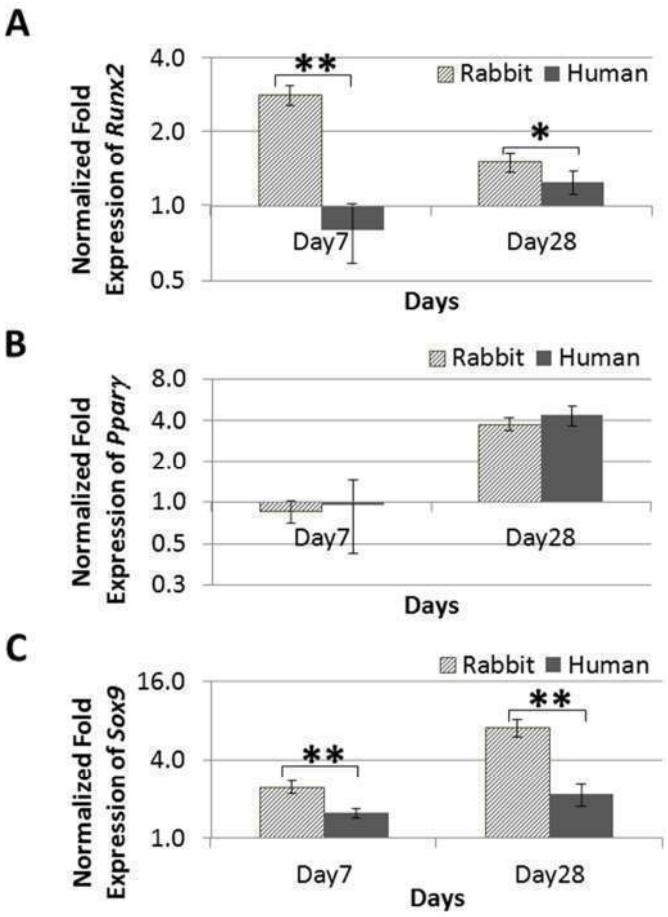

Figure 2.11 Gene expression analyses of the cultured hMSCs and rbMSCs in the temporal experiment of tri-lineage differentiation assay.

The gene expression level for osteogenic (A), adipogenic (B) and chondrogenic (C) differentiation, at day 7 and day 28 were shown. The data reflected that the relative quantification of target mRNA normalized to control samples (untreated MSCs cultured in MSC growth medium). Data was presented as $\log_2$-fold change (with error bars signifying range of standard deviation). All the differentiation markers (*Runx2*, *Pparγ* and *Sox9*) were upregulated on day 28. However, spontaneous differentiation into osteogenic and chondrogenic lineages were observed in the rbMSCs with significant early up-regulation of the respective differentiation markers (*Runx2* and *Sox9*) at day 7.

Table 2.9 A summary of rbMSCs and hMSCs characteristics.

Characteristics	rbMSC	hMSC
Plastic adherence	Yes	Yes
Morphology	Fibroblastic spindle shaped with two processes that extended in opposite directions from the cell body and grow in high density colonies.	
Ultrastructural characteristic	Cells possess a large eccentric and irregular-shaped nucleus with a prominent nucleolus. Chromatin formed a thin and dense layer inside the perinuclear cisternae. The rich inner cytoplasmic zone consists of a small amount of Golgi rough endoplasmic reticulum, mitochondria and polyribosome. The periphery of the plasma membrane displayed many small pseudopodia.	
Cell size (μm)	Length: 202.66 ±8.4 Width: 13.09±0.91	Length: 152.04±43.35 Width: 9.82±0.66
Proliferation rate	Population doubling: 6.4±1.3 h	Population doubling: 7.6±1.7 h
Phenotypic expression	Highly expressed: CD29, CD44, CD73, CD81 and CD90. Low expression: CD117, CD45 Negative expression: CD34 and HLA-DR	Highly expressed: CD29, CD44, CD73, CD81 and CD90. Negative expression: CD34, CD45, CD117 and HLA-DR
Differentiation potential (histological observation)	i. Osteogenic differentiation (Von Kossa staining): presence of intracellular deposition of calcium oxalate crystals. ii. Adipogenic differentiation (oil-red-O staining): presence of intracellular lipid droplets. iii. Chondrogenic differentiation (safranin-O staining): presence of apparent glycosaminoglycans or highly sulphated proteoglycans.	
Differentiation potential (gene expression):	i. Upregulation of osteogenic marker (*Runx2*) at day 7 and 28, upon osteogenic differentiation induction. Higher *Runx2* expression was observed in rbMSCs compared to hMSCs.	i. Upregulation of *RUNX2* at day 28, upon osteogenic differentiation induction.
	ii. Upregulation of adipogenic marker (*Pparγ*) at day 28, upon adipogenic differentiation induction. No significant difference in *Pparγ* expression between rbMSCs and hMSCs.	ii. Upregulation of *PPARγ* at day 28, upon adipogenic differentiation induction.
	iii. Upregulation of chondrogenic marker (*Sox9*) at day 7 and 28, upon chondrogenic differentiation induction. Higher *Sox9* expression was observed in rbMSC compared to hMSCs.	iii. Upregulation of *SOX9* at day 7 and 28, upon chondrogenic differentiation induction.

2.5.3 *In vivo* Transplantation

2.5.3.1 Surgical Procedure For Tendon Defect Creation and Transplantation

In brief, the surgical defect creation was conducted as follows: The surgical area was disinfected with povidon iodine topical solution 10% w/v (Unidon Solution, India) and 3 ml of 20 mg/ml lignocaine hydrochloride (Ilium, Australia) was injected subcutaneously for local anesthetic effect. A 3 cm incision was made on the shoulder and the infraspinatus tendon was exposed. The infraspinatus tendons were inspected to ensure there were no pre-existing gross lesion in the tendon or peritendinous tissues. An identical, full-thickness, window defect was dissected via ventral longitudinal incision in the central part of each infraspinatus tendon bilaterally. The proximal and distal ends of the window defect were marked with coloured (black or blue) Premilene® 3-0 non-absorbable polypropylene monofilament sutures (B. Braun, Germany) to help identify the wound site at the time of sacrifice and dissection (Figure 2.12). A silicone sheet was used to maintain the defect. After three weeks, the silicon sheet was removed and the defects were repaired. Incision closure was completed with simple suture pattern with a Ethicon 4-0 coated Vicryl undyed braided absorbable suture (Johnson & Johnson International, Brussels, Belgium).

Postoperative medication included Meloxicam injection (5 mg/ml; 0.3 mg per kg body weight; Meloxicash, India) and Kombitrim 240 (sulfamethoxazole 200 mg/ml + trimethoprim 40 mg/ml; 30 mg per kg body weight; Kela, Belgium) injection for three consecutive days in 24 h interval to minimize discomfort in the postoperative period. The activity of the animals was not restricted. The animals were fed an ordinary diet. Mobilization and walking pattern were noted daily. After 6 weeks postoperatively, the rabbits were euthanized by an over dose of pentobarbital sodium (Nebutal ® Sodium Solution; Eutha-naze (TM), Kenya.) and the infraspinatus tendons of both shoulders were harvested for histology analysis. The specimens consisted of the entire

infraspinatus tendon beginning 1 cm proximal and ending 1 cm distal to the original defect. The defect in the infraspinatus tendon was identified by removing the peritendinous fibrous tissue and locating the marker sutures. All the specimens were snapped frozen and stored in -80 ^{o}C, before used for OCT embedding. All the tissues were sectioned in the frontal longitudinal sections (8 μm-thick), including scar tissue if present, in the no repair control or repaired defects. For gene expression analysis, 15 ten-micron-cryo sections were collected in a 1.5 ml-Eppendorf® tube. Specimens were stored at -80^{o}C before further processing for total RNA isolation.

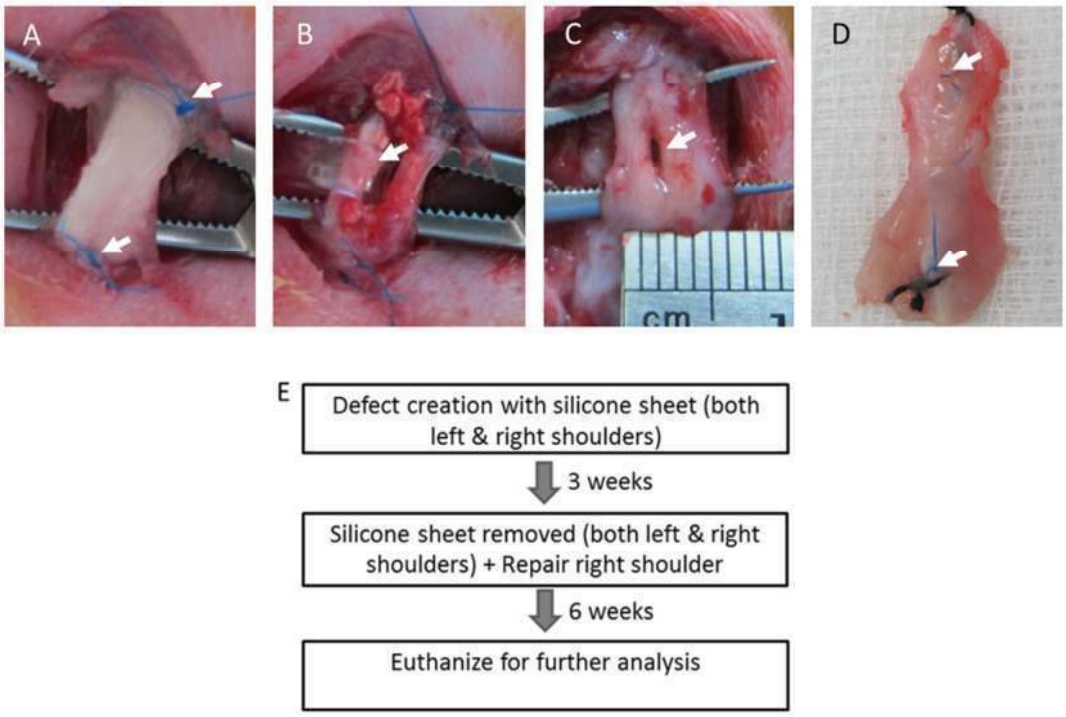

Figure 2.12 Defect creation and repair in rabbit infraspinatus tendon model.
(A) A square, full thickness defect was surgically created by removing the central one-third of the infraspinatus tendon. The proximal and distal ends of the defect area were marked by polypropylene monofilament suture at each midpoint (arrow).
(B) The defect was maintained by a silicone sheet (arrow).
(C) At three weeks post defect creation, the silicone sheet was removed and a window defect was developed (arrow) in the middle of the infraspinatus tendon.
(D) At time of recovery at six weeks post-surgical repair, the tendon defect was identify by locating the suture markers (arrow) inserted (during transplantation) at both ends of defect.
(E) The summary of the workflow from defect creation to recovery of tendon specimens at 6 weeks post-surgical repair.

2.5.3.2 Histological Scoring

Microscopically, the tendon defect area was identified by locating the marker suture (Figure 2.13). All the stained sections were scanned and analysed using Panoramic Viewer 1.14 (3DHistech, Hungary). Histological evaluations were performed with H&E and Van Gieson stained slides.

The quality of tendon repair (as observed in H&E and VG stained sections) were scored based on Watkins (1985) and Soslowsky (1996) histological scores. These scores evaluated the cellularity, vascularity and collagen density in all treatment groups compared to the control group, at 6 weeks post-surgical repair. The parameters used for histological scoring were as stated in Table 2.10 and Table 2.11 (Soslowsky et al., 1996; Watkins et al., 1985). All data were expressed as mean±standard deviation and compared by non-parametric tests due to the small sample size used in this study. The Kruskal-Wallis test which is equivalent to the analysis of variance (ANOVA) analysis and Mann-Whitney U test which is equivalent to the Student's t-test were conducted using SPSS software (SPSS). All *p*-values less than 0.05 were considered significant.

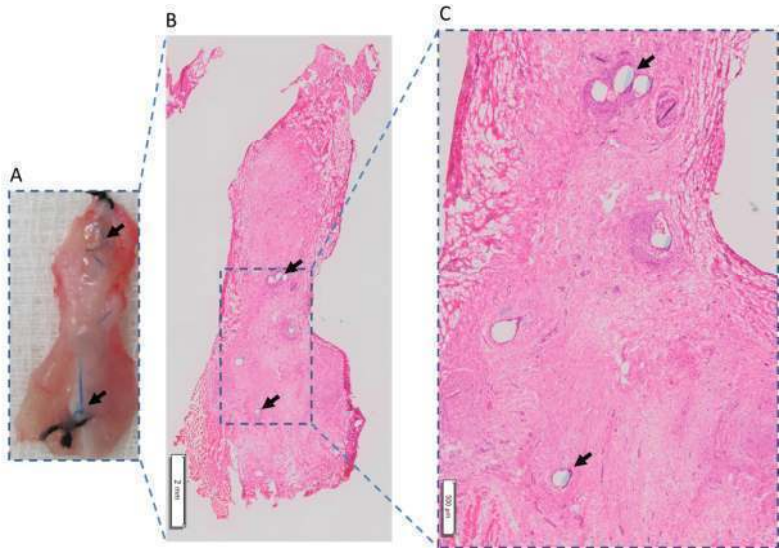

Figure 2.13 The suture markers were used to locate the defect at the time of histological analysis.
A suture marker inserted at both ends of the defect area (black arrows) during transplantation surgery, was used to identify the defect area in the hematoxylin and eosin stained tendon tissue sections (in frontal planed).
(A) The gross appearance of the infraspinatus tendon;

Figure 2.13, continued

(B) An overview of the infraspinatus tendon frontal section stained with haemaoxylin and eosin (Bar=2mm);
(C) The defect area observed at higher magnification to show the suture site (black arrows) at both ends of the defect. These sutures were used as the landmark to locate or to identify the defect site in the histology sections. (Bar=500μm).

Table 2.10 Watkins score for histological evaluation of tendon repair (Watkins, et al., 1985).

Category	Histology characteristics	Score		
		+ (Immature) =1	++ =2	+++ (Mature) = 3
A	Cellularity	Marked	Moderate	Minimal
B	Proportion of cells resembling tenocytes	<1/3	1/3-2/3	>2/3
C	Proportion of cells oriented parallel to longitudinal axis	<1/3	1/3-2/3	>2/3
D	Vascularity	Marked	Moderate	Minimal
E	Proportion of fibers of large diameter characteristics of mature tendon fibers	<1/3	1/3-2/3	>2/3
F	Proportion of fibers oriented parallel to the longitudinal axis	<1/3	1/3-2/3	>2/3
G	Wave formation	Minimal	Moderate	Marked

Table 2.11 Soslowsky score for histological evaluation of tendon repair (Soslowsky, et al., 1996).

Category	Histology Characteristic	Score			
		0	1	2	3
A	Collagen grade	Normal collagen orientated tangentially.	Mild changes with collagen fibers, < 25% disorganized.	Moderate changes in collagen, > 50% disorganized.	Marked changes in collagen, >50% disorganized.
B	Degree of angiogenesis	Normal tendon tissue.	Increase presence of capillaries.	Moderate infiltration of tissue with vessels.	
C	Cartilage formation	No cartilage formation.	Isolated hyaline cartilage nodules.	Moderate cartilage formation of 25% to 50%.	Extensive cartilage formation, > 50% of the field involved.

CHAPTER 3

RESULTS 1: EFFECT OF GDF5 ON THE TENOGENIC DIFFERENTIATION POTENTIAL OF HUMAN AND RABBIT BONE MARROW-DERIVED MESENCHYMAL STEM CELLS *IN VITRO*

Part of this chapter has been published in:

Tan S.L., Ahmad R.E., Ahmad T.S., Merican A.M., Abbas A.A., Ng W.M., Kamarul T. (2012) Effect of growth differentiation factor 5 on the proliferation and tenogenic differentiation potential of human mesenchymal stem cells in vitro. *Cells Tissues Organs* 196: 325-338.

3.0 Results 1: Effect of GDF5 on the tenogenic differentiation potential of human and rabbit bone marrow-derived mesenchymal stem cells *in vitro*

3.1 Introduction

GDF5 is a pivotal factor in tendon neoformation, and this has been demonstrated in many previous studies as summarized in Table 1.7, both in *in vitro* or *in vivo* experiments. In the early development, the tendon progenitor (TP) marker *Scx* expression is dependent on the combined conditions of the expression pattern of transcription effectors and the distance that a particular source of growth factor is able to travel (Brent et al., 2005; Brent et al., 2003). An important scenario is that when the signal molecule diffuses out from a localized signaling center, and it concurrently creates a signal concentration gradient. Cells at different distances from the source are driven to behave in a variety of different ways; according to the signal concentration that they experience (Alberts et al., 1994). In the light of GDF5 is expressed in regions of future joints during the early stages of embryological development (Storm & Kingsley, 1999), GDF5 has been shown to be an important factor during early tendon healing (Chhabra et al., 2003). It is hypothesized that GDF5 has a tenogenic differentiation induction effect in TP cells, either in the early tendon development or in tendon healing process.

Similar to other TGF-β superfamily members, GDF5 binds to the BMPR2 which in turn binds to intracellular Type I receptor (ALK2) (Nickel et al., 2005) and transmits its signal through the Smad/BMP signaling cascade. The binding of GDF5 to its receptor, forms an activated receptor complex. Smad8 is then phosphorylated by this activated receptor, which subsequently bind to Smad4. This is then followed by the translocation of the Smad8/Smad4 complex into the nucleus, which results in the regulation of selected transcription of targeted genes, which includes but not exclusively *Scx* (Bullough et al., 2008). *Scx* is a transcription factor, which will activate *Col-I* gene

expression in tenocytes thereby regulating this gene (Lejard et al., 2007). It has been speculated that the process of transcribing this gene will translate into increased COL- I production which is the most abundant protein in the tendon. Besides, other tendon candidate markers expression (i.e. tenascin C, decorin and tenomodulin) are also speculated to increase alongside with the COL-I expression.

Previous studies in tenogenic effect of GDF5 has only demonstrated for immortalized cell lines (Farng et al., 2008) and rodent adipose tissue- derived MSCs (Park et al., 2010). To date, there are limited studies investigating the isolated effect of GDF5 on MSC proliferation and tenogenic differentiation *in vitro*. The effect of GDF5 on harvested non-immortalized bone marrow-derived hMSCs, which represents the most commonly obtained source of MSCs (Hass et al., 2011), has not been previously described. A critical issue which has not been specifically addressed by previous studies is the establishment of the optimal concentration of GDF5 that can induce maximal phenotypic expression of the tenogenic hMSC *in vitro*. Therefore, this current study was conducted to determine the effect of GDF5 on the proliferation and tenogenic differentiation potential of hMSC *in vitro*. To explore this, a gradient concentration of GDF5 (0, 5, 25, 50, 100 and 500 ng/mL) was tested on the hMSCs considering that progenitor cells can differentiate into various types of mature cells, e.g., osteocytes, chondrocytes and tenocytes, in response to the amount of signal molecules received.

In view of possible animal transplantation models being used in the later *in vivo* tendon repair experiments (Chapter Four), the effect of GDF5 in bone marrow derived rabbit MSCs (rbMSCs) from New Zealand white rabbit was also examined. This is of particular importance considering that an optimal concentration must be attained in order to induce the rbMSCs into the desired tenogenic lineage. This in turn may allow the *in vivo* tendon repair to be studied when those cells were transplanted into the rabbit tendon defect area. Thus, gradient concentrations of GDF5 were also tested in rbMSCs.

3.2 Experimental Design

3.2.1 Cell Proliferation Experiment

hMSC Primary cultures (at P2, n=3) were seeded in the standard 96-well culture plates at cell density of 10^4 cells/mL and resuspended in 250 µl of culture medium. GDF5 at various concentration levels (either 0, 5, 25, 50, 100 or 500 ng/mL) were added to the cultures three days after seeding. Recombinant human GDF5 (Table 2.2) was used for hMSCs. Cells were incubated for an additional period of two days before alamarBlue® assay was commenced. Schematic diagram of experimental design for cell proliferation assay is showed in Figure 3.1.

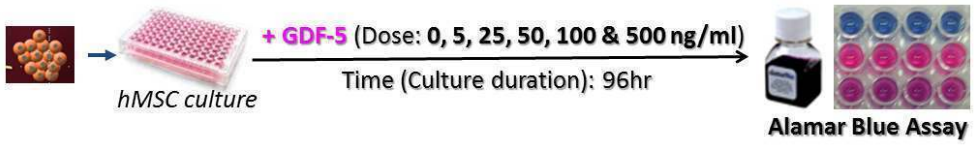

Figure 3.1 Experimental design for alamarBlue® cell proliferation assay for dose and time response experiments in human *in vitro* studies.

3.2.2 Total Soluble Collagen Assay

The MSC primary cultures (at P2, n=3) were seeded in standard 6-well culture plates at a density of 2 x 10^4 cells per well, and supplemented with recombinant GDF5 at various concentration levels (0, 5, 25, 50, 100 or 500 ng/mL). The tenocyte primary cultures (n=3) were seeded in similar density to that of MSCs and were used for comparison. These cells were not supplemented with GDF5. For dose-response analysis (in both hMSC and rbMSC), cell were observed under phase contrast microscope and total collagen expressions were measure at 96 h. The phase contrast micrographs were captured for hMSC and rbMSC cultures with or without GDF5 supplement. Based on the results obtained from dose-response experiment, only three concentrations, i.e. 0, 50 and 100 ng/mL of GDF5, were selected for further analysis which determines the collagen and gene expression levels at different time points (day 4, 7 and 10). For time response experiments, total collagen assays were conducted at day 4, 7 and 10 in hMSC

culture supplemented with 0, 50 and 100 ng/mL of GDF5. Schematic diagram of experimental design for total collagen assay is showed in Figure 3.2.

Figure 3.2 Experimental designs for total collagen assays for dose and time response experiments in human and rabbit *in vitro* studies.

3.2.3 Gene Expression Analysis

To determine the effect to GDF5 in inducing tenogenic candidate markers gene expression, hMSCs were cultured in medium supplemented with GDF5 at 0, 50 and 100 ng/mL. After 4 days, the cells were harvested for total RNA extraction and the degree of cell differentiation was determined by quantitative RT-PCR (*q*RT-PCR). This was achieved by measuring *Scx, Tnc, Col-I, Col-III, Dcn* and *Nst* gene expressions. In addition, hMSCs were cultured in DMEM supplemented with 100 ng/mL GDF5 for 7 days to determine the tenogenic lineage commitment in hMSCs post- GDF5 treatment. Cells were harvested at day 4 and 7 to evaluate the gene expression level of *Scx*, *Tnc*, *Runx2* and *Sox9*. Schematic diagram of experimental design for gene expression analysis in hMSC is showed in Figure 3.3.

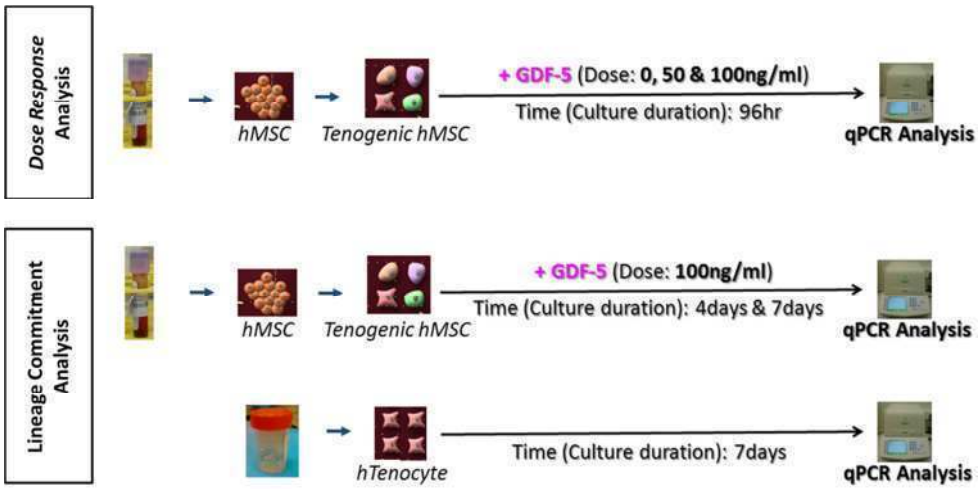

Figure 3.3 Experimental designs for gene expression analysis for dose and time response experiments in human *in vitro* studies.

In gene expression experiments conducted on rbMSC, only *Scx* and *Col-I* gene expression levels were determined for rbMSCs treated with or without GDF5. This was due to the limited molecular biology information in rabbit model at the time when this experiment was conducted. Thus, only these two genes were evaluated in rbMSCs treated with 0, 50 and 100 ng/mL of GDF5. As an extension to the gene expression analysis of these two genes, the time response analysis were conducted to determine the mRNA expression levels of these genes in rbMSC treated with 100 ng/mL of GDF5 at day 0, 4, 10 and 27. Schematic diagram of experimental design for gene expression analysis in rbMSC is showed in Figure 3.4.

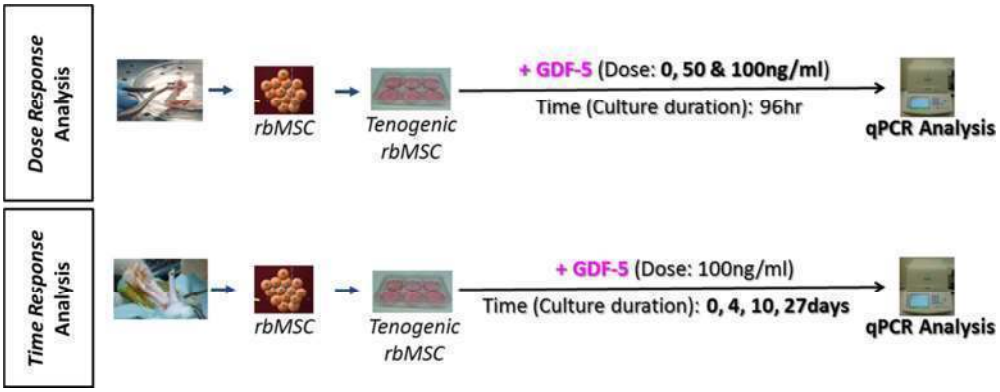

Figure 3.4 Experimental designs for gene expression analysis for dose and time response experiments in rabbit *in vitro* studies.

3.2.4 Immunofluorescence Staining

For immunofluorescence staining, hMSC (or rbMSC) as well as human (or rabbit) tenocyte were seeded on cover slips. The hMSC (or rbMSC) were cultured with and without 100 ng/mL of GDF5 for 4 days before proceeding to immunofluorescence staining. Immunofluorescence staining was conducted for candidate tenogenic markers, i.e. COL-I, SCX, TNC and TNMD. Human (or rabbit) tenocytes were used as positive control and hMSC (or rbMSC) treated with GDF5 but do not stain with primary antibodies were used as negative control.

In view of a limited number of genes analyzed in rbMSC, immunofluorescence staining for type-I collagen (COL-I) in rbMSCs cultured at different concentrations of GDF5 (0, 5, 25, 50, 100 and 500 ng/mL), and type-II and III collagen (COL-II and COL-III) in rbMSCs treated with 100 ng/mL of GDF5 were also conducted.

3.3 Results

3.3.1 hMSC Proliferation Under GDF5 Treatment

The results of alamarBlue® assay showed a pattern of an increase in cell proliferation rate at low concentrations of GDF5 (5 ng/mL) and, in contrast, the cell proliferation rate appeared to be reduced at a high GDF5 concentration (500 ng/mL). However, the differences in the hMSC proliferation between the cultures treated with or without GDF5 were not significant (Figure 3.5), suggesting that GDF5 did not alter the proliferation rate of the tenogenic- hMSCs.

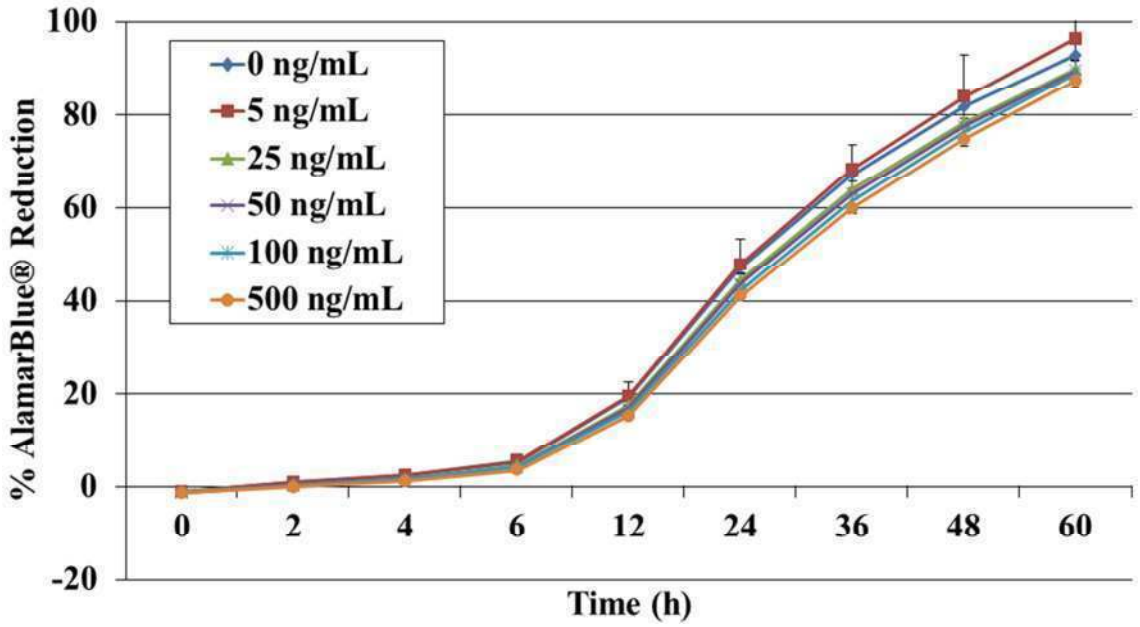

Figure 3.5 AlamarBlue® cell proliferation assay of the hMSCs cultures supplemented with different concentrations of GDF5.
There was no significant difference in cell proliferation rates as reflected by the percentage of alamarBlue® reduction by hMSC (at P2, n=3) supplemented with varying levels of GDF5.

3.3.2 Morphological Appearance of hMSC and rbMSC Under GDF5 Treatment

Images of hMSCs and rbMSC in culture with and without GDF5 supplementation were captured with a phase contrast microscope (Figure 3.6 and Figure 3.7). There were no significant differences in the gross morphological appearance between these cells, irrespective of the GDF5 concentration levels used. The rbMSCs cultured with higher concentrations of GDF5 showed more elongated appearance and more extensive network of branching in their colonies-forming than those with lower concentrations of GDF5.

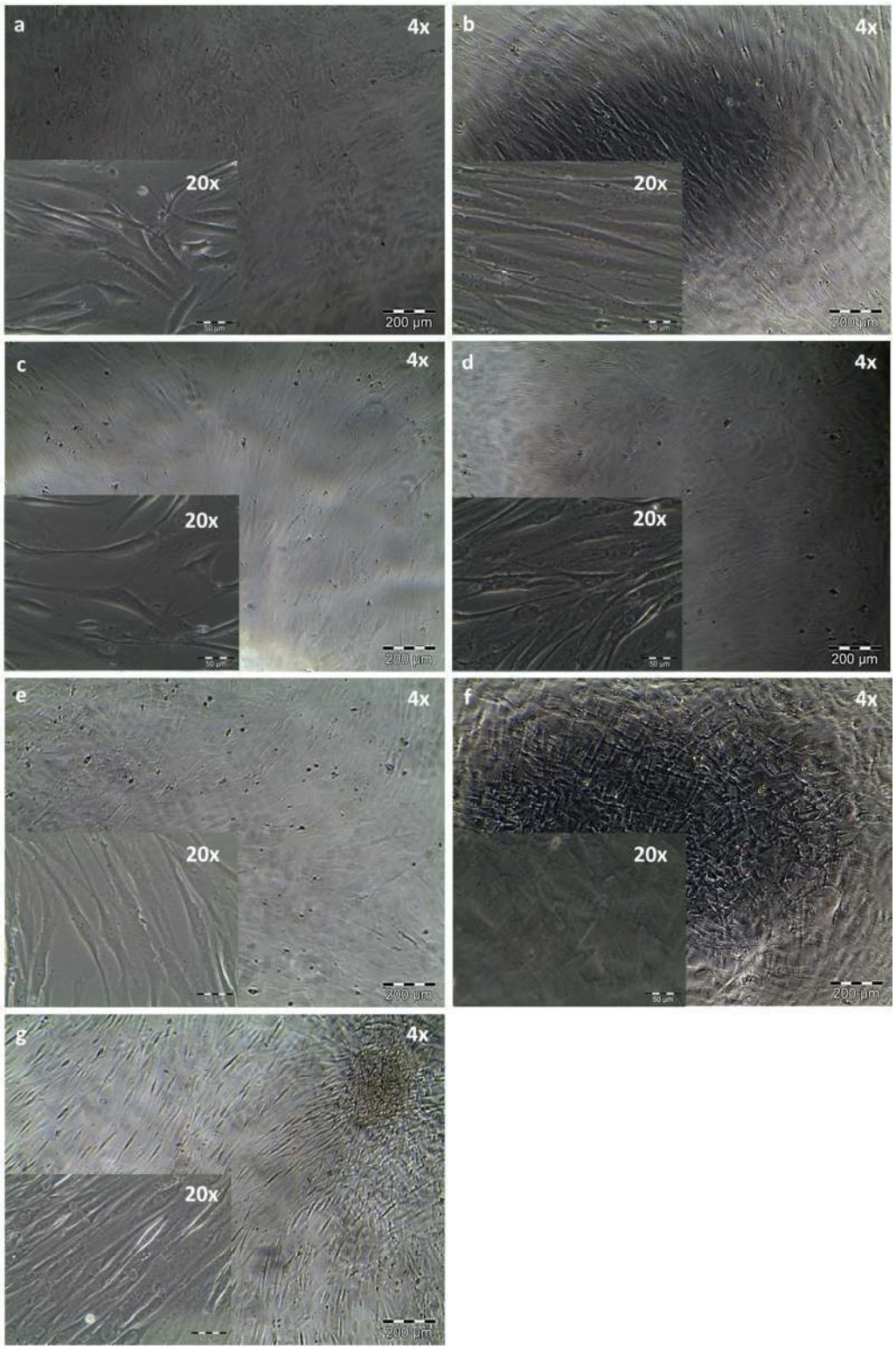

Figure 3.6 Morphological appearance of hMSC (at day 4) in culture medium supplemented with various concentrations of GDF5, i.e. (a) 0, (b) 5, (c) 25, (d) 50, (e)100, and (f) 500 ng/mL; and (g) human tenocytes.
There were no significant differences in gross appearance in the hMSC cultures with or without GDF5 supplementation. At 100 ng/mL of GDF5, cells appeared to be having similar unidirectional proliferation and fibroblastic morphology to that of the human tenocyte culture.

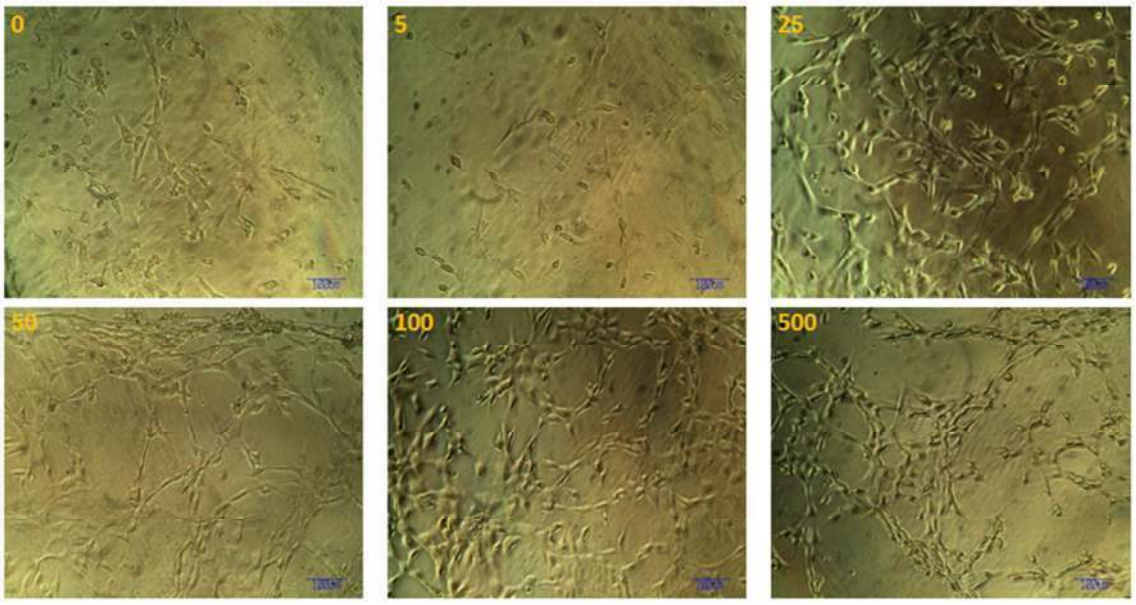

Figure 3.7 Morphological appearances of rbMSCs (at day 4) in culture medium supplemented with GDF5 at different concentrations, i.e. 0, 5, 25, 50, 100 and 500 ng/mL.
The concentrations of the GDF5 used were denoted at the left corner of each image at ng/mL. The rbMSCs showed more extensive network of branching with increase concentration of GDF5 supplemented (magnification at 10x objective).

3.3.3 Total Soluble Collagen Assay

Dose response analysis at 96 h following GDF5 supplementation revealed that total collagen was significantly increased at 100 ng/mL of GDF5 (p<0.05, Figure 3.8; Table 3.1A) in hMSC. Although rbMSC showed a significant increase at 500 ng/mL, (11.69±2.72 μg/mL; p<0.05; Table 3.1B), it also showed no significant difference compared to 100 ng/mL (Table 3.1B). Both hMSCs and rbMSCs showed no significant differences between 50 and 100 ng/mL in the total collagen expression. Based on the results obtained from this experiment, only three concentrations, i.e. 0, 50 and 100 ng/mL of GDF5, were selected for time response experiments.

In the subsequent time response experiment conducted in hMSCs, the results showed a significant increase in the total collagen expression in the culture medium from the hMSCs cultures supplemented with 100 ng/mL of GDF5 at day -4, -7 and -10, as compared to the untreated cultures (Figure 3.9). A significant increase in total

collagen expression was only observed at day -7 onwards in the hMSCs cultures treated with 50 ng/mL of GDF5. This finding demonstrates that 100 ng/mL of GDF5 is sufficient to induce a tenogenic response from hMSCs as early as day -4, but with the use of 50 ng/mL of GDF5, a longer period was required.

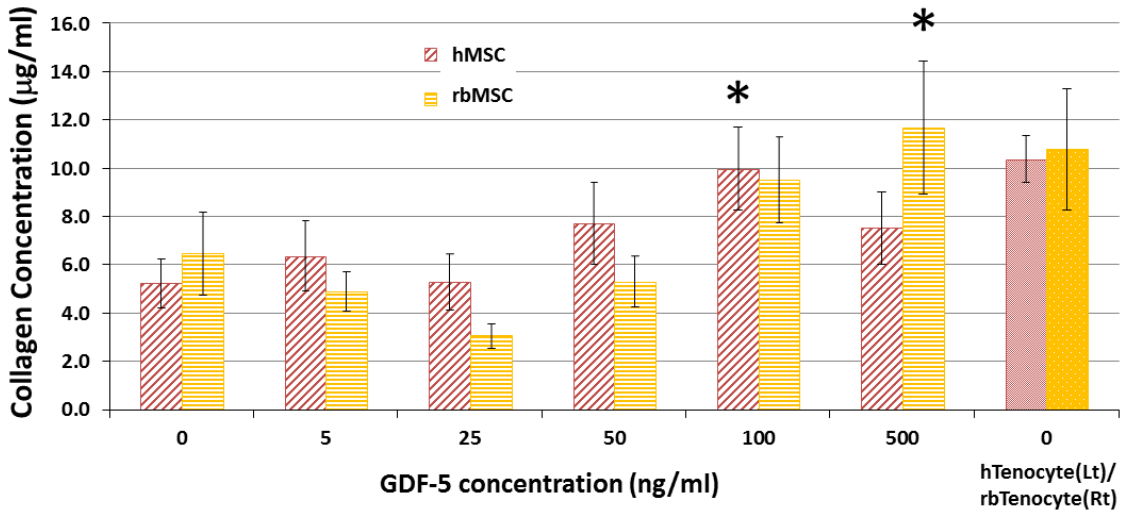

Figure 3.8 Total collagen content analysis for hMSC and rbMSC cultured with different concentrations of GDF5.
Total collagen was significantly increased in hMSC (at P2, n=3) at >100 ng/mL of GDF5 supplementation (*p<0.05).

Table 3.1 Statistical analysis of total collagen expression in hMSCs and rbMSCs cultured at different concentrations of GDF5.
Summary of least significant differences (LSD) analysis with Bonferroni adjustment for multiple pairwise comparisons of the mean total collagen differences in the culture medium of hMSCs (A) and rbMSCs (B) supplemented with different amount of GDF5. The p-value was presented at 95% confidence interval and significant value was denoted with an asterisk (* = p<0.05 and ** = p<0.01).

A

		***p*-Value**				
		Different concentration of GDF5 (ng/mL)				
		5	**25**	**50**	**100**	**500**
Different concentration of GDF5 (ng/mL)	**0**	0.515	0.978	0.157	**0.008****	0.187
	5		0.520	0.426	**0.035***	0.485
	25			0.153	**0.007****	0.183
	50				0.178	0.921
	100					0.149

Table 3.1, continued

B

		Concentrations of GDF5 (ng/mL)				
		5	**25**	**50**	**100**	**500**
Concentrations of GDF5 (ng/mL)	**0**	0.493	0.142	0.614	0.183	**0.026***
	5		0.425	0.856	**0.047***	**0.004****
	25			0.329	**0.006****	**0.000****
	50				0.069	**0.007****
	100					0.347

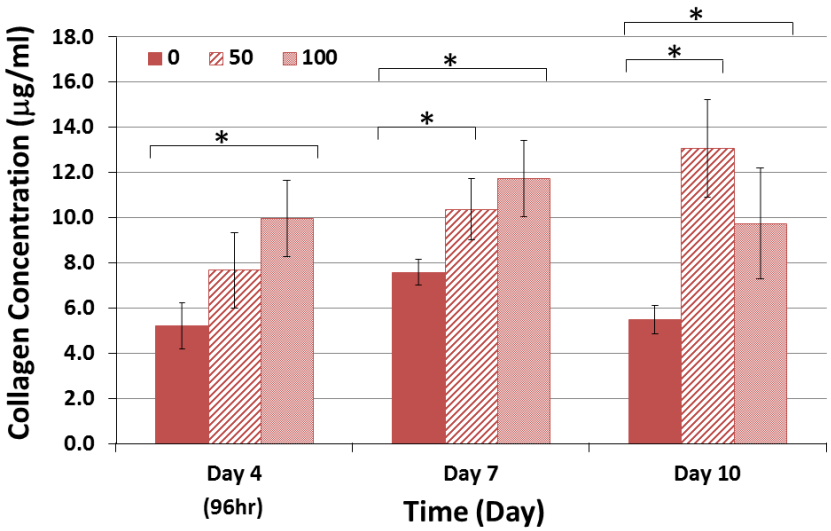

Figure 3.9 **Total collagen content for time response analysis in hMSC at three concentration levels of GDF5, i.e. 0, 50 and 100 ng/mL of GDF5.**
In comparison to hMSC without GDF5 treatment, the total collagen expression was significantly elevated (*p<0.05) in hMSCs (at P2, n=3) at 100 ng/mL of GDF5 on day 4 onwards, whilst significant increased (*p<0.05) at 50 ng/mL was only observed at day 7 onwards.

3.3.4 Gene Expression Analysis

3.3.4.1 Relative Gene Expression Analysis of hMSC Tenogenic Differentiation at mRNA Level

A. Dose Response in GDF5-Induced mRNA Expression

Gene expression analysis showed that there were significant differences in the relative gene expression levels for *Col-I* and *Col-III*, *Dcn*, *Scx*, *Tnc* and *Nst* of the hMSCs grown in 0, 50 and 100 ng/mL of GDF5 at 96 h (Figure 3.10). At 100 ng/mL of GDF5, candidate tenogenic- markers, *Col-I*, *Scx* and *Tnc*, were significantly up-regulated (2.31±0.27, 2.30±1.81 and 3.55±0.27 fold increase, respectively; Figure 3.10).

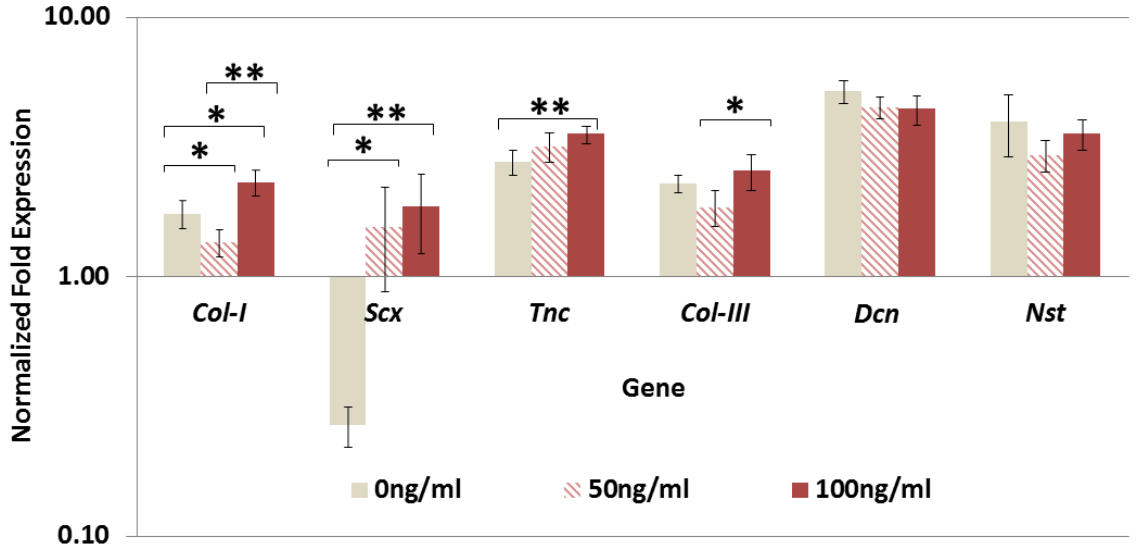

Figure 3.10 **Relative gene expression analysis of candidate tenogenic markers in hMSCs cultured with GDF5 at different concentrations (0, 50 and 100 ng/mL).**
There was a significant up-regulation of gene expression of candidate tenogenic marker genes type-I Collagen (*Col-I*), scleraxis (*Scx*), tenascin-C (*Tnc*) and type-III collagen (*Col-III*) at 100 ng/mL of GDF5 (n=3; **p*<0.05 and ***p*<0.01). (Data were presented as $\log_{10}$ fold change±S.D.)

Although the *Col-III* expressions were not significantly different in hMSCs cultured with GDF5 as compared to those without GDF5, the ratio of *Col-I* to *Col-III* appeared to be increased (Table 3.2). For *DCN* expression, there was a 4.47±0.41 fold increase at 50 ng/mL and a 4.42±0.57 fold increase at 100 ng/mL at 96 h. No significant difference in *Nst* gene expression levels was observed in all groups, demonstrating that despite undergoing tenogenic differentiation, cells maintained their original MSC gene expression.

Table 3.2 The ratios of type-I to type-III collagen (*Col-I* to *Col-III*) expression levels in hMSCs cultured at 0, 50 and 100 ng/mL of GDF5.
The ratios were derived from the qPCR data. The results showed higher ratio of type-I to type-III collagen in hMSCs cultures with 100 ng/mL of GDF5 at 96 h.

Amount of GDF-5 in hMSCs culture (ng/ml)	Ratio of Col-I to Col-III
0	0.76
50	0.73
100	0.90

B. GDF5-Induced Lineage Commitment in hMSC

The results of lineage commitment experiment showed the candidate tenogenic marker genes *Scx* and *Tnc* were up-regulated (1.86±0.63 and 5.80±0.39 fold increase, respectively) on day 4 after the GDF5 treatment (Figure 3.11 A and B). However, on day 7, only *Scx* was persistently up-regulated (1.80±0.81 fold increase), whereas the expression of *Tnc* was reduced (0.65±0.08 fold decrease; $p<0.01$). The expression of non-tenogenic marker genes *Runx2* and *Sox9* was significantly down-regulated (2.83±1.64 and 1.12±0.08 fold increase, respectively; $p<0.01$) on day 7 (Figure 4.5 C and D). These findings suggested that hMSCs were undergoing tenogenic differentiation as early as day 4 following induction by GDF5 at 100 ng/mL.

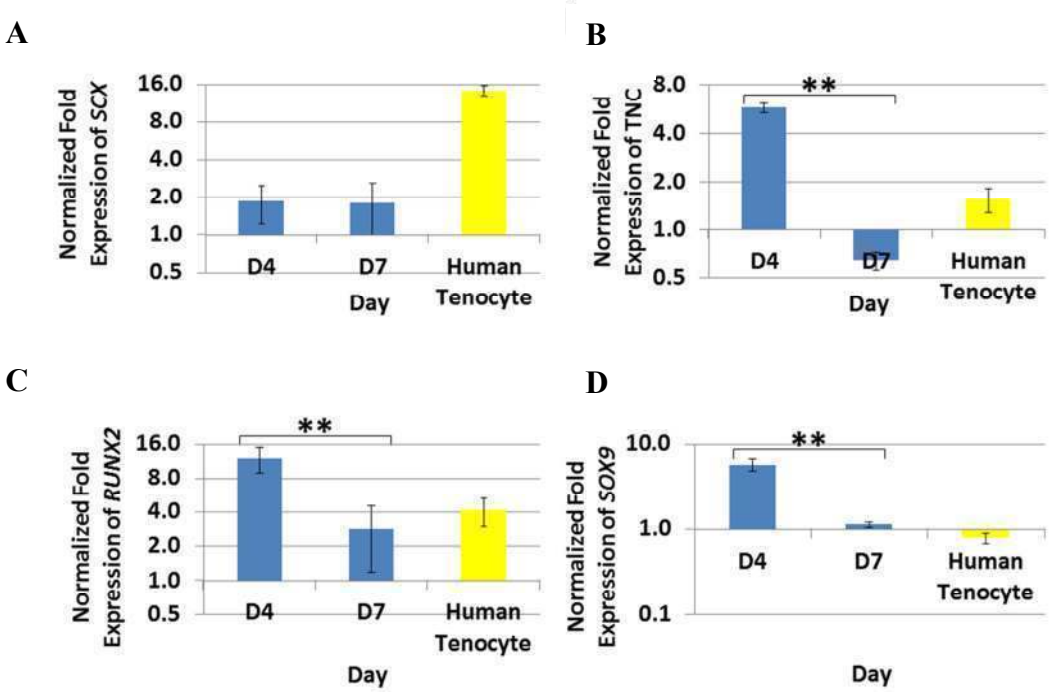

Figure 3.11 Relative gene expression analysis of cultured hMSCs in the temporal experiment at 100 ng/mL of GDF5. (A) Scleraxis (*Scx*), (B) tenascin-C (*Tnc*), (C) runt-related transcription factor 2 (*Runx2)* and (D) SRY (sex-determining region Y)-box 9 (*Sox9*).
The data reflect the relative quantification of target mRNA normalized to control samples (untreated hMSCs cultured in MSC growth medium). Data are presented in either $\log_2$- (in A, B and C) or $\log_{10}$- (in D only) scale, with error bars signifying the range of standard deviation. All the candidate tenogenic marker genes were up-regulated on day 4 (D4), but only *Scx* was persistently up-regulated on day 7 (D7). There was a significant increase in the expression of non-tenogenic marker genes (i.e. runt-related transcription factor 2 (*Runx2),* and SRY (sex-determining region Y)-box 9 (*Sox9*)) on day 4 of GDF5 treatment, which subsequently significantly down-regulated by day 7. (n=3; **$p<0.01$).

3.3.4.2 Relative Gene Expression Analysis of rbMSC Tenogenic Differentiation at mRNA Level

A. Dose Response in GDF5-Induced mRNA Expression

The *Col-I* gene was significantly (p<0.05) up-regulated in rbMSCs at a 1.30±0.06 fold in 50 ng/mL cultures and a 1.29±0.21 fold in 100 ng/mL cultures. *Col-I* gene expression was significantly down-regulated at a 1.32±0.05 fold in rbMSCs without GDF5 supplementation. The *Scx* gene expression was significantly up-regulated (p<0.05) in rbMSCs cultured with GDF5 supplementation (a 6.18±0.48 fold for 50 ng/mL and a 2.40±0.83 fold for 100 ng/mL supplemented culture; Figure 3.12). There were no significant changes in *Scx* gene expression in rbMSCs cultured at 0 ng/mL of GDF5.

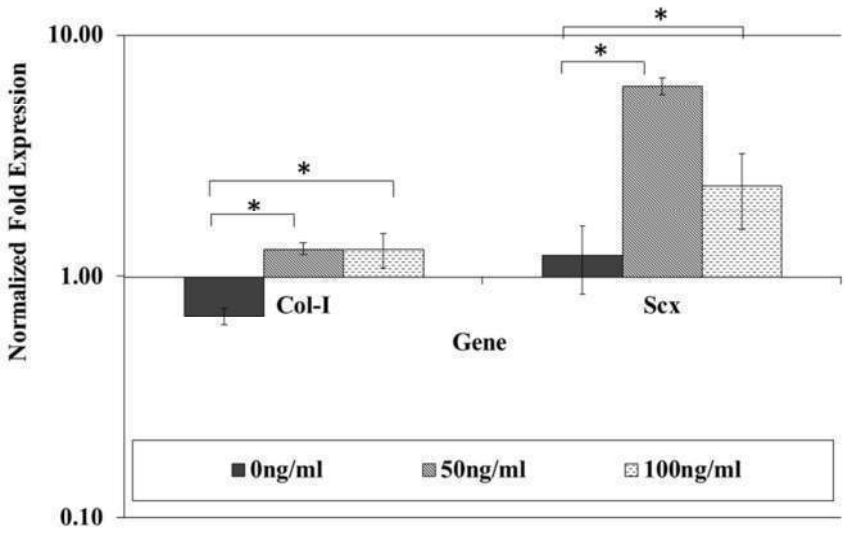

Figure 3.12 Relative gene expression analysis of candidate tenogenic markers in rbMSCs cultured with GDF5 at different concentrations (0, 50 and 100 ng/mL).
There was a significant up-regulation of gene expression of candidate tenogenic marker genes type-I Collagen (*Col-I*), and scleraxis (*Scx*), at 50 and 100 ng/mL of GDF5 (n=3; *p<0.05). (Data were presented in mean±SEM.)

B. Time Response in GDF5 Induced mRNA Expression

In the time response experiment, the *Col-I* expression was significantly (p<0.05) and persistently up-regulated on day 4 (8.76±0.71 fold) onward up to day 27 (10.34±1.09 fold) when cultured with 100 ng/mL of GDF5 supplementation. However,

the *Scx* gene expression levels was significantly and persistently up-regulated at day 4 (4.12±2.05 fold) onward up to day 10 (2.50±0.76 fold), and no significant changes on day 27 (0.69±0.63 fold; Figure 3.13).

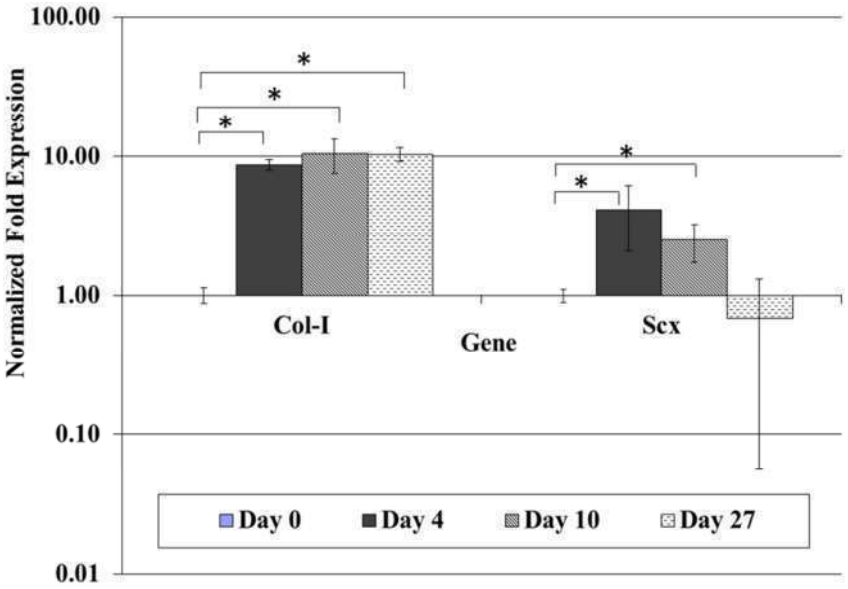

Figure 3.13 **Relative gene expression analysis of *Col-I* and *Scx* in rbMSCs cultured with 100 ng/mL GDF5 in time response experiments (day 0, 4, 10 and 27).** Both genes were up-regulated at day 4 in both concentrations, 50 and 100 ng/mL (n=3). However, only *Col-I* persistently expressed from day 4 to day 27. *Scx* showed an increased on day 4 and only persistently up-regulated up to day 10. A decrease was observed in *Scx* on day 27. (Data were presented in mean±SEM.)

3.3.5 Expression of Tenogenic Markers at Protein Level with Fluorescence Imaging

The results of immunofluorescence staining revealed that COL-I, TNMD, TNC and SCX protein expression were markedly increased in hMSCs (Figure 3.14) and rbMSCs (Figure 3.15) treated with 100 ng/mL of GDF5. These observations suggested that 100 ng/mL of GDF5 treatment able to induce hMSC and rbMSC to differentiate into tenogenic lineages. The COL-I appeared to stain around the nucleus of the rbMSCs with or without GDF5 supplement and regardless of the GDF5 concentrations (Figure 3.16 A). In the rbMSCs treated with 100 ng/mL of GDF5, only COL-I and COL-III were detected, but not COL-II. Different staining pattern of COL-I and COL-III was

observed; with COL-I expressed around the nucleus, and COL-III expression was detected as a halo-like pattern (white arrows) surrounding the nucleus (Figure 3.16 B).

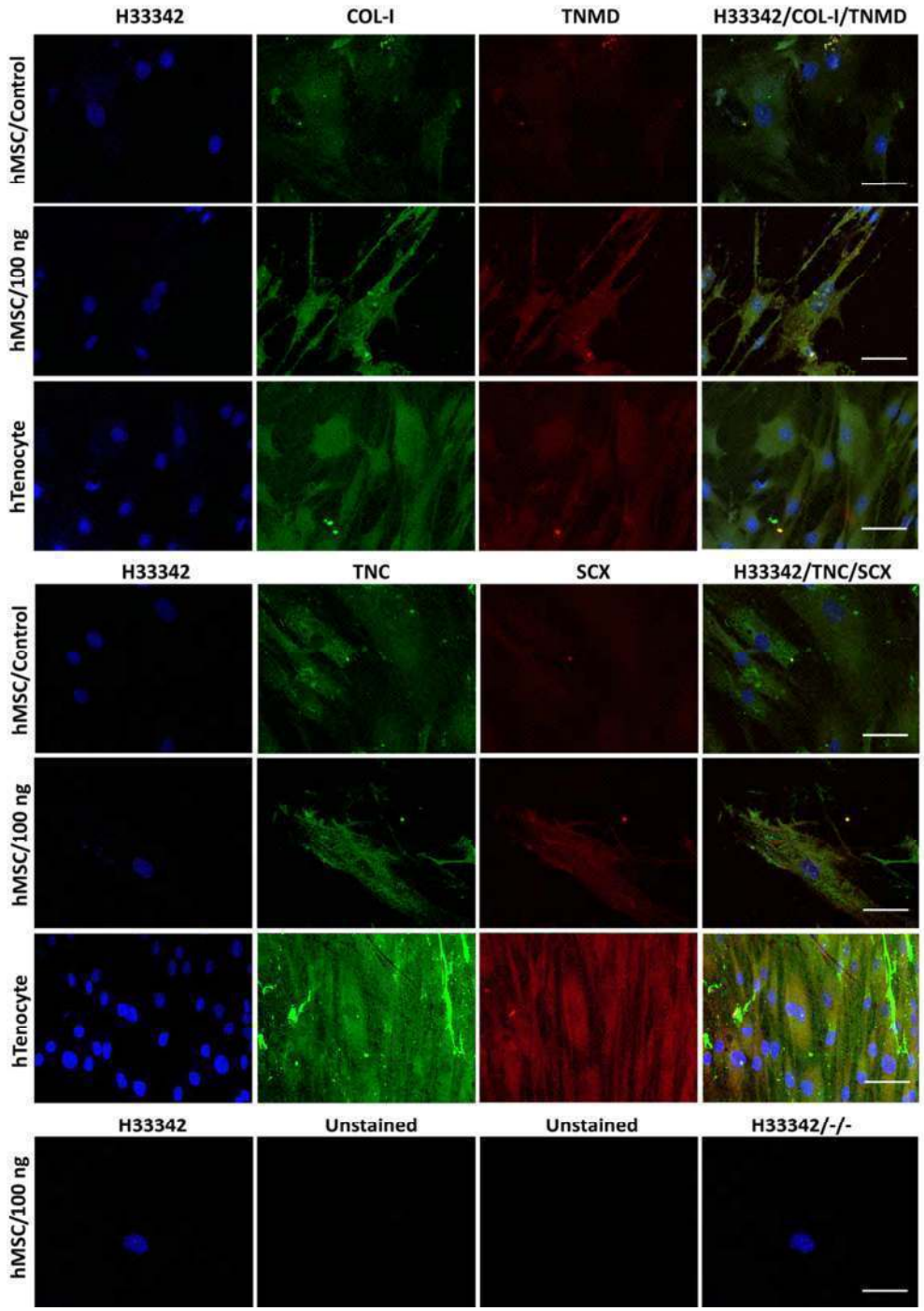

Figure 3.14 The candidate tenogenic markers (COL-I, TNMD, TNC and SCX) expression of GDF5 (100 ng/mL) treated hMSC by immunofluorescence staining.

The extent of candidate tenogenic markers expressions were increased in GDF5 treated hMSC compared to the untreated control. Images were captured at 63X objective and a scale bar (50 μm) was depicted on the right bottom corner of the overlay images.

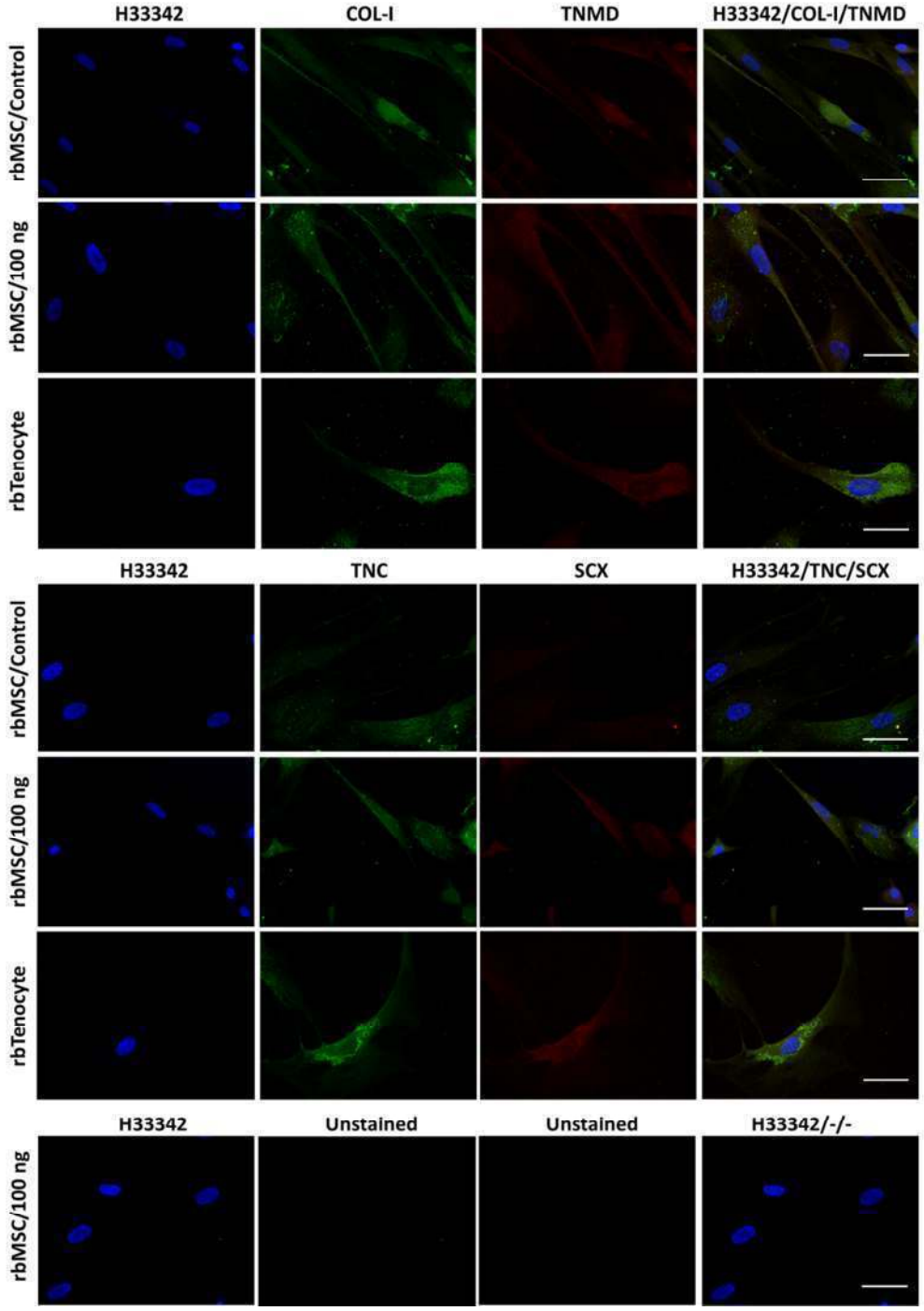

Figure 3.15 The candidate tenogenic markers (COL-I, TNMD, TNC and SCX) expression of GDF5 (100 ng/mL) treated rbMSC by immunofluorescence staining.

The extent of candidate tenogenic markers expressions were increased in GDF5 treated rbMSC compared to the untreated control. Images were captured at 63X objective and a scale bar (50 μm) was depicted on the right bottom corner of the overlay images.

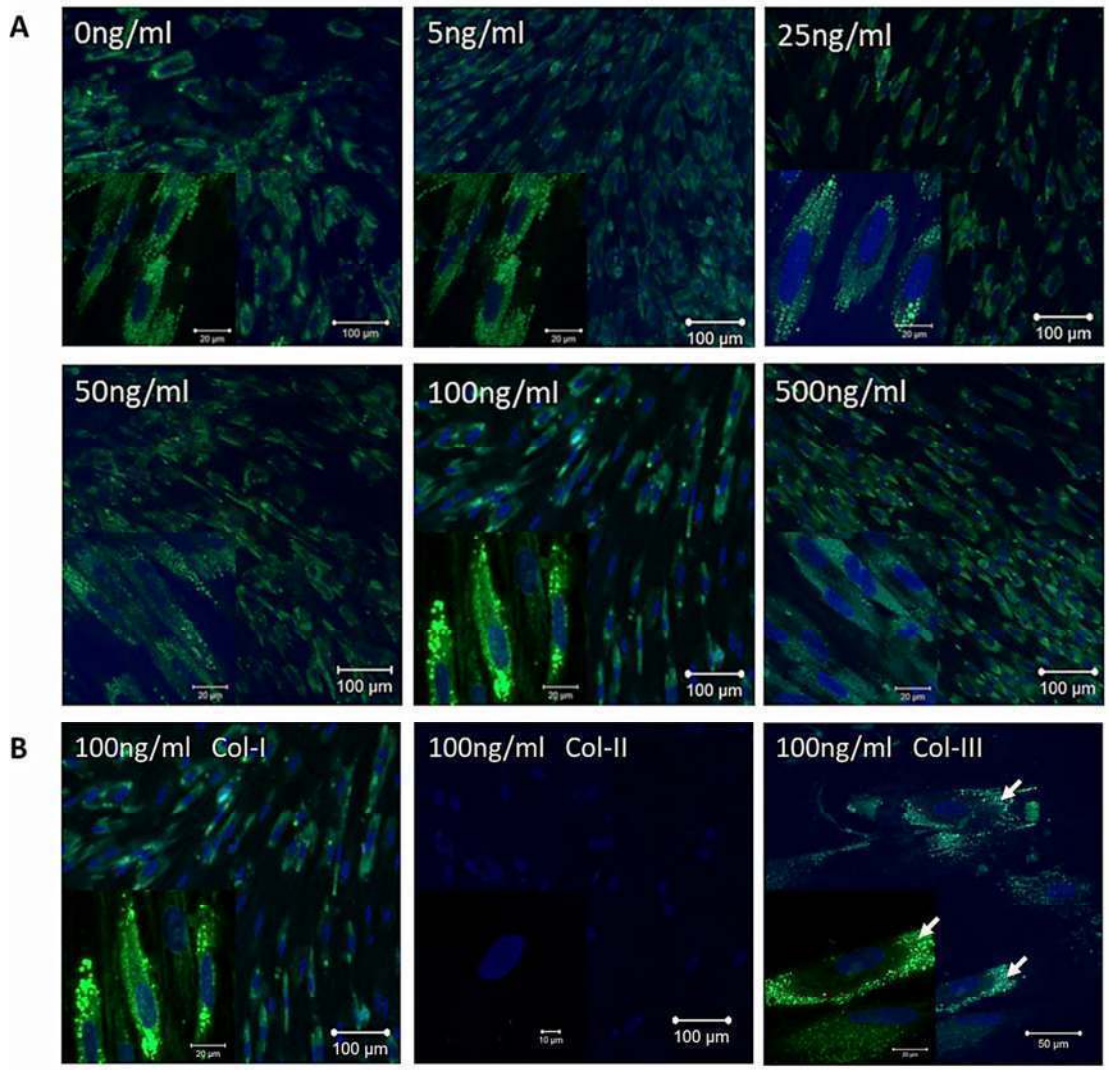

Figure 3.16 Expression of collagen type-I, II and III (COL-I, COL-II and COL-III) in rbMSCs cultured with or without GDF5 supplement.

A. COL-I immunofluorescence staining of rbMSCs supplemented with and without GDF5 (0, 5, 25, 50, 100 and 500 ng/mL, as denoted at the top left conner of each image). Positive expression was observed in all rbMSCs cultured with and without GDF5 and the expression pattern of COL-I was more intense around the nucleus in all rbMSCs, regardless of GDF5 treatment.

B. COL-I, COL-II and COL-III immunofluorescence staining (as denoted on top of each image) of rbMSC treated with 100 ng/mL of GDF5. Only COL-I and COL-III were present in rbMSCs supplemented with 100 ng/mL of GDF5, but no COL-II was detected. Different staining pattern of COL-I and COL-III was observed; with COL-I expressed more intense around the nucleus, and COL-III appeared as a halo-like pattern (white arrows) surrounding the nucleus.
Images were captured at 10X objective and 63X objective (at bottom left corner of each image).

3.4 Discussion

3.4.1 Cell Proliferation

The results of this study showed that GDF5 did not appear to influence hMSC proliferation, which is in contrast to a previous report involving the rodent adipose tissue-derived MSC primary culture (Park, et al., 2010), but in consistency with a study which uses murine bone marrow-derived stromal immortalized cell lines (Farng, et al., 2008). In a separate study reported recently, have shown that rodent adipose tissue-derived MSCs had been shown to produce faster proliferation than MSCs derived from the bone marrow (Saka et al., 2011). Nevertheless, the data presented in this current study appear to be consistent with a study which uses murine bone marrow-derived stromal immortalized cell lines (Farng, et al., 2008). Therefore, it appears that the tissue origin of the MSCs may be a predetermining factor affecting cell proliferation in the presence of GDF5. However, this needs to be confirmed by a more robust study design.

3.4.2 Candidate Tenogenic Marker Expression

Despite the fact that GDF5 does not affect the morphological appearances of hMSC or rbMSC, the supplementation of GDF5 (especially at 100 ng/mL) does affect the expression of candidate tenogenic markers. This has been shown in the results in total soluble collagen assay, gene expression and protein expression (immunofluorescence staining).

In the total soluble collagen experiment, a biphasic response was observed (significantly in rbMSC, but not significant in hMSC) where the total collagen expression showed a decrease at 25 ng/mL of GDF5 but an increase at 50 ng/mL of GDF5 (Figure 3.8). Although the observation was not significant in hMSCs total collagen expression, which may due to the small sample size (n=3), a similar biphasic response was observed in the *Col-I* gene expression levels in hMSCs (Figure 3.10). It is

suggested that this biphasic response may due to the alternate exclusion mechanism as shown in FGF signalling mechanism in early tendon development. Nevertheless, a more comprehensive experimental design is required in order to elucidate this.

In the gene expression experiments, the candidate tenogenic markers genes (*Scx* and *Tnc*) were up-regulated at day 4 of GDF5 treatment. However, at day 7, only *Scx* was persistently expressed, whereas the *Tnc* expression was reduced dramatically. It is suggested that the decrease in the *Tnc* gene expression is due to the function of this gene which is a mechanoresponsive modulator of matrix formation expressed in high tensional loading tissue. The expression of this gene may persistently express should the cells receive mechanical signals after day 4. This however, required another comprehensive study to resolve it.

Further, in the current study, there was an apparent increase in the total collagen expression in the hMSCs cultures at 100 ng/mL of GDF-5 (Figure 3.8), with no significant increase in *Col-III* gene expression (Figure 3.10). This suggests that the increase in total collagen expression observed in our study is likely to be contributed mainly by an increase in *Col-I*, but the possibility of the presence of other collagens, e.g. Collagen type II, cannot be completely ruled out. This however, would be unlikely considering that other studies have shown that the expressions of these proteins are usually of minimal quantity (Altman et al., 2002). In regards to this, one would expect to observe a relatively high *Col-I* gene expression (at mRNA level) in the GDF5-induced MSCs, however this was not the case in the both hMSCs and rbMSCs. This could be explained as the COL-I synthesis is regulated at the protein translation level, but not at the gene transcription level. This further alludes to the regulation of COL-I synthesis by the cis-acting element i.e. RNA helicase A, without affecting the expression of *Col-I* at mRNA levels (Manojlovic & Stefanovic, 2012).

It is critical to emphasize that the biology of GDF5 is still far from clear: how does GDF5 induced MSCs undergo tenogenic differentiation, and whether the GDF5-induced MSCs undergo differentiation into tendon stem cells or tenoblast or tenocytes remain unclear, as currently, there are no specific markers to distinguish these aforementioned cells. It is speculated that the MSCs may undergo a symmetrical or an asymmetrical cell division upon GDF5 treatment (Figure 3.17). This speculation remains unresolved, as there were no specific markers to distinguish them from one another. Although the differentiation mechanism involved are still unknown, the findings of this study strongly indicate that the MSCs may undergo tenogenic differentiation by GDF5 treatment.

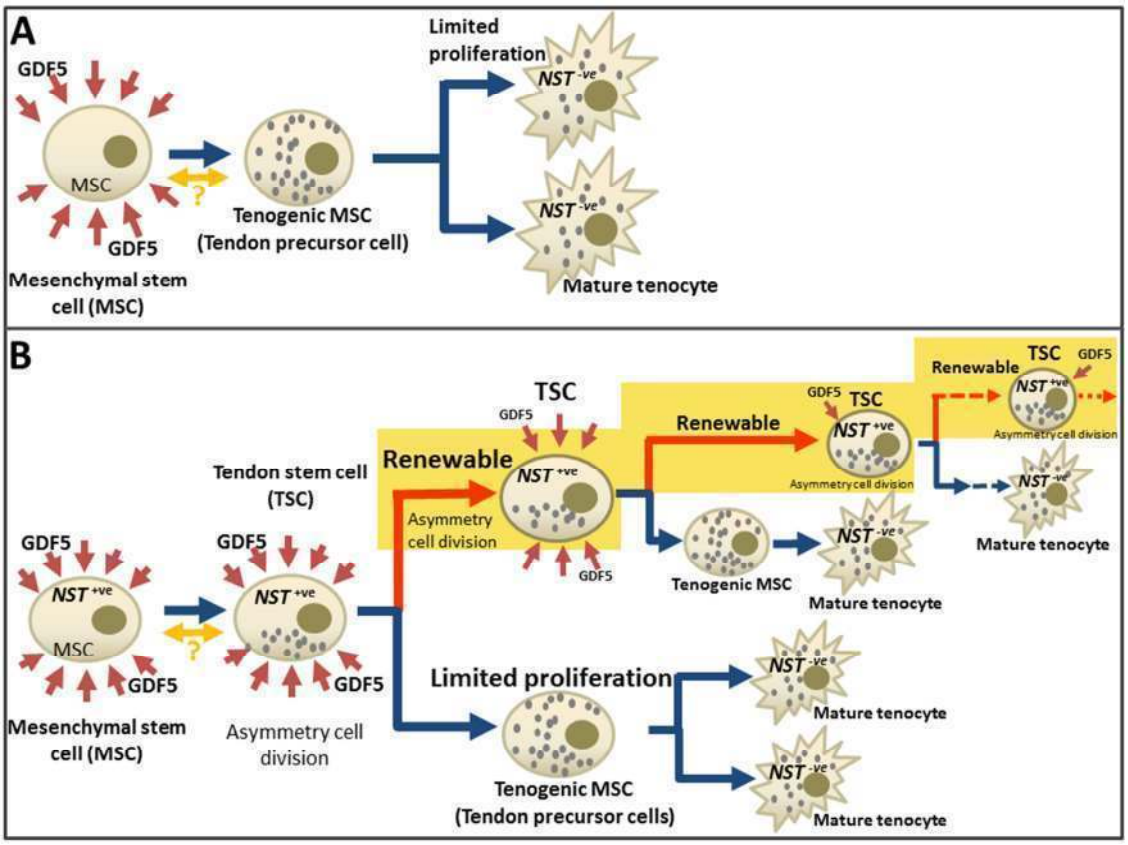

Figure 3.17 A postulated scenario of a more complex tenogenic differentiation process in MSCs under GDF5 treatment.

A. Symmerical cell division in the normally expected MSC tenogenic differentiation process.

B. An alternative condition showing the possibility of the occurrence of asymmetrical cell division resulting in two cell populations: (1) the renewable tendon stem cells (TSC) and the mature tenocyte.

3.4.3 Current Limitations

Although several limitations were identified within the present study, these were unfortunately unavoidable. Firstly, the overall experimental designs employed in this current study did not do a direct comparison between the hMSC and rbMSC. A direct comparison between hMSC and rbMSC would be useful, if both of these models are at the same level in their availability in molecular biology information. The human model has more advantage due to extensive molecular biology information, while the rabbit model has less advantage due to limited molecular biology information. Thus, in order to accommodate the information availability between the human and rabbit models, this study did not do a side by side direct comparison between hMSC and rbMSC.

Secondly, the use of total collagen assay to evaluate the tenogenic differentiation of hMSCs may not be the best method of assessment considering that many cells of mesenchymal in origin produce an abundance of extracellular collagen. The assessment of a more specific collagen, for example, type-I and type-III collagen, may be a more reasonable approach considering that these proteins are specific to tenocyte expression. However, the concentrations of these collagen types may not appear in sufficient quantities to be detected by conventional spectrophotometry analyses such as that utilized in the present study. Hence, gene expression analysis, which is a more specific and sensitive tool of assessment, was advocated in the present study. It should be noted however that gene expression analysis has its inherent limitation considering the fact that measurements are made at transcription level rather than reflecting the true level of the extracellular matrix protein that is synthesized. The decision to use total collagen assay may have been the most appropriate option in this study, since this approach has also been used in other study to evaluate the tenogenic differentiation of the fibroblasts (Sahoo et al., 2010). In other studies, changes in total collagen also appears to be correlated to the changes in the conventional hydroxyproline

assay, which is an indicator of the amount of tendon specific collagen (Taskiran et al., 1999).

3.5 Summary

The use of GDF5 induces tenogenic differentiation in hMSC and rbMSC. It appears that GDF5 at a concentration of 100 ng/mL provides the most optimal cell phenotypic response, which includes an augmented level of total collagen as well as tenogenic markers gene and protein expression, similar to that of human (or rabbit) tenocyte cultures. All the factors investigated showed that rbMSC responded in a similar way as hMSC. Table 3.3 summarized the tenogenic response observed in hMSC and rbMSC in all the experiments described in this chapter.

Table 3.3 A summary of GDF5 induced tenogenic response in hMSC and rbMSC.

No	Experiments	Response Observed in hMSC	Response Observed in rbMSC
1	**Morphological appearance**	No apparent morphological changes observed.	No apparent morphological changes observed.
2	**Total soluble collagen assay**	i. 100 ng/mL of GDF5 induced significantly higher amount of total collagen expression. ii. No significant differences were observed between the 50, 100 and 500 ng/mL of GDF5 treatment.	i. 500 ng/mL of GDF5 induced significantly higher amount of total collagen expression. ii. No significant differences were observed between the 50 and 100 ng/mL, as well as between the 100 and 500 ng/mL.
3	**Candidate tenogenic marker genes expression at mRNA level**	i. 100 ng/mL of GDF5 induced significantly (p<0.01) higher amount of candidate tenogenic marker genes expression (i.e. *Col-I*, *Scx* and *Tnc*).	i. Both *Col-I* and *Scx* gene expression were significantly (p<0.05) up-regulated in rbMSC cultures treated with 50 and 100 ng/mL of GDF5.

Table 3.3, continued

		ii. The ratio of *Col-I* to *Col-III* expression was increased in hMSCs supplemented with 100 ng/mL of GDF5. iii. Both *Scx* and *Tnc* expression were expressed in hMSCs treated with 100 ng/mL of GDF5 at day 4. iv. *Scx* was persistently expressed in hMSCs treated with GDF5 from day 4 to day 7. v. Both non-tenogenic markers (i.e. *Runx2* and *Sox9*) were significantly down-regulated (p<0.01) in hMSC treated with 100 ng/mL of GDF5.	ii. *Col-I* gene expression was significantly (p<0.05) and persistently up-regulated from day 4 to day 27. iii. *Scx* gene expression was significantly up-regulated from day 4 to 10, but reduced at day 27.
4	**Candidate tenogenic marker expression at protein level**	Candiadate tenogenic marker proteins (COL-I, TNMD, SCX and TNC) were expressed in hMSCs treated with 100 ng/mL of GDF5.	Candiadate tenogenic marker proteins (COL-I, TNMD, SCX and TNC) were expressed in rbMSCs treated with 100 ng/mL of GDF5.

CHAPTER 4

RESULTS 2: GDF5-INDUCED MESENCHYMAL STEM CELLS FOR TENDON REPAIR – USING *IN VIVO* EVALUATION IN A RABBIT INFRASPINATUS TENDON MODEL

Part of this chapter has been submitted to:

Tan S.L., Ahmad T.S., Chan C.K., Selvaratnam L., Kamarul T. (2013) Growth differentiation factor 5 (GDF5)-induced marrow stromal stem cells support superior tendon healing *in vivo*: A preliminary report. *PLOS ONE* Submitted.

4.0 Results 2: GDF5-induced mesenchymal stem cells for tendon repair – using *in vivo* evaluation in a rabbit infraspinatus tendon model

4.1 Introduction

Collectively, the previous chapter highlighted a tenogenic inductive capacity of GDF5 in hMSCs and rbMSCs that may be exploited therapeutically for tendon repair. The GDF5 induced hMSCs and rbMSCs showed expression of tenogenic marker genes and proteins *in vitro*. To date, the use of GDF5 induced MSCs in an *in vivo* model has not been explored. Questions remain whether this tenogenic MSC (TMSC) would enhance tendon repair similar to that observed in other cell-based therapies which used tenocyte (Chen et al., 2011; Chen et al., 2007), undifferentiated MSC (Awad et al., 1999; Juncosa-Melvin et al., 2006; Pacini et al., 2007) and tendon stem/progenitor (TSPC) cells (Shen et al., 2012). In instances that autologous tenocytes were used, improved COL-I expression (Chen, et al., 2007) and tendon remodelling (Chen, et al., 2011) have been observed in the healing tendons. In other cases where allogeneic MSCs loaded scaffolds were used, restoration in structure and function of rabbit tendons was found (Awad, et al., 1999; Ouyang et al., 2003). Besides, clinical use of undifferentiated MSCs in superficial digital flexor tendon repair in racehorses has been reported with no ectopic bone deposition. Furthermore, the ultrasound scanning showed that tendon fibers were correctly oriented (Pacini, et al., 2007). In addition, allogeneic TSPC-seeded knitted-collagen sponge scaffold has also been shown to enhance the efficacy of rotator cuff tendon regeneration by differentiating into tenocytes and by secreting anti-inflammatory cytokines that prevent immunological rejection (Shen, et al., 2012).

In this chapter, *in vivo* assessment of tendon repair potential of GDF5-induced MSC (TMSC) was described. To achieve this, the rabbit infraspinatus tendon was selected as a model to study tendon repair. This model was selected as a primary model due to its anatomic position where the acromion is pointed posteriorly and inferiorly

toward the infraspinatus tendon. This allows surgery on the infraspinatus tendon to be accessible and reproducible, and therefore an easy model to study the *in vivo* effect of GDF5 induced rbMSCs in tendon repair. As there is no animal model with exactly the same characteristics as those of humans, and no one animal species that we are aware represents the 'gold standard' for tendinopathy (Warden, 2007).

Although anatomically different compared to human, the rabbit models have provided valuable information regarding the etiology, pathogenesis, as well as effective surgical repair techniques (Gupta & Lee, 2007). Furthermore, rabbit infraspinatus tendons have been used to investigate the feasibility of using an acellular matrix for the regeneration of rotator cuff tendon defects (Funakoshi et al., 2006). Besides, the rabbit model is larger in size. This makes rabbit tendons more amenable to surgery and the harvesting of adequate amounts of tissue for the evaluation of useful outcome measures. Apart from that, rabbit has cellular and tissue physiology approximates that of human (Fox, 1984) and they are mild-tempered and relatively easy to handle.

This current experiment was conducted to compare the efficacy of GDF5-induced rbMSCs (day 4 with 100 ng/ml of GDF5-induced rbMSCs (P3) or tenogenic rbMSC; TMSCs) in rabbit infraspinatus tendon repair. To further strengthen the present study design, a side-by-side comparison to its counterparts, the undifferentiated MSCs and tenocytes, was conducted, apart from the control (with no repair).

4.2 Experimental Design

Rabbits (N=18) used for *in vivo* transplantation study were surgically created through a window defect, bilaterally on the infraspinatus tendon. Three weeks after defect creation, the rabbits were randomly assigned into 6 groups, and the infraspinatus tendon defects were repair with methods as listed in Table 4.1. At 6 weeks following

treatment, all the rabbits were euthanized and the infraspinatus tendons were collected for analysis. Figure 4.1 showed the overview of *in vivo* transplantation work flow.

Table 4.1 Different methods were used to repair the tendon defect at three-weeks- post defect creation.
All the right shoulders were repaired with different methods: suture only, fibrin glue (FG) only, suture with FG only, and suture with FG and 1- 2 x 10^6 cells (either tenocytes (P3), MSC (P3) or tenogenic MSC (TMSC, P3)).

Group	Type of repair	Repair Method	N
1	Non-cell-based	Suture (S) only	3
2	Non-cell-based	Fibrin glue (FG) only	3
3	Non-cell-based	S + FG only	3
4	Cell-based	S + FG + Native tenocytes (from tendon)	3
5	Cell-based	S + FG + MSCs	3
6	Cell-based	S + FG + Tenogenic MSCs (TMSC)	3

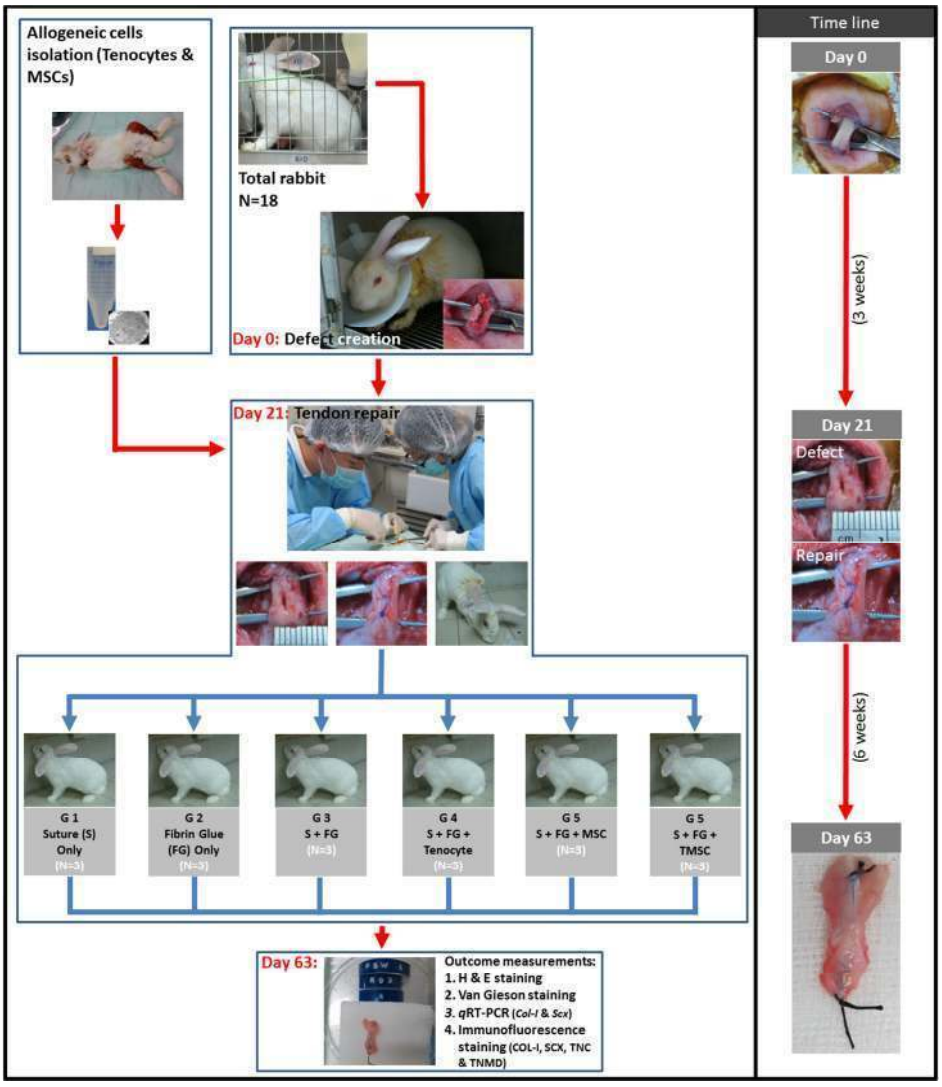

Figure 4.1 The flow chart for overall *in vivo* transplantation experimental design.

4.3 Results

4.3.1 Mobilization Observation and Gross Observation

All animals showed restricted movement during the three weeks post-defect creation. The peritendinous fibrous reaction was noticeable in all animals at three weeks after the defect creation. At time of harvest, all the animals showed equal bilateral range of motion of the shoulders. There was no detectable difference in the activity level of animals in each group. Macroscopically, there was no gross evidence of infection at the surgical site in any of the specimens (Figure 4.2). From the control (tendon defect with no repair) group to the repaired groups, the tendon defect area was filled with a pale fibrous scar (in the control and non-cell-based treatment groups) that became firmer and more organized in the cell-based treatment groups (Figure 4.2 A). Progressive tendon healing was more prominent in those treated with TMSC, where prominent tendon callus formation was observed (Figure 4.2 B). Early tendon callus formation suggested that the use of TMSC could enhance tendon neoformation.

4.3.2 Microscopic Observation

4.3.2.1 Progressive Tendon Healing as Observed by Haematoxylin and Eosin (H&E) Staining

Histological appearance in haematoxylin and eosin (H&E) stained sections of the control tendon showed increased cellularity, randomly aligned tendon cells of more plump and rounded morphology which is in contrast to the normal tendon which showed spindle-shaped tenocytes with elongated nucleus arranged in parallel alignment (Figure 4.3 A and B).

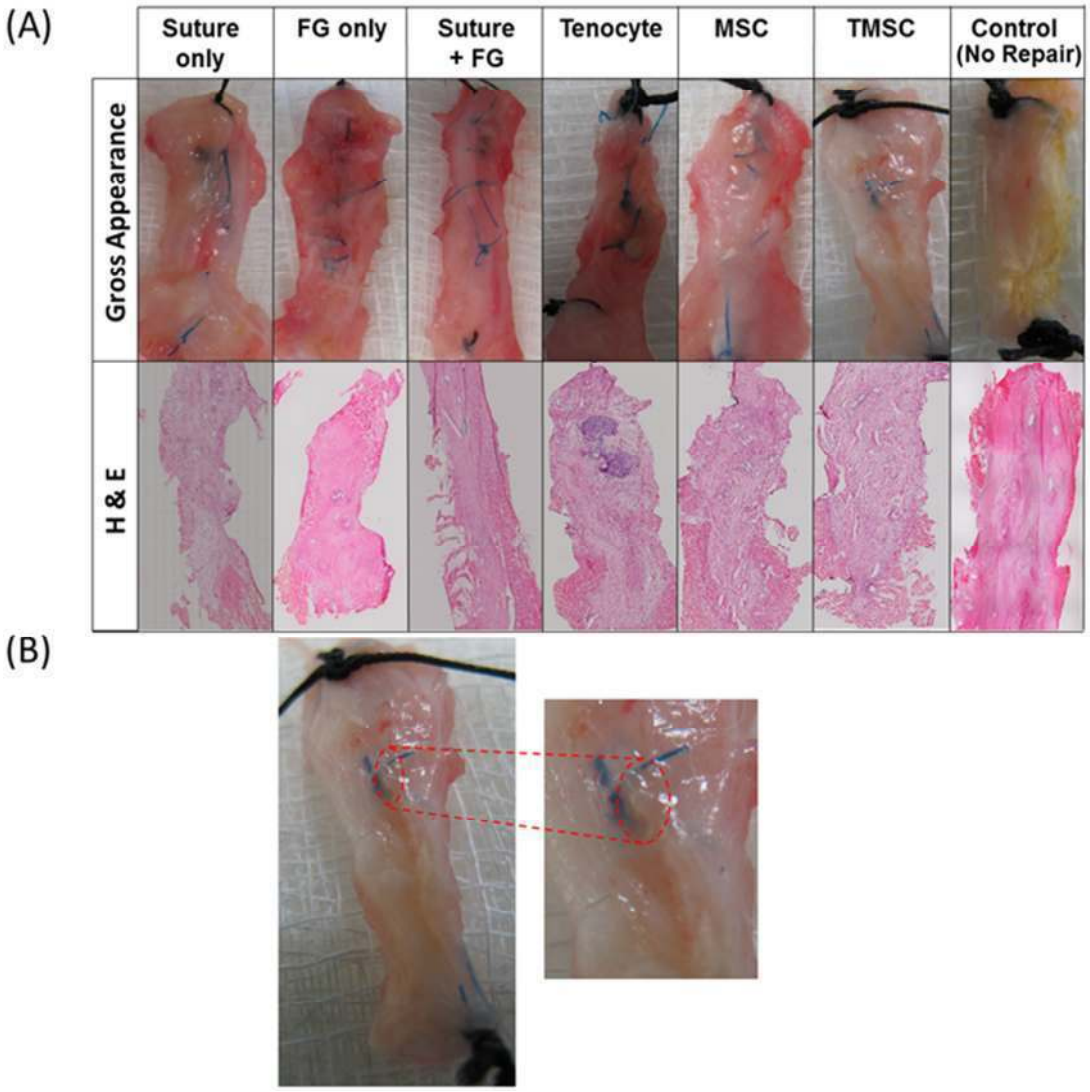

Figure 4.2 **Overview of progressive healing in tendon defects in all groups.**

(A) Macroscopic examination (Upper panel) and histological overview (Lower panel) of hematoxylin and eosin (H&E) stained tissue sections of healing tendon of all the treated and control groups. The grouping of the particular tendon specimens was denoted on top of each column of the images. FG: fibrin glue; MSC: mesenchymal stem cells, TMSC: tenogenic MSCs.

(B) Tendon callus formation was observed in the TMSC treated group. This tendon callus formation indicated early neotendon formation in TMSC group and this was not observed in any of the other groups.

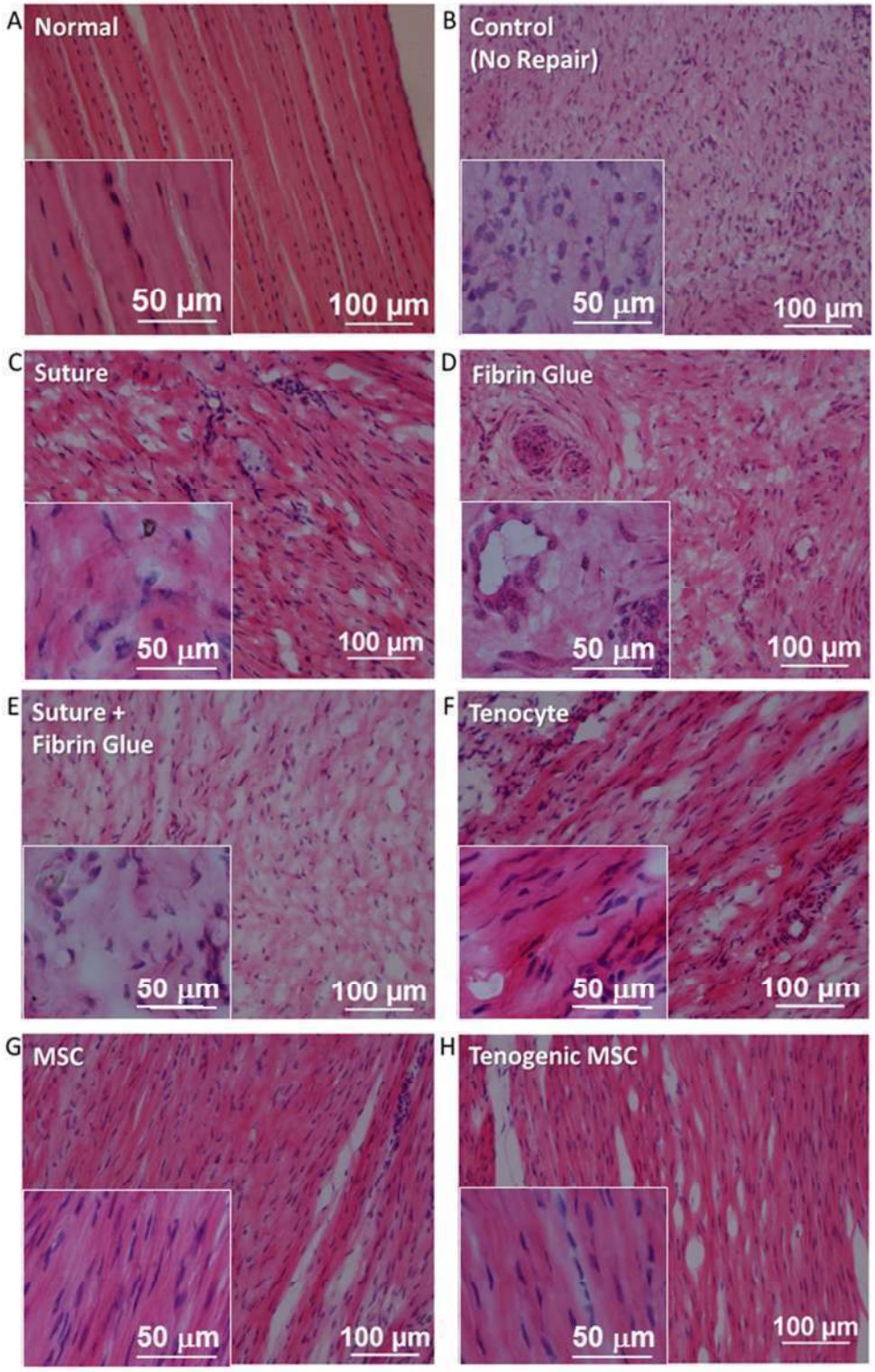

Figure 4.3 Microscopic evaluation of progressive healing in tendon defects in control (no repair) and treated groups compared to the normal tendon at six weeks following treatment.

The images showed are the longitudinal sections of tendons with hematoxylin and eosin (H&E) stain: normal tendon (A), control (no repair) (B), non-cell-based treatment groups which include suture (C), fibrin glue (FG) (D), Suture with FG (E) and cell-based treatment groups: tenocytes (F), MSC (G), and tenogenic MSC (TMSC) (H); observed at 20x objective lens (Scale bar = 100 µm).

Figure 4.3, continued

> Inset photographs showed observation at 40x objectives to depict the cell nucleus morphology and the alignment of cells with the collagen fibers (Bar = 50 μm).
> Contrasting histological appearance was observed in the normal (A) and control tendon (B), where the tendon fibroblasts became more plump, increased in number and randomly aligned in the control group as compared to the spindle-shaped tenocytes with elongated nucleus arrange in parallel alignment in normal tendon. The treated groups showed progressive healing in the defect area where the tendon collagen fibers were more orientated as observed in the non-cell-based treatment groups compared to the control and in the cell-based treatment groups compared to non-cell-based treatment groups.

Based on the histological analysis, tendon defects treated with different methods showed different stages of healing (early, moderate and mature healing) at six weeks post-surgical treatment. In normal tendon (Figure 4.3 A), spindle-shaped tenocytes with elongated nucleus (in blue colour) were resided parallel to the collagen fibers (in red colour), which were arranged in parallel alignment to the tendon's longitudinal axis. In contrast to the normal tendon histology, the control tendons (Figure 4.3 B) showed high cellularity and collagen fibers in random orientations. In addition, cells in the control tendon were more plump and rounded in shape compared to that of normal tendon. In the non-cell-based treatment groups (tendons repaired without cells; i.e. suture only, fibrin glue (FG) only, and suture with FG), their histology displayed highly disorganized collagen fibers, plump cells with rounded nuclei, and the blood vessels was evident, which indicated that the tendon were at the moderate healing stage compared to the early healing stage in the control group (Figure 4.3 C, D and E). Whereas in the cell-based treatment groups (i.e. tenocytes, MSC and TMSC), their histology showed progressive maturing of tendon healing from tenocytes to MSC to TMSC (tenocytes < MSC < TMSC). In these groups, the tendon defect area were resided with lesser and lesser cellularity, reduced in the occurrence of plump cells with rounded nuclei and an apparent decrease in disorganized collagen fibers as well as randomly aligned cells.

Within the cell-based treatment groups, TMSC group showed more mature tendon healing compared to that of tenocytes and MSC groups as evident by cells with more elongated nuclei aligned parallel to the collagen fibers which more resemble histological appearance of the normal tendon tissue (Figure 4.3 F, G and H). Besides, the collagen fibers in the TMSC group were in highly organized orientation which showed that the tendons were at the late stage of healing (Figure 4.3 H).

4.3.2.2 Progressive Tendon Healing as Observed by Van Gieson Staining

In the Van Gieson (VG) stained sections, collagen fibers was stained in bright red, while the cytoplasm, muscle and fibrin were stained in yellow, and the cell nucleus stained in blue (or grey). The mature collagen fibers in normal tendon was revealed in a deep red colour (Figure 4.4 A) and a reduced red intensity (pinkish colour) was detected for immature collagen fibers in all the other groups (none-cell-based and cell-based treatment groups). Control tendon showed a scarce distribution of collagen in the tissue (Figure 4.4 B). Yellowish muscle and fibrin was observed only in non-cell-based treatment groups. Besides, VG staining also revealed an abundance of blood vessels in the control and non-cell-based treatment groups.

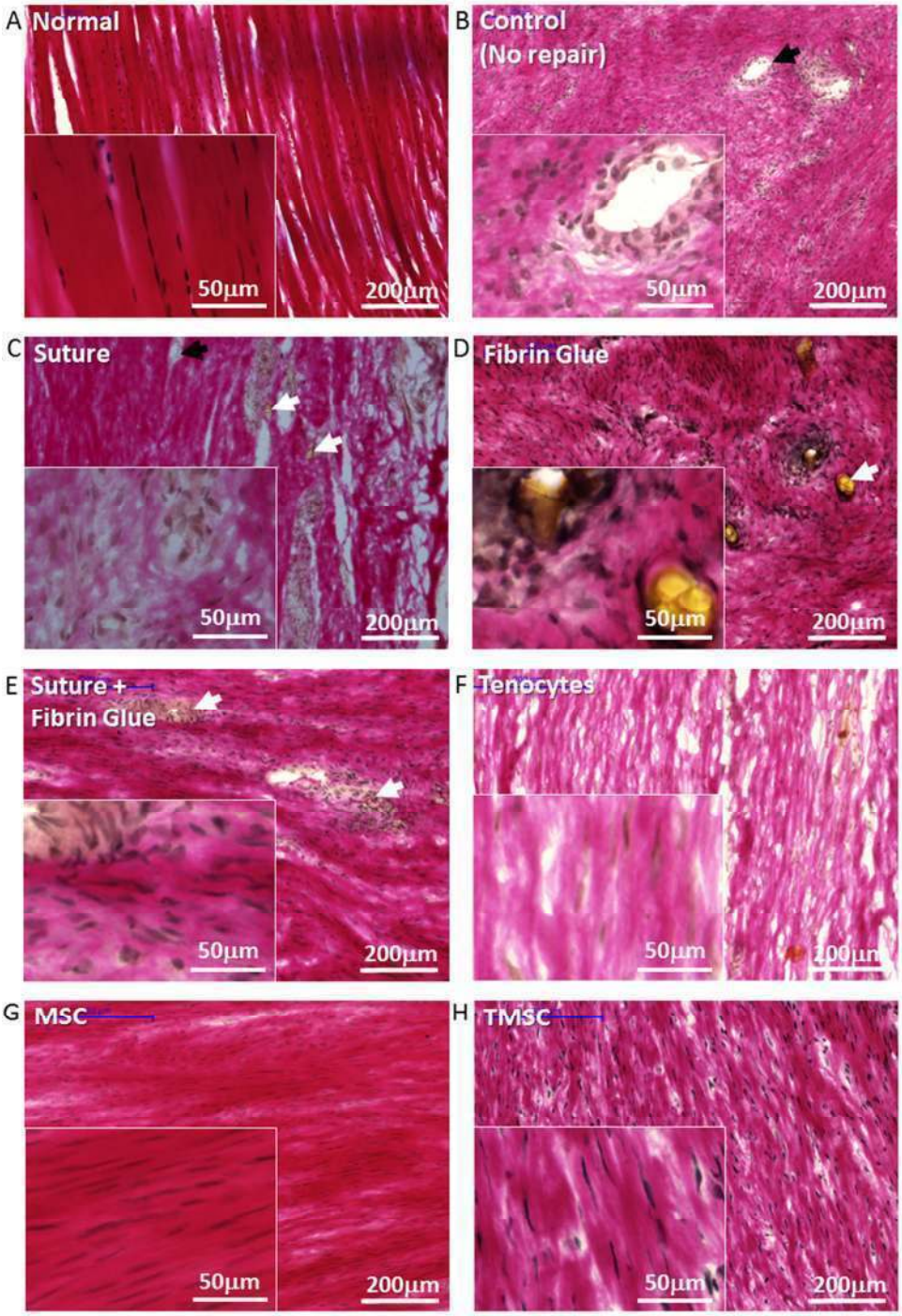

Figure 4.4 Microscopic evaluation of progressive healing in tendon defects in control (no repair) and treated groups compared to the normal tendon at six weeks following treatment.

The images showed are the longitudinal sections of tendons with Van Gieson (VG) stain: normal tendon (A), control (no repair) (B), non-cell-based treatment groups: suture (C), fibrin glue (FG) (D), Suture with FG (E) and cell-based treatment groups: tenocytes (F) , MSC (G), and tenogenic MSC (TMSC) (H); observed at 20x objective lens (Scale bar = 100 µm). Inset photographs showed observation at 40x objectives to depict the cell nucleus morphology and the alignment of cells with the collagen fibers (Bar = 50 µm). Yellowish muscle or fibrin structure (white arrows) and evident of vasculature (black arrows) were observed in the control and non-cell-based treatment groups.

4.3.2.3 Quality of Tendon Healing by Histological Scoring

The Watkins (1985) and Soslowsky (1996) scoring system were used for histological evaluation of tendon repair. Statistical analysis showed that Watkins score was significantly inversely correlated to Soslowsky score (p=0.000; r=-0.931). They were inversely correlated because in Watkins score, the higher the score, the more mature healing was observed and, for the Soslowsky score, the lower the score, the more mature healing was observed (Figure 4.5). Kruskal-Wallis test showed that there were significant differences between the treatment groups when evaluated using both Watkins score (p=0.008) and Soslowsky score (p=0.008). Pairwise Mann-Whitney U tests between all the treatment groups and control group showed that there were significant differences between the non-cell-based treatment groups (suture, FG, and suture with FG) and the cell-based treatment groups (tenocytes, MSC and TMSC), in both Watkins and Soslowsky scores (Table 4.2); except for (i) MSC vs. TMSC in Watkins score, and (ii) between the tenocytes, MSCs and TMSC in Soslowsky score.

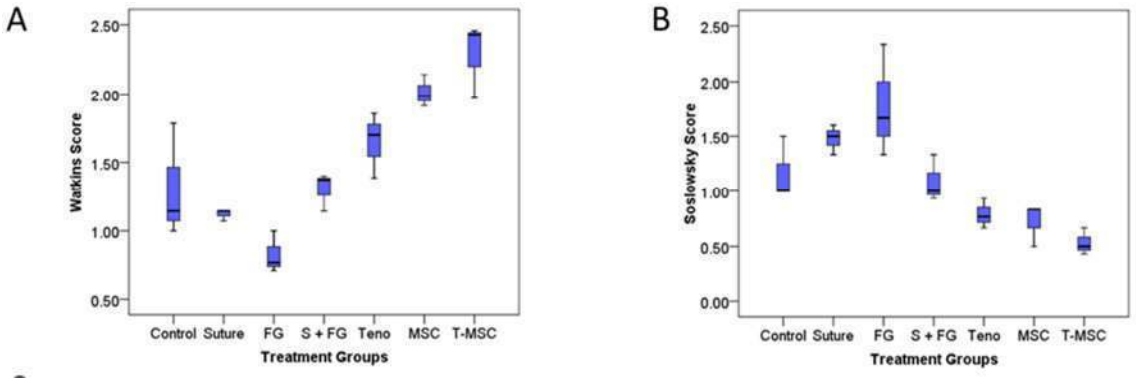

Figure 4.5 Box-plots of histological scoring for the quality of healing in tendon defects in control and treated groups.
The results showed the distribution of histological scores based on Watkins score (A) and Soslowsky score (B), for the control (no repair) and treated groups (FG:fibrin glue; S+FG: suture with FG; Teno: tenocytes). The histological scores obtained for both scoring methods were directly proportional to the methods of repair, and the quality of repair was increased in the cell-based groups (tenocytes, MSCs and TMSC) compared to the non-cell-based groups (suture, FG and suture with FG).

Table 4.2 A summary of Mann-Whitney U tests for pairwise comparisons between all the groups.
The italic font (top right of the table) indicate the *p*-value for Watkins score and the bold font (bottom left of the table) indicate the *p*-value for both scoring showed significant differences in cell-based treatment groups compared to the non-cell-based treatment groups (* $p<0.05$).

	Control	Suture (S) only	Fibrin Glue (FG) only	S + FG	S + FG + Tenocyte	S + FG + MSC	S + FG + TMSC
Control		*0.817*	*0.077*	*0.658*	*0.275*	*0.049**	*0.049**
Suture (S) only	**0.178**		*0.046**	*0.105*	*0.046**	*0.046**	*0.046**
Fibrin Glue (FG) only	**0.121**	**0.376**		*0.049**	*0.049**	*0.049**	*0.049**
S + FG	**0.487**	**0.077**	**0.077**		*0.127*	*0.049**	*0.049**
S + FG + Tenocyte	**0.046***	**0.049***	**0.049***	**0.077**		*0.049**	*0.049**
S + FG + MSC	**0.043***	**0.046***	**0.046***	**0.046***	**0.825**		*0.275*
S + FG + TMSC	**0.046***	**0.049***	**0.049***	**0.049***	**0.077**	**0.178**	

4.3.3 Expression of Candidate Tenogenic Markers at mRNA Levels Among the Cell-based Treated Groups

Relative gene expression analysis was conducted to compare the mRNA levels of two candidate tenogenic marker genes (*Col-I* and *Scx*) among the cell-based treated groups. There were significant differences in the relative gene expression levels for *Col-I* and *Scx* of tendon repaired with tenocytes, MSC and TMSC at six weeks post-surgical repair (Figure 4.6). In the TMSC group, the candidate tenogenic marker *Scx* (3.2±0.28) and *Col-I* (0.45±0.02) was significantly upregulated compared to the tenocytes and MSC groups.

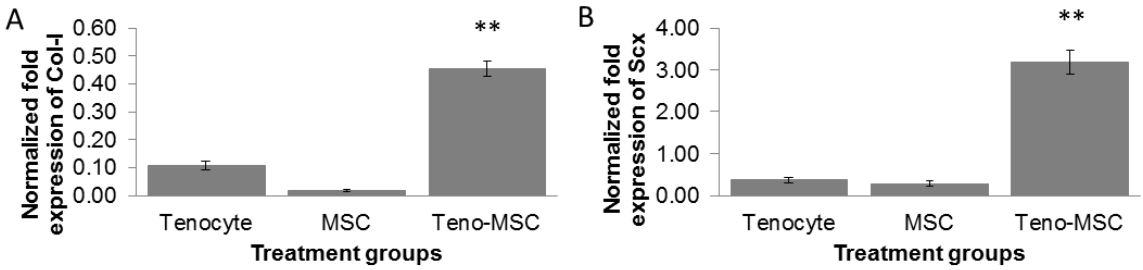

Figure 4.6 Relative gene expression analysis of type I collagen (*Col-I*) and scleraxis (*Scx*) in cell-based treatment groups (Tenocytes, MSC and TMSC) compared to the control group by qPCR analysis and normalized to GAPDH (reference gene).
Both *Col-I* (A) and *Scx* (B) showed significant increase in TMSC group compared to tenocytes and MSC groups. (Data were presented in mean±SEM.)

4.3.4 Expression of Candidate Tenogenic Markers at Protein Level Among the Cell-based Treated Groups

The immunostaining of candidate tenogenic markers (COL-I, SCX, TNC and TNMD) revealed the tissue distribution of each protein on the tendons of normal and experimental groups (Figure 4.7 and Figure 4.8). The COL-I expression showed apparent differences in the collagen-fiber-bundles appearance between the normal, control and the treated groups. In normal tendons the tendon collagen-fiber-bundles were aligned in parallel directions, contrasting to that of control tendons, where the collagens fibers were highly disorganized and no collagen-fiber-bundles could be observed. Collagen-fiber-bundles progressively aligned into parallel direction were observed in all the treatment groups. The SCX expression was higher in the treatment groups compared to the control. Some localized expression revealed as red spots in the images indicated the intracellular expressions in the tendon cells which resided along the tendon collagen fibers, and this was noticeable in the tenocytes and TMSC groups. The TNC expression on the normal tendon showed a wavy pattern of the tendon collagen fibers. These wavy patterns were also observed in the TMSC group, and in a lesser extend in the tenocytes and MSC groups. TNC expression in the control group did not show any wavy pattern.

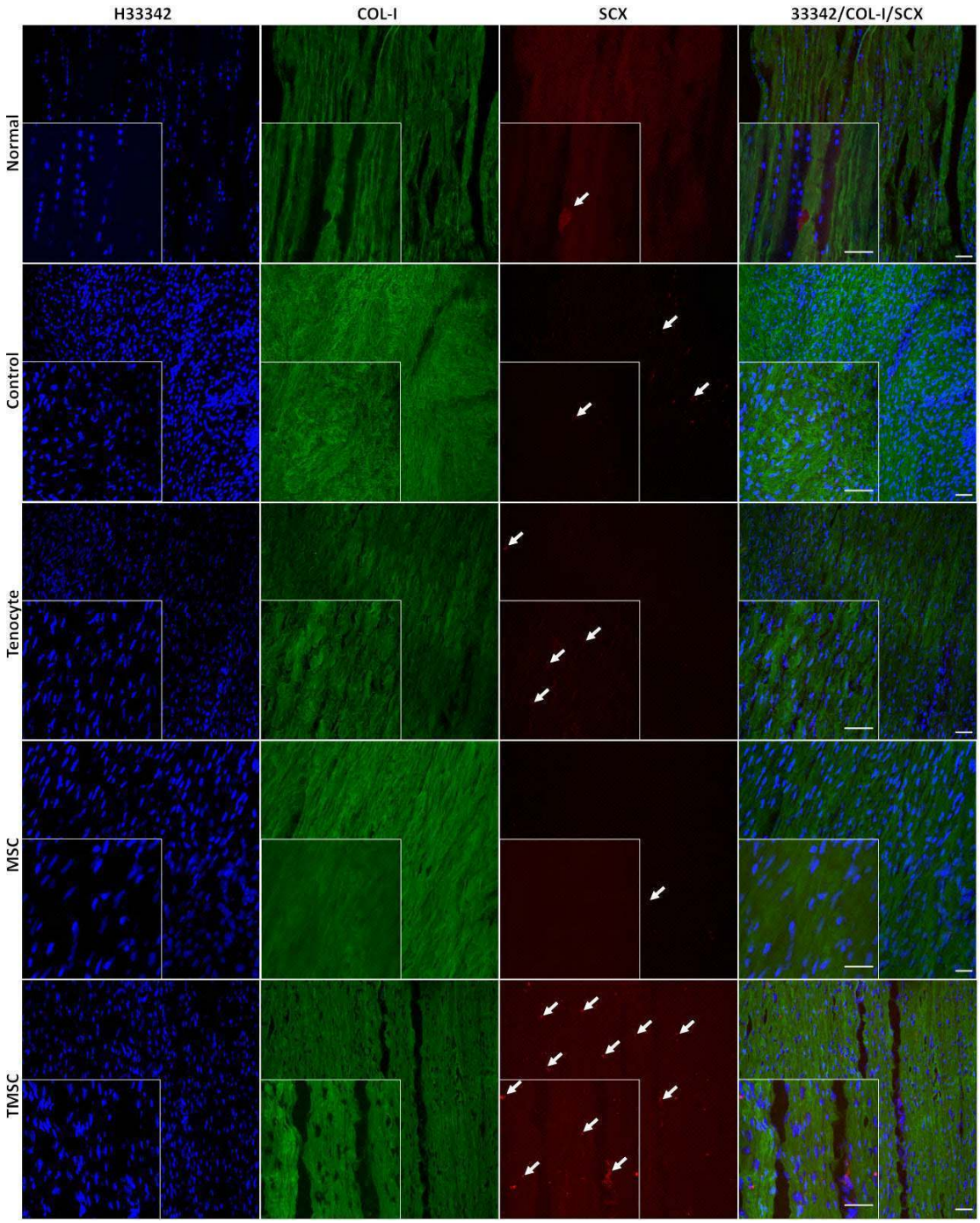

Figure 4.7 **Type-I collagen (COL-I) and scleraxis (SCX) expression on normal, control and cell-based-treated groups (normal, control, tenocytes, MSC and TMSC; indicated on the left panel) captured by laser confocal microscope.**
The expression of COL-I (depicted in green) was shown by FITC (BD Biosciences, US) reaction and SCX (depicted in red) was shown by Texas red (Santa Cruz Biotechnology, California). All the tissue sections were counterstained with Hoescht 33342 (H33342) to detect the cell nuclei (depicted in blue). All the images were captured for each channel by sequential scanning; H33342 (first panel on the left), COL-I (second panel), SCX (third panel); and the merged image of all channels (last panel on the right). Scale bar=100μm in low magnification images (20x) and 50 μm in high magnification images (100x).
The tissue distribution of both COL-I and SCX on TMSC group was comparable to that of normal tendon.

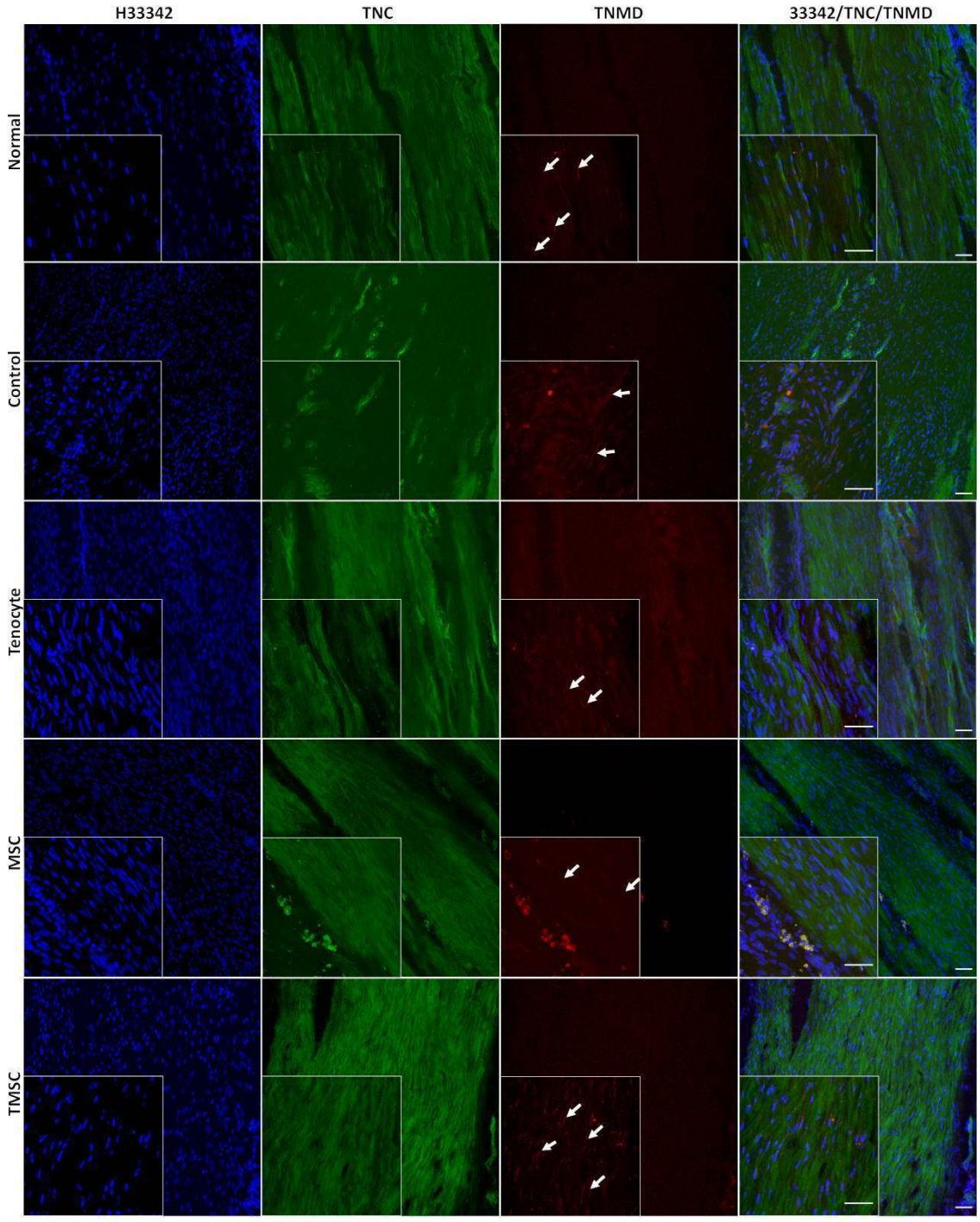

Figure 4.8 **Tenascin C (TNC) and tenomodulin (TNMD) expression on normal, control and cell-based-treated groups (normal, control, tenocytes, MSC and TMSC; indicated on the left panel) captured by laser confocal microscope.**
The expression of TNC (depicted in green) was shown by FITC (BD Biosciences, US) reaction and TNMD (depicted in red) was shown by Texas red (Santa Cruz Biotechnology, California). All the tissue sections were counterstained with Hoescht 33342 (H33342) to detect the cell nuclei (depicted in blue). All the images were captured for each channel by sequential scanning; H33342 (first panel on the left), TNC (second panel), TNMD (third panel); and the merged image of all channels (last panel on the right). Scale bar=100μm in low magnification images (20x) and 50 μm in high magnification images (100x).

Figure 4.8, continued

The localized TNMD expression (white arrows) as fine lines on the normal and TMSC specimens, but its expression on the tenocyte and MSC groups showed more coarsening lines. The control tissue showed randomly distributed TNMD expression compared to the normal and cell based treatment groups. The wavy pattern of tendon collagen fibers can be observed from the expression of both TNC and TNMD.

The TNMD expression was co-localized with the cells which resided along the tendon collagen fibers. As the mature tendon cells became elongated, and underwent changes in its cellular morphology, the intracellular TNMD was observed as thin lines aligned along the tendon fibers as depicted in the overlay images. The tissue distribution of TNMD on TMSC group was comparable to that of normal tendon, which showed the wavy pattern of the cells resided on the tendon fibers.

4.4 Discussion

The present *in vivo* study demonstrates that TMSC could augment tendon healing as compared to tenocytes and MSC. This deduction was based on the following findings: (1) early tendon callus formation in the TMSC group which was more prominent than all the other groups by macroscopic observation; (2) tendon healing in TMSC group showed cells that resembled tenocyte-like phenotype (i.e. cells with spindle-shaped and elongated nucleus) were aligned parallel to tendon's longitudinal axis; (3) collagen fibers in TMSC group were in organized orientations compared to the randomly aligned collagen fibers in the non-cell treated groups and control group; (4) VG stained section showed that tendon healing in TMSC group are at the late stage of collagen formation (mature collagen fibers formation); (5) both Watkins (1985) and Soslowsky (1996) scores demonstrated that tendons of TMSC group showed better quality of repair compared to the non-cell based treatment groups; (6) gene expression analysis showed that tendon of TMSC group expressed significantly higher *Col-I* and

Scx compared to tenocyte and MSC group; and (7) all candidate tenogenic marker proteins were expressed in the TMSC groups with the tissue distribution comparable to that observed in normal tendon.

Local tendon callus formation in the TMSC group suggested the occurrence of tendon neoformation in the site of repair. Previous study in tendon-bone junction repair in a rat model reported the observations of callus formation in the sutured tendon-bone junction at the site of repair at six weeks after surgery (Hibino et al., 2007). However, in this rabbit *in vivo* study, apparent tendon callus formation was observed in the TMSC group, but not in the suture group. This may due to the different repair model in this current study which is tendon-tendon repair but not tendon-bone junction repair. Tendon callus formation has been suggested related to the positive role play by the paratenon (Stein & Luekens, 1976) and intact periosteum (Hibino, et al., 2007) in case of tendon to bone healing. Other study in tendon-tendon healing in rat Achilles tendon has also observed with tendon callus formation after one week of repair with platelet concentrate injection (Aspenberg & Virchenko, 2004). In this current study, it is suggested that the positive factor inducing the tendon repair is the transplanted tenogenic MSC, since in the current tendon defect model did not involve paratenon or periosteum.

The results of microscopic observation showed progressive tendon healing in tendon defect sites of different repair methods. Different stages of healing as described by Soslowsky and colleagues (1996) were observed in the tendon specimens of different repair methods in this current experiment, albeit all the tendons were harvested at the same recovery time. Therefore, it is suggested that the different methods used has accelerate tendon healing at different degree. The results of this current study also showed GDF5 induced MSC (TMSC group) has better effect in accelerating the tendon healing compared to its counter parts tenocytes and undifferentiated MSC. This was

further evidenced in the tissue distribution of candidate tenogenic marker proteins, COL-I, SCX, TNC and TNMD, on the TMSC group, which were comparable to that observed in the normal tendon.

In this current experiment, the tenocytes group did not show improved tendon healing as observed in the TMSC group. This could be due to phenotypic drifting upon *in vitro* expansion (Bernard-Beaubois et al., 1997; Yao et al., 2006) of the limited number of cells obtained from the explanted tissue. In prolonged *in vitro* culture system, the isolated cells may become less proliferative and loss the expected functionality, ultimately, produced an inferior tendon repair when implanted to tendon defect area. A recent report demonstrated that GDF5 supplementation in *in vitro* tenocyte culture could augment the mRNA expression levels of extracellular matrix related genes or tenocyte phenotypic expression (Hogan et al., 2011); these GDF5 treated cells may produce enhance tendon healing when implanted *in vivo*. Nevertheless, this remains speculative and needs to be proven in a separate study.

4.4.1 Study Limitation

Several limitations were identified within the present study, these were unfortunately unavoidable. Firstly, only one time of recovery were studied in this experiment, which was 6 weeks. Previous studies in tendon repair have reported longer recovery time of 8 to 12 weeks (Soslowsky et al., 1996), or with more than one recovery time (Shen, et al., 2012). Although one recovery time at 6 weeks was used in this current experiment design, at this recovery time, different stages of repair discriminate by the different repair methods were observed. This suggested that this recovery time was appropriate to this current study. Further, a study in MSC-mediated tendon repair in rat reported at 4 weeks after surgery had also showed increased number of tenocytes and larger and more mature looking collagen fiber bundles (Awad, et al., 1999).

Secondly, use of fluorescence and bioluminescence imaging, i.e. green fluorescence protein (GFP) transfected MSCs for *in vivo* cell tracking or the use of a reporter gene system consisting of enhanced GFP (eGFP) for molecular imaging would be of advantage. The observed tendon repair in the TMSC group (i.e. tendon callus formation, collagen fibres in orientated organization and candidate tenogenic markers expression), which was not detected in all the other groups (treated and untreated control), preliminarily suggested that the observed tendon repair was due to the implantation of TMSC at the tendon defect area. However, it remains unresolved whether the implanted cells (i.e. TMSC) stimulate regeneration of damage tissue by secretion of cytokines and chemokines when engrafted into new microenvironment or by their stem-like ability to differentiate (Prockop, 2007). This could possibly be elucidated with the reporter gene system consisting eGFP to determine whether the candidate tenogenic markers expression detected at the tendon defect site is from the implanted allogeneic cells source, or from the native TSC at tendon injury site that differentiated into the tendon cells. Nevertheless, the GFP-labelled MSCs, especially those with lentiviral-based transduction (for producing a comparatively stable and longer-term GFP expression), has its own limitations; especially those using the HIV-based vectors (Van Damme et al., 2006) may induce unwanted immune response *in vivo* (Stripecke et al., 1999) as well as insertion mutagenesis (Gu et al., 2012).

Lastly, from a translational standpoint, bipeds such as non-human primates represent the most ideal species to use in tendon research as they are closest to human in terms of anatomy and physiology. However, their use is limited by ethical consideration and lack of availability which results in extraordinary high cost compared to other laboratory animals. Among the quadrupeds, rat has been suggested as an appropriate model for investigating rotator cuff disease compared to other animal model (e.g. rabbit, cow, dog etc.) due to its shoulder anatomy where the acromion is immediately adjacent

and positioned over the supraspinatus tendon as in humans (Soslowsky, et al., 1996). However the main disadvantage of rats is their relatively smaller in size compared to other model such as rabbits, which make rat tendons harvesting difficult especially for histological or mechanical outcome measures.

4.5 Summary

This *in vivo* experiment showed that TMSC or GDF5 induced rbMSC resulted in better improvement in infraspinatus tendon healing compared to that of tenocytes and undifferentiated MSC. Nevertheless, this *in vivo* model only provided an indication of its potential for tendon repair; future studies are required to evaluate the most effective postoperative weight-bearing regime for this reconstruction model and its effect on the mechanical strength of the regenerated tendon tissue. Although this study suggests that GDF5-induced MSC may be a clinically useful adjunct treatment for tendon repair, the intracellular signalling pathways activated upon GDF5 treatment in MSCs, which may be related to the observed improvement in tendon healing, remain largely unknown.

CHAPTER 5

RESULTS 3: MICROARRAY ANALYSIS OF TENOGENESIS IN HUMAN BONE MARROW-DERIVED MESENCHYMAL STEM CELLS: GDF5 MODULATE CYTOSKELETAL REMODELLING AND PROLIFERATION IN TENOGENIC hMSCs

Part of this chapter has been submitted to:

Tan S.L., Ahmad T.S., Selvaratnam L., Kamarul T. (2013) Identification of Pathways Mediating Growth Differentiation Factor 5-induced Tenogenic Differentiation in Human Bone Marrow Stromal Cells. *Stem Cells* Submitted.

5.0 Results 3: Microarray analysis of tenogenesis in human bone marrow-derived mesenchymal stem cells: GDF5 modulate cytoskeletal remodelling and proliferation in tenogenic hMSCs

5.1 Introduction

Colorimetric collagen assay, gene expression analysis and immunofluorescence staining (as described in Chapter 3), revealed that GDF5 treatment is able to induce tenogenesis in both hMSC and rbMSC. Additionally, augmented tendon healing in rabbit infraspinatus tendon defects by the GDF5-induced rbMSC was demonstrated in the *in vivo* experiments (as described in chapter 4). Having established that the GDF5 is an inductive factor for tenogenesis and that the GDF5-induced rbMSC has an impact on tendon repair, it remained to be answered the mechanisms behind the tenogensis induced by GDF5. It is reasoned in this current chapter that the signals underlying tenogenesis might be involved the transformation of the multipotent hMSCs into the tenocytic-behaviour-cells. The cellular cytoskeletal remodelling plays an essential role in tenocytes behaviour especially in response to its high tensional loading *in vivo* environment. However, whether the cytoskeletal remodelling or other signalling pathway is associated with hMSC *in vitro* tenogenesis remains to be elucidated. To explore this questions, the global gene expression profiles analysis on hMSC cultured with and without GDF5 (100 ng/ml) was conducted. Similar to the earlier study design in the earlier *in vitro* study (Chapter 3), the primary native human tenocyte culture was used as a positive control for comparison with the tenogenic hMSCs. The control hMSC and tenocytes included in the study served as undifferentiated and differentiated controls, respectively, in order to increase the specificity of genes identified as regulated by the GDF5 treatment and associated with functional tenogenesis. Gene expression profiles and signalling pathways analysis were conducted using advanced microarray analysis, including an evaluation of the pathways affected.

In the actin cytoskeleton remodelling signalling, it has been described that upon ligand binding, it induced actin polymerization at the plasma membrane, leading to the formation of lamellipodia and membrane ruffles (Nobes & Hall, 1995). The members of rho GTPases are responsible for regulating a signal transduction pathway linking extracellular growth factors to the assembly of focal adhesions and actin stress fibers (Nobes & Hall, 1995; Ridley & Hall, 1992). Furthermore, assembly and spatial organization of these highly dynamic structures of polymerized actin have been demonstrated to play a role in the differentiation of MSC (Rodriguez et al., 2004; Yourek et al., 2007). Based on the microarray analysis, the rho GTPase activating protein 29 (ARHGAP29) was one of the up-regulated and co-expressed genes in GDF5-induced hMSCs (both day 4 and day 10) and tenocytes; it was speculated that the cytoskeletal reorganization to be an important event in tenogenesis. In this current experiment, the actin cytoskeleton remodelling which involved in the control of cell shape and morphology was visualized with atomic force microscopy (AFM) live cell imaging and confocal laser scanning microscopy (CLSM) imaging. Various methods have been used to visualize the actin cytoskeleton (Small et al., 1999). The AFM imaging is a relatively novel and powerful tool that can be used for topographic imaging under physiological conditions (Radmacher et al., 1992), it is particularly suitable for viewing cytoskeletal remodelling in living cells with minimal sample preparation (no labelling, fixing or coating). The subsequent immunofluorescence imaging with CLSM allowed the confirmation of the cytoskeleton remodelling observed with the AFM analysis was the actin filaments reorganization in the differentiating hMSCs.

In addition, immunofluorescence staining of nucleostemin (NST) was conducted to determine the regulation of cell proliferation in GDF5-induced hMSCs. NST is a regulator protein of cell proliferation (Romanova et al., 2009) predominantly associated with rat neural and embryonic stem cells, and some cancer cells. Despite NST being

reported as a marker of undifferentiated human adult bone marrow stem cells that involve in regulating the proliferation of these cells (Kafienah et al., 2006), recent work however, has demonstrate that NST is in fact expressed in many normal proliferating cells (Fan et al., 2006). Nevertheless, the expression of NST is generally down-regulated in the early stage of differentiation before exit from the cell cycle (Romanova, et al., 2009). The expression of NST in differentiated bone marrow cells has also been reported as 70-90% lower than the undifferentiated cells (Kafienah, et al., 2006). Herein, the NST expression in GDF5-induced hMSC was evaluated to examine the effect of tenogenesis in hMSCs proliferation at day 4 and day 10 of induction by GDF5.

It was demonstrated here, through the global gene expression profiles analysis of tenogenic hMSC that cytoskeletal remodelling and cell adhesion signalling are essential for hMSCs tenogenic differentiation, particularly in the expression of the earliest tenogenic markers in hMSC. In the event of tenogenesis, the proliferation of hMSCs was reduced as evidenced with the reduced in nuscleostemin expression in hMSCs underwent tenogenesis. Additionally, it is proposed that EMT pathway is the putative pathway which involved in tenogenesis.

5.2 Experimental Design

Genome wide gene expressions were performed on six independent experiments with Affymetrix GeneChip® human gene 1.0 ST arrays (HuGene, Affymetrix Inc, Santa Clara, CA, USA). The global gene expression profiles for four groups of samples: control (untreated) hMSCs, day-4 GDF5-induced hMSCs, and day-10 GDF5-induced hMSCs, and human primary tenocytes cultures from hamstring tendons were evaluated. For all the four groups of sample, samples from six individual donors were analysed (six individual donors for bone marrow samples to isolate hMSCs and six individual donors for human hamstring tendon samples to isolate primary native human tenocyte). The samples collected for microarray analysis were prepared as depicted in the workflow in Figure 5.1. Microarray data (CEL intensity files) were then analysed with Limma software package for R for differentially expressed genes, and GeneGo Metacore™ Pathway Analysis Software (Thomson Reuters) for pathway analysis. The microarray data were then validated by AFM and CLSM imaging as well as QuantiGene® Plex 2.0 Assay.

5.3 Results

5.3.1 Global Gene Expression Profiles Analysis

5.3.1.1 Quality Assessment and Normalization of Microarray Data

Microarray data pre-processing analysis (Figure 5.2) showed that the target prepared hybridized efficiently and specifically onto all arrays. The signals detected for the 24 arrays were comparable to one another and no outlier was detected. The total number of features detected was 33, 297. The robust multi-array averages (RMA expression values) were used to normalize the values in each group (based on the signal intensity values). The intensities that were below background signal, absent DABG (detected above background) detection calls were omitted.

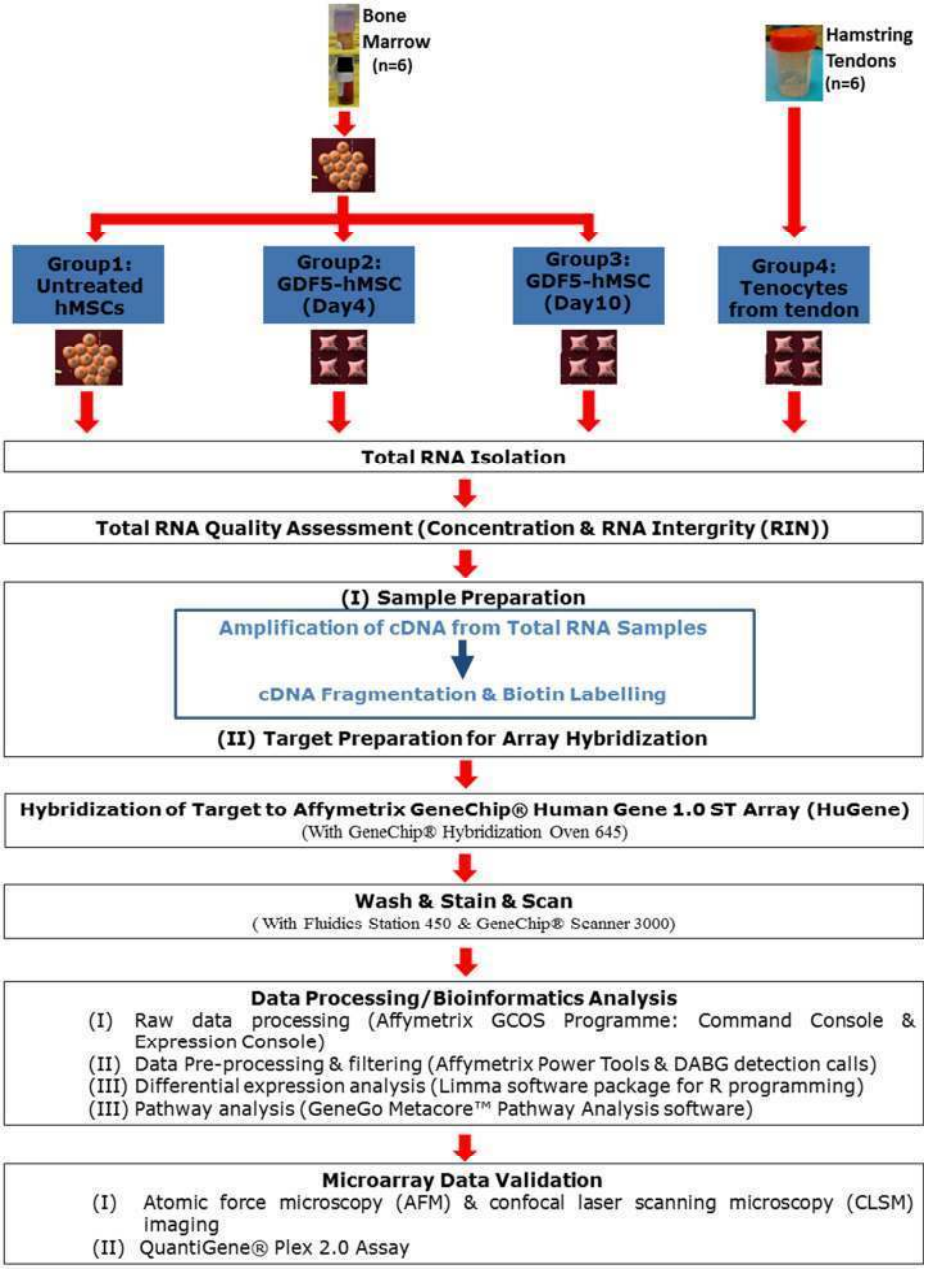

Figure 5.1 **Microarray workflow from sample preparation to data analysis and validation.**

Total RNA were extracted from all the samples and pre-determined for their concentration and integrity before proceed to cDNA amplification and labelling. All the labelled cDNA samples were used for targets preparation. The prepared targets were subsequently hybridized to the arrays, followed by washed, stained and scanned to get the image files. The captured microarray image files were analysed via GCOS (Command Console and Expression Console; Affymetrix Inc, Santa Clara, CA, USA) to get the CEL intensity files. The CEL intensity files were then summarized via data pre-processing to get the Robust Multi-array Average (RMA) signals (expression values). The significantly differentially expressed genes were detected via Limma analysis (Smyth, 2004). Pathway analysis was conducted with Partek ® Genomic Suite™ 6.6 beta and GeneGO Metacore™ Pathway Analysis software. The microarray data was validated with AFM and fluorescence imaging and QuantiGene gene expression analysis.

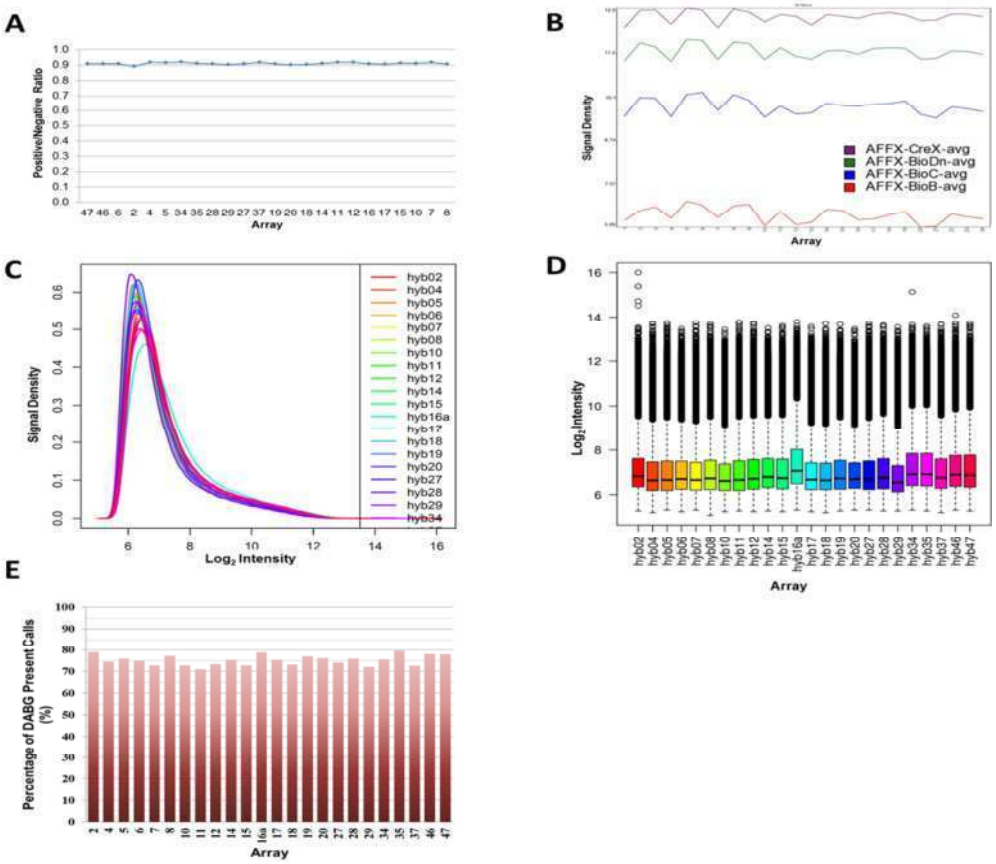

Figure 5.2 Pre-processing and quality control for microarray data.

A. Positive versus negative ratio of all arrays showed the efficiency and specificity of the hybridization in all arrays. Ideally, the value of positive versus negative control should be 1. The results showed that the efficiency and the specificity of the hybridization in all arrays were in the acceptable range (≥0.8).

B. Spike-in hybridization control plots showed similar intensity in all arrays. All arrays were able to detect the spike-in hybridization controls in accordance to their respective spike-in quantities (CreX, BioD, Bio C and Bio B), indicated that all arrays possessed comparable sensitivity in detecting the high and low abundant genes.

C. Histogram of perfect match for all arrays showed the overall higher or lower intensities in all the 24 arrays, with no saturation effects. These were the intensities of the probes, prior to normalization and not combined to the probe sets yet. The results showed a typical distribution of signal intensities; they were never normally distributed. As this is a whole genome array, a lot of cell-specific genes were not expressed, leading to a lot of probes that gave very low (or no) signal, so the distribution curves of the perfect match intensities were positively skewed.

D. Boxplots of $\log_2$ ratios for perfect match intensities of all arrays. Although some samples, e.g. "hyb02" and "hyb29" showed slightly thinker/longer tail than the other samples, all the arrays showed comparable distributions, and no sample was identified as outlier.

E. The bar chart of the percentages of detectable above background (DABG) scores for present calls in all the arrays. The percentages of DABG ranged within less than 10% difference showed that the hybridization in all arrays was of superior quality and DABG among all the arrays were comparable.

The heatmap of the RMA expression values showed the distance between all the arrays, and none of the arrays was detected as an outlier after normalization (Figure 5.3 A). The dendrogram plots based on the genes those that were significant in at least one comparison (i.e. a set of 954 probe sets) showed that the arrays were clustered into different clades in the distance tree according to their tissue origin, one clade for bone marrows derived hMSC (either with or without GDF5 treatment) and the other clade for tendon derived tenocytes (Figure 5.3 B and C). Furthermore, the principle component analysis of all 24 arrays demonstrated that the hMSCs of all donors showed the same shift in accordance with GDF5 treatment (Figure 5.4). This indicated that the discrimination of the arrays observed was not contributed by donor variations but the differences were due to the GDF5 supplementation and tissue origin of the cells (i.e. tenocytes and hMSC). Following normalization, filtering and omitting the control probes, a total of 27, 216 probe sets was retained (Table 5.1). These 27, 216 normalized intensity values of different groups were compared with the Limma package of Bioconductor (Smyth, 2004) to detect the differential gene expression with the corrected *p*-values for multiple testing using Benjamini-Hochberg method (Benjamini & Hochberg, 1995).

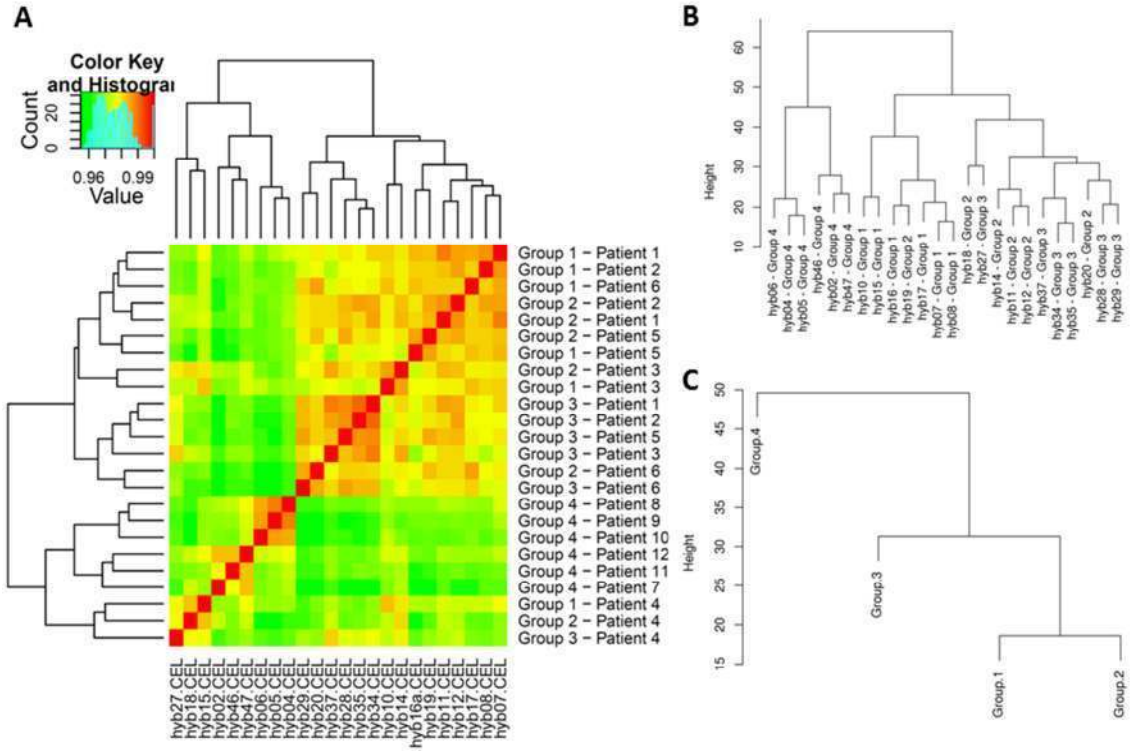

Figure 5.3 **Heatmap and dendrogram of RMA expression values.**

A. The heatmap of RMA values showed comparable level of expression of all the genes across all the 24 arrays. The tree diagram on the upper panel of the heatmap showed the distances between the samples. The colour of the heatmap indicated the between-array distances. A colour bar with scales for the heatmap is included, indicating that red corresponds to maximum distance and green to minimum distance.

B. The dendrogram plot indicates the Euclidean distance and complete linkage with all individual samples.

C. The dendrogram plot indicates the Euclidean distance and complete linkage with average of the four groups.
(Group 1: Control hMSC, Group 2: Day-4 GDF5-induced hMSC, Group 3: Day-10 GDF5-induced hMSC, Group 4: tenocytes)

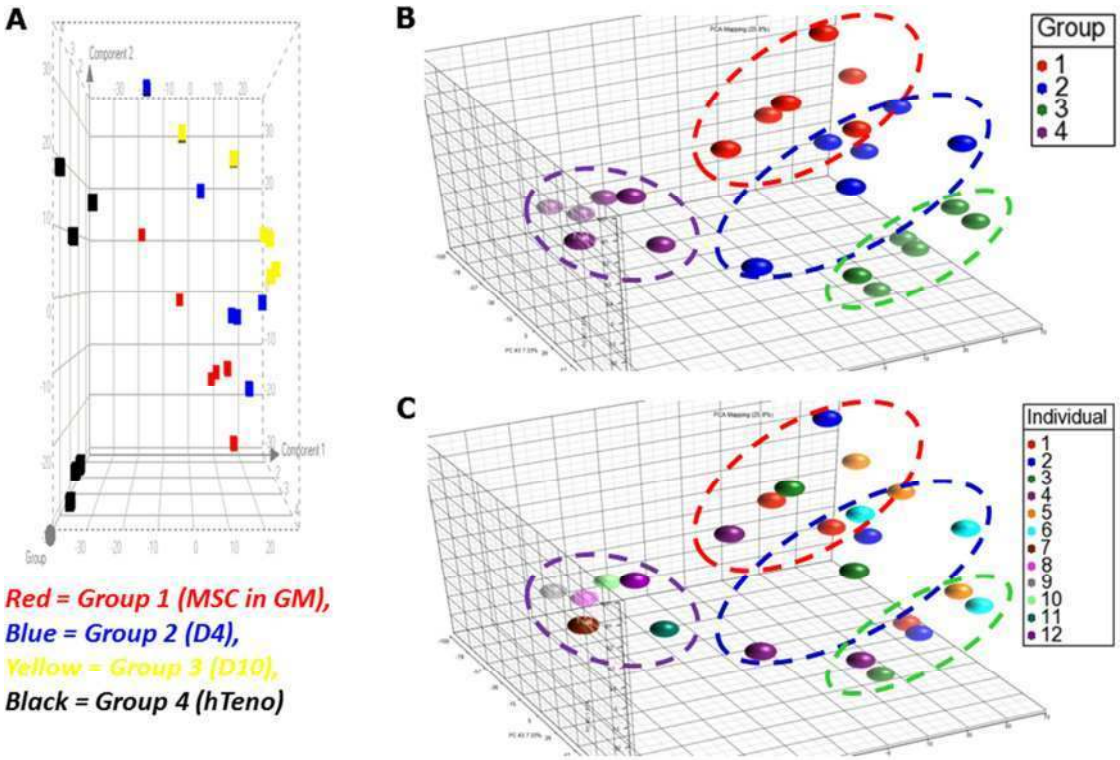

Figure 5.4 **Principle component analyses (PCA) of all 24 arrays.**
PCA analysis was performed on all samples and all probes to characterize the variability present in the data. The results showed a distinct separation between all the groups. The PCA was visualized in 2D view (A) and 3D view (B), with the different colour coded for different groups; and the 3D view (C) with the colour coded for different individual donor (In the legend, individual 1 to 6 were the bone marrow donors and individual 7 to 12 were the tendon donors). Image B and C showed that the arrays were grouped according to their experimental groups (treatment) but not according to the donor variation. (Group 1: Control hMSC, Group 2: Day-4 GDF5-induced hMSC, Group 3: Day-10 GDF5-induced hMSC, Group 4: tenocytes)

Table 5.1 Summary of total number of probe sets or genes before and after data normalization and filtering.

Probe Sets	**Total**
1. Estimated number of genes on array	28,869
2. Total distinct probe sets on the array	764,885
3. Positive control probe sets on the array	1,195
4. Negative control probe sets on the array	2,904
5. Total number of probe sets detected on chip	**33,297**
6. Total number of probe sets detected on chip but do not have a present DABG detection call	1,320
7. Total number of probe sets detected on chip after omitted control probe sets and probe sets without a present DABG detection call	27,878
8. Number of probe sets omitted after data filtering	662
9. Total number of probe sets used to assess differentially expressed genes	**27,216**

5.3.1.2 Tenogenic Gene Expression Profiles Regulated by GDF5 Treatment

The results of Limma package of Bioconductor analysis showed that the corrected *p*-value discovered slightly higher number of significant differentially expressed genes at $p<0.05$ than the uncorrected *p*-value at $p<0.001$ (Table 5.2; Appendix J), except for Group 1 vs 2. The corrected *p*-values provided a better control in the false discovery rate, thus the significant gene lists obtained based on the corrected *p*-value were used for the subsequent analysis (i.e. pathway analysis).

Table 5.2 A summary of the number of differentially expressed probe sets.

	Uncorrected *p*-value <0.001		**Corrected *p*-value<0.05**	
	Log-ratio < -1	Log-ratio > 1	Log-ratio < -1	Log-ratio > 1
Group 1 vs 4	168	159	204	182
Group 2 vs 4	211	185	268	212
Group 3 vs 4	324	264	400	291
Group 1 vs 3	139	98	152	119
Group 2 vs 3	50	8	50	8
Group 1 vs 2	19	22	12	19

(Group 1: Control hMSC, Group 2: Day-4 GDF5-induced hMSC, Group 3: Day-10 GDF5-induced hMSC, Group 4: tenocytes)

The significantly up- and down- regulated genes were presented in the Venn diagrams to show the overlap between all the comparisons with: (1) control hMSC (Group 1; Figure 5.5 A) and (2) tenocytes (Group 4; Figure 5.5 B). The Venn diagrams showed 9 genes (as compared to control hMSC; Figure 5.5 A) and 236 genes (as compared to tenocytes; Figure 5.5 B) associated with tenogenesis by GDF5 treatment; of these 3 were up-regulated and 6 were down-regulated when compared to control hMSC (Figure 5.5 A); and 130 were up-regulated and 106 were down-regulated when compared between tenocytes to hMSCs (Figure 5.5 B). In addition, numerous genes associated with tenogenesis which were modulated by GDF5 were identified in GDF5-induced hMSCs; both day 4 (21 up-regulated, 24 down-regulated) and day 10 (17 up-regulated, 9 down-regulated). The genes displayed the most significant changes

in expression patterns in the GDF5-induced hMSCs and in tenocytes were listed in Table 5.3 with their respective $\log_2$ ratio ($\log_2$ fold change).

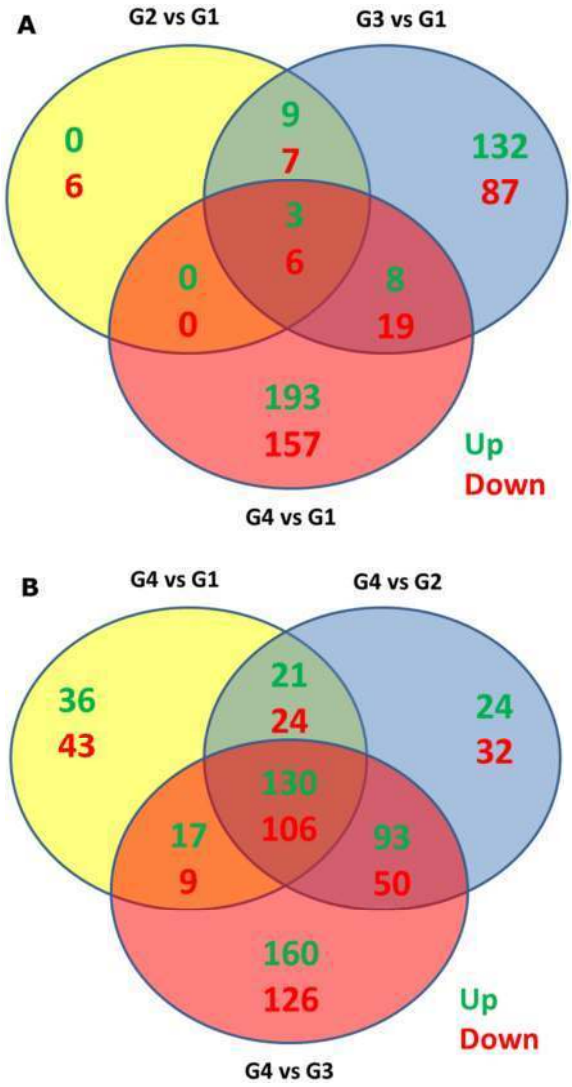

Figure 5.5 **An overview of significant overlap of differentially expressed genes observed between the GDF5-treated groups (Group 2 and 3) and the tenocytes group (group 4) in Venn diagrams.**
The microarray experiments were designed to detect differential expression of transcripts with GDF5 treatment and were compared with Venn diagrams. The list of the significantly (corrected *p*-value) up- and down- regulated genes, were used to detect the altered candidate tenogenesis genes within the GDF5-treated groups (Group 2 and 3) as depicted in the intersections or uniqueness; between all comparisons with control hMSC (as depicted in A) and tenocytes compared to all the other groups (as depicted in B).
The numbers in each section or intersections of the circles represented the total number of significantly differentially up- or down- regulated genes for the pairwise comparisons (as denoted above or below each circle). The numbers in green and red fonts indicated the significantly up- and down-regulated genes, respectively. (G1: Control hMSC; G2: Day-4 GDF5-induced hMSC; G3: Day-10 GDF5-induced hMSC; G4: tenocytes)

Table 5.3 The most significantly altered genes in the GDF5-induced hMSC and tenocytes (LR: $\log_2$ ratio, *p*-value: corrected *p*-value).

Gene Symbol	Description	Day 4 GDF-5 Induction (G2 v G1)		Day 10 GDF-5 Induction (G3 v G1)		Tenocytes (G4 v G1)		Day 10 vs Day 4 GDF-5 Induction (G3 v G2)		Tenocytes vs Day 4 GDF-5 Induction (G4 v G2)		Tenocytes vs Day 10 GDF-5 Induction (G4 v G3)	
		LR	*p*-value	LR	*p*-value	LR	*p*-value	LR	*p*-value	LR	*p*-value	LR	*p*-value
Most up-regulated in day 4 GDF-5 induced hMSC													
ASPN	asporin	**2.80**	**2.81E-03**	4.12	3.34E-06	5.05	3.68E-07	1.32	1.44E-01	2.25	4.27E-03	0.93	2.78E-01
CMKLR1	chemokine-like receptor 1	**1.99**	**1.08E-02**	2.49	1.12E-04	-0.39	6.87E-01	0.50	6.21E-01	-2.38	3.77E-04	-2.88	2.59E-05
FADS2	fatty acid desaturase 2	**1.71**	**2.38E-02**	1.75	2.40E-03	0.83	2.37E-01	0.05	9.79E-01	-0.88	1.91E-01	-0.93	1.36E-01
ACAT2	acetyl-CoA acetyltransferase 2	**1.37**	**2.41E-02**	1.16	1.16E-02	0.82	1.19E-01	-0.21	8.23E-01	-0.55	3.58E-01	-0.33	6.28E-01
CCL2	chemokine (C-C motif) ligand 2	**1.35**	**4.35E-03**	2.07	3.34E-06	1.82	3.89E-05	0.73	1.02E-01	0.48	2.94E-01	-0.25	6.52E-01
PIK3R3	phosphoinositide-3-kinase, regulatory subunit 3 gamma	**1.33**	**5.42E-03**	1.43	2.63E-04	0.74	7.20E-02	0.09	9.20E-01	-0.59	1.68E-01	-0.68	7.84E-02
SC4MOL	sterol-C4-methyl oxidase-like	**1.30**	**1.28E-02**	1.19	3.10E-03	0.36	5.41E-01	-0.11	9.13E-01	-0.94	3.01E-02	-0.83	4.46E-02
FDPS	farnesyl diphosphate synthase	**1.24**	**3.76E-02**	1.02	2.11E-02	0.06	9.54E-01	-0.22	8.08E-01	-1.17	1.42E-02	-0.96	3.66E-02
TIPARP	TCDD-inducible poly(ADP-ribose) polymerase	**1.11**	**3.40E-03**	1.09	4.00E-04	0.23	6.00E-01	-0.02	9.82E-01	-0.87	5.99E-03	-0.85	5.03E-03
SQLE	squalene epoxidase	**1.10**	**1.02E-02**	1.42	7.32E-05	0.55	1.49E-01	0.32	5.51E-01	-0.55	1.36E-01	-0.87	9.22E-03
Most up-regulated in day 10 GDF-5 induced hMSC													
ASPN	asporin	2.80	2.81E-03	**4.12**	**3.34E-06**	5.05	3.68E-07	1.32	1.44E-01	2.25	4.27E-03	0.93	2.78E-01
MX1	myxovirus (influenza virus) resistance 1	0.18	9.58E-01	**3.35**	**5.01E-04**	0.22	9.19E-01	3.17	3.50E-03	0.04	9.88E-01	-3.14	1.29E-03
HERC6	hect domain and RLD 6	0.15	9.49E-01	**3.02**	**3.10E-05**	0.09	9.55E-01	2.87	3.81E-04	-0.06	9.65E-01	-2.93	5.22E-05
OAS1	2',5'-oligoadenylate synthetase 1, 40/46kDa	0.39	8.69E-01	**2.99**	**4.91E-04**	1.68	6.76E-02	2.60	7.05E-03	1.29	1.82E-01	-1.31	1.48E-01
CCL26	chemokine (C-C motif) ligand 26	-0.09	9.60E-01	**2.89**	**2.22E-06**	-0.14	8.94E-01	2.98	1.36E-05	-0.05	9.64E-01	-3.03	1.06E-06
KRT14	keratin 14	0.90	4.67E-01	**2.87**	**1.31E-04**	0.47	6.74E-01	1.97	1.39E-02	-0.43	7.09E-01	-2.40	1.08E-03
TNFAIP6	tumor necrosis factor, alpha-induced protein 6	0.19	9.24E-01	**2.68**	**5.39E-05**	1.69	9.61E-03	2.49	6.98E-04	1.50	2.01E-02	-0.99	1.23E-01
DPT	dermatopontin	1.52	9.56E-02	**2.68**	**1.24E-04**	-1.11	1.38E-01	1.16	1.51E-01	-2.63	3.17E-04	-3.79	2.56E-06
IFIT1	interferon-induced protein with tetratricopeptide repeats 1	-0.04	9.93E-01	**2.58**	**7.82E-03**	0.28	8.96E-01	2.62	2.00E-02	0.32	8.67E-01	-2.30	2.16E-02
HTR2A	5-hydroxytryptamine (serotonin) receptor 2A	0.43	8.43E-01	**2.58**	**1.73E-03**	-1.31	1.69E-01	2.14	2.21E-02	-1.75	4.85E-02	-3.89	2.91E-05

Table 5.3 continued

Gene Symbol	Description	Day 4 GDF-5 Induction (G2 v G1)		Day 10 GDF-5 Induction (G3 v G1)		Tenocytes (G4 v G1)		Day 10 vs Day 4 GDF-5 Induction (G3 v G2)		Tenocytes vs Day 4 GDF-5 Induction (G4 v G2)		Tenocytes vs Day 10 GDF-5 Induction (G4 v G3)	
		LR	*p*-value	LR	*p*-value	LR	*p*-value	LR	*p*-value	LR	*p*-value	LR	*p*-value
Most up-regulated in tenocytes													
ASPN	asporin	2.80	2.81E-03	4.12	3.34E-06	**5.05**	**3.68E-07**	1.32	1.44E-01	2.25	4.27E-03	0.93	2.78E-01
RPS4Y1	ribosomal protein S4, Y-linked 1	-0.09	9.79E-01	-0.04	9.83E-01	**4.64**	**2.26E-05**	0.05	9.86E-01	4.73	1.23E-05	4.68	9.54E-06
EIF1AY	eukaryotic translation initiation factor 1A, Y-linked	0.02	9.97E-01	0.02	9.92E-01	**4.49**	**2.58E-05**	0.00	1.00E+00	4.47	1.98E-05	4.47	1.32E-05
DDX3Y	DEAD (Asp-Glu-Ala-Asp) box polypeptide 3, Y-linked	0.14	9.62E-01	0.12	9.39E-01	**4.24**	**3.45E-05**	-0.02	9.94E-01	4.10	4.14E-05	4.12	2.34E-05
RBP4	retinol binding protein 4, plasma	0.21	8.40E-01	0.37	4.26E-01	**4.23**	**1.95E-10**	0.16	8.42E-01	4.03	3.89E-10	3.86	9.62E-10
THBS4	thrombospondin 4	0.05	9.89E-01	0.30	8.11E-01	**4.04**	**2.16E-05**	0.26	8.85E-01	3.99	1.65E-05	3.73	2.54E-05
FGL2	fibrinogen-like 2	-0.49	9.01E-01	2.42	5.03E-02	**3.96**	**3.59E-03**	2.91	4.20E-02	4.45	1.03E-03	1.54	2.89E-01
PRG4	proteoglycan 4	0.25	9.62E-01	-0.89	6.73E-01	**3.89**	**1.47E-02**	-1.14	6.56E-01	3.64	2.06E-02	4.78	1.69E-03
OGN	osteoglycin	1.56	4.92E-01	1.36	3.47E-01	**3.57**	**8.85E-03**	-0.20	9.56E-01	2.01	1.64E-01	2.21	9.50E-02
MEOX2	mesenchyme homeobox 2	0.97	4.17E-01	0.54	5.63E-01	**3.51**	**3.30E-05**	-0.44	7.39E-01	2.54	9.87E-04	2.98	1.16E-04

Table 5.3 continued

Gene Symbol	Description	Day 4 GDF-5 Induction (G2 v G1)		Day 10 GDF-5 Induction (G3 v G1)		Tenocytes (G4 v G1)		Day 10 vs Day 4 GDF-5 Induction (G3 v G2)		Tenocytes vs Day 4 GDF-5 Induction (G4 v G2)		Tenocytes vs Day 10 GDF-5 Induction (G4 v G3)	
		LR	*p* -value	LR	*p* -value	LR	*p* -value	LR	*p* -value	LR	*p* -value	LR	*p* -value
Most down-regulated in day 4 GDF-5 induced hMSC													
MT2A	metallothionein 2A	**-1.34**	**2.05E-05**	-0.79	8.36E-04	0.37	1.81E-01	0.55	4.21E-02	1.71	1.38E-07	1.16	1.71E-05
	Unknown transcript (Transcript cluster ID: 8162531)	**-1.38**	**9.01E-05**	-1.03	3.45E-04	0.44	1.74E-01	0.35	3.70E-01	1.82	5.65E-07	1.47	7.17E-06
TFRC	transferrin receptor (p90, CD71)	**-1.45**	**1.22E-03**	-0.76	2.96E-02	-0.49	2.52E-01	0.69	1.10E-01	0.96	1.17E-02	0.27	5.95E-01
ACAN	aggrecan	**-1.46**	**1.03E-02**	-2.22	1.32E-05	-1.37	4.24E-03	-0.76	1.65E-01	0.09	9.24E-01	0.85	6.15E-02
STC1	stanniocalcin 1	**-1.49**	**1.17E-02**	-1.45	1.58E-03	-1.07	3.12E-02	0.04	9.75E-01	0.42	5.09E-01	0.38	5.43E-01
ID3	inhibitor of DNA binding 3	**-1.57**	**9.01E-05**	-1.38	5.62E-05	0.07	9.21E-01	0.19	7.42E-01	1.64	1.22E-05	1.45	3.74E-05
PODXL	podocalyxin-like	**-1.69**	**1.26E-02**	-1.92	4.07E-04	2.01	6.39E-04	-0.23	8.37E-01	3.70	1.91E-07	3.93	5.75E-08
HMOX1	heme oxygenase (decycling) 1	**-1.73**	**1.89E-02**	-2.21	2.12E-04	0.57	4.61E-01	-0.48	6.10E-01	2.30	2.73E-04	2.78	1.84E-05
ITGA8	integrin, alpha 8	**-1.86**	**5.42E-03**	-2.99	2.63E-06	-3.06	3.72E-06	-1.14	6.34E-02	-1.20	3.13E-02	-0.06	9.57E-01
NEFM	neurofilament, medium polypeptide	**-2.23**	**3.53E-02**	-2.55	1.45E-03	-2.44	5.04E-03	-0.32	8.51E-01	-0.22	8.94E-01	0.11	9.52E-01
Most down-regulated in day 10 GDF-5 induced hMSC													
ASPM	asp homolog, microcephaly associated	-1.19	3.42E-01	**-2.37**	**2.26E-03**	0.77	4.74E-01	-1.18	2.42E-01	1.96	1.83E-02	3.14	1.93E-04
TOP2A	topoisomerase (DNA) II alpha 170kDa	-1.32	2.65E-01	**-2.42**	**1.61E-03**	0.38	7.82E-01	-1.10	2.80E-01	1.70	3.82E-02	2.80	5.47E-04
KIF20A	kinesin family member 20A	-1.44	2.41E-01	**-2.55**	**1.60E-03**	0.09	9.65E-01	-1.11	3.09E-01	1.52	8.52E-02	2.63	1.57E-03
MKI67	antigen identified by monoclonal antibody Ki-67	-1.80	1.29E-01	**-2.55**	**2.05E-03**	0.49	7.22E-01	-0.75	5.79E-01	2.29	9.78E-03	3.04	5.19E-04
NEFM	neurofilament, medium polypeptide	-2.23	3.53E-02	**-2.55**	**1.45E-03**	-2.44	5.04E-03	-0.32	8.51E-01	-0.22	8.94E-01	0.11	9.52E-01
ANLN	anillin, actin binding protein	-1.61	2.29E-01	**-2.68**	**2.37E-03**	0.17	9.35E-01	-1.07	4.01E-01	1.78	6.39E-02	2.84	1.81E-03
IL7R	interleukin 7 receptor	-2.08	8.20E-02	**-2.74**	**1.51E-03**	-2.08	2.62E-02	-0.66	6.58E-01	0.00	9.99E-01	0.67	5.87E-01
DLGAP5	discs, large (Drosophila) homolog-associated protein 5	-1.80	1.56E-01	**-2.99**	**8.20E-04**	-0.02	9.94E-01	-1.19	3.23E-01	1.78	6.28E-02	2.97	1.18E-03
ITGA8	integrin, alpha 8	-1.86	5.42E-03	**-2.99**	**2.63E-06**	-3.06	3.72E-06	-1.14	6.34E-02	-1.20	3.13E-02	-0.06	9.57E-01
SLC14A1	solute carrier family 14 (urea transporter), member 1	-0.03	9.95E-01	**-3.03**	**4.19E-04**	-1.38	1.50E-01	-3.00	2.34E-03	-1.35	1.53E-01	1.65	5.37E-02

Table 5.3 continued

Gene Symbol	Description	Day 4 GDF-5 Induction (G2 v G1)		Day 10 GDF-5 Induction (G3 v G1)		Tenocytes (G4 v G1)		Day 10 vs Day 4 GDF-5 Induction (G3 v G2)		Tenocytes vs Day 4 GDF-5 Induction (G4 v G2)		Tenocytes vs Day 10 GDF-5 Induction (G4 v G3)	
		LR	*p*-value	LR	*p*-value	LR	*p*-value	LR	*p*-value	LR	*p*-value	LR	*p*-value
Most down-regulated in tenocytes													
TSPAN18	tetraspanin 18	-0.05	9.87E-01	-1.49	5.82E-02	**-3.05**	**5.65E-04**	-1.43	1.35E-01	-3.00	5.37E-04	-1.57	5.16E-02
ITGA8	integrin, alpha 8	-1.86	5.42E-03	-2.99	2.63E-06	**-3.06**	**3.72E-06**	-1.14	6.34E-02	-1.20	3.13E-02	-0.06	9.57E-01
FMO3	flavin containing monooxygenase 3	0.37	9.25E-01	-0.30	8.88E-01	**-3.12**	**1.53E-02**	-0.67	7.67E-01	-3.49	6.12E-03	-2.82	1.96E-02
PDE5A	phosphodiesterase 5A, cGMP-specific	-0.24	8.85E-01	-1.44	8.82E-03	**-3.31**	**3.72E-06**	-1.19	7.04E-02	-3.07	7.02E-06	-1.87	1.26E-03
DEPDC6	DEP domain containing 6	0.15	9.62E-01	0.04	9.84E-01	**-3.35**	**7.16E-04**	-0.11	9.65E-01	-3.49	3.80E-04	-3.38	3.44E-04
ANKRD1	ankyrin repeat domain 1 (cardiac muscle)	-1.02	6.25E-01	0.03	9.90E-01	**-3.41**	**2.81E-03**	1.05	5.19E-01	-2.39	3.12E-02	-3.44	1.37E-03
ANK3	ankyrin 3, node of Ranvier (ankyrin G)	0.42	6.51E-01	0.46	3.99E-01	**-3.59**	**4.09E-08**	0.04	9.80E-01	-4.01	4.57E-09	-4.05	3.80E-09
VCAM1	vascular cell adhesion molecule 1	0.54	7.83E-01	0.83	3.85E-01	**-3.92**	**5.05E-05**	0.29	8.74E-01	-4.46	7.02E-06	-4.75	2.30E-06
SRGN	serglycin	-0.12	9.64E-01	-0.40	7.22E-01	**-4.41**	**3.72E-06**	-0.28	8.64E-01	-4.29	4.22E-06	-4.01	6.81E-06
IGF2	insulin-like growth factor 2 (somatomedin A)	-0.03	9.93E-01	-1.27	8.51E-02	**-6.40**	**6.21E-09**	-1.24	1.70E-01	-6.37	4.57E-09	-5.13	1.18E-07
Co-expressed genes (Up- or down- regulated in all day 4, 10 GDF-5-induced hMSC and tenocytes)													
ASPN	asporin	2.80	2.81E-03	4.12	3.34E-06	5.05	3.68E-07	1.32	1.44E-01	2.25	4.27E-03	0.93	2.78E-01
ARHGAP29	Rho GTPase activating protein 29	1.10	1.30E-02	1.03	2.66E-03	1.94	6.10E-06	-0.07	9.36E-01	0.85	2.10E-02	0.92	8.74E-03
CCL2	chemokine (C-C motif) ligand 2	1.35	4.35E-03	2.07	3.34E-06	1.82	3.89E-05	0.73	1.02E-01	0.48	2.94E-01	-0.25	6.52E-01
ENO2	enolase 2 (gamma, neuronal)	-1.30	2.22E-03	-1.69	1.32E-05	-1.02	5.41E-03	-0.39	4.17E-01	0.28	5.63E-01	0.68	4.84E-02
STC1	stanniocalcin 1	-1.49	1.17E-02	-1.45	1.58E-03	-1.07	3.12E-02	0.04	9.75E-01	0.42	5.09E-01	0.38	5.43E-01
ACAN	aggrecan	-1.46	1.03E-02	-2.22	1.32E-05	-1.37	4.24E-03	-0.76	1.65E-01	0.09	9.24E-01	0.85	6.15E-02
C7orf69	chromosome 7 open reading frame 69	-1.32	3.08E-02	-1.26	5.29E-03	-1.57	2.02E-03	0.05	9.69E-01	-0.26	7.39E-01	-0.31	6.57E-01
NEFM	neurofilament, medium polypeptide	-2.23	3.53E-02	-2.55	1.45E-03	-2.44	5.04E-03	-0.32	8.51E-01	-0.22	8.94E-01	0.11	9.52E-01
ITGA8	integrin, alpha 8	-1.86	5.42E-03	-2.99	2.63E-06	-3.06	3.72E-06	-1.14	6.34E-02	-1.20	3.13E-02	-0.06	9.57E-01

Among the significantly co-expressed genes by GDF5-induced hMSCs and tenocytes, asporin (ASPN) and integrin alpha 8 (ITGA8) were found to be among the top most up- and down- regulated genes, respectively (Table 5.3). Besides, neurofilament medium polypeptide (NEFM) was among the most significantly down-regulated genes in day-4 and day-10 GDF5-induced hMSCs, although not appeared to be the top most down-regulated genes in tenocytes, it was significantly down-regulated in tenocytes. Besides, the rho GTPase activating protein 29 (ARHGAP29) and chemokine (C-C motif) ligand 2 (CCL2) were up-regulated and co-expressed in all the GDF5 treated hMSCs and tenocytes. These genes have been reported to associate with actin cytoskeleton reorganization (stress fibers formation) (Stamatovic et al., 2003). Overall, all the co-expressed genes were involved direct or indirectly with collagen fibrillogenesis (Velling et al., 2002) and cytoskeletal remodelling signalling (Moon & Zheng, 2003; Stamatovic, et al., 2003). Therefore, these findings suggested a crucial role played by collagen fibrillogenesis and cytoskeletal remodelling in directing hMSC into tenogenic cell fate. A complete list of genes significantly modulated during tenogenesis by GDF5 treatment can be found in Appendix K.

5.3.1.3 Tenogenesis Pathways Associated with GDF5-induced hMSC

In this section, the complex signalling mechanisms involved in GDF5-induced hMSCs (day 4 and day 10) and in native tenocytes, as captured by pathway analysis are presented (Table 5.4). The pathway analysis was based on the significantly up- or down-regulated gene lists where corrected-p<0.05 and at least fold change of 2 (or $\log_2$ ratio at least 1.0 for up-regulated genes) or fold change less than 0.5 (or $\log_2$ ratio less than -1.0 for down-regulated genes). A total of 8 pathways (p<0.001) were regulated at day 4 of induction by GDF5.

Table 5.4 Pathways regulated by GDF5-induced tenogensis in hMSC.

Pathway regulated in hMSC at day 4 of 100 ng/ml GDF5 treatment (Total= 8 pathways)

Pathway name	Genes involved	*p*-value
Cholesterol biosynthesis	FDPS↑, SC4MOL↑, ERG1↑	3.603E-04
Glycolysis and gluconeogenesis p.3 / Human version	ENO↓, ENO2↓	6.822E-04
Glycolysis and gluconeogenesis p.3	ENO↓, ENO2↓	6.822E-04
Immune response_TREM1 signalling pathway	PI3K reg class IA↑, CCL2↑	4.092E-03
Immune response_IL-17 signalling pathways	PI3K reg class IA↑, CCL2↑	4.229E-03
Glycolysis and gluconeogenesis (short map)	ENO2↓	5.096E-03
Development_VEGF signaling via VEGFR2 - generic cascades	PI3K reg class IA↑, CCL2↑	8.143E-03
Regulation of lipid metabolism_Insulin regulation of fatty acid methabolism	PI3K reg class IA↑, FADS2↑	9.105E-03

Pathway regulated in hMSC at day 10 of 100 ng/ml GDF5 treatment (Total= 21 pathways)

Pathway name	Genes involved	*p*-value
Cell cycle_Role of APC in cell cycle regulation	PLK1↓, BUBR1↓, Aurora-A↓, Cyclin A↓, Cyclin B↓, Nek2A↓, Securin↓, APC↓, CDC18L(CDC6)↑	3.540E-10
Cell cycle_The metaphase checkpoint	Survivin↓, Aurora-A↓, Nek2A↓, PLK1↓, BUB1↓, BUBR1↓, AF15q14↓, CENP-F↓	2.731E-08
Cell cycle_Chromosome condensation in prometaphase	Cyclin A↓, Cyclin B↓, CAP-G↓, Aurora-A↓, CAP-G/G2↓, Condensin↓, TOP2↓	3.203E-07
Cholesterol Biosynthesis	IDI1↑, HMGCS1↑, HMDH↑, ERG1↑, FDPS↑, SC4MOL↑, SC5D↑	2.325E-04
Cell cycle_Initiation of mitosis	PLK1↓, Wee1↓, FOXM1↓, Cyclin B2↓	3.811E-04
Immune response_Antiviral actions of Interferons	OAS1↑, OAS2↑, OAS3↑, 2′-5′-oligoadenylate synthetase↑, MxA↑	7.921E-04
Cell cycle_Role of Nek in cell cycle regulation	PI3K reg class IA↑, Nek2A↓, tubulin beta↑, Aurora-A↓	1.004E-03
Cell cycle_Spindle assembly and chromosome separation	Anaphase-promoting complex (APC)↓, Nek2A↓, Securin↓, Aurora-A↓	1.130E-03
Development_Angiopoietin - Tie2 signaling	Angiopoietin 3↑, PI3K reg class IA↑, Grb14↑, Survivin↓	1.415E-03
Development_TGF-beta-dependent induction of EMT via SMADs	Endothelin-1↓, SMAD3↓, ID2↓, E-cadherin↑	1.415E-03
Cytoskeleton remodeling_Keratin filaments	Tubulin beta↑, Keratin 14↑, Keratin 16↑, Kereatin 17↑	1.575E-03
Cell cycle_Regulation of G1/S transition (part 1)	Anaphase-promoting complex (APC) ↓, PP2A regulatory↑, SMAD3↓, Cyclin A↓, CDK6↑	1.931E-03
Cell cycle_Cell cycle (generic schema)	CDK6↑, CyclinA↓, Cyclin B↓	3.038E-03

Table 5.4 continued

Immune response_NF-AT signaling and leukocyte interactions	NF-AT1↑, cPAL2↑, Ca(II) channel↑, Eotaxin↑	3.914E-03
Immune response _CCR3 signaling in eosinophils	Eotaxin↑, Eotaxin 3↑, Rac2↓, MyHC↑, Myosin II ↑	4.553E-03
Arachidonic acid production	FADS1↑, PA24A↑, cPLA2↑, PLA2↑	5.290E-03
DNA damage_ATM / ATR regulation of G2 / M checkpoint	Wee1↓, Cyclin A↓, Cyclin B↓	5.643E-03
Cell cycle_Transition and termination of DNA replication	Cyclin A↓, TOP1 alpha↓, TOP2↓	6.966E-03
Immune response_Innate immune response to RNA viral infection	TLR3↓, RIG-I↓, MDA-5↓	6.966E-03
Cell cycle_Role of SCF complex in cell cycle regulation	APC↓, PLK1↓, Wee1↓	7.690E-03
Immune response_TREM1 signaling pathway	TLR4↓, PI3K reg class IA↑, CCL2↑, NFATC2↑	9.488E-03

Pathway regulated in tenocytes (Total= 18 pathways)

Pathway name	**Genes involved**	***p*-value**
Immune response_Alternative complement pathway	C3↑, C3a↑, iC3b↑, C3c↑, C3dg↑, C3b↑, C5 convertase (C3bBb)↑, Clusterin↑	1.129E-07
Immune response_Lectin induced complement pathway	C3↑, C3a↑, C3b↑, C3c↑, C3dg↑, iC3b↑, DAF↑, C5 convertase (C2aC4bC3b)↑	7.265E-07
Immune response_Classical complement pathway	C3↑, C3a↑, C3b↑, C3c↑, C3dg↑, iC3b↑, DAF↑, C5 convertase (C2aC4bC3b)↑	1.166E-06
Development_Regulation of epithelial-to-mesenchymal transition (EMT)	HGF↓, WNT↓, Jagged1↓, TGF-beta 3↑, Endothelin-1↓, ENDRA↓, ACTA2 ↓	5.553E-05
Immune response_MIF-mediated glucocorticoid regulation	I-kB↑, NFKBIA↑, IL-8↑, VCAM↓	3.282E-04
Development_TGF-beta-dependent induction of EMT via SMADs	Endothelin-1↓ , TGF-beta↑, TGF-beta 3↑, Jagged1↓	2.010E-03
Transcription_Role of AP-1 in regulation of cellular metabolism	ITGA2↑, TSG-6↑, GCL cat↑, GCL reg↑	2.733E-03
Apoptosis and survival_Lymphotoxin-beta receptor signaling	IL-8↑, I-kB↑, VCAM↓, SDF-1↓	3.951E-03
Cell adhesion_Ephrin signaling	Ephrin-B↓, Ephrin-B receptors↑, Ephrin-B receptor 1↑, Ephrin-A receptors↓	5.075E-03
Immune response_PGE2 signaling in immune response	PGE2R2↑, PGES↓, IL-8↑, HGF↓	5.075E-03
Development_TGF-beta-dependent induction of EMT via RhoA, PI3K and ILK.	TGF-beta 3↑, ACTA2↓, I-kB↑, Actin↓	5.492E-03
Immune response_Histamine H1 receptor signaling in immune response	IL-8↑, VCAM1↓, NFKBIA↑, I-kB↑	6.394E-03
Muscle contraction_Relaxin signaling pathway	Endothelin-1↓, PDE4D↑, NFKBIA↑, I-kB↑	6.394E-03
Development_PEDF signaling	PEDF (serpinF1)↑, NFKBIA↑, c-IAP2↑, BDNF↓	6.881E-03

Table 5.4 continued

Development_Cross-talk between VEGF and Angiopoietin 1 signaling pathways	VCAM1↓, I-kB↑, Angiopoietin 1↓	7.347E-03
Development_S1P2 and S1P3 receptors in cell proliferation and differentiation	ACTA2↓, Transgelin↓, Actin↓	7.347E-03
Immune response_HMGB1/RAGE signaling pathway	VCAM1↓, I-kB↑, NFKBIA↑, IL-8↑	9.068E-03
Muscle contraction_GPCRs in the regulation of smooth muscle tone	Endothelin-1↓, ENDRA↓, PGE2R2↑, MRLC↓, Myosin II↓	9.278E-03

Pathway regulated in GDF5-induced hMSC (day 4 and day 10) (Total= 3 pathways)

Pathway name	**Change**	***p*-value**		
		GDF5-induced hMSC (Day 4)	**GDF5-induced hMSC (Day 10)**	**Day 10 vs day 4**
Development_Angiopoietin - Tie2 signaling	+	5.622E-2	1.415E-3	8.316E-2
Development_TGF-beta-dependent induction of EMT via SMADs	+	5.622E-2	1.415E-3	8.316E-2
Immune response_IL-13 signaling via JAK-STAT	+	7.019E-2	2.393E-2	5.175E-3

Pathway regulated in GDF5-induced hMSC (day 4 and day 10) and tenocytes (Total= 11 pathways)

Pathway name	**Change**	***p*-value**		
		GDF5-induced hMSC (Day 4)	**GDF5-induced hMSC (Day 10)**	**Tenocytes**
Glycolysis and gluconeogenesis p.3 / Human version	-	6.822E-4	4.463E-2	5.296E-2
Glycolysis and gluconeogenesis p.3	-	6.822E-4	4.463E-2	5.296E-2
Cell cycle_Role of Nek in cell cycle regulation	+	5.152E-2	1.004E-3	8.790E-2
Development_Angiopoietin - Tie2 signaling	+	5.622E-2	1.415E-3	1.024E-1
Development_TGF-beta-dependent induction of EMT via SMADs	+	5.622E-2	1.415E-3	2.010E-3
Immune response_TREM1 signaling pathway	+	4.092E-3	9.488E-3	1.313E-2
Immune response_IL-17 signaling pathways	+	4.229E-3	2.078E-1	1.390E-2
Glycolysis and gluconeogenesis (short map)	-	5.096E-3	6.630E-2	2.738E-1
Development_PEDF signaling	+	7.787E-2	5.030E-1	6.881E-3
Development_VEGF signaling via VEGFR2 - generic cascades	+	8.143E-3	1.155E-1	3.765E-1

Table 5.4 continued

Regulation of lipid metabolism_Insulin regulation of fatty acid methabolism	+	9.105E-3	3.592E-1	7.538E-1

Pathway regulated in tenocytes compared to GDF5-induced hMSC (day 4 and day 10) (Total= 41 pathways)

Pathway name	**Change**	***p*-value**		
		Tenocytes vs control hMSC	**Tenocytes vs GDF5-induced hMSC (Day4)**	**Tenocytes vs GDF5-induced hMSC (Day 10)**
Cell cycle_Chromosome condensation in prometaphase	+	2.806E-1	1.132E-7	2.303E-12
Cell cycle_Role of APC in cell cycle regulation	+	3.948E-1	1.365E-1	1.134E-8
Cell cycle_Initiation of mitosis	+	5.699E-2	8.134E-6	1.519E-8
Immune response_Alternative complement pathway	+	1.129E-7	1.866E-1	7.618E-4
Immune response_Lectin induced complement pathway	+	7.265E-7	2.614E-1	1.259E-2
Immune response_Classical complement pathway	+	1.166E-6	2.840E-1	1.602E-2
Development_TGF-beta-dependent induction of EMT via SMADs	+	2.010E-3	1.576E-1	4.825E-6
Development_Regulation of epithelial-to-mesenchymal transition (EMT)	-	5.553E-5	2.906E-4	1.190E-5
Immune response_MIF-mediated glucocorticoid regulation	+	3.282E-4	6.401E-5	2.618E-5
Immune response_Histamine H1 receptor signaling in immune response	+	6.394E-3	4.521E-5	2.313E-3
Cell adhesion_ECM remodeling	+	4.671E-2	7.675E-5	6.418E-4
Cell cycle_Role of Nek in cell cycle regulation	+	8.790E-2	1.365E-1	2.501E-4
DNA damage_ATM/ATR regulation of G1/S checkpoint	+	3.948E-1	1.365E-1	2.501E-4
Cell cycle_Sister chromatid cohesion	+	2.918E-1	9.471E-3	3.251E-4
GTP metabolism	-	5.128E-2	7.298E-4	6.803E-2
Transcription_Role of AP-1 in regulation of cellular metabolism	+	2.733E-3	9.389E-4	2.968E-1
Cell cycle_Role of SCF complex in cell cycle regulation	+	3.656E-1	4.481E-1	1.245E-3
Apoptosis and survival_Lymphotoxin-beta receptor signaling	+	3.951E-3	1.491E-3	1.179E-1
Transcription_Role of VDR in regulation of genes involved in osteoporosis	-	6.889E-2	3.513E-1	1.683E-3
Immune response_IL-1 signaling pathway	+	3.059E-2	1.842E-3	1.306E-1
Development_TGF-beta-dependent induction of EMT via RhoA, PI3K and ILK.	+	5.492E-3	6.578E-2	1.851E-3

Table 5.4 continued

Development_NOTCH1-mediated pathway for NF-KB activity modulation	+	1.546E-2	4.689E-3	2.597E-3
Immune response_Gastrin in inflammatory response	+	2.216E-2	2.639E-3	1.348E-1
Immune response_HMGB1/RAGE signaling pathway	+	9.068E-3	4.206E-3	1.729E-2
Cell adhesion_Cell-matrix glycoconjugates	+	1.174E-1	4.104E-2	4.270E-3
Airway smooth muscle contraction in asthma	-	5.606E-2	1.041E-1	5.062E-3
Cell adhesion_Ephrin signaling	+	5.075E-3	1.269E-2	3.898E-2
Immune response_PGE2 signaling in immune response	+	5.075E-3	1.269E-2	1.372E-1
Immune response_Role of PKR in stress-induced antiviral cell response	+	5.853E-2	5.753E-3	2.229E-1
Cell adhesion_Tight junctions	+	1.803E-2	5.772E-3	2.754E-1
Cell adhesion_Cadherin-mediated cell adhesion	+	6.113E-2	1.507E-2	5.953E-3
Muscle contraction_Delta-type opioid receptor in smooth muscle contraction	-	6.113E-2	1.507E-2	5.953E-3
Development_S1P2 and S1P3 receptors in cell proliferation and differentiation	-	7.347E-3	1.507E-2	5.953E-3
Muscle contraction_Relaxin signaling pathway	+	6.394E-3	1.582E-2	1.574E-1
Development_PEDF signaling	+	6.881E-3	6.341E-1	5.080E-2
Immune response_IL-17 signaling pathways	+	1.390E-2	7.148E-3	2.804E-2
Development_Cross-talk between VEGF and Angiopoietin 1 signaling pathways	+	7.347E-3	1.507E-2	3.704E-2
Cell adhesion_PLAU signaling	+	1.226E-1	7.691E-3	2.455E-2
Transport_Macropinocytosis regulation by growth factors	+	7.437E-2	3.841E-2	8.979E-3
Muscle contraction_GPCRs in the regulation of smooth muscle tone	-	9.278E-3	2.627E-2	9.435E-3
Apoptosis and survival_Granzyme A signaling	+	3.755E-1	2.220E-2	9.983E-3
Cell cycle_Chromosome condensation in prometaphase	+	2.806E-1	1.132E-7	2.303E-12

↑ Up-regulated; ↓ Down-regulated

Of particular relevance is the activation of vascular endothelial growth factor (VEGF) signalling via VEGFR2 generic cascade. VEGF is found expressed in tendon sheath fibroblasts and the expression of VEGF is increased in early tendon healing process (Bidder et al., 2000). Besides, it has been suggested as one of the important regulators of gene activation (Kjaer, 2004). Activation of this pathway may thus potentially be involved in early stage of tenogenesis induced by GDF5. Besides, a down-regulation in the glycolysis and gluconeogenesis pathway was found. Although, there is no study available focusing on the role of glycolysis during early hMSC differentiation, this observation can be explained by MSCs are more glycolytic than differentiated fibroblasts (Funes et al., 2007).

At day 10 of GDF5 treatment, a total of 21 pathways (p<0.001) were regulated, among which cell cycle related signalling pathways (i.e. the metaphase checkpoint signalling, chromosome condensation in prometaphase signalling, initiation of mitosis signalling as well as spindle assembly and chromosome separation signalling) were down-regulated and development related TGF-β-dependent induction of EMT via SMADs signalling, angiopoietin - Tie2 signalling, cytoskeleton remodelling keratin filaments signalling, arachidonic acid production signalling were activated. Extensive cell-cell contact or depletion of nutrients from the culture medium has been shown to induce transient/reversible growth arrest (or cell cycle arrest). However, a more physiological mechanism, a reciprocal regulation of cell proliferation and differentiation occurs (Owen et al., 1990), when cells undergo differentiation. The growth arrest in the G_1 phase of the cell cycle has been reported to be associated with expression of the differentiated phenotype in many cell types (Filipak et al., 1989; Myster & Duronio, 2000; Nadal-Ginard, 1978); and the stem cells must growth arrest (predifferentiation growth arrest) at a distinct cell cycle state prior to differentiation (Filipak, et al., 1989). Thus, the down-regulation of cell cycle related pathways at day 10 of GDF5 treatment

was not unexpected. Whereas, the developmental related pathway, EMT pathway in particular, plays crucial roles in the formation of body plan (a characteristic process of vertebrate gastrulation) (Behr et al., 2005) and in the differentiation process of multiple tissue and organs (Thiery et al., 2009). The occurrence of EMT has been reported in mesodermal fate program, where the somites (one of the transient structures) will undergo secondary EMT, leading to the generation of mesenchymal cells that differentiate into specific cell types, i.e. tendon (Acloque et al., 2009; Thiery, et al., 2009). In addition, amniotic epithelial cells can stepwise differentiate *in vitro* into tenocytes through EMT (Barboni et al., 2012). Therefore, it is suggested that the EMT may be required for the adult stem cells (ie. hMSC) to differentiate into tenogenic lineage. Angiopoietin - Tie2 signalling pathway has been demonstrated to play a critical role in the maintenance of hematopoietic stem cells in a quiescent state in the bone marrow niche (Arai et al., 2004) and it also has a protective effect on MSC which is crucial to MSC survival (Liu et al., 2008). The activation of angiopoietin - Tie2 signalling together with the down regulation of cell cycle related pathway, may suggest that the angiopoietin - Tie2 signalling plays a protective role when the hMSC exit the cell cycle and undergo differentiation. Rapid keratin-network adaptation has recently been reported to be crucial in migrating cells and for adaptation to varying environment conditions for example, during development or under mechanical stress in epithelia (Kolsch et al., 2010) and hepatocyte (Galarneau et al., 2007; Loranger et al., 1997). The activation of cytoskeleton remodelling related keratin filaments signalling in this current experiment may suggest a crucial role of keratin filament reorganization in hMSCs during early tenogenic differentiation. The arachidonic acid production signalling is suggested to play an important role in tenocyte behaviour (Cilli et al., 2004; Khan et al., 2005). This is because the arachidonic acid is an initial molecule in a cascade that involved phospholipase A_2 (PLA_2) and produces prostaglandin-E_2 (PGE_2) (Kaiser,

1999). This PGE_2 has an effect in the proliferation and collagen production of human tendon fibroblast (Cilli, et al., 2004). Thus, the activation of arachidonic acid signalling in the GDF5-induced hMSCs may play an essential role in collagen production during tenogenesis. Further, cytosolic PLA_2 ($cPLA_2$) and secretory PLA_2 ($sPLA_2$) are involved in the production of other inflammatory mediators, apart from the PGE_2. Therefore, this could possibly explain the occurrence of the immune response pathways identified in this current experiment (Table 5.4).

The GDF5-induced hMSC (day 4 and 10) and tenocytes together showed regulation of 11 pathways. Down-regulation of glycolysis signalling in the GDF5-induced hMSCs is thereby relevant to tenogenesis, as the tenocytes also demonstrated a down-regulation in the glycolysis signalling, similar to that observed in the day-4 GDF5-induced hMSC. This again explained that the hMSCs are more glycolytic than primary human tenocytes. Thus, upon induction by GDF5, the hMSCs underwent tenogenesis, which subsequently exhibited lower glycolytic activities than the control hMSCs. In addition, of particular relevance was the activation of development related angiopoietin - Tie2 signalling, TGF-beta-dependent induction of EMT via SMADs, VEGF signalling via VEGFR2 and pigment epithelium-derived factor (PEDF) signalling. It is suggested that activation of these pathways would promotes tenogenic differentiation. The activation of PEDF signalling was relevant for it has a crucial role in angiogenesis inhibition (Bouck, 2002). Activation of this pathway may potentially be involved in the response of hMSC to the angiogenesis effect of GDF5 (Yamashita et al., 1997). It is important to emphasize that tenomodulin, as one of the tenogenic markers, is also an anti-angiogenic molecule (Oshima et al., 2003; Shukunami et al., 2005). In addition, the PEDF is a new identified adipokine. At physiological concentration, this protein also inhibits adipocyte differentiation, and down regulates the adipocyte markers (Wang et al., 2009). Therefore, the activation of

this PEDF signalling pathway was suggested to be crucial to promote tenogenesis in GDF5-induced hMSCs via inhibition on both angiogenesis and adipogenic differentiation. Furthermore, the cell adhesion signalling and cytoskeletal remodelling signalling were also activated in the GDF5-induced hMSCs and in native tenocytes (not shown in table); despite at a lower significance level (p=0.01 and p=0.05, respectively). These pathways were associated with tenocyte behaviour as cell adhesion and cytoskeletal remodelling are particularly important in the survival of the tendon cells which reside in the high tensional loading tissue.

As an extension to determine the pathways associated with the late tenogenic differentiation or mature tenocytes, the significantly up- or down regulated gene lists obtained from comparing tenocytes to GDF5-induced hMSC were analyzed. In matured tenocytes, the activated pathways were: (i) development related TGF-β-dependent induction of EMT via SMADs signalling, TGF-β-dependent induction of EMT via RhoA, PI3K and ILK signalling, PEDF signalling, cross-talk between VEGF and angiopoietin 1 signalling, (ii) cell adhesion related ECM remodelling signalling, cell-matrix glycoconjugates signalling, Ephrin signalling, tight junctions signalling, cadherin-mediated cell adhesion signalling, PLAU signalling and (iii) cell cycle related (i.e. chromosome condensation in prometaphase signalling, role of APC in cell cycle regulation signalling, initiation of mitosis signalling, ATM/ATR regulation of G1/S checkpoint signalling, sister chromatid cohesion signalling and role of SCF complex in cell cycle regulation signalling) pathways. Whereas, the down-regulated pathways were muscle contraction delta-type opioid receptor in smooth muscle signalling, muscle contraction related GPCRs in the regulation of smooth muscle tone signalling, and development related S1P2 and S1P3 receptors in cell proliferation and differentiation signalling. The activated pathways which were development related were consistent to the pathways identified from the day-4 or day-10 GDF5-induced hMSCs, except the

PEDF signalling. PEDF signalling was only up-regulated at in the tenocytes. This suggests that the PEDF signalling may be involved in the late tenogenic differentiation or in mature tenocytes phenotypes. However, in contrary to the effect of day 10 GDF5 treatment (or early tenogenesis), the cell cycle related pathways were up-regulated in the mature tenocytes. Activation of cell cycle signalling in tenocytes suggests that active maintenance of cell-cycle as an important aspect of the differentiated tenocytes and there may be a temporal coupling between withdrawal from the cell cycle and tenogenic differentiation as previously described in stem cells differentiation events (Filipak, et al., 1989; Myster & Duronio, 2000). A reciprocal and functionally coupled relationship between proliferation and differentiation has been demonstrated in fetal calvarial derived osteoblasts (Owen, et al., 1990). It is, therefore, postulated that there is a reciprocal mechanism for coordinating the temporal sequence of cell cycle and differentiation events during tenogenesis, which remains to be explored.

Apart from the development and cell cycle related signalling, the activated pathways also involved ECM remodelling signalling and cell adhesion signalling which were two crucial phenotypes that the mature tenocytes must possess. These characteristics are crucial for the tenocytes to maintain its integrity and physical resistance to mechanical stress in their native tendon tissue. Hence, the conversion of biochemical signals (GDF5 induction) into the cytoskeletal remodelling is important for maturation of tenogenic hMSCs, especially in cytoskeletal-ECM linkage. The pathways related to ECM remodelling via direct or indirect connections between internal actin cytoskeleton and ECM in tenocytes were such as cell adhesion related integrin inside-out signalling, cytoskeleton remodelling signalling and regulation of actin cytoskeleton by Rho GTPases signalling, which involved significantly regulated transcripts, i.e. type-I collagen, alpha-2/beta-1 integrin, alpha-10/beta-1 integrin, actin and laminin 1. The regulation of actin cytoskeleton by Rho GTPases signalling has been implicated in

lamellipodium and stress fiber formation in mammalian cells (Kaibuchi et al., 1999; Nobes & Hall, 1995). Activation of this pathway may thus potentially be involved in the lamellipodium and stress fiber formation in the mature tenocytes. Other cell adhesion related pathways activated in the mature tenocytes (cell-matrix glycoconjugates, ephrin signalling, tight junctions, cadherin-mediated cell adhesion and PLAU signalling) also play an important role in cytoskeleton-ECM linkage in tenocytes. Down regulation of muscle contraction and development related signalling were consistent with mature tenocyte phenotype.

5.3.1.4 Candidate Tenogenic and Non-Tenogenic Markers Expression Profiles

Apart from the most significantly up- or down- regulated genes and pathways, the changes in the expression profiles in ECM related genes as well as candidate tenogenic and non-tenogenic marker genes in GDF5-induced hMSCs were also analysed. Graphical representation of $\log_2$ ratios detected by microarray analysis is shown in Figure 5.6. Among these genes, type-I collagen alpha 1 (*Col-I a1*), type-II collagen alpha 1 (*Col-II*), type-III collagen alpha 1 (*Col-III a1*) and matrix metallopeptidase 3 (*Mmp3*) were related to ECM; thrombospondin 4 (*Thbs4*), mohawk homeobox (*Mkx*), tenomodulin (*Tnmd*), scleraxis (*Scx*) and tenascin C (*Tnc*) were candidate tenogenic marker genes; peroxisome proliferator-activated receptor gamma (*Pparg*), SRY (Sex determining region Y)-box 9 (*Sox9*), cartilage oligomeric matrix protein (*Comp*), Runt-related transcription factor 2 (*Runx2*), bone gamma-carboxyglutamate protein (*Bglap*) and alkaline phosphatase liver (*Alpl*) were the non-tenogenic marker genes; and c-fos induced growth factor (*Figf* or *Vegf-d*) were related to chondrogenesis (Bluteau et al., 2007), osteogenesis (Orlandini et al., 2006) and tenocyte proliferation (Luo et al., 2009).

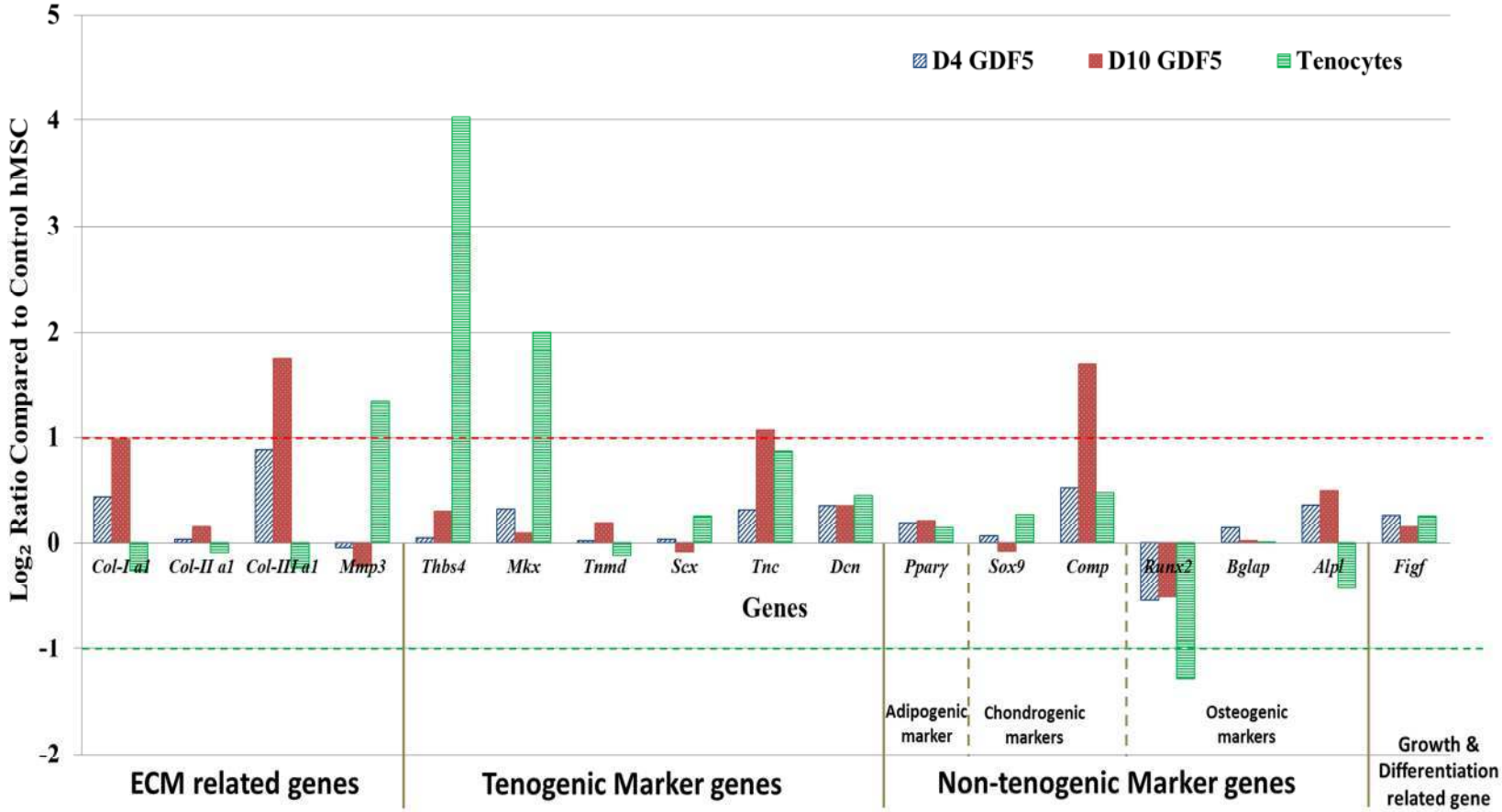

Figure 5.6 Expression levels of the ECM related, candidate tenogenic and non-tenogenic marker genes based on microarray analysis.
The graphical representation of genes (n=16) displaying changes in expression patterns in hMSC in response to GDF5 treatment with their respective $\log_2$ ratio based on microarray analysis. The genes which showed at least fold change of 2 ($\log_2$ ratio=1, red dotted line) and fold change of less than 0.5 ($\log_2$ ratio=-1, green dotted line) were regarded as significantly up- and down- regulated genes respectively.

The *Col-I* and *Col-III* were significantly up-regulated in the day-10 GDF5-induced hMSCs, among the ECM related genes. A down-regulation of *Col-I* in tenocytes indicated that the production of *Col-I* were reduced in mature tenocytes compared to the control hMSC and the early differentiating tenogenic hMSCs. Nevertheless, the *Mmp3*, which play a role in the normal maintenance and remodelling of tendon ECM, was up-regulated in the tenocytes, but weakly expressed in the GDF5-induced hMSCs.

Among the tenogenic marker genes, only *Tnc* was detected as up-regulated in the GDF5-induced hMSCs. Whereas in the mature tenocytes, the *Thbs4* and *Mkx* was detected as highly up-regulated transcript compared to the other genes. The expression level of *Tnc* in tenocytes was higher than the control hMSCs despite not being above the cut-off level. The non-tenogenic marker genes were generally weakly expressed among the GDF5-induced hMSC and tenocytes, except for *Comp* and *Runx2*. The expression levels of *Comp* was significantly up-regulated in day-10 GDF5-induced hMSC, while the *Runx2* was significantly down regulated in tenocytes. The rest of the other genes, including the *Figf*, were detected as weakly expressed and not significantly up- or down- regulated.

5.3.2 AFM and CLSM Imaging in hMSCs During Tenogenesis

5.3.2.1 Cytoskeletal Remodelling in GDF5-induced hMSCs

The control hMSCs, day-4 GDF5-induced hMSCs, day-10 GDF5-induced hMSCs and tenocytes were cultured in respective media and scanned with AFM imaging. Upon differentiation, there were evident differences in the topography between undifferentiated hMSCs and their GDF5-induced counterparts (Figure 5.7). Overall, the scanning in topography revealed a higher height scale in control hMSCs as compared to

that of the GDF5 treated hMSCs and tenocytes, which may particularly related to their cytoskeleton organization.

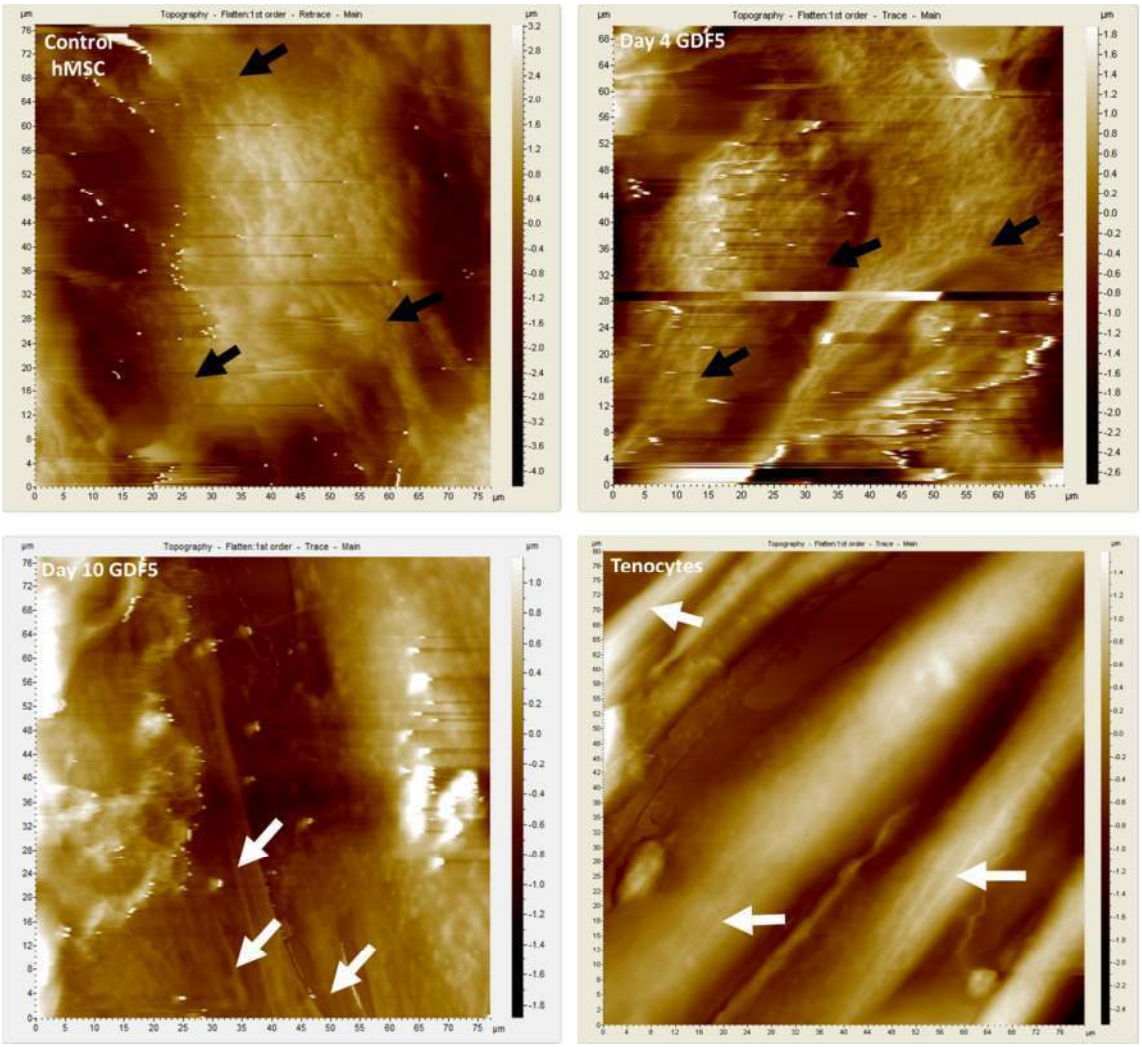

Figure 5.7 Cytoskeleton reorganization in hMSCs visualized by AFM.
Representative AFM topography scanning of control hMSCs (left upper), hMSCs at day 4 of induction by GDF5 (right upper), hMSCs at day 10 of induction by GDF5 (left lower) and tenocyte. In the topography images, brighter colour indicated higher distance off of substrate (cover slip). The panel on the right side of each image indicated the height scale (z-scale) of the topography. There was a marked difference in the topography (cytoskeleton organization) of the control hMSCs compared to the hMSCs exposed to GDF5. The topography of control hMSCs had a larger z-scale; apparently possessed higher morphology. Both control hMSCs and day-4 GDF5-induced hMSCs showed detailed tree-like web structure of presumably the actin network under the cell membrane especially at the leading edges which strongly attached on the cover slip (black arrowheads). The GDF5-induced hMSCs possessed more flatten morphology because they adhered more strongly via the stress fibers that could be visualized just under the surface of the cell membrane (white arrowheads). The detailed structure of presumably the actin cytoskeleton (actin bundles or stress fibers) could be observed in the day-10 GDF5-induced hMSCs and tenocytes.

At day-4 GDF5-induced hMSCs, similar cell surface topography to that of control hMSCs were observed, with a tree-like web structure of presumably actin network. There was a tremendous change in cell surface topography of day-10 GDF5-induced hMSCs. The day-10 GDF5-induced hMSCs showed similar cell surface topography to that of tenocytes, which both revealed bundle structure of presumably the stress fibers at the leading edge. These results suggests that the hMSCs underwent tenogenesis and continued reorganizing their cytoskeleton which allowed them to adhere more strongly to the substrate (cover slip) and subsequently displayed a more flatten morphology compared to the control hMSCs. To further confirm that the structures visualized under AFM were actin filaments, fluorescence imaging was conducted.

The fluorescence images obtained by CLSM (Figure 5.8) shadowed those images obtained by AFM imaging (Figure 5.7). The CLSM analysis demonstrated that the GDF5-induced hMSCs possessed stress fiber arrays which localised primarily next to the cell attachment site (Figure 5.8). However the abundance of this stress fiber arrays appeared low in the control hMSCs, which displayed more cortical cytoplasmic actin (or actin filament meshwork). Following extended GDF5 treatment on day 10, hMSCs displayed long, thin stress fibres, similar to that in tenocytes. These observations suggested that GDF5-induced a reorganization of actin structures which involved F-actin polymerization and restructuring of cortical actin elements to newly formed stress fibres.

5.3.2.2 Down Regulation of Nucleostemin in Early Stage of Tenogenesis in hMSCs

The nucleostemin (NST) expression was decreased in day-4 and day-10 GDF5-induced hMSCs (Figure 5.8), but persistently expressed in the untreated hMSC (at day 4 and day 10). The NST expression was also remained high in tenocytes.

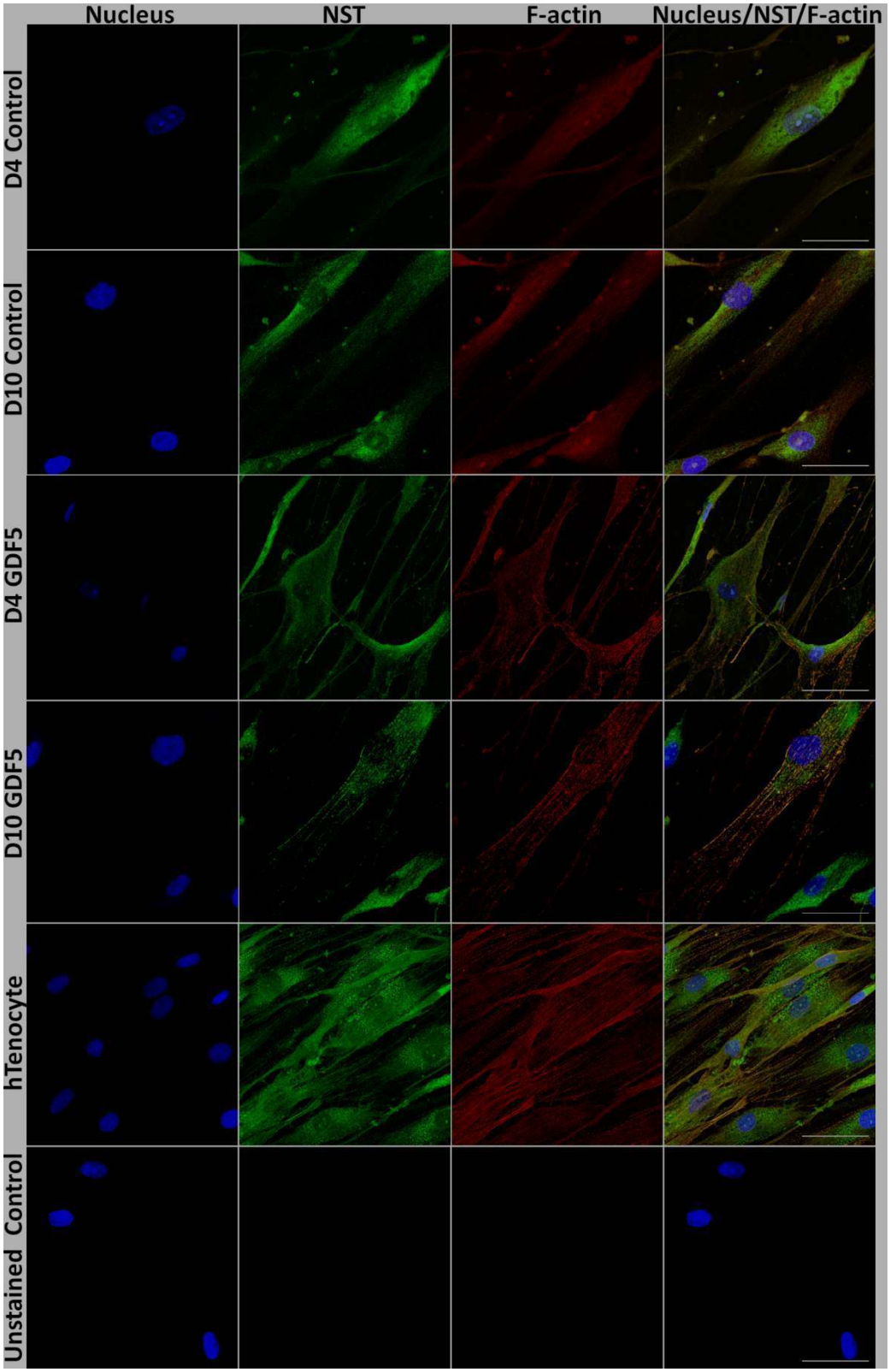

Figure 5.8 Actin cytoskeleton reorganization and nucleostemin (NST) expression in hMSCs upon induction by GDF5 captured with confocal laser scanning microscope.

Representative images of sequential scanning: nucleus stained with Hoescht 33342 (first panel on the left), nucleostemin (NST) (with indirect FITC stain; second panel) and actin fibres (direct staining which specifically stained cellular F-actin; third panel) and the merged image of all channels (last panel on the right). Scale bar=50μm (at 100x objective).

GDF5-induced hMSCs showed a reduction in the NST expression, which is parallel with the cytoskeletal reorganization. This finding suggests that the proliferation of hMSCs was reduced upon tenogenic differentiations.

5.3.2.3 Gene Expression Validation with QuantiGene® Plex 2.0 Assay

In order to validate the gene expression profiling results from microarray analysis, selected candidate tenogenic marker and non-tenogenic marker genes were quantified using QuantiGene® Plex 2.0 Assay (n=6). Among the 12 targets measured, only 9 targets were detected above the limit of detection (LOD). Three targets (*Col2a1*, *Figf* and *Tnmd*) were detected as absent calls in all the samples, hence were excluded from fold change analysis. The rest of the other 9 targets were detected in all the samples (all the 6 samples in each group), except *Scx* and *Mmp3* were only detected in 3 samples among the 6 samples measured (Figure 5.9).

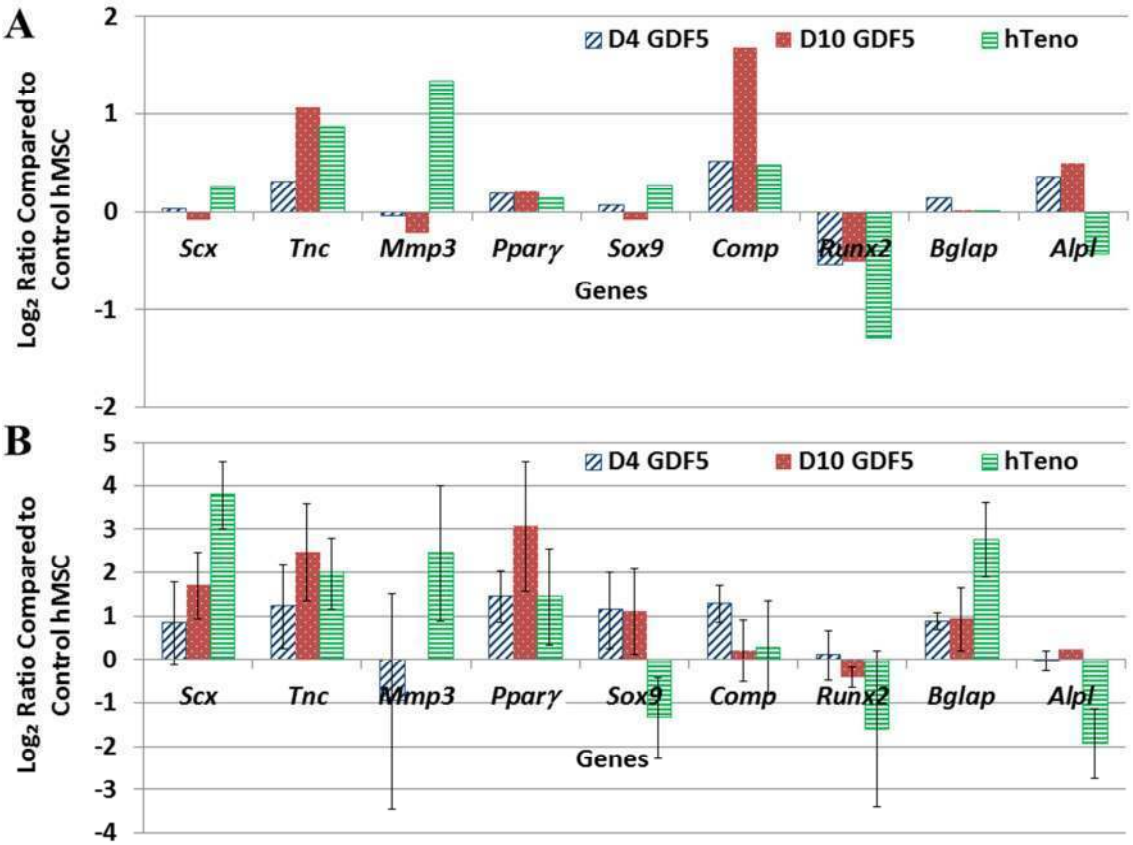

Figure 5.9 Expression levels of selected candidate tenogenic and non-tenogenic marker genes (n=9) based on microarray and QuantiGene® Plex 2.0 Assay.

Figure 5.9, continued

(A) The graphical representation of genes expression patterns in hMSCs in response to induction by GDF5; with their respective $\log_2$ ratio based on microarray analysis.
(B) Gene expression profiles independently validated using QuantiGene® Plex assay presented in $\log_2$ ratio. Expression variation for each gene was visualized with standard deviation.

The gene expression levels detected with QuantiGene® Plex assay was relatively higher compared to that of microarray analysis. Overall, the gene expression profiles obtained from QuantiGene® Plex assay were consistent with the microarray results in *Tnc*, *Mmp3*, *Runx2* and *Alpl*, but showed some differences in the expression profiles for *Scx*, *Pparγ*, *Sox9*, *Comp* and *Bglap*. Considering that *Scx* and *Mmp3* were derived from three biological samples compared to that of microarray which was derived from six bioloigical samples, the variation in the expression profiles was not unexpected. Whereas the *Pparγ*, *Sox9* and *Bglap* were all weakly expressed genes, thus the differences detected may result from the detection limit and sensitivity of the different platforms, which subsequently affected interplatform reproducibility of differentially expressed genes. Nonetheless, the discordant results could also be due to the probes (for each quantitative platform used) were probing different sequence locations in the genes (in *Pparγ*, *Sox9* and *Bglap)*. This discordant gene expression data, however, could only be minimized if probes of different platforms are custom designed to detect the same location of the genes. From these results, collectively, the microarray data has been validated with the QuantiGene® Plex assay thus supporting the use and interpretation of expression profiles and pathways information based on the microarray results.

5.4 Discussion

Herein, the molecular signalling pathways regulated during GDF5-induced tenogenesis were identified. Firstly, the top differentially expressed genes in GDF5-induced hMSCs and tenocytes were identified, i.e. ASPN, ARHGAP29 and CCL2 were the up-regulated genes; ENO2, STC1, ACAN, C7orf69, NEFM and ITGA8 were the consistently down-regulated in GDF5-induced hMSCs and tenocytes. Secondly, through the global gene expression profiles analysis, several pathways were identified as important pathways for tenogenesis: (i) the glycolysis and gluconeogenesis signalling pathways were down regulated upon GDF5 treatment in hMSC and in tenocytes; (ii)The cell cycle related signalling pathways were also down-regulated in the day-10 GDF5-induced hMSCs; (iii) The activated pathways which may be crucial in tenogenesis were angiopoietin-Tie2 signalling, TGF-beta-dependent induction of EMT via SMADS signalling, PEDF signalling and VEGF signalling via VEGFR2; (iii) The cell adhesion and cytoskeleton remodelling signalling pathways were identified as important pathways at the late tenogenic differentiation stage or in mature tenocytes; (iv) the EMT pathway is identified as the putative pathway which is involved in GDF5-induced tenogenesis. Thirdly, among the candidate tenogenic marker genes, *Col-I*, *Col-III* and *Tnc* were up-regulated in the day-10 GDF5-induced hMSCs; while the *Runx2* was the down-regulated non-tenogenic marker genes. Contradictory, *Comp* was also up-regulated in day-10 GDF5-induced hMSCs. Fourthly, the AFM and fluorescence imaging evidence the cytoskeletal remodelling events in the GDF5-induced hMSCs. Fifthly, a reduction in the proliferation of GDF5-induced hMSCs was evidenced by reduced NST expression in GDF5-induced hMSCs. Lastly, the QuantiGene® Plex 2.0 Assay validated the expression of the candidate tenogenic and non-tenogenic marker genes and showed consistent results with microarray analysis, except: (i) the *Pparγ* which was detected weakly expressed in all groups in microarray analysis, was detected

as up-regulated in the day-10 GDF5-induced group; (ii) the *Comp* were detected as up-regulated in day-4 GDF5-induced hMSCs compared to weakly expressed as detected in microarray analysis; and (iii) the *Bglap* were detected as up-regulated in tenocytes compared to weakly expressed as detected in microarray analysis.

Aspn is among the top up-regulated transcript which co-expressed in the GDF5-induced hMSCs and in tenocytes. This gene has been reported as one of the top molecular markers expressed in human mature tendon (Jelinsky et al., 2010). Thus, *Aspn* may play a crucial role from the early tenogenesis to the late mature tenocyte. In contrary to the occurrence in mature tendon, the *Aspn* has also been demonstrated with a role in osteoblast-driven collagen mineralization, which increases the *Osterix* and *Runx2* expression (Kalamajski et al., 2009). However, in this current study, the expression of *Runx2* was not up-regulated, suggesting that the asporin might play other role in the GDF5-induced hMSCs rather than promoting the osteoblastic function. Further, asporin has been reported as a negative regulator of TGF-β in cartilage, which inhibits TGF-β-induced expression of cartilage matrix genes in ATDC5 cells (Kizawa et al., 2005), and in *in vitro* mouse model for chondrogenesis (Shukunami et al., 1997; Shukunami et al., 1996). Conversely, in articular cartilage cells, knockdown of asporin increases the expression of cartilage markers and TGF-β1; in turn, TGF-β1 stimulates asporin expression; which suggested the asporin and TGF-β1 form a regulatory feedback loop (Nakajima et al., 2007). The high abundance of asporin expression detected in the GDF5-induced hMSCs and tenocytes may thus play a role to suppress the chondrogenic phenotype while promoting the tenogenic expression, i.e. *Tnc* expression, in the differentiating hMSCs.

A previous study reported in human tendon found that *Thbs4, Tnmd*, *Dcn* and *Mkx* were among the top molecular markers of mature human tendon (Jelinsky, et al., 2010). Consistent to that reported by Jelinsky and colleagues (2010), this current

experiment also found *Thbs4* and *Mkx* as the top most up-regulated transcripts in tenocytes, apart from *Aspn*. However, the *Thbs4* and *Mkx* were not up-regulated in the GDF5-induced hMSCs. Previous study in murine mesenchymal stem cell line C3H10T1/2 (clone 8) reported that an unknown mechanism, which associated with BMP type I receptor (BMPR-I i.e. ALK3), is involved in inhibiting BMP12-induced *Thbs4* mRNA expression (Berasi et al., 2011). Therefore, it is suggested that a similar BMPR-mediated signalling may be involved and resulted in the low mRNA expression of *Thbs4* in the GDF5-induced hMSCs. In addition, it has been reported that an establishment of the muscle-tendon junction is required for the elevated level of *Thbs4* in tendon cells (Charvet et al., 2012). The *Mkx* is a late tenogenic marker, which will only be elevated in mature tenocyte (Ito et al., 2010; Liu et al., 2010), hence, not up-regulated in the GDF5-induced tenogenic hMSCs.

Cytoskeletal remodelling signalling and cell adhesion signalling were identified as essential signalling pathways for hMSCs tenogenic differentiation, particularly in the expression of the earliest tenogenic markers in hMSC. Development of the cellular cytoskeleton during the tenogenic differentiation has been shown by previous study in uniaxial-cyclic-stretched hMSCs, with observations of actin stress fibers in the stretched hMSCs (Morita et al., 2012). This effect however, was also observed in this current experiment in the GDF5-induced hMSCs. Therefore, it is suggested that the cytoskeleton remodelling is an essential event in tenogenesis and for the tenocyte phenotypic expression.

In the event of tenogenesis, the proliferation of hMSCs was reduced as evidenced with the reduced in NST expression in hMSCs undergoing tenogenesis. This finding is therefore relevant to the pathway analysis which demonstrated a down-regulation in the cell cycle related signalling pathways in the GDF5-induced hMSCs. The available evidence reported that growth arrest in G_1 phase of the cell cycle is

associated with expression of the differentiated phenotype in many cell types (Hong & Yaffe, 2006; Nadal-Ginard, 1978). Hence, it is suggested that a temporal coupling of cell cycle arrest and terminal differentiation occurs during the tenogenic differentiation in hMSCs. However, a more comprehensive study is required in order to show how the temporal and reciprocal coordination of cell-cycle arrest and tenogenic differentiation is achieved. This would subsequently contribute to the identification of known developmental regulators or pathways that directly link these two events, particularly in hMSC tenogenic differentiation.

5.4.1 Study Limitation

A possible limitation of this study model is that the hMSCs derived from the elderly donors (bone marrow donor) were compared to the tenocytes derived from the young donors (hamstring tendon donors). While this current study being invaluable in the understanding of the molecular mechanisms in human MSCs tenogenesis, it remain unknown whether the similar observation would be seen if hMSCs and tenocytes derived from the young donors of same age group were used. The bone marrow samples collected in this study were obtained from the patients undergoing intramedullary nailing, which majority of them were from elderly group. It has been reported that the cells from aged population may have reduced ability to self-renew and differentiate (Kretlow et al., 2008; Roobrouck et al., 2008). However, in this study, the MSCs derived from elderly donors were not compared to the tenocytes derived from the aged donors. This alludes to the observation of inferior cell biological characteristics in tenocytes derived from elderly donors (Klatte-Schulz et al., 2012). Thus, support the use of tenocytes from young donors for a better positive control cells, albeit the use the hMSCs from the elderly donors for tenogenic differentiation experiments. Thereby, this *in vitro* model is useful for the understanding of MSC tenogenesis.

Another possible limitation in this current experiment is that the assessment of cytoskeleton rearrangement by CLSM were not conducted on the same area or same sample scanned by AFM. Ideally, a better experimental approach to evidence the AFM topography results is to assess the same area scanned by AFM for CLSM imaging. However, due to the limitation in the equipment used in the current experiment, the assessment of cytoskeleton rearrangement on the same cell or same scanned area by the AFM was not possible. Nevertheless, the samples independently prepared for AFM and CLSM in the current experiment allowed an independent validation of AFM results by CLSM. Further, the independent sample preparation for AFM and CLSM imaging allowed the advantages of minimally prepared cultured cells (i.e. without any staining) to be used for AFM live cell imaging, hence reflected closer to the physiological condition. Nonetheless, the AFM instrument used for live cells imaging in this study, does not have the analysis module for quantifying or measuring the cellular elasticity, which would otherwise greatly improve the strength of the AFM imaging data, especially in evaluating the changes in cytoskeleton organization.

5.5 Summary

In conclusion, this study shed light on the possible signalling pathways involved in GDF5-induced hMSC tenogenesis and showed that the cytoskeleton remodelling occurred in the early tenogenic differentiation parallel with a reduction in cell proliferation. The top most up- or down- regulated genes identified in early tenogenenic hMSCs or in late mature tenocytes can potentially to be used as molecular markers in future studies related to tenogenic differentiation. Nevertheless, much remains to be explored about the tenogenesis events in hMSCs, for instance, the cell adhesion force change during the MSC-to-tenocyte differentiation.

CHAPTER 6

DISCUSSION

6.0 DISCUSSION

6.1 Summary of the Findings

Collectively, this study consists of three main parts. Firstly, the *in vitro* study of tenogenic inducing effects of GDF5 in hMSCs and rbMSCs was conducted. The cell proliferation experiments showed no significant differences in the cell proliferation rate between the hMSCs cultured at different concentrations of GDF5 (0, 5, 25, 50, 100 and 500 ng/ml). In determining the potential for tenogenic differentiation, the total collagen assays revealed that GDF5 elicited a biphasic response in both hMSCs and rbMSCs at the gradient concentrations tested. The hMSCs cultured at 100 ng/mL of GDF5 demonstrated a significant increase in total collagen levels comparable to that of tenocyte culture ($p<0.05$). On the other hand, despite only showing a significant increase in total collagen level in cultures supplemented with 500 ng/ml of GDF5, rbMSC showed no significant difference to hMSCs at 100 ng/mL of GDF5. Furthermore, hMSCs cultured at 100 ng/mL of GDF5 demonstrated significant up-regulation in the candidate tenogenic marker genes (*Scx*, *Tnc* and *Col-I*; $p<0.05$) whilst a significant down-regulation of the non-tenogenic marker genes (*Runx2* and *Sox 9*; $p<0.05$) at day 7 was observed. Similarly, in rbMSCs, a significant up-regulation in *Scx* and *Col-I* gene expression levels were detected at 100 ng/ml of GDF5. Immunofluorescence staining also revealed an increase in COL-I, TNMD, TNC and SCX expression in day 4 hMSCs and rbMSCs cultures treated with 100 ng/ml of GDF5. However, a significant down-regulation ($p<0.05$) in the *Scx* gene expression levels in rbMSCs at day 27 was detected despite having a significantly persistent *Col-I* up-regulation throughout day 4 to day 27.

Secondly, an *in vivo* pilot study in a rabbit infraspinatus tendon model was conducted to evaluate the potential of using tenogenically differentiated MSCs (TMSC; at the optimized response dosage of 100 ng/mL of GDF5) in clinical applications. H&E

and VG staining revealed significant differences in the quality of repair between the non-cell-based treatment groups (tendons repaired without cells; i.e. suture only, fibrin glue (FG) only, and suture with FG) and the cell-based treatment groups (i.e. tenocytes, MSC and TMSC). The TMSCs treated group displayed more mature tendon healing as compared to that of tenocytes and MSC groups with prominent tendon callus formation. Besides, improved healing in TMSC was also evidenced by cells with more elongated nuclei aligned parallel to the collagen fibers which more resemble histological appearance of the normal tendon tissue. In addition, the collagen fibers in the TMSC group were in highly organized orientation which showed that the tendons were at the late stage of healing process. Further analysis by comparing the gene expressions and protein expressions in cell-based treatment groups showed augmented gene expression levels (*Scx* and *Col-I*) and higher intensity in protein expression (COL-I, SCX, TNC and TNMD) in the tendon repaired with TMSC.

Lastly, the differentially expressed genes between the control hMSCs (G1) and hMSCs cultured at 100 ng/mL GDF5 for 4 days (G2), hMSCs cultured at 100 ng/mL GDF5 at 10 days (G3), and native tenocyte cultures (G4) were identified and the signaling pathways potentially involved in tenogenesis events were also identified. In this global gene expression analysis, a list of 27,216 genes was analyzed. Significant differences in 954 (3.51% of the overall human transcriptome) genes were observed at corrected *p*-values (Corr *p*) of less than 0.05 (using Benjamini-Hochberg correction to control the false discovery rate). When these significant gene lists were analyzed with GeneGo Metacore™ Pathway Analysis, these genes were identified to be involved in specific pathways (i.e. cytoskeleton remodeling, cell adhesion, and extracellular matrix related pathways) that are closely related to the native behavior of tenocytes *in vivo* such as the adhesion of tenocytes to the tendon collagen fibers for survival under high tensional loading environment. In addition, several signaling pathways which may be

crucial for tendon development were identified, i.e. development related TGF-β-dependent induction of EMT via SMADs signalling, TGF-β-dependent induction of EMT via RhoA, PI3K and ILK signalling, PEDF signalling, cross-talk between VEGF and angiopoietin 1 signalling pathways. Further, the cytoskeleton remodeling in GDF5-induced hMSCs were evidenced with AFM and CSLM imaging. CSLM also revealed a reduction in NST expression in the differentiating hMSCs which indicated a reduced cell proliferation rate in the GDF5-induced hMSCs. The microarray data was validated with independent QuantiGene® Plex assay thus supporting the use and interpretation of the inferred gene expression profiles and pathways information.

6.2 GDF5-induced Tenogenesis in MSC

The findings of the *in vitro* studies in hMSCs and rbMSCs appeared to be supported by a previous study by Park and colleagues (2010) which demonstrated that at 100 ng/mL of GDF5 there was a significant increase in TNMD and TNC expression at protein level, compared to that of 10 ng/mL or lesser (Park et al., 2010). Further, the biphasic response in the total collagen expression where an observation of a decrease at 25 ng/ml and an increased at 50 ng/ml of GDF5 (Figure 4.3 A), was similar to that reported in bovine chondrocyte COL-I expression at low concentration of GDF5 (Appel et al., 2009). This could possibly be explained as the GDF5 has a biphasic effect in inducing the collagen expression, particularly the COL-I expression, hence promoting differentiation into different phenotypes (chondrocytes and tenocytes) at different concentration levels of GDF5 and there is an alternate exclusion mechanism occurs (when differentiation into one cell fate (i.e. chondrocytes) is blocked, the other (i.e. tenocytes) is adopted). Nevertheless, a more comprehensive study, which includes analysis at protein level, is required in order to evidence this.

In the *q*RT-PCR analysis, the results showed an up-regulation in *Col-I*, *Scx* and *Tnc* gene expression at mRNA levels in day 4 GDF5-induced hMSCs. These genes were continuously up-regulated to day 7 of induction by GDF5, except *Tnc* which showed a down-regulation. However, in comparison to the microarray and the QuantiGene® Plex assay, the *Tnc* expression was up-regulated at day 10 of induction by GDF-5. The temporal expression profile observed in this study was however similar to that observed in a rodent MSC model, which demonstrated a down-regulation of *Tnc* on day 6 upon GDF-5 treatment which eventually increased on day 9 and day 12 (Park, et al., 2010). Since *Tnc* is a late tenogenic marker, hence the up-regulation of this gene in the hMSCs at the latter time point (day 10) is particularly relevant. This finding was consistent to that observed in other study in rodent MSC model (Park, et al., 2010). The increased expression of this gene at a late phase of tendon development has also recently been documented in a study comparing the *Tnc* expression in tendon from the embryonic period to that observed at day 14 postnatal (Liu et al., 2011). The most studied function of *Tnc* is its modulation of cell adhesion and cell spreading (Chiquet-Ehrismann & Tucker, 2004). The up-regulation in the *Tnc* expression may be related to its function in regulating cell shapes through the suppression of focal adhesion kinase and RhoA activity, which both have an influence on the actin cytoskeleton (Chiquet-Ehrismann & Tucker, 2004; Chiquet et al., 2003). It is hypothesized that the up-regulation of the *Tnc* may be involved in releasing tensile stress to avoid overstretching when the hMCS actively reorganized their cytoskeletal or forming the stress fiber upon induction by GDF5.

The increase in *Scx* and *Col-I* gene expression at mRNA level is an expected outcome of tenogenic MSC differentiation process. However, it is interesting to note that *Dcn* expression was not up-regulated during tenogenic differentiation (neither in the qRT-PCR, microarray nor QuantiGene® Plex assay), which may have been related to

the monolayer conditions used in this experiment (Yao et al., 2006). Culture conditions play a critical role in modulating the synthesis, assembly and organization of extracellular matrix components. In a 3D environment, *Dcn* is also able to modulate BMP/TGFβ pathway through interaction with lipoprotein-receptor related protein (Cabello-Verrugio & Brandan, 2007) and regulates matrix organization and mechanical characteristics of the three dimensional collagen matrices (Ferdous et al., 2007). This nonetheless may not be the case in the present study, as previous studies have shown that an increase in *Dcn* expression in monolayer rodent MSC cultures is not unexpected (Park, et al., 2010).

Nevertheless, while this current study has determined the tenogenic phenotype of the GDF5-induced MSCs, it will thus be an important line of future investigation to examine how stable is the GDF5-induced tenogenic MSCs. Are the GDF5-induced MSCs 'permanently' committed to the tenogenic lineage? Will the GDF5-induced tenogenic MSCs undergo trans-differentiation when cultured in the trilineage differentiation medium (i.e. adipogenic, osteogenic and chondrogenic medium)? Would the GDF5-induced MSCs persistently maintain their tenogenic phenotype after the initial treatment with GDF5? In addition, this current study was focused on the gene expression at mRNA level, the expression at protein level was only determined qualitatively with immunostaining analysis. Hence, based on the findings of gene expression analysis at mRNA level of this study, future study should focused and explored further at protein expression analysis, in order to reveal the biological significant of the changes detected in this current study.

6.3 Effect of Tenogenic-MSCs in Tendon Regeneration

The results of the pilot study found significant improvement in tendon defects repaired with TMSC. The tendon callus formation, occurrence of the tenocyte-like cells

with elongated nucleus and collagen fibers in parallel orientation to tendon's long axis were only observed in the TMSC repaired tendon but not in that of the control tendon. This indicates that the injected TMSC were capable of producing tendon matrix, thus may have been integrated into the repair tissue. However, this would require a cell tracking study to further support this finding.

It is plausible that the improved tendon healing observed in the TMSC repair group was resultant from the active involvement of TMSC in tendon healing process, such as, inflammation, proliferation, differentiation and ECM remodeling. When implanted into tendon defect area, the behavior of TMSC at the repair site is postulated directed by a complex set of micro-environment factors (soluble and substrate bound cues in the ECM and intracellular signaling) in the defect area. TMSC eventually participated in tendon repair in two speculative manners: (i) by proliferation to appropriate number of cells and subsequent differentiation into mature tenocytes for tendon healing, and (ii) by mediating the behavior of cells involved in the repair process through paracrine signaling, similar to that previously reported foe MSC in wound healing (Chen et al., 2008b; Wu et al., 2007). It is suggested that TMSC secreted trophic factors that are highly stimulatory to tendon ECM production, i.e. TGFβ (Beredjiklian et al., 2003) and BMP2 (Thomopoulos et al., 2012), which can play a role in regulating differentiation and healing kinetics (Sharma & Snedeker, 2012). However, the interaction between TMSC paracrine signaling and ECM cues and how they affect progenitor cell differentiation at the healing tendon remain to be elucidated.

Paracrine factors plays a crucial role in tenogenic differentiation (Barboni, et al., 2012; Sharma & Snedeker, 2012) and tendon healing (Chen et al., 2008a). Although it remain unclear of the exact paracrine system involved in TMSC induced tendon healing, current study indicated that the TMSC able to improve tendon healing better compared to its counterparts (repair by tenocytes nad undifferentiated MSC). As an

extension from this current study, future study should explore further with the use of a reporter gene system consisting of eGFP for molecular imaging. This ultimately would allow the determination of whether the observed tendon healing occurred due to the differentiation capability of the implanted TMSCs into mature tenocytes or by the secretion of cytokines and chemokines by the implanted TMSC at the repair site. Conversely, the native tenocytes from the surrounding of tendon defect area may release the paracrine factors which influence the implanted TMSC to enhance tendon healing, e.g. by ECM remodelling. Apart from *in vivo* study, this could also possibly be tested in an *in vitro* co-culture system of GDF5-induced MSCs and tenocytes; by seeding one cell type in the transwell chambers and the other in the plate wells, to elucidate the potential mutual or reciprocal effects of these two cell types.

Apart from the paracrine effect, from this current study, question remains that whether or not the FG matrix provides another stimulating effect on the TMSC or tenocytes. Although previous study have shown that FG may be used as an injectable scaffold to deliver more viable cells directly into infacted myocardium (Christman et al., 2004), the effect of the fibrin matrix on the injected TMSCs have not been explored.

6.4 Potential Therapeutic Approaches

The observation from the current temporal experiment indicates that it may be appropriate to utilize the GDF-5 induced hMSC collected at day 4 for further clinical application, in view of the fact that the hMSCs has already been differentiated into tenocytes, as indicated by the significant up-regulation of the candidate tenogenic marker gene and protein expression at this time point.

CHAPTER 7

CONCLUSION

7.0 CONCLUSION

The results of this study demonstrated that the GDF5-induced hMSCs differentiated along the tenogenic lineage as evidenced by the colorimetric assay, qRT-PCR, and immunofluorescent staining. The results of the *in vivo* experiments suggest that GDF5-induced rbMSCs were superior in promoting tendon repair as compared to its counterpart, the undifferentiated rbMSCs and tenocytes. This finding supports the idea that tenogenic differentiated MSC may be a preferred source of cells in cell based therapy for tendon repair in the future. Further, the newly identified high abundant genes in the global gene expression analysis may be used as tenogenic differentiation markers in future studies. The identified signaling pathways which were involved in hMSCs tenogenesis would provide a better understanding of the molecular events in tendon formation. This ultimately may allow enhancement in future tendon treatment strategies.

CHAPTER 8

REFERENCES

8.0 REFERENCES

Acloque, H., Adams, M. S., Fishwick, K., Bronner-Fraser, M., & Nieto, M. A. (2009). Epithelial-mesenchymal transitions: the importance of changing cell state in development and disease. *J Clin Invest, 119*(6), 1438-1449.

Alberton, P., Popov, C., Pragert, M., Kohler, J., Shukunami, C., Schieker, M., et al. (2012). Conversion of human bone marrow-derived mesenchymal stem cells into tendon progenitor cells by ectopic expression of scleraxis. *Stem Cells Dev, 21*(6), 846-858.

Alberts, B., D, B., Lewis, J., Raff, M., Roberts, K., & Watson, J. D. (1994). *Molecular Biology of the Cell* (3rd ed.). New York: Garland Science.

Altman, G. H., Horan, R. L., Lu, H. H., Moreau, J., Martin, I., Richmond, J. C., et al. (2002). Silk matrix for tissue engineered anterior cruciate ligaments. *Biomaterials, 23*(20), 4131-4141.

Amiel, D., Frank, C., Harwood, F., Fronek, J., & Akeson, W. (1984). Tendons and ligaments: a morphological and biochemical comparison. *J Orthop Res, 1*(3), 257-265.

Appel, B., Baumer, J., Eyrich, D., Sarhan, H., Toso, S., Englert, C., et al. (2009). Synergistic effects of growth and differentiation factor-5 (GDF-5) and insulin on expanded chondrocytes in a 3-D environment. *Osteoarthritis Cartilage, 17*(11), 1503-1512.

Arai, F., Hirao, A., Ohmura, M., Sato, H., Matsuoka, S., Takubo, K., et al. (2004). Tie2/angiopoietin-1 signaling regulates hematopoietic stem cell quiescence in the bone marrow niche. *Cell, 118*(2), 149-161.

Aspenberg, P. (2007). Stimulation of tendon repair: mechanical loading, GDFs and platelets. A mini-review. *Int Orthop, 31*(6), 783-789.

Aspenberg, P., & Forslund, C. (1999). Enhanced tendon healing with GDF 5 and 6. *Acta Orthop Scand, 70*(1), 51-54.

Aspenberg, P., & Virchenko, O. (2004). Platelet concentrate injection improves Achilles tendon repair in rats. *Acta Orthop Scand, 75*(1), 93-99.

Aune, A. K., Holm, I., Risberg, M. A., Jensen, H. K., & Steen, H. (2001). Four-strand hamstring tendon autograft compared with patellar tendon-bone autograft for anterior cruciate ligament reconstruction. A randomized study with two-year follow-up. *Am J Sports Med, 29*(6), 722-728.

Awad, H. A., Butler, D. L., Boivin, G. P., Smith, F. N., Malaviya, P., Huibregtse, B., et al. (1999). Autologous mesenchymal stem cell-mediated repair of tendon. *Tissue Eng, 5*(3), 267-277.

Barboni, B., Curini, V., Russo, V., Mauro, A., Di Giacinto, O., Marchisio, M., et al. (2012). Indirect co-culture with tendons or tenocytes can program amniotic epithelial cells towards stepwise tenogenic differentiation. *PLoS One, 7*(2), e30974.

Basile, P., Dadali, T., Jacobson, J., Hasslund, S., Ulrich-Vinther, M., Soballe, K., et al. (2008). Freeze-dried tendon allografts as tissue-engineering scaffolds for Gdf5 gene delivery. *Mol Ther, 16*(3), 466-473.

Becker, U., Nowack, H., Gay, S., & Timpl, R. (1976). Production and specificity of antibodies against the aminoterminal region in type III collagen. *Immunology, 31*(1), 57-65.

Behr, R., Heneweer, C., Viebahn, C., Denker, H. W., & Thie, M. (2005). Epithelial-mesenchymal transition in colonies of rhesus monkey embryonic stem cells: a model for processes involved in gastrulation. *Stem Cells, 23*(6), 805-816.

Beitzel, K., McCarthy, M. B., Cote, M. P., Chowaniec, D., Falcone, L. M., Falcone, J. A., et al. (2012). Rapid isolation of human stem cells (connective progenitor cells) from the distal femur during arthroscopic knee surgery. *Arthroscopy, 28*(1), 74-84.

Benjamin, M., Kaiser, E., & Milz, S. (2008). Structure-function relationships in tendons: a review. *J Anat, 212*(3), 211-228.

Benjamini, Y., & Hochberg, Y. (1995). Controlling the false discovery rate: a practical and powerful approach to multiple testing. *J. Roy. Statist. Soc. Ser. B, 57*(1), 289-300.

Berasi, S. P., Varadarajan, U., Archambault, J., Cain, M., Souza, T. A., Abouzeid, A., et al. (2011). Divergent activities of osteogenic BMP2, and tenogenic BMP12 and BMP13 independent of receptor binding affinities. *Growth Factors, 29*(4), 128-139.

Beredjiklian, P. K., Favata, M., Cartmell, J. S., Flanagan, C. L., Crombleholme, T. M., & Soslowsky, L. J. (2003). Regenerative versus reparative healing in tendon: a study of biomechanical and histological properties in fetal sheep. *Ann Biomed Eng, 31*(10), 1143-1152.

Berenson, M. C., Blevins, F. T., Plaas, A. H., & Vogel, K. G. (1996). Proteoglycans of human rotator cuff tendons. *J Orthop Res, 14*(4), 518-525.

Bernard-Beaubois, K., Hecquet, C., Houcine, O., Hayem, G., & Adolphe, M. (1997). Culture and characterization of juvenile rabbit tenocytes. *Cell Biol Toxicol, 13*(2), 103-113.

Bi, Y., Ehirchiou, D., Kilts, T. M., Inkson, C. A., Embree, M. C., Sonoyama, W., et al. (2007). Identification of tendon stem/progenitor cells and the role of the extracellular matrix in their niche. *Nat Med, 13*(10), 1219-1227.

Bidder, M., Towler, D. A., Gelberman, R. H., & Boyer, M. I. (2000). Expression of mRNA for vascular endothelial growth factor at the repair site of healing canine flexor tendon. *J Orthop Res, 18*(2), 247-252.

Bluteau, G., Julien, M., Magne, D., Mallein-Gerin, F., Weiss, P., Daculsi, G., et al. (2007). VEGF and VEGF receptors are differentially expressed in chondrocytes. *Bone, 40*(3), 568-576.

Boker, W., Yin, Z., Drosse, I., Haasters, F., Rossmann, O., Wierer, M., et al. (2008). Introducing a single-cell-derived human mesenchymal stem cell line expressing hTERT after lentiviral gene transfer. *J Cell Mol Med, 12*(4), 1347-1359.

Bolt, P., Clerk, A. N., Luu, H. H., Kang, Q., Kummer, J. L., Deng, Z. L., et al. (2007). BMP-14 gene therapy increases tendon tensile strength in a rat model of Achilles tendon injury. *J Bone Joint Surg Am, 89*(6), 1315-1320.

Boquest, A. C., & Collas, P. (2012). Obtaining freshly isolated and cultured mesenchymal stem cells from human adipose tissue. *Methods Mol Biol, 879*, 269-278.

Bouck, N. (2002). PEDF: anti-angiogenic guardian of ocular function. *Trends Mol Med, 8*(7), 330-334.

Boyer, M. I. (2005). Flexor tendon biology. *Hand Clin, 21*(2), 159-166.

Boyer, M. I., Goldfarb, C. A., & Gelberman, R. H. (2005). Recent progress in flexor tendon healing. The modulation of tendon healing with rehabilitation variables. *J Hand Ther, 18*(2), 80-85.

Brent, A. E., Braun, T., & Tabin, C. J. (2005). Genetic analysis of interactions between the somitic muscle, cartilage and tendon cell lineages during mouse development. *Development, 132*(3), 515-528.

Brent, A. E., Schweitzer, R., & Tabin, C. J. (2003). A somitic compartment of tendon progenitors. *Cell, 113*(2), 235-248.

Brent, A. E., & Tabin, C. J. (2004). FGF acts directly on the somitic tendon progenitors through the Ets transcription factors Pea3 and Erm to regulate scleraxis expression. *Development, 131*(16), 3885-3896.

Bullough, R., Finnigan, T., Kay, A., Maffulli, N., & Forsyth, N. R. (2008). Tendon repair through stem cell intervention: cellular and molecular approaches. *Disabil Rehabil, 30*(20-22), 1746-1751.

Buxton, P., Edwards, C., Archer, C. W., & Francis-West, P. (2001). Growth/differentiation factor-5 (GDF-5) and skeletal development. *J Bone Joint Surg Am, 83-A Suppl 1*(Pt 1), S23-30.

Cabello-Verrugio, C., & Brandan, E. (2007). A novel modulatory mechanism of transforming growth factor-beta signaling through decorin and LRP-1. *J Biol Chem, 282*(26), 18842-18850.

Canseco, J. A., Kojima, K., Penvose, A. R., Ross, J. D., Obokata, H., Gomoll, A. H., et al. (2012). Effect on Ligament Marker Expression by Direct-Contact Co-culture of Mesenchymal Stem Cells and Anterior Cruciate Ligament Cells. *Tissue Eng Part A, 18*(23-24), 2549-2558.

Caplan, A. I., & Bruder, S. P. (2001). Mesenchymal stem cells: building blocks for molecular medicine in the 21st century. *Trends Mol Med, 7*(6), 259-264.

Chang, S. C., Hoang, B., Thomas, J. T., Vukicevic, S., Luyten, F. P., Ryba, N. J., et al. (1994). Cartilage-derived morphogenetic proteins. New members of the transforming growth factor-beta superfamily predominantly expressed in long bones during human embryonic development. *J Biol Chem, 269*(45), 28227-28234.

Charvet, B., Ruggiero, F., & Le Guellec, D. (2012). The development of the myotendinous junction. A review. *Muscles Ligaments Tendons J, 2*(2), 53-63.

Chen, C. H., Cao, Y., Wu, Y. F., Bais, A. J., Gao, J. S., & Tang, J. B. (2008a). Tendon healing in vivo: gene expression and production of multiple growth factors in early tendon healing period. *J Hand Surg Am, 33*(10), 1834-1842.

Chen, G., Zhang, S. X., & Zhang, Z. Z. (2011a). Over-expression of has2 in synovium-derived mesenchymal stem cells may prevent adhesions following surgery of the digital flexor tendons. *Medic Hypothesis, 76*(3), 314-316.

Chen, J., Xu, J., Wang, A., & Zheng, M. (2009). Scaffolds for tendon and ligament repair: review of the efficacy of commercial products. *Expert Rev Med Devices, 6*(1), 61-73.

Chen, J., Yu, Q., Wu, B., Lin, Z., Pavlos, N. J., Xu, J., et al. (2011b). Autologous tenocyte therapy for experimental Achilles tendinopathy in a rabbit model. *Tissue Eng Part A, 17*(15-16), 2037-2048.

Chen, J. M., Willers, C., Xu, J., Wang, A., & Zheng, M. H. (2007). Autologous tenocyte therapy using porcine-derived bioscaffolds for massive rotator cuff defect in rabbits. *Tissue Eng, 13*(7), 1479-1491.

Chen, L., Tredget, E. E., Wu, P. Y., & Wu, Y. (2008b). Paracrine factors of mesenchymal stem cells recruit macrophages and endothelial lineage cells and enhance wound healing. *PLoS One, 3*(4), e1886.

Cheng, L., Hammond, H., Ye, Z., Zhan, X., & Dravid, G. (2003). Human adult marrow cells support prolonged expansion of human embryonic stem cells in culture. *Stem Cells, 21*(2), 131-142.

Chhabra, A., Tsou, D., Clark, R. T., Gaschen, V., Hunziker, E. B., & Mikic, B. (2003). GDF-5 deficiency in mice delays Achilles tendon healing. *J Orthop Res, 21*(5), 826-835.

Chiquet-Ehrismann, R., & Tucker, R. P. (2004). Connective tissues: signalling by tenascins. *Int J Biochem Cell Biol, 36*(6), 1085-1089.

Chiquet, M., Renedo, A. S., Huber, F., & Fluck, M. (2003). How do fibroblasts translate mechanical signals into changes in extracellular matrix production? *Matrix Biol, 22*(1), 73-80.

Choi, S. A., Lee, J. Y., Wang, K. C., Phi, J. H., Song, S. H., Song, J., et al. (2012). Human adipose tissue-derived mesenchymal stem cells: characteristics and therapeutic potential as cellular vehicles for prodrug gene therapy against brainstem gliomas. *Eur J Cancer, 48*(1), 129-137.

Chong, A. K., Ang, A. D., Goh, J. C., Hui, J. H., Lim, A. Y., Lee, E. H., et al. (2007). Bone marrow-derived mesenchymal stem cells influence early tendon-healing in a rabbit achilles tendon model. *J Bone Joint Surg Am, 89*(1), 74-81.

Christman, K. L., Fok, H. H., Sievers, R. E., Fang, Q., & Lee, R. J. (2004). Fibrin glue alone and skeletal myoblasts in a fibrin scaffold preserve cardiac function after myocardial infarction. *Tissue Eng, 10*(3-4), 403-409.

Cilli, F., Khan, M., Fu, F., & Wang, J. H. (2004). Prostaglandin E2 affects proliferation and collagen synthesis by human patellar tendon fibroblasts. *Clin J Sport Med, 14*(4), 232-236.

Clark, R. T., Johnson, T. L., Schalet, B. J., Davis, L., Gaschen, V., Hunziker, E. B., et al. (2001). GDF-5 deficiency in mice leads to disruption of tail tendon form and function. *Connect Tissue Res, 42*(3), 175-186.

Coleman, C. M., & Tuan, R. S. (2003). Functional role of growth/differentiation factor 5 in chondrogenesis of limb mesenchymal cells. *Mech Dev, 120*(7), 823-836.

Colter, D. C., Class, R., DiGirolamo, C. M., & Prockop, D. J. (2000). Rapid expansion of recycling stem cells in cultures of plastic-adherent cells from human bone marrow. *Proc Natl Acad Sci U S A, 97*(7), 3213-3218.

Colter, D. C., Sekiya, I., & Prockop, D. J. (2001). Identification of a subpopulation of rapidly self-renewing and multipotential adult stem cells in colonies of human marrow stromal cells. *Proc Natl Acad Sci U S A, 98*(14), 7841-7845.

Comley, A. S., & Krishnan, J. (1999). Donor site morbidity after quadriceps tendon harvest for rotator cuff repair. *Aust N Z J Surg, 69*(11), 808-810.

Connell, D., Datir, A., Alyas, F., & Curtis, M. (2009). Treatment of lateral epicondylitis using skin-derived tenocyte-like cells. *Br J Sports Med, 43*(4), 293-298.

Cui, Y., Hackenmiller, R., Berg, L., Jean, F., Nakayama, T., Thomas, G., et al. (2001). The activity and signaling range of mature BMP-4 is regulated by sequential cleavage at two sites within the prodomain of the precursor. *Genes Dev, 15*(21), 2797-2802.

Cui, Y., Jean, F., Thomas, G., & Christian, J. L. (1998). BMP-4 is proteolytically activated by furin and/or PC6 during vertebrate embryonic development. *EMBO J, 17*(16), 4735-4743.

Date, H., Furumatsu, T., Sakoma, Y., Yoshida, A., Hayashi, Y., Abe, N., et al. (2010). GDF-5/7 and bFGF activate integrin alpha2-mediated cellular migration in rabbit ligament fibroblasts. *J Orthop Res, 28*(2), 225-231.

de Malttos Carvalho, A., Alves, A. L. G., de Oliveira, P. G. G., Alvarez, L. E. C., Amorim, R. L., Hussni, C. A., et al. (2011). Use of Adipose Tissue-Derived Mesenchymal Stem Cells for Experimental Tendinitis Therapy in Equines. *J Equine Vet Sci, 31*, 26-34.

Del Bue, M., Ricco, S., Ramoni, R., Conti, V., Gnudi, G., & Grolli, S. (2008). Equine adipose-tissue derived mesenchymal stem cells and platelet concentrates; their association in vitro and in vivo. *Vet Res Comm, 32*(1), 51-55.

Dines, J. S., Weber, L., Razzano, P., Prajapati, R., Timmer, M., Bowman, S., et al. (2007). The effect of growth differentiation factor-5-coated sutures on tendon repair in a rat model. *J Shoulder Elbow Surg, 16*(5 Suppl), S215-221.

Djouad, F., Plence, P., Bony, C., Tropel, P., Apparailly, F., Sany, J., et al. (2003). Immunosuppressive effect of mesenchymal stem cells favors tumor growth in allogeneic animals. *Blood, 102*(10), 3837-3844.

Docheva, D., Hunziker, E. B., Fassler, R., & Brandau, O. (2005). Tenomodulin is necessary for tenocyte proliferation and tendon maturation. *Mol Cell Biol, 25*(2), 699-705.

Docheva, D., Padula, D., Popov, C., Mutschler, W., Clausen-Schaumann, H., & Schieker, M. (2008). Researching into the cellular shape, volume and elasticity of mesenchymal stem cells, osteoblasts and osteosarcoma cells by atomic force microscopy. *J Cell Mol Med, 12*(2), 537-552.

Dominici, M., Le Blanc, K., Mueller, I., Slaper-Cortenbach, I., Marini, F., Krause, D., et al. (2006). Minimal criteria for defining multipotent mesenchymal stromal cells. The International Society for Cellular Therapy position statement. *Cytotherapy, 8*(4), 315-317.

Duance, V. C., Restall, D. J., Beard, H., Bourne, F. J., & Bailey, A. J. (1977). The location of three collagen types in skeletal muscle. *FEBS Lett, 79*(2), 248-252.

Erlacher, L., Ng, C. K., Ullrich, R., Krieger, S., & Luyten, F. P. (1998). Presence of cartilage-derived morphogenetic proteins in articular cartilage and enhancement of matrix replacement in vitro. *Arthritis Rheum, 41*(2), 263-273.

Evans, J. H., & Barbenel, J. C. (1975). Structural and mechanical properties of tendon related to function. *Equine Vet J, 7*(1), 1-8.

Fan, Y., Liu, Z., Zhao, S., Lou, F., Nilsson, S., Ekman, P., et al. (2006). Nucleostemin mRNA is expressed in both normal and malignant renal tissues. *Br J Cancer, 94*(11), 1658-1662.

Farng, E., Urdaneta, A. R., Barba, D., Esmende, S., & McAllister, D. R. (2008). The effects of GDF-5 and uniaxial strain on mesenchymal stem cells in 3-D culture. *Clin Orthop Relat Res, 466*(8), 1930-1937.

Fenwick, S. A., Hazleman, B. L., & Riley, G. P. (2002). The vasculature and its role in the damaged and healing tendon. *Arthritis Res, 4*(4), 252-260.

Ferdous, Z., Wei, V. M., Iozzo, R., Hook, M., & Grande-Allen, K. J. (2007). Decorin-transforming growth factor- interaction regulates matrix organization and mechanical characteristics of three-dimensional collagen matrices. *J Biol Chem, 282*(49), 35887-35898.

Filipak, M., Estervig, D. N., Tzen, C. Y., Minoo, P., Hoerl, B. J., Maercklein, P. B., et al. (1989). Integrated control of proliferation and differentiation of mesenchymal stem cells. *Environ Health Perspect, 80*, 117-125.

Fox, R. R. (1984). The rabbit as a research subject. *The Physiologist, 27*(6), 393-402.

Francis-West, P. H., Abdelfattah, A., Chen, P., Allen, C., Parish, J., Ladher, R., et al. (1999). Mechanisms of GDF-5 action during skeletal development. *Development, 126*(6), 1305-1315.

Frank, C., Shrive, N., Hiraoka, H., Nakamura, N., Kaneda, Y., & Hart, D. (1999). Optimisation of the biology of soft tissue repair. *J Sci Med Sport, 2*(3), 190-210.

Friedenstein, A. J., Deriglasova, U. F., Kulagina, N. N., Panasuk, A. F., Rudakowa, S. F., Luria, E. A., et al. (1974). Precursors for fibroblasts in different populations of hematopoietic cells as detected by the in vitro colony assay method. *Exp Hematol, 2*(2), 83-92.

Fu, W. L., Zhang, J. Y., Fu, X., Duan, X. N., Leung, K. K., Jia, Z. Q., et al. (2012). Comparative study of the biological characteristics of mesenchymal stem cells from bone marrow and peripheral blood of rats. *Tissue Eng Part A, 18*(17-18), 1793-1803.

Fukuta, S., Oyama, M., Kavalkovich, K., Fu, F. H., & Niyibizi, C. (1998). Identification of types II, IX and X collagens at the insertion site of the bovine achilles tendon. *Matrix Biol, 17*(1), 65-73.

Funakoshi, T., Majima, T., Suenaga, N., Iwasaki, N., Yamane, S., & Minami, A. (2006). Rotator cuff regeneration using chitin fabric as an acellular matrix. *J Shoulder Elbow Surg, 15*(1), 112-118.

Funes, J. M., Quintero, M., Henderson, S., Martinez, D., Qureshi, U., Westwood, C., et al. (2007). Transformation of human mesenchymal stem cells increases their dependency on oxidative phosphorylation for energy production. *Proc Natl Acad Sci U S A, 104*(15), 6223-6228.

Fyfe, I., & Stanish, W. D. (1992). The use of eccentric training and stretching in the treatment and prevention of tendon injuries. *Clin Sports Med, 11*(3), 601-624.

Galarneau, L., Loranger, A., Gilbert, S., & Marceau, N. (2007). Keratins modulate hepatic cell adhesion, size and G1/S transition. *Exp Cell Res, 313*(1), 179-194.

Gu, E., Chen, W. Y., Gu, J., Burridge, P., & Wu, J. C. (2012). Molecular imaging of stem cells: tracking survival, biodistribution, tumorigenicity, and immunogenicity. *Theranostics, 2*(4), 335-345.

Gulotta, L. V., Chaudhury, S., & Wiznia, D. (2012). Stem cells for augmenting tendon repair. *Stem Cells Int, 2012*, 291431.

Gupta, R., & Lee, T. Q. (2007). Contributions of the different rabbit models to our understanding of rotator cuff pathology. *J Shoulder Elbow Surg, 16*(5 Suppl), S149-157.

Gurkan, U. A., Cheng, X., Kishore, V., Uquillas, J. A., & Akkus, O. (2010). Comparison of morphology, orientation, and migration of tendon derived fibroblasts and bone marrow stromal cells on electrochemically aligned collagen constructs. *J Biomed Mater Res A, 94*(4), 1070-1079.

Gurtner, G. C., Werner, S., Barrandon, Y., & Longaker, M. T. (2008). Wound repair and regeneration. *Nature, 453*(7193), 314-321.

Harris, M. T., Butler, D. L., Boivin, G. P., Florer, J. B., Schantz, E. J., & Wenstrup, R. J. (2004). Mesenchymal stem cells used for rabbit tendon repair can form ectopic bone and express alkaline phosphatase activity in constructs. *J Orthop Res, 22*(5), 998-1003.

Hass, R., Kasper, C., Bohm, S., & Jacobs, R. (2011). Different populations and sources of human mesenchymal stem cells (MSC): A comparison of adult and neonatal tissue-derived MSC. *Cell Commun Signal, 9*, 12.

Hegedus, E. J., Cook, C., Brennan, M., Wyland, D., Garrison, J. C., & Driesner, D. (2010). Vascularity and tendon pathology in the rotator cuff: a review of literature and implications for rehabilitation and surgery. *Br J Sports Med, 44*(12), 838-847.

Herpin, A., Lelong, C., & Favrel, P. (2004). Transforming growth factor-beta-related proteins: an ancestral and widespread superfamily of cytokines in metazoans. *Dev Comp Immunol, 28*(5), 461-485.

Hess, G. P., Cappiello, W. L., Poole, R. M., & Hunter, S. C. (1989). Prevention and treatment of overuse tendon injuries. *Sports Med, 8*(6), 371-384.

Hibino, N., Hamada, Y., Sairyo, K., Yukata, K., Sano, T., & Yasui, N. (2007). Callus formation during healing of the repaired tendon-bone junction. A rat experimental model. *J Bone Joint Surg Br, 89*(11), 1539-1544.

Hoerstrup, S. P., Kadner, A., Melnitchouk, S., Trojan, A., Eid, K., Tracy, J., et al. (2002). Tissue engineering of functional trileaflet heart valves from human marrow stromal cells. *Circulation, 106*(12 Suppl 1), I143-150.

Hoffmann, A., Pelled, G., Turgeman, G., Eberle, P., Zilberman, Y., Shinar, H., et al. (2006). Neotendon formation induced by manipulation of the Smad8 signalling pathway in mesenchymal stem cells. *J Clin Invest, 116*(4), 940-952.

Hogan, M., Girish, K., James, R., Balian, G., Hurwitz, S., & Chhabra, A. B. (2011). Growth differentiation factor-5 regulation of extracellular matrix gene expression in murine tendon fibroblasts. *J Tissue Eng Regen Med, 5*(3), 191-200.

Hong, J. H., & Yaffe, M. B. (2006). TAZ: a beta-catenin-like molecule that regulates mesenchymal stem cell differentiation. *Cell Cycle, 5*(2), 176-179.

Hotten, G., Neidhardt, H., Jacobowsky, B., & Pohl, J. (1994). Cloning and expression of recombinant human growth/differentiation factor 5. *Biochem Biophys Res Commun, 204*(2), 646-652.

Hotten, G. C., Matsumoto, T., Kimura, M., Bechtold, R. F., Kron, R., Ohara, T., et al. (1996). Recombinant human growth/differentiation factor 5 stimulates mesenchyme aggregation and chondrogenesis responsible for the skeletal development of limbs. *Growth Factors, 13*(1-2), 65-74.

Huang, S., Wang, S., Bian, C., Yang, Z., Zhou, H., Zeng, Y., et al. (2012). Upregulation of miR-22 promotes osteogenic differentiation and inhibits adipogenic differentiation of human adipose tissue-derived mesenchymal stem cells by repressing HDAC6 protein expression. *Stem Cells Dev, 21*(13), 2531-2540.

Iozzo, R. V., & Murdoch, A. D. (1996). Proteoglycans of the extracellular environment: clues from the gene and protein side offer novel perspectives in molecular diversity and function. *FASEB J, 10*(5), 598-614.

Ito, Y., Toriuchi, N., Yoshitaka, T., Ueno-Kudoh, H., Sato, T., Yokoyama, S., et al. (2010). The Mohawk homeobox gene is a critical regulator of tendon differentiation. *Proc Natl Acad Sci U S A, 107*(23), 10538-10542.

Itoh, S., Kanno, S., Gai, Z., Suemoto, H., Kawakatsu, M., Tanishima, H., et al. (2008). Trps1 plays a pivotal role downstream of Gdf5 signaling in promoting chondrogenesis and apoptosis of ATDC5 cells. *Genes Cells, 13*(4), 355-363.

James, R., Kesturu, G., Balian, G., & Chhabra, A. B. (2008). Tendon: biology, biomechanics, repair, growth factors, and evolving treatment options. *J Hand Surg Am, 33*(1), 102-112.

James, R., Kumbar, S. G., Laurencin, C. T., Balian, G., & Chhabra, A. B. (2011). Tendon tissue engineering: adipose-derived stem cell and GDF-5 mediated regeneration using electrospun matrix systems. *Biomed Mater, 6*(2), 025011.

Janmey, P. A. (1991). Mechanical properties of cytoskeletal polymers. *Curr Opin Cell Biol, 3*(1), 4-11.

Jelinsky, S. A., Archambault, J., Li, L., & Seeherman, H. (2010). Tendon-selective genes identified from rat and human musculoskeletal tissues. *J Orthop Res, 28*(3), 289-297.

Joyce, N. C., Harris, D. L., Markov, V., Zhang, Z., & Saitta, B. (2012). Potential of human umbilical cord blood mesenchymal stem cells to heal damaged corneal endothelium. *Mol Vis, 18*, 547-564.

Jozsa, L., Kannus, P., Balint, J. B., & Reffy, A. (1991). Three-dimensional ultrastructure of human tendons. *Acta Anat (Basel), 142*(4), 306-312.

Juncosa-Melvin, N., Boivin, G. P., Gooch, C., Galloway, M. T., West, J. R., Dunn, M. G., et al. (2006). The effect of autologous mesenchymal stem cells on the biomechanics and histology of gel-collagen sponge constructs used for rabbit patellar tendon repair. *Tissue Eng, 12*(2), 369-379.

Kafienah, W., Mistry, S., Williams, C., & Hollander, A. P. (2006). Nucleostemin is a marker of proliferating stromal stem cells in adult human bone marrow. *Stem Cells, 24*(4), 1113-1120.

Kaibuchi, K., Kuroda, S., & Amano, M. (1999). Regulation of the cytoskeleton and cell adhesion by the Rho family GTPases in mammalian cells. *Annu Rev Biochem, 68*, 459-486.

Kaiser, E. (1999). Phospholipase A2: its usefulness in laboratory diagnostics. *Crit Rev Clin Lab Sci, 36*(2), 65-163.

Kalamajski, S., Aspberg, A., Lindblom, K., Heinegard, D., & Oldberg, A. (2009). Asporin competes with decorin for collagen binding, binds calcium and promotes osteoblast collagen mineralization. *Biochem J, 423*(1), 53-59.

Kardon, G. (1998). Muscle and tendon morphogenesis in the avian hind limb. *Development, 125*(20), 4019-4032.

Kassis, I., Zangi, L., Rivkin, R., Levdansky, L., Samuel, S., Marx, G., et al. (2006). Isolation of mesenchymal stem cells from G-CSF-mobilized human peripheral blood using fibrin microbeads. *Bone Marrow Transplant, 37*(10), 967-976.

Ker, E. D., Chu, B., Phillippi, J. A., Gharaibeh, B., Huard, J., Weiss, L. E., et al. (2011). Engineering spatial control of multiple differentiation fates within a stem cell population. *Biomaterials, 32*(13), 3413-3422.

Khan, M. H., Li, Z., & Wang, J. H. (2005). Repeated exposure of tendon to prostaglandin-E2 leads to localized tendon degeneration. *Clin J Sport Med, 15*(1), 27-33.

Kim, J., Shin, J. M., Jeon, Y. J., Chung, H. M., & Chae, J. I. (2012). Proteomic validation of multifunctional molecules in mesenchymal stem cells derived from human bone marrow, umbilical cord blood and peripheral blood. *PLoS One, 7*(5), e32350.

Kirkendall, D. T., & Garrett, W. E. (1997). Function and biomechanics of tendons. *Scand J Med Sci Sports, 7*(2), 62-66.

Kishore, V., Bullock, W., Sun, X., Van Dyke, W. S., & Akkus, O. (2012). Tenogenic differentiation of human MSCs induced by the topography of electrochemically aligned collagen threads. *Biomaterials, 33*(7), 2137-2144.

Kizawa, H., Kou, I., Iida, A., Sudo, A., Miyamoto, Y., Fukuda, A., et al. (2005). An aspartic acid repeat polymorphism in asporin inhibits chondrogenesis and increases susceptibility to osteoarthritis. *Nat Genet, 37*(2), 138-144.

Kjaer, M. (2004). Role of extracellular matrix in adaptation of tendon and skeletal muscle to mechanical loading. *Physiol Rev, 84*(2), 649-698.

Klatte-Schulz, F., Pauly, S., Scheibel, M., Greiner, S., Gerhardt, C., Schmidmaier, G., et al. (2012). Influence of age on the cell biological characteristics and the stimulation potential of male human tenocyte-like cells. *Eur Cell Mater, 24*, 74-89.

Kolsch, A., Windoffer, R., Wurflinger, T., Aach, T., & Leube, R. E. (2010). The keratin-filament cycle of assembly and disassembly. *J Cell Sci, 123*(Pt 13), 2266-2272.

Kornak, U., & Mundlos, S. (2003). Genetic disorders of the skeleton: a developmental approach. *Am J Hum Genet, 73*(3), 447-474.

Kotzsch, A., Nickel, J., Seher, A., Sebald, W., & Muller, T. D. (2009). Crystal structure analysis reveals a spring-loaded latch as molecular mechanism for GDF-5-type I receptor specificity. *EMBO J, 28*(7), 937-947.

Kretlow, J. D., Jin, Y. Q., Liu, W., Zhang, W. J., Hong, T. H., Zhou, G., et al. (2008). Donor age and cell passage affects differentiation potential of murine bone marrow-derived stem cells. *BMC Cell Biol, 9*, 60.

Kuo, C. K., & Tuan, R. S. (2008). Mechanoactive tenogenic differentiation of human mesenchymal stem cells. *Tissue Eng Part A, 14*(10), 1615-1627.

Lawler, J. (1986). The structural and functional properties of thrombospondin. *Blood, 67*(5), 1197-1209.

Leadbetter, W. B. (1992). Cell-matrix response in tendon injury. *Clin Sports Med, 11*(3), 533-578.

Lee, I. C., Wang, J. H., Lee, Y. T., & Young, T. H. (2007). The differentiation of mesenchymal stem cells by mechanical stress or/and co-culture system. *Biochem Biophys Res Commun, 352*(1), 147-152.

Lee, J. Y., Zhou, Z., Taub, P. J., Ramcharan, M., Li, Y., Akinbiyi, T., et al. (2011). BMP-12 treatment of adult mesenchymal stem cells in vitro augments tendon-like tissue formation and defect repair in vivo. *PLoS One, 6*(3), e17531.

Lejard, V., Brideau, G., Blais, F., Salingcarnboriboon, R., Wagner, G., Roehrl, M. H., et al. (2007). Scleraxis and NFATc regulate the expression of the pro-alpha1(I) collagen gene in tendon fibroblasts. *J Biol Chem, 282*(24), 17665-17675.

Liu, C. F., Aschbacher-Smith, L., Barthelery, N. J., Dyment, N., Butler, D., & Wylie, C. (2011a). What we should know before using tissue engineering techniques to repair injured tendons: a developmental biology perspective. *Tissue Eng Part B Rev, 17*(3), 165-176.

Liu, C. F., Aschbacher-Smith, L., Bathelery, N. J., Dyment, N., Butler, D. L., & Wylie, C. (2011b). Spatial and temporal expression of molecular markers and cell signals during normal development of the mouse patellar tendon. *Tissue Eng Part A*.

Liu, W., Watson, S. S., Lan, Y., Keene, D. R., Ovitt, C. E., Liu, H., et al. (2010). The atypical homeodomain transcription factor Mohawk controls tendon morphogenesis. *Mol Cell Biol, 30*(20), 4797-4807.

Liu, X. B., Jiang, J., Gui, C., Hu, X. Y., Xiang, M. X., & Wang, J. A. (2008). Angiopoietin-1 protects mesenchymal stem cells against serum deprivation and hypoxia-induced apoptosis through the PI3K/Akt pathway. *Acta Pharmacol Sin, 29*(7), 815-822.

Loranger, A., Duclos, S., Grenier, A., Price, J., Wilson-Heiner, M., Baribault, H., et al. (1997). Simple epithelium keratins are required for maintenance of hepatocyte integrity. *Am J Pathol, 151*(6), 1673-1683.

Lorda-Diez, C. I., Montero, J. A., Martinez-Cue, C., Garcia-Porrero, J. A., & Hurle, J. M. (2009). Transforming growth factors beta coordinate cartilage and tendon differentiation in the developing limb mesenchyme. *J Biol Chem, 284*(43), 29988-29996.

Luo, Q., Song, G., Song, Y., Xu, B., Qin, J., & Shi, Y. (2009). Indirect co-culture with tenocytes promotes proliferation and mRNA expression of tendon/ligament related genes in rat bone marrow mesenchymal stem cells. *Cytotechnology, 61*(1-2), 1-10.

Luyten, F. P. (1997). Cartilage-derived morphogenetic protein-1. *Int J Biochem Cell Biol, 29*(11), 1241-1244.

Maffulli, N., Ewen, S. W., Waterston, S. W., Reaper, J., & Barrass, V. (2000). Tenocytes from ruptured and tendinopathic achilles tendons produce greater quantities of type III collagen than tenocytes from normal achilles tendons. An in vitro model of human tendon healing. *Am J Sports Med, 28*(4), 499-505.

Maffulli, N., Longo, U. G., Maffulli, G. D., Khanna, A., & Denaro, V. (2011). Achilles tendon ruptures in diabetic patients. *Arch Orthop Trauma Surg, 131*(1), 33-38.

Manojlovic, Z., & Stefanovic, B. (2012). A novel role of RNA helicase A in regulation of translation of type I collagen mRNAs. *RNA, 18*(2), 321-334.

Mazzocca, A. D., McCarthy, M. B., Chowaniec, D., Cote, M. P., Judson, C. H., Apostolakos, J., et al. (2011). Bone marrow-derived mesenchymal stem cells obtained during arthroscopic rotator cuff repair surgery show potential for tendon cell differentiation after treatment with insulin. *Arthroscopy, 27*(11), 1459-1471.

Mehr, D., Pardubsky, P. D., Martin, J. A., & Buckwalter, J. A. (2000). Tenascin-C in tendon regions subjected to compression. *J Orthop Res, 18*(4), 537-545.

Mienaltowski, M. J., Adams, S. M., & Birk, D. E. (2013). Regional differences in stem cell/progenitor cell populations from the mouse achilles tendon. *Tissue Eng Part A, 19*(1-2), 199-210.

Mikic, B., Rossmeier, K., & Bierwert, L. (2009). Sexual dimorphism in the effect of GDF-6 deficiency on murine tendon. *J Orthop Res, 27*(12), 1603-1611.

Mikic, B., Schalet, B. J., Clark, R. T., Gaschen, V., & Hunziker, E. B. (2001). GDF-5 deficiency in mice alters the ultrastructure, mechanical properties and composition of the Achilles tendon. *J Orthop Res, 19*(3), 365-371.

Miller, R. R., & McDevitt, C. A. (1991). Thrombospondin in ligament, meniscus and intervertebral disc. *Biochim Biophys Acta, 1115*(1), 85-88.

Minami, A., Ishii, S., Ogino, T., Oikawa, T., & Kobayashi, H. (1982). Effect of the immunological antigenicity of the allogeneic tendons on tendon grafting. *Hand, 14*(2), 111-119.

Moon, S. Y., & Zheng, Y. (2003). Rho GTPase-activating proteins in cell regulation. *Trends Cell Biol, 13*(1), 13-22.

Morita, Y., Mukai, T., Ju, Y., & Watanabe, S. (2012). Evaluation of Stem Cell-to-Tenocyte Differentiation By Atomic Force Microscopy to Measure Cellular Elastic Moduli. *Cell Biochem Biophys*.

Morotome, Y., Goseki-Sone, M., Ishikawa, I., & Oida, S. (1998). Gene expression of growth and differentiation factors-5, -6, and -7 in developing bovine tooth at the root forming stage. *Biochem Biophys Res Commun, 244*(1), 85-90.

Moutsatsos, I. K., Turgeman, G., Zhou, S., Kurkalli, B. G., Pelled, G., Tzur, L., et al. (2001). Exogenously regulated stem cell-mediated gene therapy for bone regeneration. *Mol Ther, 3*(4), 449-461.

Myster, D. L., & Duronio, R. J. (2000). To differentiate or not to differentiate? *Curr Biol, 10*(8), R302-304.

Nadal-Ginard, B. (1978). Commitment, fusion and biochemical differentiation of a myogenic cell line in the absence of DNA synthesis. *Cell, 15*(3), 855-864.

Nakajima, M., Kizawa, H., Saitoh, M., Kou, I., Miyazono, K., & Ikegawa, S. (2007). Mechanisms for asporin function and regulation in articular cartilage. *J Biol Chem, 282*(44), 32185-32192.

Nakamura, K., Shirai, T., Morishita, S., Uchida, S., Saeki-Miura, K., & Makishima, F. (1999). p38 mitogen-activated protein kinase functionally contributes to chondrogenesis induced by growth/differentiation factor-5 in ATDC5 cells. *Exp Cell Res, 250*(2), 351-363.

Nellas, Z. J., Loder, B. G., & Wertheimer, S. J. (1996). Reconstruction of an Achilles tendon defect utilizing an Achilles tendon allograft. *J Foot Ankle Surg, 35*(2), 144-148.

Neuhuber, B., Swanger, S. A., Howard, L., Mackay, A., & Fischer, I. (2008). Effects of plating density and culture time on bone marrow stromal cell characteristics. *Exp Hematol, 36*(9), 1176-1185.

Nickel, J., Kotzsch, A., Sebald, W., & Mueller, T. D. (2005). A single residue of GDF-5 defines binding specificity to BMP receptor IB. *J Mol Biol, 349*(5), 933-947.

Nishitoh, H., Ichijo, H., Kimura, M., Matsumoto, T., Makishima, F., Yamaguchi, A., et al. (1996). Identification of type I and type II serine/threonine kinase receptors for growth/differentiation factor-5. *J Biol Chem, 271*(35), 21345-21352.

Nishiwaki, S., Nakayama, T., Saito, S., Mizuno, H., Ozaki, T., Takahashi, Y., et al. (2012). Efficacy and safety of human adipose tissue-derived mesenchymal stem cells for supporting hematopoiesis. *Int J Hematol, 96*(3), 295-300.

Nobes, C. D., & Hall, A. (1995). Rho, rac, and cdc42 GTPases regulate the assembly of multimolecular focal complexes associated with actin stress fibers, lamellipodia, and filopodia. *Cell, 81*(1), 53-62.

Nutton, R. W., McLean, I., & Melville, E. (1999). Tendon allografts in knee ligament surgery. *J R Coll Surg Edinb, 44*(4), 236-240.

O'Brien, M. (1992). Functional anatomy and physiology of tendons. *Clin Sports Med, 11*(3), 505-520.

Orlandini, M., Spreafico, A., Bardelli, M., Rocchigiani, M., Salameh, A., Nucciotti, S., et al. (2006). Vascular endothelial growth factor-D activates VEGFR-3 expressed in osteoblasts inducing their differentiation. *J Biol Chem, 281*(26), 17961-17967.

Oshima, Y., Shukunami, C., Honda, J., Nishida, K., Tashiro, F., Miyazaki, J., et al. (2003). Expression and localization of tenomodulin, a transmembrane type chondromodulin-I-related angiogenesis inhibitor, in mouse eyes. *Invest Ophthalmol Vis Sci, 44*(5), 1814-1823.

Ouyang, H. W., Goh, J. C., Thambyah, A., Teoh, S. H., & Lee, E. H. (2003). Knitted poly-lactide-co-glycolide scaffold loaded with bone marrow stromal cells in repair and regeneration of rabbit Achilles tendon. *Tissue Eng, 9*(3), 431-439.

Owen, T. A., Aronow, M., Shalhoub, V., Barone, L. M., Wilming, L., Tassinari, M. S., et al. (1990). Progressive development of the rat osteoblast phenotype in vitro: reciprocal relationships in expression of genes associated with osteoblast proliferation and differentiation during formation of the bone extracellular matrix. *J Cell Physiol, 143*(3), 420-430.

Pacini, S., Spinabella, S., Trombi, L., Fazzi, R., Galimberti, S., Dini, F., et al. (2007). Suspension of bone marrow-derived undifferentiated mesenchymal stromal cells for repair of superficial digital flexor tendon in race horses. *Tissue Eng, 13*(12), 2949-2955.

Park, A., Hogan, M. V., Kesturu, G. S., James, R., Balian, G., & Chhabra, A. B. (2010). Adipose-derived mesenchymal stem cells treated with growth differentiation factor-5 express tendon-specific markers. *Tissue Eng Part A, 16*(9), 2941-2951.

Pfaffl, M. W. (2001). A new mathematical model for relative quantification in real-time RT-PCR. *Nucleic Acids Res, 29*(9), e45.

Pierini, M., Dozza, B., Lucarelli, E., Tazzari, P. L., Ricci, F., Remondini, D., et al. (2012). Efficient isolation and enrichment of mesenchymal stem cells from bone marrow. *Cytotherapy, 14*(6), 686-693.

Platt, M. O., Wilder, C. L., Wells, A., Griffith, L. G., & Lauffenburger, D. A. (2009). Multipathway kinase signatures of multipotent stromal cells are predictive for osteogenic differentiation: tissue-specific stem cells. *Stem Cells, 27*(11), 2804-2814.

Prime, S. S., Pring, M., Davies, M., & Paterson, I. C. (2004). TGF-beta signal transduction in oro-facial health and non-malignant disease (part I). *Crit Rev Oral Biol Med, 15*(6), 324-336.

Prockop, D. J. (2007). "Stemness" does not explain the repair of many tissues by mesenchymal stem/multipotent stromal cells (MSCs). *Clin Pharmacol Ther, 82*(3), 241-243.

Provenzano, P. P., & Vanderby, R., Jr. (2006). Collagen fibril morphology and organization: implications for force transmission in ligament and tendon. *Matrix Biol, 25*(2), 71-84.

Pryce, B. A., Watson, S. S., Murchison, N. D., Staverosky, J. A., Dunker, N., & Schweitzer, R. (2009). Recruitment and maintenance of tendon progenitors by TGFbeta signaling are essential for tendon formation. *Development, 136*(8), 1351-1361.

Radmacher, M., Tillamnn, R. W., Fritz, M., & Gaub, H. E. (1992). From molecules to cells: imaging soft samples with the atomic force microscope. *Science, 257*(5078), 1900-1905.

Rees, S. G., Flannery, C. R., Little, C. B., Hughes, C. E., Caterson, B., & Dent, C. M. (2000). Catabolism of aggrecan, decorin and biglycan in tendon. *Biochem J, 350 Pt 1*, 181-188.

Ridley, A. J., & Hall, A. (1992). The small GTP-binding protein rho regulates the assembly of focal adhesions and actin stress fibers in response to growth factors. *Cell, 70*(3), 389-399.

Riley, G. P., Harrall, R. L., Constant, C. R., Chard, M. D., Cawston, T. E., & Hazleman, B. L. (1994a). Glycosaminoglycans of human rotator cuff tendons: changes with age and in chronic rotator cuff tendinitis. *Ann Rheum Dis, 53*(6), 367-376.

Riley, G. P., Harrall, R. L., Constant, C. R., Chard, M. D., Cawston, T. E., & Hazleman, B. L. (1994b). Tendon degeneration and chronic shoulder pain: changes in the collagen composition of the human rotator cuff tendons in rotator cuff tendinitis. *Ann Rheum Dis, 53*(6), 359-366.

Rodrigues, M., Griffith, L. G., & Wells, A. (2010). Growth factor regulation of proliferation and survival of multipotential stromal cells. *Stem Cell Res Ther, 1*(4), 32.

Rodriguez, J. P., Gonzalez, M., Rios, S., & Cambiazo, V. (2004). Cytoskeletal organization of human mesenchymal stem cells (MSC) changes during their osteogenic differentiation. *J Cell Biochem, 93*(4), 721-731.

Roelen, B. A., & Dijke, P. (2003). Controlling mesenchymal stem cell differentiation by TGFBeta family members. *J Orthop Sci, 8*(5), 740-748.

Romanova, L., Grand, A., Zhang, L., Rayner, S., Katoku-Kikyo, N., Kellner, S., et al. (2009). Critical role of nucleostemin in pre-rRNA processing. *J Biol Chem, 284*(8), 4968-4977.

Roobrouck, V. D., Ulloa-Montoya, F., & Verfaillie, C. M. (2008). Self-renewal and differentiation capacity of young and aged stem cells. *Exp Cell Res, 314*(9), 1937-1944.

Rosenbaum, A. J., Grande, D. A., & Dines, J. S. (2008). The use of mesenchymal stem cells in tissue engineering. A global assessment. *Organogenesis, 4*(1), 23-27.

Roufosse, C. A., Direkze, N. C., Otto, W. R., & Wright, N. A. (2004). Circulating mesenchymal stem cells. *Int J Biochem Cell Biol, 36*(4), 585-597.

Rui, Y. F., Lui, P. P., Li, G., Fu, S. C., Lee, Y. W., & Chan, K. M. (2010). Isolation and characterization of multipotent rat tendon-derived stem cells. *Tissue Eng Part A, 16*(5), 1549-1558.

Sahoo, S., Ang, L. T., Cho-Hong Goh, J., & Toh, S. L. (2010). Bioactive nanofibers for fibroblastic differentiation of mesenchymal precursor cells for ligament/tendon tissue engineering applications. *Differentiation, 79*(2), 102-110.

Saiga, K., Furumatsu, T., Yoshida, A., Masuda, S., Takihira, S., Abe, N., et al. (2010). Combined use of bFGF and GDF-5 enhances the healing of medial collateral ligament injury. *Biochem Biophys Res Commun, 402*(2), 329-334.

Saka, Y., Furuhashi, K., Katsuno, T., Kim, H., Ozaki, T., Iwasaki, K., et al. (2011). Adipose-derived stromal cells cultured in a low-serum medium, but not bone marrow-derived stromal cells, impede xenoantibody production. *Xenotransplantation, 18*(3), 196-208.

Schellenberg, A., Lin, Q., Schuler, H., Koch, C. M., Joussen, S., Denecke, B., et al. (2011). Replicative senescence of mesenchymal stem cells causes DNA-methylation changes which correlate with repressive histone marks. *Aging (Albany NY), 3*(9), 873-888.

Schnabel, L. V., Lynch, M. E., van der Meulen, M. C., Yeager, A. E., Kornatowski, M. A., & Nixon, A. J. (2009). Mesenchymal stem cells and insulin-like growth factor-I gene-enhanced mesenchymal stem cells improve structural aspects of healing in equine flexor digitorum superficialis tendons. *J Orthop Res, 27*(10), 1392-1398.

Schneider, P. R., Buhrmann, C., Mobasheri, A., Matis, U., & Shakibaei, M. (2011). Three-dimensional high-density co-culture with primary tenocytes induces tenogenic differentiation in mesenchymal stem cells. *J Orthop Res, 29*(9), 1351-1360.

Schwabe, G. C., & Mundlos, S. (2004). Genetics of congenital hand anomalies. *Handchir Mikrochir Plast Chir, 36*(2-3), 85-97.

Schweitzer, R., Chyung, J. H., Murtaugh, L. C., Brent, A. E., Rosen, V., Olson, E. N., et al. (2001). Analysis of the tendon cell fate using Scleraxis, a specific marker for tendons and ligaments. *Development, 128*(19), 3855-3866.

Schweitzer, R., Zelzer, E., & Volk, T. (2010). Connecting muscles to tendons: tendons and musculoskeletal development in flies and vertebrates. *Development, 137*(17), 2807-2817.

Scott, A., Lian, O., Roberts, C. R., Cook, J. L., Handley, C. J., Bahr, R., et al. (2008). Increased versican content is associated with tendinosis pathology in the patellar tendon of athletes with jumper's knee. *Scand J Med Sci Sports, 18*(4), 427-435.

Seemann, P., Schwappacher, R., Kjaer, K. W., Krakow, D., Lehmann, K., Dawson, K., et al. (2005). Activating and deactivating mutations in the receptor interaction site of GDF5 cause symphalangism or brachydactyly type A2. *J Clin Invest, 115*(9), 2373-2381.

Sekiya, I., Larson, B. L., Smith, J. R., Pochampally, R., Cui, J. G., & Prockop, D. J. (2002). Expansion of human adult stem cells from bone marrow stroma: conditions that maximize the yields of early progenitors and evaluate their quality. *Stem Cells, 20*(6), 530-541.

Settle, S. H., Jr., Rountree, R. B., Sinha, A., Thacker, A., Higgins, K., & Kingsley, D. M. (2003). Multiple joint and skeletal patterning defects caused by single and double mutations in the mouse Gdf6 and Gdf5 genes. *Dev Biol, 254*(1), 116-130.

Sharma, P., & Maffulli, N. (2005). Tendon injury and tendinopathy: healing and repair. *J Bone Joint Surg Am, 87*(1), 187-202.

Sharma, R. I., & Snedeker, J. G. (2010). Biochemical and biomechanical gradients for directed bone marrow stromal cell differentiation toward tendon and bone. *Biomaterials, 31*(30), 7695-7704.

Sharma, R. I., & Snedeker, J. G. (2012). Paracrine interactions between mesenchymal stem cells affect substrate driven differentiation toward tendon and bone phenotypes. *PLoS One, 7*(2), e31504.

Shen, W., Chen, J., Yina, Z., Chen, X., Liua, H., Heng, B. C., et al. (2012). Allogenous tendon stem/progenitor cells in silk scaffold for functional shoulder repair. *Cell Transplant, 21*(5), 943-958.

Shimaoka, H., Dohi, Y., Ohgushi, H., Ikeuchi, M., Okamoto, M., Kudo, A., et al. (2004). Recombinant growth/differentiation factor-5 (GDF-5) stimulates osteogenic differentiation of marrow mesenchymal stem cells in porous hydroxyapatite ceramic. *J Biomed Mater Res A, 68*(1), 168-176.

Shukunami, C., Ishizeki, K., Atsumi, T., Ohta, Y., Suzuki, F., & Hiraki, Y. (1997). Cellular hypertrophy and calcification of embryonal carcinoma-derived chondrogenic cell line ATDC5 in vitro. *J Bone Miner Res, 12*(8), 1174-1188.

Shukunami, C., Oshima, Y., & Hiraki, Y. (2005). Chondromodulin-I and tenomodulin: a new class of tissue-specific angiogenesis inhibitors found in hypovascular connective tissues. *Biochem Biophys Res Commun, 333*(2), 299-307.

Shukunami, C., Shigeno, C., Atsumi, T., Ishizeki, K., Suzuki, F., & Hiraki, Y. (1996). Chondrogenic differentiation of clonal mouse embryonic cell line ATDC5 in vitro: differentiation-dependent gene expression of parathyroid hormone (PTH)/PTH-related peptide receptor. *J Cell Biol, 133*(2), 457-468.

Shukunami, C., Takimoto, A., Oro, M., & Hiraki, Y. (2006). Scleraxis positively regulates the expression of tenomodulin, a differentiation marker of tenocytes. *Dev Biol, 298*(1), 234-247.

Silver, F. H., Freeman, J. W., & Seehra, G. P. (2003). Collagen self-assembly and the development of tendon mechanical properties. *J Biomech, 36*(10), 1529-1553.

Sini, P., Denti, A., Tira, M. E., & Balduini, C. (1997). Role of decorin on in vitro fibrillogenesis of type I collagen. *Glycoconj J, 14*(7), 871-874.

Small, J., Rottner, K., Hahne, P., & Anderson, K. I. (1999). Visualising the actin cytoskeleton. *Microsc Res Tech, 47*(1), 3-17.

Smith, J. R., Pochampally, R., Perry, A., Hsu, S. C., & Prockop, D. J. (2004). Isolation of a highly clonogenic and multipotential subfraction of adult stem cells from bone marrow stroma. *Stem Cells, 22*(5), 823-831.

Smyth, G. K. (2004). Linear models and empirical bayes methods for assessing differential expression in microarray experiments. *Stat Appl Genet Mol Biol, 3*, Article3.

Soslowsky, L. J., Carpenter, J. E., DeBano, C. M., Banerji, I., & Moalli, M. R. (1996). Development and use of an animal model for investigations on rotator cuff disease. *J Shoulder Elbow Surg, 5*(5), 383-392.

Stamatovic, S. M., Keep, R. F., Kunkel, S. L., & Andjelkovic, A. V. (2003). Potential role of MCP-1 in endothelial cell tight junction 'opening': signaling via Rho and Rho kinase. *J Cell Sci, 116*(22), 4615-4628.

Stein, S. R., & Luekens, C. A. (1976). Methods and rationale for closed treatment of Achilles tendon ruptures. *Am J Sports Med, 4*(4), 162-169.

Storm, E. E., Huynh, T. V., Copeland, N. G., Jenkins, N. A., Kingsley, D. M., & Lee, S. J. (1994). Limb alterations in brachypodism mice due to mutations in a new member of the TGF beta-superfamily. *Nature, 368*(6472), 639-643.

Storm, E. E., & Kingsley, D. M. (1999). GDF5 coordinates bone and joint formation during digit development. *Dev Biol, 209*(1), 11-27.

Stripecke, R., Carmen Villacres, M., Skelton, D., Satake, N., Halene, S., & Kohn, D. (1999). Immune response to green fluorescent protein: implications for gene therapy. *Gene Ther, 6*(7), 1305-1312.

Tan, S. L., Ahmad, R. E., Ahmad, T. S., Merican, A. M., Abbas, A. A., Ng, W. M., et al. (2012). Effect of Growth Differentiation Factor 5 on the Proliferation and Tenogenic Differentiation Potential of Human Mesenchymal Stem Cells in vitro. *Cells Tissues Organs, 196*, 325-338.

Tan, S. L., Sulaiman, S., Pingguan-Murphy, B., Selvaratnam, L., Tai, C. C., & Kamarul, T. (2011). Human amnion as a novel cell delivery vehicle for chondrogenic mesenchymal stem cells. *Cell Tissue Bank, 12*(1), 59-70.

Tashiro, T., Hiraoka, H., Ikeda, Y., Ohnuki, T., Suzuki, R., Ochi, T., et al. (2006). Effect of GDF-5 on ligament healing. *J Orthop Res, 24*(1), 71-79.

Taskiran, D., Taskiran, E., Yercan, H., & Kutay, F. Z. (1999). Quantification of Total Collagen in Rabbit Tendon by the Sirius Red Method. *Tr J Med Sci, 29*, 7-9.

Thiery, J. P., Acloque, H., Huang, R. Y., & Nieto, M. A. (2009). Epithelial-mesenchymal transitions in development and disease. *Cell, 139*(5), 871-890.

Thomopoulos, S., Kim, H. M., Silva, M. J., Ntouvali, E., Manning, C. N., Potter, R., et al. (2012). Effect of bone morphogenetic protein 2 on tendon-to-bone healing in a canine flexor tendon model. *J Orthop Res, 30*(11), 1702-1709.

Toma, C., Pittenger, M. F., Cahill, K. S., Byrne, B. J., & Kessler, P. D. (2002). Human mesenchymal stem cells differentiate to a cardiomyocyte phenotype in the adult murine heart. *Circulation, 105*(1), 93-98.

Towler, D. A., & Gelberman, R. H. (2006). The alchemy of tendon repair: a primer for the (S)mad scientist. *J Clin Invest, 116*(4), 863-866.

Van Damme, A., Thorrez, L., Ma, L., Vandenburgh, H., Eyckmans, J., Dell'Accio, F., et al. (2006). Efficient lentiviral transduction and improved engraftment of human bone marrow mesenchymal cells. *Stem Cells, 24*(4), 896-907.

Vangsness, C. T., Jr., Garcia, I. A., Mills, C. R., Kainer, M. A., Roberts, M. R., & Moore, T. M. (2003). Allograft transplantation in the knee: tissue regulation, procurement, processing, and sterilization. *Am J Sports Med, 31*(3), 474-481.

Velling, T., Risteli, J., Wennerberg, K., Mosher, D. F., & Johansson, S. (2002). Polymerization of type I and III collagens is dependent on fibronectin and enhanced by integrins alpha 11beta 1 and alpha 2beta 1. *J Biol Chem, 277*(40), 37377-37381.

Violini, S., Ramelli, P., Pisani, L. F., Gorni, C., & Mariani, P. (2009). Horse bone marrow mesenchymal stem cells express embryo stem cell markers and show the ability for tenogenic differentiation by in vitro exposure to BMP-12. *BMC Cell Biol, 10*, 29.

Vogel, K. G., & Heinegard, D. (1985). Characterization of proteoglycans from adult bovine tendon. *J Biol Chem, 260*(16), 9298-9306.

Waggett, A. D., Ralphs, J. R., Kwan, A. P., Woodnutt, D., & Benjamin, M. (1998). Characterization of collagens and proteoglycans at the insertion of the human Achilles tendon. *Matrix Biol, 16*(8), 457-470.

Wang, J. H. (2000). Substrate deformation determines actin cytoskeleton reorganization: A mathematical modeling and experimental study. *J Theor Biol, 202*(1), 33-41.

Wang, J. H. (2006). Mechanobiology of tendon. *J Biomech, 39*(9), 1563-1582.

Wang, J. H., Goldschmidt-Clermont, P., Wille, J., & Yin, F. C. (2001). Specificity of endothelial cell reorientation in response to cyclic mechanical stretching. *J Biomech, 34*(12), 1563-1572.

Wang, M., Wang, J. J., Li, J., Park, K., Qian, X., Ma, J. X., et al. (2009). Pigment epithelium-derived factor suppresses adipogenesis via inhibition of the MAPK/ERK pathway in 3T3-L1 preadipocytes. *Am J Physiol Endocrinol Metab, 297*(6), E1378-1387.

Wang, Q.-W., Chen, Z.-L., & Piao, Y.-J. (2005). Mesenchymal stem cells differentiate into tenocytes by bone morphogenetic protein (BMP) 12 gene transfer. *J Biosci Bioeng, 100*(4), 418-422.

Warden, S. J. (2007). Animal models for the study of tendinopathy. *Br J Sports Med, 41*(4), 232-240.

Watkins, J. P., Auer, J. A., Gay, S., & Morgan, S. J. (1985). Healing of surgically created defects in the equine superficial digital flexor tendon: collagen-type transformation and tissue morphologic reorganization. *Am J Vet Res, 46*(10), 2091-2096.

Williams, I. F., McCullagh, K. G., & Silver, I. A. (1984). The distribution of types I and III collagen and fibronectin in the healing equine tendon. *Connect Tissue Res, 12*(3-4), 211-227.

Wolfman, N. M., Hattersley, G., Cox, K., Celeste, A. J., Nelson, R., Yamaji, N., et al. (1997). Ectopic induction of tendon and ligament in rats by growth and differentiation factors 5, 6, and 7, members of the TGF-beta gene family. *J Clin Invest, 100*(2), 321-330.

Wu, B., Chen, J., Rosa, T. D., Yu, Q., Wang, A., Xu, J., et al. (2010). Cellular response and extracellular matrix breakdown in rotator cuff tendon rupture. *Arch Orthop Trauma Surg, 131*(3), 405-411.

Wu, Y., Chen, L., Scott, P. G., & Tredget, E. E. (2007). Mesenchymal stem cells enhance wound healing through differentiation and angiogenesis. *Stem Cells, 25*(10), 2648-2659.

Xu, B., Song, G., & Ju, Y. (2011). Effect of focal adhesion kinase on the regulation of realignment and tenogenic differentiation of human mesenchymal stem cells by mechanical stretch. *Connect Tissue Res, 52*(5), 373-379.

Xu, B., Song, G., Ju, Y., Li, X., Song, Y., & Watanabe, S. (2012). RhoA/ROCK, cytoskeletal dynamics, and focal adhesion kinase are required for mechanical stretch-induced tenogenic differentiation of human mesenchymal stem cells. *J Cell Physiol, 227*(6), 2722-2729.

Yamashita, H., Shimizu, A., Kato, M., Nishitoh, H., Ichijo, H., Hanyu, A., et al. (1997). Growth/differentiation factor-5 induces angiogenesis in vivo. *Exp Cell Res, 235*(1), 218-226.

Yang, G., Crawford, R. C., & Wang, J. H. (2004). Proliferation and collagen production of human patellar tendon fibroblasts in response to cyclic uniaxial stretching in serum-free conditions. *J Biomech, 37*(10), 1543-1550.

Yao, L., Bestwick, C. S., Bestwick, L. A., Maffulli, N., & Aspden, R. M. (2006). Phenotypic drift in human tenocyte culture. *Tissue Eng, 12*(7), 1843-1849.

Yin, Z., Chen, X., Chen, J. L., Shen, W. L., Hieu Nguyen, T. M., Gao, L., et al. (2010). The regulation of tendon stem cell differentiation by the alignment of nanofibers. *Biomaterials, 31*(8), 2163-2175.

Yoon, J. H., & Halper, J. (2005). Tendon proteoglycans: biochemistry and function. *J Musculoskelet Neuronal Interact, 5*(1), 22-34.

You, L., Kruse, F. E., Pohl, J., & Volcker, H. E. (1999). Bone morphogenetic proteins and growth and differentiation factors in the human cornea. *Invest Ophthalmol Vis Sci, 40*(2), 296-311.

Yourek, G., Hussain, M. A., & Mao, J. J. (2007). Cytoskeletal changes of mesenchymal stem cells during differentiation. *ASAIO J, 53*(2), 219-228.

Zeng, Q., Li, X., Beck, G., Balian, G., & Shen, F. H. (2007). Growth and differentiation factor-5 (GDF-5) stimulates osteogenic differentiation and increases vascular endothelial growth factor (VEGF) levels in fat-derived stromal cells in vitro. *Bone, 40*(2), 374-381.

Zhang, G., Ezura, Y., Chervoneva, I., Robinson, P. S., Beason, D. P., Carine, E. T., et al. (2006). Decorin regulates assembly of collagen fibrils and acquisition of biomechanical properties during tendon development. *J Cell Biochem, 98*(6), 1436-1449.

Zhang, J., & Wang, J. H. (2010). Platelet-rich plasma releasate promotes differentiation of tendon stem cells into active tenocytes. *Am J Sports Med, 38*(12), 2477-2486.

Zuzarte-Luis, V., Montero, J. A., Rodriguez-Leon, J., Merino, R., Rodriguez-Rey, J. C., & Hurle, J. M. (2004). A new role for BMP5 during limb development acting through the synergic activation of Smad and MAPK pathways. *Dev Biol, 272*(1), 39-52.

CHAPTER 9

APPENDICES

APPENDIX A1

University of Malaya Medical Centre (UMMC) Ethics Approval Letter

JAWATANKUASA ETIKA PERUBATAN
PUSAT PERUBATAN UNIVERSITI MALAYA
ALAMAT: LEMBAH PANTAI, 59100 KUALA LUMPUR, MALAYSIA
TELEFON: 03-79494422 FAKSIMILI: 03-79545682

NAME OF ETHICS COMMITTEE/IRB: Medical Ethics Committee, University Malaya Medical Centre ADDRESS: LEMBAH PANTAI 59100 KUALA LUMPUR	ETHICS COMMITTEE/IRB REFERENCE NUMBER: 602.22
PROTOCOL NO: UM-009-07 TITLE: The Investigation Of Rotator Cuff Tendionpathies In Human And Determining The Feasibility Of Using Tissue Engineering Methods Using Outologous Fibroblast And Mesenchymal Stem Cells For The Repair Of Rotator Cuff Tears.	
PRINCIPAL INVESTIGATOR: Dr. Tunku Kamarul Zaman b Tunku Zainol Abidin TELEPHONE: KOMTEL:	SPONSOR:

The following item [✓] have been received and reviewed in connection with the above study to be conducted by the above investigator.

[✓] Borang Permohonan Pindaan Penyelidikan	Ver date: 7 July 2007
[ ] Protocol Amendment	Ver date:
[ ] Investigator's Brochure	Ver date:
[✓] Consent Form for Patients and their relatives	Ver date:
[✓] Patient Information Sheet	Ver date:
[ ] Advertisement/Payment & Compensation to Subjects	Ver date:
[ ] Investigator(s) CV's (if applicable)	

and have been [✓]

[✓] Approved
[ ] Conditionally approved (identify item and specify modification below or in accompanying letter)
[ ] Rejected (identify item and specify reasons below or in accompanying letter)

Comments:

Date of approval : 25th July 2007

.....
PROF. LOOI LAI MENG
Chairman
Medical Ethics Committee

APPENDIX A2

Donors Demographic Details

Table 1 Basic demographics and the origin of tissue samples for hMSCs cultures from the donors.

Donor	Age (year)	Gender	Sampling Site	Experiments
1 (h79)	53	Female	Bone marrow from femur	For comparison with rbMSC characteristics.
2 (h63)	60	Female	Bone marrow from tibia	
3 (h65)	74	Female	Bone marrow from tibia	
4 (h9)	69	Male	Bone marrow from femur	For *in vitro* tenogenic differentiation with GDF-5 induction in hMSC (collagen assay and qPCR).
5 (h19)	67	Female	Bone marrow from femur	
6 (h23)	75	Male	Bone marrow from femur	
7 (hST1)	19	Male	Hamstring tendon	As positive control for *in vitro* tenogenic differentiation of hMSC (collagen assay and qPCR).
8 (0217m)	28	Male	Hamstring tendon	
9 (0223b)	21	Male	Hamstring tendon	
10 (h78)	63	Female	Bone marrow from femur	For *in vitro* tenogenic differentiation with GDF-5 induction in hMSC (microarray analysis) and imaging analysis.
11 (h79)	53	Female	Bone marrow from tibia	
12 (h74)	75	Female	Bone marrow from tibia	
13 (h76)	62	Female	Bone marrow from tibia	
14 (h83)	85	Female	Bone marrow from femur	
15 (h90)	65	Female	Bone marrow from tibia	
16 (02h23)	21	Male	Hamstring tendon	As positive control for *in vitro* tenogenic differentiation of hMSC (microarray analysis) and imaging analysis.
17 (02h16)	20	Male	Hamstring tendon	
18 (02h27)	29	Female	Hamstring tendon	
19 (02h33)	26	Male	Hamstring tendon	
20 (02h07)	23	Male	Hamstring tendon	
21 (02h17)	28	Male	Hamstring tendon	

APPENDIX B

Animal Care and Use Committee, Faculty of Medicine, University of Malaya Ethics Approval Letter

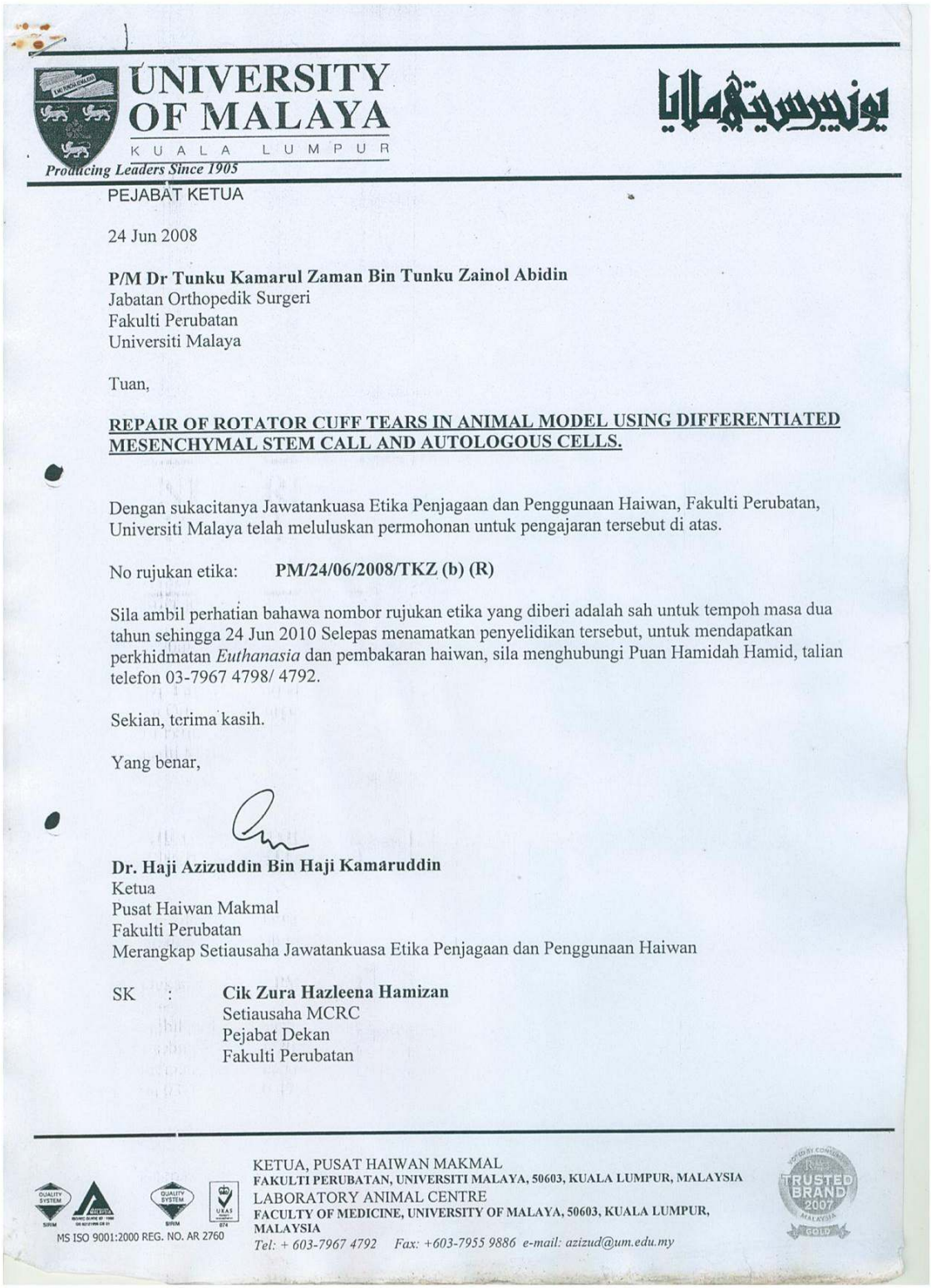

UNIVERSITY OF MALAYA
KUALA LUMPUR
Producing Leaders Since 1905

يونيورسيتي مالايا

PEJABAT KETUA

24 Jun 2008

P/M Dr Tunku Kamarul Zaman Bin Tunku Zainol Abidin
Jabatan Orthopedik Surgeri
Fakulti Perubatan
Universiti Malaya

Tuan,

REPAIR OF ROTATOR CUFF TEARS IN ANIMAL MODEL USING DIFFERENTIATED MESENCHYMAL STEM CALL AND AUTOLOGOUS CELLS.

Dengan sukacitanya Jawatankuasa Etika Penjagaan dan Penggunaan Haiwan, Fakulti Perubatan, Universiti Malaya telah meluluskan permohonan untuk pengajaran tersebut di atas.

No rujukan etika: **PM/24/06/2008/TKZ (b) (R)**

Sila ambil perhatian bahawa nombor rujukan etika yang diberi adalah sah untuk tempoh masa dua tahun sehingga 24 Jun 2010 Selepas menamatkan penyelidikan tersebut, untuk mendapatkan perkhidmatan *Euthanasia* dan pembakaran haiwan, sila menghubungi Puan Hamidah Hamid, talian telefon 03-7967 4798/ 4792.

Sekian, terima kasih.

Yang benar,

Dr. Haji Azizuddin Bin Haji Kamaruddin
Ketua
Pusat Haiwan Makmal
Fakulti Perubatan
Merangkap Setiausaha Jawatankuasa Etika Penjagaan dan Penggunaan Haiwan

SK : **Cik Zura Hazleena Hamizan**
Setiausaha MCRC
Pejabat Dekan
Fakulti Perubatan

MS ISO 9001:2000 REG. NO. AR 2760

KETUA, PUSAT HAIWAN MAKMAL
FAKULTI PERUBATAN, UNIVERSITI MALAYA, 50603, KUALA LUMPUR, MALAYSIA
LABORATORY ANIMAL CENTRE
FACULTY OF MEDICINE, UNIVERSITY OF MALAYA, 50603, KUALA LUMPUR, MALAYSIA
Tel: + 603-7967 4792 Fax: +603-7955 9886 e-mail: azizud@um.edu.my

TRUSTED BRAND 2007 MALAYSIA GOLD

APPENDIX C

Preparation of Trilineage Differentiation Medium

I. Preparing StemPro® Osteogenesis Differentiation medium (Invitrogen, Carlsbad, California, USA)

Osteogenesis differentiation medium	**Final Conc.**	**For 100 ml**
StemPro® Osteocyte/Chondrocyte Differentiation Basal medium	1X	90 ml
StemPro® Osteogenesis supplement	1X	10 ml
Gentamicin (10 mg/ml)	5 μg/ml	50 μl

II. Preparing StemPro® Adipogenesis Differentiation medium (Invitrogen, Carlsbad, California, USA)

Osteogenesis differentiation medium	**Final Conc.**	**For 100 ml**
StemPro® Adipocyte Differentiation Basal medium	1X	90 ml
StemPro® Adipogenesis supplement	1X	10 ml
Gentamicin (10 mg/ml)	5 μg/ml	50 μl

III. Preparing standard chondrogenesis differentiation medium

Standard chondrogenesis medium were prepared according to standard method previously described by Mackay et al. 1998 (Tissue Engineering (1998) 4(4): 415) as follow:

DMEM-high glucose supplemented with 10 ng/ml TGF-β3 (Invitrogen-Gibco, USA), 100nM dexamethasone (Sigma–Aldrich, USA), 50 μg/ml ascorbic acid-2-phosphate (Sigma–Aldrich, USA), 100 μg/ml sodium pyruvate (Invitrogen-Gibco, USA), 40 μg/ml proline (Sigma–Aldrich, USA) and 1X ITS (Sigma–Aldrich, USA).

APPENDIX D

Optimization of Primers for *q*RT-PCR

Protocol:

To determine the optimal annealing temperature of each primer set, gradient PCR was conducted. 2 μL of each dilution was added to 20 μL of PCR reaction mixture, containing 10 uL iQ^{TM} SYBR® Green Supermix (Bio-Rad Laboratories, Inc., Hercules, CA), 0.6 μL cDNA samples, and 0.2 μM of each primer (forward and reverse primers; Table 2.4). The amplification protocol was as follows: an initial denaturation and activation step at 95^{o}C for 30 s followed by 40 cycles of 95^{o}C for 15 s and gradient temperature ranging from 55 ^{o}C to 65^{o}C for 45 s. Following amplification, a melting curve program was carried out to confirm the presence of a single product (55-95^{o}C with a heating rate of 0.5^{o}C per second and a continuous fluorescence measurement). Data was analysed with the CFX manager software. The optimum annealing temperature was determined based on the cycle threshold (C_t) value at different annealing temperature. Primers used for *q*RT-PCR in rabbit samples, which derived from human or other animal sequences, were checked for its specificity via DNA sequencing analysis.

Sequencing results of primers used for rabbit *q*RT-PCR:

>glyceraldehyde_3_phosphate_dehydrogenase_1st_BASE_248889_A1_A_f.ab1
GNGCGAGGGCAGTCATCCCTGAGCTGACGGGAAGCTCACTGGCATGGCCTTCCGTGTCCCCACTGCCA
ACGTGTCAGTGGTGGACCTGACCTGCCGTCTAGAAAAACCTGCCAAATATGATGACATCAAGAAGGTG
GTGAAGCAGGCGTCGGAGA

>scleraxis_homolog_B_1st_BASE_248891_B1_B_f.ab1
NNNNNNNNNNNCGCAACNTCTCATCCTTGGAGAGCTTGCGGTTCGGCGGGCTTCGGTGGGGATCAG
CGTGCGCAGCGCCGTGAAGGCCGTGTTCACGCTGTTGGTGCGGTCTCGCTCGCGCGCGTTCGCCGTGT
GCCGCTG

>collagen_type I_alpha 1_1st_BASE_248893_E1_E_f.ab1
NNTGTCAGGCTCCTGGCTCTCCTGGTGACAAGGTCCCTCTGGAGCCTCTGGTCCTGCTGGTCCCCGAGG
TCCCCCTGGCTCTGCTGGTGCTCCTGGCAAAGATGGACTCAACGGTCTCCCTGGCCCCATTGGGCCCCC
TGGTCCTCGCGGTCGCACTGGTGATGCTGGTCCTGTTGGTCCCCCCGGCCCTCCTGGACCTCCTGGTCC
CCCTGGTCCTCCCAGCGCTGGTTCGACTTCAGCTTCCTGCCCCAGCCACCTCAAGAGAAGGCTCACGAT
GGTGGCCGCTACTACCGGGCTGATGATGCCAATTGTGGTTCGA

APPENDIX E1

Electropherogram of Total RNA Samples Used for Microarray Experiment

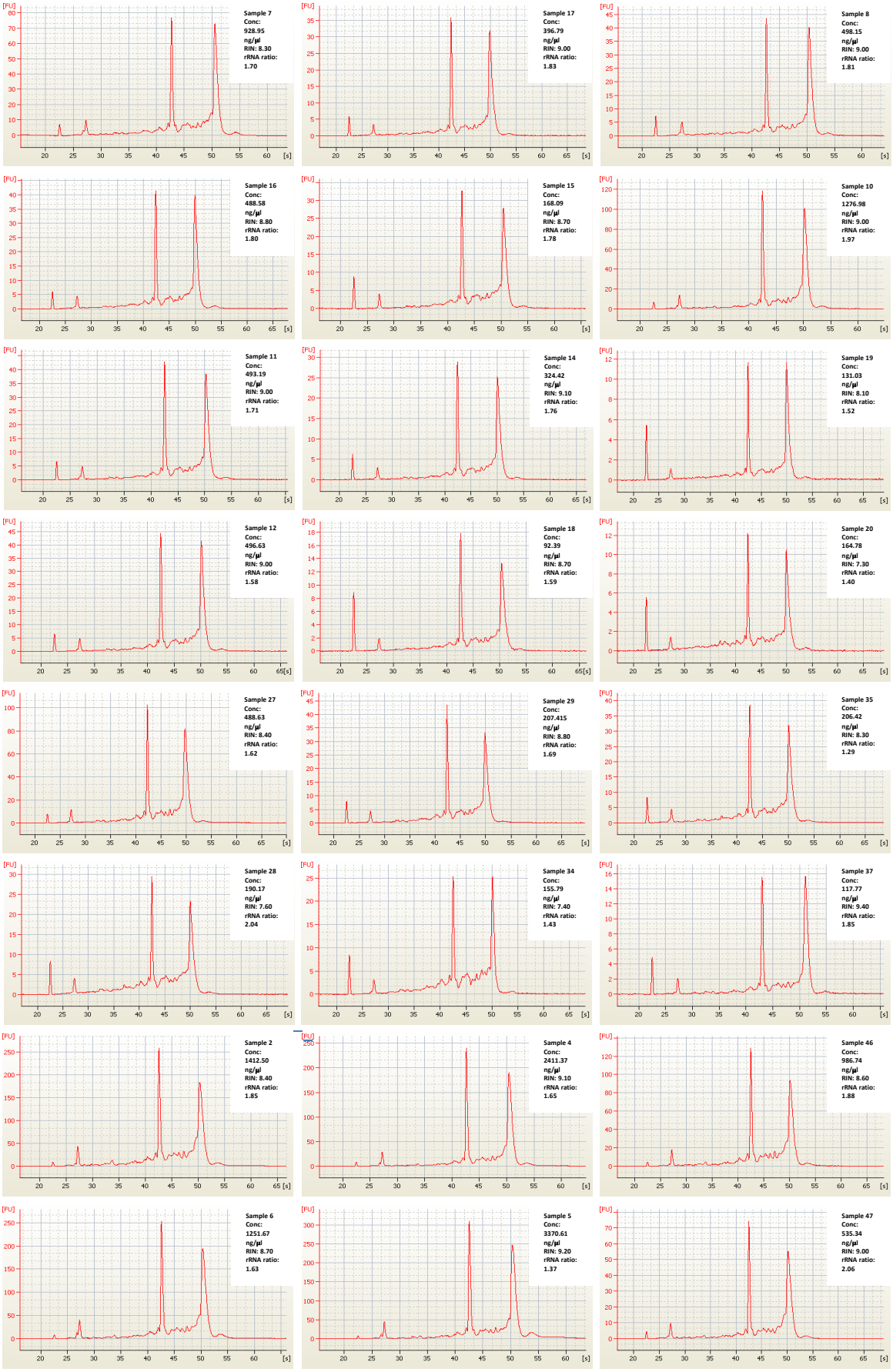

APPENDIX E2

Quality and Integrity of Total RNA Samples and Their Respective cDNA Concentration Amplified From 200 ng of Total RNA

The quality control tests of total RNA was conducted with Agilent Bioanalyzer and Nanodrop spectrophotometry. In this study, only total RNA with high purity and integrity (with no evidence of degradation) were used for the microarray experiment in order to prevent any false positive or false negative results contributed by the low quality total RNA. Overall, the integrity of total RNA samples as indicated by RIN was 8.62±0.56; and the purity as indicated by A260/A280 ratios was 2.10±0.03, to ensured excellent amplification for microarray hybridization. Two hundred nanogram of total RNA were used and the concentrations of cDNA after amplification by the Applaus™ WT-Amp ST System (NuGEN Technologies, Inc, San Carlos, CA, USA) for microarray target preparation were as indicated in the table below.

Sample No	Total RNA concentration (ng/μl)	Ratio A_{260}/A_{280}	RNA Integrity Number (RIN)	Concentration of cDNA (μg/μl)
2	2266.1	2.10	8.40	1.250
4	1209.7	2.08	9.10	0.625
5	2171.9	2.08	9.20	0.500
6	1698.4	2.10	8.70	0.417
7	411.1	2.07	8.30	0.357
8	202.9	2.08	9.00	0.313
10	584.3	2.07	9.00	0.250
11	284.8	2.09	9.00	0.227
12	177.1	2.09	9.00	0.208
14	116.7	2.10	9.10	0.179
15	138.1	2.10	8.70	0.167
16	175.8	2.10	8.80	0.156
17	127.4	2.09	9.00	0.147
18	53.9	2.20	8.70	0.139
19	41.2	2.19	8.10	0.132
20	52.6	2.14	7.30	0.125
27	93.6	2.10	8.40	0.093
28	140.2	2.10	7.60	0.089
29	113.0	2.10	8.80	0.086
34	141.1	2.10	7.40	0.074
35	302.6	2.10	8.30	0.071
37	94.3	2.10	9.40	0.068
46	1327	2.10	8.60	0.054
47	584	2.10	9.00	0.053

APPENDIX F

QuantiGene® Plex 2.0 Assay (11904 Human) Reagent System

Bead Number	Gene Symbol	Genbank Accession No	Seq Length	Probe set region	Type	Target Name
13	RUNX2	NM_004348	5720	648-1082	Target	Runt-related transcription factor 2
14	MMP3	NM_002422	1828	1119-1775	Target	Matrix metallopeptidase 3
20	SCXA	NM_001008271	606	251-574	Target	Homo sapiens scleraxis homolog A (mouse) (SCXA)
21	COMP	NM_000095	2471	1420-1842	Target	Homo sapiens cartilage oligomeric matrix protein (COMP), mRNA
25	PGK1	NM_000291	2439	1609-2233	HKG	Phosphoglycerate kinase 1 (Medium High abundant HKG)
27	COL2A1	NM_001844	5087	1788-2258	Target	Type-II alpha 1 (primary osteoarthritis, spomdyloepiphyseal dysplasia, congenital)
30	FIGF	NM_004469	2128	835-1476	Target	c-fos induced growth factor (vascular endothelial growth factor D)
34	HPRT1	NM_000194	1435	102-646	HKG	Hypoxanthine phophoribosyltransferase 1 (Medium abundant HKG)
43	ALPL	NM_000478	2596	1075-1617	Target	Alkaline phosphatase, liver/bone/kidney
44	BGLAP	NM_199173	552	113-477	Target	Bone gamma-carboxyglutamate (gla) protein
45	PPARG	NM_005037	1818	567-1044	Target	Peroxisome proliferative activated receptor, gamma
46	TNC	NM_002160	8605	2687-3165	Target	Tenascin C
53	SOX9	NM_000346	3963	1607-2274	Target	SRY(Sex determining region Y)-box 9 (campomelic dysplasia, autosomal sex-reversal)
56	TNMD	NM_022144	1360	301-1020	Target	Homo sapiens tenomodulin (TNMD)
57	TBP	NM_003194	1921	277-822	HKG	TATA box binding protein (Low abundant HKG)

APPENDIX G1

Unstained Control Used to Adjust the PMT Voltage for Flow Cytometry Analysis

1. Dot plot of an example of unstained control used to adjust the PMT voltage:

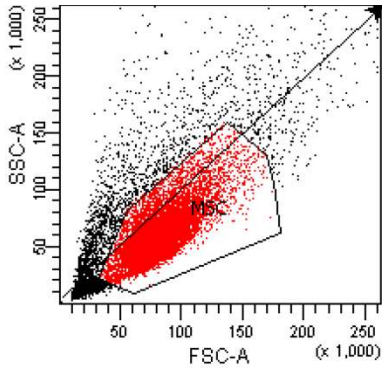

2. PMT voltages were adjusted with the unstained control tube before recording the single-stained control (with BD CompBead).
   Histograms of fluorescence signals detected for the unstained control after adjusted the PMT voltage:

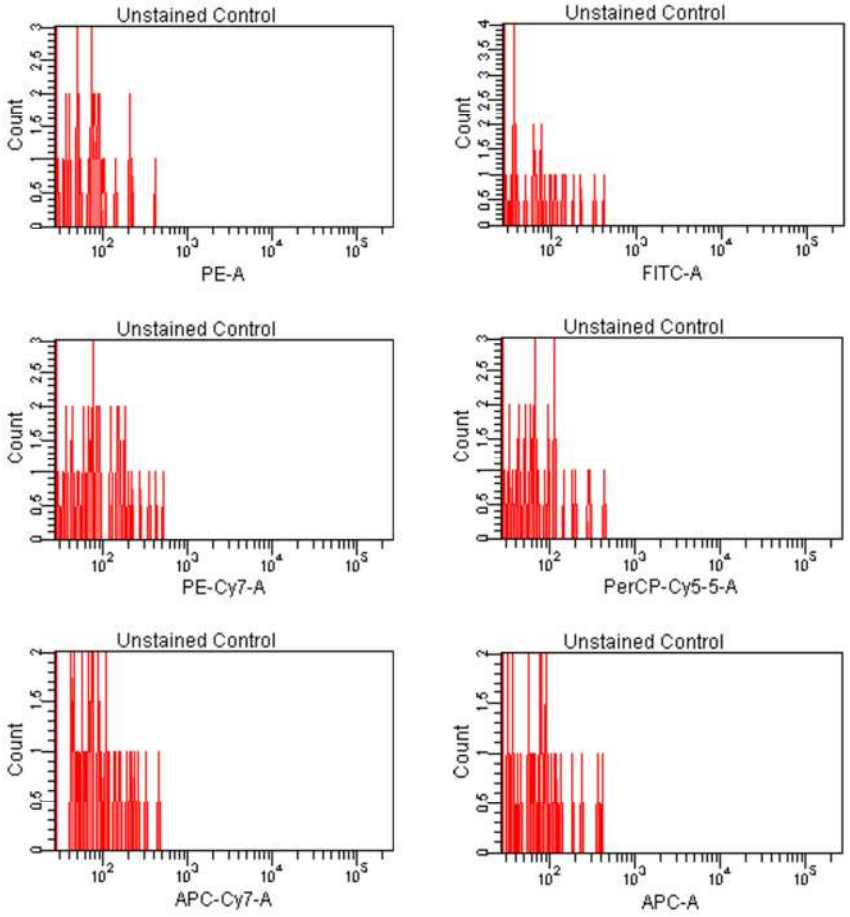

APPENDIX G2

Examples of the Gated Histogram of Single-stained Controls (BD CompBead)

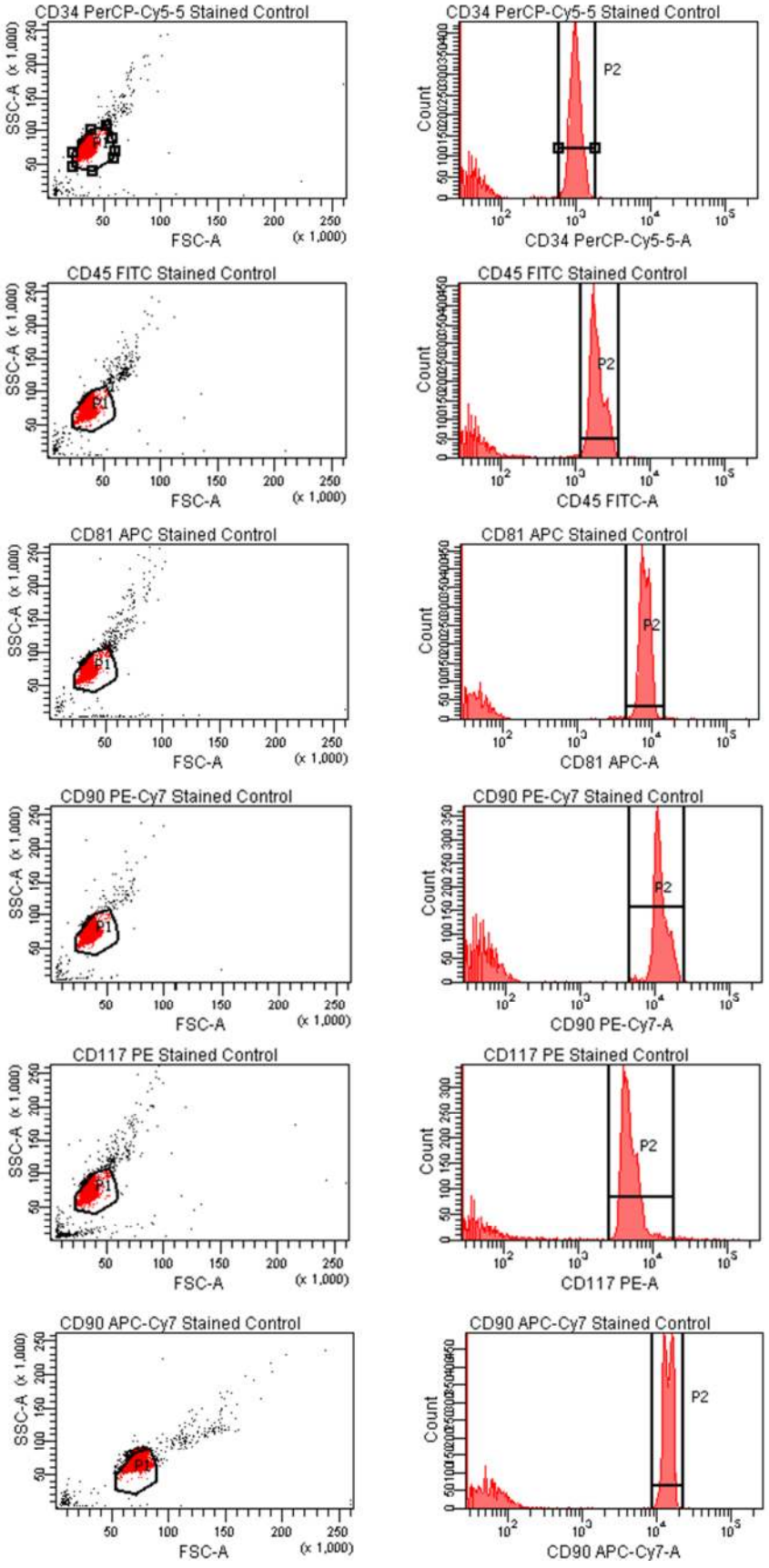

APPENDIX H

Preparation of Staining Solutions

I. Preparing 1% (w/v) Eosin Y Stain

Eosin Y	10.0 g
Distilled water	200 ml
95% ethanol	800 ml

All the components were mixed to dissolve and the stock solution was stored at room temperature. The eosin solution was filtered prior to use.

II. Preparing Oil Red O Stain

An oil red O stock solution was prepared by adding 300 mg of Oil Red O powder to 100 mL of 99% isopropanol. This stock solution is only stable for one year from the date it was made.

In the fume hood, 3 parts of Oil Red O stock solution was mixed with 2 parts of deionized water. The mixture was incubated for 10 min at room temperature. This working solution must be prepared prior to use because it is only stable for 2 hours.

The Oil Red O working solution was completely filtered through the Whatman filter paper in a funnel above a vessel before used for staining.

III. Preparing Safranin O and Fast green Stain

1. Modified Weigert's iron hematoxylin

Stock solution A (This stock solution is only stable for 4 months):

Hematoxylin	10.0 g
80% Ethanol	500.0 ml

Stock solution B (This stock solution is only stable for 4 months):

Ferric chloride	20.0 g
Distilled water	475.0 ml
Hydrochloride acid (36.5-38%)	5.0 ml

Working Modified Weigert's iron hematoxylin (This working solution is only stable for 1 week)

Equal parts of stock A and B were mixed.

2. 1.0% acid-alcohol

70% ethanol	500.0 ml
Hydrochloride acid (36.5-38%)	5.0 ml

3. 0.02% Fast green

Fast green	0.05 g
Distilled water	250.0 ml

4. 1.0% acetic acid

70% ethanol	100.0 ml
Acetic acid, glacial	1.0 ml

5. 1% safranin O

Safranin O	2.5 g
Distilled water	250.0 ml

APPENDIX I1

Comparison of hMSCs and rbMSCs Phenotypic Expression

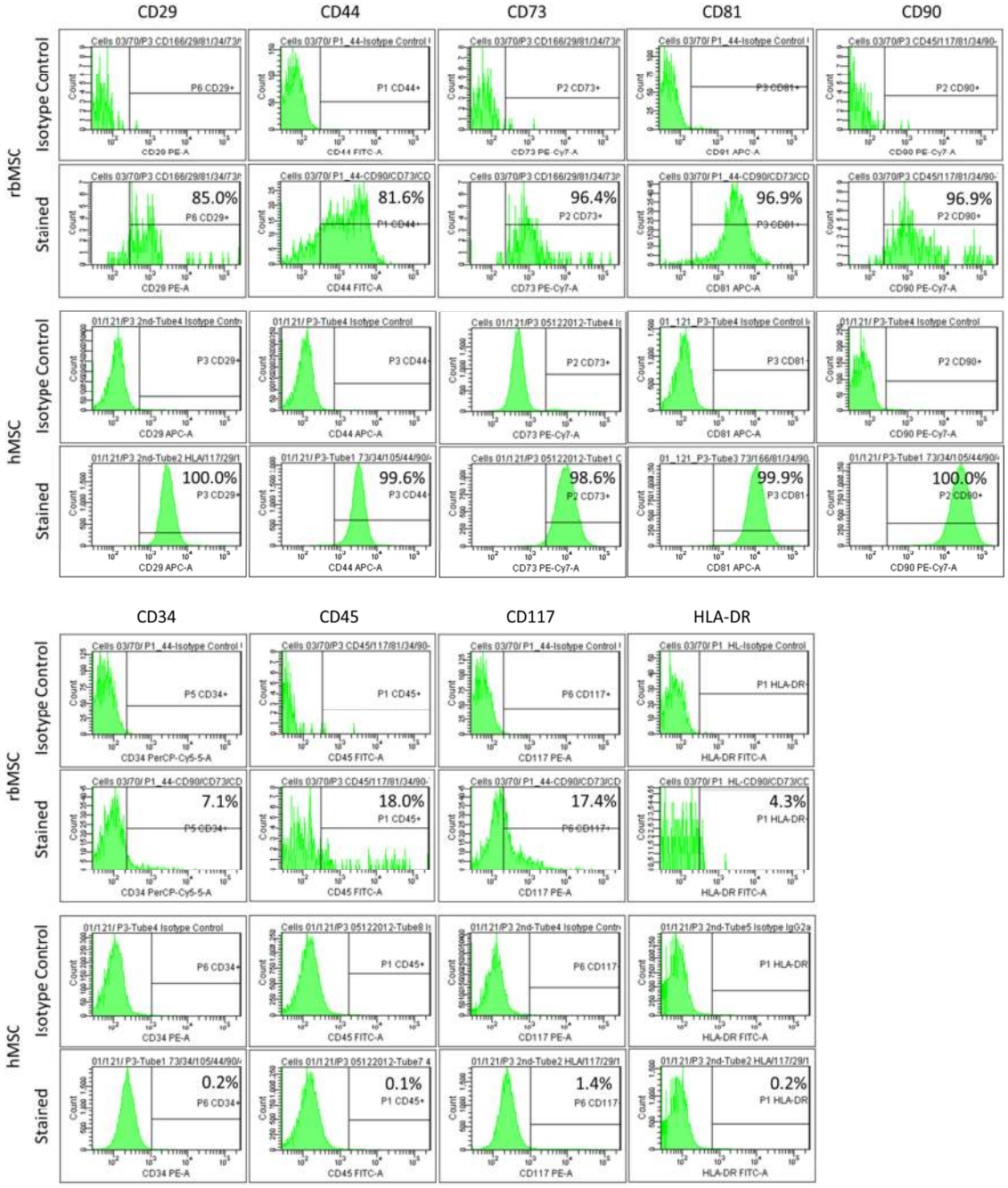

The hMSCs and rbMSCs were stained with antibodies against the indicated antigens (labeled on top of the figures) and analyzed by flow cytometry. Representative histograms are displayed. The y axis indicated the event count, and the x axis indicated the mean fluorescence intensity in a log (10^0 to 10^5) scale. The isotype control histograms are shown above their respective stained sample histograms. The results showed that rbMSCs expressed CD29, CD44, CD73, CD81, CD90, but do not expressed CD34, CD45, CD177 and HLA-DR.

APPENDIX I2

Expression of CD105, CD166, CD14 and CD19 on hMSCs

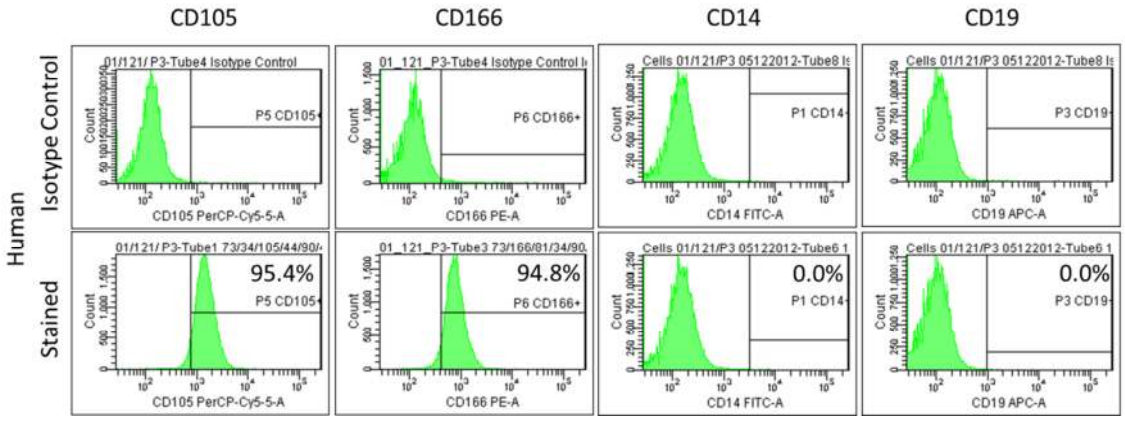

Representative histograms are displayed. The y axis indicated the event count, and the x axis indicated the mean fluorescence intensity in a log (10^0 to 10^5) scale. The isotype control histograms are shown above their respective stained sample histograms. The results showed that hMSCs expressed CD105 and CD166 but does not expressed CD14 and CD19. Representative histograms illustrate relative number of cells vs. mean fluorescence intensity.

APPENDIX J

Volcano Plots of Log_2-ratios vs $-Log_{10}$ *p*-value for Uncorrected *p*-value (Left) and the Corrected *p*-value (Right)

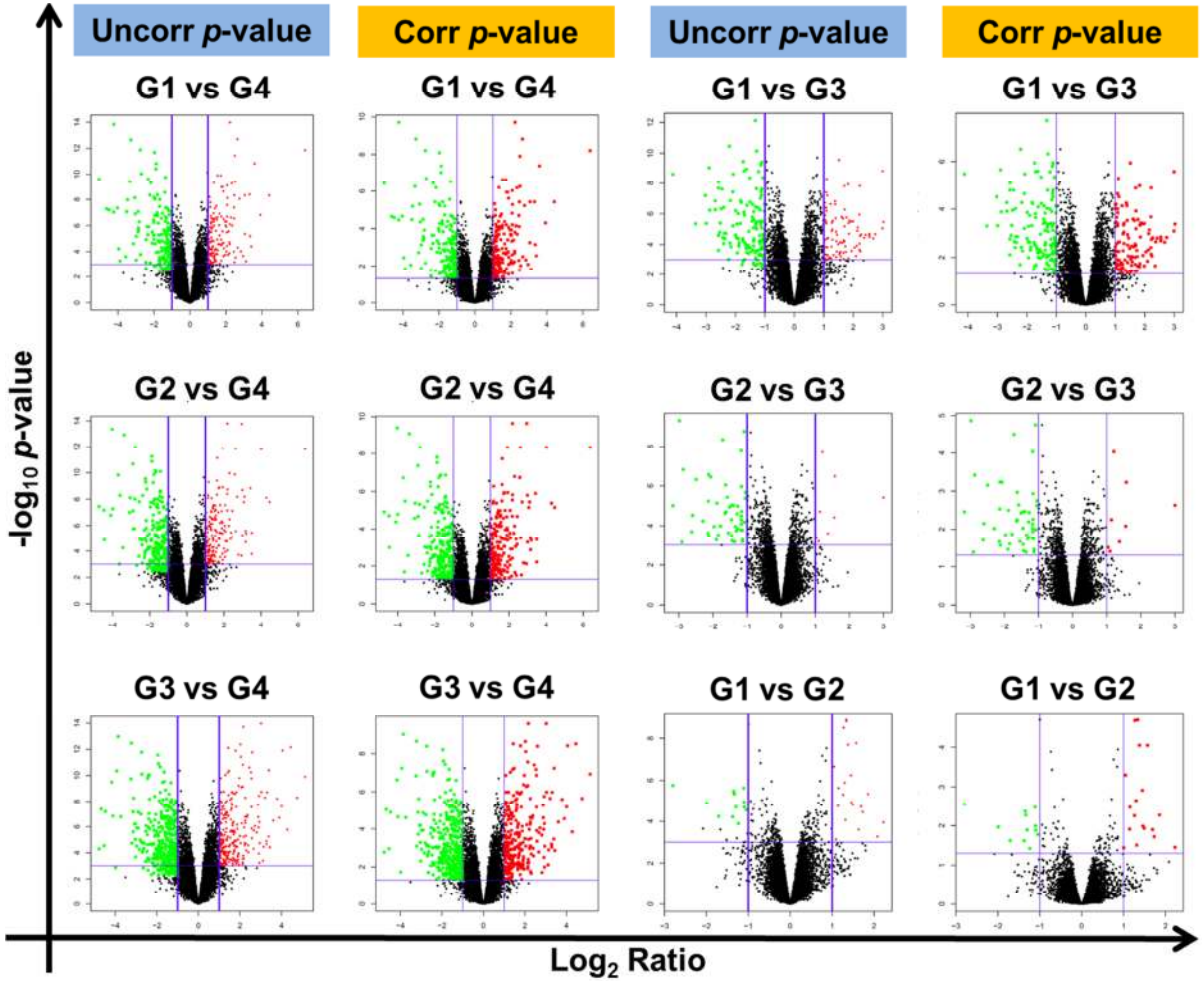

The green-dots and red-dots represent the down- and up-regulated, respectively

APPENDIX K

List of Genes Modulated in hMSCs by GDF5 Treatment and Genes Modulated in Tenocytes (Total: 954 genes)

			Estimate				Log-ratio						p-value (corr)					
UT ID	NCBI Ref No	Gene Symbol	G1	G2	G3	G4	G2/G1	G3/G1	G4/G1	G4/G2	G4/G3	G3/G2	G2/G1	G3/G1	G4/G1	G4/G2	G4/G3	G3/G2
8017885	NM_007168	ABCA8	5.9	5.6	5.3	3.9	-0.28	-0.56	-2.02	-1.74	-1.46	-0.28	8.16E-01	2.92E-01	2.28E-04	8.87E-04	2.94E-03	7.53E-01
7961710	NM_005691	ABCC9	4.8	4.1	3.6	3.7	-0.75	-1.24	-1.10	-0.35	0.15	-0.50	4.16E-01	1.95E-02	6.60E-02	6.88E-01	8.88E-01	5.77E-01
7985786	NM_013227	ACAN	9.2	7.8	7.0	7.8	-1.46	-2.22	-1.37	0.09	0.85	-0.76	1.03E-02	1.32E-05	4.24E-03	9.24E-01	6.15E-02	1.65E-01
8123137	NM_005891	ACAT2	7.4	8.8	8.6	8.3	1.37	1.16	0.82	-0.55	-0.33	-0.21	2.41E-02	1.16E-02	1.19E-01	3.58E-01	6.28E-01	8.23E-01
7957386	NM_024560	ACSS3	7.6	7.5	6.9	5.7	-0.08	-0.65	-1.87	-1.79	-1.22	-0.58	9.58E-01	1.18E-01	8.53E-05	1.11E-04	3.43E-03	2.88E-01
7929026	NM_001141945	ACTA2	5.5	5.9	5.4	4.5	0.40	-0.12	-1.01	-1.41	-0.89	-0.52	6.14E-01	8.63E-01	1.90E-02	1.18E-03	2.80E-02	3.43E-01
7934906	NM_001141946	ACTA2	11.5	11.7	11.5	9.4	0.23	0.00	-2.07	-2.30	-2.07	-0.23	7.63E-01	9.98E-01	9.38E-07	1.64E-07	5.28E-07	6.96E-01
7987315	NM_005159	ACTC1	6.0	5.4	5.2	7.5	-0.69	-0.81	1.41	2.10	2.22	-0.12	7.10E-01	4.32E-01	1.48E-01	2.04E-02	9.97E-03	9.60E-01
8045587	NM_001616	ACVR2A	8.5	9.5	9.7	6.4	0.95	1.15	-2.16	-3.11	-3.31	0.20	2.51E-01	3.03E-02	4.06E-04	3.65E-06	1.07E-06	8.65E-01
8047788	NM_003812	ADAM23	5.2	5.5	5.8	7.5	0.36	0.69	2.33	1.98	1.65	0.33	8.14E-01	3.18E-01	6.20E-04	2.56E-03	7.72E-03	7.82E-01
8111387	NM_030955	ADAMTS12	4.7	5.2	6.2	4.6	0.51	1.51	-0.17	-0.68	-1.68	1.00	6.57E-01	5.95E-03	8.80E-01	3.32E-01	3.33E-03	1.45E-01
8116272	NM_014244	ADAMTS2	7.9	7.9	8.1	7.0	-0.02	0.22	-0.93	-0.91	-1.15	0.25	9.89E-01	6.73E-01	1.98E-02	2.12E-02	2.40E-03	7.13E-01
8088560	NM_182920	ADAMTS9	4.6	5.3	5.6	4.2	0.67	0.99	-0.48	-1.15	-1.48	0.32	8.75E-03	1.40E-05	2.38E-02	3.27E-06	5.75E-08	1.98E-01
8154512	NM_001040272	ADAMTSL1	6.3	6.0	5.5	6.9	-0.28	-0.75	0.61	0.89	1.37	-0.48	6.63E-01	1.24E-02	7.02E-02	6.89E-03	6.15E-05	2.26E-01
8154491	NM_001040272	ADAMTSL1	6.9	6.7	5.9	7.7	-0.19	-1.02	0.74	0.93	1.75	-0.83	8.51E-01	5.53E-03	7.38E-02	2.00E-02	3.21E-05	5.91E-02
7985522	NM_207517	ADAMTSL3	3.9	3.9	3.9	5.7	-0.01	0.03	1.88	1.89	1.84	0.04	9.93E-01	9.42E-01	4.09E-08	3.05E-08	3.67E-08	9.45E-01
8096116	NM_032717	AGPAT9	3.5	3.6	3.5	4.5	0.08	-0.03	1.02	0.94	1.05	-0.11	9.24E-01	9.55E-01	7.16E-04	1.44E-03	2.83E-04	8.43E-01
7981514	NM_138420	AHNAK2	7.2	7.4	6.9	9.1	0.12	-0.31	1.89	1.77	2.21	-0.43	9.67E-01	8.08E-01	2.65E-02	3.53E-02	6.03E-03	7.79E-01
8131614	NM_001621	AHR	9.3	9.7	9.6	8.6	0.33	0.24	-0.70	-1.03	-0.94	-0.09	3.21E-01	3.12E-01	2.38E-03	2.78E-05	5.57E-05	8.39E-01
8121277	NM_001624	AIM1	4.0	4.3	5.1	6.3	0.25	1.03	2.23	1.98	1.20	0.78	7.80E-01	5.65E-03	3.72E-06	1.31E-05	2.14E-03	8.41E-02
7902452	NM_174858	AK5	7.2	6.8	6.5	8.1	-0.41	-0.75	0.83	1.24	1.58	-0.34	7.95E-01	3.09E-01	3.11E-01	8.25E-02	1.69E-02	7.94E-01
7973850	NM_004274	AKAP6	4.8	4.3	4.2	5.7	-0.50	-0.61	0.97	1.47	1.58	-0.11	5.68E-01	2.08E-01	5.14E-02	2.69E-03	8.78E-04	9.19E-01
7935230	NM_002860	ALDH18A1	7.7	7.9	8.3	7.3	0.18	0.65	-0.37	-0.55	-1.02	0.47	7.48E-01	6.91E-03	1.97E-01	3.54E-02	1.34E-04	1.12E-01
8155327	NM_000692	ALDH1B1	9.9	10.3	10.2	9.1	0.38	0.23	-0.79	-1.17	-1.02	-0.14	6.29E-01	6.74E-01	6.34E-02	4.85E-03	9.23E-03	8.68E-01
8013660	NM_005165	ALDOC	6.0	5.4	4.9	5.2	-0.52	-1.04	-0.80	-0.28	0.25	-0.52	1.89E-01	2.24E-04	6.40E-03	4.46E-01	4.81E-01	1.05E-01
8023528	NM_052947	ALPK2	8.0	8.1	8.3	6.8	0.10	0.26	-1.19	-1.29	-1.45	0.16	9.56E-01	7.06E-01	1.85E-02	1.02E-02	2.54E-03	8.77E-01
7962579	NM_001143668	AMIGO2	6.7	5.6	6.4	5.2	-1.13	-0.32	-1.50	-0.37	-1.18	0.81	1.16E-01	6.52E-01	6.40E-03	6.36E-01	2.20E-02	2.12E-01
8152297	NM_001146	ANGPT1	6.8	6.7	6.3	5.6	-0.09	-0.49	-1.21	-1.13	-0.72	-0.41	9.61E-01	3.95E-01	2.22E-02	3.16E-02	1.82E-01	6.17E-01
7922598	NM_004673	ANGPTL1	4.4	5.4	6.8	4.6	0.94	2.39	0.22	-0.72	-2.17	1.45	2.96E-01	9.68E-05	8.46E-01	3.10E-01	3.61E-04	2.61E-02
8164200	NM_012098	ANGPTL2	6.8	6.8	6.4	8.2	0.08	-0.35	1.45	1.37	1.80	-0.43	9.76E-01	7.14E-01	3.98E-02	4.90E-02	6.40E-03	7.18E-01
7951195	NM_178127	ANGPTL5	4.2	4.2	4.0	7.0	-0.03	-0.23	2.85	2.88	3.08	-0.20	9.94E-01	8.51E-01	3.26E-04	2.29E-04	6.63E-05	9.04E-01
7897675	NM_021146	ANGPTL7	3.4	3.5	3.3	5.9	0.06	-0.09	2.45	2.40	2.54	-0.15	9.90E-01	9.60E-01	1.74E-02	1.86E-02	8.58E-03	9.56E-01
7933772	NM_020987	ANK3	8.1	8.5	8.5	4.5	0.42	0.46	-3.59	-4.01	-4.05	0.04	6.51E-01	3.99E-01	4.09E-08	4.57E-09	3.80E-09	9.80E-01
8008609	NM_153228	ANKFN1	4.3	4.2	3.9	3.2	-0.03	-0.34	-1.04	-1.02	-0.71	-0.31	9.88E-01	5.49E-01	2.61E-02	2.79E-02	1.26E-01	6.88E-01
7934979	NM_014391	ANKRD1	8.8	7.8	8.9	5.4	-1.02	0.03	-3.41	-2.39	-3.44	1.05	6.25E-01	9.90E-01	2.81E-03	3.12E-02	1.37E-03	5.19E-01
8098604	NM_181726	ANKRD37	7.1	6.3	6.4	5.8	-0.79	-0.70	-1.27	-0.48	-0.57	0.09	2.18E-01	1.10E-01	5.98E-03	3.80E-01	2.37E-01	9.34E-01
8060949	NM_022096	ANKRD5	5.2	5.2	4.9	4.2	0.07	-0.30	-0.94	-1.01	-0.64	-0.37	9.62E-01	5.77E-01	3.36E-02	2.06E-02	1.48E-01	5.82E-01
8132318	NM_018685	ANLN	8.5	6.9	5.9	8.7	-1.61	-2.68	0.17	1.78	2.84	-1.07	2.29E-01	2.37E-03	9.35E-01	6.39E-02	1.81E-03	4.01E-01
8095986	NM_005139	ANXA3	3.2	3.2	3.3	4.4	0.04	0.13	1.26	1.22	1.13	0.09	9.78E-01	8.50E-01	4.30E-03	4.89E-03	6.18E-03	9.32E-01
8047300	NM_001159	AOX1	6.0	5.6	5.0	6.7	-0.42	-0.97	0.73	1.15	1.70	-0.55	7.90E-01	1.62E-01	4.05E-01	1.18E-01	1.10E-02	6.18E-01
8017210	NM_003916	AP1S2	6.1	5.8	5.7	7.4	-0.30	-0.46	1.24	1.54	1.70	-0.16	6.10E-01	1.37E-01	2.55E-04	1.35E-05	2.89E-06	7.83E-01
8146159	NM_001134296	AP3M2	6.2	5.9	5.7	5.1	-0.29	-0.40	-1.05	-0.76	-0.64	-0.12	6.78E-01	2.69E-01	3.76E-03	3.16E-02	5.81E-02	8.78E-01
8073062	NM_004900	APOBEC3B	5.0	4.5	3.9	4.6	-0.57	-1.11	-0.43	0.13	0.67	-0.54	3.33E-01	2.36E-03	3.60E-01	8.46E-01	7.51E-02	2.58E-01
8072735	NM_145343	APOL1	6.2	6.0	7.5	4.1	-0.14	1.37	2.03	1.89	3.40	1.51	9.24E-01	2.43E-03	1.18E-04	2.12E-04	5.75E-08	3.73E-03
8132118	NM_198098	AQP1	4.0	4.1	4.9	5.2	0.16	0.93	1.17	1.01	0.24	0.77	8.67E-01	5.25E-03	1.81E-03	5.47E-03	6.32E-01	5.11E-02
7982358	NM_014783	ARHGAP11A	6.4	5.8	4.7	7.3	-0.68	-1.69	0.82	1.50	2.51	-1.01	5.28E-01	3.27E-03	2.42E-01	1.53E-02	8.76E-05	1.59E-01
7982287	NM_001039841	ARHGAP11B	5.4	4.7	4.4	5.8	-0.72	-1.04	0.32	1.04	1.36	-0.32	2.76E-01	1.19E-02	6.13E-01	2.06E-02	1.74E-03	6.60E-01
8108873	NM_015071	ARHGAP26	6.3	6.3	5.7	6.8	0.05	-0.51	0.56	0.51	1.08	-0.56	9.78E-01	3.37E-01	3.45E-01	3.98E-01	2.27E-02	4.02E-01
8019964	NM_001010000	ARHGAP28	5.8	7.2	7.1	5.4	1.36	1.22	-0.43	-1.80	-1.66	-0.14	1.42E-01	5.77E-02	6.72E-01	9.33E-03	1.11E-02	9.32E-01
7917850	NM_004815	ARHGAP29	7.0	8.1	8.0	9.0	1.10	1.03	1.94	0.85	0.92	-0.07	1.30E-02	2.66E-03	6.10E-06	2.10E-02	8.74E-03	9.36E-01
8112033	NM_019087	ARL15	6.7	6.9	7.3	6.1	0.24	0.58	-0.55	-0.79	-1.13	0.34	7.34E-01	7.01E-02	1.31E-01	2.00E-02	7.57E-04	4.93E-01
8059854	NM_005737	ARL4C	8.3	8.2	8.9	7.2	-0.07	0.58	-1.15	-1.08	-1.72	0.64	9.74E-01	3.71E-01	5.78E-02	7.30E-02	2.40E-03	4.22E-01
7932744	NM_018076	ARMC4	3.4	3.2	3.3	4.7	-0.15	-0.04	1.36	1.51	1.40	0.11	9.22E-01	9.65E-01	5.80E-03	2.12E-03	2.63E-03	9.26E-01
8113073	NM_020801	ARRDC3	9.3	9.4	8.8	10.1	0.06	-0.48	0.82	0.76	1.30	-0.54	9.59E-01	1.67E-01	2.10E-02	3.07E-02	2.43E-04	1.94E-01
7986350	NM_183376	ARRDC4	6.6	7.0	7.0	5.3	0.44	0.40	-1.27	-1.72	-1.68	-0.04	3.04E-01	1.62E-01	7.96E-05	1.30E-06	1.18E-06	9.60E-01
7930181	NM_020682	AS3MT	6.8	6.3	5.7	6.3	-0.41	-1.07	-0.48	-0.08	0.59	-0.67	4.16E-01	4.05E-04	1.53E-01	8.95E-01	5.07E-02	5.07E-02
7923086	NM_018136	ASPM	6.2	5.1	3.9	7.0	-1.19	-2.37	0.77	1.96	3.14	-1.18	3.42E-01	2.26E-03	4.74E-01	1.83E-02	1.93E-04	2.42E-01
8162394	NM_017680	ASPN	3.6	6.4	7.7	8.7	2.80	4.12	5.05	2.25	0.93	1.32	2.81E-03	3.34E-06	3.68E-07	4.27E-03	2.78E-01	1.44E-01
8152668	NM_014109	ATAD2	6.9	6.6	6.2	7.2	-0.27	-0.66	0.36	0.63	1.02	-0.39	8.28E-01	1.93E-01	6.20E-01	2.79E-01	3.52E-02	6.20E-01
8006187	NM_024857	ATAD5	4.5	4.3	4.2	5.5	-0.24	-0.35	0.96	1.20	1.31	-0.11	8.69E-01	6.19E-01	9.49E-02	2.91E-02	1.21E-02	9.34E-01
8092849	NM_024524	ATP13A3	9.8	9.4	9.5	8.6	-0.42	-0.30	-1.17	-0.75	-0.87	0.12	3.10E-01	3.06E-01	1.29E-04	7.63E-03	1.45E-03	8.31E-01
7907160	NM_001677	ATP1B1	8.9	8.9	9.3	8.3	-0.01	0.41	-0.60	-0.60	-1.01	0.41	9.98E-01	5.23E-01	3.42E-01	3.40E-01	4.63E-02	6.16E-01
8067167	NM_198433	AURKA	6.3	5.2	4.5	6.4	-1.13	-1.82	0.09	1.22	1.91	-0.69	4.19E-01	2.47E-02	9.64E-01	2.05E-01	2.20E-02	6.13E-01
7923034	NM_003783	B3GALT2	5.4	5.5	4.5	4.0	0.16	-0.88	-1.40	-1.56	-0.52	-1.04	9.24E-01	9.83E-02	1.24E-02	4.85E-03	4.26E-01	9.22E-02
8084206	NM_032047	B3GNT5	3.3	3.2	3.1	4.4	-0.12	-0.18	1.15	1.27	1.34	-0.07	9.17E-01	7.21E-01	2.29E-03	7.57E-04	2.83E-04	9.39E-01
8066939	NM_004776	B4GALT5	7.6	7.7	7.7	8.7	0.13	0.12	1.15	1.03	1.03	-0.01	9.09E-01	8.38E-01	2.28E-03	5.11E-03	3.25E-03	9.94E-01
8058695	NM_000465	BARD1	5.5	5.2	4.6	6.2	-0.28	-0.95	0.66	0.94	1.60	-0.67	7.09E-01	5.05E-03	8.54E-02	1.10E-02	3.47E-05	1.06E-01
7978595	NM_013448	BAZ1A	7.1	6.9	7.0	8.0	-0.12	-0.02	0.97	1.09	0.99	0.10	8.20E-01	9.62E-01	1.12E-04	1.81E-05	4.08E-05	8.12E-01
7976567	NM_000710	BDKRB1	5.9	5.1	4.2	7.2	-0.85	-1.75	1.29	2.14	3.04	-0.90	4.91E-01	9.28E-03	9.07E-02	3.58E-03	6.46E-05	3.43E-01
7976560	NM_000623	BDKRB2	5.3	5.3	4.6	5.8	0.07	-0.63	0.51	0.44	1.15	-0.70	9.71E-01	2.65E-01	4.71E-01	5.52E-01	2.87E-02	3.16E-01
7947230	NM_170732	BDNF	4.9	4.3	3.9	3.9	-0.60	-0.99	-1.03	-0.43	-0.04	-0.39	1.39E-01	5.67E-04	1.02E-03	1.86E-01	9.50E-01	3.01E-01
8120362	NM_152731	BEND6	5.8	6.6	6.4	7.1	0.83	0.66	1.36	0.53	0.70	-0.17	1.42E-01	1.02E-01	1.75E-03	2.62E-01	8.63E-02	8.36E-01
8174201	NM_018476	BEX1	6.5	6.8	6.9	4.0	0.31	0.44	-2.47	-2.78	-2.91	0.13	9.24E-01	7.72E-01	1.74E-02	6.87E-03	3.16E-03	9.60E-01
8106494	NM_017614	BHMT2	7.1	7.7	8.0	5.8	0.57	0.90	-1.36	-1.92	-2.26	0.34	5.42E-01	6.80E-02	1.07E-02	4.25E-04	4.19E-05	7.05E-01
7943413	NM_001165	BIRC3	5.7	6.1	5.8	6.9	0.44	0.13	1.24	0.80	1.11	-0.31	5.70E-01	8.54E-01	4.47E-03	6.41E-02	6.36E-03	6.57E-01
8018860	NM_001168	BIRC5	6.7	5.5	4.6	6.8	-1.28	-2.09	0.05	1.33	2.15	-0.82	3.75E-01	1.45E-02	9.81E-01	1.89E-01	1.53E-02	5.65E-01
8116818	NM_001718	BMP6	5.3	5.6	5.7	6.6	0.35	0.39	1.27	0.92	0.89	0.03	6.31E-01	3.65E-01	1.67E-03	1.86E-02	1.67E-02	9.77E-01
7991080	NM_001717	BNC1	5.0	5.0	5.5	6.2	-0.05	0.48	1.20	1.25	0.72	0.53	9.68E-01	1.72E-01	1.27E-03	6.75E-04	3.52E-02	2.12E-01
8136341	NM_199186	BPGM	7.1	7.3	7.7	6.5	0.26	0.63	-0.61	-0.87	-1.24	0.37	5.75E-01	7.62E-03	1.82E-02	9.21E-04	1.01E-05	2.34E-01
7968484	NM_000059	BRCA2	5.3	5.0	5.5	6.4	-0.36	0.20	1.08	1.45	0.88	0.56	8.18E-01	8.54E-01	1.26E-01	3.02E-02	2.05E-01	5.82E-01

			Estimate				Log-ratio						p-value (corr)					
UT ID	NCBI Ref No	Gene Symbol	G1	G2	G3	G4	G2/G1	G3/G1	G4/G1	G4/G2	G4/G3	G3/G2	G2/G1	G3/G1	G4/G1	G4/G2	G4/G3	G3/G2
8035304	NM_004335	BST2	3.9	3.9	4.9	3.7	0.02	1.00	-0.20	-0.21	-1.20	0.99	9.93E-01	2.60E-03	7.27E-01	6.95E-01	6.78E-04	9.42E-03
8117476	NM_006994	BTN3A3	6.7	7.0	7.5	6.4	0.30	0.74	-0.30	-0.60	-1.04	0.44	7.02E-01	3.73E-02	5.64E-01	1.40E-01	4.50E-03	3.86E-01
8054580	NM_004336	BUB1	5.9	4.6	4.3	6.1	-1.31	-1.52	0.23	1.54	1.75	-0.21	2.59E-01	4.14E-02	8.80E-01	5.84E-02	2.14E-02	9.06E-01
7982663	NM_001211	BUB1B	5.8	4.4	3.8	6.2	-1.37	-1.99	0.40	1.77	2.39	-0.62	3.39E-01	2.28E-02	8.05E-01	6.70E-02	8.10E-03	6.96E-01
7928882	NM_006829	C10orf116	6.7	6.6	6.4	7.5	-0.15	-0.37	0.74	0.89	1.11	-0.21	7.74E-01	1.11E-01	2.80E-03	3.54E-04	1.76E-05	5.54E-01
7943711	NM_207645	C11orf87	6.3	6.8	6.7	5.4	0.45	0.37	-0.98	-1.43	-1.35	-0.08	5.47E-01	4.46E-01	2.34E-02	1.03E-03	1.15E-03	9.33E-01
7968351	NM_032849	C13orf33	6.0	6.8	6.5	7.2	0.79	0.46	1.22	0.43	0.77	-0.34	1.33E-01	2.56E-01	2.51E-03	3.57E-01	4.11E-02	5.80E-01
7978776	NM_018353	C14orf106	5.4	5.1	5.2	6.3	-0.34	-0.29	0.87	1.21	1.16	0.05	4.84E-01	3.50E-01	3.13E-03	8.71E-05	8.89E-05	9.47E-01
7980496	NM_152446	C14orf145	5.3	5.2	4.9	6.1	-0.18	-0.47	0.75	0.93	1.22	-0.29	9.03E-01	4.04E-01	1.73E-01	7.04E-02	1.09E-02	7.45E-01
8001178	BC056676	C16orf87	6.3	6.6	7.1	5.9	0.32	0.76	-0.44	-0.76	-1.20	0.44	7.02E-01	4.94E-02	3.91E-01	7.30E-02	2.64E-03	4.42E-01
8021286	NM_173529	C18orf54	4.8	5.1	4.6	5.7	0.32	-0.16	0.87	0.55	1.03	-0.48	7.51E-01	8.26E-01	7.15E-02	3.12E-01	2.04E-02	4.68E-01
7908161	NM_030806	C1orf21	7.5	7.5	6.7	8.1	-0.02	-0.78	0.55	0.58	1.33	-0.76	9.88E-01	1.27E-02	1.23E-01	1.03E-01	1.29E-04	3.90E-02
7905147	NM_024579	C1orf54	7.8	7.6	6.5	5.4	-0.14	-1.28	-2.33	-2.19	-1.05	-1.14	9.00E-01	4.53E-04	6.61E-07	1.52E-06	3.78E-03	5.58E-03
8111443	NM_181435	C1QTNF3	3.5	4.5	6.1	3.9	0.93	2.58	0.37	-0.56	-2.21	1.64	2.39E-01	1.66E-05	6.50E-01	4.09E-01	1.07E-04	6.03E-03
8068083	NM_020152	C21orf7	7.3	7.8	7.6	6.0	0.52	0.33	-1.31	-1.83	-1.64	-0.19	5.59E-01	6.06E-01	9.01E-03	3.85E-04	7.89E-04	8.46E-01
8033257	NM_000064	C3	4.7	5.7	5.5	6.9	0.98	0.78	2.20	1.22	1.43	-0.20	5.49E-01	4.65E-01	1.83E-02	2.33E-01	1.21E-01	9.26E-01
8102587	NM_024574	C4orf31	6.9	7.5	6.9	4.3	0.54	0.01	-2.66	-3.20	-2.66	-0.54	7.83E-01	9.98E-01	3.17E-03	4.25E-04	1.67E-03	7.18E-01
8163839	NM_001735	C5	4.5	4.7	3.8	5.3	0.20	-0.65	0.82	0.62	1.47	-0.86	8.15E-01	5.81E-02	2.80E-02	1.07E-01	1.01E-04	3.00E-02
8113504	NM_004772	C5orf13	10.2	10.5	10.5	9.4	0.36	0.35	-0.73	-1.09	-1.08	-0.01	6.93E-01	5.27E-01	1.36E-01	1.71E-02	1.32E-02	9.91E-01
8107194	BC009203	C5orf30	6.1	6.2	6.1	7.3	0.11	0.02	1.24	1.14	1.22	-0.09	9.38E-01	9.81E-01	4.41E-03	7.91E-03	2.89E-03	9.32E-01
8113103	NM_001145678	C5orf36	5.3	5.9	6.3	5.2	0.62	1.01	-0.10	-0.72	-1.10	0.39	1.51E-01	8.69E-04	8.72E-01	2.43E-02	4.92E-04	3.51E-01
8113097	NM_001145678	C5orf36	6.8	7.4	7.7	6.7	0.66	0.93	-0.11	-0.76	-1.04	0.28	9.56E-02	1.08E-03	8.48E-01	1.15E-02	5.30E-04	5.42E-01
8126853	NM_001013732	C6orf138	5.4	6.5	6.0	4.2	1.05	0.56	-1.25	-2.30	-1.82	-0.49	1.46E-01	3.24E-01	2.08E-02	6.99E-05	6.06E-04	5.42E-01
8135734	NM_024913	C7orf58	6.7	6.5	6.3	8.2	-0.13	-0.32	1.58	1.71	1.90	-0.19	9.68E-01	8.40E-01	1.36E-01	9.47E-02	4.53E-02	9.37E-01
8132710	NM_025031	C7orf69	5.2	3.8	3.9	3.6	-1.32	-1.26	-1.57	-0.26	-0.31	0.05	3.08E-02	5.29E-03	2.02E-03	7.39E-01	6.57E-01	9.69E-01
8151369	NM_153225	C8orf84	6.2	6.2	6.1	4.7	0.00	-0.17	-1.52	-1.52	-1.35	-0.17	9.99E-01	8.81E-01	2.34E-02	2.12E-02	3.18E-02	9.11E-01
8162624	NM_153698	C9orf21	6.1	6.2	6.6	7.2	0.03	0.50	1.09	1.06	0.59	0.47	9.78E-01	5.73E-02	2.75E-04	2.90E-04	2.63E-02	1.44E-01
7971590	NM_030925	CAB39L	4.2	5.0	5.2	4.6	0.81	1.06	0.49	-0.32	-0.57	0.26	2.29E-01	1.43E-02	4.04E-01	6.41E-01	2.59E-01	7.58E-01
7901993	NM_020925	CACHD1	6.8	6.6	6.8	7.9	-0.25	-0.07	1.07	1.33	1.14	0.19	8.02E-01	9.30E-01	1.53E-02	2.64E-03	6.38E-03	8.25E-01
7926506	NM_201596	CACNB2	3.6	3.8	3.6	4.9	0.19	-0.05	1.25	1.07	1.30	-0.23	8.67E-01	9.51E-01	3.24E-03	1.01E-02	1.24E-03	7.50E-01
8055872	NM_000726	CACNB4	5.2	5.7	6.6	6.4	0.44	1.32	1.13	0.69	-0.19	0.88	7.29E-01	1.73E-02	6.92E-02	3.28E-01	8.52E-01	2.23E-01
7951807	NM_014333	CADM1	6.6	6.7	7.6	6.5	0.14	1.03	-0.11	-0.25	-1.14	0.89	9.26E-01	1.86E-02	9.07E-01	7.35E-01	1.13E-02	9.28E-02
8057578	NM_005795	CALCRL	5.4	6.0	5.9	4.2	0.56	0.53	-1.20	-1.76	-1.73	-0.03	5.43E-01	3.45E-01	2.24E-02	9.42E-04	7.23E-04	9.84E-01
7913237	NM_018584	CAMK2N1	6.8	7.4	7.3	8.3	0.57	0.46	1.42	0.84	0.96	-0.12	5.53E-01	4.70E-01	1.03E-02	1.45E-01	6.92E-02	9.27E-01
8053417	NM_001747	CAPG	6.2	5.8	5.5	7.4	-0.35	-0.64	1.20	1.55	1.84	-0.29	7.30E-01	1.84E-01	1.50E-02	1.72E-03	1.94E-04	7.27E-01
7982757	NM_170589	CASC5	5.9	4.5	3.6	6.3	-1.40	-2.24	0.45	1.85	2.69	-0.84	3.04E-01	8.75E-03	7.67E-01	4.85E-02	2.63E-03	5.49E-01
8089261	NM_170662	CBLB	9.0	8.3	8.0	8.5	-0.65	-1.00	-0.46	0.19	0.54	-0.35	3.13E-02	6.63E-05	6.95E-02	5.61E-01	2.05E-02	2.50E-01
8023575	NM_133459	CCBE1	5.9	5.3	5.0	6.6	-0.63	-0.85	0.73	1.37	1.58	-0.22	4.65E-01	9.06E-02	2.07E-01	9.50E-03	1.82E-03	8.35E-01
7903049	NM_206886	CCDC18	4.1	3.9	3.9	5.4	-0.27	-0.22	1.30	1.57	1.52	0.06	6.29E-01	5.55E-01	7.46E-05	4.83E-06	5.46E-06	9.37E-01
7942941	NM_001156474	CCDC81	4.2	5.0	5.0	3.8	0.80	0.81	-0.44	-1.23	-1.24	0.01	1.73E-01	4.27E-02	4.14E-01	4.09E-03	2.56E-03	9.92E-01
8006445	NM_002986	CCL11	4.4	4.6	6.4	4.5	0.22	2.00	0.07	-0.15	-1.93	1.78	9.15E-01	1.65E-03	9.66E-01	9.08E-01	2.94E-03	1.36E-02
8006433	NM_002982	CCL2	8.3	9.7	10.4	10.1	1.35	2.07	1.82	0.48	-0.25	0.73	4.35E-03	3.34E-06	3.89E-05	2.94E-01	6.52E-01	1.02E-01
8140358	NM_006072	CCL26	3.7	3.7	6.6	3.6	-0.09	2.89	-0.14	-0.05	-3.03	2.98	9.60E-01	2.22E-06	8.94E-01	9.64E-01	1.06E-06	1.36E-05
8102643	NM_001237	CCNA2	7.3	6.0	5.5	7.3	-1.21	-1.76	0.05	1.27	1.81	-0.54	3.36E-01	2.29E-02	9.78E-01	1.57E-01	2.30E-02	7.02E-01
7983969	NM_004701	CCNB2	6.2	5.0	4.3	6.9	-1.22	-1.94	0.68	1.91	2.63	-0.72	3.00E-01	8.38E-03	5.22E-01	1.74E-02	8.45E-04	5.54E-01
7953200	NM_001759	CCND2	5.7	6.2	6.5	4.4	0.45	0.82	-1.32	-1.77	-2.14	0.37	8.30E-01	3.93E-01	1.61E-01	4.28E-02	9.49E-03	8.27E-01
8120719	NM_133493	CD109	7.8	8.0	7.9	8.9	0.18	0.05	1.09	0.91	1.04	-0.13	8.23E-01	9.31E-01	1.54E-03	5.93E-03	1.24E-03	8.47E-01
8001657	NM_001004195	CD200	4.1	4.5	4.3	3.4	0.40	0.27	-0.70	-1.10	-0.97	-0.13	6.76E-01	6.04E-01	1.96E-01	2.45E-02	3.86E-02	9.02E-01
7949588	NM_020404	CD248	8.9	9.3	9.4	7.4	0.38	0.49	-1.54	-1.92	-2.02	0.11	2.51E-01	2.22E-02	2.29E-07	4.57E-09	2.28E-09	8.08E-01
8133876	NM_001001548	CD36	6.5	7.1	7.2	3.9	0.63	0.74	-2.54	-3.16	-3.28	0.11	7.72E-01	5.26E-01	9.75E-03	1.37E-03	6.33E-04	9.65E-01
7909332	NM_001114752	CD55	7.0	7.0	7.0	8.4	-0.01	0.02	1.40	1.41	1.39	0.02	9.98E-01	9.89E-01	3.94E-02	3.54E-02	2.93E-02	9.91E-01
8004510	NM_001251	CD68	9.1	8.7	7.8	9.2	-0.48	-1.29	0.04	0.53	1.33	-0.81	4.82E-01	9.02E-04	9.62E-01	2.52E-01	8.97E-04	7.62E-02
7953291	NM_001769	CD9	8.8	9.0	9.2	9.9	0.19	0.35	1.01	0.82	0.66	0.16	8.89E-01	5.50E-01	3.85E-02	9.93E-02	1.80E-01	8.77E-01
8051573	NM_006449	CDC42EP3	9.4	9.4	9.1	8.0	-0.08	-0.33	-1.44	-1.36	-1.11	-0.25	9.54E-01	4.55E-01	3.87E-04	5.37E-04	2.46E-03	6.95E-01
8071212	NM_001178010	CDC45	4.7	4.2	4.1	5.5	-0.46	-0.55	0.79	1.25	1.34	-0.09	7.03E-01	4.07E-01	2.41E-01	3.66E-02	1.77E-02	9.53E-01
8007071	NM_001254	CDC6	7.3	7.5	8.3	7.6	0.24	1.03	0.35	0.11	-0.68	0.79	8.69E-01	4.35E-02	6.70E-01	9.23E-01	2.46E-01	2.36E-01
8145418	NM_152562	CDCA2	5.0	4.5	4.0	5.8	-0.49	-1.02	0.86	1.35	1.88	-0.53	7.04E-01	9.15E-02	2.26E-01	3.36E-02	2.11E-03	5.85E-01
8138489	NM_018719	CDCA7L	7.0	6.6	7.0	7.8	-0.44	-0.01	0.79	1.23	0.80	0.43	5.56E-01	9.87E-01	6.90E-02	3.59E-03	4.62E-02	4.75E-01
8086517	NM_022842	CDCP1	5.8	5.1	4.8	6.0	-0.66	-0.95	0.20	0.86	1.15	-0.29	5.25E-01	9.59E-02	8.54E-01	1.81E-01	4.31E-02	7.92E-01
7996837	NM_004360	CDH1	3.9	4.3	5.0	3.6	0.41	1.12	-0.26	-0.67	-1.38	0.71	5.74E-01	2.81E-03	6.57E-01	1.10E-01	5.37E-04	1.20E-01
8104663	NM_004932	CDH6	9.0	8.8	8.9	6.8	-0.14	-0.04	-2.20	-2.06	-2.16	0.10	9.58E-01	9.79E-01	5.95E-03	9.07E-03	4.09E-03	9.60E-01
7927710	NM_001786	CDK1	3.6	3.3	3.1	4.4	-0.26	-0.43	0.83	1.09	1.26	-0.17	8.70E-01	5.47E-01	2.06E-01	7.14E-02	2.45E-02	8.93E-01
8140955	NM_001259	CDK6	6.8	7.2	7.8	6.7	0.42	1.07	-0.07	-0.50	-1.14	0.65	5.22E-01	2.69E-03	9.31E-01	2.48E-01	2.06E-03	1.42E-01
7974404	NM_005192	CDKN3	6.9	5.7	4.6	7.1	-1.17	-2.23	0.23	1.40	2.46	-1.06	2.96E-01	1.80E-03	8.76E-01	7.29E-02	9.75E-04	2.58E-01
8012951	NM_006382	CDRT1	4.9	4.6	5.9	4.3	-0.29	1.00	-0.66	-0.37	-1.66	1.29	7.60E-01	1.29E-02	1.69E-01	5.31E-01	1.94E-04	6.36E-03
8102076	NM_001813	CENPE	4.9	4.3	4.0	6.0	-0.64	-0.91	1.11	1.75	2.02	-0.27	6.38E-01	2.05E-01	1.52E-01	1.46E-02	3.34E-03	8.52E-01
7909708	NM_016343	CENPF	6.9	5.2	4.7	7.5	-1.73	-2.21	0.53	2.26	2.74	-0.48	1.16E-01	3.96E-03	6.64E-01	6.37E-03	7.64E-04	7.37E-01
7970624	NM_018451	CENPJ	5.6	5.5	6.0	6.6	-0.05	0.49	1.02	1.07	0.53	0.54	9.70E-01	2.68E-01	1.88E-02	1.21E-02	2.50E-01	3.18E-01
8112376	NM_022145	CENPK	4.9	4.6	4.3	6.2	-0.32	-0.59	1.34	1.66	1.93	-0.27	8.68E-01	4.83E-01	7.12E-02	2.12E-02	5.08E-03	8.51E-01
8121911	NM_001012507	CENPW	4.8	4.3	4.1	5.2	-0.51	-0.75	0.32	0.83	1.07	-0.24	5.85E-01	1.34E-01	6.72E-01	1.22E-01	2.80E-02	8.03E-01
8095187	NM_025009	CEP135	6.6	6.2	6.3	7.3	-0.36	-0.24	0.77	1.13	1.01	0.12	3.57E-01	4.07E-01	3.84E-03	6.05E-05	1.41E-04	7.95E-01
7929334	NM_018131	CEP55	6.2	5.1	4.4	6.8	-1.12	-1.83	0.64	1.75	2.47	-0.71	3.98E-01	1.84E-02	5.87E-01	3.84E-02	2.40E-03	5.82E-01
8158250	NM_016174	CERCAM	7.3	7.4	7.8	6.3	0.09	0.52	0.93	1.02	1.45	0.43	9.03E 01	3.01E 02	6.09E 04	1.80E 04	1.56E 06	1.54E 01
8001457	NM_001025195	CES1	6.4	6.8	7.0	4.8	0.34	0.60	-1.58	-1.92	-2.18	0.26	8.84E-01	5.57E-01	6.37E-02	2.04E-02	5.94E-03	8.85E-01
7908459	NM_000186	CFH	9.7	10.1	10.3	9.2	0.46	0.61	-0.44	-0.90	-1.05	0.15	3.14E-01	3.41E-02	1.99E-01	3.74E-03	6.23E-04	7.99E-01
7934916	NM_003956	CH25H	4.3	4.9	4.5	6.0	0.69	0.30	1.77	1.08	1.47	-0.39	4.13E-01	6.77E-01	1.33E-03	4.26E-02	3.73E-03	6.43E-01
8068478	NM_005441	CHAF1B	5.8	5.3	5.1	6.2	-0.43	-0.61	0.48	0.91	1.09	-0.18	5.39E-01	1.13E-01	3.15E-01	2.33E-02	4.56E-03	8.14E-01
7923547	NM_001276	CHI3L1	7.7	7.9	6.2	10.2	0.21	-1.45	2.53	2.32	3.99	-1.67	9.73E-01	4.87E-01	1.99E-01	2.45E-01	1.85E-02	5.28E-01
8020179	NM_020412	CHMP1B	7.6	7.2	7.0	8.2	-0.43	-0.66	0.60	1.02	1.26	-0.23	4.44E-01	3.95E-02	1.01E-01	3.28E-03	2.96E-04	6.85E-01
8056890	NM_001822	CHN1	7.7	7.9	8.1	6.4	0.21	0.43	-1.30	-1.52	-1.73	0.21	9.01E-01	5.43E-01	2.57E-02	8.67E-03	1.90E-03	8.56E-01
8067969	NM_024944	CHODL	3.4	3.4	3.5	4.8	-0.05	0.05	1.36	1.42	1.31	0.10	9.34E-01	8.87E-01	2.96E-07	1.38E-07	2.52E-07	7.86E-01
8174513	NM_145234	CHRDL1	4.5	5.1	5.9	7.9	0.52	1.38	3.33	2.82	1.96	0.86	5.97E-01	4.97E-03	5.50E-07	4.83E-06	2.66E-04	1.63E-01
7966878	NM_007174	CIT	5.9	5.8	4.8	6.8	-0.11	-1.17	0.82	0.93	1.99	-1.06	9.62E-01	8.95E-02	3.48E-01	2.52E-01	4.09E-03	2.23E-01
7969243	NM_018204	CKAP2	8.5	8.2	7.8	8.8	-0.30	-0.66	0.37	0.68	1.03	-0.35	7.31E-01	1.01E-01	4.89E-01	1.22E-01	9.28E-03	5.80E-01
8054702	NM_152515	CKAP2L	5.1	4.2	3.6	6.0	-0.86	-1.49	0.89	1.75	2.38	-0.63	6.10E-01	8.53E-02	4.45E-01	5.79E-02	6.28E-03	6.76E-01
8156290	NM_001827	CKS2	8.4	7.8	7.1	8.3	-0.61	-1.24	-0.05	0.56	1.19	-0.63	6.34E-01	4.94E-02	9.73E-01	5.36E-01	7.03E-02	5.30E-01
8083887	NM_005602	CLDN11	6.2	6.3	6.0	8.2	0.09	-0.16	1.99	1.90	2.15	-0.25	9.78E-01	9.18E-01	2.72E-02	3.26E-02	1.08E-02	8.98E-01
8102877	NM_004362	CLGN	4.4	4.2	3.7	7.8	-0.14	-0.70	3.47	3.61	4.17	-0.56	9.51E-01	3.19E-01	6.42E-06	3.27E-06	2.39E-07	5.81E-01
7914851	NM_022111	CLSPN	5.8	4.9	4.6	6.5	-0.93	-1.26	0.65	1.58	1.91	-0.33	5.74E-01	1.64E-01	6.15E-01	9.42E-02	2.79E-02	8.61E-01

			Estimate				Log-ratio						p-value (corr)					
UT ID	NCBI Ref No	Gene Symbol	G1	G2	G3	G4	G2/G1	G3/G1	G4/G1	G4/G2	G4/G3	G3/G2	G2/G1	G3/G1	G4/G1	G4/G2	G4/G3	G3/G2
8149927	NM_001831	CLU	7.2	7.7	7.1	10.3	0.55	-0.07	3.14	2.59	3.21	-0.62	8.09E-01	9.69E-01	1.92E-03	8.34E-03	8.22E-04	7.07E-01
8124307	NR_002174	CMAH	5.3	6.2	6.0	5.0	0.91	0.73	-0.24	-1.15	-0.97	-0.18	1.11E-01	7.33E-02	7.21E-01	7.72E-03	1.77E-02	8.31E-01
7966089	NM_001142343	CMKLR1	5.8	7.8	8.3	5.4	1.99	2.49	-0.39	-2.38	-2.88	0.50	1.08E-02	1.12E-04	6.87E-01	3.77E-04	2.59E-05	6.21E-01
8166355	NM_014927	CNKSR2	4.4	4.2	4.4	7.1	-0.21	-0.02	2.70	2.91	2.72	0.18	8.31E-01	9.75E-01	1.94E-07	4.36E-08	8.47E-08	8.08E-01
8025918	NM_001299	CNN1	6.1	7.2	6.9	5.1	1.12	0.81	-0.96	-2.08	-1.77	-0.31	1.33E-01	1.34E-01	9.97E-02	3.31E-04	1.10E-03	7.47E-01
8088866	NM_020872	CNTN3	3.5	3.4	3.5	5.1	-0.10	-0.04	1.58	1.68	1.62	0.06	9.54E-01	9.68E-01	3.13E-03	1.46E-03	1.33E-03	9.62E-01
8056343	NM_014900	COBLL1	5.8	6.2	7.1	6.4	0.33	1.22	0.53	0.20	-0.69	0.89	3.44E-01	2.68E-06	2.19E-02	4.92E-01	1.71E-03	5.90E-04
7968711	NM_020751	COG6	8.4	8.6	9.1	8.0	0.16	0.73	-0.41	-0.57	-1.13	0.56	7.44E-01	1.06E-03	9.76E-02	1.51E-02	1.07E-05	2.52E-02
7918064	NM_001854	COL11A1	6.7	7.2	7.4	5.6	0.45	0.65	-1.08	-1.53	-1.73	0.20	7.55E-01	3.72E-01	1.27E-01	2.16E-02	6.54E-03	8.90E-01
8148070	NM_021110	COL14A1	8.2	9.1	9.6	9.1	0.91	1.37	0.94	0.03	-0.43	0.46	7.57E-02	3.70E-04	1.90E-02	9.72E-01	3.36E-01	3.83E-01
8156783	NM_001855	COL15A1	4.9	5.3	6.2	5.3	0.41	1.31	0.41	0.00	-0.90	0.90	7.89E-01	3.69E-02	6.93E-01	9.99E-01	2.00E-01	2.88E-01
8016646	NM_000088	COL1A1	8.7	9.2	9.7	8.5	0.43	0.98	-0.26	-0.69	-1.24	0.55	5.28E-01	6.96E-03	6.56E-01	8.91E-02	1.25E-03	2.62E-01
8046922	NM_000090	COL3A1	7.2	8.0	8.9	6.9	0.88	1.74	-0.23	-1.12	-1.97	0.85	1.54E-02	1.14E-06	5.74E-01	3.66E-04	1.38E-07	8.38E-03
7972750	NM_001845	COL4A1	7.0	6.8	7.2	4.9	-0.18	0.18	-2.11	-1.93	-2.30	0.37	9.41E-01	8.88E-01	7.12E-03	1.25E-02	2.10E-03	7.98E-01
7970033	NM_001846	COL4A2	7.1	6.9	7.1	5.6	-0.19	0.01	-1.46	-1.27	-1.47	0.20	9.18E-01	9.93E-01	1.48E-02	3.17E-02	9.01E-03	8.74E-01
8057620	NM_000393	COL5A2	6.4	7.0	7.7	6.1	0.51	1.29	-0.32	-0.83	-1.61	0.78	1.77E-01	1.66E-05	3.40E-01	3.06E-03	1.06E-06	9.30E-03
8069269	NM_001848	COL6A1	7.9	8.3	9.2	8.2	0.45	1.32	0.26	-0.19	-1.06	0.87	3.88E-01	9.34E-05	5.72E-01	7.10E-01	1.17E-03	1.52E-02
8021946	NM_130386	COLEC12	4.9	5.3	5.1	7.1	0.39	0.13	2.11	1.72	1.98	-0.26	7.93E-01	9.05E-01	1.78E-03	8.50E-03	1.70E-03	8.44E-01
8035517	NM_000095	COMP	7.4	7.9	9.0	7.8	0.52	1.69	0.48	-0.05	-1.21	1.17	7.65E-01	2.06E-02	6.93E-01	9.79E-01	1.26E-01	2.20E-01
8016390	NM_016429	COPZ2	9.3	9.6	9.7	8.6	0.27	0.35	-0.72	-0.99	-1.06	0.07	5.40E-01	1.64E-01	5.34E-03	1.99E-04	5.39E-05	8.93E-01
8136200	NM_016352	CPA4	7.8	6.9	6.4	6.9	-0.94	-1.42	-0.91	0.03	0.51	-0.48	3.30E-01	1.62E-02	2.03E-01	9.83E-01	5.29E-01	6.36E-01
8098204	NM_001873	CPE	6.4	7.0	8.0	5.7	0.67	1.62	-0.62	-1.29	-2.24	0.95	5.93E-01	9.76E-03	4.78E-01	6.12E-02	8.11E-04	2.58E-01
7964834	NM_001874	CPM	4.1	3.4	3.4	5.3	-0.62	-0.69	1.22	1.84	1.91	-0.07	3.80E-01	1.18E-01	8.17E-03	1.48E-04	5.64E-05	9.52E-01
7936835	NM_198148	CPXM2	4.0	4.0	4.1	6.4	0.03	0.11	2.43	2.41	2.32	0.09	9.93E-01	9.26E-01	1.16E-03	1.06E-03	9.50E-04	9.64E-01
7921099	NM_001878	CRABP2	4.7	6.1	7.1	6.0	1.43	2.37	1.27	-0.15	-1.10	0.95	1.89E-01	1.39E-03	1.29E-01	9.23E-01	1.75E-01	3.59E-01
8146967	NM_031461	CRISPLD1	5.5	5.8	6.4	4.6	0.29	0.83	-0.95	-1.24	-1.77	0.53	9.07E-01	3.62E-01	3.45E-01	1.67E-01	2.52E-02	7.05E-01
8149574	NM_018371	CSGALNACT1	4.3	4.4	4.0	5.0	0.13	-0.33	0.68	0.55	1.01	-0.46	9.37E-01	6.05E-01	2.34E-01	3.62E-01	3.63E-02	5.46E-01
7923378	NM_004078	CSRP1	8.9	9.2	9.1	7.8	0.30	0.23	-1.11	-1.41	-1.34	-0.07	8.05E-01	7.59E-01	3.44E-02	6.53E-03	6.60E-03	9.60E-01
7965090	NM_001321	CSRP2	6.6	7.0	8.0	5.7	0.37	1.38	-0.87	-1.25	-2.25	1.01	7.19E-01	3.08E-03	9.68E-02	1.30E-02	2.56E-05	7.02E-02
7950906	NM_001814	CTSC	4.3	4.2	4.4	7.6	-0.10	0.06	3.28	3.38	3.22	0.16	9.32E-01	9.26E-01	1.52E-09	8.08E-10	2.22E-09	8.25E-01
7945666	NM_001909	CTSD	8.6	8.2	8.1	7.1	-0.47	-0.58	-1.51	-1.05	-0.93	-0.11	5.54E-01	1.91E-01	1.14E-03	1.89E-02	2.75E-02	9.12E-01
8095697	NM_001511	CXCL1	5.5	5.6	6.0	7.0	0.11	0.50	1.52	1.41	1.01	0.39	9.12E-01	1.14E-01	4.11E-05	7.82E-05	1.58E-03	3.64E-01
7933194	NM_000609	CXCL12	9.1	8.9	8.9	8.0	-0.12	-0.17	-1.09	-0.97	-0.92	-0.05	9.31E-01	7.97E-01	1.27E-02	2.44E-02	2.49E-02	9.65E-01
8011713	NM_022059	CXCL16	5.4	4.9	5.2	4.2	-0.47	-0.24	-1.26	-0.78	-1.01	0.23	4.90E-01	6.56E-01	2.84E-03	5.90E-02	8.97E-03	7.42E-01
8100994	NM_002089	CXCL2	4.2	4.2	4.0	6.2	-0.03	-0.15	1.99	2.02	2.14	-0.12	9.88E-01	8.70E-01	6.38E-04	4.49E-04	1.55E-04	9.29E-01
7923516	NM_016243	CYB5R1	8.0	8.0	8.0	7.0	-0.06	-0.01	-1.00	-0.94	-1.00	0.05	9.54E-01	9.89E-01	1.90E-03	2.75E-03	1.08E-03	9.44E-01
8018754	NM_134268	CYGB	6.9	5.9	6.4	5.3	-0.99	-0.44	-1.62	-0.63	-1.18	0.54	5.17E-02	2.96E-01	1.93E-04	1.36E-01	2.34E-03	2.74E-01
8176698	NM_001005852	CYorf15A	3.2	3.1	3.1	4.5	-0.07	-0.07	1.31	1.39	1.38	0.00	9.53E-01	9.06E-01	4.02E-04	1.80E-04	1.15E-04	9.98E-01
7988767	NM_031226	CYP19A1	3.4	3.3	3.2	4.4	-0.12	-0.16	1.04	1.16	1.20	-0.04	9.33E-01	8.15E-01	2.39E-02	1.08E-02	5.58E-03	9.73E-01
7974697	NM_014992	DAAM1	6.2	6.9	7.1	6.1	0.73	0.95	-0.12	-0.86	-1.07	0.21	1.30E-04	1.14E-06	5.80E-01	5.06E-06	1.38E-07	3.08E-01
7974689	NM_016651	DACT1	8.1	8.0	8.2	6.3	-0.05	0.15	-1.75	-1.70	-1.90	0.20	9.87E-01	8.98E-01	1.42E-02	1.56E-02	4.84E-03	8.98E-01
8156199	NM_004938	DAPK1	8.1	8.4	7.8	6.4	0.31	-0.32	-1.73	-2.05	-1.42	-0.63	7.86E-01	6.30E-01	1.16E-03	1.65E-04	3.88E-03	3.39E-01
8121685	NM_173674	DCBLD1	7.8	7.5	8.2	7.0	-0.26	0.44	-0.82	-0.56	-1.26	0.70	7.16E-01	2.02E-01	1.89E-02	1.21E-01	2.81E-04	6.65E-02
8000028	NM_173475	DCUN1D3	6.6	7.1	7.3	6.1	0.52	0.70	-0.51	-1.03	-1.21	0.18	9.79E-02	2.08E-03	3.86E-02	7.52E-05	6.81E-06	6.55E-01
7928308	NM_019058	DDIT4	5.3	4.7	4.2	4.8	-0.68	-1.12	-0.52	0.16	0.60	-0.44	2.95E-01	5.67E-03	3.22E-01	8.31E-01	1.84E-01	4.83E-01
8101952	NM_145244	DDIT4L	3.9	4.1	3.7	5.3	0.14	-0.19	1.36	1.22	1.56	-0.33	8.63E-01	6.24E-01	6.27E-05	1.76E-04	5.59E-06	4.28E-01
8176624	NM_001122665	DDX3Y	3.3	3.5	3.4	7.5	0.14	0.12	4.24	4.10	4.12	-0.02	9.62E-01	9.39E-01	3.45E-05	4.14E-05	2.34E-05	9.94E-01
8120679	NM_010665	DDX43	4.2	4.4	4.3	5.2	0.17	0.15	1.06	0.89	0.91	-0.01	8.04E-01	8.07E-01	1.08E-02	3.05E-02	2.04E-02	9.91E-01
8160559	NM_014314	DDX58	5.7	6.3	7.7	6.1	0.67	1.99	0.46	-0.22	-1.53	1.32	4.18E-01	1.40E-04	5.05E-01	8.07E-01	2.44E-03	1.88E-02
8103563	NM_017631	DDX60	4.3	4.5	5.8	4.5	0.26	1.54	0.29	0.02	-1.26	1.28	8.29E-01	1.10E-03	7.13E-01	9.83E-01	8.37E-03	1.66E-02
8103601	NM_001012967	DDX60L	5.9	5.9	7.0	6.3	0.01	1.14	0.41	0.40	-0.73	1.13	9.98E-01	1.31E-02	5.50E-01	5.59E-01	1.48E-01	3.53E-02
7916898	NM_001114120	DEPDC1	4.3	3.5	3.2	5.0	-0.81	-1.10	0.66	1.47	1.75	-0.29	5.32E-01	1.28E-01	5.01E-01	5.05E-02	1.28E-02	8.47E-01
8148059	NM_022783	DEPDC6	7.9	8.1	7.9	4.6	0.15	0.04	-3.35	-3.49	-3.38	-0.11	9.62E-01	9.84E-01	7.16E-04	3.80E-04	3.44E-04	9.65E-01
7968800	NM_178009	DGKH	5.3	5.1	5.1	6.4	-0.22	-0.20	1.05	1.26	1.25	0.01	6.69E-01	5.11E-01	1.95E-04	1.36E-05	1.10E-05	9.87E-01
8143154	NM_004717	DGKI	4.9	4.7	5.4	5.7	-0.11	0.54	0.89	1.00	0.34	0.66	9.34E-01	2.24E-01	4.95E-02	2.33E-02	5.45E-01	2.12E-01
8022640	NM_000791	DHFR	6.4	5.6	5.2	6.3	-0.75	-1.22	-0.11	0.64	1.11	-0.47	3.86E-01	1.72E-02	9.28E-01	3.25E-01	3.61E-02	5.83E-01
7912537	NM_004753	DHRS3	6.2	5.5	4.5	6.3	-0.79	-1.70	0.08	0.87	1.79	-0.91	1.96E-01	1.21E-04	9.33E-01	5.07E-02	9.46E-05	6.24E-02
7927631	NM_012242	DKK1	8.9	7.7	7.2	7.8	-1.22	-1.73	-1.06	0.17	0.68	-0.51	3.81E-01	3.87E-02	3.25E-01	9.28E-01	5.66E-01	7.45E-01
7971653	NR_002612	DLEU2	4.2	4.2	3.9	5.6	-0.07	-0.30	1.39	1.46	1.69	-0.23	9.56E-01	4.97E-01	5.19E-04	2.30E-04	2.59E-05	7.23E-01
7979307	NM_014750	DLGAP5	6.5	4.7	3.5	6.5	-1.80	-2.99	-0.02	1.78	2.97	-1.19	1.56E-01	8.20E-04	9.94E-01	6.28E-02	1.18E-03	3.23E-01
8016609	NM_005220	DLX3	5.8	4.7	4.5	4.7	-1.06	-1.26	-1.14	-0.07	0.12	-0.19	2.20E-01	2.66E-02	7.33E-02	9.55E-01	9.18E-01	8.83E-01
8141140	NM_005221	DLX5	7.5	6.8	7.1	5.9	-0.64	-0.39	-1.55	-0.91	-1.15	0.25	6.51E-01	7.00E-01	4.08E-02	2.83E-01	1.17E-01	8.75E-01
8171921	NM_000109	DMD	5.8	6.1	5.9	4.7	0.32	0.11	-1.03	-1.35	-1.14	-0.21	7.79E-01	8.98E-01	4.91E-02	8.40E-03	1.89E-02	8.32E-01
8158183	NM_004408	DNM1	4.4	4.3	4.4	5.3	-0.12	-0.05	0.89	1.00	0.94	0.06	8.94E-01	9.19E-01	4.32E-03	1.21E-03	1.42E-03	9.30E-01
8169541	NM_144658	DOCK11	7.4	7.0	6.7	8.2	-0.47	-0.69	0.78	1.24	1.47	-0.22	3.00E-01	1.45E-02	1.23E-02	1.41E-04	1.17E-05	6.56E-01
8021695	NM_152721	DOK6	3.8	4.1	4.5	3.4	0.26	0.66	-0.43	-0.69	-1.09	0.39	6.37E-01	1.40E-02	1.74E-01	1.71E-02	2.17E-04	2.74E-01
7922130	NM_001937	DPT	6.3	7.9	9.0	5.2	1.52	2.68	-1.11	-2.63	-3.79	1.16	9.56E-02	1.24E-04	1.38E-01	3.17E-04	2.56E-06	1.51E-01
8020779	NM_001943	DSG2	3.9	3.5	3.5	5.9	-0.42	-0.40	1.96	2.38	2.36	0.03	5.99E-01	4.20E-01	5.36E-05	3.29E-06	2.65E-06	9.84E-01
8116780	NM_004415	DSP	9.5	9.5	10.1	8.7	-0.02	0.59	-0.84	-0.82	-1.42	0.60	9.95E-01	3.04E-01	1.51E-01	1.55E-01	5.86E-03	4.09E-01
8082075	NM_138287	DTX3L	6.4	6.6	7.6	6.8	0.22	1.16	0.40	0.18	-0.76	0.94	8.36E-01	3.94E-03	4.79E-01	8.08E-01	7.05E-02	4.52E-02
7924450	NM_007207	DUSP10	7.6	7.0	6.5	5.1	-0.63	-1.14	-2.50	-1.88	-1.36	-0.51	2.83E-01	2.29E-03	5.50E-07	2.22E-05	5.87E-04	3.14E-01
7943442	NM_001377	DYNC2H1	7.7	7.2	6.7	7.3	-0.53	-1.04	-0.43	0.10	0.61	-0.51	3.54E-01	2.69E-03	3.36E-01	8.87E-01	9.43E-02	2.64E-01
7947110	NM_024680	E2F8	4.0	3.8	3.6	4.8	0.23	0.36	0.78	1.00	1.14	0.14	8.77E-01	5.81E-01	1.65E-01	5.63E-02	2.08E-02	9.08E-01
8115543	NM_024007	EBF1	8.7	8.9	8.8	7.3	0.20	0.10	-1.32	-1.52	-1.42	-0.10	8.40E-01	8.84E-01	1.41E-03	2.67E-04	3.57E-04	9.12E-01
8167305	NM_006579	EBP	7.5	8.3	8.0	7.2	0.79	0.53	-0.35	-1.13	-0.88	-0.25	2.08E-01	2.43E-01	5.71E-01	1.12E-02	3.89E-02	7.45E-01
8116921	NM_001955	EDN1	6.7	6.6	5.2	5.5	-0.12	-1.49	-1.16	-1.04	0.33	-1.37	9.52E-01	4.17E-03	4.32E-02	6.89E-02	6.83E-01	2.22E-02
8097692	NM_001957	EDNRA	6.2	6.4	6.6	4.7	0.23	0.38	-1.53	-1.76	-1.91	0.16	9.22E-01	7.12E-01	4.46E-02	1.87E-02	7.22E-03	9.30E-01
8049187	NM_025202	EFHD1	7.7	7.8	8.2	6.8	0.03	0.44	-0.92	-0.95	-1.36	0.41	9.89E-01	5.16E-01	1.30E-01	1.09E-01	1.17E-02	6.58E-01
7972713	NM_004093	EFNB2	6.0	7.3	7.7	4.1	1.30	1.74	-1.86	-3.17	-3.61	0.44	2.90E-01	2.43E-02	2.88E-02	3.08E-04	4.29E-05	7.71E-01
7985555	NM_024580	EFTUD1	6.2	5.6	6.1	6.7	-0.55	-0.09	0.48	1.04	0.58	0.46	4.15E-01	8.96E-01	3.46E-01	1.51E-02	1.91E-01	4.35E-01
7933872	NM_000399	EGR2	8.1	9.6	9.5	7.2	1.52	1.37	-0.92	-2.44	-2.28	-0.15	9.61E-02	3.50E-02	2.46E-01	7.05E-04	8.59E-04	9.27E-01
8176719	NM_004681	EIF1AY	3.1	3.1	3.1	7.6	0.02	0.02	4.49	4.47	4.47	0.00	9.97E-01	9.92E-01	2.58E-05	1.98E-05	1.32E-05	1.00E+00
7957665	NM_005230	ELK3	7.8	7.6	7.7	8.6	-0.19	-0.07	0.82	1.01	0.89	0.12	8.11E-01	9.05E-01	1.56E-02	2.84E-03	5.58E-03	8.62E-01
8139057	NM_014800	ELMO1	3.6	3.9	3.6	4.6	0.36	0.06	1.08	0.72	1.01	-0.29	6.63E-01	9.32E-01	1.20E-02	1.01E-01	1.16E-02	6.73E-01
7917182	NM_022159	ELTD1	7.3	7.2	7.4	5.6	0.00	0.14	-1.66	-1.66	-1.81	0.15	9.99E-01	9.04E-01	2.01E-02	1.88E-02	7.26E-03	9.30E-01
8112007	NM_198449	EMB	5.1	5.1	5.5	3.8	0.01	0.36	-1.26	-1.27	-1.62	0.35	9.98E-01	2.84E-01	2.36E-04	1.81E-04	5.59E-06	4.18E-01
7999387	NM_001424	EMP2	9.1	8.7	8.1	9.7	-0.40	-1.00	0.63	1.03	1.63	-0.61	2.92E-01	9.68E-05	1.53E-02	1.67E-04	2.18E-07	2.71E-02
7953532	NM_001975	ENO2	6.4	5.1	4.7	5.4	-1.30	-1.69	-1.02	0.28	0.68	-0.39	2.22E-03	1.32E-05	5.41E-03	5.63E-01	4.84E-02	4.17E-01
7971311	NM_017993	ENOX1	4.0	4.5	5.0	4.6	0.59	1.05	0.68	0.09	-0.37	0.47	5.27E-01	3.28E-02	2.65E-01	9.32E-01	6.04E-01	5.67E-01

			Estimate				Log-ratio						p-value (corr)					
UT ID	NCBI Ref No	Gene Symbol	G1	G2	G3	G4	G2/G1	G3/G1	G4/G1	G4/G2	G4/G3	G3/G2	G2/G1	G3/G1	G4/G1	G4/G2	G4/G3	G3/G2
8120061	NM_014936	ENPP4	5.2	5.1	5.4	4.3	-0.04	0.20	-0.86	-0.83	-1.07	0.24	9.78E-01	6.74E-01	1.81E-02	2.18E-02	2.16E-03	6.88E-01
7929511	NM_001776	ENTPD1	4.1	4.6	4.5	3.6	0.46	0.42	-0.56	-1.01	-0.98	-0.04	6.38E-01	4.78E-01	3.72E-01	4.90E-02	4.52E-02	9.81E-01
7929750	NM_020354	ENTPD7	5.7	6.0	7.0	5.8	0.23	1.31	0.10	-0.13	-1.21	1.08	7.95E-01	5.17E-04	8.94E-01	8.53E-01	1.56E-03	1.02E-02
8113512	NM_022140	EPB41L4A	3.8	4.1	3.8	5.4	0.23	-0.01	1.57	1.34	1.58	-0.25	8.20E-01	9.86E-01	6.09E-04	2.42E-03	2.92E-04	7.42E-01
8095723	NM_001013442	EPGN	3.2	3.6	5.5	6.0	0.47	2.32	2.88	2.41	0.56	1.84	7.87E-01	1.39E-03	4.26E-04	2.05E-03	5.81E-01	2.52E-02
8081081	NM_005233	EPHA3	5.8	5.7	6.7	4.1	-0.07	0.91	-1.67	-1.60	-2.58	0.97	9.81E-01	2.24E-01	2.57E-02	2.98E-02	4.47E-04	2.93E-01
8082846	NM_004441	EPHB1	4.4	4.1	4.2	5.6	-0.33	-0.28	1.16	1.49	1.44	0.04	5.74E-01	4.38E-01	6.09E-04	2.64E-05	2.48E-05	9.60E-01
7971296	NM_001002264	EPSTI1	3.7	3.9	5.6	4.0	0.20	1.82	0.28	0.08	-1.54	1.63	8.64E-01	5.39E-05	6.62E-01	9.23E-01	4.10E-04	1.07E-03
7933509	NM_000124	ERCC6	8.4	9.1	9.9	7.4	0.67	1.51	-1.03	-1.70	-2.53	0.84	1.79E-01	5.91E-05	5.98E-03	2.62E-05	6.68E-08	3.38E-02
8070297	NM_001136154	ERG	5.5	5.1	4.9	7.1	-0.39	-0.55	1.66	2.05	2.21	-0.16	8.08E-01	4.99E-01	1.77E-02	3.17E-03	1.04E-03	9.19E-01
8055969	NM_001009959	ERMN	3.6	4.2	5.5	3.0	0.56	1.90	-0.65	-1.21	-2.55	1.35	5.42E-01	1.86E-04	2.72E-01	1.92E-02	7.17E-06	1.39E-02
7912157	NM_018948	ERRFI1	9.5	9.1	8.1	9.1	-0.42	-1.39	-0.36	0.06	1.03	-0.97	4.60E-01	7.32E-05	4.04E-01	9.32E-01	1.94E-03	8.85E-03
8145570	NM_001017420	ESCO2	3.6	3.3	3.3	4.7	-0.25	-0.28	1.18	1.42	1.46	-0.04	9.12E-01	7.98E-01	1.31E-01	5.48E-02	3.61E-02	9.86E-01
8112045	NM_007036	ESM1	5.2	4.9	4.1	6.7	-0.35	-1.11	1.42	1.78	2.53	-0.76	8.24E-01	7.82E-02	3.51E-02	7.63E-03	1.77E-04	4.00E-01
7952601	NM_001143820	ETS1	7.2	6.7	6.5	7.6	-0.47	-0.68	0.42	0.89	1.09	-0.20	2.63E-01	1.14E-02	1.94E-01	2.49E-03	2.09E-04	6.68E-01
8068593	NM_005239	ETS2	5.5	5.3	5.1	7.2	-0.13	-0.36	1.74	1.87	2.10	-0.23	9.34E-01	5.45E-01	6.35E-04	2.45E-04	3.94E-05	7.99E-01
8138289	NM_004956	ETV1	5.7	5.7	5.5	7.5	-0.05	-0.20	1.75	1.80	1.96	-0.16	9.87E-01	8.70E-01	2.20E-02	1.71E-02	6.64E-03	9.31E-01
7968658	NM_181503	EXOSC8	6.2	6.1	6.5	7.2	-0.06	0.26	0.97	1.03	0.72	0.31	9.70E-01	6.52E-01	2.74E-02	1.79E-02	9.40E-02	6.56E-01
8151310	NM_000503	EYA1	5.7	5.8	5.7	4.4	0.16	0.01	-1.31	-1.47	-1.32	-0.15	9.25E-01	9.95E-01	1.74E-02	6.99E-03	1.07E-02	8.98E-01
8143663	NM_004456	EZH2	5.5	4.9	5.0	6.2	-0.62	-0.51	0.69	1.32	1.20	0.12	3.45E-01	2.60E-01	1.37E-01	2.74E-03	4.09E-03	9.03E-01
8112731	NM_004101	F2RL2	4.8	3.9	3.9	5.8	-0.94	-0.89	0.95	1.89	1.84	0.05	2.43E-01	9.74E-02	1.06E-01	1.02E-03	8.19E-04	9.77E-01
7948420	NM_001444	FABP5	6.7	6.7	7.6	7.9	-0.02	0.94	1.18	1.20	0.23	0.97	9.93E-01	7.10E-02	3.67E-02	3.06E-02	7.89E-01	1.25E-01
8147049	NM_001444	FABP5	6.8	6.8	7.7	7.9	-0.03	0.91	1.16	1.19	0.25	0.94	9.91E 01	8.02E 02	3.91E 02	3.16E 02	7.75E 01	1.36E 01
7948612	NM_013402	FADS1	8.1	9.2	9.4	9.0	1.11	1.28	0.86	-0.25	-0.42	0.17	1.11E-01	8.09E-03	1.23E-01	7.68E-01	5.33E-01	8.81E-01
7940565	NM_004265	FADS2	7.5	9.2	9.3	8.3	1.71	1.75	0.83	-0.88	-0.93	0.05	2.38E-02	2.40E-03	2.37E-01	1.91E-01	1.36E-01	9.79E-01
7940147	NM_198947	FAM111B	5.5	4.2	4.0	6.1	-1.26	-1.53	0.61	1.87	2.14	-0.27	3.61E-01	7.28E-02	6.42E-01	3.89E-02	1.25E-02	8.93E-01
7922846	NM_052966	FAM129A	6.2	5.9	6.3	8.0	-0.38	0.03	1.71	2.09	1.68	0.41	8.17E-01	9.84E-01	1.41E-02	2.64E-03	1.01E-02	7.34E-01
8106626	AY358256	FAM151B	6.4	6.8	7.3	5.7	0.38	0.91	-0.69	-1.07	-1.60	0.53	4.52E-01	1.80E-03	2.79E-02	7.66E-04	4.64E-06	1.39E-01
8143127	NM_205855	FAM180A	7.3	6.2	6.5	7.9	-1.15	-0.81	0.59	1.74	1.40	0.34	3.40E-03	7.43E-03	8.39E-02	4.83E-06	4.90E-05	4.65E-01
8103415	NM_001128424	FAM198B	7.0	7.5	7.7	6.2	0.49	0.73	-0.77	-1.26	-1.50	0.24	5.58E-01	1.07E-01	1.23E-01	7.54E-03	1.08E-03	7.80E-01
8130993	NM_020223	FAM20C	6.6	6.5	6.4	7.5	-0.18	-0.23	0.85	1.04	1.08	-0.05	6.41E-01	2.81E-01	1.29E-04	8.62E-06	3.50E-06	9.17E-01
8121601	NM_153711	FAM26E	7.6	8.0	8.2	6.4	0.35	0.59	-1.23	-1.58	-1.82	0.24	6.10E-01	9.20E-02	1.28E-03	6.99E-05	7.17E-06	6.94E-01
8050427	NM_030797	FAM49A	4.2	4.2	4.1	6.0	-0.07	-0.14	1.76	1.83	1.89	-0.07	9.75E-01	8.96E-01	5.23E-03	3.19E-03	1.52E-03	9.69E-01
8129763	NM_001099286	FAM54A	5.1	4.3	4.0	6.1	-0.84	-1.07	1.00	1.84	2.07	-0.23	5.11E-01	1.42E-01	2.39E-01	1.42E-02	3.92E-03	8.84E-01
7917728	NM_001006605	FAM69A	8.1	8.4	8.4	7.1	0.25	0.25	-1.06	-1.31	-1.31	0.00	6.38E-01	4.28E-01	3.59E-04	2.16E-05	1.45E-05	1.00E+00
7919591	AB096683	FAM72D	4.8	4.2	4.0	5.7	-0.63	-0.81	0.87	1.50	1.68	-0.18	6.28E-01	2.52E-01	2.72E-01	2.94E-02	1.02E-02	9.09E-01
7904452	AB096683	FAM72D	5.5	5.0	4.7	6.2	-0.55	-0.79	0.63	1.18	1.41	-0.23	5.99E-01	1.62E-01	3.66E-01	3.92E-02	9.21E-03	8.37E-01
7909146	AB096683	FAM72D	5.5	5.0	4.7	6.1	-0.50	-0.79	0.62	1.12	1.41	-0.28	6.46E-01	1.67E-01	3.79E-01	5.41E-02	1.01E-02	7.88E-01
8039928	AB096683	FAM72D	5.3	4.8	4.6	5.9	-0.48	-0.76	0.60	1.08	1.36	-0.28	6.45E-01	1.60E-01	3.68E-01	5.07E-02	9.15E-03	7.81E-01
8077731	NM_033084	FANCD2	3.5	3.3	3.3	4.3	-0.26	-0.27	0.74	1.00	1.01	-0.01	8.48E-01	7.23E-01	2.14E-01	6.70E-02	4.97E-02	9.96E-01
7931281	NM_145235	FANK1	8.0	7.9	7.8	6.5	-0.04	-0.12	-1.47	-1.43	-1.35	-0.07	9.67E-01	7.96E-01	1.69E-05	1.53E-05	2.04E-05	9.13E-01
8073775	NM_006486	FBLN1	7.5	7.2	6.9	8.4	-0.23	-0.58	0.98	1.21	1.56	-0.35	8.85E-01	3.50E-01	1.08E-01	3.67E-02	4.84E-03	7.26E-01
8077970	NM_001004019	FBLN2	5.6	5.6	5.5	6.5	-0.01	-0.13	0.88	0.89	1.01	-0.11	9.95E-01	8.18E-01	1.46E-02	1.21E-02	3.24E-03	8.79E-01
7980908	NM_006329	FBLN5	10.0	10.4	10.7	9.6	0.45	0.74	-0.39	-0.84	-1.12	0.28	4.39E-01	2.89E-02	3.88E-01	2.08E-02	1.46E-03	6.19E-01
8113800	NM_001999	FBN2	4.7	4.3	4.4	5.7	-0.34	-0.24	1.05	1.39	1.30	0.09	8.34E-01	8.09E-01	1.35E-01	3.56E-02	3.94E-02	9.58E-01
8099449	NR_036464	FBXL5	7.9	8.9	8.8	7.7	1.00	0.92	-0.18	-1.18	-1.10	-0.08	2.05E-05	9.65E-06	4.68E-01	5.42E-07	1.06E-06	8.32E-01
8150002	NM_172366	FBXO16	4.9	5.1	5.6	3.7	0.25	0.74	-1.13	-1.37	-1.87	0.50	8.19E-01	8.62E-02	1.43E-02	2.72E-03	7.34E-05	4.25E-01
8130374	NM_012177	FBXO5	6.5	6.1	5.8	7.6	0.39	0.74	1.13	1.52	1.87	0.34	7.37E 01	1.79E 01	4.43E 02	5.81E 03	6.12E 04	7.14E 01
7905986	NM_002004	FDPS	7.7	9.0	8.8	7.8	1.24	1.02	0.06	-1.17	-0.96	-0.22	3.76E-02	2.11E-02	9.54E-01	1.42E-02	3.66E-02	8.08E-01
8064904	NM_017671	FERMT1	3.7	3.7	3.9	4.7	-0.02	0.17	1.01	1.03	0.85	0.18	9.88E-01	6.11E-01	2.28E-04	1.57E-04	7.55E-04	6.63E-01
7954729	NM_139241	FGD4	5.9	5.7	5.0	6.2	-0.17	-0.88	0.25	0.42	1.13	-0.71	9.25E-01	1.16E-01	7.98E-01	6.03E-01	4.04E-02	3.43E-01
7965541	NM_018351	FGD6	5.3	5.1	4.9	6.7	-0.17	-0.40	1.38	1.55	1.78	-0.23	9.23E-01	5.65E-01	1.64E-02	6.34E-03	1.25E-03	8.37E-01
7983630	NM_002009	FGF7	9.4	9.5	9.2	8.3	0.07	-0.21	-1.13	-1.20	-0.91	-0.28	9.38E-01	5.39E-01	2.40E-04	9.56E-05	1.06E-03	4.92E-01
8140463	NM_006682	FGL2	5.6	5.2	8.1	9.6	-0.49	2.42	3.96	4.45	1.54	2.91	9.01E-01	5.03E-02	3.59E-03	1.03E-03	2.89E-01	4.20E-02
7939052	NM_203371	FIBIN	4.1	4.1	3.7	4.8	-0.03	-0.39	0.72	0.75	1.11	-0.36	9.87E-01	4.49E-01	1.38E-01	1.14E-01	9.84E-03	6.07E-01
8056323	NM_018086	FIGN	5.3	5.4	5.5	3.9	0.13	0.14	-1.43	-1.56	-1.57	0.01	8.87E-01	7.63E-01	7.59E-05	1.81E-05	1.12E-05	9.91E-01
8127646	NM_015687	FILIP1	3.8	3.9	5.0	3.7	0.17	1.22	-0.10	-0.27	-1.32	1.05	8.18E-01	1.02E-04	8.66E-01	5.11E-01	5.34E-05	2.38E-03
8138834	NM_017946	FKBP14	7.5	8.0	8.5	7.3	0.51	1.07	-0.15	-0.66	-1.22	0.55	5.22E-02	4.48E-06	6.23E-01	1.89E-03	1.06E-06	1.30E-02
8125919	NM_001145775	FKBP5	5.1	5.1	5.2	6.5	-0.01	0.10	1.37	1.38	1.27	0.11	9.95E-01	8.46E-01	1.15E-04	7.87E-05	1.35E-04	8.66E-01
7920165	NM_002016	FLG	6.9	7.7	8.6	5.4	0.73	1.70	-1.58	-2.31	-3.28	0.97	7.29E-01	7.49E-02	1.46E-01	2.19E-02	8.99E-04	5.11E-01
8074168	ENST00000400192	FLJ39632	6.4	6.0	6.4	5.3	-0.33	0.08	-1.08	-0.75	-1.15	0.40	6.19E-01	8.98E-01	2.98E-03	3.36E-02	8.34E-04	3.92E-01
7977452	ENST00000400192	FLJ39632	6.5	6.2	6.6	5.4	-0.35	0.05	-1.17	-0.82	-1.22	0.40	5.94E-01	9.30E-01	1.57E-03	2.09E-02	5.30E-04	4.02E-01
8080714	NM_001164317	FLNB	8.8	8.4	7.5	7.8	-0.37	-1.27	-1.04	-0.67	0.23	-0.90	6.38E-01	1.06E-03	1.24E-02	1.19E-01	6.98E-01	4.20E-02
7976073	NM_013231	FLRT2	7.7	7.6	7.9	8.9	-0.06	0.18	1.25	1.31	1.08	0.23	9.80E-01	8.67E-01	5.47E-02	3.96E-02	8.15E-02	8.56E-01
7987145	NM_001103184	FMN1	5.4	5.3	5.7	6.9	-0.08	0.36	1.57	1.65	1.22	0.43	9.67E-01	6.07E-01	4.78E-03	2.68E-03	1.86E-02	6.10E-01
8045736	NM_052905	FMNL2	6.8	6.6	6.8	8.1	-0.16	-0.02	1.30	1.46	1.32	0.14	8.00E-01	9.74E-01	2.22E-05	3.65E-06	8.46E-06	7.72E-01
7907249	NM_006894	FMO3	6.4	6.8	6.1	3.3	0.37	-0.30	-3.12	-3.49	-2.82	-0.67	9.25E-01	8.88E-01	1.53E-02	6.12E-03	1.96E-02	7.67E-01
8098103	NM_020840	FNIP2	7.5	7.2	7.9	6.3	-0.30	0.39	-1.20	-0.90	-1.58	0.69	8.47E-01	6.23E-01	5.75E-02	1.74E-01	6.78E-03	4.07E-01
7949532	NM_005438	FOSL1	6.8	6.7	6.4	7.4	-0.15	-0.39	0.61	0.77	1.01	-0.24	7.72E-01	7.96E-02	1.06E-02	1.51E-03	5.04E-05	4.72E-01
7960340	NM_202002	FOXM1	5.7	4.9	4.6	6.6	-0.80	-1.10	0.81	1.61	1.91	-0.30	3.50E-01	3.52E-02	1.95E-01	4.43E-03	6.27E-04	7.68E-01
7980680	NM_001085471	FOXN3	7.6	7.6	7.1	8.5	-0.06	-0.53	0.89	0.96	1.42	-0.46	9.57E-01	1.08E-01	9.41E-03	4.91E-03	5.96E-05	2.72E-01
7932132	NM_018027	FRMD4A	5.5	5.9	5.9	4.6	0.36	0.41	-0.88	-1.24	-1.29	0.05	4.15E-01	1.32E-01	2.46E-03	5.22E-05	1.92E-05	9.45E-01
8080745	NM_015123	FRMD4B	4.2	4.3	4.1	6.2	0.06	-0.11	2.00	1.94	2.11	-0.17	9.77E-01	9.18E-01	1.09E-03	1.21E-03	3.35E-04	8.98E-01
8169235	ENST00000276185	FRMPD3	4.0	3.9	3.8	4.9	-0.03	-0.12	0.94	0.97	1.06	-0.09	9.85E-01	8.61E-01	2.77E-02	2.09E-02	8.15E-03	9.28E-01
7917954	NM_001013660	FRRS1	7.1	7.1	6.6	5.8	-0.06	-0.51	-1.29	-1.23	-0.78	-0.45	9.63E-01	2.27E-01	2.66E-03	3.33E-03	5.06E-02	4.34E-01
8057506	NM_001463	FRZB	4.9	5.1	4.5	4.1	0.22	-0.43	-0.82	-1.04	-0.39	-0.65	8.70E-01	4.51E-01	1.21E-01	3.81E-02	5.43E-01	3.04E-01
7909441	NM_015714	G0S2	5.7	5.3	5.1	6.4	-0.34	-0.53	0.68	1.01	1.21	-0.19	7.20E-01	2.55E-01	1.67E-01	2.46E-02	5.19E-03	8.26E-01
8162777	NM_005458	GABBR2	3.9	4.0	3.9	5.2	0.12	-0.04	1.34	1.22	1.38	-0.15	9.18E-01	9.57E-01	6.09E-04	1.24E-03	2.41E-04	8.34E-01
8045776	NM_052917	GALNT13	3.3	3.3	3.4	5.1	-0.02	0.04	1.80	1.82	1.76	0.05	9.93E-01	9.62E-01	5.70E-05	3.92E-05	3.35E-05	9.60E-01
8081810	NM_001130064	GAP43	5.0	6.0	6.2	4.8	1.07	1.23	-0.14	-1.21	-1.37	0.16	1.07E-01	7.89E-03	8.88E-01	1.62E-02	4.60E-03	8.84E-01
7979269	NM_000161	GCH1	3.2	3.3	3.8	4.7	0.15	0.68	1.51	1.37	0.83	0.54	9.54E-01	4.04E-01	4.39E-02	6.88E-02	3.11E-01	6.51E-01
8127158	NM_001498	GCLC	7.1	7.0	7.2	8.3	-0.06	0.16	1.24	1.30	1.08	0.22	9.57E-01	7.30E-01	3.94E-04	1.86E-04	8.29E-04	6.85E-01
7917779	NM_002061	GCLM	5.9	6.7	7.3	7.1	0.83	1.38	1.18	0.34	-0.20	0.55	8.17E-02	1.49E-04	1.92E-03	4.59E-01	7.03E-01	2.10E-01
8112668	NM_016591	GCNT4	5.9	6.4	5.4	4.2	0.53	-0.45	-1.65	-2.17	-1.19	-0.98	5.00E-01	3.68E-01	6.46E-04	2.07E-05	6.58E-03	5.06E-02
7983890	NM_001018100	GCOM1	3.6	3.7	3.6	4.8	0.03	-0.04	1.17	1.14	1.20	-0.06	9.87E-01	9.63E-01	5.48E-03	5.74E-03	2.46E-03	9.54E-01
8027002	NM_004864	GDF15	5.9	5.4	4.8	5.4	-0.52	-1.03	-0.48	0.04	0.55	-0.51	4.17E-01	5.25E-03	3.15E-01	9.60E-01	1.79E-01	3.15E-01
8116418	NM_005110	GFPT2	5.5	5.6	5.2	7.1	0.07	-0.33	1.64	1.56	1.97	-0.41	9.78E-01	7.51E-01	2.74E-02	3.27E-02	4.86E-03	7.51E-01
7936494	NM_005264	GFRA1	4.8	5.2	5.5	7.1	0.37	0.65	2.29	1.92	1.64	0.28	7.74E-01	2.78E-01	2.28E-04	1.14E-03	3.16E-03	7.90E-01
8174103	NM_001128127	GK	6.1	6.3	6.3	7.2	0.12	0.12	1.03	0.90	0.90	0.00	9.30E-01	8.70E-01	2.58E-02	4.89E-02	3.68E-02	9.99E-01

			Estimate				Log-ratio						p-value (corr)					
UT ID	NCBI Ref No	Gene Symbol	G1	G2	G3	G4	G2/G1	G3/G1	G4/G1	G4/G2	G4/G3	G3/G2	G2/G1	G3/G1	G4/G1	G4/G2	G4/G3	G3/G2
8155192	NM_022343	GLIPR2	8.2	9.0	8.9	7.6	0.73	0.70	-0.60	-1.33	-1.30	-0.03	1.61E-02	2.50E-03	1.78E-02	4.25E-06	4.01E-06	9.66E-01
8159900	NM_152629	GLIS3	5.4	5.4	5.6	6.7	-0.04	0.23	1.33	1.37	1.10	0.27	9.84E-01	7.67E-01	1.28E-02	9.61E-03	2.83E-02	7.77E-01
8098006	NM_000824	GLRB	4.3	4.8	5.4	4.6	0.53	1.04	0.24	-0.29	-0.80	0.51	3.04E-01	1.66E-03	6.38E-01	5.35E-01	1.68E-02	2.33E-01
7965941	NM_031302	GLT8D2	7.6	8.2	8.3	8.7	0.59	0.62	1.07	0.48	0.45	0.03	4.09E-01	1.64E-01	1.89E-02	3.73E-01	3.87E-01	9.82E-01
8154951	NM_002065	GLUL	7.7	7.5	6.9	8.7	-0.21	-0.82	0.97	1.18	1.79	-0.61	7.86E-01	1.01E-02	5.98E-03	8.84E-04	4.64E-06	1.24E-01
7922689	NM_002065	GLUL	6.4	6.3	5.9	7.0	-0.09	-0.54	0.62	0.71	1.16	-0.45	8.96E-01	1.60E-02	1.23E-02	3.63E-03	1.30E-05	1.04E-01
7948354	NM_145016	GLYATL2	3.6	3.4	3.2	4.4	-0.12	-0.37	0.85	0.97	1.22	-0.25	8.95E-01	2.52E-01	7.47E-03	2.17E-03	1.39E-04	6.10E-01
8036710	NM_004877	GMFG	6.7	5.8	5.0	4.6	-0.90	-1.65	-2.07	-1.17	-0.42	-0.75	1.54E-01	2.99E-04	6.27E-05	1.21E-02	4.52E-01	1.70E-01
8114787	NM_005471	GNPDA1	6.3	5.5	5.3	6.2	-0.76	-1.04	-0.13	0.63	0.90	-0.28	1.69E-01	5.71E-03	8.62E-01	1.48E-01	1.98E-02	6.85E-01
7936322	NM_020918	GPAM	6.1	5.5	5.3	4.9	-0.69	-0.86	-1.20	-0.51	-0.34	-0.18	2.35E-01	2.09E-02	3.98E-03	2.67E-01	5.11E-01	8.22E-01
8122365	NM_020455	GPR126	3.3	3.3	3.4	5.4	-0.10	0.04	2.10	2.20	2.06	0.14	9.59E-01	9.69E-01	4.41E-04	2.12E-04	2.79E-04	9.13E-01
7974372	NM_001099652	GPR137C	4.2	4.0	4.1	5.2	-0.15	-0.12	0.99	1.14	1.11	0.03	9.09E-01	8.67E-01	2.37E-02	8.66E-03	7.10E-03	9.82E-01
8056837	NM_001033045	GPR155	5.3	5.6	6.4	5.1	0.22	1.07	-0.23	-0.45	-1.30	0.85	8.55E-01	1.35E-02	7.67E-01	4.50E-01	4.03E-03	1.12E-01
7954065	NM_003979	GPRC5A	6.7	6.4	4.9	7.3	-0.28	-1.84	0.55	0.83	2.38	-1.56	8.33E-01	4.69E-04	4.24E-01	1.55E-01	3.47E-05	8.28E-03
8109333	NM_002084	GPX3	5.8	5.7	5.2	6.6	-0.11	-0.58	0.74	0.85	1.32	-0.47	9.47E-01	2.35E-01	1.54E-01	8.73E-02	4.08E-03	4.95E-01
7901460	NM_015696	GPX7	7.6	8.0	8.3	7.2	0.48	0.74	-0.42	-0.89	-1.16	0.27	3.88E-01	2.30E-02	3.18E-01	1.17E-02	8.45E-04	6.35E-01
8056327	NM_004490	GRB14	3.8	4.3	5.2	4.4	0.50	1.38	0.56	0.07	-0.82	0.89	5.00E-01	7.73E-04	2.56E-01	9.41E-01	4.69E-02	6.22E-02
7925452	NM_022469	GREM2	6.8	6.3	6.1	7.8	-0.57	-0.72	1.01	1.57	1.72	-0.15	4.16E-01	8.68E-02	2.40E-02	5.37E-04	1.31E-04	8.70E-01
8169717	NM_007325	GRIA3	6.5	6.5	7.0	5.8	-0.02	0.51	-0.69	-0.67	-1.20	0.53	9.87E-01	8.52E-02	2.72E-02	2.96E-02	1.44E-04	1.37E-01
8121225	NM_175768	GRIK2	5.7	5.7	6.1	4.2	0.01	0.38	-1.52	-1.53	-1.90	0.36	9.98E-01	7.31E-01	5.51E-02	4.91E-02	9.76E-03	8.01E-01
7918379	NM_000849	GSTM3	7.1	7.6	7.4	6.0	0.52	0.27	-1.11	-1.62	-1.38	-0.24	2.13E-01	4.09E-01	4.06E-04	3.22E-06	1.52E-05	5.91E-01
7941936	NM_000852	GSTP1	9.8	9.7	9.7	8.8	-0.11	-0.12	-1.01	-0.90	-0.88	-0.01	9.14E-01	8.14E-01	4.00E-03	9.05E-03	6.78E-03	9.91E-01
8007973	NM_000857	GUCY1B3	4.9	6.1	6.8	4.1	1.18	1.90	0.82	2.00	2.72	0.72	2.13E 01	2.43E 03	2.95E 01	3.14E 03	8.89E 05	4.33E 01
8080964	NM_001080393	GXYLT2	7.4	8.2	8.3	6.7	0.77	0.87	-0.76	-1.52	-1.63	0.10	1.97E-01	2.82E-02	8.82E-02	5.58E-04	1.82E-04	9.17E-01
8045009	NM_002101	GYPC	6.0	5.9	5.3	6.6	-0.12	-0.76	0.58	0.70	1.33	-0.63	9.22E-01	4.27E-02	1.92E-01	9.18E-02	7.48E-04	1.77E-01
7929438	NM_018063	HELLS	4.5	3.6	3.8	5.3	-0.91	-0.79	0.78	1.69	1.57	0.11	3.85E-01	2.51E-01	3.28E-01	1.20E-02	1.36E-02	9.45E-01
8096335	NM_017912	HERC6	4.7	4.9	7.7	4.8	0.15	3.02	0.09	-0.06	-2.93	2.87	9.49E-01	3.10E-05	9.55E-01	9.65E-01	5.22E-05	3.81E-04
8121850	NM_012259	HEY2	4.4	4.9	5.1	4.0	0.53	0.78	-0.38	-0.91	-1.15	0.24	5.85E-01	1.38E-01	6.23E-01	1.03E-01	2.36E-02	8.11E-01
8140556	NM_000601	HGF	6.2	6.8	6.4	4.6	0.60	0.22	-1.59	-2.18	-1.81	-0.37	6.94E-01	8.57E-01	3.89E-02	3.87E-03	1.14E-02	7.87E-01
8097628	NM_022475	HHIP	4.1	3.7	3.6	5.3	-0.40	-0.43	1.23	1.63	1.66	-0.03	7.78E-01	5.94E-01	6.29E-02	1.10E-02	6.74E-03	9.89E-01
8124380	NM_005325	HIST1H1A	5.4	4.8	4.4	5.8	-0.57	-0.94	0.48	1.05	1.42	-0.37	7.04E-01	2.08E-01	6.67E-01	1.96E-01	4.67E-02	7.88E-01
8124430	NM_005320	HIST1H1D	5.9	5.4	5.1	7.1	-0.49	-0.83	1.20	1.69	2.03	-0.34	6.23E-01	1.03E-01	2.67E-02	1.79E-03	1.73E-04	7.04E-01
8117377	NM_005321	HIST1H1E	8.2	7.5	7.2	8.5	-0.68	-0.96	0.33	1.01	1.29	-0.28	2.18E-01	7.56E-03	5.19E-01	9.76E-03	7.70E-04	6.60E-01
8117426	NM_003524	HIST1H2BH	6.6	6.2	6.0	7.4	-0.36	-0.60	0.80	1.16	1.40	-0.24	7.88E-01	3.41E-01	2.31E-01	5.32E-02	1.25E-02	8.34E-01
8124388	NM_003537	HIST1H3B	4.2	3.7	3.5	5.3	-0.46	-0.63	1.17	1.64	1.80	-0.16	8.06E-01	5.17E-01	1.86E-01	4.48E-02	1.90E-02	9.32E-01
8124531	NM_003533	HIST1H3I	6.1	5.0	4.2	6.5	-1.11	-1.87	0.42	1.53	2.29	-0.76	1.27E-01	3.79E-04	5.70E-01	4.81E-03	5.27E-05	2.52E-01
8117368	NM_003542	HIST1H4C	6.3	5.7	5.1	6.5	-0.62	-1.16	0.27	0.89	1.43	-0.54	4.99E-01	1.98E-02	7.55E-01	1.14E-01	5.58E-03	4.89E-01
7919642	NM_175065	HIST2H2AB	6.0	5.9	5.5	6.6	-0.15	-0.51	0.56	0.71	1.07	-0.36	8.83E-01	1.49E-01	1.54E-01	5.34E-02	2.20E-03	4.87E-01
8059838	NM_018410	HJURP	6.0	5.1	4.9	6.3	-0.88	-1.14	0.31	1.19	1.44	-0.26	3.57E-01	5.06E-02	7.62E-01	6.06E-02	1.46E-02	8.32E-01
8178884	NM_006120	HLA-DMA	6.2	6.3	5.8	5.2	0.13	-0.39	-0.93	-1.06	-0.54	-0.52	8.46E-01	1.40E-01	9.22E-04	1.86E-04	3.40E-02	8.22E-02
8180086	NM_006120	HLA-DMA	6.2	6.3	5.8	5.2	0.13	-0.39	-0.93	-1.06	-0.54	-0.52	8.46E-01	1.40E-01	9.22E-04	1.86E-04	3.40E-02	8.22E-02
8179519	NM_002121	HLA-DPB1	5.2	4.7	4.5	4.2	-0.49	-0.65	-1.02	-0.53	-0.37	-0.16	5.70E-01	1.73E-01	3.66E-02	3.54E-01	5.47E-01	8.77E-01
8103728	NM_001130688	HMGB2	8.6	8.0	7.0	9.1	-0.57	-1.60	0.45	1.02	2.06	-1.04	4.30E-01	2.57E-04	4.20E-01	2.28E-02	1.92E-05	3.12E-02
8106280	NM_000859	HMGCR	7.5	8.8	8.9	7.9	1.27	1.41	0.38	-0.89	-1.03	0.14	9.04E-02	7.44E-03	6.51E-01	1.43E-01	6.32E-02	9.17E-01
8111941	NM_001098272	HMGCS1	7.4	9.1	9.4	8.0	1.67	1.96	0.63	-1.04	-1.33	0.29	5.38E-02	2.24E-03	4.75E-01	1.56E-01	4.22E-02	8.26E-01
8109712	NM_001142556	HMMR	5.9	4.3	3.7	6.3	-1.54	-2.22	0.45	2.00	2.67	-0.67	2.26E-01	7.41E-03	7.55E-01	2.64E-02	2.14E-03	6.40E-01
8072678	NM_002133	HMOX1	8.7	6.9	6.5	9.2	-1.73	-2.21	0.57	2.30	2.78	-0.48	1.89E-02	2.12E-04	4.61E-01	2.73E-04	1.84E-05	6.10E-01
8045499	NM_006895	HNMT	5.6	5.7	5.2	4.3	0.03	-0.44	-1.34	-1.37	-0.90	-0.46	9.85E-01	1.87E-01	1.97E-04	1.24E-04	4.68E-03	2.57E-01
7956271	NM_003725	HSD17B6	5.5	6.6	6.4	3.2	1.08	0.86	-2.35	-3.43	-3.21	-0.22	1.77E-01	1.32E-01	2.00E-04	1.30E-06	2.27E-06	8.54E-01
8042283	NM_014181	HSPC159	7.0	7.7	8.1	7.5	0.66	1.04	0.41	-0.25	-0.63	0.38	2.02E-01	2.59E-03	3.63E-01	6.40E-01	8.05E-02	4.65E-01
7971526	NM_000621	HTR2A	5.3	5.8	7.9	4.0	0.43	2.58	-1.31	-1.75	-3.89	2.14	8.43E-01	1.73E-03	1.69E-01	4.85E-02	2.91E-05	2.21E-02
8096281	NM_004967	IBSP	6.5	4.9	4.3	4.3	-1.63	-2.15	-2.20	-0.56	-0.04	-0.52	5.38E-02	7.32E-04	1.59E-03	5.27E-01	9.78E-01	6.17E-01
8025601	NM_000201	ICAM1	4.9	4.7	4.6	5.7	-0.16	-0.25	0.82	0.98	1.07	-0.10	9.21E-01	7.27E-01	1.32E-01	5.96E-02	2.75E-02	9.37E-01
8040103	NM_002166	ID2	7.6	6.5	6.0	8.0	-1.05	-1.51	0.41	1.45	1.92	-0.47	5.06E-04	1.14E-06	1.40E-01	2.20E-06	2.41E-08	1.08E-01
7913655	NM_002167	ID3	6.4	4.9	5.0	6.5	-1.57	-1.38	0.07	1.64	1.45	0.19	9.01E-05	5.62E-05	9.21E-01	1.22E-05	3.74E-05	7.42E-01
7931754	NM_004508	IDI1	7.9	8.8	8.9	8.3	0.94	1.02	0.43	-0.52	-0.59	0.07	7.07E-02	6.15E-03	3.90E-01	2.56E-01	1.50E-01	9.39E-01
8178435	NM_003897	IER3	7.2	8.2	8.2	7.2	1.05	1.04	0.05	-1.00	-0.99	-0.01	1.67E-02	1.96E-03	9.51E-01	5.56E-03	3.92E-03	9.96E-01
7976443	NM_001130080	IFI27	5.5	5.2	6.8	4.6	-0.32	1.30	-0.96	-0.64	-2.26	1.62	7.93E-01	8.84E-03	8.59E-02	3.06E-01	5.79E-05	5.58E-03
8026971	NM_006332	IFI30	8.7	8.0	7.5	6.9	-0.79	-1.20	-1.88	-1.09	-0.68	-0.41	4.31E-01	3.83E-02	3.37E-03	8.95E-02	3.32E-01	6.94E-01
7902553	NM_006417	IFI44	6.3	6.6	8.7	6.9	0.32	2.45	0.65	0.32	-1.80	2.13	7.87E-01	1.66E-05	2.95E-01	6.82E-01	6.09E-04	5.79E-04
7902541	NM_006820	IFI44L	5.8	6.0	8.3	6.3	0.24	2.54	0.58	0.34	-1.96	2.29	9.25E-01	1.23E-03	6.30E-01	8.11E-01	1.30E-02	9.53E-03
7914127	NM_002038	IFI6	5.5	6.0	7.7	5.3	0.49	2.21	-0.24	-0.73	-2.44	1.72	3.37E-01	3.11E-07	6.28E-01	3.24E-02	3.89E-08	3.08E-05
8056285	NM_022168	IFIH1	6.0	6.1	7.6	6.0	0.10	1.65	-0.02	-0.12	-1.67	1.54	9.61E-01	4.65E-03	9.89E-01	9.22E-01	5.55E-03	2.19E-02
7929065	NM_001548	IFIT1	6.0	6.0	8.6	6.3	-0.04	2.58	0.28	0.32	-2.30	2.62	9.93E-01	7.82E-03	8.96E-01	8.67E-01	2.16E-02	2.00E-02
7929052	NM_001031683	IFIT3	6.9	7.1	8.8	7.4	0.20	1.94	0.51	0.31	-1.43	1.74	9.41E-01	1.03E-02	6.82E-01	8.25E-01	7.31E-02	5.20E-02
7937335	NM_003641	IFITM1	6.0	5.5	7.6	5.1	-0.50	1.63	-0.93	-0.43	-2.56	2.14	7.03E-01	6.40E-03	1.95E-01	6.51E-01	1.23E-04	2.92E-03
7937772	NM_000612	IGF2	10.0	10.0	8.7	3.6	-0.03	-1.27	-6.40	-6.37	-5.13	-1.24	9.93E-01	8.51E-02	6.21E-09	4.57E-09	1.18E-07	1.70E-01
8048205	NM_000597	IGFBP2	6.4	6.8	6.4	5.2	0.38	-0.04	-1.22	-1.60	-1.19	-0.42	7.38E-01	9.71E-01	2.45E-02	3.00E-03	1.98E-02	6.19E-01
8058857	NM_000599	IGFBP5	8.1	9.7	10.3	8.1	1.60	2.19	0.06	-1.54	-2.13	0.59	1.46E-01	3.76E-03	9.76E-01	6.19E-02	6.16E-03	6.57E-01
7955694	NM_002178	IGFBP6	7.9	7.8	6.9	8.1	-0.17	-1.08	0.21	0.38	1.29	-0.91	7.36E-01	2.31E-05	5.02E-01	1.30E-01	2.89E-06	8.99E-04
8100541	NM_001553	IGFBP7	9.2	9.3	9.4	8.3	0.12	0.22	-0.86	-0.97	-1.08	0.11	8.91E-01	5.28E-01	4.50E-03	1.23E-03	2.73E-04	8.59E-01
8100827	NM_144646	IGJ	3.8	3.7	3.2	5.0	-0.09	-0.54	1.22	1.30	1.76	-0.45	9.64E-01	4.03E-01	3.87E-02	2.41E-02	1.69E-03	6.14E-01
8091537	NM_178822	IGSF10	3.3	3.2	3.2	4.5	-0.07	-0.10	1.23	1.29	1.32	-0.03	9.73E-01	9.23E-01	3.09E-02	2.08E-02	1.27E-02	9.87E-01
8043995	NM_000877	IL1R1	8.5	8.3	7.9	9.5	-0.19	-0.51	1.04	1.22	1.54	-0.32	9.15E-01	4.39E-01	8.28E-02	3.40E-02	5.07E-03	7.51E-01
8084794	NM_002182	IL1RAP	5.4	6.0	6.7	5.9	0.61	1.39	0.57	-0.05	-0.82	0.78	3.00E-01	3.54E-04	2.01E-01	9.56E-01	3.03E-02	7.94E-02
8104901	NM_002185	IL7R	7.9	5.8	5.2	5.8	-2.08	-2.74	-2.08	0.00	0.67	-0.66	8.20E-02	1.51E-03	2.62E-02	9.99E-01	5.87E-01	6.58E-01
8095680	NM_000584	IL8	4.3	4.4	4.6	5.5	0.05	0.30	1.14	1.09	0.85	0.25	9.78E-01	6.66E-01	2.90E-02	3.47E-02	9.53E-02	7.97E-01
7930208	NM_032727	INA	5.1	6.0	6.0	4.3	0.83	0.88	-0.78	-1.62	-1.66	0.04	1.55E-01	2.88E-02	8.25E-02	3.54E-04	1.69E-04	9.71E-01
8137526	NM_005542	INSIG1	7.4	8.5	8.6	8.2	1.12	1.25	0.86	-0.26	-0.39	0.13	1.61E-01	2.20E-02	1.86E-01	7.91E-01	6.35E-01	9.26E-01
8044766	NM_016133	INSIG2	7.3	7.2	7.6	5.5	-0.10	0.32	-1.72	-1.62	-2.05	0.42	9.01E-01	2.13E-01	2.29E-07	4.41E-07	7.82E-09	1.61E-01
7904761	NM_003637	ITGA10	4.7	4.4	4.2	5.4	-0.26	-0.48	0.73	0.99	1.22	-0.22	8.12E-01	3.37E-01	1.48E-01	3.48E-02	6.68E-03	7.99E-01
8105267	NM_002203	ITGA2	4.7	5.0	5.4	6.7	0.31	0.70	2.02	1.71	1.32	0.39	7.67E-01	1.28E-01	9.65E-05	4.76E-04	3.56E-03	5.92E-01
8046695	NM_000885	ITGA4	6.5	7.0	7.0	4.5	0.49	0.46	-2.09	-2.58	-2.55	-0.03	4.29E-01	2.46E-01	5.17E-06	1.87E-07	1.38E-07	9.78E-01
8046380	NM_000210	ITGA6	8.3	8.4	8.0	9.5	0.17	-0.25	1.27	1.10	1.52	-0.42	8.67E-01	5.93E-01	1.25E-03	3.63E-03	9.24E-05	4.06E-01
7932254	NM_003638	ITGA8	6.6	4.8	3.6	3.6	-1.86	-2.99	-3.06	-1.20	-0.06	-1.14	5.42E-03	2.63E-06	3.72E-06	3.13E-02	9.57E-01	6.34E-02
7931977	NM_030569	ITIH5	5.5	6.2	6.8	4.8	0.70	1.33	-0.68	-1.39	-2.02	0.63	4.34E-01	9.73E-03	2.97E-01	1.33E-02	3.32E-04	4.07E-01
8064978	NM_000214	JAG1	7.9	8.4	8.7	6.4	0.46	0.80	-1.54	-2.00	-2.34	0.34	6.41E-01	1.14E-01	4.12E-03	2.67E-04	2.68E-05	7.05E-01
8068024	NM_021219	JAM2	5.5	6.0	5.7	4.6	0.54	0.26	-0.91	-1.46	-1.17	-0.29	6.45E-01	7.85E-01	1.84E-01	1.98E-02	5.17E-02	8.07E-01
8171248	NM_000216	KAL1	5.7	6.4	7.9	3.5	0.71	2.17	-2.28	-2.99	-4.45	1.46	3.75E-01	5.39E-05	7.12E-05	1.62E-06	3.04E-09	9.30E-03

			Estimate				Log-ratio						p-value (corr)					
UT ID	NCBI Ref No	Gene Symbol	G1	G2	G3	G4	G2/G1	G3/G1	G4/G1	G4/G2	G4/G3	G3/G2	G2/G1	G3/G1	G4/G1	G4/G2	G4/G3	G3/G2
7953274	NM_000217	KCNA1	5.0	4.9	4.9	6.2	-0.06	-0.11	1.27	1.32	1.37	-0.05	9.63E-01	8.59E-01	1.02E-03	5.26E-04	2.32E-04	9.59E-01
8135705	NM_012281	KCND2	4.6	4.1	4.0	3.4	-0.50	-0.64	-1.17	-0.66	-0.52	-0.14	5.61E-01	1.82E-01	1.74E-02	2.13E-01	3.38E-01	8.95E-01
8048749	NM_080671	KCNE4	5.9	5.9	6.3	4.7	-0.01	0.44	-1.18	-1.17	-1.62	0.45	9.98E-01	3.30E-01	5.90E-03	5.41E-03	1.57E-04	4.41E-01
7924071	NM_172362	KCNH1	5.5	4.6	4.5	3.2	-0.91	-0.94	-2.22	-1.31	-1.28	-0.03	2.40E-01	6.66E-02	1.61E-04	1.59E-02	1.28E-02	9.87E-01
8009502	NM_000891	KCNJ2	4.6	4.3	4.1	5.9	-0.34	-0.57	1.20	1.54	1.77	-0.23	6.45E-01	1.34E-01	2.62E-03	1.75E-04	2.04E-05	7.35E-01
8115756	NM_004137	KCNMB1	5.3	5.9	5.7	4.2	0.63	0.38	-1.12	-1.76	-1.50	-0.25	3.91E-01	5.00E-01	1.94E-02	3.80E-04	1.16E-03	7.62E-01
8155487	NR_003674	KGFLP1	9.2	9.3	9.0	8.1	0.17	-0.13	-1.03	-1.20	-0.90	-0.30	8.53E-01	8.14E-01	4.80E-03	1.04E-03	8.10E-03	5.90E-01
8161423	NR_003674	KGFLP1	9.2	9.3	9.0	8.1	0.17	-0.13	-1.03	-1.20	-0.90	-0.30	8.53E-01	8.14E-01	4.80E-03	1.04E-03	8.10E-03	5.90E-01
8161455	NR_003674	KGFLP1	9.2	9.3	9.0	8.1	0.17	-0.13	-1.03	-1.20	-0.90	-0.30	8.53E-01	8.14E-01	4.80E-03	1.04E-03	8.10E-03	5.90E-01
8067839	NR_003674	KGFLP1	9.4	9.6	9.3	8.5	0.19	-0.08	-0.91	-1.10	-0.83	-0.27	7.60E-01	8.60E-01	1.92E-03	2.29E-04	2.46E-03	5.15E-01
8148448	NM_006558	KHDRBS3	6.3	6.5	6.4	5.2	0.24	0.10	-1.13	-1.36	-1.22	-0.14	8.43E-01	9.04E-01	2.14E-02	4.81E-03	7.76E-03	8.95E-01
7989647	NM_014736	KIAA0101	5.5	4.1	3.5	5.4	-1.48	-2.04	-0.10	1.38	1.94	-0.56	1.77E-01	5.88E-03	9.54E-01	9.86E-02	1.13E-02	6.74E-01
7932826	NM_020848	KIAA1462	7.4	7.7	8.4	7.7	0.34	1.01	0.27	-0.07	-0.74	0.68	4.34E-01	1.45E-04	4.21E-01	9.00E-01	3.89E-03	1.83E-02
8089372	NM_020890	KIAA1524	5.7	5.4	5.3	6.8	-0.35	-0.45	1.07	1.42	1.52	-0.10	7.25E-01	3.96E-01	2.84E-02	3.28E-03	1.15E-03	9.30E-01
8022996	NM_020964	KIAA1632	7.2	6.9	6.2	7.5	-0.34	-1.03	0.28	0.62	1.31	-0.69	3.90E-01	6.35E-05	3.54E-01	1.41E-02	4.14E-06	9.75E-03
7929258	NM_004523	KIF11	6.5	5.5	5.2	7.2	-0.93	-1.24	0.72	1.64	1.96	-0.32	4.24E-01	6.89E-02	4.32E-01	2.34E-02	4.73E-03	8.19E-01
7923189	NM_014875	KIF14	4.4	3.7	3.5	5.4	-0.70	-0.89	1.04	1.74	1.92	-0.18	4.91E-01	1.32E-01	1.03E-01	4.12E-03	1.11E-03	8.89E-01
8079237	NM_020242	KIF15	3.9	3.4	3.3	4.8	-0.48	-0.61	0.87	1.36	1.48	-0.12	7.58E-01	4.70E-01	3.03E-01	6.55E-02	3.18E-02	9.45E-01
7947248	NM_031217	KIF18A	6.1	5.1	4.9	6.5	-0.93	-1.12	0.48	1.41	1.60	-0.18	4.34E-01	1.20E-01	6.61E-01	6.02E-02	2.34E-02	9.15E-01
8108301	NM_005733	KIF20A	7.0	5.5	4.4	7.0	-1.44	-2.55	0.09	1.52	2.63	-1.11	2.41E-01	1.60E-03	9.65E-01	8.52E-02	1.57E-03	3.09E-01
7929078	NM_016195	KIF20B	5.5	5.0	4.7	6.5	-0.52	-0.82	0.98	1.50	1.80	-0.30	6.89E-01	2.12E-01	1.69E-01	2.15E-02	4.03E-03	8.09E-01
8168146	NM_012310	KIF4A	6.5	5.3	5.0	6.8	-1.27	-1.53	0.23	1.50	1.76	-0.26	1.55E-01	1.17E-02	8.52E-01	2.35E-02	5.40E-03	8.44E-01
7965322	NM_000899	KITLG	6.0	5.7	6.2	7.2	0.30	0.20	1.18	1.48	0.98	0.50	8.30E 01	8.27E 01	4.61E 02	1.07E 02	8.15E 02	5.75E 01
7972003	NM_007249	KLF12	7.6	7.4	7.3	6.5	-0.20	-0.38	-1.17	-0.97	-0.79	-0.19	7.16E-01	1.34E-01	5.94E-05	3.77E-04	1.95E-03	6.63E-01
8174654	NM_033495	KLHL13	5.3	4.5	4.2	4.0	-0.81	-1.09	-1.31	-0.51	-0.23	-0.28	2.12E-02	1.44E-04	4.11E-05	8.66E-02	5.29E-01	5.07E-01
8084219	NM_017644	KLHL24	8.3	7.7	7.2	7.3	-0.58	-1.09	-1.01	-0.42	0.09	-0.51	4.55E-01	1.26E-02	3.84E-02	4.96E-01	9.27E-01	4.38E-01
7959408	NM_014708	KNTC1	4.6	4.3	4.3	5.4	-0.27	-0.29	0.79	1.06	1.09	-0.02	8.18E-01	6.59E-01	1.42E-01	3.44E-02	2.28E-02	9.88E-01
8015366	NM_000526	KRT14	6.2	7.1	9.1	6.7	0.90	2.87	0.47	-0.43	-2.40	1.97	4.67E-01	1.31E-04	6.74E-01	7.09E-01	1.08E-03	1.39E-02
8015376	NM_005557	KRT16	5.6	6.8	8.1	5.3	1.20	2.52	-0.29	-1.49	-2.81	1.32	2.75E-01	4.75E-04	8.24E-01	4.85E-02	2.09E-04	1.20E-01
8013465	NR_029393	KRT16P3	5.2	5.7	6.4	5.3	0.55	1.29	0.16	-0.39	-1.12	0.74	3.32E-01	4.23E-04	8.02E-01	4.06E-01	2.15E-03	7.96E-02
8015387	NM_000422	KRT17	5.3	5.6	6.4	5.3	0.30	1.06	-0.04	-0.34	-1.10	0.76	6.86E-01	2.43E-03	9.62E-01	4.79E-01	2.33E-03	6.68E-02
8154725	NM_000224	KRT18	5.4	5.3	6.1	4.8	-0.08	0.75	-0.56	-0.48	-1.31	0.83	9.64E-01	1.43E-01	3.88E-01	4.75E-01	8.72E-03	1.77E-01
8015196	NM_030967	KRTAP1-1	7.2	6.6	6.5	6.1	-0.65	-0.73	-1.11	-0.46	-0.38	-0.08	1.56E-01	1.95E-02	1.58E-03	2.16E-01	3.10E-01	9.19E-01
8019578	NM_030967	KRTAP1-1	7.2	6.6	6.5	6.1	-0.65	-0.73	-1.11	-0.46	-0.38	-0.08	1.56E-01	1.95E-02	1.58E-03	2.16E-01	3.10E-01	9.19E-01
8015187	NM_030967	KRTAP1-1	9.6	8.6	8.2	7.9	-0.96	-1.42	-1.65	-0.69	-0.23	-0.46	1.73E-01	3.11E-03	2.03E-03	2.31E-01	7.76E-01	5.58E-01
8015179	NM_031957	KRTAP1-5	8.9	7.8	7.3	6.8	-1.05	-1.58	-2.02	-0.97	-0.45	-0.52	3.12E-01	1.50E-02	5.01E-03	2.10E-01	6.51E-01	6.41E-01
8019588	NM_031957	KRTAP1-5	8.9	7.8	7.3	6.8	-1.05	-1.58	-2.02	-0.97	-0.45	-0.52	3.12E-01	1.50E-02	5.01E-03	2.10E-01	6.51E-01	6.41E-01
8022176	NM_005559	LAMA1	4.8	4.2	4.5	6.0	-0.56	-0.32	1.19	1.74	1.51	0.24	4.31E-01	5.54E-01	8.21E-03	1.86E-04	5.78E-04	7.60E-01
8121949	NM_000426	LAMA2	6.4	7.0	7.3	7.9	0.57	0.88	1.50	0.93	0.62	0.31	5.81E-01	1.11E-01	9.44E-03	1.20E-01	3.32E-01	7.62E-01
7908072	NM_005562	LAMC2	3.9	3.9	3.9	6.8	0.02	-0.03	2.87	2.85	2.90	-0.05	9.95E-01	9.83E-01	2.63E-04	2.29E-04	1.19E-04	9.81E-01
7914270	NM_006762	LAPTM5	6.8	6.0	5.3	7.0	-0.81	-1.56	0.18	1.00	1.74	-0.74	5.78E-01	3.87E-02	9.13E-01	2.81E-01	2.37E-02	5.39E-01
8041206	NM_030915	LBH	7.0	6.2	6.3	5.9	-0.75	-0.65	-1.08	-0.33	-0.43	0.10	1.52E-01	7.63E-02	6.33E-03	5.28E-01	3.29E-01	9.09E-01
7902074	NM_002303	LEPR	9.5	9.6	9.1	8.0	0.03	-0.40	-1.53	-1.56	-1.13	-0.42	9.85E-01	2.70E-01	6.61E-05	4.29E-05	8.60E-04	3.49E-01
8092707	NM_018192	LEPREL1	6.9	6.5	5.9	8.1	-0.39	-0.99	1.18	1.57	2.17	-0.60	7.33E-01	4.81E-02	3.00E-02	3.57E-03	8.90E-05	4.05E-01
8018975	NM_005567	LGALS3BP	6.4	6.4	7.1	5.0	0.00	0.73	-1.40	-1.40	-2.14	0.74	9.98E-01	5.78E-03	2.22E-05	1.53E-05	2.73E-08	1.67E-02
8099685	NM_018176	LGI2	3.8	3.8	3.7	5.4	0.07	-0.03	1.68	1.61	1.72	-0.10	9.68E-01	9.72E-01	1.33E-03	1.63E-03	5.78E-04	9.32E-01
7947199	NM_018490	LGR4	6.8	7.7	8.4	7.6	0.94	1.63	0.80	-0.14	-0.83	0.69	9.54E-03	2.53E-06	8.19E-03	7.72E-01	3.86E-03	3.20E-02
8112803	NM_005779	LHFPL2	7.0	6.7	7.2	8.1	-0.22	0.27	1.10	1.32	0.83	0.49	8.73E-01	6.96E-01	3.39E-02	9.94E-03	1.00E-01	5.08E-01
8094789	NM_014988	LIMCH1	6.9	7.1	7.3	5.9	0.13	0.39	-0.97	-1.11	-1.36	0.25	9.26E-01	4.81E-01	4.25E-02	1.86E-02	2.63E-03	7.62E-01
8077490	NM_014583	LMCD1	8.8	8.4	8.7	6.7	-0.34	-0.06	-2.05	-1.71	-1.99	0.28	7.84E-01	9.51E-01	4.67E-04	2.26E-03	3.24E-04	7.80E-01
8107706	NM_005573	LMNB1	5.9	4.8	4.7	6.6	-1.12	-1.20	0.72	1.84	1.91	-0.08	2.40E-01	5.50E-02	3.84E-01	6.08E-03	2.88E-03	9.65E-01
7923386	NM_012134	LMOD1	7.3	7.6	6.9	4.8	0.27	-0.36	-2.45	-2.71	-2.09	-0.62	8.26E-01	5.65E-01	2.04E-05	3.65E-06	6.10E-05	3.39E-01
8091735	NM_001168214	LOC401097	3.7	4.5	4.8	2.9	0.79	1.03	-0.81	-1.60	-1.84	0.24	6.73E-01	3.08E-01	5.30E-01	1.10E-01	4.49E-02	9.13E-01
7945663	NM_001170820	LOC402778	6.1	6.2	6.1	4.8	0.15	-0.03	-1.27	-1.42	-1.24	-0.19	9.38E-01	9.79E-01	4.42E-02	2.12E-02	3.57E-02	8.90E-01
8160431	NR_027054	LOC554202	4.2	4.1	3.9	5.4	-0.10	-0.28	1.16	1.26	1.44	-0.18	9.36E-01	5.57E-01	3.58E-03	1.44E-03	2.34E-04	8.03E-01
8077499	AF086709	LOH3CR2A	5.2	4.8	5.2	3.9	-0.42	0.05	-1.33	-0.91	-1.38	0.47	7.84E-01	9.68E-01	5.62E-02	2.27E-01	3.24E-02	6.69E-01
8053231	NM_032603	LOXL3	5.6	5.3	6.4	6.0	-0.33	0.81	0.39	0.72	-0.42	1.14	7.28E-01	5.50E-02	5.17E-01	1.32E-01	4.34E-01	1.83E-02
8163257	NM_057159	LPAR1	9.1	9.1	8.8	9.9	0.02	-0.33	0.76	0.74	1.09	-0.35	9.78E-01	9.49E-02	5.19E-04	5.37E-04	3.64E-06	1.40E-01
7903214	NM_014839	LPPR4	5.3	6.4	7.2	4.5	1.11	1.87	-0.80	-1.91	-2.68	0.76	2.75E-01	3.70E-03	3.32E-01	5.99E-03	1.57E-04	4.21E-01
7948332	NM_004811	LPXN	4.6	4.4	4.8	5.8	-0.24	0.18	1.19	1.43	1.02	0.41	7.59E-01	7.30E-01	1.46E-03	1.77E-04	3.28E-03	3.90E-01
8174610	NM_020871	LRCH2	5.9	6.3	6.0	7.0	0.41	0.08	1.09	0.68	1.01	-0.33	6.53E-01	9.24E-01	2.38E-02	1.88E-01	2.56E-02	6.71E-01
7950555	NM_001128922	LRRC32	7.1	6.6	7.6	5.8	-0.50	0.50	-1.33	-0.83	-1.83	1.00	2.83E-01	1.02E-01	1.18E-04	8.84E-03	1.06E-06	3.66E-03
7984569	NM_017691	LRRC49	5.8	6.2	5.5	7.0	0.37	-0.29	1.17	0.80	1.46	-0.66	7.23E-01	6.66E-01	2.20E-02	1.34E-01	2.60E-03	2.96E-01
8147079	NM_033402	LRRCC1	4.7	4.9	4.6	5.8	0.18	-0.07	1.06	0.88	1.13	-0.25	8.27E-01	9.09E-01	2.67E-03	1.03E-02	8.01E-04	6.57E-01
8049528	NM_001137550	LRRFIP1	7.4	7.2	8.4	8.4	-0.16	0.97	0.98	1.14	0.01	1.13	9.20E-01	4.08E-02	6.33E-02	2.64E-02	9.96E-01	4.13E-02
8049532	NM_001137550	LRRFIP1	5.1	5.3	6.8	6.4	0.18	1.61	1.26	1.09	-0.35	1.44	9.30E-01	6.44E-03	5.61E-02	1.05E-01	7.12E-01	3.83E-02
8049540	NM_001137550	LRRFIP1	5.0	5.1	6.4	6.2	0.16	1.39	1.27	1.11	-0.12	1.22	9.41E-01	2.98E-02	7.50E-02	1.28E-01	9.32E-01	1.19E-01
8135488	NM_001099660	LRRN3	4.8	5.0	6.4	4.8	0.20	1.57	-0.02	-0.23	-1.59	1.36	9.13E-01	5.85E-03	9.89E-01	8.33E-01	7.09E-03	4.17E-02
8089714	NM_002338	LSAMP	6.7	7.1	6.3	4.9	0.44	-0.37	-1.74	-2.18	-1.37	-0.81	5.18E-01	3.90E-01	6.27E-05	2.84E-06	4.61E-04	6.04E-02
8148572	NM_002346	LY6E	5.7	5.8	7.0	5.4	0.11	1.28	-0.26	-0.37	-1.54	1.17	9.31E-01	8.51E-04	6.71E-01	4.85E-01	1.84E-04	7.24E-03
8056113	NM_002349	LY75	3.6	3.6	3.5	4.6	0.03	-0.09	1.00	0.96	1.08	-0.12	9.85E-01	9.08E-01	2.45E-02	2.77E-02	9.24E-03	9.02E-01
8146500	NM_002350	LYN	5.9	5.6	5.9	4.8	-0.35	-0.01	-1.17	-0.82	-1.16	0.34	7.50E-01	9.91E-01	2.34E-02	1.24E-01	1.66E-02	6.92E-01
8045664	NM_177964	LYPD6B	6.8	6.5	5.9	5.0	-0.23	-0.92	-1.82	-1.59	-0.90	-0.68	8.52E-01	4.19E-02	4.04E-04	1.30E-03	5.17E-02	2.48E-01
8066266	NM_005461	MAFB	5.1	4.8	4.7	6.4	-0.32	-0.42	1.32	1.64	1.74	-0.10	8.64E-01	6.55E-01	7.33E-02	2.12E-02	1.02E-02	9.59E-01
8088602	NM_015520	MAGI1	7.9	7.3	7.1	6.7	-0.67	-0.87	-1.20	-0.52	-0.33	-0.20	5.38E-02	9.03E-04	8.07E-05	6.21E-02	2.74E-01	6.64E-01
8054479	NM_005434	MALL	6.0	5.6	4.9	7.3	-0.45	-1.08	1.32	1.76	2.40	-0.64	7.20E-01	5.42E-02	3.10E-02	3.48E-03	1.05E-04	4.45E-01
8166925	NM_000240	MAOA	4.6	4.7	5.5	4.2	0.10	0.87	-0.39	-0.50	-1.26	0.77	9.01E-01	9.02E-04	1.95E-01	7.93E-02	2.00E-05	9.42E-03
8129804	NM_005923	MAP3K5	5.3	4.9	4.4	5.5	-0.36	-0.90	0.19	0.55	1.09	-0.54	5.70E-01	5.25E-03	7.31E-01	1.39E-01	1.36E-03	1.90E-01
8101587	NM_138982	MAPK10	4.5	4.9	4.6	3.8	0.44	0.13	-0.65	-1.10	-0.78	-0.31	6.12E-01	8.67E-01	2.12E-01	1.95E-02	8.81E-02	6.88E-01
8043187	NM_005911	MAT2A	10.2	10.2	9.6	10.6	-0.01	-0.66	0.37	0.38	1.03	-0.65	9.93E-01	9.57E-03	2.34E-01	2.08E-01	2.32E-04	2.90E-02
8147516	NM_002380	MATN2	5.7	5.6	5.5	7.9	-0.07	-0.20	2.17	2.23	2.37	-0.13	9.57E-01	6.74E-01	6.40E-07	3.31E-07	9.31E-08	8.50E-01
8124166	NM_001080480	MBOAT1	4.2	4.0	4.0	5.5	-0.18	-0.17	1.35	1.53	1.53	0.00	8.91E-01	7.99E-01	3.13E-03	8.26E-04	5.43E-04	9.97E-01
8050160	NM_138799	MBOAT2	7.4	7.3	6.6	8.2	-0.05	-0.75	0.78	0.83	1.53	-0.70	9.58E-01	4.10E-03	6.76E-03	3.47E-03	2.63E-06	2.05E-02
8146357	NM_005914	MCM4	5.3	5.0	5.2	6.1	-0.29	-0.09	0.83	1.12	0.92	0.20	7.59E-01	9.02E-01	6.06E-02	9.76E-03	2.43E-02	8.09E-01
8141395	NM_005916	MCM7	6.0	5.1	5.1	6.4	-0.86	-0.91	0.44	1.30	1.36	-0.05	2.96E-01	8.57E-02	5.60E-01	1.97E-02	1.04E-02	9.71E-01
8060813	NM_032485	MCM8	6.4	6.1	6.4	7.2	-0.36	-0.06	0.80	1.16	0.86	0.30	7.84E-01	9.55E-01	2.19E-01	4.80E-02	1.43E-01	7.74E-01
8155214	NM_014791	MELK	6.8	6.1	6.0	7.5	-0.69	-0.82	0.66	1.35	1.49	-0.13	5.53E-01	2.12E-01	4.18E-01	3.95E-02	1.68E-02	9.32E-01
8138353	NM_005924	MEOX2	5.8	6.8	6.3	9.3	0.97	0.54	3.51	2.54	2.98	-0.44	4.17E-01	5.63E-01	3.30E-05	9.87E-04	1.16E-04	7.39E-01
8136248	NM_002402	MEST	8.9	8.9	9.0	7.7	-0.02	0.06	-1.23	-1.21	-1.28	0.08	9.92E-01	9.38E-01	3.61E-03	3.43E-03	1.30E-03	9.38E-01

			Estimate				Log-ratio						p-value (corr)					
UT ID	NCBI Ref No	Gene Symbol	G1	G2	G3	G4	G2/G1	G3/G1	G4/G1	G4/G2	G4/G3	G3/G2	G2/G1	G3/G1	G4/G1	G4/G2	G4/G3	G3/G2
8135601	NM_001127500	MET	8.0	7.8	7.2	8.9	-0.18	-0.72	0.99	1.16	1.71	-0.55	7.71E-01	3.94E-03	5.51E-04	7.19E-05	2.39E-07	6.65E-02
8013341	NM_001198695	MFAP4	6.7	7.9	8.7	7.5	1.25	2.08	0.86	-0.39	-1.22	0.83	1.46E-01	6.28E-04	2.30E-01	6.78E-01	4.48E-02	3.03E-01
7969574	NR_030754	MIR622	5.4	5.2	5.9	4.5	-0.21	0.49	-0.90	-0.69	-1.39	0.70	8.88E-01	3.93E-01	9.80E-02	2.32E-01	5.14E-03	2.79E-01
7937020	NM_002417	MKI67	6.4	4.7	3.9	6.9	-1.80	-2.55	0.49	2.29	3.04	-0.75	1.29E-01	2.05E-03	7.22E-01	9.78E-03	5.19E-04	5.79E-01
7932733	NM_173576	MKX	6.4	6.7	6.5	8.4	0.32	0.09	2.00	1.68	1.91	-0.23	7.63E-01	9.14E-01	1.35E-04	6.86E-04	1.12E-04	7.99E-01
8083494	NM_007288	MME	7.9	6.9	7.9	10.3	-0.99	0.02	2.45	3.44	2.43	1.02	6.46E-01	9.92E-01	3.53E-02	2.81E-03	2.57E-02	5.58E-01
7951271	NM_002421	MMP1	4.2	3.7	3.6	5.8	-0.47	-0.59	1.53	2.00	2.12	-0.11	8.00E-01	5.53E-01	6.79E-02	1.36E-02	6.30E-03	9.58E-01
7963946	NM_002429	MMP19	6.5	6.8	7.0	5.2	0.31	0.46	-1.33	-1.64	-1.79	0.15	3.32E-01	2.03E-02	6.40E-07	1.85E-08	3.80E-09	6.81E-01
7951284	NM_002422	MMP3	3.7	3.6	3.5	5.0	-0.04	-0.21	1.34	1.38	1.55	-0.17	9.87E-01	8.48E-01	5.81E-02	4.65E-02	1.75E-02	9.14E-01
8097857	NM_032117	MND1	4.6	3.8	4.1	5.2	-0.76	-0.46	0.65	1.41	1.11	0.30	3.73E-01	4.74E-01	3.24E-01	1.11E-02	3.59E-02	7.59E-01
8129573	NM_015529	MOXD1	5.6	5.7	5.6	8.7	0.02	-0.04	3.07	3.06	3.12	-0.06	9.96E-01	9.68E-01	5.04E-06	4.22E-06	2.38E-06	9.70E-01
7932765	NM_173496	MPP7	4.1	4.5	4.3	5.3	0.37	0.23	1.19	0.82	0.96	-0.14	6.69E-01	7.08E-01	7.87E-03	6.60E-02	2.12E-02	8.83E-01
7946589	NM_130385	MRVI1	5.1	5.3	5.0	4.3	0.23	-0.15	-0.78	-1.00	-0.63	-0.38	7.46E-01	7.63E-01	2.09E-02	2.64E-03	4.73E-02	4.01E-01
8151334	NM_005098	MSC	6.5	6.5	7.6	5.9	0.05	1.10	-0.61	-0.66	-1.70	1.05	9.82E-01	4.35E-02	4.03E-01	3.42E-01	2.49E-03	1.14E-01
8110084	NM_002449	MSX2	5.5	5.5	6.3	4.9	0.08	0.79	-0.59	-0.67	-1.38	0.71	9.70E-01	2.21E-01	4.74E-01	3.87E-01	2.28E-02	4.12E-01
7995797	NM_175617	MT1E	7.6	7.0	6.7	7.7	-0.57	-0.92	0.08	0.65	1.00	-0.35	2.85E-02	3.48E-05	8.34E-01	2.40E-03	1.45E-05	1.61E-01
7995838	NM_005952	MT1X	5.8	4.8	5.1	6.4	-1.00	-0.65	0.60	1.60	1.25	0.35	3.63E-02	7.27E-02	1.49E-01	1.06E-04	8.99E-04	5.50E-01
8095376	NM_005953	MT2A	9.5	8.2	8.7	9.9	-1.27	-0.74	0.40	1.67	1.14	0.53	2.13E-05	1.34E-03	1.31E-01	1.38E-07	1.72E-05	4.80E-02
7995783	NM_005953	MT2A	10.8	9.5	10.1	11.2	-1.34	-0.75	0.34	1.67	1.08	0.59	2.05E-05	1.35E-03	2.27E-01	1.38E-07	3.42E-05	2.54E-02
8095362	NM_005953	MT2A	10.0	8.6	9.2	10.3	-1.34	-0.79	0.37	1.71	1.16	0.55	2.05E-05	8.36E-04	1.81E-01	1.38E-07	1.71E-05	4.21E-02
8152764	NM_014751	MTSS1	6.2	5.0	4.3	5.9	-1.22	-1.99	-0.32	0.91	1.67	-0.77	1.11E-01	4.00E-04	7.30E-01	1.41E-01	2.74E-03	2.94E-01
8156919	NM_001018116	MURC	4.6	4.7	5.6	4.7	0.04	1.01	0.12	0.08	-0.88	0.97	9.79E-01	5.96E-03	8.70E-01	9.15E-01	1.95E-02	2.27E-02
8068713	NM_002462	MX1	3.9	4.1	7.3	4.2	0.18	3.35	0.22	0.04	-3.14	3.17	9.58E-01	5.01E-04	9.19E-01	9.88E-01	1.29E-03	3.50E-03
8068697	NM_002463	MX2	4.2	4.5	6.6	3.6	0.28	2.40	-0.55	-0.83	-2.95	2.12	9.20E-01	3.94E-03	6.81E-01	4.71E-01	8.19E-04	2.75E-02
8171172	NM_015419	MXRA5	7.5	8.7	9.7	9.4	1.18	2.23	1.88	0.69	-0.36	1.05	5.06E-01	2.03E-02	8.40E-02	6.46E-01	8.38E-01	4.83E-01
7988444	NM_016132	MYEF2	5.7	5.7	5.0	6.0	-0.05	-0.70	0.31	0.36	1.01	-0.65	9.75E-01	6.36E-02	5.70E-01	4.91E-01	8.11E-03	1.59E-01
8012475	NM_005964	MYH10	7.5	7.5	7.1	8.3	0.02	-0.38	0.78	0.76	1.17	-0.40	9.86E-01	1.84E-01	8.03E-03	8.97E-03	9.84E-05	2.58E-01
7999674	NM_022844	MYH11	4.5	6.0	6.8	4.4	1.53	2.36	-0.05	-1.58	-2.41	0.83	1.78E-01	2.39E-03	9.79E-01	6.22E-02	2.61E-03	4.84E-01
8062312	NM_006097	MYL9	10.4	10.3	10.2	8.6	-0.01	-0.15	-1.76	-1.74	-1.61	-0.13	9.92E-01	7.19E-01	1.15E-06	1.18E-06	2.38E-06	8.12E-01
7927827	NM_032578	MYPN	5.7	4.9	4.3	4.9	-0.81	-1.41	-0.72	0.09	0.69	-0.60	5.48E-01	4.67E-02	4.59E-01	9.55E-01	4.53E-01	6.12E-01
8094719	NM_018177	N4BP2	5.4	5.4	5.3	6.4	-0.01	-0.13	0.93	0.94	1.06	-0.11	9.94E-01	8.33E-01	1.57E-02	1.30E-02	3.81E-03	8.93E-01
7972601	NM_052867	NALCN	5.9	5.9	5.6	4.7	-0.07	-0.32	-1.22	-1.14	-0.90	-0.24	9.61E-01	5.70E-01	7.91E-03	1.13E-02	3.60E-02	7.63E-01
8142120	NM_005746	NAMPT	8.2	7.9	7.8	9.1	-0.26	-0.31	0.94	1.21	1.26	-0.05	7.44E-01	4.79E-01	1.36E-02	1.67E-03	7.49E-04	9.62E-01
7933084	NM_005746	NAMPT	8.4	8.0	8.0	9.3	-0.35	-0.36	0.93	1.29	1.29	0.00	6.37E-01	4.21E-01	1.90E-02	1.34E-03	8.30E-04	9.97E-01
8173917	NM_004538	NAP1L3	5.3	5.9	6.3	5.1	0.61	1.01	-0.19	-0.80	-1.20	0.40	2.41E-01	2.79E-03	7.43E-01	2.82E-02	7.81E-04	4.14E-01
7901123	NM_002482	NASP	7.3	6.9	7.1	8.0	-0.36	-0.13	0.77	1.13	0.90	0.23	6.02E-01	8.24E-01	4.74E-02	3.00E-03	1.23E-02	7.19E-01
7938834	NM_182964	NAV2	6.8	5.7	5.5	7.6	-1.14	-1.30	0.80	1.94	2.10	-0.16	1.22E-02	3.89E-04	3.92E-02	7.02E-06	1.90E-06	8.29E-01
8152119	NM_001040624	NCALD	4.3	4.3	4.3	5.6	0.07	0.10	1.40	1.33	1.30	0.03	9.24E-01	7.92E-01	2.72E-06	4.19E-06	3.65E-06	9.70E-01
7943892	NM_181351	NCAM1	4.0	4.4	3.9	5.5	0.44	-0.14	1.47	1.03	1.61	-0.58	7.79E-01	9.08E-01	3.93E-02	1.71E-01	1.56E-02	5.92E-01
8067985	NM_004540	NCAM2	6.0	5.8	6.4	3.5	-0.20	0.41	-2.46	-2.26	-2.87	0.61	9.08E-01	5.48E-01	7.75E-05	1.65E-04	5.54E-06	4.32E-01
8094278	NM_022346	NCAPG	7.6	6.4	5.5	8.2	-1.20	-2.12	0.58	1.79	2.70	-0.92	3.20E-01	4.89E-03	6.15E-01	2.86E-02	7.64E-04	4.06E-01
8144153	NM_017760	NCAPG2	5.2	4.7	4.5	5.6	-0.51	-0.66	0.45	0.96	1.11	-0.15	6.19E-01	2.33E-01	5.41E-01	8.80E-02	3.22E-02	8.98E-01
8043602	NM_015341	NCAPH	5.2	4.6	4.3	6.0	-0.63	-0.91	0.77	1.40	1.69	-0.29	6.85E-01	2.53E-01	4.31E-01	8.00E-02	2.25E-02	8.56E-01
8055323	NM_207363	NCKAP5	4.8	5.4	5.0	4.2	0.61	0.21	-0.66	-1.27	-0.87	-0.40	4.70E-01	7.85E-01	2.52E-01	1.24E-02	7.87E-02	6.14E-01
8005191	BC027986	NCRNA00188	9.1	8.7	8.0	8.7	-0.37	-1.10	-0.40	-0.04	0.70	-0.73	2.38E-01	5.06E-06	7.38E-02	9.38E-01	1.05E-03	2.38E-03
8019857	NM_006101	NDC80	5.0	4.2	3.7	5.8	-0.80	-1.35	0.76	1.56	2.11	-0.55	5.62E-01	6.08E-02	4.30E-01	4.35E-02	4.03E-03	6.57E-01
8153002	NM_001135242	NDRG1	6.9	6.5	6.4	7.5	-0.39	-0.52	0.60	0.99	1.12	-0.12	5.76E-01	1.83E-01	1.54E-01	1.10E-02	2.92E-03	8.84E-01
8109203	NM_001543	NDST1	7.6	7.9	8.3	7.2	0.32	0.69	-0.41	-0.73	-1.10	0.37	4.65E-01	4.84E-03	1.45E-01	5.71E-03	6.15E-05	2.56E-01
8021376	NM_001144967	NEDD4L	6.4	6.3	5.7	7.1	-0.09	-0.66	0.74	0.84	1.41	-0.57	9.71E-01	4.12E-01	4.08E-01	3.25E-01	4.15E-02	6.10E-01
8123936	NM_001142393	NEDD9	5.8	5.7	6.0	4.3	-0.13	0.24	-1.51	-1.39	-1.75	0.37	9.39E-01	7.40E-01	4.25E-03	7.42E-03	5.90E-04	6.59E-01
8145361	NM_005382	NEFM	7.1	4.9	4.6	4.7	-2.23	-2.55	-2.44	-0.22	0.11	-0.32	3.53E-02	1.45E-03	5.04E-03	8.94E-01	9.52E-01	8.51E-01
8098423	NM_018248	NEIL3	4.9	4.5	4.0	5.3	-0.36	-0.86	0.47	0.84	1.33	-0.49	7.48E-01	9.06E-02	4.92E-01	1.35E-01	8.38E-03	5.31E-01
8085867	NM_199347	NEK10	6.6	5.7	5.0	6.2	-0.93	-1.68	-0.43	0.50	1.25	-0.75	2.96E-01	2.84E-03	6.22E-01	5.31E-01	2.96E-02	3.40E-01
7924096	NM_002497	NEK2	5.1	4.2	3.9	5.3	-0.91	-1.21	0.27	1.18	1.47	-0.30	3.12E-01	3.29E-02	8.01E-01	5.71E-02	1.11E-02	7.95E-01
8157761	NM_001145001	NEK6	6.7	6.3	6.4	5.6	-0.31	-0.23	-1.09	-0.78	-0.86	0.09	2.90E-01	2.84E-01	4.72E-06	2.43E-04	4.38E-05	8.22E-01
7908543	NM_133494	NEK7	9.5	9.8	9.9	8.8	0.27	0.34	-0.71	-0.98	-1.04	0.06	8.01E-01	5.60E-01	1.65E-01	3.74E-02	1.93E-02	9.59E-01
8067040	NM_012340	NFATC2	4.7	5.7	6.3	5.5	1.00	1.55	0.76	-0.24	-0.78	0.54	3.03E-01	1.08E-02	3.35E-01	8.33E-01	2.75E-01	5.92E-01
7901788	NM_001134673	NFIA	7.1	7.5	7.4	8.3	0.42	0.34	1.20	0.78	0.87	-0.09	6.23E-01	5.43E-01	9.44E-03	1.01E-01	4.86E-02	9.37E-01
8160138	NM_001190737	NFIB	6.3	6.9	7.1	9.1	0.61	0.77	2.81	2.20	2.05	0.16	6.28E-01	2.67E-01	1.20E-04	1.30E-03	1.65E-03	9.20E-01
7978644	NM_020529	NFKBIA	7.5	7.1	7.2	8.6	-0.35	-0.33	1.09	1.44	1.42	0.02	6.09E-01	4.28E-01	3.62E-03	1.93E-04	1.42E-04	9.86E-01
8129888	NM_001144060	NHSL1	4.5	4.5	4.7	6.0	0.09	0.20	1.50	1.41	1.30	0.11	9.54E-01	7.54E-01	1.41E-03	2.07E-03	2.84E-03	9.12E-01
8083968	NM_014932	NLGN1	4.3	4.6	3.9	6.7	0.25	-0.38	2.38	2.13	2.77	-0.63	8.82E-01	6.19E-01	2.28E-04	5.71E-04	1.83E-05	4.46E-01
7946334	NM_176821	NLRP10	4.8	5.0	5.7	4.6	0.19	0.91	-0.21	-0.40	-1.12	0.72	8.37E-01	8.69E-03	7.17E-01	3.77E-01	2.09E-03	8.64E-02
8114354	NM_003551	NME5	6.7	7.0	6.6	5.6	0.28	-0.07	-1.07	-1.35	-1.01	-0.35	6.38E-01	9.02E-01	1.09E-03	6.99E-05	1.04E-03	4.17E-01
8055702	NM_004688	NMI	4.8	5.1	6.0	5.6	0.25	1.18	0.77	0.52	-0.41	0.93	7.84E-01	1.74E-03	6.13E-02	2.44E-01	3.83E-01	3.10E-02
7932227	NM_004808	NMT2	8.0	7.6	6.9	7.6	-0.37	-1.08	-0.38	-0.01	0.70	-0.71	4.95E-01	4.97E-04	3.22E-01	9.94E-01	2.20E-02	4.21E-02
8022531	NM_000271	NPC1	8.1	7.3	7.3	8.3	-0.89	-0.84	0.18	1.07	1.02	0.05	2.32E-01	9.18E-02	8.52E-01	4.22E-02	4.08E-02	9.73E-01
7986329	NM_021005	NR2F2	7.4	7.5	7.5	6.2	0.16	0.14	-1.17	-1.33	-1.31	-0.02	8.18E-01	7.31E-01	1.58E-04	2.56E-05	1.96E-05	9.84E-01
8103094	NM_000901	NR3C2	4.1	4.3	4.5	5.3	0.20	0.48	1.22	1.02	0.74	0.27	7.65E-01	1.12E-01	2.53E-04	1.35E-03	1.17E-02	5.67E-01
7955589	NM_002135	NR4A1	5.5	5.7	5.3	6.5	0.22	-0.19	0.98	0.77	1.17	-0.41	7.02E-01	5.87E-01	7.81E-04	6.19E-03	5.68E-05	2.28E-01
8055952	NM_006186	NR4A2	5.3	4.9	5.0	7.2	-0.37	-0.28	1.87	2.23	2.15	0.09	8.11E-01	7.73E-01	5.42E-03	9.32E-04	8.70E-04	9.59E-01
8156848	NM_006981	NR4A3	4.6	4.4	4.5	5.8	-0.19	-0.14	1.17	1.35	1.31	0.05	8.64E-01	8.27E-01	5.75E-03	1.35E-03	1.19E-03	9.67E-01
8047738	NM_201266	NRP2	6.5	6.2	5.7	7.6	0.30	0.81	1.11	1.41	1.92	0.51	8.12E 01	1.17E 01	4.28E 02	8.94E 03	3.41E 04	5.12E 01
8156134	NM_006180	NTRK2	7.4	8.0	8.4	6.6	0.58	1.00	-0.87	-1.45	-1.87	0.42	4.62E-01	2.30E-02	7.79E-02	2.64E-03	1.29E-04	5.59E-01
7991186	NM_001007156	NTRK3	3.9	4.5	5.2	3.5	0.60	1.31	-0.38	-0.98	-1.69	0.71	3.04E-01	6.01E-04	4.55E-01	1.36E-02	5.20E-05	1.19E-01
7966026	NM_014840	NUAK1	6.5	6.5	6.7	4.8	-0.02	0.17	-1.74	-1.72	-1.91	0.19	9.95E-01	8.52E-01	2.29E-03	2.12E-03	5.16E-04	8.73E-01
7906930	NM_145697	NUF2	5.3	4.0	3.6	6.1	-1.30	-1.64	0.81	2.11	2.45	-0.33	3.57E-01	5.96E-02	5.08E-01	2.26E-02	5.72E-03	8.61E-01
7982889	NM_016359	NUSAP1	6.5	5.5	4.8	7.2	-1.02	-1.73	0.72	1.75	2.45	-0.70	3.00E-01	5.11E-03	3.79E-01	9.40E-03	2.76E-04	4.50E-01
7958884	NM_016816	OAS1	4.7	5.1	7.7	6.4	0.39	2.99	1.68	1.29	-1.31	2.60	8.69E-01	4.91E-04	6.76E-02	1.82E-01	1.48E-01	7.05E-03
7958913	NM_002535	OAS2	4.8	5.3	7.3	4.4	0.50	2.57	-0.35	-0.86	-2.92	2.07	6.06E-01	8.22E-06	6.42E-01	1.20E-01	1.78E-06	5.90E-04
7958895	NM_006187	OAS3	3.8	4.0	5.5	4.1	0.12	1.70	0.23	0.11	-1.47	1.58	9.35E-01	2.22E-04	7.60E-01	9.01E-01	1.22E-03	2.28E-03
8098441	NM_001080477	ODZ3	6.1	5.9	6.9	7.7	-0.17	0.77	1.65	1.82	0.88	0.94	9.32E-01	2.41E-01	1.14E-02	4.81E-03	1.89E-01	2.22E-01
8120602	NM_024576	OGFRL1	5.9	5.7	5.7	7.1	-0.25	-0.24	1.17	1.42	1.41	0.01	5.82E-01	3.89E-01	2.93E-05	1.82E-06	1.35E-06	9.87E-01
8162373	NM_033014	OGN	4.2	5.8	5.6	7.8	1.56	1.36	3.57	2.01	2.21	-0.20	4.92E-01	3.47E-01	8.85E-03	1.64E-01	9.50E-02	9.56E-01
8033818	NM_058164	OLFM2	6.2	6.7	7.9	5.9	0.54	1.70	-0.23	-0.77	-1.94	1.16	2.30E-01	2.63E-06	6.01E-01	1.46E-02	4.26E-07	1.17E-03
8162388	NM_005014	OMD	4.1	6.1	6.5	7.1	2.08	2.43	2.99	0.91	0.56	0.35	5.17E-02	2.22E-03	7.42E-04	3.72E-01	6.30E-01	8.35E-01
8084814	NM_198184	OSTN	3.3	3.6	4.5	3.3	0.30	1.20	-0.07	-0.37	-1.27	0.90	8.08E-01	1.28E-02	9.54E-01	6.25E-01	1.10E-02	1.33E-01
8085138	NM_000916	OXTR	6.1	6.7	6.9	5.7	0.54	0.80	-0.41	-0.95	-1.21	0.26	5.63E-01	1.14E-01	5.68E-01	7.55E-02	1.50E-02	7.89E-01
8113981	NM_004199	P4HA2	8.9	8.6	9.4	8.3	-0.38	0.48	-0.61	-0.23	-1.09	0.86	4.19E-01	9.18E-02	4.27E-02	5.66E-01	2.62E-04	7.24E-03

			Estimate				Log-ratio						p-value (corr)					
UT ID	NCBI Ref No	Gene Symbol	G1	G2	G3	G4	G2/G1	G3/G1	G4/G1	G4/G2	G4/G3	G3/G2	G2/G1	G3/G1	G4/G1	G4/G2	G4/G3	G3/G2
8095221	NM_001079525	PAICS	7.2	6.5	6.9	7.7	-0.65	-0.25	0.55	1.20	0.80	0.40	1.48E-01	5.36E-01	1.18E-01	4.94E-04	1.13E-02	3.54E-01
7903227	NM_017734	PALMD	6.3	7.4	8.2	5.3	1.04	1.88	-1.02	-2.06	-2.90	0.84	3.45E-01	5.02E-03	2.07E-01	4.71E-03	1.05E-04	3.87E-01
7947512	NM_015430	PAMR1	6.3	6.5	4.9	6.7	0.17	-1.40	0.37	0.20	1.77	-1.57	8.75E-01	2.98E-04	4.74E-01	7.57E-01	2.75E-05	5.90E-04
8163672	NM_002581	PAPPA	9.8	9.8	10.3	8.5	-0.07	0.43	-1.34	-1.27	-1.76	0.49	9.50E-01	1.64E-01	8.85E-05	1.27E-04	1.30E-06	1.74E-01
8157487	NM_002581	PAPPA	8.7	8.7	9.3	7.2	0.00	0.63	-1.51	-1.51	-2.14	0.63	9.99E-01	5.58E-02	9.37E-05	7.36E-05	4.77E-07	1.13E-01
7907572	NM_020318	PAPPA2	5.4	4.9	5.2	6.2	-0.42	-0.20	0.80	1.23	1.00	0.22	7.21E-01	8.21E-01	2.06E-01	3.22E-02	7.08E-02	8.45E-01
8102214	NM_005443	PAPSS1	8.4	8.7	8.7	7.5	0.31	0.29	-0.83	-1.14	-1.12	-0.02	3.22E-01	1.64E-01	2.95E-04	4.25E-06	3.80E-06	9.72E-01
8082100	NM_017554	PARP14	6.8	7.0	8.2	7.2	0.27	1.44	0.43	0.16	-1.01	1.17	7.74E-01	3.96E-04	4.18E-01	8.25E-01	1.10E-02	9.30E-03
8105191	NM_001178055	PARP8	6.5	6.8	6.8	3.8	0.32	0.38	-2.64	-2.96	-3.02	0.06	5.36E-01	1.90E-01	1.52E-09	2.32E-10	2.63E-10	9.27E-01
8090018	NM_031458	PARP9	5.9	6.3	7.7	6.4	0.41	1.80	0.51	0.10	-1.29	1.39	6.21E-01	6.12E-05	3.26E-01	9.03E-01	2.36E-03	3.43E-03
8105495	NR_028508	PART1	3.4	3.3	3.4	4.8	-0.09	-0.03	1.35	1.43	1.38	0.06	9.18E-01	9.50E-01	2.04E-05	6.21E-06	6.95E-06	9.33E-01
8149955	NM_018492	PBK	5.8	4.4	3.4	6.5	-1.42	-2.35	0.67	2.09	3.02	-0.93	4.27E-01	2.27E-02	6.95E-01	6.67E-02	4.85E-03	5.91E-01
8097449	NM_032961	PCDH10	5.4	5.3	5.8	4.3	-0.16	0.36	-1.16	-1.00	-1.52	0.52	9.31E-01	6.35E-01	5.48E-02	1.01E-01	6.64E-03	5.59E-01
8091243	NM_013363	PCOLCE2	8.5	9.0	8.9	9.9	0.56	0.48	1.41	0.84	0.93	-0.09	6.08E-01	4.93E-01	1.89E-02	1.90E-01	1.14E-01	9.57E-01
8113234	NM_000439	PCSK1	4.8	4.3	4.1	6.4	-0.50	-0.70	1.68	2.19	2.38	-0.20	5.94E-01	1.69E-01	1.59E-03	7.82E-05	1.71E-05	8.50E-01
8155898	NM_001190482	PCSK5	4.4	4.9	5.8	4.3	0.43	1.32	-0.11	-0.54	-1.44	0.90	4.37E-02	2.05E-08	6.41E-01	1.64E-03	3.04E-09	1.76E-05
8154245	NM_025239	PDCD1LG2	6.9	6.9	7.9	6.5	-0.01	0.91	-0.41	-0.40	-1.32	0.92	9.98E-01	8.40E-02	5.94E-01	6.03E-01	1.17E-02	1.50E-01
8138888	NM_001191058	PDE1C	9.1	9.1	8.8	8.0	0.07	-0.27	-1.04	-1.10	-0.76	-0.34	9.60E-01	5.77E-01	9.41E-03	5.16E-03	4.23E-02	5.75E-01
7954293	NM_000921	PDE3A	7.9	7.6	7.5	5.2	-0.31	-0.39	-2.76	-2.45	-2.37	-0.08	7.89E-01	5.33E-01	5.89E-06	2.13E-05	2.06E-05	9.55E-01
7902104	NM_002600	PDE4B	5.5	5.2	5.8	6.3	-0.25	0.38	0.88	1.13	0.49	0.63	8.56E-01	5.57E-01	1.20E-01	3.48E-02	4.38E-01	3.67E-01
8102532	NM_001083	PDE5A	8.7	8.4	7.2	5.4	-0.24	-1.44	-3.31	-3.07	-1.87	-1.19	8.85E-01	8.82E-03	3.72E-06	7.02E-06	1.26E-03	7.04E-02
8095080	NM_006206	PDGFRA	9.8	9.6	9.2	10.3	-0.13	-0.56	0.50	0.63	1.06	-0.43	8.83E-01	4.94E-02	1.21E-01	4.13E-02	4.74E-04	2.44E-01
8144802	NM_006207	PDGFRL	4.8	4.9	4.9	7.2	0.13	0.16	2.42	2.29	2.26	0.03	9.75E 01	9.37E 01	4.29E 02	5.35E 02	4.38E 02	9.92E 01
7935180	NM_020992	PDLIM1	7.7	8.0	8.2	5.9	0.29	0.43	-1.85	-2.13	-2.27	0.14	9.26E-01	7.74E-01	7.67E-02	3.47E-02	1.75E-02	9.58E-01
8134339	NM_015068	PEG10	5.7	5.8	5.9	7.0	0.13	0.18	1.36	1.24	1.19	0.05	9.28E-01	7.96E-01	3.43E-03	6.34E-03	6.13E-03	9.65E-01
8150901	NM_006211	PENK	7.9	8.1	6.9	8.0	0.19	-1.02	0.01	-0.18	1.03	-1.21	7.24E-01	9.65E-05	9.83E-01	6.34E-01	1.09E-04	9.28E-05
7965040	NM_007350	PHLDA1	8.2	8.1	7.3	8.3	-0.07	-0.94	0.07	0.13	1.01	-0.87	9.59E-01	7.09E-03	9.36E-01	8.45E-01	5.58E-03	3.18E-02
7915787	NM_003629	PIK3R3	6.9	8.2	8.3	7.6	1.33	1.43	0.74	-0.59	-0.68	0.09	5.42E-03	2.63E-04	7.20E-02	1.68E-01	7.84E-02	9.20E-01
8009353	NM_181671	PITPNC1	5.3	4.7	4.6	6.5	-0.60	-0.69	1.19	1.79	1.88	-0.09	2.34E-01	3.55E-02	1.27E-03	8.62E-06	3.48E-06	9.11E-01
7948987	NM_007069	PLA2G16	7.3	6.6	6.3	5.9	-0.72	-1.04	-1.43	-0.71	-0.39	-0.32	3.04E-01	1.76E-02	3.51E-03	1.64E-01	5.16E-01	6.85E-01
7908351	NM_024420	PLA2G4A	6.2	6.5	7.2	6.5	0.38	1.09	0.37	-0.01	-0.72	0.71	6.55E-01	7.09E-03	5.37E-01	9.92E-01	9.37E-02	1.62E-01
7928429	NM_002658	PLAU	6.1	6.8	7.1	6.1	0.71	1.01	-0.06	-0.77	-1.08	0.31	2.67E-01	1.21E-02	9.50E-01	8.95E-02	1.01E-02	6.71E-01
8037374	NM_002659	PLAUR	7.7	7.0	7.3	8.1	-0.69	-0.41	0.41	1.10	0.82	0.28	3.05E-01	4.26E-01	5.03E-01	1.71E-02	6.63E-02	7.25E-01
7961440	NM_024829	PLBD1	4.6	4.9	5.1	5.7	0.33	0.49	1.06	0.73	0.56	0.16	5.26E-01	8.02E-02	6.75E-04	1.40E-02	4.69E-02	7.52E-01
7929388	NM_016341	PLCE1	7.5	8.3	8.4	9.0	0.74	0.86	1.47	0.73	0.61	0.12	4.20E-01	1.24E-01	1.19E-02	2.64E-01	3.57E-01	9.30E-01
8078187	NM_015184	PLCL2	5.3	5.6	5.3	6.4	0.32	-0.03	1.10	0.79	1.13	-0.34	7.65E-01	9.79E-01	2.35E-02	1.18E-01	1.34E-02	6.63E-01
8041644	NM_172069	PLEKHH2	4.7	5.0	5.5	5.9	0.30	0.74	1.14	0.84	0.40	0.44	6.55E-01	2.20E-02	1.76E-03	1.71E-02	3.08E-01	3.32E-01
8160297	NM_001122	PLIN2	9.0	7.7	7.1	8.9	-1.26	-1.82	-0.04	1.22	1.79	-0.56	5.59E-03	1.09E-05	9.66E-01	1.55E-03	1.43E-05	2.15E-01
7994109	NM_005030	PLK1	6.3	5.2	4.7	6.4	-1.13	-1.55	0.07	1.20	1.62	-0.42	2.93E-01	2.13E-02	9.68E-01	1.18E-01	2.00E-02	7.41E-01
8112202	NM_006622	PLK2	8.4	8.9	8.1	9.6	0.48	-0.24	1.21	0.73	1.45	-0.72	4.93E-01	6.69E-01	4.36E-03	8.80E-02	4.59E-04	1.30E-01
8097356	NM_014264	PLK4	4.9	4.5	4.2	6.1	-0.43	-0.74	1.18	1.61	1.93	-0.32	8.55E-01	4.82E-01	2.52E-01	8.51E-02	2.55E-02	8.64E-01
8014768	NM_020405	PLXDC1	5.2	6.4	7.0	5.8	1.17	1.77	0.54	-0.64	-1.24	0.60	4.13E-01	3.43E-02	6.97E-01	6.20E-01	1.86E-01	6.91E-01
8090591	NM_015103	PLXND1	6.2	6.1	6.3	5.1	-0.13	0.01	-1.13	-1.01	-1.15	0.14	8.18E-01	9.73E-01	2.00E-05	6.35E-05	7.17E-06	7.22E-01
8021470	NM_021127	PMAIP1	4.5	4.5	4.4	7.5	-0.05	-0.11	3.04	3.08	3.15	-0.06	9.86E-01	9.24E-01	4.40E-05	2.62E-05	1.36E-05	9.73E-01
7901535	NM_153703	PODN	6.7	6.9	7.4	5.7	0.21	0.74	-0.97	-1.18	-1.72	0.54	8.98E-01	1.64E-01	8.35E-02	2.98E-02	1.14E-03	4.92E-01
8142981	NM_001018111	PODXL	7.6	5.9	5.6	9.6	-1.69	-1.92	2.01	3.70	3.93	-0.23	1.26E-02	4.07E-04	6.39E-04	1.91E-07	5.75E-08	8.37E-01
8089875	NM_199420	POLQ	3.7	3.3	3.3	4.3	-0.37	-0.42	0.62	0.99	1.04	-0.05	7.06E-01	4.45E-01	2.65E-01	4.26E-02	2.37E-02	9.69E-01
7916493	NM_003713	PPAP2B	8.3	8.3	7.6	9.1	0.03	-0.69	0.85	0.82	1.53	-0.71	9.84E-01	2.06E-02	9.44E-03	1.11E-02	1.27E-05	4.07E-02
8036473	NM_033256	PPP1R14A	5.5	5.8	5.7	4.4	0.31	0.18	-1.09	-1.40	-1.27	-0.13	8.23E-01	8.43E-01	6.89E-02	1.58E-02	2.09E-02	9.26E-01
8082869	NM_002718	PPP2R3A	6.6	6.5	7.7	7.6	-0.05	1.12	0.99	1.04	-0.14	1.17	9.56E-01	2.26E-05	2.28E-04	1.05E-04	7.10E-01	9.28E-05
7991406	NM_003981	PRC1	7.6	6.4	5.5	7.7	-1.22	-2.14	0.11	1.33	2.25	-0.92	2.05E-01	1.04E-03	9.39E-01	5.66E-02	8.60E-04	2.85E-01
7908924	NM_002725	PRELP	6.4	6.9	6.6	7.8	0.57	0.23	1.47	0.90	1.24	-0.34	5.71E-01	7.80E-01	9.83E-03	1.31E-01	2.07E-02	7.25E-01
7908312	NM_005807	PRG4	7.1	7.4	6.2	11.0	0.25	-0.89	3.89	3.64	4.78	-1.14	9.62E-01	6.73E-01	1.47E-02	2.06E-02	1.69E-03	6.56E-01
7962375	NM_153026	PRICKLE1	7.9	8.1	8.0	5.4	0.12	0.10	-2.50	-2.62	-2.60	-0.02	9.01E-01	8.47E-01	1.24E-08	4.57E-09	4.07E-09	9.85E-01
7964271	NM_000946	PRIM1	6.1	5.8	5.7	7.1	-0.26	-0.39	0.99	1.25	1.38	-0.13	8.72E-01	6.16E-01	1.27E-01	4.12E-02	1.72E-02	9.30E-01
7919305	NM_005399	PRKAB2	7.4	7.8	7.7	6.4	0.37	0.23	-1.03	-1.40	-1.26	-0.14	4.16E-01	4.95E-01	6.09E-04	1.26E-05	3.08E-05	7.93E-01
8008784	NM_018304	PRR11	7.1	6.1	5.5	7.5	-1.06	-1.68	0.42	1.48	2.10	-0.62	3.82E-01	1.96E-02	7.36E-01	6.41E-02	5.10E-03	6.09E-01
8120932	NM_001170423	PRSS35	3.8	4.1	4.6	3.6	0.29	0.84	-0.20	-0.49	-1.03	0.54	4.64E-01	4.02E-04	5.51E-01	4.55E-02	5.27E-05	4.05E-02
7932584	NM_020200	PRTFDC1	5.7	5.6	5.4	6.5	-0.13	-0.38	0.78	0.91	1.16	-0.25	9.07E-01	3.32E-01	3.33E-02	1.20E-02	1.05E-03	6.75E-01
8037283	NM_002780	PSG4	5.0	4.2	3.7	4.9	-0.83	-1.30	-0.06	0.77	1.23	-0.47	1.96E-01	2.66E-03	9.51E-01	1.13E-01	5.37E-03	4.81E-01
8037272	NM_002781	PSG5	7.7	6.4	5.4	7.4	-1.29	-2.27	-0.27	1.02	2.00	-0.98	2.35E-01	1.54E-03	8.45E-01	2.28E-01	6.13E-03	3.15E-01
8037251	NM_002783	PSG7	7.4	6.3	5.8	7.2	-1.15	-1.66	-0.26	0.89	1.41	-0.51	2.56E-01	9.89E-03	8.40E-01	2.60E-01	3.57E-02	6.48E-01
8160238	NM_033222	PSIP1	7.1	7.2	6.6	8.1	0.07	-0.53	1.04	0.96	1.57	-0.60	9.53E-01	1.14E-01	3.73E-03	5.71E-03	2.47E-05	1.30E-01
7926356	NM_001001484	PTER	7.0	6.8	6.5	7.9	-0.22	-0.51	0.90	1.11	1.41	-0.29	7.67E-01	1.11E-01	8.07E-03	1.09E-03	5.30E-05	5.61E-01
7974366	NM_000956	PTGER2	3.8	3.8	3.9	6.6	-0.03	0.03	2.76	2.79	2.73	0.06	9.81E-01	9.62E-01	6.21E-09	4.57E-09	4.07E-09	9.42E-01
8164580	NM_004878	PTGES	7.3	6.7	6.5	4.8	-0.58	-0.75	-2.47	-1.89	-1.72	-0.17	4.18E-01	7.86E-02	3.72E-06	8.71E-05	1.63E-04	8.51E-01
7902527	NM_001039585	PTGFR	6.2	6.5	6.0	7.3	0.31	-0.17	1.12	0.81	1.29	-0.48	6.77E-01	7.51E-01	3.59E-03	3.01E-02	5.19E-04	3.17E-01
7904293	NM_020440	PTGFRN	6.2	6.7	6.4	7.3	0.45	0.15	1.10	0.65	0.95	-0.30	2.90E-01	7.05E-01	3.48E-04	2.35E-02	8.04E-04	4.65E-01
8160346	NM_001010915	PTPLAD2	6.4	6.7	6.1	7.3	0.29	-0.35	0.84	0.55	1.19	-0.64	6.41E-01	3.14E-01	1.08E-02	1.04E-01	2.83E-04	7.86E-02
8109639	NM_004219	PTTG1	6.1	5.1	4.6	6.3	-0.99	-1.56	0.17	1.15	1.73	-0.58	3.04E-01	9.18E-03	8.99E-01	8.64E-02	5.58E-03	5.64E-01
8083594	NM_002852	PTX3	8.4	7.6	7.0	7.3	-0.83	-1.42	-1.08	-0.25	0.34	-0.59	1.96E-01	1.14E-03	2.10E-02	7.23E-01	5.81E-01	3.16E-01
8021301	NM_004163	RAB27B	7.0	6.2	5.9	4.2	-0.83	-1.14	-2.84	-2.00	-1.70	-0.31	6.60E-01	2.61E-01	4.80E-03	4.30E-02	7.62E-02	8.83E-01
7950899	NM_022337	RAB38	3.8	3.9	4.1	5.7	0.12	0.31	1.89	1.78	1.58	0.19	8.70E-01	2.60E-01	9.40E-08	1.87E-07	8.22E-07	6.57E-01
7916112	NM_002867	RAB3B	8.0	7.0	6.2	8.0	-1.02	-1.85	-0.05	0.97	1.80	-0.83	2.51E-01	1.44E-03	9.69E-01	1.40E-01	2.52E-03	2.81E-01
8075910	NM_002872	RAC2	7.1	6.3	5.6	5.3	-0.77	-1.55	-1.86	-1.09	-0.31	-0.79	3.88E-01	3.44E-03	1.71E-03	5.98E-02	7.16E-01	2.67E-01
7963157	NM_013277	RACGAP1	6.7	6.2	5.8	7.0	-0.54	-0.93	0.33	0.86	1.25	-0.39	4.82E-01	2.77E-02	6.13E-01	6.19E-02	4.03E-03	5.77E-01
7953218	NM_001130862	RAD51AP1	5.4	4.7	4.4	6.2	-0.67	-1.02	0.79	1.46	1.81	-0.35	7.02E-01	2.50E-01	4.81E-01	1.05E-01	2.78E-02	8.39E-01
7907657	NM_152663	RALGPS2	7.1	7.0	6.1	7.7	-0.17	-1.01	0.56	0.73	1.57	-0.84	8.86E-01	8.27E-03	2.37E-01	9.22E-02	2.07E-04	6.75E-02
8111569	NM_001161429	RANBP3L	3.9	4.6	5.1	3.7	0.65	1.13	-0.25	-0.90	-1.37	0.48	5.89E-01	6.89E-02	8.34E-01	2.16E-01	2.79E-02	6.54E-01
8141843	NM_006989	RASA4	6.3	7.0	6.4	8.1	0.68	0.16	1.77	1.09	1.61	-0.52	2.82E-01	8.14E-01	1.42E-04	1.09E-02	2.04E-04	3.50E-01
7965226	NM_005447	RASSF9	4.8	5.3	5.3	3.7	0.44	0.45	-1.12	-1.56	-1.57	0.01	5.43E-01	2.97E-01	7.32E-03	2.83E-04	1.70E-04	9.94E-01
8066136	NM_002895	RBL1	6.9	6.3	6.2	7.5	-0.55	-0.71	0.56	1.11	1.27	-0.16	5.20E-01	1.42E-01	3.39E-01	2.39E-02	6.79E-03	8.79E-01
7904751	BC017770	RBM8A	5.0	5.6	5.8	6.1	0.56	0.76	1.06	0.51	0.30	0.20	3.81E-01	4.71E-02	1.04E-02	2.77E-01	5.74E-01	7.87E-01
7935116	NM_006744	RBP4	4.2	4.4	4.6	8.5	0.21	0.37	4.23	4.03	3.86	0.16	8.40E-01	4.26E-01	1.95E-10	3.89E-10	9.62E-10	8.42E-01
8126760	NM_005822	RCAN2	7.2	7.7	7.0	6.6	0.43	-0.28	-0.59	-1.02	-0.31	-0.71	6.54E-01	6.86E-01	3.24E-01	4.43E-02	6.59E-01	2.52E-01
8146921	NM_172037	RDH10	7.3	7.8	8.6	8.2	0.48	1.31	0.84	0.36	-0.47	0.83	6.92E-01	1.83E-02	2.09E-01	6.88E-01	5.48E-01	2.64E-01
8128894	NM_002912	REV3L	6.8	7.0	6.9	7.8	0.19	0.10	1.04	0.85	0.94	-0.09	8.83E-01	8.96E-01	2.45E-02	6.68E-02	3.07E-02	9.36E-01
7968563	NM_002915	RFC3	5.6	5.1	5.3	6.4	-0.50	-0.38	0.79	1.29	1.17	0.11	6.38E-01	5.79E-01	1.98E-01	2.04E-02	2.64E-02	9.31E-01
8106210	NM_001080479	RGNEF	5.0	4.7	4.4	5.5	-0.35	-0.62	0.43	0.78	1.06	-0.27	5.44E-01	4.09E-02	2.45E-01	1.68E-02	9.95E-04	5.93E-01

			Estimate				Log-ratio						p-value (corr)					
UT ID	NCBI Ref No	Gene Symbol	G1	G2	G3	G4	G2/G1	G3/G1	G4/G1	G4/G2	G4/G3	G3/G2	G2/G1	G3/G1	G4/G1	G4/G2	G4/G3	G3/G2
7908409	NM_002923	RGS2	5.0	4.7	4.9	6.6	-0.27	-0.15	1.58	1.85	1.73	0.11	7.88E-01	8.23E-01	5.72E-04	7.91E-05	1.07E-04	9.07E-01
7974902	NM_020663	RHOJ	7.6	8.5	8.6	8.2	0.92	1.02	0.62	-0.30	-0.40	0.10	1.59E-01	2.26E-02	2.62E-01	6.79E-01	5.16E-01	9.32E-01
8020806	NM_017831	RNF125	3.5	3.5	3.3	4.5	0.07	-0.11	1.00	0.93	1.11	-0.18	9.18E-01	7.10E-01	3.24E-05	6.22E-05	4.28E-06	5.91E-01
7946569	NM_016422	RNF141	8.3	8.0	7.7	7.3	-0.23	-0.54	-1.00	-0.77	-0.47	-0.30	5.24E-01	5.32E-03	2.34E-05	3.89E-04	1.89E-02	2.27E-01
8102938	NM_020724	RNF150	6.1	6.2	6.3	5.1	0.06	0.19	-1.04	-1.10	-1.23	0.13	9.71E-01	7.90E-01	3.16E-02	2.09E-02	6.78E-03	9.00E-01
8105585	NM_001113561	RNF180	5.7	5.7	5.9	3.7	-0.01	0.19	-2.07	-2.06	-2.26	0.20	9.98E-01	7.45E-01	1.51E-05	1.02E-05	2.30E-06	7.95E-01
7914603	NM_153341	RNF19B	6.0	6.5	7.1	6.8	0.51	1.15	0.86	0.34	-0.30	0.64	2.32E-01	1.28E-04	5.34E-03	3.30E-01	4.03E-01	5.07E-02
7901969	NM_005012	ROR1	7.7	8.3	8.8	8.0	0.57	1.11	0.29	-0.28	-0.82	0.53	6.35E-02	1.66E-05	3.09E-01	3.07E-01	5.63E-04	3.80E-02
8176375	NM_001008	RPS4Y1	3.5	3.4	3.5	8.2	-0.09	-0.04	4.64	4.73	4.68	0.05	9.79E-01	9.83E-01	2.26E-05	1.23E-05	9.54E-06	9.86E-01
8040223	NM_001165931	RRM2	5.7	4.7	4.1	6.1	-1.02	-1.69	0.35	1.37	2.04	-0.67	4.93E-01	3.97E-02	8.21E-01	1.43E-01	1.50E-02	6.33E-01
8040080	NM_080657	RSAD2	3.3	3.4	5.3	3.5	0.06	1.94	0.13	0.07	-1.81	1.88	9.76E-01	5.15E-04	9.14E-01	9.54E-01	1.37E-03	3.17E-03
8120043	NM_001024630	RUNX2	7.3	6.8	6.8	6.0	-0.54	-0.51	-1.28	-0.75	-0.78	0.03	4.75E-01	2.86E-01	5.48E-03	1.15E-01	7.77E-02	9.81E-01
8122634	NM_001030060	SAMD5	4.9	5.3	5.5	4.4	0.34	0.55	-0.50	-0.84	-1.05	0.21	6.22E-01	1.21E-01	2.28E-01	2.26E-02	2.98E-03	7.42E-01
8140967	NM_017654	SAMD9	8.2	8.2	9.3	8.5	-0.06	1.11	0.22	0.27	-0.89	1.17	9.68E-01	5.48E-03	7.59E-01	6.67E-01	3.08E-02	1.15E-02
8140971	NM_152703	SAMD9L	7.6	8.1	9.1	8.1	0.47	1.51	0.51	0.04	-1.00	1.04	2.82E-01	4.48E-06	9.89E-02	9.42E-01	6.63E-04	1.80E-03
8058091	NM_015265	SATB2	8.9	9.0	9.3	7.8	0.13	0.45	-1.07	-1.20	-1.52	0.33	9.32E-01	3.82E-01	2.53E-02	1.13E-02	9.51E-04	6.70E-01
8036103	NM_001166034	SBSN	5.9	4.8	4.7	5.9	-1.09	-1.22	-0.03	1.06	1.19	-0.13	1.89E-01	2.83E-02	9.85E-01	8.63E-02	3.75E-02	9.27E-01
8098195	NM_006745	SC4MOL	7.8	9.1	9.0	8.2	1.30	1.19	0.36	-0.94	-0.83	-0.11	1.28E-02	3.10E-03	5.41E-01	3.01E-02	4.46E-02	9.13E-01
7944656	NM_006918	SC5DL	7.3	8.0	8.3	7.6	0.76	1.03	0.30	-0.46	-0.73	0.26	1.42E-01	4.03E-03	5.70E-01	2.98E-01	4.93E-02	6.77E-01
8145555	NM_016240	SCARA3	5.2	5.1	4.8	7.2	-0.15	-0.43	2.00	2.16	2.44	-0.28	8.83E-01	2.58E-01	4.85E-06	1.46E-06	1.38E-07	6.37E-01
8171758	NR_023358	SCARNA9L	5.2	5.0	4.9	6.1	-0.28	-0.33	0.83	1.11	1.16	-0.05	7.66E-01	5.18E-01	5.54E-02	9.01E-03	4.21E-03	9.65E-01
8059345	NM_003469	SCG2	3.7	3.4	4.3	3.2	-0.36	0.55	-0.48	-0.12	-1.03	0.91	2.48E-01	5.11E-03	2.86E-02	7.14E-01	1.12E-05	3.21E-04
7982366	NM_001144757	SCG5	4.9	5.0	4.4	5.5	0.07	0.48	0.53	0.46	1.01	0.55	9.61E 01	3.24E 01	3.25E 01	4.14E 01	1.94E 02	3.51E 01
8103736	NM_007281	SCRG1	6.1	6.8	7.6	8.9	0.63	1.52	2.75	2.12	1.23	0.89	7.79E-01	1.18E-01	6.89E-03	3.49E-02	2.51E-01	5.62E-01
8118890	NM_152753	SCUBE3	8.2	7.7	8.1	6.3	-0.49	-0.17	-1.95	-1.46	-1.78	0.33	7.46E-01	8.91E-01	7.12E-03	4.29E-02	8.62E-03	8.08E-01
8147461	NM_002998	SDC2	9.4	9.7	10.0	8.9	0.33	0.61	-0.45	-0.78	-1.06	0.28	2.80E-01	1.68E-03	3.24E-02	3.27E-04	5.09E-06	2.70E-01
7919984	NM_003944	SELENBP1	6.7	6.8	6.3	5.7	0.13	-0.41	-0.93	-1.06	-0.52	-0.54	8.99E-01	2.39E-01	7.91E-03	2.36E-03	1.36E-01	1.78E-01
8140668	NM_006080	SEMA3A	7.0	7.4	7.8	4.7	0.30	0.75	-2.37	-2.67	-3.11	0.45	9.38E-01	6.43E-01	6.11E-02	3.00E-02	7.79E-03	8.59E-01
8174692	NM_145799	SEPT6	5.0	4.9	4.9	6.2	-0.08	-0.11	1.24	1.32	1.36	-0.03	9.20E-01	7.63E-01	2.26E-05	7.02E-06	3.65E-06	9.59E-01
8029969	NM_003009	SEPW1	7.2	7.8	7.4	6.3	0.65	0.23	-0.88	-1.53	-1.11	-0.42	1.11E-01	5.27E-01	5.24E-03	1.08E-05	3.15E-04	2.78E-01
8021635	NM_001143818	SERPINB2	7.6	7.5	8.9	4.6	-0.01	1.32	-2.95	-2.94	-4.28	1.34	9.98E-01	2.39E-01	8.21E-03	7.69E-03	1.42E-04	3.51E-01
8003667	NM_002615	SERPINF1	7.3	8.1	8.6	8.8	0.79	1.28	1.56	0.77	0.28	0.49	5.39E-01	6.18E-02	3.58E-02	3.87E-01	8.14E-01	6.88E-01
7909503	NM_019605	SERTAD4	5.6	6.2	6.4	4.1	0.63	0.83	-1.46	-2.09	-2.29	0.20	5.84E-01	1.89E-01	2.33E-02	1.24E-03	3.16E-04	8.83E-01
7951077	NM_144665	SESN3	9.0	9.3	9.0	8.2	0.35	0.05	-0.82	-1.17	-0.86	-0.30	6.45E-01	9.47E-01	4.72E-02	3.77E-03	2.37E-02	6.33E-01
8103254	NM_003013	SFRP2	5.3	5.5	7.4	7.0	0.25	2.15	1.68	1.43	-0.47	1.90	9.23E-01	5.34E-03	4.99E-02	1.00E-01	7.04E-01	3.53E-02
8109490	NM_000337	SGCD	7.3	7.8	8.0	8.3	0.54	0.75	1.04	0.50	0.29	0.21	2.43E-01	1.18E-02	2.00E-03	1.51E-01	4.68E-01	7.02E-01
8129677	NM_001143676	SGK1	7.0	6.9	6.9	7.9	-0.11	-0.13	0.92	1.03	1.05	-0.02	8.26E-01	6.23E-01	4.97E-05	8.62E-06	4.65E-06	9.70E-01
8085754	NM_001012410	SGOL1	4.1	3.3	3.2	4.9	-0.76	-0.87	0.87	1.63	1.73	-0.10	5.42E-01	2.30E-01	2.93E-01	2.12E-02	1.01E-02	9.57E-01
8047288	NM_152524	SGOL2	4.6	4.4	4.5	5.5	-0.26	-0.12	0.90	1.16	1.02	0.14	8.30E-01	8.87E-01	8.47E-02	2.09E-02	3.31E-02	8.99E-01
8144880	NM_022071	SH2D4A	7.7	7.0	7.2	8.0	-0.77	-0.56	0.27	1.04	0.83	0.21	1.57E-01	1.59E-01	6.41E-01	9.94E-03	3.01E-02	7.72E-01
8120833	NM_031469	SH3BGRL2	5.2	5.6	5.2	4.3	0.33	-0.08	-0.93	-1.26	-0.85	-0.41	6.78E-01	9.08E-01	2.20E-02	1.98E-03	2.56E-02	4.74E-01
8165723	NM_000451	SHOX	4.3	4.4	4.2	5.5	0.13	-0.06	1.23	1.10	1.29	-0.19	8.72E-01	9.10E-01	1.42E-04	3.80E-04	3.94E-05	7.12E-01
8176297	NM_000451	SHOX	4.3	4.4	4.2	5.5	0.13	-0.06	1.23	1.10	1.29	-0.19	8.72E-01	9.10E-01	1.42E-04	3.80E-04	3.94E-05	7.12E-01
7944049	NM_001040455	SIDT2	8.3	8.4	8.4	7.0	0.05	0.07	-1.28	-1.33	-1.34	0.02	9.61E-01	8.97E-01	1.18E-04	6.14E-05	3.08E-05	9.87E-01
8060418	NM_001040022	SIRPA	5.9	5.6	5.6	6.8	-0.26	-0.29	0.95	1.20	1.23	-0.03	7.81E-01	5.76E-01	2.34E-02	3.60E-03	1.99E-03	9.82E-01
8021187	NM_001039535	SKA1	3.4	3.1	2.9	3.9	-0.30	-0.49	0.54	0.84	1.03	-0.19	7.28E-01	2.35E-01	2.34E-01	3.93E-02	7.41E-03	7.95E-01
7970513	NM_145061	SKA3	4.6	4.0	3.5	5.6	-0.59	-1.11	1.02	1.61	2.13	-0.52	6.98E-01	1.29E-01	2.28E-01	3.31E-02	3.24E-03	6.73E-01
8021081	NM_001128588	SLC14A1	8.8	8.8	5.8	7.5	-0.03	-3.03	-1.38	-1.35	1.65	-3.00	9.95E-01	4.19E-04	1.50E-01	1.53E-01	5.37E-02	2.34E-03
7933750	NM_194298	SLC16A9	3.6	3.9	3.5	4.9	0.25	-0.09	1.23	0.97	1.32	-0.35	6.96E-01	8.58E-01	3.46E-04	2.64E-03	7.34E-05	4.32E-01
8104930	NM_004172	SLC1A3	6.0	7.2	7.5	6.8	1.15	1.46	0.74	-0.41	-0.72	0.31	1.61E-01	8.99E-03	3.01E-01	6.37E-01	2.75E-01	7.81E-01
8123246	NM_021977	SLC22A3	5.1	4.2	4.6	3.3	-0.93	-0.55	-1.80	-0.87	-1.25	0.38	2.43E-01	3.65E-01	1.88E-03	1.43E-01	1.87E-02	6.83E-01
8087224	NM_000387	SLC25A20	5.3	5.2	5.6	4.5	-0.06	0.31	-0.73	-0.66	-1.04	0.38	9.54E-01	3.65E-01	2.40E-02	3.81E-02	8.48E-04	3.66E-01
7915472	NM_006516	SLC2A1	7.9	7.3	7.7	6.7	-0.55	-0.19	-1.15	-0.59	-0.96	0.37	3.38E-01	7.32E-01	3.60E-03	1.46E-01	8.49E-03	5.11E-01
7951485	NM_017515	SLC35F2	3.8	3.7	3.7	5.0	-0.11	-0.16	1.17	1.28	1.33	-0.05	9.01E-01	6.97E-01	2.73E-04	7.63E-05	2.98E-05	9.48E-01
7962516	NM_030674	SLC38A1	8.7	8.5	8.5	10.1	-0.25	-0.25	1.31	1.56	1.56	0.00	8.89E-01	7.88E-01	4.03E-02	1.27E-02	8.74E-03	9.98E-01
8101992	NM_022154	SLC39A8	6.0	6.0	6.8	7.4	-0.04	0.73	1.35	1.39	0.62	0.77	9.85E-01	9.94E-02	4.30E-03	2.90E-03	1.96E-01	1.52E-01
7965964	NM_032148	SLC41A2	7.5	7.9	8.5	7.7	0.42	1.01	0.23	-0.19	-0.78	0.59	2.34E-01	7.32E-05	4.77E-01	5.71E-01	1.32E-03	2.90E-02
7948229	NM_017611	SLC43A3	6.8	5.7	5.0	8.2	-1.09	-1.77	1.47	2.57	3.25	-0.68	9.47E-02	2.74E-04	3.84E-03	6.90E-06	1.45E-07	2.69E-01
8025672	NM_020428	SLC44A2	8.5	8.7	8.9	7.3	0.22	0.36	-1.17	-1.39	-1.54	0.14	7.04E-01	2.08E-01	1.56E-04	1.34E-05	2.89E-06	7.88E-01
7970793	NM_181785	SLC46A3	6.2	6.3	6.6	5.4	0.11	0.39	-0.82	-0.93	-1.21	0.28	9.49E-01	5.18E-01	1.19E-01	6.70E-02	1.07E-02	7.51E-01
8144786	NM_003046	SLC7A2	3.4	3.4	3.4	4.7	-0.04	0.02	1.33	1.37	1.31	0.07	9.86E-01	9.85E-01	4.60E-02	3.55E-02	3.56E-02	9.69E-01
8091260	NM_173653	SLC9A9	5.3	5.9	5.4	6.8	0.55	0.01	1.48	0.93	1.48	-0.54	7.24E-01	9.96E-01	5.27E-02	2.70E-01	3.84E-02	6.54E-01
8094301	NM_004787	SLIT2	7.0	7.3	8.2	8.7	0.27	1.25	1.67	1.40	0.42	0.98	8.74E-01	3.37E-02	9.54E-03	2.84E-02	6.35E-01	1.94E-01
8115691	NM_003062	SLIT3	7.2	7.9	8.4	8.1	0.66	1.14	0.83	0.17	-0.32	0.48	3.39E-01	6.87E-03	8.29E-02	8.35E-01	6.13E-01	4.52E-01
7984364	NM_005902	SMAD3	8.4	8.2	7.3	8.5	-0.19	-1.12	0.05	0.24	1.17	-0.93	7.24E-01	3.10E-05	9.25E-01	4.61E-01	2.05E-05	1.33E-03
7971015	NM_001127217	SMAD9	6.3	5.7	5.7	6.9	-0.66	-0.65	0.57	1.22	1.22	0.00	7.57E-02	1.28E-02	5.36E-02	7.41E-05	4.71E-05	9.97E-01
8156982	NM_001042551	SMC2	7.9	7.4	7.6	8.4	-0.48	-0.31	0.53	1.00	0.84	0.17	4.83E-01	5.28E-01	2.58E-01	1.36E-02	3.13E-02	8.31E-01
8083709	NM_005496	SMC4	8.3	8.0	8.1	9.1	-0.25	-0.22	0.83	1.09	1.06	0.03	5.59E-01	4.15E-01	1.09E-03	4.70E-05	3.94E-05	9.61E-01
8123446	NM_022138	SMOC2	5.1	5.8	6.6	3.6	0.64	1.45	-1.49	-2.13	-2.94	0.81	8.24E-01	2.37E-01	2.89E-01	8.69E-02	1.03E-02	6.86E-01
7920873	NR_002974	SNORA42	7.7	7.6	7.0	6.5	-0.09	-0.69	-1.19	-1.10	-0.50	-0.60	9.35E-01	2.96E-02	8.76E-04	1.55E-03	1.48E-01	1.22E-01
8139482	NR_002919	SNORA5A	5.7	5.4	5.3	4.6	-0.32	-0.37	-1.15	-0.83	-0.78	-0.05	7.62E-01	5.26E-01	1.90E-02	9.88E-02	1.02E-01	9.71E-01
8059708	NR_002921	SNORA75	5.2	4.6	4.1	3.2	-0.56	-1.05	-1.98	-1.42	-0.93	-0.49	5.01E-01	2.06E-02	1.95E-04	3.98E-03	4.74E-02	4.94E-01
7981982	NR_003332	SNORD116-17	7.1	7.4	7.1	6.3	0.27	0.01	-0.81	-1.08	-0.82	-0.25	6.47E-01	9.86E-01	8.78E-03	6.19E-04	4.91E-03	5.88E-01
7981986	NR_003332	SNORD116-17	7.1	7.4	7.1	6.3	0.27	0.01	-0.81	-1.08	-0.82	-0.25	6.47E-01	9.86E-01	8.78E-03	6.19E-04	4.91E-03	5.88E-01
7981951	NR_003317	SNORD116-2	4.8	5.5	4.7	4.3	0.64	-0.12	-0.46	-1.11	-0.35	-0.76	1.55E-01	8.22E-01	2.18E-01	1.23E-03	3.73E-01	3.47E-02
7981953	NR_003318	SNORD116-3	6.9	7.4	7.0	6.0	0.53	0.13	-0.87	-1.40	-1.00	-0.40	2.63E-01	7.96E-01	7.97E-03	6.89E-05	1.46E-03	3.41E-01
7981966	NR_003318	SNORD116-3	6.9	7.4	7.0	6.0	0.53	0.13	-0.87	-1.40	-1.00	-0.40	2.63E-01	7.96E-01	7.97E-03	6.89E-05	1.46E-03	3.41E-01
7981958	NR_003320	SNORD116-5	5.7	6.3	5.8	4.9	0.62	0.16	-0.78	-1.40	-0.93	-0.47	3.03E-01	8.04E-01	6.52E-02	8.83E-04	1.66E-02	3.99E-01
7981962	NR_003320	SNORD116-5	5.7	6.3	5.8	4.9	0.62	0.16	-0.78	-1.40	-0.93	-0.47	3.03E-01	8.04E-01	6.52E-02	8.83E-04	1.66E-02	3.99E-01
7981960	NR_003321	SNORD116-6	4.7	4.9	4.4	3.8	0.28	-0.31	-0.89	-1.17	-0.58	-0.59	7.44E-01	5.21E-01	2.85E-02	3.61E-03	1.52E-01	2.22E-01
7981964	NR_003323	SNORD116-8	6.8	7.2	6.8	5.7	0.38	-0.03	-1.13	-1.51	-1.11	-0.40	5.32E-01	9.69E-01	1.54E-03	5.89E-05	9.91E-04	3.81E-01
7952339	NR_001453	SNORD14C	5.2	5.2	5.1	6.2	0.00	-0.12	0.96	0.96	1.08	-0.12	9.98E-01	8.75E-01	3.11E-02	2.94E-02	9.93E-03	9.03E-01
8030362	NR_000020	SNORD33	8.2	8.5	8.4	7.2	0.37	0.22	-0.93	-1.30	-1.16	-0.15	5.28E-01	5.99E-01	6.29E-03	2.28E-04	5.22E-04	8.21E-01
8005200	NR_003043	SNORD49B	5.8	5.5	4.7	5.9	-0.25	-1.08	0.12	0.37	1.20	-0.82	6.25E-01	9.98E-05	8.09E-01	2.26E-01	3.94E-05	5.78E-03
8059712	NR_004398	SNORD82	4.3	4.0	3.6	5.0	-0.26	-0.60	0.72	0.98	1.33	-0.35	7.93E-01	1.57E-01	1.15E-01	2.36E-02	1.58E-03	6.07E-01
7957551	NM_003877	SOCS2	6.4	6.1	5.5	7.1	-0.29	-0.89	0.75	1.04	1.64	-0.61	4.59E-01	1.49E-04	2.15E-03	5.94E-05	6.58E-08	1.67E-02
8130556	NM_001024465	SOD2	9.0	8.8	8.6	9.8	-0.24	-0.41	0.81	1.06	1.22	-0.16	8.85E-01	5.88E-01	2.28E-01	8.81E-02	3.30E-02	9.02E-01
8104035	NM_021069	SORBS2	6.8	6.7	6.7	4.5	-0.04	-0.06	-2.23	-2.19	-2.17	-0.02	9.53E-01	8.55E-01	1.95E-10	2.32E-10	2.63E-10	9.73E-01
7918323	NM_002959	SORT1	8.7	8.8	8.4	6.8	0.07	-0.26	-1.86	-1.93	-1.60	-0.33	9.54E-01	4.97E-01	2.38E-06	1.18E-06	8.40E-06	4.84E-01

			Estimate				Log-ratio						p-value (corr)					
UT ID	NCBI Ref No	Gene Symbol	G1	G2	G3	G4	G2/G1	G3/G1	G4/G1	G4/G2	G4/G3	G3/G2	G2/G1	G3/G1	G4/G1	G4/G2	G4/G3	G3/G2
8059650	NM_080424	SP110	6.2	6.1	7.3	6.6	-0.09	1.07	0.41	0.50	-0.66	1.16	9.46E-01	2.76E-03	3.83E-01	2.47E-01	7.84E-02	5.45E-03
8013671	NM_006461	SPAG5	4.4	3.8	3.6	5.1	-0.62	-0.85	0.65	1.27	1.51	-0.23	6.17E-01	1.98E-01	4.41E-01	5.91E-02	1.71E-02	8.65E-01
8095021	NM_145263	SPATA18	6.9	7.6	7.4	6.5	0.68	0.54	-0.36	-1.03	-0.90	-0.14	2.24E-02	1.57E-02	1.81E-01	7.87E-05	2.55E-04	7.48E-01
8056572	NM_020675	SPC25	3.6	3.2	3.0	4.3	-0.36	-0.56	0.70	1.06	1.26	-0.20	7.94E-01	4.12E-01	3.33E-01	8.95E-02	2.92E-02	8.79E-01
8089627	NM_144718	SPICE1	5.0	5.1	5.9	4.8	0.09	0.85	-0.27	-0.35	-1.11	0.76	9.06E-01	2.98E-04	3.62E-01	1.74E-01	1.71E-05	3.43E-03
8096301	NM_001040058	SPP1	4.7	4.6	5.6	4.0	-0.12	0.89	-0.77	-0.65	-1.65	1.00	9.61E-01	2.13E-01	3.76E-01	4.74E-01	1.38E-02	2.46E-01
8060997	NM_018327	SPTLC3	7.4	7.7	6.8	8.2	0.28	-0.67	0.81	0.53	1.48	-0.95	8.68E-01	3.06E-01	2.52E-01	5.15E-01	1.19E-02	1.99E-01
8148280	NM_003129	SQLE	8.4	9.5	9.8	8.9	1.10	1.42	0.55	-0.55	-0.87	0.32	1.02E-02	7.32E-05	1.49E-01	1.36E-01	9.22E-03	5.51E-01
7927964	NM_002727	SRGN	10.7	10.6	10.3	6.3	-0.12	-0.40	-4.41	-4.29	-4.01	-0.28	9.64E-01	7.22E-01	3.72E-06	4.22E-06	6.81E-06	8.64E-01
8168749	NM_014467	SRPX2	6.2	6.6	6.3	5.4	0.42	0.13	-0.74	-1.16	-0.87	-0.29	5.22E-01	8.21E-01	5.56E-02	2.36E-03	1.47E-02	6.30E-01
7961757	NM_003034	ST8SIA1	4.5	5.6	6.3	5.4	1.11	1.83	0.91	-0.19	-0.92	0.72	1.33E-01	4.91E-04	1.14E-01	8.37E-01	8.49E-02	2.89E-01
7961755	NM_003034	ST8SIA1	3.4	4.3	5.2	3.9	0.91	1.74	0.49	-0.41	-1.25	0.83	3.44E-01	3.05E-03	5.71E-01	6.51E-01	3.86E-02	2.94E-01
7929012	NM_020799	STAMBPL1	4.9	4.8	4.8	6.6	-0.09	-0.06	1.68	1.77	1.74	0.04	9.30E-01	9.22E-01	1.86E-05	6.02E-06	5.40E-06	9.70E-01
8113491	NM_139164	STARD4	6.7	7.8	8.3	6.3	1.15	1.67	-0.36	-1.51	-2.04	0.53	1.75E-01	3.58E-03	7.04E-01	1.48E-02	8.18E-04	5.80E-01
8057771	NM_003151	STAT4	6.4	6.8	6.7	5.0	0.36	0.29	-1.37	-1.72	-1.66	-0.07	7.40E-01	6.67E-01	8.17E-03	9.42E-04	8.78E-04	9.60E-01
8149825	NM_003155	STC1	5.2	3.7	3.7	4.1	-1.49	-1.45	-1.07	0.42	0.38	0.04	1.17E-02	1.58E-03	3.12E-02	5.09E-01	5.43E-01	9.75E-01
8115851	NM_003714	STC2	9.0	8.0	8.0	7.6	-0.96	-1.03	-1.40	-0.44	-0.37	-0.06	1.57E-01	2.79E-02	6.37E-03	5.10E-01	5.74E-01	9.62E-01
8134030	NM_012449	STEAP1	5.5	5.0	5.6	6.7	-0.44	0.17	1.26	1.70	1.09	0.61	7.46E-01	8.72E-01	5.26E-02	7.54E-03	7.68E-02	5.13E-01
8134036	NM_152999	STEAP2	5.6	5.4	5.3	7.1	-0.17	-0.32	1.52	1.68	1.84	-0.16	9.27E-01	6.89E-01	1.20E-02	4.81E-03	1.46E-03	9.08E-01
8140840	NM_024636	STEAP4	5.5	5.4	3.5	8.0	-0.05	-2.00	2.54	2.59	4.54	-1.95	9.95E-01	1.55E-01	8.73E-02	7.71E-02	1.12E-03	2.71E-01
7915926	NM_001048166	STIL	5.3	5.0	5.2	6.1	-0.29	-0.05	0.81	1.10	0.86	0.24	8.19E-01	9.59E-01	1.64E-01	4.14E-02	1.04E-01	8.14E-01
8093858	NM_018401	STK32B	5.4	5.6	6.5	5.6	0.22	1.10	0.21	-0.01	-0.89	0.88	9.01E-01	4.27E-02	8.43E-01	9.98E-01	1.29E-01	2.04E-01
7954511	NM_015000	STK38L	9.2	9.4	9.6	8.5	0.23	0.44	0.73	0.96	1.17	0.21	8.80E 01	4.89E 01	2.25E 01	8.35E 02	2.21E 02	8.45E 01
7913869	NM_203401	STMN1	7.1	6.2	5.4	7.1	-0.85	-1.71	0.02	0.87	1.72	-0.85	2.62E-01	6.57E-04	9.88E-01	1.11E-01	8.11E-04	1.59E-01
8140386	NM_016086	STYXL1	6.7	6.5	6.0	5.7	-0.21	-0.69	-1.02	-0.81	-0.33	-0.48	7.13E-01	6.63E-03	5.20E-04	3.63E-03	2.82E-01	1.26E-01
7932796	NM_021738	SVIL	6.7	7.1	6.4	7.8	0.37	-0.32	1.14	0.77	1.46	-0.69	8.05E-01	7.21E-01	8.74E-02	2.97E-01	1.66E-02	4.34E-01
7917322	NM_032184	SYDE2	6.4	6.7	6.7	5.2	0.31	0.26	-1.19	-1.50	-1.45	-0.05	5.97E-01	4.95E-01	4.55E-04	2.18E-05	2.28E-05	9.45E-01
7974920	NM_182914	SYNE2	4.8	4.3	4.9	5.8	-0.42	0.12	1.01	1.43	0.89	0.54	2.43E-01	7.33E-01	2.14E-04	2.07E-06	4.27E-04	4.67E-02
8097080	NM_133477	SYNPO2	5.4	5.7	5.5	4.6	0.32	0.07	-0.85	-1.17	-0.93	-0.24	5.37E-01	8.84E-01	4.18E-03	1.59E-04	1.11E-03	5.85E-01
7909494	NR_027458	SYT14	5.2	4.0	3.8	4.7	-1.13	-1.35	-0.49	0.64	0.86	-0.21	2.58E-01	3.65E-02	6.22E-01	4.69E-01	2.49E-01	8.86E-01
8093500	NM_006342	TACC3	4.9	4.5	4.2	5.5	-0.42	-0.79	0.58	1.00	1.37	-0.37	7.53E-01	2.05E-01	4.62E-01	1.21E-01	1.97E-02	7.33E-01
7944082	NM_001001522	TAGLN	9.2	9.4	8.9	7.0	0.14	-0.29	-2.21	-2.35	-1.92	-0.44	9.51E-01	7.77E-01	2.03E-03	9.32E-04	3.88E-03	7.12E-01
8045889	NM_033394	TANC1	6.6	7.0	7.1	6.1	0.39	0.53	-0.55	-0.93	-1.07	0.14	6.91E-01	3.10E-01	3.59E-01	6.00E-02	2.12E-02	8.99E-01
8054308	NM_001102426	TBC1D8	4.9	4.8	4.6	5.6	-0.06	-0.30	0.76	0.82	1.06	-0.24	9.61E-01	5.03E-01	4.67E-02	2.83E-02	3.24E-03	7.10E-01
8169186	NM_017752	TBC1D8B	7.6	7.6	8.1	7.1	0.00	0.50	-0.50	-0.50	-1.00	0.50	9.98E-01	5.10E-02	7.82E-02	7.58E-02	2.83E-04	1.04E-01
8165911	NM_005647	TBL1X	6.4	6.0	5.5	6.7	-0.33	-0.83	0.36	0.69	1.19	-0.50	3.63E-01	2.98E-04	1.54E-01	3.48E-03	5.58E-06	4.88E-02
7958262	NM_152772	TCP11L2	7.5	7.0	5.9	7.5	-0.49	-1.62	0.05	0.54	1.67	-1.13	6.81E-01	3.63E-03	9.71E-01	4.88E-01	3.76E-03	9.16E-02
8135576	NM_015641	TES	9.1	9.4	9.6	8.5	0.29	0.50	-0.66	-0.95	-1.16	0.20	6.57E-01	1.39E-01	6.41E-02	5.91E-03	6.89E-04	7.33E-01
8017582	NM_018469	TEX2	7.6	7.9	8.7	7.4	0.23	1.11	-0.19	-0.42	-1.30	0.87	4.57E-01	1.14E-06	4.45E-01	2.84E-02	9.36E-08	1.22E-04
8057599	NM_006287	TFPI	8.3	8.3	8.1	6.4	-0.03	-0.25	-1.95	-1.92	-1.70	-0.22	9.86E-01	6.89E-01	1.17E-04	1.10E-04	2.71E-04	7.99E-01
8141016	NM_006528	TFPI2	6.0	5.7	5.0	6.7	-0.32	-1.01	0.69	1.01	1.70	-0.70	9.03E-01	2.65E-01	5.67E-01	3.28E-01	4.26E-02	6.10E-01
8093053	NM_003234	TFRC	9.3	7.9	8.6	8.8	-1.45	-0.76	-0.49	0.96	0.27	0.69	1.22E-03	2.96E-02	2.52E-01	1.17E-02	5.95E-01	1.10E-01
7909789	NM_001135599	TGFB2	8.8	9.3	8.7	9.8	0.50	-0.07	0.98	0.48	1.05	-0.57	4.54E-01	9.24E-01	1.85E-02	3.21E-01	7.42E-03	2.58E-01
7980316	NM_003239	TGFB3	5.4	6.1	6.2	6.4	0.71	0.84	1.05	0.34	0.21	0.13	2.04E-01	2.31E-02	9.82E-03	5.26E-01	7.26E-01	8.80E-01
8066214	NM_004613	TGM2	8.3	8.0	8.7	6.5	-0.32	0.35	-1.87	-1.55	-2.22	0.67	8.63E-01	7.14E-01	8.28E-03	2.61E-02	1.08E-03	5.09E-01
8130867	NM_003247	THBS2	10.0	10.0	10.0	8.8	0.05	-0.03	-1.19	-1.24	-1.15	-0.08	9.77E-01	9.72E-01	1.74E-02	1.19E-02	1.36E-02	9.45E-01
8106573	NM_003248	THBS4	4.5	4.5	4.8	8.5	0.05	0.30	4.04	3.99	3.73	0.26	9.89E-01	8.11E-01	2.16E-05	1.65E-05	2.54E-05	8.85E-01
8085797	NM_001128176	THRB	4.6	4.8	4.8	6.4	0.21	0.18	1.80	1.58	1.62	-0.04	7.65E-01	6.91E-01	3.72E-06	1.36E-05	7.09E-06	9.65E-01
8096411	NM_145715	TIGD2	5.1	4.5	4.4	4.0	-0.63	-0.73	-1.14	-0.51	-0.41	-0.10	2.02E-02	5.77E-04	9.88E-06	2.23E-02	5.72E-02	8.11E-01
8083569	NM_015508	TIPARP	8.7	9.8	9.8	9.0	1.11	1.09	0.23	-0.87	-0.85	-0.02	3.40E-03	4.00E-04	6.00E-01	5.99E-03	5.03E-03	9.82E-01
8155707	NM_004817	TJP2	6.0	5.9	6.2	7.1	-0.10	0.25	1.15	1.25	0.89	0.35	8.95E-01	3.59E-01	4.97E-05	1.25E-05	4.09E-04	2.62E-01
8013771	NM_138463	TLCD1	4.9	5.3	6.0	5.0	0.43	1.13	0.07	-0.36	-1.06	0.70	1.04E-01	1.56E-06	8.45E-01	8.27E-02	3.50E-06	1.80E-03
8098611	NM_003265	TLR3	6.4	6.9	7.4	6.8	0.45	1.00	0.36	-0.10	-0.65	0.55	5.94E-01	1.84E-02	5.76E-01	9.16E-01	1.72E-01	3.66E-01
8157524	NR_024168	TLR4	7.8	7.0	6.6	7.2	-0.86	-1.23	-0.66	0.20	0.57	-0.37	2.14E-02	7.32E-05	3.40E-02	6.45E-01	4.92E-02	3.47E-01
8091411	NM_014220	TM4SF1	9.4	9.6	8.9	10.3	0.17	-0.45	0.92	0.75	1.37	-0.62	8.37E-01	1.99E-01	8.97E-03	3.22E-02	1.25E-04	1.15E-01
7996860	NM_024562	TMCO7	6.2	6.5	6.9	5.3	0.29	0.72	-0.94	-1.22	-1.66	0.44	7.35E-01	5.14E-02	2.02E-02	2.41E-03	6.10E-05	4.17E-01
8007483	NM_145041	TMEM106A	5.8	5.7	6.3	5.3	-0.05	0.54	-0.47	-0.42	-1.01	0.59	9.61E-01	9.58E-02	2.09E-01	2.78E-01	1.99E-03	1.23E-01
7954985	NM_032256	TMEM117	6.4	6.9	7.6	6.4	0.45	1.15	-0.03	-0.48	-1.18	0.70	2.39E-01	4.22E-05	9.61E-01	8.17E-02	3.47E-05	1.58E-02
8103226	NM_152680	TMEM154	4.9	5.0	4.7	6.2	0.09	-0.23	1.33	1.24	1.56	-0.31	9.44E-01	6.45E-01	6.65E-04	1.11E-03	6.10E-05	5.88E-01
8138337	NM_001004320	TMEM195	3.2	3.3	3.2	5.2	0.09	0.02	1.97	1.88	1.95	-0.07	8.98E-01	9.57E-01	8.15E-09	1.54E-08	6.12E-09	8.98E-01
7979524	NM_001017970	TMEM30B	5.7	5.9	6.0	6.7	0.28	0.39	1.03	0.75	0.64	0.11	7.79E-01	4.43E-01	2.19E-02	1.03E-01	1.54E-01	9.14E-01
8081288	NM_018004	TMEM45A	8.3	8.2	8.3	7.3	-0.17	0.01	-0.99	-0.82	-1.00	0.19	7.02E-01	9.72E-01	5.70E-05	3.80E-04	2.21E-05	5.85E-01
7957737	NM_001032283	TMPO	6.4	6.4	6.0	7.1	-0.04	-0.38	0.67	0.71	1.05	-0.34	9.82E-01	4.78E-01	1.82E-01	1.45E-01	1.61E-02	6.43E-01
8163637	NM_002160	TNC	8.9	9.2	10.0	9.8	0.32	1.06	0.87	0.56	-0.19	0.75	6.80E-01	3.04E-03	2.57E-02	1.81E-01	7.46E-01	8.07E-02
8045688	NM_007115	TNFAIP6	8.1	8.3	10.8	9.8	0.19	2.68	1.69	1.50	-0.99	2.49	9.24E-01	5.39E-05	9.61E-03	2.01E-02	1.23E-01	6.98E-04
8149749	NM_003840	TNFRSF10D	7.9	7.9	6.8	7.6	-0.03	-1.13	-0.40	-0.37	0.73	-1.10	9.87E-01	1.28E-02	5.55E-01	5.96E-01	1.43E-01	3.97E-02
7968015	NM_148957	TNFRSF19	6.0	6.6	5.9	5.2	0.62	-0.10	-0.81	-1.43	-0.71	-0.72	9.79E-02	8.19E-01	5.65E-03	1.02E-05	9.48E-03	1.88E-02
8092095	NM_015028	TNIK	5.1	4.4	4.6	3.6	-0.66	-0.45	-1.54	-0.88	-1.09	0.21	4.72E-01	4.88E-01	6.40E-03	1.35E-01	4.05E-02	8.52E-01
8139500	NM_022748	TNS3	5.5	5.1	5.2	4.3	-0.50	-0.34	-1.21	-0.71	-0.87	0.15	2.77E-01	2.98E-01	2.99E-04	2.30E-02	3.89E-03	7.88E-01
8113120	BC028919	TOB2	9.7	9.5	9.1	10.4	-0.21	-0.64	0.62	0.82	1.25	-0.43	8.37E-01	1.04E-01	1.65E-01	4.64E-02	1.55E-03	4.43E-01
8165707	BC028919	TOB2	9.7	9.5	9.1	10.4	-0.21	-0.64	0.62	0.82	1.25	-0.43	8.37E-01	1.04E-01	1.65E-01	4.64E-02	1.55E-03	4.43E-01
8014974	NM_001067	TOP2A	8.2	6.9	5.8	8.6	-1.32	-2.42	0.38	1.70	2.80	-1.10	2.65E-01	1.61E-03	7.82E-01	3.82E-02	5.47E-04	2.80E-01
8143643	NM_022445	TPK1	4.8	5.3	5.9	5.3	0.53	1.19	0.51	-0.02	-0.68	0.66	3.00E-01	3.96E-04	1.77E-01	9.83E-01	4.06E-02	8.66E-02
8075106	NM_003595	TPST2	7.4	7.5	7.9	6.6	0.12	0.51	-0.71	-0.83	-1.23	0.40	9.09E-01	1.17E-01	3.84E-02	1.42E-02	3.00E-04	3.77E-01
7909545	NM_145759	TRAF5	5.6	6.2	6.1	5.1	0.67	0.50	-0.44	-1.12	-0.94	-0.18	2.14E-01	1.98E-01	3.36E-01	3.84E-03	1.03E-02	8.07E-01
8012953	NM_006470	TRIM16	6.5	6.5	7.1	6.1	-0.04	0.60	-0.45	-0.41	-1.04	0.63	9.65E-01	8.77E-03	8.40E-02	1.15E-01	5.59E-05	1.68E-02
8005475	NM_001037330	TRIM16L	6.9	7.0	7.7	6.5	0.12	0.80	-0.41	-0.53	-1.21	0.68	8.58E-01	1.39E-03	1.58E-01	4.82E-02	2.21E-05	1.74E-02
8104234	NM_004237	TRIP13	5.6	4.8	4.8	6.3	-0.80	-0.85	0.72	1.52	1.57	-0.05	5.75E-01	3.13E-01	4.86E-01	5.92E-02	3.88E-02	9.85E-01
7971104	NM_016179	TRPC4	5.7	5.1	5.0	3.9	-0.60	-0.69	-1.82	-1.22	-1.12	-0.10	1.50E-01	1.34E-02	1.15E-06	1.71E-04	2.69E-04	8.80E-01
8152453	NM_014112	TRPS1	7.3	7.4	7.4	8.3	0.08	0.06	1.01	0.93	0.95	-0.02	9.58E-01	9.41E-01	2.67E-02	3.93E-02	2.60E-02	9.87E-01
8063437	NM_173485	TSHZ2	5.7	5.9	5.2	6.8	0.15	-0.49	1.06	0.91	1.55	-0.64	9.56E-01	6.11E-01	2.13E-01	2.99E-01	3.25E-02	5.85E-01
7954653	NM_001080509	TSPAN11	5.2	5.2	4.5	5.9	-0.05	-0.76	0.71	0.76	1.46	-0.71	9.81E-01	1.54E-01	2.45E-01	1.98E-01	4.54E-03	2.97E-01
8142524	NM_012338	TSPAN12	4.7	5.1	5.8	4.5	0.46	1.12	-0.20	-0.66	-1.32	0.66	3.97E-01	7.44E-04	7.21E-01	6.41E-02	2.03E-04	9.13E-02
8131600	NM_014399	TSPAN13	4.7	4.9	5.6	4.2	0.17	0.88	-0.49	-0.66	-1.38	0.72	9.18E-01	7.94E-02	4.71E-01	2.74E-01	6.61E-03	2.79E-01
7939559	NM_130783	TSPAN18	7.4	7.3	5.9	4.3	-0.05	-1.49	-3.05	-3.00	-1.57	-1.43	9.87E-01	5.82E-02	5.65E-04	5.37E-04	5.16E-02	1.35E-01
7918857	NM_005725	TSPAN2	7.4	7.8	8.2	6.1	0.43	0.79	-1.34	-1.76	-2.13	0.37	8.52E-01	4.36E-01	1.71E-01	5.15E-02	1.22E-02	8.35E-01
8101828	NM_005723	TSPAN5	7.5	7.8	8.0	8.6	0.26	0.53	1.09	0.83	0.56	0.27	6.28E-01	4.72E-02	3.58E-04	3.98E-03	4.07E-02	5.29E-01
8120838	NM_003318	TTK	4.6	3.7	3.5	5.5	-0.89	-1.10	0.84	1.73	1.95	-0.21	5.93E-01	2.31E-01	4.70E-01	5.92E-02	2.35E-02	9.18E-01
8116649	NM_001069	TUBB2A	8.7	9.3	9.8	9.4	0.56	1.13	0.71	0.14	-0.43	0.57	2.52E-01	5.15E-04	4.23E-02	7.99E-01	2.37E-01	1.42E-01

			Estimate				Log-ratio						p-value (corr)					
UT ID	NCBI Ref No	Gene Symbol	G1	G2	G3	G4	G2/G1	G3/G1	G4/G1	G4/G2	G4/G3	G3/G2	G2/G1	G3/G1	G4/G1	G4/G2	G4/G3	G3/G2
8116653	NM_001069	TUBB2A	8.7	9.3	9.8	9.4	0.56	1.13	0.71	0.14	-0.43	0.57	2.52E-01	5.15E-04	4.23E-02	7.99E-01	2.37E-01	1.42E-01
7905428	NM_020127	TUFT1	5.5	5.8	6.0	4.6	0.33	0.53	-0.85	-1.18	-1.38	0.20	5.06E-01	5.28E-02	4.80E-03	1.59E-04	1.45E-05	6.83E-01
7904726	NM_006472	TXNIP	9.9	10.0	9.5	7.8	0.11	-0.39	-2.06	-2.17	-1.67	-0.50	9.60E-01	6.52E-01	2.51E-03	1.26E-03	8.10E-03	6.26E-01
8019842	NM_001071	TYMS	7.9	7.2	6.3	8.2	-0.71	-1.54	0.34	1.05	1.88	-0.83	5.31E-01	1.01E-02	7.47E-01	1.25E-01	2.76E-03	3.23E-01
8063043	NM_181802	UBE2C	4.9	4.6	4.3	5.6	-0.28	-0.54	0.75	1.03	1.29	-0.26	8.24E-01	3.40E-01	2.05E-01	5.53E-02	1.04E-02	7.88E-01
8094778	NM_004181	UCHL1	9.6	9.6	10.0	8.9	0.01	0.39	-0.68	-0.70	-1.07	0.38	9.95E-01	3.79E-01	1.12E-01	9.83E-02	5.66E-03	5.30E-01
7906995	NM_012474	UCK2	7.5	7.8	8.6	7.8	0.32	1.11	0.36	0.04	-0.75	0.79	4.28E-01	3.09E-05	1.98E-01	9.42E-01	2.23E-03	3.96E-03
7950307	NM_003355	UCP2	4.4	4.6	4.1	5.2	0.16	-0.30	0.82	0.66	1.12	-0.46	8.81E-01	5.06E-01	3.67E-02	1.00E-01	2.49E-03	3.54E-01
8122724	NM_025218	ULBP1	5.2	5.0	4.8	7.2	-0.21	-0.43	1.93	2.14	2.35	-0.21	9.07E-01	5.64E-01	1.92E-03	5.56E-04	1.29E-04	8.61E-01
7928189	NM_170744	UNC5B	6.3	6.5	6.7	5.6	0.20	0.39	-0.67	-0.87	-1.06	0.19	8.82E-01	4.82E-01	1.94E-01	7.04E-02	1.76E-02	8.39E-01
8032284	NM_006830	UQCR11	6.9	6.9	6.6	5.9	-0.06	-0.36	-1.07	-1.01	-0.71	-0.30	9.55E-01	2.24E-01	4.78E-04	6.62E-04	9.37E-03	4.60E-01
8074606	NM_017414	USP18	4.5	4.9	6.2	4.5	0.34	1.61	-0.03	-0.37	-1.64	1.27	6.60E-01	8.09E-05	9.75E-01	4.75E-01	8.39E-05	3.62E-03
7952249	NM_004205	USP2	4.4	4.4	4.4	5.4	-0.06	0.01	0.96	1.03	0.95	0.08	9.45E-01	9.82E-01	1.22E-03	4.99E-04	7.22E-04	9.02E-01
8097098	NM_019050	USP53	9.2	9.3	9.4	8.0	0.14	0.24	-1.16	-1.30	-1.40	0.10	9.30E-01	7.48E-01	2.49E-02	1.10E-02	4.29E-03	9.37E-01
8176578	NM_004654	USP9Y	3.2	3.2	3.2	6.1	-0.02	-0.02	2.88	2.90	2.90	0.00	9.95E-01	9.89E-01	3.24E-05	2.13E-05	1.43E-05	1.00E+00
8177137	NM_007125	UTY	3.2	3.3	3.1	4.6	0.12	-0.07	1.46	1.33	1.52	-0.19	9.18E-01	9.21E-01	3.48E-04	6.75E-04	1.06E-04	7.90E-01
7903358	NM_001078	VCAM1	9.0	9.6	9.9	5.1	0.54	0.83	-3.92	-4.46	-4.75	0.29	7.83E-01	3.85E-01	5.05E-05	7.02E-06	2.30E-06	8.74E-01
7962689	NM_001017535	VDR	5.9	5.9	6.4	5.0	0.05	0.51	-0.85	-0.91	-1.37	0.46	9.52E-01	3.17E-02	1.49E-03	6.58E-04	3.50E-06	1.16E-01
8088979	NM_016206	VGLL3	9.8	9.9	9.7	8.1	0.15	-0.08	-1.64	-1.79	-1.56	-0.23	8.84E-01	8.96E-01	4.21E-05	1.02E-05	3.64E-05	7.11E-01
8042086	NM_006296	VRK2	5.9	6.2	6.3	6.9	0.39	0.48	1.03	0.64	0.55	0.09	2.88E-01	4.04E-02	1.58E-04	1.13E-02	2.11E-02	8.68E-01
7983306	NM_024908	WDR76	6.9	6.0	5.5	7.5	-0.85	-1.33	0.69	1.53	2.02	-0.49	4.42E-01	3.46E-02	4.22E-01	2.44E-02	2.14E-03	6.60E-01
7938364	BX641032	WEE1	5.2	4.8	4.4	5.7	-0.39	-0.84	0.50	0.89	1.34	-0.45	7.33E-01	1.10E-01	4.73E-01	1.16E-01	9.44E-03	5.93E-01
7938366	BX641032	WEE1	5.4	4.7	4.1	5.7	-0.72	-1.33	0.30	1.02	1.63	-0.61	4.45E-01	1.28E-02	7.49E-01	8.95E-02	3.52E-03	4.52E-01
8088180	NM_003392	WNT5A	6.3	6.0	5.5	4.9	-0.25	-0.73	-1.38	-1.13	-0.65	-0.48	8.67E-01	1.93E-01	1.54E-02	4.69E-02	2.96E-01	5.80E-01
8004184	NM_017523	XAF1	7.3	7.6	9.0	7.7	0.26	1.71	0.42	0.16	-1.29	1.45	8.04E-01	1.54E-04	4.77E-01	8.44E-01	3.20E-03	3.43E-03
7936284	NM_020383	XPNPEP1	8.1	8.0	8.3	7.3	-0.08	0.25	-0.79	-0.71	-1.04	0.33	9.20E-01	3.46E-01	1.92E-03	3.85E-03	5.34E-05	2.89E-01
7949577	NM_020470	YIF1A	6.9	6.9	7.1	5.9	0.01	0.19	-1.04	-1.04	-1.23	0.19	9.98E-01	7.28E-01	9.35E-03	8.26E-03	1.30E-03	7.99E-01
8023871	NM_175907	ZADH2	6.5	6.5	6.3	7.5	-0.06	-0.23	0.95	1.01	1.18	-0.17	9.44E-01	4.44E-01	5.45E-04	2.25E-04	2.23E-05	7.03E-01
7943715	NM_033390	ZC3H12C	5.7	5.8	5.6	7.4	0.08	-0.15	1.68	1.60	1.83	-0.23	9.35E-01	7.37E-01	6.23E-06	9.20E-06	1.07E-06	6.49E-01
8144758	NM_016353	ZDHHC2	8.1	8.2	7.6	8.7	0.05	-0.49	0.55	0.51	1.05	-0.54	9.49E-01	1.51E-02	1.32E-02	2.19E-02	1.31E-05	2.19E-02
7926916	NM_030751	ZEB1	8.5	8.9	8.4	9.5	0.33	-0.12	0.93	0.60	1.06	-0.46	5.83E-01	8.08E-01	5.98E-03	7.89E-02	1.14E-03	2.69E-01
8028652	NM_003407	ZFP36	7.4	7.8	7.3	8.3	0.43	-0.06	0.94	0.51	1.01	-0.50	6.46E-01	9.42E-01	6.59E-02	4.03E-01	3.37E-02	4.87E-01
8147837	NM_012082	ZFPM2	4.3	4.4	4.2	6.6	0.09	-0.10	2.32	2.23	2.42	-0.19	9.34E-01	8.72E-01	3.68E-07	5.42E-07	1.01E-07	7.70E-01
8176384	NM_003411	ZFY	3.5	3.6	3.5	5.1	0.08	0.06	1.58	1.50	1.52	-0.02	9.50E-01	9.24E-01	7.67E-05	1.09E-04	5.79E-05	9.87E-01
7995258	NM_003414	ZNF267	5.5	5.8	6.3	6.5	0.28	0.79	1.02	0.74	0.23	0.51	7.24E-01	2.44E-02	8.27E-03	5.48E-02	6.69E-01	2.84E-01
8085774	NM_024697	ZNF385D	5.3	5.6	5.6	8.3	0.29	0.34	2.99	2.70	2.65	0.05	9.41E-01	8.64E-01	1.34E-02	2.35E-02	1.94E-02	9.88E-01
8039044	NR_028343	ZNF415	5.4	5.4	5.0	4.4	0.00	-0.41	-1.03	-1.03	-0.63	-0.40	9.98E-01	2.20E-01	2.19E-03	1.95E-03	4.46E-02	3.44E-01
8107591	NM_207317	ZNF474	3.5	3.7	4.8	3.4	0.19	1.28	-0.12	-0.32	-1.40	1.09	6.12E-01	4.85E-07	6.83E-01	1.42E-01	6.82E-08	1.76E-05
8022612	NM_015461	ZNF521	5.8	6.1	5.8	8.0	0.23	0.00	2.14	1.91	2.14	-0.23	9.50E-01	9.99E-01	5.13E-02	8.29E-02	3.60E-02	9.27E-01
8027348	ENST00000327867	ZNF730	4.3	4.2	4.4	5.8	-0.10	0.06	1.46	1.56	1.41	0.16	9.57E-01	9.55E-01	8.44E-03	4.31E-03	6.99E-03	8.95E-01
8047763	---		7.7	7.4	6.4	9.0	-0.30	-1.32	1.37	1.67	2.69	-1.01	8.98E-01	8.47E-02	1.06E-01	3.85E-02	7.09E-04	3.26E-01
8117018	---		3.3	3.0	3.2	4.6	-0.33	-0.12	1.27	1.59	1.38	0.21	6.95E-01	8.63E-01	3.05E-03	2.50E-04	7.08E-04	7.83E-01
7913803	---		3.7	4.3	3.8	4.9	0.55	0.03	1.18	0.63	1.15	-0.52	5.30E-01	9.79E-01	2.05E-02	2.70E-01	1.57E-02	4.53E-01
8156358	---		5.4	5.5	4.9	6.5	0.09	-0.55	1.09	1.00	1.64	-0.65	9.61E-01	3.84E-01	6.48E-02	9.29E-02	2.92E-03	4.05E-01
7999362	---		4.2	4.7	4.5	5.2	0.58	0.33	1.06	0.49	0.73	-0.25	4.65E-01	5.77E-01	2.84E-02	4.06E-01	1.25E-01	7.79E-01
8047401	---		6.5	6.8	6.7	7.5	0.33	0.20	1.03	0.70	0.84	-0.14	6.39E-01	7.00E-01	6.17E-03	6.21E-02	1.73E-02	8.58E-01
8157191	---		4.5	3.8	4.0	5.6	-0.72	-0.54	1.03	1.76	1.57	0.19	2.51E-01	2.29E-01	2.01E-02	1.65E-04	3.48E-04	8.25E-01
8045804	---		9.2	9.2	8.5	10.2	-0.05	-0.68	0.98	1.03	1.67	-0.63	9.86E-01	3.38E-01	1.75E-01	1.43E-01	8.38E-03	5.15E-01
7896748	---		4.8	4.9	4.4	5.8	0.08	-0.41	0.96	0.87	1.37	-0.50	9.59E-01	4.63E-01	5.68E-02	8.27E-02	3.50E-03	4.74E-01
8045533	---		4.2	4.2	3.8	5.2	0.00	-0.45	0.95	0.96	1.40	-0.44	9.98E-01	3.55E-01	3.58E-02	3.23E-02	1.25E-03	4.92E-01
8142763	---		5.2	4.4	4.6	6.1	-0.84	-0.60	0.86	1.70	1.46	0.25	3.13E-01	3.21E-01	1.63E-01	2.84E-03	7.03E-03	8.21E-01
7944970	---		3.8	4.7	5.9	4.2	0.91	2.09	0.34	-0.57	-1.74	1.18	1.46E-01	2.31E-05	5.98E-01	2.85E-01	2.08E-04	1.78E-02
7911337	---		10.5	10.3	9.8	11.4	-0.19	-0.74	0.85	1.04	1.59	-0.55	9.27E-01	2.90E-01	2.61E-01	1.40E-01	1.17E-02	5.91E-01
7973871	---		10.5	10.3	9.8	11.4	-0.19	-0.74	0.85	1.04	1.59	-0.55	9.27E-01	2.90E-01	2.61E-01	1.40E-01	1.17E-02	5.91E-01
8165696	---		10.5	10.3	9.8	11.4	-0.19	-0.74	0.85	1.04	1.59	-0.55	9.27E-01	2.90E-01	2.61E-01	1.40E-01	1.17E-02	5.91E-01
7928821	---		5.6	4.7	5.1	6.4	-0.86	-0.50	0.81	1.67	1.31	0.36	3.97E-01	5.13E-01	2.82E-01	1.02E-02	3.33E-02	7.56E-01
8154207	---		5.1	4.2	5.1	5.8	-0.84	0.02	0.68	1.52	0.66	0.86	3.04E-01	9.82E-01	2.91E-01	6.32E-03	2.77E-01	1.88E-01
7911339	---		8.3	8.4	7.5	9.0	0.07	-0.79	0.67	0.60	1.46	-0.86	9.78E-01	2.77E-01	4.49E-01	5.11E-01	2.76E-02	3.42E-01
8165698	---		8.3	8.4	7.5	9.0	0.07	-0.79	0.67	0.60	1.46	-0.86	9.78E-01	2.77E-01	4.49E-01	5.11E-01	2.76E-02	3.42E-01
8114211	---		7.7	8.8	9.2	8.4	1.15	1.56	0.77	-0.37	-0.79	0.41	1.55E-01	4.70E-03	2.57E-01	6.72E-01	2.06E-01	6.70E-01
8107204	---		8.1	7.9	7.5	8.6	-0.17	-0.62	0.52	0.69	1.15	-0.45	8.58E-01	7.63E-02	2.07E-01	6.71E-02	1.48E-03	3.50E-01
8108180	---		8.2	8.0	7.6	8.7	-0.17	-0.59	0.49	0.66	1.08	-0.42	8.30E-01	5.30E-02	1.73E-01	4.65E-02	8.00E-04	3.11E-01
8116651	---		8.4	8.9	9.5	9.1	0.44	1.06	0.71	0.27	-0.35	0.62	4.42E-01	1.51E-03	5.12E-02	5.84E-01	4.02E-01	1.26E-01
8148325	---		5.1	4.6	4.1	5.0	-0.51	-1.00	-0.16	0.36	0.85	-0.49	3.70E-01	3.65E-03	8.06E-01	4.50E-01	1.68E-02	2.95E-01
8162531	---		9.2	7.8	8.2	9.7	-1.38	-1.03	0.44	1.82	1.47	0.35	9.01E-05	3.45E-04	1.74E-01	5.65E-07	7.17E-06	3.70E-01
8146647	---		5.0	4.5	3.9	4.7	-0.54	-1.09	-0.29	0.25	0.79	-0.54	5.51E-01	2.15E-02	7.14E-01	7.60E-01	1.20E-01	4.43E-01
8083592	---		5.9	6.0	4.8	6.3	0.04	-1.12	0.41	0.37	1.52	-1.16	9.85E-01	3.17E-02	6.07E-01	6.54E-01	4.56E-03	6.04E-02
8149248	---		5.1	4.7	3.9	4.1	-0.32	-1.19	-0.97	-0.65	0.22	-0.87	7.94E-01	1.66E-02	8.43E-02	2.99E-01	7.95E-01	1.66E-01
8169233	---		3.8	4.7	4.2	3.3	0.96	0.45	-0.47	-1.43	-0.91	-0.51	1.56E-01	4.33E-01	4.66E-01	4.43E-03	5.79E-02	4.69E-01
8131867	---		8.4	8.9	8.7	7.6	0.49	0.35	-0.83	-1.31	-1.17	-0.14	6.83E-01	6.65E-01	2.18E-01	2.89E-02	4.06E-02	9.19E-01
8084213	---		6.9	7.3	7.3	6.0	0.42	0.46	-0.89	-1.31	-1.35	0.04	4.57E-01	1.80E-01	1.02E-02	2.69E-04	1.25E-04	9.65E-01
7922400	---		9.1	9.2	8.9	8.2	0.08	-0.24	-0.93	-1.00	-0.68	-0.32	9.41E-01	5.29E-01	5.03E-03	2.16E-03	2.64E-02	4.89E-01
7919600	---		6.4	6.6	5.9	5.2	0.14	-0.51	-1.24	-1.38	-0.73	-0.65	9.39E-01	4.27E-01	3.12E-02	1.50E-02	2.21E-01	3.97E-01

APPENDIX L

List of Related Publications, Proceedings and Awards

A. LIST OF RELATED PUBLICATIONS

1. **Tan S.L.,** Ahmad T.S., Chan C.K., Selvaratnam L., Kamarul T. (2013) Growth differentiation factor 5 (GDF5)-induced marrow stromal stem cells support superior tendon healing in vivo: A preliminary report. *PLOS ONE* (Submitted).

2. **Tan S.L.,** Ahmad T.S., Selvaratnam L., Kamarul T. (2013) Identification of Pathways Mediating Growth Differentiation Factor 5-induced Tenogenic Differentiation in Human Bone Marrow Stromal Cells. *Stem Cells* (Submitted).

3. **Tan S.L.,** Ahmad T.S., Selvaratnam L. & Kamarul T. (2013) Isolation, characterization and the multi-lineage differentiation potential of rabbit bone marrow-derived mesenchymal stem cells. *Journal of Anatomy* 222: 437-450.

4. **Tan S.L.,** Ahmad R.E., Ahmad T.S., Merican A.M., Abbas A.A., Ng W.M., et al. (2012) Effect of growth differentiation factor 5 on the proliferation and tenogenic differentiation potential of human mesenchymal stem cells in vitro. *Cells Tissues Organs* 196: 325-338.

5. Kamarul Tunku, **Sik-Loo Tan**, Selvaratnam Lakshmi, Tai Cheh-Chin, (2009) The effect of growth and differentiation factor 5 in tenogenic differentiation. *European Cells and Materials* 18 (Suppl. 1): 47.

B. LIST OF PROCEEDINGS

1. **Sik Loo Tan**; Azhar Mahmood Merican; Azlina Amir Abbas; Wuey Min Ng; Chee Ken Chan; Raja Hisyam; Selvaratnam Lakshmi; Cheh Chin Tai; Elina Raja Ahmad; Sara Tunku; Kamarul Tunku. 2011. 'Optimizing Tenogenic Differentiation of Human Mesenchymal Stem Cells using Growth & Differentiation Factor-5'. 57th Annual Meeting of the Orthopaedic Research Society (ORS), on 13th-16thJanuary, 2011, at Long Beach, CA, United State. Pp1759.

2. **Sik-Loo Tan**, Lakshmi Selvaratnam, Cheh-Chin Tai & T. Kamarul. 2010. 'Tenogenic Expression of Differentiated Mesenchymal Stem Cells is Dependant on Growth and Differentiation Factor-5'. 56th Annual Meeting of the Orthopaedic Research Society (ORS), on 6th-9th March, 2010, at Morial Convention Center (Hall H), New Orleans, United State. Pg1090.

3. **Sik-Loo Tan**, Lakshmi Selvaratnam, Cheh-Chin Tai & T. Kamarul. 2009. 'Ultrastructural Analysis and Identification of Rabbit Bone Marrow Derived Mesenchymal Stem Cells'. 7th Annual Meeting of International Society of Stem Cell Research, on 8th to 11th July 2009, at Centre Convencions Barcelona, Barcelona, Spain. Pp226.

4. **Sik-Loo Tan**, Lakshmi Selvaratnam, Cheh-Chin Tai & T. Kamarul. 2009. Digital Imaging of bone marrow derived mesenchymal stem cells. 16th International Student Congress of Medical Sciences, 2nd - 5th June 2009, University Medical Center Groningen, Groningen, The Netherlands. Pp78.

C. LIST OF AWARDS

1. Best Basic Science Poster Award (MOA 2013 Poster Presentation)
   Sik-Loo Tan, TS Ahmad, WM Ng, AM Merican, AA Abbas, L Selvaratnam & T Kamarul.
   Title: Confocal laser scanning microscopy and atomic force microscopy imaging of growth differentiation factor 5-induced human mesenchymal stem cells (hMSCs).
2. 2nd Runner Up Best Basic Science Poster Award (MOA 2012 Poster Presentation)
   S-L Tan, TS Ahmad, WM Ng, AA Abbas, L Selvaratnam & T Kamarul.
   Title: Microarray Identification of Differentially Expressed Genes Mediating Differentiation of Human-Bone-Marrow-Derived Mesenchymal Stem Cells Under Growth Differentiation Factor 5 (GDF-5) Induction.
3. Excellent Poster Presentation Award (Asian Reproductive Biotechnology Society-The 7th Annual Conference 2010)
   Sik Loo Tan; Lakshmi Selvaratnam; Azhar Mahmood Merican,; Azlina Amir Abbas,; Wuey Min Ng; Cheh-Chin Tai; Raja Elina Ahmad, Tunku Sara Ahmad; Tunku Kamarul.
   Title: *In vitro* tenogenic differentiation potential of human mesenchymal stem cells using growth & differentiation factor-5.
4. 1st Prize – Advances in Stem Cell Therapy 2009 (Poster Presentation)
   Tan, S-L; Merican, AM; Abas, AA; Ng, W-M; Selvaratnam, L; Tai, C-C; Kamarul, T.
   Title: Comparison of the Effect of GDF-5 on Human and Rabbit Bone Marrow Derived Mesenchymal Stem Cells.
5. International Society of Stem cells Research 2009-Travel Award
   Sik-Loo Tan, Lakshmi Selvaratnam, Cheh-Chin Tai & T. Kamarul.
   Title: Ultrastructural Analysis and Identification of Rabbit Bone Marrow Derived Mesenchymal Stem Cells.

D. PATENTS

1. Tenogenic medium for mesenchymal stem cells differentation into tenogenic lineage (PI2012002249).

E. RESEARCH FELLOWSHIP

1. 16th International Student Congress of Medical Sciences (ISCOMS) Research Fellowship, 2009, in Academy Institute for International Development of Transfusion Medicine (IDTM), Groningen, the Netherlands.

2. 8thDr Ranjeet Bhagwan Singh National Fellowship on "Human Embryonic Stem Cell: Culture and Maintenance". Under the programme of the Dr Ranjeet Bhagwan Singh Medical Trust Fund, co-organized by Academy of Science Malaysia, MOSTI and International Medical University.

APPENDIX M

Publication in Journal of Anatomy

Journal of Anatomy

J. Anat. (2013) **222**, pp437–450 doi: 10.1111/joa.12032

Isolation, characterization and the multi-lineage differentiation potential of rabbit bone marrow-derived mesenchymal stem cells

Sik-Loo Tan,[1] Tunku Sara Ahmad,[1] Lakshmi Selvaratnam[2] and Tunku Kamarul[1]

[1]*Tissue Engineering Group, National Orthopaedics Centre of Excellence in Research & Learning, Department of Orthopaedic Surgery, Faculty of Medicine, University of Malaya, Kuala Lumpur, Malaysia*
[2]*School of Medicine & Health Sciences, Monash University, Sunway Campus, Subang Jaya, Selangor, Malaysia*

Abstract

Mesenchymal stem cells (MSCs) are recognized by their plastic adherent ability, fibroblastic-like appearance, expression of specific surface protein markers, and are defined by their ability to undergo multi-lineage differentiation. Although rabbit bone marrow-derived MSCs (rbMSCs) have been used extensively in previous studies especially in translational research, these cells have neither been defined morphologically and ultrastructurally, nor been compared with their counterparts in humans in their multi-lineage differentiation ability. A study was therefore conducted to define the morphology, surface marker proteins, ultrastructure and multi-lineage differentiation ability of rbMSCs. Herein, the primary rbMSC cultures of three adult New Zealand white rabbits (at least 4 months old) were used for three independent experiments. rbMSCs were isolated using the gradient-centrifugation method, an established technique for human MSCs (hMSCs) isolation. Cells were characterized by phase contrast microscopy observation, transmission electron microscopy analysis, reverse transcriptase-polymerase chain reaction (PCR) analysis, immunocytochemistry staining, flow cytometry, alamarBlue® assay, histological staining and quantitative (q)PCR analysis. The isolated plastic adherent cells were in fibroblastic spindle-shape and possessed eccentric, irregular-shaped nuclei as well as rich inner cytoplasmic zones similar to that of hMSCs. The rbMSCs expressed CD29, CD44, CD73, CD81, CD90 and CD166, but were negative (or dim positive) for CD34, CD45, CD117 and HLD-DR. Despite having similar morphology and phenotypic expression, rbMSCs possessed significantly larger cell size but had a lower proliferation rate as compared with hMSCs. Using established protocols to differentiate hMSCs, rbMSCs underwent osteogenic, adipogenic and chondrogenic differentiation. Interestingly, differentiated rbMSCs demonstrated higher levels of osteogenic (*Runx2*) and chondrogenic (*Sox9*) gene expressions than that of hMSCs ($P < 0.05$). There was, however, no difference in the adipogenic (*Pparγ*) expressions between these cell types ($P > 0.05$). rbMSCs possess similar morphological characteristics to hMSCs, but have a higher potential for osteogenic and chondrogenic differentiation, despite having a lower cell proliferation rate than hMSCs. The characteristics reported here may be used as a comprehensive set of criteria to define or characterize rbMSCs.

Key words: cell differentiation; cell therapy; mesenchymal stem cells; orthopaedics; tendon; tissue engineering.

Introduction

Mesenchymal stem cells (MSCs) are multipotent cells that can undergo multi-lineage differentiation. Due to this, many studies have been conducted with the ultimate aim to harness the potential of these cells for many possible applications, especially for translational research (Dashtdar et al. 2011; Tay et al. 2011). The use of rabbit MSCs (rbMSCs) has been described in many previous studies, and has recently been very popular with many scientists, due to a readily available supply of this animal. Furthermore, it has been described that these cells possess cellular and tissue physiology that closely resemble human

Correspondence
Sik-Loo Tan, Tissue Engineering Group, National Orthopaedics Centre of Excellence in Research & Learning, Department of Orthopaedic Surgery, Faculty of Medicine, University of Malaya, Kuala Lumpur, Malaysia. E: tansikloo@yahoo.com

Presented in abstract form at the 2009 International Society for Stem Cell Research (ISSCR) 7th Annual Meeting, Barcelona, Spain, July 2009. This manuscript also represents a portion of a thesis to be submitted by S.-L. Tan to the Department of Orthopaedic Surgery, University of Malaya as partial fulfillment of the requirements for a PhD degree
Accepted for publication *28 January 2013*

MSCs (hMSCs; Fox, 1984; Warden, 2007). In *in vivo* models, the rabbit has the advantage over other animals due to its relatively larger size compared with the rat or mouse. It is inexpensive and is relatively easy to handle compared with other larger animal models, such as dogs, goats or sheep. However, unlike hMSCs, there is not much in the literature about the basic characteristics that define rbMSCs (Gupta & Lee, 2007; Warden, 2007; Amini et al. 2012). Despite being readily available, many researchers are in a dilemma when it comes to using rbMSCs as the validity of studies conducted using these cells may be questioned. This is especially true because rbMSCs, until today, remain largely undefined. Furthermore, whilst these cells may have certain potentials that mimic MSCs, they may in fact be merely progenitor cells that may have been isolated during the harvesting process (Chong et al. 2011). This further creates other issues as the outcome of many experiments may turn out to be unreliable because the cell population used would then be of a mixed type. It is therefore imperative that the identification and characterization of MSCs from different tissue origins (Koerner et al. 2006; Laitinen & Laine, 2007; Bunnell et al. 2008) or different species (Zeng et al. 2006; Nadri et al. 2007; Neupane et al. 2008) must be clearly defined in order to validate any studies in which they are used.

According to the International Society for Cellular Therapy (ISCT), MSCs are defined as cells that are: (i) plastic adherent; (ii) express CD105, CD73 and CD90, whilst lacking in the expression of CD45, CD34, CD14 or CD11b, CD79α or CD19 and HLA-DR surface molecules; and (iii) can differentiate into osteogenic, chondrogenic and adipogenic lineages (Dominici et al. 2006). In previous literature, MSCs obtained from rabbits have been shown to be able to adhere to plastic surfaces and undergo tri-lineage differentiation (Owen et al. 1987; Sahoo et al. 2010). Although MSC surface protein markers have been reported extensively in human (Chamberlain et al. 2007; Haasters et al. 2009), murine (Tropel et al. 2004; Nadri et al. 2007) and rodent (Marcus et al. 2008; Karaoz et al. 2009) cells, identification of these cells in other animal models such as rabbit (Amini et al. 2012) has not been widely published. This is mainly due to the lack of molecular biology information and the limited availability of the monoclonal antibodies (mAbs) necessary for the characterization of these cells. Furthermore, there have not been any studies that have made a comparison between the ability of rbMSCs to express various differentiation genes, for example osteogenic or chondrogenic, as compared with hMSCs. This information is important because many studies, such as those of translational models, would require the fundamental understanding of the differences between these two sources to ensure accurate interpretation of the data obtained.

This study was therefore conducted to isolate and characterize rbMSCs isolated using a commonly practiced method described by the majority of studies, i.e. gradient centrifugation technique. These cells are then identified and recognized through: (i) their morphology observed by phase contrast microscopy; (ii) ultrastructural analysis using transmission electron microscopy (TEM) analysis; (iii) CD marker expression, detected using immunostaining, reverse transcriptase-polymerase chain reaction (RT-PCR) and flow cytometry analysis; and (iv) differentiation ability using a commercial assay (osteogenic, adipogenic and chondrogenic differentiation assay). The differentiation potential of both cell types was compared using gene expression analysis techniques.

Materials and methods

rbMSC isolation

Rabbit bone marrow was harvested from New Zealand white rabbits with the protocol approved by the Animal Care and Use Committee, Faculty of Medicine, University of Malaya (PM/24/06/2008/TKZ). Three adult New Zealand white rabbits (at least 4 months old) were killed by an overdose of pentobarbital sodium (Nebutal® Sodium Solution; Boehringer, Ingelheim, Germany). Rabbit bone marrow was isolated from the tibial and femoral bones, and resuspended in 2 mL of phosphate-buffered saline (PBS; pH 7.2; Invitrogen-Gibco, USA). The bone marrow suspension was layered on 3 mL Ficoll-Paque™ Premium (density: 1.077 g mL^{-1}; GE Healthcare, Sweden) for gradient centrifugation at 400 g for 30 min in a 15-mL centrifuge tube.

The mononuclear layer (second top layer) was collected and then washed twice using Dulbecco's modified Eagle's medium (DMEM)-low glucose (DMEM-LG; 1000 mg L^{-1} D-Glucose; Invitrogen-Gibco) supplemented with antibiotic/antimycotic 1% (v/v; Invitrogen-Gibco). Next, the isolated mononuclear cells were cultured in growth medium [DMEM-LG (Invitrogen-Gibco) supplemented with 10% foetal bovine serum (Invitrogen-Gibco), antibiotic/antimycotic (Invitrogen-Gibco) 1% (v/v) and 200 mM GlutaMAX™-I (Invitrogen-Gibco)] in T75 tissue culture flasks (Nunc™, USA). The medium was changed at day 5 after primary culture to remove the non-adherent cells. The subsequent medium change was conducted at 3-day intervals. For comparison, human bone marrow was harvested from three adult donors (Table S1) undergoing intramedullary nailing of the femur or tibia in the University of Malaya Medical Center, and used for comparison with rbMSCs in the downstream experiments. hMSCs were isolated and expanded *in vitro* as previously described (Tan et al. 2012). Ethics approval to conduct this study was granted by the University of Malaya Medical Center Ethics Committee (reference no. 602.22).

Measurement of cell lengths and widths

Photographs were taken at representative areas of culture plates. The length and the maximum widths (cell body width) perpendicular to the long axes of individual cells were measured using ImageJ 1.46r software (National Institute of Mental Health, Maryland, USA). At least eight representative cells were measured from each independent experiment. Data were presented as mean ± standard error of mean. The statistical analysis was performed using SPSS Statistic software (version 19). Student's *t*-test (two-sided, unpaired)

was carried out to compare the differences in mean values, and a P-value < 0.05 was taken as significant.

rbMSC characterization by ultrastructural analysis

For electron microscopy, the medium was discarded from the culture flask containing rbMSC (or hMSC) at 70–80% confluence. The cells were rinsed twice with PBS (pH 7.2) (Invitrogen-Gibco) before being trypsinized and scraped from the flask with a cell scraper, centrifuged at 800 *g* for 10 min to form a cell pellet at the bottom of the centrifuge tube. The cell pellet was then fixed in 4% glutaraldehyde overnight before being further processed. The pellet was washed three times in 0.1 M cacodylate buffer (pH 7.4; Merck AG, Darmstadt, Germany),[i] prior to, and post-secondary fixation for 2 h at room temperature in a mixture of osmium tetraoxide : cacodylate buffer (1 : 1). The pellet was kept overnight in 0.1 M cacodylate buffer (pH 7.4; Merck AG). The next day, the pellet was washed with uranyl acetate for 10 min, followed by three washes with double-distilled water. Then, the pellet was dehydrated through a graded ethanol series (35, 50, 70 and 95%) for 10 min each; 100% for 15 min, three times; propylene oxide and epoxy resin mixture (1 : 0 for 15 min twice; 1 : 1 for 1 h; and 1 : 3 for 2 h), and in fresh epoxy resin, overnight, on the rotary mixer (Ted Pella, Redding, CA, USA), at 0.2 g. The specimen was then embedded in epoxy resin for semithin and ultrathin sectioning with an ultramicrotome (Reichert Ultracuts; Leica Microsystems, Vienna, Austria). Images were obtained with a TEM (Leo Libra 120; Carl Zeiss SMT AG, Oberkochen, Germany). Electron micrographs were prepared by the Electron Microscope Unit in University of Malaya.

rbMSC characterization by immunocytochemistry staining

Rabbit MSCs at P1 or P2 were seeded on a coverslip and used for CD44 immunocytochemistry staining. Briefly, the rbMSC cells were washed twice with cold PBS. Two-hundred microlitres of diluted (dilution at 1 : 1000) mouse mAb against rabbit CD44 surface antigen (Chemicon® International, Germany) used for staining was applied on to the cells and incubated in a humid chamber for 30 min. The cells were then washed again, twice, with cold PBS. Subsequently, the cells were stained with anti-mouse IgG allophycocyanin-conjugated Goat F (ab')$_2$ and counterstained with nucleus stain before mounting. Fluorescence images were captured using NIKON-ECLIPSE-TI-U microscope (Nikon, Japan) and NIS-ELEMENT AR software (Nikon).

rbMSC characterization by RT-PCR

Total RNA was extracted from 1×10^6 cells of 70–80% confluent rbMSC primary culture (P1–P3) using AllPrep DNA/RNA/Protein Mini kit[g] according to manufacturer's instructions and treated with RNase-free DNase I (Qiagen GmbH, Hilden, Germany). The gene-specific primers for RT-PCR were designed according to the mRNA sequence obtained from CD29 of *Felis catus* (GenBank accession FCU27351), and CD166, CD45 and CD34 of *Oryctolagus cuniculus* (GenBank accession Y13243, XM_002717662 and XM_002717543, respectively) using the *Primer Premier v5.0* (Table 1). The RT-PCR reactions were carried out using Superscript™ III One-Step RT-PCR System with Platinum® Taq DNA Polymerase kit (Invitrogen, Carlsbad, CA, USA). The RT-PCR reactions were prepared according to the manufacturer's instructions (with some modifications) in a final volume of 25 μL with 12.5 μL 2 × reaction mix, 1 μL (or 1 μg) of total RNA, 10 μM of each primer, 1 μL of Superscript™ III RT/Platinum® Taq Mix. The RT step involved incubation at 42 °C for 60 min. The amplification protocol was as follows: an initial denaturation of 94 °C for 2 min followed by 35 cycles of 94 °C for 15 s, 58 °C for 30 s and 72 °C for 30 s. Negative control tubes for each gene that contained water instead of template RNA or cDNA were also run under the same conditions. Glyceraldehyde-3-phosphate dehydrogenase (GAPDH) was used as internal control and RNA from mononuclear cells was used as positive control. To confirm the absence of primer-dimers and other spurious products, the PCR products were evaluated using an Experion™ automated microfluidic electrophoresis system (BioRad) as described in the manufacturer's protocol. This provides high-resolution banding patterns of the separated DNA molecules as well as the quantitative output of their relative abundance. Briefly, a small aliquot (~1 μL) of PCR product or DNA ladder was loaded into the sample well or ladder well on the DNA 1 K chip

Table 1 Primers used for RT-PCR and qPCR analysis.

Gene	Forward primer sequence	Reverse primer sequence	Amplicon size (bp)	GenBank accession no
RT-PCR				
CD29	5′-CAAGAAGGAATGCCTACGTC-3′	5′-CAATGCCACCAAGTTTCCCAT-3′	720	FCU27351
CD166	5′-GCTCCCCAGTATTTATTGCCTTC-3′	5′-GTAGCACCT TTCCATTCCTGTA-3′	345	Y13243
CD45	5′-AGGTAGTAGATGTTTTCCAAGTAGTGA-3′	5′-ACTTGTCCATTCTGGGCAGGGTAG-3′	130	XM_002717662
CD34	5′-AGAACTTTCCAGCATGTTCCAGTTTATG-3′	5′-GGCTTGCCACATCTTGCTCGGTGA-3′	95	XM_002717543
qPCR				
Col-I	5′-CTGACTGGAAGAGCGGAGAG-3′	5′-TCTGGGCAATGCTGGGCTGTGTGGG-3′	129	AY633663 (Tan et al. 2012)
Scx	5′-CAG CGG CAC ACG GCG AAC -3′	5′-CGT TGC CCA GGT GCG AGA TG -3′	165	BK000280 (Kuo & Tuan, 2008)
Ppar–γ	5′-AGCAAAGAAGTCGCCATCC-3′	5′-CGTTCAAGTCAAGGCTCACA-3′	118	NM_001082148
Runx2	5′-TCAGGCATGTCCCTCGGTAT-3′	5′-TGGCAGGTAGGTATGGTAGTGG-3′	54	AY598934
Sox9	5′-AGAGCGAAGAGGACAAGTTCCCCGT-3′	5′-ATGGGCACCAGCGTCCAGTCGTAG C-3′	85	XM_002719499
RT-PCR and qPCR				
GAPDH	5′-AACATCATCCCTGCCTCTACTG-3′	5′-CTCCGACGCCTGCTTCAC-3′	196	NM_002046 (Kuo & Tuan, 2008)

Table 2 Fluorescence-conjugated monoclonal antibodies used for immunophenotyping of rbMSC and hMSC.

Antigens	Fluorochrome-conjugate	Manufacturer	Applications
CD29	Non-conjugated	Abcam, UK	Rabbit only
CD29	APC	BD Biosciences, USA	Human only
CD44	Non-conjugated	SeroTec, USA	Rabbit only
CD44	APC	BD Biosciences, USA	Human only
CD73	PE-Cy™ 7	eBioscience, CA, USA	Rabbit only
CD73	PE-Cy™7	BD Biosciences, USA	Human only
CD73	FITC	BD Biosciences, USA	Human only
CD81	APC	BD Biosciences, USA	Rabbit and Human
CD90	PE-Cy™ 7	BD Biosciences, USA	Rabbit and Human
CD34	PerCP-Cy5.5	Santa Cruz Biotechnology, CA, USA	Rabbit only
CD34	PE	BD Biosciences, USA	Human only
CD34	PerCP-Cy5.5	BD Biosciences, USA	Human only
CD45	Non-conjugated	Gentaur Molecular Products, Belgium	Rabbit only
CD45	APC-H7	BD Biosciences, USA	Human only
CD117	PE	BD Biosciences, USA	Rabbit and Human
HLA-DR	FITC	BD Biosciences, USA	Rabbit and Human

(Bio-Rad, Hercules, CA, USA) and analysed with the Experion™ automated electrophoresis system (Bio-Rad). An electropherogram and a virtual gel were generated by the Experion software analysis tool when the run was completed for each sample, and the sizing of the PCR product was performed automatically based on the DNA standard electropherogram.

Flow cytometry analysis

Both rbMSCs and hMSCs at P2 or P3 were trypsinized at 70–80% confluence for phenotypic characterization using fluorescence-activated cell sorting (BD FACS Cantor II, BD Biosciences, USA). The cells were resuspended in PBS (pH 7.2) at a concentration of 10^7 cells mL^{-1}. A 100-μL cell suspension was transferred into each 5-mL polystyrene round-bottomed tube for incubation on ice with the optimum dilution of fluorochrome-conjugated mAbs or tandem dye-conjugated mAbs (Table 2). Alternatively, the cells were preincubated with non-conjugated mAbs followed by a secondary rat anti-mouse IgG–FITC or IgG–PE or IgG–APC and the fluorescence-conjugated mAb, at 4 °C for 30 min. The MSC-positive antigens included in the phenotyping profile were: CD29, CD44, CD73, CD81 and CD90.1. To discriminate MSCs from haematopoietic stem and progenitor cells, isolates were stained for CD34, CD45, CD117 and HLA-DR. All mAbs were immunoglobulin G_1 (IgG_1) isotype except for HLA-DR, which is immunoglobulin G_{2b} (IgG_{2b}). After 30 min of incubation, cells were washed using 2 mL PBS. Non-specific fluorescence emission was detected by incubating cells with fluorescence-conjugated isotype control. At least 10 000 events were captured by the system. Flow cytometry data were analysed using CELLQUEST software (Becton Dickinson). Gating was performed to exclude cell debris and unwanted aggregates (FSC/SSC dotplot). Non-specific isotype control (IgG_1 or IgG_{2a}) was used to determine the background fluorescence emission, if any.

AlamarBlue® cell proliferation assay

Cell proliferation was assessed using the alamarBlue® assay based on the colorimetric quantitative analytical principle. Both rbMSCs and hMSCs (at P2 or P3, $n = 3$) were seeded in standard 96-well culture plates at a cell density of 7.5×10^4 cells mL^{-1} in 250 μL of cell culture medium. Cells were incubated for 4 h before 25 μL of alamarBlue® reagent (Invitrogen-Gibco) was added into the medium. Culture plates were protected from light using aluminium foil. Absorbance readings at 570 and 600 nm were obtained using a spectrophotometer (Epoch; Biotek, USA) at various time points, i.e. at 0, 2, 4, 6, 12, 24, 36, 48, 60, 72, 84 and 96 h. Three independent experiments were performed, each in quadruplicate using 96-well plates. As a negative control, alamarBlue® reagent was added into the medium without cells. Data were presented as the mean ± standard deviation. Statistical analysis was analysed with SPSS (version 17) software. Comparisons of mean values between rbMSCs and hMSCs at various time points were conducted using Mann–Whitney *U*-test. Statistical significance was accepted at $P < 0.05$.

rbMSC differentiation assay

To further elucidate that the isolated rbMSCs have multi-lineage differentiation potential, rbMSCs were differentiated into tri-lineages (osteogenic, adipogenic and chondrogenic lineages) using the standard induction media. Osteogenic and adipogenic differentiation of rbMSCs was accomplished using commercially available standard differentiation induction media, namely STEMPRO® osteogenesis differentiation kit and STEMPRO® adipogenesis differentiation kit (Invitrogen-Gibco) in accordance with the manufacturer's protocol. Chondrogenic differentiation of rbMSCs was accomplished by using a modified protocol outlined by Mackay et al. (1998). The chondrogenic medium was prepared to that which was previously described (Tan et al. 2011). Cells were trypsinized, washed using PBS (pH 7.2; Invitrogen-Gibco) and then seeded in serum-free chondrogenic medium as previously described (Tan et al. 2011). The medium was changed at 3-day intervals. Differentiation potential was assessed by histological staining, i.e. Von Kossa staining for osteogenic differentiation; oil-red-O staining for adipogenic differentiation and safranin-O staining for chondrogenic differentiation; at day 28 of differentiation induction.

For gene expression analysis, cells were trypsinized at day 7 and day 28, and used for total RNA isolation. Quantitative RT-PCR (qPCR) was conducted as previously described (Tan et al. 2011).

Results

rbMSC isolation and culture

Isolation of rbMSCs was achieved by using the Ficoll-Paque gradient centrifugation. This technique stratified the MSC-like populations cells into a single layer, which allowed us to extract a high concentration of MSCs more effectively (Neagu et al. 2005). To aid the selection of rbMSC only,

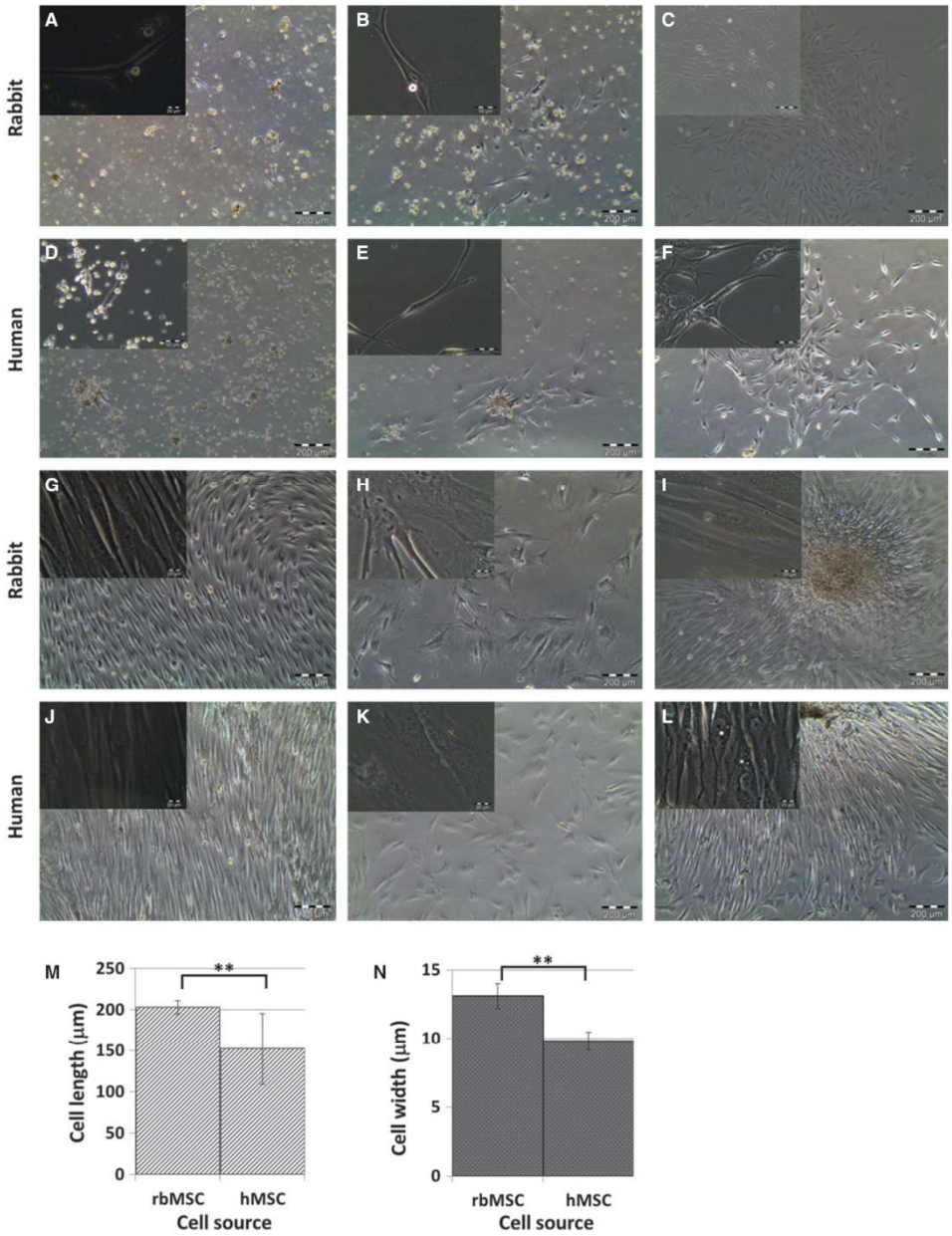

Fig. 1 Morphology of primary culture of rabbit and human bone marrow-derived mesenchymal stem cells (rbMSC and hMSC, respectively) observed under phase contrast microscope at 4 × objective (images of 40 × objectives were shown on the left upper corner of each image). Representative images from three independently performed experiments were shown (A–L). The cell length and width of eight representative cells from each individual experiment ($n = 3$) were measured and data are presented as mean ± standard error of the mean (M, N). Cells were fibroblastic spindle-shaped at days 4, 7, 10 and 24 in rbMSC cultures (A, B, C and G, respectively), and in hMSCs cultures (D, E, F and J, respectively). Some non-fibroblastic flat cells were observed in rbMSC (H) cultures and hMSC cultures (K) upon sub-culturing (P1 onwards). The majority of the cells remained fibroblastic spindle-shaped in rbMSCs (I) and hMSCs (L) upon sub-culturing from P1 to P3. The rbMSCs possessed significantly higher cell length (M) and cell width (N) compared with hMSCs ($P < 0.05$).

harvested cells were then seeded onto plastic cell culture flasks. Only those that adhered to the flask surfaces were maintained (Fig. 1A,B). After at least four medium changes over a period of 8–12 days, which resulted in the removal of the majority if not all non-adherent cells (Fig. 1C), the remaining cells appeared to have heterogeneous fibroblas-

tic-like appearance and formed distinct colonies on flask surfaces (Fig. 1C). This cell type appeared to form the majority of the cell population observed in cultures thereafter (Fig. 1G). These observations were similar to that of hMCS cultures (Fig. 1D–G). In the subsequent passages, i.e. P1 to P3, cultures with low proliferative (prolonged passage time), large polygonal and flattened cells with short or no processes (Fig. 1H,K) were discarded. The rbMSC-like cultures demonstrated increased proliferation, gradually and uniformly maintaining a homogeneous fibroblastic morphology. Cells from both rbMSCs and hMSCs were mainly of spindle-shaped appearance and elongated morphology with two processes that extended in opposite directions from a small cell body (Fig. 1B,E). These appearances were consistent and similar in both rbMSCs and hMSCs, with both cells not demonstrating any particular distinctive features that can conclusively define one from the other. Although cells appeared to be stretched with long and thin processes, these cells tended to group in close contact, parallel arrangement and grow in high-density colonies (Fig. 1I,L).

Table 3 A summary of similarities and differences between rbMSCs and hMSCs.

	Characteristics	rbMSC	hMSC
1	Isolation method	Gradient centrifugation using Ficoll-Paque™ Premium (density: 1.077 g mL^{-1})	
2	Plastic adherence	Yes	
3	Morphology	Fibroblastic spindle-shaped with two processes that extended in opposite directions from the cell body and grow in high-density colonies	
4	Ultrastructural characteristic	A large eccentric and irregular-shaped nucleus with a prominent nucleolus. Chromatin formed a thin and dense layer inside the perinuclear cisternae A rich inner cytoplasmic zone A small amount of Golgi rough endoplasmic reticulum, mitochondria and polyribosome The periphery of the plasma membrane displayed many small pseudopodia	
5	Cell size (μm)	Length: 202.66 ± 8.4 Width: 13.09 ± 0.91	Length: 152.04 ± 43.35 Width: 9.82 ± 0.66
6	Proliferation rate	Significantly lower than hMSC before 48 h Population doubling: 6.4 ± 1.3 h	Significantly higher than rbMSC after 48 h Population doubling: 7.6 ± 1.7 h
7	Phenotypic expression	Highly expressed: CD29, CD44, CD73, CD81 and CD90 Low expression: CD117, CD45 Negative expression: CD34 and HLA-DR	Highly expressed: CD29, CD44, CD73, CD81 and CD90 Negative expression: CD34, CD45, CD117 and HLA-DR
8	Differentiation conditions	StemPro® osteogenesis differentiation medium for osteogenic differentiation induction StemPro® adipogenesis differentiation medium for adipogenic differentiation induction Chondrogenic medium was prepared according to protocol outlined by Mackay et al. (1998)	
9	Differentiation potential (histological observation)	Osteogenic differentiation: Revealed by Von Kossa staining, which showed intracellular deposition of calcium oxalate crystals Adipogenic differentiation: Revealed by oil-red-O staining with presence of intracellular lipid droplets Chondrogenic differentiation: Revealed by safranin-O staining with presence of apparent glycosaminoglycans or highly sulphated proteoglycans	
10	Differentiation potential (gene expression)	Upregulation of osteogenic marker (*Runx2*) at days 7 and 28, upon osteogenic differentiation induction. Higher *Runx2* expression was observed in rbMSCs compared with hMSCs Upregulation of adipogenic marker (*Pparγ*) at day 28, upon adipogenic differentiation induction. No significant difference in *Pparγ* expression between rbMSCs and hMSCs Upregulation of chondrogenic marker (*Sox9*) at days 7 and 28, upon chondrogenic differentiation induction. Higher *Sox9* expression was observed in rbMSC compared with hMSCs	Upregulation of *RUNX2* at day 28, upon osteogenic differentiation induction Upregulation of *PPARγ* at day 28, upon adipogenic differentiation induction Upregulation of *SOX9* at days 7 and 28, upon chondrogenic differentiation induction

hMSC, human mesenchymal stem cell; rbMSC, rabbit mesenchymal stem cell.

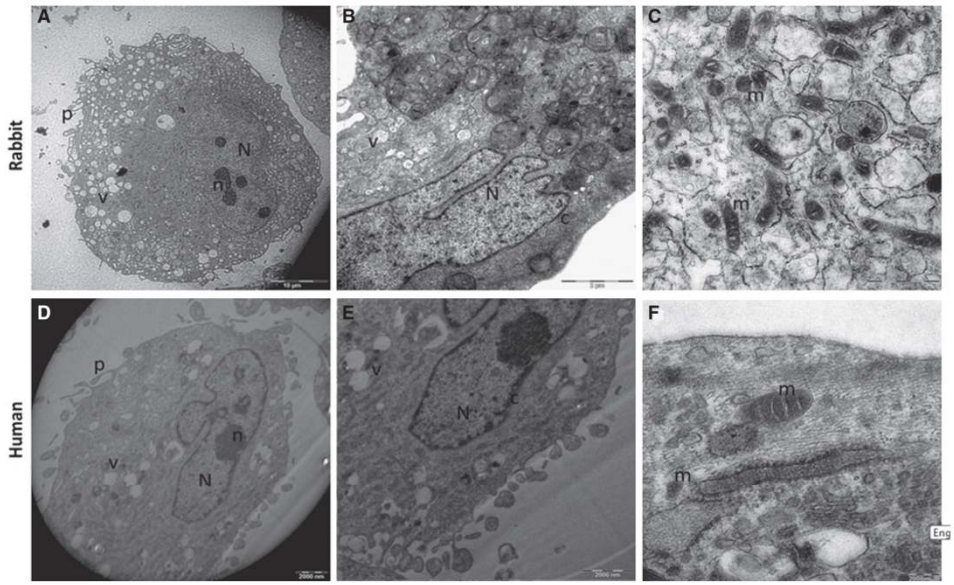

Fig. 2 TEM analysis of the ultrastructure of rbMSCs and hMSCs. Representative images of rbMSCs and hMSCs ultrastructure were shown. Both rbMSCs and hMSCs showed similar ultrastructure features. An eccentric and irregular-shaped nucleus (N), usually with multiple nucleoli (n), with various mitochondrial profiles (m), and small vacuoles (v) in rbMSCs (A, B) and hMSCs (D, E). Chromatin formed a thin and dense layer inside the perinuclear cisternae (c), and the plasma membrane formed many thin pseudopodia (p). Mitochondria showed both a rounded and elongated profile with thick cristae in both rbMSCs (C) and hMSCs (F).

However, there were cells that were widely dispersed; most of these cells formed colonies eventually. A summary of the description and similarities between these cells is presented in Table 3. These rbMSC-like cells were maintained and subcultured up to P3 for downstream analysis.

Although similar in their morphological appearance, the rbMSCs cell length ($202.66 \pm 8.40\ \mu m$) and width ($13.09 \pm 0.91\ \mu m$) were significantly longer and wider than hMSCs ($152.04 \pm 43.35\ \mu m$ in length; $9.82 \pm 0.66\ \mu m$ in width; $P < 0.01$; Fig. 1M,N).

rbMSC ultrastructural analysis

In the ultrastructural analysis, rbMSCs displayed phenotypic appearances that were indistinguishable from hMSCs (Fig. 2). They were relatively uniform in their ultrastructural characteristics. Generally, both rbMSCs and hMSCs possessed a large, eccentric, irregular-shaped nucleus and a rich inner cytoplasmic zone (Fig. 2A,B,D,E). The nucleus showed multiple nucleoli, and the chromatin formed a thin and dense layer inside the perinuclear cisternae. The periphery of the plasma membrane displayed many small pseudopodia in both rbMSCs and hMSCs (Fig. 2A,D). In addition, within the rich cytoplasm region (Fig. 2A,B), a small amount of Golgi rough endoplasmic reticulum as well as a modest number of mitochondrial with different profiles (rounded and elongated profile with thick cristae) were present. There was neither fat globules in the cells nor ultrastuctural disruption, denoting that no cells were at the senescence stage of development.

rbMSC surface markers expression

Immunofluorescence staining to detect CD44 surface markers was positive for rbMSCs (Fig. 3A). RT-PCR analysis demonstrated a positive expression for CD29 and CD166 in rbMSCs (Fig. 3B), but was negative for other surface markers (CD45 and CD34; Fig. 3B). GAPDH was used as the housekeeping gene, whilst positive and negative controls were also performed for the surface protein markers: CD29, CD166, CD45 and CD34 (data not shown).

Flow cytometry analysis

Based on the mAbs available for rbMSC, this study elucidates that rbMSCs express multiple markers of MSCs. The cultured rbMSCs revealed positive for CD29, CD44, CD73, CD81 and CD90, but were negative (or dim positive) for CD34, CD45, CD117 and HLA-DR (Table 4A). In the multi-colour, at least 70% of rbMSCs expressed double-positive expression, double-negative or co-expressed positive and negative markers as compared with 90% of that in hMSCs. These analyses are summarized in Table 4B.

Important note: there were no other markers that were tested on these cells that yielded negative or positive results

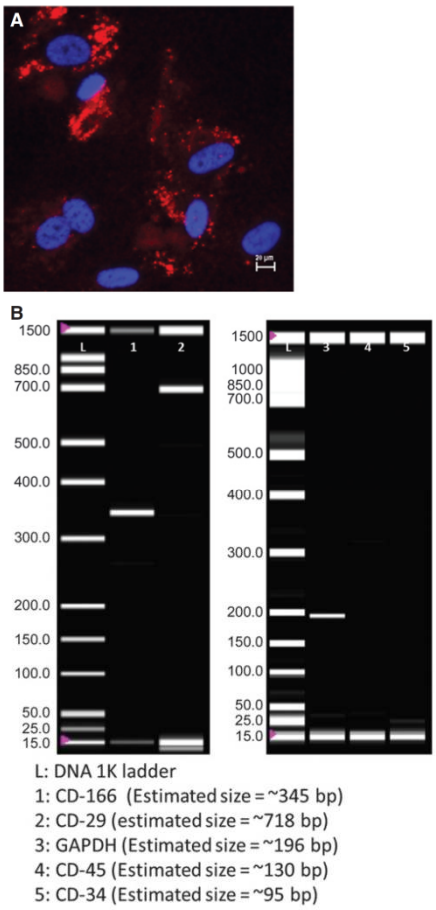

Fig. 3 Immunofluorescence staining image for positive expression of CD44 [in red, anti-mouse IgG allophycocyanin-conjugated goat F $(ab')_2$] counterstained with nucleus stain (in blue) in both rbMSC and hMSC. (B) RT-PCR analysis for CD166 (lane 1), CD29 (lane 2), CD45 (lane 4), CD34 (lane 5) and GAPDH (in lane 3). Lane L indicates the DNA ladder. The presence of amplicon in lanes 1–3 indicated positive expression of the corresponding genes, and the absence of amplicon in lanes 4 and 5 denoted that these genes were not expressed.

in both the flow cytometry and immunohistochemistry analyses.

AlamarBlue® cell proliferation assay

The results of alamarBlue® assay showed a growth curve of rbMSC and hMSC, both appearing as a typical 'S-shaped curve' seen in many cell cultures (Fig. 4). No significant differences were observed in the alamarBlue® reduction in both rbMSCs and hMSCs during the 'lag phase' of cell proliferation. However, as the cells enter into their exponential 'log phase', rbMSCs showed significantly lower ($P < 0.05$) cell proliferation than hMSCs, at 48 h during the cell culture. The rbMSCs reached a plateau phase at 72 h, as compared with 48 h in hMSCs. The population doubling times of rbMSCs and hMSCs were 6.4 ± 1.3 and 7.6 ± 1.7 h, respectively. However, there were no significant differences between the two ($P > 0.05$).

rbMSC tri-lineage differentiation assay

Using the osteogenic differentiation assay, the presence of calcium oxalates was clearly observed from the Von Kossa staining on the differentiated rbMSCs, which was not present in the undifferentiated cells (Fig. 5A). The use of safranin-O aided the detection of proteoglycan deposition in chondrogenic-induced rbMSCs; however, this was negative in the control group (Fig. 5B). Adipogenesis of rbMSCs was detected by staining intracellular lipid droplets using oil-red-O (Fig. 5C) in the adipogenic-induced rbMSC cultures. This was also absent in the undifferentiated rbMSCs. These observations suggest that rbMSCs have the potential to undergo the tri-lineage, i.e. osteogenic, chondrogenic and adipogenic, differentiation required to fulfill the characteristics of MSCs. As compared with cultured hMSCs, these cells appear to have similar characteristics.

Gene expression quantification analysis of rbMSC tri-lineage differentiation potential

rbMSCs expressed significantly higher *Runx2* (osteogenic marker) and *Sox9* (chondrogenic marker) expression on both day 7 and day 28 as compared with that of hMSC ($P < 0.05$). In adipogenic medium, both rbMSCs and hMSCs showed similarly elevated *Pparγ* (adipogenic marker) gene expression levels on day 28 ($P > 0.05$; Fig. 6). A summary of gene expression levels in rbMSC tri-lineage differentiation potential as compared with hMSCs is described in Table 3.

Discussion

The present study demonstrates that similar techniques used to isolate hMSCs may be used to isolate rbMSCs. We identified that rbMSCs possess characteristics similar to those of hMSCs based on the following findings: (i) the rbMSCs were adherent to plastic and demonstrated fibroblastic spindle shape with two processes that extended in opposite directions from the cell body as observed under phase contract microscope (Fig. 1B); (ii) the ultrastructural characteristics and morphology observed using TEM were similar to that of hMSCs; (iii) the specific antigens expression in rbMSCs identified using immunohistology staining, RT-PCR and flow cytometry were similar to that defined in hMSC, i.e. $CD29^+$, $CD44^+$, $CD73^+$, $CD81^+$, $CD90^+$, $CD166^+$, $CD34^-$ (dim), $CD45^-$ (dim), $CD117^-$ (dim) and $HLA\text{-}DR^-$ expression; and (iv) histology staining (Von Kossa, safranin-O and staining oil-red-O) indicates that rbMSCs are able to undergo tri-lineage differentiation when cultured using the appropriate differentiation medium for osteogenic,

Table 4 Summary of flow cytometry analysis for (A) single marker and (B) co-expression of two markers.

A

Cell type	$CD29^+$ (%)	$CD44^+$ (%)	$CD73^+$ (%)*	$CD81^+$ (%)	$CD90^+$ (%)*	$CD34^+$ (%)*	$CD45^+$ (%)*	$CD117^+$ (%)	$HLA\text{-}DR^+$ (%)*
rbMSC	85.0	81.6	96.4	96.9	96.9	7.1	18.0	17.4	4.3
hMSC	100.0	99.6	98.6	99.9	100.0	0.2	0.1	1.4	0.2

B

Antigens	rbMSC (%)	hMSC (%)
$CD29^+$ and $CD34^-$*	78.4	99.8
$CD44^+$ and $CD73^+$*	70.9	93.7
$CD44^+$ and $CD34^-$*	82.1	98.4
$CD90^+$* and $CD73^+$*	70.1	96.4
$CD90^+$* and $CD81^+$	89.8	100.0
$CD90^+$* and $CD34^-$*	89.8	97.3
$CD90^+$* and $CD45^-$*	81.6	92.0
$CD90^+$* and $CD117^-$	79.6	99.0
$CD73^+$* and $CD81^+$	75.0	99.5
$CD73^+$* and $CD34^-$*	83.2	97.7
$CD73^+$* and $CD117^-$	71.2	98.6
$CD81^+$ and $CD34^-$*	91.8	98.0
$CD81^+$ and $CD117^-$	76.9	98.6
$CD81^+$ and $HLA\text{-}DR^-$*	76.3	99.4
$CD34^-$* and $CD45^-$*	76.2	91.0
$CD34^-$* and $CD117^-$	77.3	97.0
$CD45^-$* and $HLA\text{-}DR^-$*	72.0	97.7

MSC-positive antigens (+): CD29 (Integrin β1), CD44 (H-CAM, PGP-1), CD73 (Ecto-5′-nucleotidase, NT5E), CD81 (TAPA-I) and CD90 (Thy-1). MSC-negative antigens (−): CD34. CD45 (leukocyte common antigen, Ly-5), CD117 (SCF R, c-Kit) and HLA-DR (MHC Class-II).
*CD markers that are prerequisite by ISCT criteria.
hMSC, human mesenchymal stem cell; rbMSC, rabbit mesenchymal stem cell.

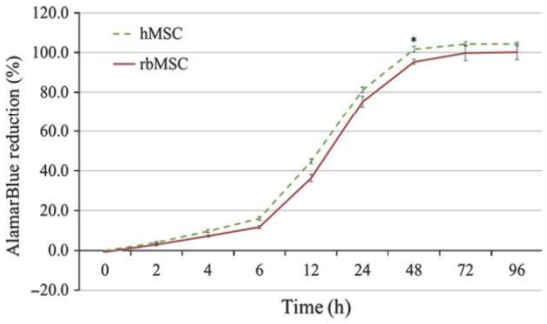

Fig. 4 AlamarBlue® cell proliferation assay of rabbit mesenchymal stem cells (rbMSCs) and human (h)MSCs cultures. There were no significant differences in cell proliferation rates at the lag phase and plateau phase, but the hMSCs showed significantly higher alamarBlue® reduction at the log phase, after 48 h ($P < 0.05$).

adipogenic and chondrogenic differentiation. Nevertheless, there are differences that are worth mentioning. Our results demonstrate that between rbMSCs in hMSC: (i) the cell size of rbMSCs was significantly larger than hMSCs ($P < 0.05$); (ii) the cell proliferation of rbMSCs was lower than that of hMSCs ($P < 0.05$); and (iii) the *Runx2* (osteogenic marker) and *Sox9* (chondrogenic marker) gene expressions levels were significantly higher in rbMSCs at day 7 and 28 as compared with that of hMSC ($P < 0.05$). All the similarities and differences between rbMSCs and hMSCs were also summarized in Table 3.

Based on the current technique used to isolate rbMSCs, it appears that at P3, both rbMSCs and hMSCs produced sufficient cells for analyses, specifically for flow cytometry and qPCR, to be conducted successfully. However, the present study did not measure cell quantity in order to determine the yield potential of the technique used, as this was outside the scope of the study. Consistent with previous reports, fibroblastic rbMSCs cultured in this study tend to form cell colonies, arranged in parallel assembly, and grow in high-density colonies, similar to those observed in human (Castro-Malaspina et al. 1980), mouse (Friedenstein et al. 1982; Mori et al. 1987), rat (Fu et al. 2012) and rabbit (Owen et al. 1987) MSCs. The high-density colony characteristics were also similar to those observed in other matured cell types (Selvaratnam et al. 2005). In this study, the

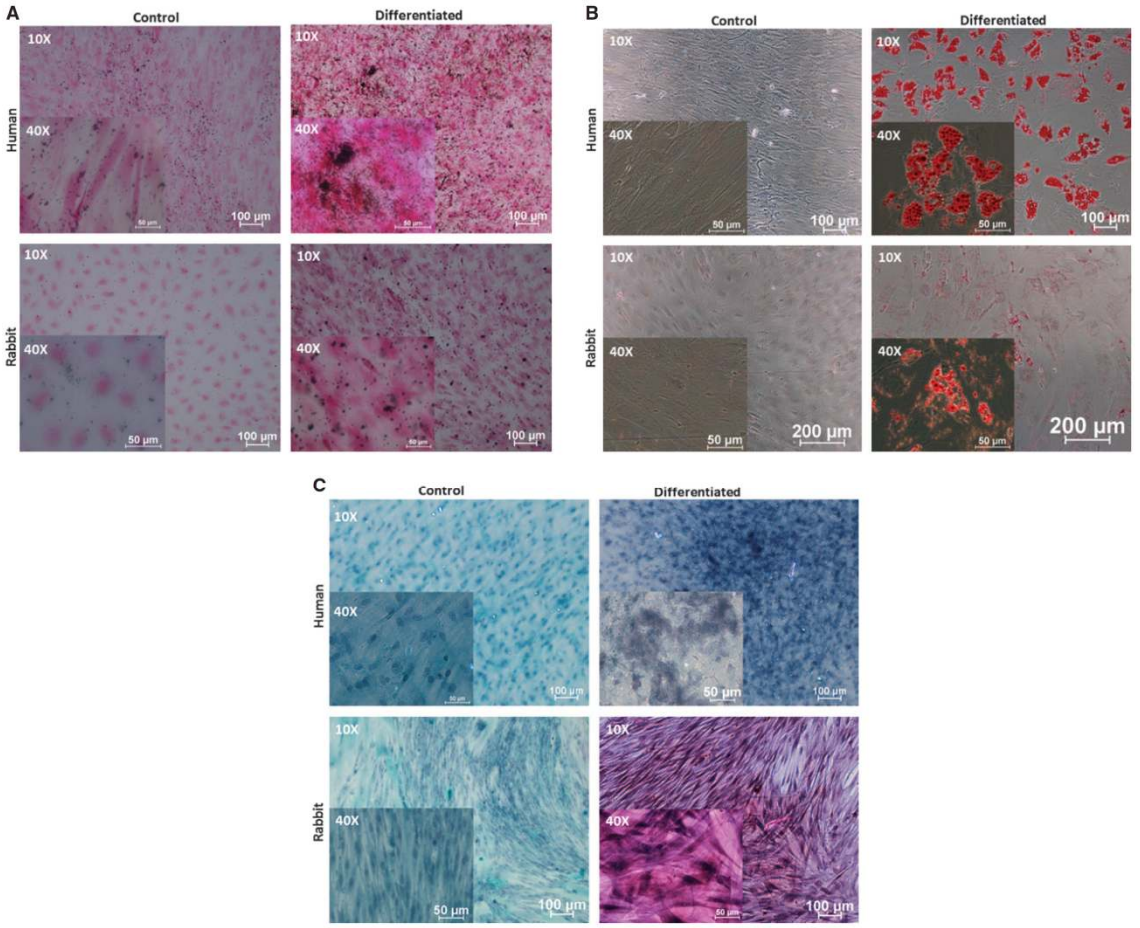

Fig. 5 Tri-lineage differentiations of primary rbMSCs. (A) Osteogenic differentiation of rbMSC and hMSC (as positive control) for 28 days. rbMSC and hMSC were cultured in standard MSC growth medium (control cultures) or osteogenic induction medium. Lower images: intracellular deposition of calcium oxalate crystals (black colour signifies) in osteogenic-rbMSCs as revealed by Von Kossa staining (right). No accumulation of calcium oxalate crystals was observed in uninduced control rbMSC culture stained with Von Kossa staining for comparison (left). Upper images: positive control of adipogenic differentiation in hMSCs (right) and non-induced control hMSC (left) stained with oil-red-O staining. Magnifications were denoted at the upper left corner of the images. (B) Adipogenic differentiation assay of rbMSC and hMSC (as positive control) for 28 days. rbMSC and hMSC were cultured in standard MSC growth medium (control cultures) or adipogenic induction medium. Lower images: presence of intracellular accumulated lipid droplets (red colour in the image) in adipogenic-rbMSCs as revealed by oil-red-O staining (right). No accumulation of lipid droplets was observed in non-induced control rbMSC culture stained with oil-red-O staining for comparison (left). Upper images: positive control of adipogenic differentiation in hMSCs (right) and uninduced control hMSC (left) stained with oil-red-O staining. Magnifications were denoted at the upper left corner of the images. (C) Chondrogenic differentiation assay of rbMSC and hMSC (as positive control) for 28 days. rbMSC and hMSC were cultured in standard MSC growth medium (control cultures) or chondrogenic induction medium. Lower images: presence of glycosaminoglycans or highly sulphated proteoglycans (pinkish colour in the image) in chondrogenic-rbMSCs as revealed by safranin-O staining (right). No accumulation of glycosaminoglycans was observed in non-induced rbMSC culture stained with safranin-O for comparison (left). Upper images: positive control of chondrogenic differentiation in hMSCs (right) and non-induced control hMSC (left) stained with safranin-O. Magnifications were denoted at the upper left corner of the images.

rbMSCs cultures that demonstrated large flat cells upon sub-culturing were discarded because the typical larger flat cellular morphology has been reported as: (i) senescent MSC (Cheng et al. 2003; Schellenberg et al. 2011; Fu et al. 2012); and (ii) associated with low proliferative rate and were less potential or characterized as 'mature' (Colter et al. 2000, 2001; Sekiya et al. 2002; Neuhuber et al. 2008). Besides, morphological heterogeneity has also been associated with different stages of cell differentiation rather than the existence of distinct cell types or subtypes (Sekiya et al. 2002; Smith et al. 2004; Docheva et al. 2008). This further alludes to the importance of culturing the subset of rbMSCs that is more homogeneous, proliferative and exhibits fibroblastic spindle-shaped for the downstream applications.

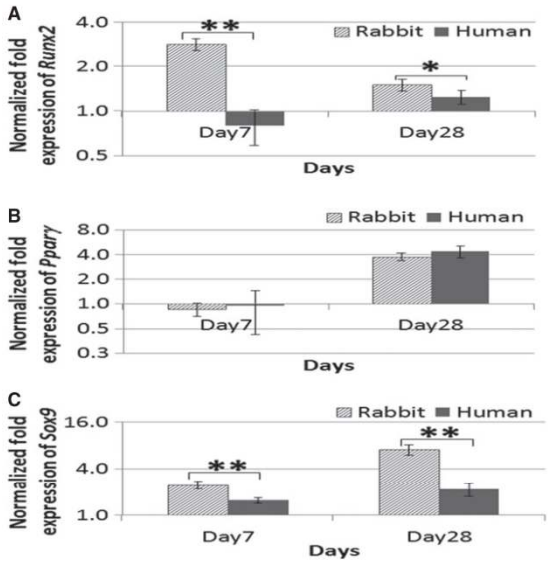

Fig. 6 Gene expression analysis of the cultured rbMSCs in the temporal experiment of tri-lineage differentiation assay, osteogenic (a), adipogenic (b) and chondrogenic (c) differentiation, at day 7 and day 28. The data reflected that the relative quantification of target mRNA normalized to control samples (untreated MSCs cultured in MSC growth medium). Data were presented as $\log_2$-fold change (with error bars signifying range of standard deviation). All the differentiation markers (*Runx2*, *Pparγ* and *Sox9*) were upregulated on day 28. However, spontaneous differentiation into osteogenic and chondrogenic lineages was observed in the rbMSCs with significant early upregulation of the respective differentiation markers (*Runx2* and *Sox9*) at day 7.

To determine the characteristics of rbMSC, electron microscopy has been an invaluable tool that has allowed us to make effective identification of rbMSCs based on the surface and internal morphological appearance that were similar to hMSCs. Our observations indicate that rbMSC and hMSC ultrastructures appeared similar to that previously reported in hMSC (Castro-Malaspina et al. 1980; Raimondo et al. 2006; Li et al. 2008). Raimondo et al. (2006) and Castro-Malaspina et al. (1980) described the hMSC as having a large, eccentric and irregular-shaped nucleus. In addition to the morphology of the nucleus, hMSC has been reported as being uni-nucleated (Raimondo et al. 2006), which was similar to that found in rbMSC. Similarly, mitochondria of various profiles (Raimondo et al. 2006; Li et al. 2008) and Golgi apparatus with typical stacks of flattened cisternae (Raimondo et al. 2006) were also observed in rbMSC (data not shown). The presence of pseudopodia surrounding the entire plasma membrane of rbMSCs has also been reported in rat MSC (Castro-Malaspina et al. 1980) and hMSC (Raimondo et al. 2006).

According to the ISCT guidelines (Dominici et al. 2006), one of the criteria that defines hMSC is phenotypic co-expression of CD105, CD90 and CD73 (> 95%), and lack of CD34, CD45, CD14, CD79 and HLA-DR (< 2%). Within the assessed hMSC donor cells, flow cytometry results showed that the cell culture populations consistently fulfilled all hMSC criteria (Table 3), including CD105, CD14 and CD19 (only tested in hMSCs; Supplementary #3). In comparison, the rbMSCs fulfilled the positive marker criteria set for hMSC (CD73 and CD90), but partly fulfilled the negative marker criteria set for hMSC (CD34, CD45 and HLA-DR) where dim expressions of the surface markers were observed for CD34 and CD45. A previous study demonstrated that bone marrow-derived MSCs in culture have a heterogeneous CD34 and CD45 phenotype that changes under *in vitro* conditions (Kaiser et al. 2007). This may explain the occurrence of $CD34^+$ and $CD45^+$ observed in rbMSCs. Whereas for the other CD markers evaluated, i.e. CD117 was also detected as dimly positive in rbMSCs (17.4%) whilst in hMSCs, this was negative (1.4%). On the contrary, CD81 was highly positive in rbMSCs (96.9%) as well as hMSCs (99.9%). CD29 and CD44 were also observed as being highly positive in rbMSCs (85% and 81.6%, respectively) and hMSCs (100 and 99.6%, respectively).

The expression of CD117 by MSCs is controversial. It has been previously reported in murine MSCs, and the expression levels have been demonstrated to decrease during extended serial passage (Meirelles LDA and NARDI, 2003). In isolated adipose tissue-derived stem cells, CD117 and HLA-DR expression have also been reported (Varma et al. 2007; Rebelatto et al. 2008). However, contrasting results have been reported in mouse MSC where negative expression of CD117 was observed (Nadri et al. 2007). This may be due to the loss of CD117 upon *in vitro* expansion (Meirelles LDA and NARDI, 2003). It is therefore logical to deduce that CD117 should be used as a potential marker of rbMSCs to determine if this expression would be lost in long-term cell cultures.

The rbMSCs are $CD44^+$ cells (Fig. 1B), similar to that previously reported in murine (Nadri et al. 2007) and canine (Seo et al. 2009) MSCs; and are $CD29^+$, which is consistent with that reported in rodent (Karaoz et al. 2009) and canine MSCs (Seo et al. 2009). Our findings also demonstrate that $CD166^+$ was present in rbMSCs, which is similar to that reported for human bone marrow- and cord blood-derived MSCs (Goodwin et al. 2001), and ovine bone marrow-derived MSCs (McCarty et al. 2009). Nevertheless, $CD166^+$ has been described as an inconsistent marker, as this protein gradually decreases over many passages in murine epiphysis-derived MSCs (Cheng et al. 2012). Whether this may be the case for rbMSCs remains to be elucidated, hence the loss of detection of this surface marker may not be enough to exclude the presence of rbMSCs.

The present study demonstrated that the cells obtained using the described method conformed to the criteria set by ISCT guidelines (Dominici et al. 2006), with the exception of several protein markers that are not available for testing. In this study, both qualitative and quantitative assays were used to determine the *in vitro* multi-lineage developmental potential of rbMSCs and hMSCs after *in vitro* exposure to

specific culture conditions. The hMSCs demonstrated a greater propensity to differentiate into the osteogenic and adipogenic lineages than rbMSCs based on the qualitative (histological staining) results. Induced hMSCs presented more prominent deposition of calcium oxalate crystals and more mature adipocytes (more lipid vacuoles present) than the induced rbMSCs under the same culture conditions. Only tiny amounts of calcium oxalate crystals or tiny lipid vacuoles were observed in rbMSCs after 28 days of induction. These observations suggest that differentiation occurs in rbMSC cultures but takes longer than hMSCs. In contrast, gene expression analysis demonstrates that rbMSCs express higher levels of osteogenic and chondrogenic marker gene expression by day 28. However, the adipogenic marker gene expression was similar to hMSC. The high expression of *Runx2* gene in rbMSC at day 7, but appears lower by day 28, may explain the observations of tiny calcium oxalate crystals on day 28 in rbMSCs. We can therefore suggest from the observation of this experiment, that the response of rbMSCs in osteogenic induction is more acute (by day 7) than hMSCs, but subsequently gradually decreases as it is kept in cultures longer. It may be the case that the regulation of adipogenic differentiation of rbMSCs is controlled at the protein translation level, and thus for the reason for not being able to observe large lipid vacuole despite having increased *Pparγ* expression levels. Nevertheless, the higher *Sox9* expression levels in rbMSCs than hMSCs were consistent and appear to correspond to the increased intensity of the glycosaminoglycans observed from the safranin-O staining.

What is of interest in this study is that similar protocols and preparations used for hMSCs may be used for rbMSC differentiation without the need for any modification. This alludes to the fact that rbMSCs possess similar behaviour and capabilities as hMSCs, which is a strong point that supports the use of this cell in many studies. This is a quality that is especially important for translational research. However, there is a need to be cautious when interpreting the data of cellular differentiation as our study has demonstrated that rbMSCs appear to have the ability to express a higher level of osteogenic and chondrogenic gene expressions than that of hMSCs. Besides, the proliferation rate of rbMSCs was significantly lower than that of hMSCs. Because telomere length and telomerase activity are in relation to cell proliferation and aging, we postulated that hMSCs telomere length and telomerase activity are both greater than rbMSCs. Nevertheless, this speculation needs to be substantiated in further studies, which at the present time is not within the scope of current study.

With the results of the present study supporting our earlier hypothesis that rbMSCs can be isolated using established methods meant for hMSCs and that they possess similar characteristics to these cells, we propose that the set criteria that define hMSCs would be applicable to define rbMSCs, whilst using the present report as a reference. The criteria should include the plastic adherent behaviour, the described morphological appearances, selected CD markers expressed, and the ability to undergo tri-lineage differentiation. These criteria are summarized in Table 5.

Table 5 Summary of characteristics of rbMSC.

Minimum criteria to define rbMSC		
Adherent to plastic in standard culture conditions		
Fibroblastic spindle-shaped with two processes that extended in opposite directions from the cell body and grow in high-density colonies when cultured under standard culture conditions		
Phenotype (as revealed by flow cytometry analysis)	Positive CD29 CD44 CD73 CD81 CD90 CD117	Negative CD34 CD45 HLA-DR
Capable to undergo *in vitro* differentiation into osteogenic, chondrogenic and adipogenic lineages (as revealed by histological staining) when cultured in the appropriate differentiation medium		

rbMSC, rabbit mesenchymal stem cell.

Several unavoidable limitations were also identified. Firstly, isolation of rbMSCs was merely selected based on their plastic adherence characteristic. It would have been more accurate if antibody-specific approaches were utilized (Friedenstein et al. 1976; Taylor et al. 2007). Isolation and purification of rbMSCs using this method, however, was not available due to limited availability of mAbs for the rabbit model, particularly for those specific to MSCs surface molecules, i.e. CD105 (endoglin). In the future, it is hoped that these antibodies may become available (i.e. CD166 and CD105), thus producing more convincing results using more efficient isolation methods. Future study should also include CD166 (or other markers) in flow cytometry analysis once the mAb becomes available for rbMSCs. Secondly, not all the CD markers set to define hMSC were evaluated in rbMSCs, i.e. CD105, CD14 and CD19 (Dominici et al. 2006). This however, was hampered due to the scarcity in rabbit molecular biology information and limitations in the mAbs available for stem cell surface markers immunostaining. To overcome this problem, the use of gene expression analysis obtained by determining mRNA levels using gene-specific primers was an acceptable option for the present study. Custom-designed gene-specific primers for CD29, CD166, CD45 and CD34 based on their corresponding mRNA sequence information were designed from available information of *Oryctolagus cuniculus* or *Felis catus* or *Homo sapiens*. This was obtained from the NCBI GenBank database; and was helpful in defining the rbMSCs.

Conclusion

rbMSCs can be isolated using methods described previously for hMSCs. rbMSCs appear to have similar characteristics to that of hMSCs, and conform to most of the standards set by ISCT. Based on the results presented here and with reference to the ISCT guidelines (Dominici et al. 2006), we summarized that the minimum characteristics of rbMSCs in Table 5 should be used as a reference tool for future researchers, although we caution that revisions to the definitions or criteria should be made regularly as new data or new technologies emerge. Nevertheless, these criteria should suffice as the baseline that best identifies rbMSCs in view of the current state of knowledge. It is important to note that several differences between rbMSCs and hMSCs need to be acknowledged, for example proliferation, osteogenic/chondrogenic expressions, and that caution should be used when interpreting or translating data from rabbits to humans.

Acknowledgements

This study was supported by HIR-MOHE research grant initiative, eScience Grant (12-02-03-2017), UMRG (RG093/09HTM) and University of Malaya postgraduate student grant (PS167/2008C, PS360/2009B and PS219/2010A). We also thank the University of Malaya for a PhD thesis scholarship for the first author.

Conflict of interest

The authors indicate no potential conflicts of interest.

Authors' contribution

T.S.L. designed and performed experiments, acquired and analysed data as well as wrote the manuscript; L.S. supervised on data analysis/interpretation; T.S.A. and T.K.Z. supervised the experiment design, provided reagents and revised the manuscript critically; all authors were involved in final approval of the version to be submitted for reviewing/publication.

References

Amini AR, Laurencin CT, Nukavarapu SP (2012) Differential analysis of peripheral blood- and bone marrow-derived endothelial progenitor cells for enhanced vascularization in bone tissue engineering. *J Orthop Res* **30**, 1507–1515.

Bunnell BA, Flaat M, Gagliardi C, Patel B, Ripoll C (2008) Adipose-derived stem cells: isolation, expansion and differentiation. *Methods* **45**, 115–120.

Castro-Malaspina H, Gay RE, Resnick G, et al. (1980) Characterization of human bone marrow fibroblast colony-forming cells (CFU-F) and their progeny. *Blood* **56**, 289–301.

Chamberlain G, Fox J, Ashton B, Middleton J (2007) Concise review: mesenchymal stem cells: their phenotype, differentiation capacity, immunological features, and potential for homing. *Stem Cells* **25**, 2739–2749.

Cheng CC, Lian WS, Hsiao FS, et al. (2012) Isolation and characterization of novel murine epiphysis derived mesenchymal stem cells. *PLoS One* **7**, e36085.

Cheng L, Hammond H, Ye Z, Zhan X, Dravid G (2003) Human adult marrow cells support prolonged expansion of human embryonic stem cells in culture. *Stem Cells* **21**, 131–142.

Chong PP, Selvaratnam L, Abbas AA, Kamarul T (2011)Human peripheral blood derived mesenchymal stem cells demonstrate similar characteristics and chondrogenic differentiation potential to bone marrow derived mesenchymal stem cells. *J Orthop Res* **30**, 634–642.

Colter DC, Class R, Digirolamo CM, Prockop DJ (2000) Rapid expansion of recycling stem cells in cultures of plastic-adherent cells from human bone marrow. *Proc Natl Acad Sci USA* **97**, 3213–3218.

Colter DC, Sekiya I, Prockop DJ (2001) Identification of a subpopulation of rapidly self-renewing and multipotential adult stem cells in colonies of human marrow stromal cells. *Proc Natl Acad Sci USA* **98**, 7841–7845.

Dashtdar H, Rothan HA, Tay T, et al. (2011) A preliminary study comparing the use of allogenic chondrogenic predifferentiated and undifferentiated mesenchymal stem cells for the repair of full thickness articular cartilage defects in rabbits. *J Orthop Res* **29**, 1336–1342.

Docheva D, Padula D, Popov C, Mutschler W, Clausen-Schaumann H, Schieker M (2008) Researching into the cellular shape, volume and elasticity of mesenchymal stem cells, osteoblasts and osteosarcoma cells by atomic force microscopy. *J Cell Mol Med* **12**, 537–552.

Dominici M, Le Blanc K, Mueller I, et al. (2006) Minimal criteria for defining multipotent mesenchymal stromal cells. The International Society for Cellular Therapy position statement. *Cytotherapy* **8**, 315–317.

Fox RR (1984) The rabbit as a research subject. *The Physiologist* **27**, 393–402.

Friedenstein AJ, Gorskaja JF, Kulagina NN (1976) Fibroblast precursors in normal and irradiated mouse hematopoietic organs. *Exp Hematol* **4**, 267–274.

Friedenstein AJ, Latzinik NW, Grosheva AG, Gorskaya UF (1982) Marrow microenvironment transfer by heterotopic transplantation of freshly isolated and cultured cells in porous sponges. *Exp Hematol* **10**, 217–227.

Fu WL, Zhang JY, Fu X, et al. (2012) Comparative study of the biological characteristics of mesenchymal stem cells from bone marrow and peripheral blood of rats. *Tissue Eng Part A* **18**, 1793–1803.

Goodwin HS, Bicknese AR, Chien SN, Bogucki BD, Quinn CO, Wall DA (2001) Multilineage differentiation activity by cells isolated from umbilical cord blood: expression of bone, fat, and neural markers. *Biol Blood Marrow Transplant* **7**, 581–588.

Gupta R, Lee TQ (2007) Contributions of the different rabbit models to our understanding of rotator cuff pathology. *J Shoulder Elbow Surg* **16**, S149–S157.

Haasters F, Prall WC, Anz D, et al. (2009) Morphological and immunocytochemical characteristics indicate the yield of early progenitors and represent a quality control for human stem cell culturing. *J Anat* **214**, 759–767.

Kaiser S, Hackanson B, Follo M, et al. (2007) BM cells giving rise to MSC in culture have a heterogeneous CD34 and CD45 phenotype. *Cytotherapy* **9**, 439–450.

Karaoz E, Aksoy A, Ayhan S, Sariboyaci AE, Kaymaz F, Kasap M (2009) Characterization of mesenchymal stem cells from rat bone marrow: ultrastructural properties, differentiation potential and immunophenotypic markers. *Histochem Cell Biol* **132**, 533–546.

Koerner J, Nesic D, Romero JD, Brehm W, Mainil-Varlet P, Grogan SP (2006) Equine peripheral blood-derived progenitors in comparison to bone marrow-derived mesenchymal stem cells. *Stem Cells* **24**, 1613–1619.

Kuo CK, Tuan RS (2008) Mechanoactive tenogenic differentiation of human mesenchymal stem cells. *Tissue Eng Part A* **14**, 1615–1627.

Laitinen A, Laine J (2007)Isolation of mesenchymal stem cells from human cord blood. *Curr Protoc Stem Cell Biol* **1**, 2A.3.1–2A.3.7.

Li Y, Zhang C, Xiong F, et al. (2008) Comparative study of mesenchymal stem cells from C57BL/10 and mdx mice. *BMC Cell Biol* **9**, 24.

Mackay AM, Beck SC, Murphy JM, Barry FP, Chichester CO, Pittenger MF (1998) Chondrogenic differentiation of cultured human mesenchymal stem cells from marrow. *Tissue Eng* **4**, 415–428.

Marcus AJ, Coyne TM, Rauch J, Woodbury D, Black IB (2008) Isolation, characterization, and differentiation of stem cells derived from the rat amniotic membrane. *Differentiation* **76**, 130–144.

McCarty RC, Gronthos S, Zannettino AC, Foster BK, Xian CJ (2009) Characterisation and developmental potential of ovine bone marrow derived mesenchymal stem cells. *J Cell Physiol* **219**, 324–333.

Meirelles LDA S, Nardi NB(2003)Murine marrow-derived mesenchymal stem cell: isolation, in vitro expansion, and characterization. *Br J Haematol*, **123**, 702–711.

Mori M, Sadahira Y, Awai M (1987) Characteristics of bone marrow fibroblastic colonies (CFU-F) formed in collagen gel. *Exp Hematol* **15**, 1115–1120.

Nadri S, Soleimani M, Hosseni RH, Massumi M, Atashi A, Izadpanah R (2007) An efficient method for isolation of murine bone marrow mesenchymal stem cells. *Int J Dev Biol* **51**, 723–729.

Neagu M, Suciu E, Ordodi V (2005) Human mesenchymal stem cells as basic tools for tissue engineering: isolation and culture. *Romanian J Biophys* **15**, 29–34.

Neuhuber B, Swanger SA, Howard L, Mackay A, Fischer I (2008) Effects of plating density and culture time on bone marrow stromal cell characteristics. *Exp Hematol* **36**, 1176–1185.

Neupane M, Chang CC, Kiupel M, Yuzbasiyan-Gurkan V (2008) Isolation and characterization of canine adipose-derived mesenchymal stem cells. *Tissue Eng Part A* **14**, 1007–1015.

Owen ME, Cave J, Joyner CJ (1987) Clonal analysis in vitro of osteogenic differentiation of marrow CFU-F. *J Cell Sci* **87**(Pt 5), 731–738.

Raimondo S, Penna C, Pagliaro P, Geuna S (2006) Morphological characterization of GFP stably transfected adult mesenchymal bone marrow stem cells. *J Anat* **208**, 3–12.

Rebelatto CK, Aguiar AM, Moretao MP, et al. (2008) Dissimilar differentiation of mesenchymal stem cells from bone marrow, umbilical cord blood, and adipose tissue. *Exp Biol Med (Maywood)* **233**, 901–913.

Sahoo S, Ang LT, Cho-Hong Goh J, Toh SL (2010)Bioactive nanofibers for fibroblastic differentiation of mesenchymal precursor cells for ligament/tendon tissue engineering applications. *Differentiation*, **79**, 102–110.

Schellenberg A, Lin Q, Schuler H, et al. (2011) Replicative senescence of mesenchymal stem cells causes DNA-methylation changes which correlate with repressive histone marks. *Aging (Albany NY)* **3**, 873–888.

Sekiya I, Larson BL, Smith JR, Pochampally R, Cui JG, Prockop DJ (2002) Expansion of human adult stem cells from bone marrow stroma: conditions that maximize the yields of early progenitors and evaluate their quality. *Stem Cells* **20**, 530–541.

Selvaratnam L, Abd Rahim S, Kamarul T, et al. (2005)Colonies in engineered articular cartilage express superior differentiation. *Med J Malaysia* **60**, Suppl C, 49–52.

Seo MS, Jeong YH, Park JR, et al. (2009) Isolation and characterization of canine umbilical cord blood-derived mesenchymal stem cells. *J Vet Sci* **10**, 181–187.

Smith JR, Pochampally R, Perry A, Hsu SC, Prockop DJ (2004) Isolation of a highly clonogenic and multipotential subfraction of adult stem cells from bone marrow stroma. *Stem Cells* **22**, 823–831.

Tan S. L., Ahmad R. E., Ahmad T. S., et al. (2012) Effect of growth differentiation factor 5 on the proliferation and tenogenic differentiation potential of human mesenchymal stem cells in vitro. *Cells Tissues Organs* **196**, 325–338.

Tan SL, Sulaiman S, Pingguan-Murphy B, Selvaratnam L, Tai CC, Kamarul T (2011) Human amnion as a novel cell delivery vehicle for chondrogenic mesenchymal stem cells. *Cell Tissue Bank* **12**, 59–70.

Tay LX, Ahmad RE, Dashtdar H, et al. (2011) Treatment outcomes of alginate-embedded allogenic mesenchymal stem cells vs. autologous chondrocytes for the repair of focal articular cartilage defects in a rabbit model. *Am J Sports Med* **40**, 83–90.

Taylor SE, Smith RK, Clegg PD (2007) Mesenchymal stem cell therapy in equine musculoskeletal disease: scientific fact or clinical fiction? *Equine Vet J* **39**, 172–180.

Tropel P, Noel D, Platet N, Legrand P, Benabid AL, Berger F (2004) Isolation and characterisation of mesenchymal stem cells from adult mouse bone marrow. *Exp Cell Res* **295**, 395–406.

Varma MJ, Breuls RG, Schouten TE, et al. (2007) Phenotypical and functional characterization of freshly isolated adipose tissue-derived stem cells. *Stem Cells Dev* **16**, 91–104.

Warden SJ (2007) Animal models for the study of tendinopathy. *Br J Sports Med* **41**, 232–240.

Zeng L, Rahrmann E, Hu Q, et al. (2006) Multipotent adult progenitor cells from swine bone marrow. *Stem Cells* **24**, 2355–2366.

Supporting Information

Additional Supporting Information may be found in the online version of this article:

Table S1 Basic demographics and the origin of tissue samples (both for hMSCs and the primary native hTeno cultures) from the donors.

Fig. S1. Comparison of rbMSCs and hMSCs phenotypic expression.

Fig. S2. Expression of CD105, CD166, CD14 and CD19 on hMSCs.

APPENDIX N

Publication in Cells Tissues Organs

Original Paper

Cells Tissues Organs

Cells Tissues Organs 2012;196:325–338
DOI: 10.1159/000335693

Received: August 15, 2011
Accepted after revision: December 12, 2011
Published online: May 30, 2012

Effect of Growth Differentiation Factor 5 on the Proliferation and Tenogenic Differentiation Potential of Human Mesenchymal Stem Cells in vitro

Sik-Loo Tan[a] Raja Elina Ahmad[b] Tunku Sara Ahmad[a] Azhar M. Merican[a]
Azlina A. Abbas[a] Wuey Min Ng[a] Tunku Kamarul[a]

[a]Tissue Engineering Group, National Orthopaedic Centre of Excellence for Research and Learning, Department of Orthopaedic Surgery, and [b]Department of Physiology, Faculty of Medicine, University of Malaya, Kuala Lumpur, Malaysia

Key Words
Tendon · Tissue engineering · Cell-based therapy · Orthopedics · Mesenchymal stem cell

Abstract
The use of growth differentiation factor 5 (GDF-5) in damaged tendons has been shown to improve tendon repair. It has been hypothesized that further improvements may be achieved when GDF-5 is used to promote cell proliferation and induce tenogenic differentiation in human bone marrow-derived mesenchymal stem cells (hMSCs). However, the optimal conditions required to produce these effects on hMSCs have not been demonstrated in previous studies. A study to determine cell proliferation and tenogenic differentiation in hMSCs exposed to different concentrations of GDF-5 (0, 5, 25, 50, 100 and 500 ng/ml) was thus conducted. No significant changes were observed in the cell proliferation rate in hMSCs treated at different concentrations of GDF-5. GDF-5 appeared to induce tenogenic differentiation at 100 ng/ml, as reflected by (1) a significant increase in total collagen expression, similar to that of the primary native human tenocyte culture; (2) a significant upregulation in candidate tenogenic marker gene expression, i.e. scleraxis, tenascin-C and type-I collagen; (3) the ratio of type-I collagen to type-III collagen expression was elevated to levels similar to that of human tenocyte cultures, and (4) a significant downregulation of the non-tenogenic marker genes runt-related transcription factor 2 and sex determining region Y (SRY)-box 9

Abbreviations used in this paper

BMP	bone morphogenetic protein
COL-I	type-I collagen
COL-III	type-III collagen
DCN	decorin
DMEM	Dulbecco's modified Eagle's medium
ECM	extracellular matrix
GDF-5	growth differentiation factor 5
hMSC	human mesenchymal stem cell
hTeno	human tenocyte
MSC	mesenchymal stem cell
NST	nucleostemin
PBS	phosphate-buffered saline
qRT-PCR	quantitative RT-PCR
RUNX2	runt-related transcription factor 2
SCX	scleraxis
SOX9	SRY (sex determining region Y)-box 9
TNC	tenascin-C

KARGER

Fax +41 61 306 12 34
E-Mail karger@karger.ch
www.karger.com

1422–6405/12/1964–0325$38.00/0

Accessible online at:
www.karger.com/cto

Dr. T. Kamarul
National Orthopaedics Centre of Excellent Research and Learning
Department of Orthopaedic Surgery, Faculty of Medicine, Tissue Engineering Group
University of Malaya, Kuala Lumpur 50603 (Malaysia)
Tel. +603 7967 7548, E-Mail tkzrea@yahoo.com

at day 7 of GDF-5 induction, further excluding hMSC differentiation into other lineages. In conclusion, GDF-5 does not alter the proliferation rates of hMSCs, but, instead, induces an optimal tenogenic differentiation response at 100 ng/ml.

Introduction

Tendon damage resulting from trauma contributes to a large number of soft tissue injury cases reported each year [Butler et al., 2004]. At present, surgical repair of damaged tendon is the only viable option to restore tissue integrity. However, this method does not completely return the damaged tendon to its preinjured state [Butler et al., 2004]. It has been demonstrated that natural tissue healing of tendons appears to be limited due to poor vascularity [Bergljung, 1970]. This in turn results in a higher tendency for the damaged tendon to undergo tissue degeneration [Romeo et al., 1999]. Recent endeavours in tendon tissue engineering have harnessed the potential of cell-based therapy to promote tendon regeneration. It has been hypothesized that the application of cells to damaged sites will produce superior tissue repair, overcoming the limitations of the natural healing processes [Obaid and Connell, 2010]. Mesenchymal stem cells (MSCs) present a great potential for this type of treatment modality due to their ability to proliferate and differentiate into progenitors of different mesenchymal tissues including tenocyte [Lee and Hui, 2006], while avoiding excessive morbidity to the donor site. However, it has been previously reported that transplantation of undifferentiated MSCs may produce complications such as the formation of ectopic bone in situ [Harris et al., 2004]. To overcome such issues, a number of tissue engineering approaches are presently being developed to induce tenogenic differentiation in human MSCs (hMSCs), or to produce controlled differentiation of hMSCs into the desired tenogenic lineage prior to transplantation. An example of such an approach is the use of growth factors [Farng et al., 2008].

The presence of growth factors has been regarded as an important component in the healing of lacerated tendons [Lou et al., 2001]. This has been supported by recent findings demonstrating that several soluble growth factors, e.g. basic fibroblast growth factor [Sahoo et al., 2010], growth differentiation factor 5 (GDF-5) [Farng et al., 2008] and bone morphogenetic protein 12 (BMP-12 or GDF-7) [Wang et al., 2005; Violini et al., 2009], are able to induce tenogenic differentiation in MSCs. Among these, GDF-5, which is a member of the human BMP family, has been identified as a key biological molecule that can accelerate tendon healing [Aspenberg and Forslund, 1999]. However, presently, there are limited studies investigating the isolated effect of GDF-5 on hMSC proliferation and differentiation in vitro. Previous reports examining the effects of GDF-5 on MSCs were limited to studies with immortalized cell lines [Farng et al., 2008] and rodent adipose tissue-derived MSCs [Park et al., 2010]. The effect of GDF-5 on harvested non-immortalized bone marrow-derived hMSCs, which represents the most commonly obtained source of MSCs [Hass et al., 2011], has not been previously described. A critical issue which has not been specifically addressed by previous studies is the establishment of the optimal concentration of GDF-5 that can induce maximal phenotypic expression of the tenogenic hMSC in vitro. This is of particular importance considering that an optimal condition must be attained in order to effectively repair the damaged tendon. Moreover, this knowledge would be of particular interest since it has been suggested that harvested bone marrow-derived hMSCs may respond differently to GDF-5 as compared to the immortalized cell line [Farng et al., 2008] or to MSCs from different sources [Musina et al., 2006]. Furthermore, bone marrow-derived MSCs have been shown to produce higher amounts of collagen as compared to cells originating from other tissues, possibly resulting in superior tissue repair [Van Eijk et al., 2004]. Therefore, this study was conducted to determine the optimal culture condition for hMSC tenogenic differentiation using GDF-5 as an induction factor and to elucidate the effect of GDF-5 on tenogenic hMSC proliferation. A gradient of GDF-5 concentration was tested, considering that progenitor cells can differentiate into various types of mature cells, e.g. osteocytes, chondrocytes and tenocytes, in response to the amount of signal molecules received. We speculate that the hMSCs will differentiate into mature tenocytes in response to a particular concentration of GDF-5 within the range tested, which remains to be established.

To confirm the occurrence of tenogenic differentiation in hMSCs, a few candidate tenogenic marker genes, which include transcription factor scleraxis *(SCX)* and extracellular matrix (ECM) genes tenascin-C *(TNC)*, type-I collagen *(COL-I)*, type-III collagen *(COL-III)* and decorin *(DCN)* were investigated in the present study. These genes were selected in accordance with previous reports indicating that GDF-5 acts as a molecular cue that regulates tenocyte-specific transcription factor, particularly *SCX* [Schweitzer et al., 2001], through the

Smad/BMP signaling cascade [Bullough et al., 2008], which in turn regulates the expression of *COL-I* in tendon tissues [Lejard et al., 2007]. In addition, the expression of genes such as *TNC,* a mechanoresponsive modulator of matrix formation expressed in high tensional loading tissue such as tendons and ligaments, as well as the ratio of *COL-I* to *COL-III* have been previously used as indicators of the tenogenic characteristics in tendon tissues and tenocyte cultures [Maffulli et al., 2000; Yao et al., 2006].

In addition, in the current study, non-tenogenic marker genes, i.e. (1) runt-related transcription factor 2 *(RUNX2),* a transcription factor which is essential for osteoblast differentiation [Komori, 2006, 2010], (2) sex determining region Y (SRY)-box 9 *(SOX9),* a transcriptional activator for chondrocyte-specific gene such as type-II collagen [Lefebvre et al., 1997; Haller et al., 2011] for chondrocyte differentiation [Bi et al., 2001; Akiyama et al., 2004; Pan et al., 2008], and (3) nucleostemin *(NST),* a general stem cell marker gene which has been previously reported to be absent in terminally differentiated cells such as tenocytes [Tsai and McKay, 2002; Zhang and Wang, 2010a], were also analyzed to rule out the possibilities that the cells may undergo differentiation into lineage other than tenogenic lineage. These genes have been analyzed in a previous study to confirm the exclusive occurrence of tenogenic differentiation in patella tendon-derived stem cells treated with platelet-rich plasma [Zhang and Wang, 2010b]. To further strengthen the present study design, primary native human tenocyte (hTeno) culture was used as a positive control for comparison with the tenogenic differentiated hMSCs.

Materials and Methods

hMSC Isolation and Culture

Ethics approval to conduct this study was granted by the University of Malaya Medical Center Ethics Committee (reference No. 602.22). Human bone marrow was harvested from 3 adult donors (table 1) undergoing intramedullary nailing in the University of Malaya Medical Center. Informed consent was obtained from each donor. hMSCs were isolated from bone marrow samples and expanded in vitro following methods that had been previously established [Tan et al., 2011]. A volume of 2 ml of bone marrow was diluted with 2 ml of phosphate-buffered saline (PBS; pH 7.2) and layered onto 3 ml of Ficoll-Paque Premium (GE Healthcare, Sweden) before undergoing gradient centrifugation at 2,200 rpm for 30 min (Eppendorf 5810R).

The mononuclear layer (second top layer) was then collected and washed twice with Dulbecco's modified Eagle's medium (DMEM) low glucose (Invitrogen-Gibco, USA) supplemented with antibiotic/antimycotic 1% (v/v; Invitrogen-Gibco). The isolated mononuclear cells were cultured in growth medium [DMEM low glucose supplemented with 10% fetal bovine serum, antibiotic/antimycotic 1% (v/v) and 200 mM GlutaMAX™-I (Invitrogen-Gibco)] and transferred into T75 tissue culture flasks (Nunc™, USA). The medium was changed at day 5 to remove non-adherent cells, and the subsequent medium change was conducted at 3-day intervals.

Table 1. Basic demographics and the origin of tissue samples (both for hMSCs and the primary native hTeno cultures) from the donors

Donor	Age years	Gender	Sample
1	69	male	bone marrow from femur
2	67	female	bone marrow from femur
3	75	male	bone marrow from femur
4	19	male	Hamstring tendon
5	28	male	Hamstring tendon
6	21	male	Hamstring tendon

To determine whether the cells obtained consisted of pure MSCs, various tests including immunohistochemical staining for specific cell surface markers, cell morphological analyses and the ability of the isolated cells to undergo tri-lineage differentiation, i.e. chondrogenic, adipogenic and osteogenic differentiation, were conducted. The methods used are described in our previous publications [Kamarul et al., 2009a, 2009b].

Primary Native hTeno Isolation and Culture

Adult human hamstring tendons free of pathology (n = 3) were obtained from donors who underwent ligamentous reconstruction of the knees and arthroplasty of the knee(s) (table 1). Written informed consent was obtained from each donor. The hamstring tendons that were obtained were kept in PBS supplemented with penicillin-streptomycin 1% (v/v; Invitrogen-Gibco) before further processing. The tendon specimens were processed using the methods modified from Zhang and Wang [2010a]. Briefly, the tendons were minced into approximately 1 mm^3 in size under a sterile condition. The explants were then transferred into a 15-ml falcon tube with 0.4 mg/ml type I collagenase in PBS (pH 7.2) and incubated at 37°C in a humidified atmosphere of 5% CO_2 for 2 h to allow for the enzymatic digestion process to occur. The specimens were subsequently centrifuged at 1,800 rpm at 15°C for 5 min. The supernatant was then removed and the pellet was washed twice with 10 ml PBS. Following that, the digested explants were cultured in T75 tissue culture flasks (Nunc) with DMEM high glucose (4.5 g/l glucose; Invitrogen-Gibco), supplemented with 10% fetal bovine serum (Invitrogen-Gibco), 100 units/ml penicillin-streptomycin and 200 mM GlutaMAX-I (Invitrogen-Gibco). Cultures were incubated at 37°C in a humidified atmosphere of 5% CO_2 and supplemented with fresh culture medium at 3-day intervals. Forty-eight hours after culturing, the digested tissues were discarded and the outgrown cells were maintained at 80–90% of confluency for subculture using trypsin digestion. These primary native hTeno cultures (P2 or P3) were used

as positive controls in the subsequent total collagen and gene expression experiments. The cells isolated appeared to have fibroblastic morphology, similar to that reported by Zhang and Wang [2010a] in rabbit tenocyte culture.

AlamarBlue® Cell Proliferation Analysis of hMSC under GDF-5 Induction

Cell proliferation was assessed using the AlamarBlue assay based on the colorimetric quantitative analytical principle. hMSCs (at P2, n = 3) were seeded in the standard 96-well culture plates at a cell density of 10^4 cells/ml and resuspended in 250 μl of culture medium. GDF-5 at various concentration levels (either 0, 5, 25, 50, 100 or 500 ng/ml) were added to the cultures 3 days after seeding. Cells were incubated for an additional period of 2 days before 25 μl of AlamarBlue reagent (Invitrogen-Gibco) was added to the medium. Culture plates were protected from light with aluminium foil. Absorbance readings at 570 and 600 nm were obtained using a spectrophotometer (Epoch; Biotek, USA) at various time points, i.e. at 0, 2, 4, 6, 12 and 24, 36, 48 and 60 h. Untreated hMSCs cultured in MSC growth medium were used as controls. Three independent experiments were performed, each in octuplicates in the 96-well plates.

Tenogenic Differentiation and Total Collagen Colorimetric Quantification

hMSCs (at P2, n = 3) were seeded in standard 6-well culture plates at a density of 2×10^4 cells per well, with serum-free DMEM supplemented with recombinant human GDF-5 at various concentration levels (0, 5, 25, 50, 100 or 500 ng/ml; Abcam, Inc., Cambridge, UK). The hTeno cultures isolated from tendon tissues were seeded in similar densities to that of hMSCs and were used for comparison. These cells were not supplemented with GDF-5. For dose-response analysis, total collagen expressions were measured at 96 h. Based on the results obtained from this experiment, only three concentrations, i.e. 0, 50 and 100 ng/ml of GDF-5, were selected for further analysis which determines the collagen and gene expression levels at different time points (day 4, 7 and 10).

For time response experiments, total collagen assays were conducted at day 4, 7 and 10 in hMSC culture supplemented with 0, 50 and 100 ng/ml of GDF-5. Total soluble collagen in the culture medium was quantified with colorimetric Sircol™ soluble collagen assay (Biocolor, Ireland). Briefly, the cell culture medium was mixed with Sircol dye reagent with vigorous agitation in a 1.5-ml microcentrifuge tube for 30 min. The mixture was then centrifuged for 10 min at 10,000 *g* to collect the collagen-dye complex at the bottom of the centrifuge tubes. The unbound dye solutions were later removed by draining the tubes. Subsequently, 1 ml of the alkaline reagent was added to each microcentrifuge tube. As the unbound dye dissolved, the absorbance of the samples was measured at 540 nm. The collagen content in the medium was calculated based on the standard curve plot, with *COL-I* supplied with the kit as the reference sample. In both the dose- and time-response experiments, three independent experiments, each in triplicate, were performed. Data were presented as the mean ± SD. Statistical analysis was analyzed with SPSS (version 17) software. Comparisons of mean values between the different concentrations and various time points were conducted using one-way analysis of variance. Statistical significance was accepted when the p value was <0.05.

Quantitative RT-PCR for GDF-5 Dose-Dependent Relative Gene Expression Analysis

To induce the expression of tenogenic specific phenotypes, hMSCs were cultured in DMEM supplemented with GDF-5 at 0, 50 and 100 ng/ml. After 4 days, the degree of cell differentiation was determined by quantitative RT-PCR (qRT-PCR). This was achieved by measuring *SCX, TNC, COL-I, COL-III, DCN* and *NST* gene expressions. Total RNA was extracted from the hMSC cultures, with and without GDF-5 supplementation. In this study, 1 μg of total RNA was reverse-transcribed into cDNA with the transcriptor high-fidelity cDNA synthesis kit (Roche Diagnostics GmbH, Mannheim, Germany). qRT-PCR was performed with a Bio-Rad CFX96™ real-time detection system (Bio-Rad Laboratories, Inc., Hercules, Calif., USA) in a final volume of 20 μl with 10 μl iQ™ SYBR® Green Supermix (Bio-Rad Laboratories), 0.6 μl cDNA samples, and 0.2 μM of each primer (for *COL-I α1* or *COL-I, COL-III, SCX, TNC, DCN* and *NST;* table 2). The amplification protocol was as follows: an initial denaturation and activation step at 95°C for 30 s followed by 40 cycles of 95°C for 15 s and 61°C for 45 s. A melting curve program was carried out routinely to confirm the presence of a single product (55–95°C with a heating rate of 0.5°C per second and a continuous fluorescence measurement). The annealing temperature at 61°C was derived empirically with temperature gradients. To estimate amplification efficiency, a standard curve was generated for each target molecule via 5-fold serial dilution of a cDNA pool containing the target gene sequences. Data were analyzed with the CFX manager software. A relative quantification method (with corrected PCR efficiency) [Pfaffl, 2001] was performed. All the data were normalized to GAPDH, which was used as our reference gene, after correcting for differences in amplification efficiency (as recommended in the CFX manager package). Data were presented as $\log_{10}$-fold change (±SD) of relative quantification of target mRNA relative to control samples (untreated hMSCs). Student's t tests were employed to determine the differences between the untreated and GDF-5-treated samples. For all comparisons, the statistical significance was accepted at 95% confidence interval ($p < 0.05$).

qRT-PCR for GDF-5 Temporal-Dependent Relative Gene Expression Analysis

To determine the tenogenic lineage commitment in hMSCs treated with 100 ng/ml GDF-5, hMSCs were cultured in DMEM supplemented with 100 ng/ml GDF-5 for 7 days. Cells were harvested at day 4 and 7 for total RNA isolation. Total RNA from the hTeno cultures (P2 or P3) was also isolated and used as positive control, whilst the untreated hMSCs cultured in MSC growth medium were used as negative controls. Similar qRT-PCR protocols as described above were used to analyze the expression of *SCX, TNC* and two non-tenogenic markers: the osteogenic marker *RUNX2* and the chondrogenic marker *SOX9* in GDF-5-treated and -untreated hMSCs as well as in hTeno. Data were presented as $\log_{10}$ (or $\log_2$)-fold change (mean ± SD) of relative quantification of target mRNA relative to negative control samples (untreated hMSCs).

Table 2. Primers used for qRT-PCR analysis

Gene	Primer sequence	Size bp	GenBank accession No./reference
GAPDH	5′-AAC ATC ATC CCT GCC TC TAC TG-3′ 5′-CTC CGA CGC CTG CTT CAC-3′	196	NM_002046 [Kuo and Tuan, 2008]
COL-I	5′-CTG ACT GGA AGA GCG GAG AG-3′ 5′- TCT GGG CAA TGC TGG GCT GTG TGG G-3′	129	AY633663
SCX	5′-CAG CGG CAC ACG GCG AAC-3′ 5′-CGT TGC CCA GGT GCG AGA TG-3′	165	BK000280 [Kuo and Tuan, 2008]
NST	5′-ATG ACC TGC CAT AAG CGG TAT-3′ 5′-AAG GGA GCA CTG TTT GGA ACT-3′	131	AK315484
COL-III	5′-CAG CGG TTC TCC AGG CAA GG-3′ 5′-CTC CAG TGA TCC CAG CAA TCC C-3′	179	NM_000090 [Kuo and Tuan, 2008]
DEC	5′-CTC TGC TGT TGA CAA TGG CTC TCT-3′ 5′-TGG ATG GCT GTA TCT CCC AGT ACT-3′	257	NM_133505 [Kuo and Tuan, 2008] NM_133504 [Kuo and Tuan, 2008] NM_001920 [Kuo and Tuan, 2008] NM_133503 [Kuo and Tuan, 2008]
TNC	5′-GGG TCC TCA AGA AAG TCA TCC G-3′ 5′-CTG ACT CCA GAT CCA CCG AAC-3′	62	NM 002160

Results

In vitro Characteristics of the Expanded hMSC

Three to 5 days following the plating of bone marrow mononuclear cells onto the plastic surface of the cell culture flasks, discrete fibroblastic cell colonies with a low degree of cellular heterogeneity appeared to develop in the culture. Over time, there was a gradual shift in cell morphology, with an increasing number of fibroblastic cells and a decreasing quantity of the heterogeneous cells (such as polygonal cells) in the culture. Thus, the final homogeneous cell population obtained at the end of P2 was used for the succeeding differentiation assay to minimize the possible variation contributed by the heterogeneous cell populations.

The isolated cells appeared to conform to the characteristics expected of MSCs, i.e. (1) spindle-shaped plastic adherent features; (2) positive markers for CD44, CD105 and CD166 while being devoid of CD34 and CD45, and (3) able to undergo tri-lineage differentiation, namely chondrogenic, osteogenic and adipogenic differentiation (data not shown) [Kamarul et al., 2009a, 2009b].

hMSC Differentiation Using GDF-5 Induction

Images of hMSCs in culture with and without GDF-5 supplementation were captured using phase contrast microscopy (fig. 1). There were no significant differences in the gross morphological appearance between these cells, irrespective of the GDF-5 concentration levels used.

Dose and Temporal Effects in hMSC Proliferation under GDF-5 Induction

The effects of different GDF-5 concentrations on the proliferation rate of hMSCs at different time points were reflected by the absorbance readings obtained from the AlamarBlue assay. There was a pattern of an increase in cell proliferation rate at low concentrations of GDF-5 (5 ng/ml) and, in contrast, the cell proliferation rate appeared to be reduced at a high GDF-5 concentration (500 ng/ml). However, the differences in the hMSC proliferation between the cultures treated with or without GDF-5 were not significant (fig. 2), suggesting that GDF-5 did not alter the proliferation rate of the tenogenic hMSCs.

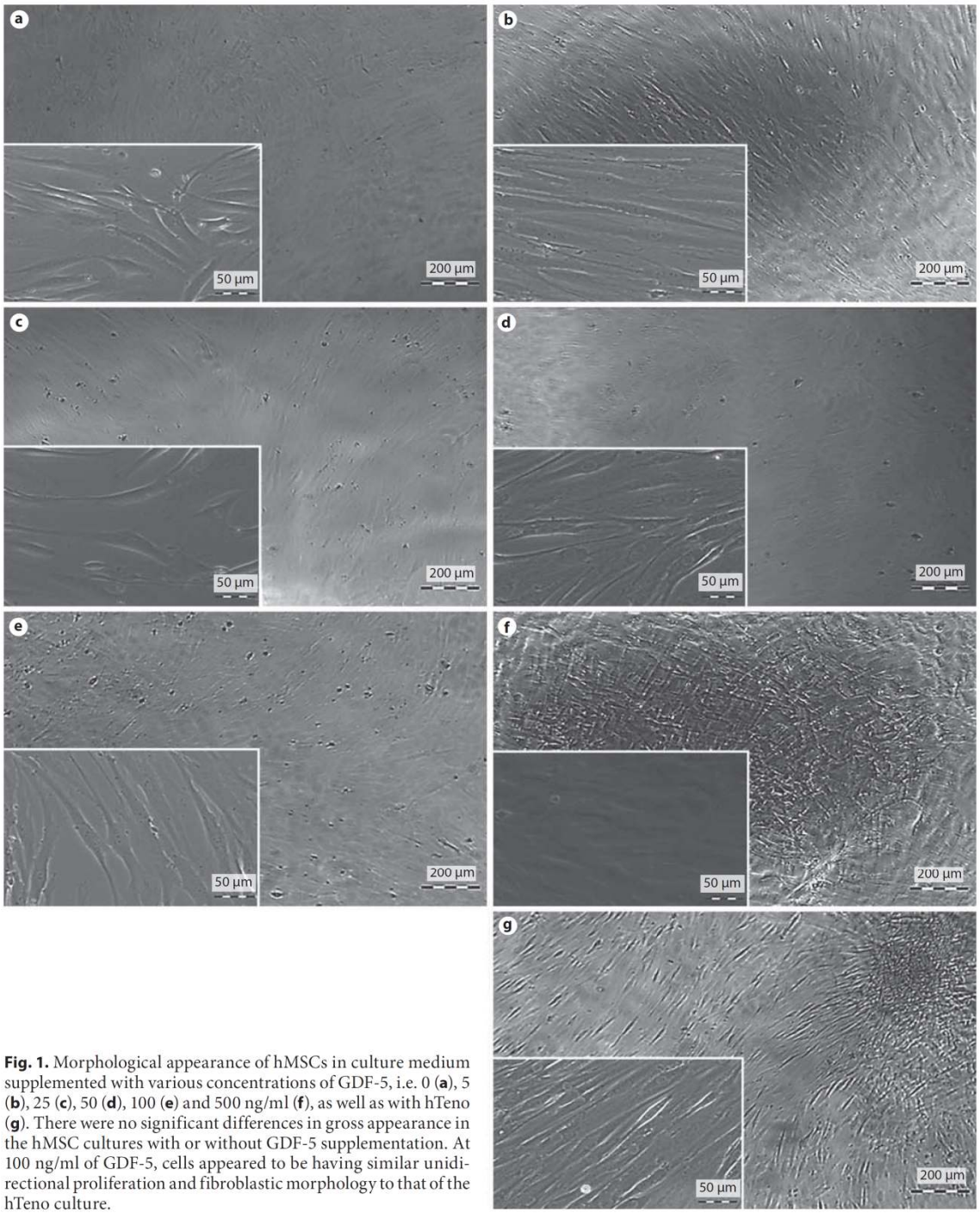

Fig. 1. Morphological appearance of hMSCs in culture medium supplemented with various concentrations of GDF-5, i.e. 0 (**a**), 5 (**b**), 25 (**c**), 50 (**d**), 100 (**e**) and 500 ng/ml (**f**), as well as with hTeno (**g**). There were no significant differences in gross appearance in the hMSC cultures with or without GDF-5 supplementation. At 100 ng/ml of GDF-5, cells appeared to be having similar unidirectional proliferation and fibroblastic morphology to that of the hTeno culture.

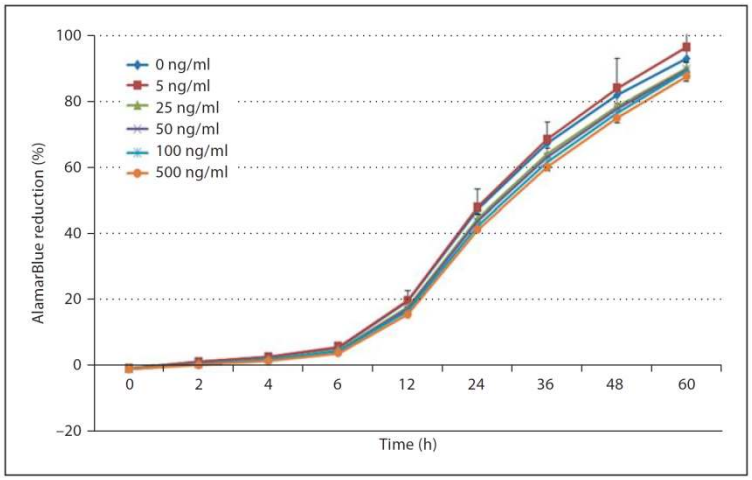

Fig. 2. AlamarBlue cell proliferation assay of the hMSC cultures supplemented with different concentrations of GDF-5. There was no significant difference in cell proliferation rates as reflected by the percentage of AlamarBlue reduction by hMSCs supplemented with varying levels of GDF-5.

Dose Response of GDF-5 Induced Total Collagen Expression in hMSCs

The results of total collagen assay of the hMSC culture supernatant revealed that at 100 ng/ml, GDF-5 induced a significantly higher total collagen concentration (9.98 ± 1.70 μg/ml; $p < 0.05$; table 3) as compared to that at concentration levels of 0, 5 and 25 ng/ml (fig. 3a). This expression level was comparable to that observed in the hTeno culture (10.39 ± 2.32 μg/ml). Expression levels of total collagen were significantly lower than the hTeno cultures in all other concentrations of GDF-5. There were no significant differences in the total collagen concentration between the hMSC cultures in all other GDF-5 concentration levels (table 3).

The subsequent time-response experiments showed a significant increase in the total collagen expression in the culture medium from the hMSC cultures supplemented with 100 ng/ml of GDF-5 at day 4, 7 and 10, as compared to the untreated cultures (fig. 3b). A significant increase in total collagen expression was only observed at day 7 onwards in the hMSC cultures treated with 50 ng/ml of GDF-5. This finding demonstrates that 100 ng/ml of GDF-5 is sufficient to induce a tenogenic response from hMSCs as early as day 4, but with the use of 50 ng/ml of GDF-5, a longer period was required.

Relative Gene Expression Analysis of hMSC Tenogenic Differentiation

There were significant differences in the relative gene expression levels for *COL-I* and *COL-III, DCN, SCX, TNC* and *NST* of the hMSCs grown in 0, 50 and 100 ng/ml of GDF-5 at 96 h (fig. 4). At 100 ng/ml of GDF-5, candidate tenogenic markers, *COL-I, SCX* and *TNC,* were significantly upregulated (2.31± 0.27, 2.30 ± 1.81 and 3.55 ± 0.27 fold increase, respectively; fig. 4).

There was a significantly higher expression of *DCN,* the genes related to collagen fiber formation *(COL-III)* and matrix assembly [Zhang et al., 2006], at 96 h as compared to 0 h ($p < 0.05$). There was a 1.84 ± 0.28

Table 3. Statistical analysis of total collagen expression in hMSCs cultured at different concentrations of GDF-5

	Concentrations of GDF-5				
	5 ng/ml	25 ng/ml	50 ng/ml	100 ng/ml	500 ng/ml
Concentrations of GDF-5					
0 ng/ml	0.515	0.978	0.157	*0.008***	0.187
5 ng/ml		0.520	0.426	*0.035**	0.485
25 ng/ml			0.153	*0.007***	0.183
50 ng/ml				0.178	0.921
100 ng/ml					0.149

Data given are p values. Summary of the least significant difference analysis with Bonferroni adjustment for multiple pairwise comparisons of the mean total collagen differences in the culture medium of hMSCs supplemented with different amounts of GDF-5. The p values are presented at 95% confidence intervals and the significant values are denoted with an asterisk. * $p < 0.05$; ** $p < 0.01$.

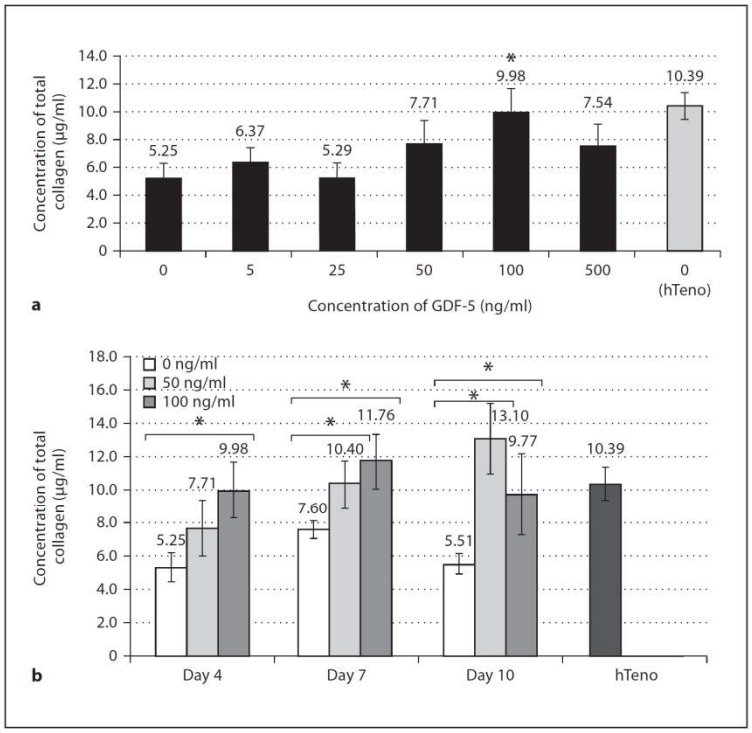

Fig. 3. Total collagen content analysis for hMSCs cultured with different concentrations of GDF-5. **a** Dose-response analysis at 96 h following GDF-5 supplementation. The total collagen expression in hMSCs was significantly increased at 100 ng/ml of GDF-5 (* $p < 0.05$). **b** Time-response analysis at three concentration levels of GDF-5, i.e. 0, 50 and 100 ng/ml. In comparison to hMSCs without GDF-5 induction, the total collagen expression was significantly elevated (* $p < 0.05$) in hMSCs at 100 ng/ml of GDF-5 on day 4 onwards, whilst significant increase (* $p < 0.05$) at 50 ng/ml was only observed at day 7 onwards.

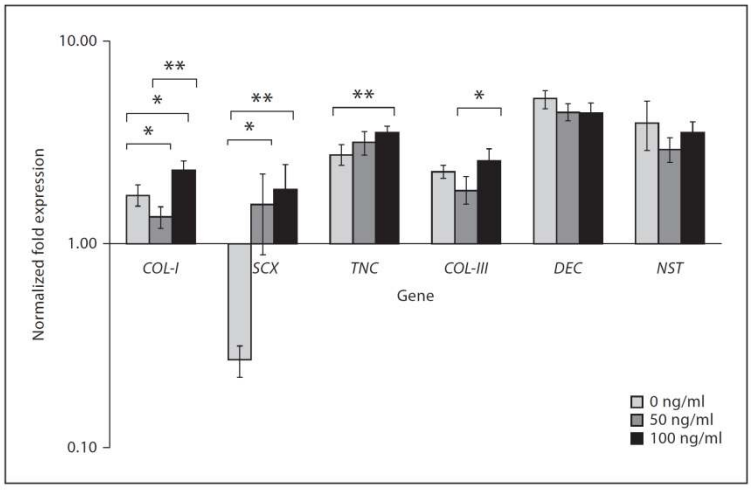

Fig. 4. Gene expression analysis of candidate tenogenic markers in hMSCs cultured with GDF-5 at different concentrations (0, 50 and 100 ng/ml). There was a significant upregulation of gene expression of candidate tenogenic marker genes *COL-I, SCX, TNC* and *COL-III* at 100 ng/ml of GDF-5. * $p < 0.05$; ** $p < 0.01$.

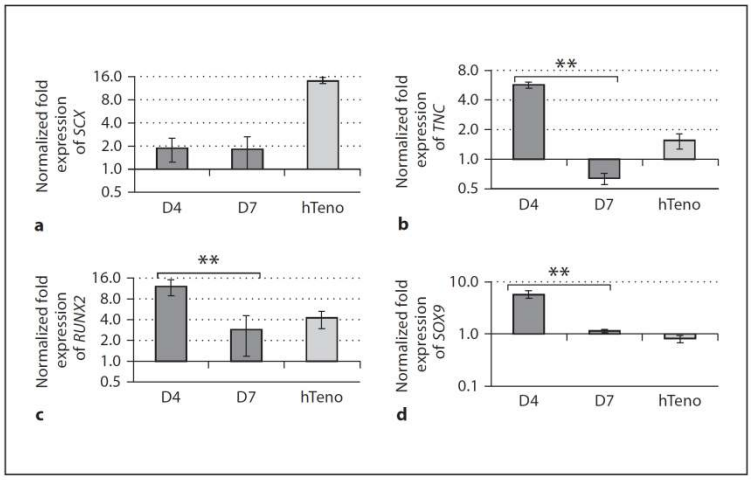

Fig. 5. Gene expression analysis of cultured hMSCs in the temporal experiment at 100 ng/ml of GDF-5 for *SCX* (**a**), *TNC* (**b**), *RUNX2* (**c**) and *SOX9* (**d**). The data reflect the relative quantification of target mRNA normalized to control samples (untreated hMSCs cultured in MSC growth medium). Data are presented as $\log_{10}$ (or $\log_2$)-fold change (with error bars signifying the range of SDs). All the candidate tenogenic marker genes were upregulated on day 4 (D4), but only *SCX* was persistently upregulated on day 7 (D7). There was a significant increase in the expression of non-tenogenic marker genes (i.e. *RUNX2* and *SOX9*) on day 4 of GDF-5 induction, which subsequently was significantly downregulated by day 7 (n = 3). $^{**}p < 0.01$.

fold increase in the *COL-III* expression at 50 ng/ml and a 2.56 ± 0.41 fold increase at 100 ng/ml at 96 h. Although the *COL-III* expressions were not significantly different in hMSCs cultured with GDF-5 as compared to those without GDF-5, the ratio of *COL-I* to *COL-III* appeared to be increased (online suppl. table, www.karger.com/doi/10.1159/000335693). For *DCN* expression, there was a 4.47 ± 0.41 fold increase at 50 ng/ml and a 4.42 ± 0.57 fold increase at 100 ng/ml at 96 h. No significant difference in *NST* gene expression levels was observed in all groups, demonstrating that despite undergoing tenogenic differentiation, cells maintained their original MSC gene expression.

Having established significant increment in the candidate tenogenic marker gene expression at 100 ng/ml of GDF-5, we further analyzed the temporal effect of GDF-5 at that concentration level on hMSC differentiation. In the temporal analysis, the candidate tenogenic marker genes *SCX and TNC* were upregulated on day 4 after the GDF-5 treatment (fig. 5a, b). However, on day 7, only *SCX* was persistently upregulated, whereas the expression of *TNC* was reduced ($p < 0.01$). The expression of non-tenogenic marker genes *RUNX2 and SOX9* was significantly downregulated ($p < 0.01$) on day 7 (fig. 5c, d). These findings suggested that hMSCs were undergoing tenogenic differentiation as early as day 4 following GDF-5 induction at 100 ng/ml.

Discussion

The present study demonstrates that 100 ng/ml of GDF-5 provided the optimal concentration required to induce tenogenic differentiation of bone marrow-derived hMSCs. This deduction was based on the following findings: (1) total collagen was significantly higher in cultures with GDF-5 concentrations of ≥50 ng/ml; (2) however, only the concentration of 100 ng/ml in hMSC cultures produced similar levels of total collagen to that of the hTeno cultures. hMSC cultures with GDF-5 concentrations >100 ng/ml produced significantly less total collagen than the hTeno cultures; (3) within the range of GDF-5 concentrations tested, only concentrations of 100 ng/ml produced significantly higher amounts of collagen as early as day 4; (4) *COL-I, SCX* and *TNC* genes in the hMSCs were only upregulated at this concentration; (5) the ratio of *COL-I* to *COL-III* was highest in hMSC cultures supplemented with 100 ng/ml of GDF-5, and (6) non-tenogenic genes, such as *RUNX2* and *SOX9,* were significantly reduced on day 7 of GDF-5 induction. These findings appear to be supported by a previous study [Park et al., 2010], demonstrating that at 100 ng/ml, there was a significant increase in protein expression of tenomodulin, TNC, Smad-8 and matrix metalloproteinase-13, compared to that of ≤10 ng/ml. At higher concentrations, i.e. 1,000 ng/ml, these genes were downregulated instead [Park et al., 2010]. Although our study did not utilize such high concentrations, at concentrations of 500 ng/ml, the total collagen concentration from the hMSC cultures ap-

peared to be significantly lower than that of the hTeno cultures and hMSC cultures at a concentration of 100 ng/ml. This precluded the need for further experiments beyond the concentration level of 500 ng/ml. It is unclear as to why there was no linear pattern of dose-response relationship in this study. It can be speculated that at higher concentrations of GDF-5, the antagonistic effects of GDF-5 may have resulted in a decrease in collagen production, as observed in other studies using other growth factors, for example, transforming growth factor-β [Ghosh et al., 2001]. However, this remains speculative and needs to be proven in a separate study.

It is interesting to note that GDF-5 did not appear to influence hMSC proliferation in the present study, which is in contrast to a previous report involving the rodent adipose tissue-derived MSC primary culture [Park et al., 2010]. In addition, in a separate study, the rodent adipose tissue-derived MSCs have been reported to produce faster proliferation than those derived from the bone marrow [Saka et al., 2011]. Nevertheless, the data presented in this study appear to be consistent with a study which uses murine bone marrow-derived stromal immortalized cell lines [Farng et al., 2008]. Therefore, it appears that the tissue of origin of the MSCs may be a predetermining factor affecting cell proliferation in the presence of GDF-5. However, this needs to be confirmed by a more robust study design. In addition to tissue of origin, other factors such as species [Reilly et al., 2007] and the amount of serum used for cell culture [Saka et al., 2011] may also play an important role in determining the response of bone marrow-derived hMSCs to GDF-5. The effects of GDF-5 on MSC proliferation have not been previously explained by a specific cellular mechanistic pathway which may be involved following GDF-5 receptor stimulation. However, there are several possibilities that could be considered. GDF-5 has been shown to bind specifically to three different receptors: serine/threonine kinase receptor type 1 (BMPR1b) or serine/threonine kinase receptor type 2 which could be either BMPR2 or ACTR2a [Nishitoh et al., 1996]. The activation of any one of these receptors may induce the expression of ID1 and ID3 via the Smad-dependent and mitogen-activated protein kinase-independent pathway in the regulation of transcription for cell cycle or cell proliferation control [Chen et al., 2006]. This could be expected considering that mitogen-activated protein kinase is an important signaling pathway that regulates cell proliferation [Zhang and Liu, 2002].

The changes in the candidate tenogenic marker genes (such as *SCX, TNC, COL-I* and *COL-III*) as observed in our study strongly suggest that the expression of the main proteins produced by tenocytes, i.e. *COL-I, COL-III, TNC and DCN,* is also present in the tenogenic differentiated hMSCs. It is plausible that the process of tenogenic differentiation induced by GDF-5 at 100 ng/ml in the present study involves a similar Smad/BMP signal transduction mechanism to that reported previously [Nishitoh et al., 1996]. However, this needs to be substantiated by a more comprehensive study.

The increase in *SCX* and *COL-I* is an expected outcome of the tenogenic MSC differentiation process. However, it is interesting to note that *DCN* expression was not upregulated during tenogenic differentiation, which may have been related to the monolayer conditions used in this experiment [Yao et al., 2006]. Culture conditions play a critical role in modulating the synthesis, assembly and organization of ECM components. In a 3D environment, *DCN* is also able to modulate the BMP/transforming growth factor-β pathway through interaction with lipoprotein receptor-related protein [Cabello-Verrugio and Brandan, 2007] and regulates matrix organization and mechanical characteristics of the 3D collagen matrices [Ferdous et al., 2007]. Nonetheless, this may not be the case in the present study, as previous studies have shown that an increase in *DCN* expression in monolayer rodent MSC cultures is not unexpected [Park et al., 2010].

During the course of tenogenic differentiation, the expression of *TNC* can be expected to be persistently upregulated at a later time point, potentially reaching a level similar to that observed in the hTeno cultures. In this study, the *TNC* expression in hMSCs at day 7 of GDF-5 induction appeared to be reduced (fig. 5). However, the temporal expression profile observed in this study was similar to that observed in a rodent MSC model, which demonstrated downregulation of *TNC* on day 6 upon GDF-5 induction which eventually increased on day 9 and day 12 [Park et al., 2010]. Since *TNC* is a late tenogenic marker, we suspect that the expression of this gene would be upregulated in the hMSCs if our experiment were extended to a longer period of time, as observed in the previous rodent MSC model [Park et al., 2010]. The increased expression of this gene at a late phase of tendon development has recently been documented in a study comparing the *TNC* expression in tendon from the embryonic period to that observed at day 14 postnatally [Liu et al., 2012]. The observation from our temporal experiment implicates that it may have been appropriate to utilize the GDF-5-induced hMSCs collected at day 4 for further clinical application, in view of the fact that the hMSCs have already been differentiated into tenocytes, as indicated by the significant upregulation of the *TNC*

gene expression at this time point. However, a more rigorous study needs to be conducted in order to confirm this.

In this study, although no significant differences were observed in *COL-III* gene expression levels in hMSCs induced with GDF-5, the ratio of *COL-I* and *COL-III* was highest in hMSC cultures supplemented with 100 ng/ml of GDF-5 (online suppl. table), suggesting that at this concentration, hMSCs underwent optimal differentiation along the tenogenic lineage. In the current study, there was an apparent increase in the total collagen expression in the hMSC cultures at 100 ng/ml of GDF-5 (fig. 3), with no significant increase in *COL-III* gene expression (fig. 4). This suggests that the increase in total collagen expression observed in our study is likely mainly due to an increase in *COL-I,* but the possibility of the presence of other collagens, e.g. collagen type II, cannot be ruled out completely. However, this would be unlikely considering that other studies have shown that the expressions of these proteins are usually of minimal quantity [Altman et al., 2002].

An interesting finding from the present study is the presence of persistent expression of *NST* in tenogenic differentiation of hMSCs. The *NST* gene is a highly specific gene found in MSCs that may also be present in embryonic stem cells and various primitive cells found in the bone marrow. However, this gene is absent in differentiated lineage committed cells found in most adult tissues [Tsai and McKay, 2002]. It has been previously observed that *NST* expression will decrease rapidly as soon as MSCs (or tendon stem cells) undergo tenogenic transformation [Zhang and Wang, 2010b]. However, this was not observed in the present study. There are at least 2 possible explanations for this contrasting result: (1) the duration of the experiment in the present study may be too short to observe any reduction in the *NST* gene expression. Should our experiment be extended to a longer period, we suspect that a decrease in *NST* gene expression may have been observed since the NST^+ MSCs may have been attenuated when mixed with the increasing population of the NST^- mature tenocytes. (2) The transformation of MSCs from their undifferentiated progenitor origins to tenogenic committed cells in the presence of GDF-5 may be a complex process. In normal circumstances, under GDF-5 induction, hMSCs would be expected to differentiate into tenogenic MSCs, which would subsequently undergo symmetrical cell division and mature into tenocytes (fig. 6a). However, an alternative, more complex, cell differentiation process may have occurred. In this condition, it is plausible that hMSCs might first transform into tendon stem cells, which would undergo asymmetrical cell division resulting in two different cell populations, i.e. tendon stem cells and mature tenocytes. The persistence of tendon stem cells that possess self-renewable capability would therefore retain (or increase) the *NST* gene expression throughout the differentiation process (fig. 6b). In both scenarios, it is not known whether the tenogenic differentiation is still reversible, such that the tenogenic hMSCs might regress to become undifferentiated hMSCs again. This speculation needs to be further substantiated by a more comprehensive study, for example, using flow cytometry quantification analysis.

Although several limitations were identified within the present study, these were unfortunately unavoidable. Firstly, the use of total collagen assay to evaluate the tenogenic differentiation of hMSCs may not have been the best method of assessment considering that many cells of mesenchymal origin produce an abundance of collagen extracellularly. The assessment of a more specific collagen, for example, COL-I and COL-III, may have been a more reasonable approach considering that these proteins are specific to tenocyte expression. However, the concentrations of these collagen types may not appear in sufficient quantities to be detected by conventional spectrophotometry analyses such as that utilized in the present study. Hence, gene expression analysis, which is a more specific and sensitive tool of assessment, was advocated in the present study. It should be noted that gene expression analysis has its inherent limitation considering the fact that measurements are made at the transcription level rather than reflecting the true level of the ECM protein that is synthesized. The decision to use total collagen assay may have been the most appropriate option in this study, since this approach has also been used in other study to evaluate the tenogenic differentiation of the fibroblasts [Sahoo et al., 2010]. In other studies, changes in total collagen also appear to be correlated to the changes in the conventional hydroxyproline assay, which is an indicator of the amount of tendon-specific collagen [Taskiran et al., 1999]. Secondly, although the data presented here are novel in view of the absence of previous data on primary human bone marrow-derived MSCs undergoing tenogenic differentiation under GDF-5 induction, it would also be useful to carry out direct comparisons between the hMSC derived from the human bone marrow with that of the MSC lines or the primary MSC culture from animal models to further explore the potential influence of tissue of origin on the effect of GDF-5 on the cells. Lastly, one of the commonly used tenogenic marker genes, tenomodulin [Docheva et al., 2005], was not analyzed in this study. Tenomodulin is a type II transmembrane glycoprotein that has been reported to be pre-

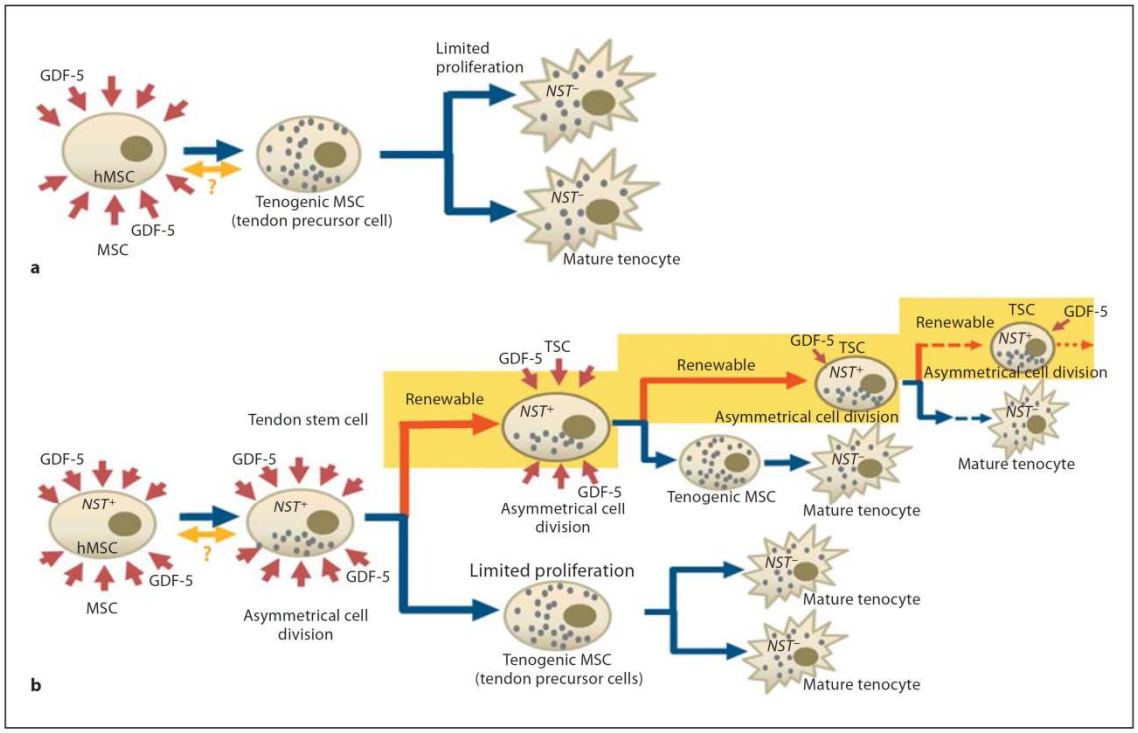

Fig. 6. A postulated scenario of a more complex tenogenic differentiation process in hMSC under GDF-5 induction. **a** Symmetrical cell division in the normally expected hMSC tenogenic differentiation process. **b** An alternative condition showing the possibility of the occurrence of asymmetrical cell division resulting in two cell populations: (1) the renewable tendon stem cells (TSC) with the persistence of *NST* gene (*NST*$^+$) expression, and (2) the mature tenocyte without the *NST* genes (*NST*$^-$).

dominantly expressed in tendons and ligaments. In this study, although we did not include tenomodulin in our analysis, we have analyzed the expression of *SCX* which is also a tenogenic marker that positively regulates tenomodulin expression in a tendon lineage-dependent manner [Shukunami et al., 2006]. In addition, the expression of tenomodulin has previously been detected in other tissues such as cartilage, bone marrow and fat tissue [Jelinsky et al., 2010]. Considering that our hMSC primary culture was derived from bone marrow, the analysis of this gene may not have been as relevant as it would have been when using MSCs derived from other tissues.

In conclusion, this study has shown that the use of GDF-5 induces tenogenic differentiation in hMSCs without significant alteration in the cell proliferation rates. It appears that GDF-5 at a concentration of 100 ng/ml provides the most optimal cell phenotypic response, which includes an augmented level of total collagen and tenogenic marker gene expression, as well as a reduced non-tenogenic marker gene expression, similar to that observed in hTeno cultures.

Acknowledgements

This research was supported by eScience Grant (12-02-03-2017), HIR-MOHE and University of Malaya postgraduate student grants (PS167/2008C, PS360/2009B and PS219/2010A). We thank the University of Malaya for supporting the scholarship PhD thesis of the first author.

Disclosure Statement

The authors indicate no potential conflicts of interest.

References

Akiyama, H., J.P. Lyons, Y. Mori-Akiyama, X. Yang, R. Zhang, Z. Zhang, J.M. Deng, M.M. Taketo, T. Nakamura, R.R. Behringer, P.D. McCrea, B. de Crombrugghe (2004) Interactions between Sox9 and beta-catenin control chondrocyte differentiation. Genes Dev *18:* 1072–1087.

Altman, G.H., R.L. Horan, H.H. Lu, J. Moreau, I. Martin, J.C. Richmond, D.L. Kaplan (2002) Silk matrix for tissue engineered anterior cruciate ligaments. Biomaterials *23:* 4131–4141.

Aspenberg, P., C. Forslund (1999) Enhanced tendon healing with GDF 5 and 6. Acta Orthop Scand *70:* 51–54.

Bergljung, L. (1970) Vascular reactions in tendon healing. Stereomicroangiographic studies of tendon suturing techniques and tendon transplantation. Angiology *21:* 375–384.

Bi, W., W. Huang, D.J. Whitworth, J.M. Deng, Z. Zhang, R.R. Behringer, B. de Crombrugghe (2001) Haploinsufficiency of Sox9 results in defective cartilage primordia and premature skeletal mineralization. Proc Natl Acad Sci USA *98:* 6698–6703.

Bullough, R., T. Finnigan, A. Kay, N. Maffulli, N.R. Forsyth (2008) Tendon repair through stem cell intervention: cellular and molecular approaches. Disabil Rehabil *30:* 1746–1751.

Butler, D.L., N. Juncosa, M.R. Dressler (2004) Functional efficacy of tendon repair processes. Annu Rev Biomed Eng *6:* 303–329.

Cabello-Verrugio, C., E. Brandan (2007) A novel modulatory mechanism of transforming growth factor-beta signaling through decorin and LRP-1. J Biol Chem *282:* 18842–18850.

Chen, X., A. Zankl, F. Niroomand, Z. Liu, H.A. Katus, L. Jahn, C. Tiefenbacher (2006) Upregulation of ID protein by growth and differentiation factor 5 (GDF5) through a Smad-dependent and MAPK-independent pathway in HUVSMC. J Mol Cell Cardiol *41:* 26–33.

Docheva, D., E.B. Hunziker, R. Fassler, O. Brandau (2005) Tenomodulin is necessary for tenocyte proliferation and tendon maturation. Mol Cell Biol *25:* 699–705.

Farng, E., A.R. Urdaneta, D. Barba, S. Esmende, D.R. McAllister (2008) The effects of GDF-5 and uniaxial strain on mesenchymal stem cells in 3-D culture. Clin Orthop Relat Res *466:* 1930–1937.

Ferdous, Z., V.M. Wei, R. Iozzo, M. Hook, K.J. Grande-Allen (2007) Decorin-transforming growth factor interaction regulates matrix organization and mechanical characteristics of three-dimensional collagen matrices. J Biol Chem *282:* 35887–35898.

Ghosh, A.K., W. Yuan, Y. Mori, S. Chen, J. Varga (2001) Antagonistic regulation of type I collagen gene expression by interferon-gamma and transforming growth factor-beta. Integration at the level of p300/CBP transcriptional coactivators. J Biol Chem *276:* 11041–11048.

Haller, R., R. Schwanbeck, S. Martini, K. Bernoth, J. Kramer, U. Just, J. Rohwedel (2011) Notch1 signaling regulates chondrogenic lineage determination through Sox9 activation. Cell Death Differ *19:* 461–469.

Harris, M.T., D.L. Butler, G.P. Boivin, J.B. Florer, E.J. Schantz, R.J. Wenstrup (2004) Mesenchymal stem cells used for rabbit tendon repair can form ectopic bone and express alkaline phosphatase activity in constructs. J Orthop Res *22:* 998–1003.

Hass, R., C. Kasper, S. Bohm, R. Jacobs (2011) Different populations and sources of human mesenchymal stem cells (MSC): a comparison of adult and neonatal tissue-derived MSC. Cell Commun Signal *9:* 12.

Jelinsky, S.A., J. Archambault, L. Li, H. Seeherman (2010) Tendon-selective genes identified from rat and human musculoskeletal tissues. J Orthop Res *28:* 289–297.

Kamarul, T., P. Chong, L. Selvaratnam, C.C. Tai, A.A. Abbas (2009a) Quantitative real-time PCR analysis for chondrogenic differentiation of human mesenchymal stem cell in alginate scaffolds. Eur Cell Mater *18(suppl 1):* 44.

Kamarul, T., S.L. Tan, L. Selvaratnam, C.C. Tai (2009b) The effect of growth and differentiation factor 5 in tenogenic differentiation. Eur Cell Mater *18(suppl 1):* 47.

Komori, T. (2006) Regulation of osteoblast differentiation by transcription factors. J Cell Biochem *99:* 1233–1239.

Komori, T. (2010) Regulation of osteoblast differentiation by Runx2. Adv Exp Med Biol *658:* 43–49.

Kuo, C.K., R.S. Tuan (2008) Mechanoactive tenogenic differentiation of human mesenchymal stem cells. Tissue Eng Part A *14:* 1615–1627.

Lee, E.H., J.H. Hui (2006) The potential of stem cells in orthopaedic surgery. J Bone Joint Surg Br *88:* 841–851.

Lefebvre, V., W. Huang, V.R. Harley, P.N. Goodfellow, B. de Crombrugghe (1997) SOX9 is a potent activator of the chondrocyte-specific enhancer of the pro alpha1(II) collagen gene. Mol Cell Biol *17:* 2336–2346.

Lejard, V., G. Brideau, F. Blais, R. Salingcarnboriboon, G. Wagner, M.H. Roehrl, M. Noda, D. Duprez, P. Houillier, J. Rossert (2007) Scleraxis and NFATc regulate the expression of the pro-alpha1(I) collagen gene in tendon fibroblasts. J Biol Chem *282:* 17665–17675.

Liu, C.F., L. Aschbacher-Smith, N.J. Bathelery, N. Dyment, D.L. Butler, C. Wylie (2012) Spatial and temporal expression of molecular markers and cell signals during normal development of the mouse patellar tendon. Tissue Eng Part A *18:* 598–608.

Lou, J., Y. Tu, M. Burns, M.J. Silva, P. Manske (2001) BMP-12 gene transfer augmentation of lacerated tendon repair. J Orthop Res *19:* 1199–1202.

Maffulli, N., S.W. Ewen, S.W. Waterston, J. Reaper, V. Barrass (2000) Tenocytes from ruptured and tendinopathic achilles tendons produce greater quantities of type III collagen than tenocytes from normal achilles tendons. An in vitro model of human tendon healing. Am J Sports Med *28:* 499–505.

Musina, R.A., E.S. Bekchanova, A.V. Belyavskii, G.T. Sukhikh (2006) Differentiation potential of mesenchymal stem cells of different origin. Bull Exp Biol Med *141:* 147–151.

Nishitoh, H., H. Ichijo, M. Kimura, T. Matsumoto, F. Makishima, A. Yamaguchi, H. Yamashita, S. Enomoto, K. Miyazono (1996) Identification of type I and type II serine/threonine kinase receptors for growth/differentiation factor-5. J Biol Chem *271:* 21345–21352.

Obaid, H., D. Connell (2010) Cell therapy in tendon disorders: what is the current evidence? Am J Sports Med *38:* 2123–2132.

Pan, Q., Y. Yu, Q. Chen, C. Li, H. Wu, Y. Wan, J. Ma, F. Sun (2008) Sox9, a key transcription factor of bone morphogenetic protein-2-induced chondrogenesis, is activated through BMP pathway and a CCAAT box in the proximal promoter. J Cell Physiol *217:* 228–241.

Park, A., M.V. Hogan, G.S. Kesturu, R. James, G. Balian, A.B. Chhabra (2010) Adipose-derived mesenchymal stem cells treated with growth differentiation factor-5 express tendon-specific markers. Tissue Eng Part A *16:* 2941–2951.

Pfaffl, M.W. (2001) A new mathematical model for relative quantification in real-time RT-PCR. Nucleic Acids Res *29:* e45.

Reilly, G.C., S. Radin, A.T. Chen, P. Ducheyne (2007) Differential alkaline phosphatase responses of rat and human bone marrow derived mesenchymal stem cells to 45S5 bioactive glass. Biomaterials *28:* 4091–4097.

Romeo, A.A., D.W. Hang, B.R. Bach Jr., S. Shott (1999) Repair of full thickness rotator cuff tears. Gender, age, and other factors affecting outcome. Clin Orthop Relat Res 243–255.

Sahoo, S., L.T. Ang, J. Cho-Hong Goh, S.L. Toh (2010) Bioactive nanofibers for fibroblastic differentiation of mesenchymal precursor cells for ligament/tendon tissue engineering applications. Differentiation *79:* 102–110.

Saka, Y., K. Furuhashi, T. Katsuno, H. Kim, T. Ozaki, K. Iwasaki, M. Haneda, W. Sato, N. Tsuboi, Y. Ito, S. Matsuo, T. Kobayashi, S. Maruyama (2011) Adipose-derived stromal cells cultured in a low-serum medium, but not bone marrow-derived stromal cells, impede xenoantibody production. Xenotransplantation *18:* 196–208.

Schweitzer, R., J.H. Chyung, L.C. Murtaugh, A.E. Brent, V. Rosen, E.N. Olson, A. Lassar, C.J. Tabin (2001) Analysis of the tendon cell fate using scleraxis, a specific marker for tendons and ligaments. Development *128:* 3855–3866.

Shukunami, C., A. Takimoto, M. Oro, Y. Hiraki (2006) Scleraxis positively regulates the expression of tenomodulin, a differentiation marker of tenocytes. Dev Biol *298:* 234–247.

Tan, S.L., S. Sulaiman, B. Pingguan-Murphy, L. Selvaratnam, C.C. Tai, T. Kamarul (2011) Human amnion as a novel cell delivery vehicle for chondrogenic mesenchymal stem cells. Cell Tissue Bank *12:* 59–70.

Taskiran, D., E. Taskiran, H. Yercan, F.Z. Kutay (1999) Quantification of total collagen in rabbit tendon by the Sirius red method. Tr J Med Sci *29:* 7–9.

Tsai, R.Y., R.D. McKay (2002) A nucleolar mechanism controlling cell proliferation in stem cells and cancer cells. Genes Dev *16:* 2991–3003.

Van Eijk, F., D.B. Saris, J. Riesle, W.J. Willems, C.A. Van Blitterswijk, A.J. Verbout, W.J. Dhert (2004) Tissue engineering of ligaments: a comparison of bone marrow stromal cells, anterior cruciate ligament, and skin fibroblasts as cell source. Tissue Eng *10:* 893–903.

Violini, S., P. Ramelli, L.F. Pisani, C. Gorni, P. Mariani (2009) Horse bone marrow mesenchymal stem cells express embryo stem cell markers and show the ability for tenogenic differentiation by in vitro exposure to BMP-12. BMC Cell Biol *10:* 29.

Wang, Q.W., Z.L. Chen, Y.J. Piao (2005) Mesenchymal stem cells differentiate into tenocytes by bone morphogenetic protein (BMP) 12 gene transfer. J Biosci Bioeng *100:* 418–422.

Yao, L., C.S. Bestwick, L.A. Bestwick, N. Maffulli, R.M. Aspden (2006) Phenotypic drift in human tenocyte culture. Tissue Eng *12:* 1843–1849.

Zhang, G., Y. Ezura, I. Chervoneva, P.S. Robinson, D.P. Beason, E.T. Carine, L.J. Soslowsky, R.V. Iozzo, D.E. Birk (2006) Decorin regulates assembly of collagen fibrils and acquisition of biomechanical properties during tendon development. J Cell Biochem *98:* 1436–1449.

Zhang, J., J.H. Wang (2010a) Characterization of differential properties of rabbit tendon stem cells and tenocytes. BMC Musculoskelet Disord *11:* 10.

Zhang, J., J.H. Wang (2010b) Platelet-rich plasma releasate promotes differentiation of tendon stem cells into active tenocytes. Am J Sports Med *38:* 2477–2486.

Zhang, W., H.T. Liu (2002) MAPK signal pathways in the regulation of cell proliferation in mammalian cells. Cell Res *12:* 9–18.

APPENDIX O

Proceeding in European Cells and Materials

European Cells and Materials Vol. 18. Suppl. 1, 2009 (page 47) ISSN 1473-2262

The Effect of Growth and Differentiation Factor 5 in Tenogenic Differentiation

T Kamarul[1], S-L Tan[1], Lakshmi Selvaratnam[2], C-C Tai[1]

[1]Tissue Engineering Department (TEG), Department of Orthopaedic Surgery, Faculty of Medicine, University of Malaya, Kuala Lumpur, Malaysia.

[2]School of Medicine & Health Sciences, Monash University, Sunway Campus, Selangor, Malaysia.

INTRODUCTION: Growth and differentiation factor 5 (GDF-5 or bone morphogenetic proteins 14) is a multifunctional protein molecule that plays an important role in tissue differentiation [1]. Although its role in tendon repair has been described, it use *in vitro* tenogenic differentiation from MSC has not been determined. Owing to the limitation in getting allograft for tendon repair, mesenchymal stem cell provides an alternative cell based therapy for damaged tendons. We therefore conducted an *in vitro* trial to isolate, characterize, proliferate and differentiate rabbit bone marrow derived MSCs with GDF-5 in view of future *in vivo* applications.

METHODS: Rabbit MSCs isolated from rabbit bone marrow via gradient centrifugation methods and expanded using cell culture techniques were used in this study. Total RNA were extracted from MSCs and further analyzed using our custom designed primers based on sequence information attained from GenBank database. Concurrently, MSCs fixed and embedded in epon were viewed using transmision electron microsope (TEM). To study the possibility of tenogenic differentiation, MSCs seeded in six-well culture plates were maintained in culture medium supplemented with GDF-5 at different concentrations for 4 days. The collagen expression of the MSCs was determined using Sircol™ collagen assay. Real-time PCR was conducted to assessed the gene expression profile of the type-I collagen and Scleraxis in MSC in growth medium, differentiation medium with and without GDF-5, and tenocyte.

RESULTS: Plastic adherent mononuclear cells appear heterogeneous with the majority of cells possessing fibroblastic morphology. The mononuclear cells isolated expressed CD29 and CD166 proteins but were negative for CD 45, which is similar to that reported previously. TEM images demonstrated ultra structures which may be of interest for further biological understanding. Collagen expression in MSC appears to up-regulated with increasing GDF-5 concentrations (table 1). MSC grown in tenogenic medium showed an increase in their gene expression in type-I collagen and Scleraxis as compared to undifferentiated MSC and autologous cultured tenocytes.

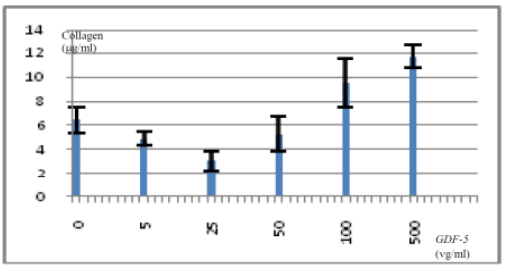

Table 1: Collagen expression of tenogenic MSC quantified by Sircol Collagen assay kit.

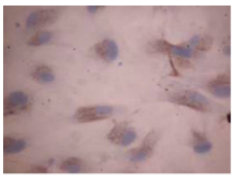

Fig. 2: Collagen type-I expression in rabbit MSC after induced by tenogenic medium (400X magnification).

DISCUSSION & CONCLUSIONS: Our technique of MSC isolation appears to produce replicable results validated using our characterization methods. Previous study reported that GDF-5 plays an important role in tendon repair[1,2]. In our study, tenogenic differentiation appears achievable and is useful for future clinical application namely in tendon repair using differentiated MSCs.

REFERENCES: [1] Chhabra A. et al. J Ortho Res, 2003, 21 826-35. [2] Rodeo SA., Technique in Orthopaedics, 2007; 22(1): 10-13.

ACKNOWLEDGEMENTS: This project is funded by E-Science 12-02-03-2017.

APPENDIX P

Oral Abstract for ISCOM 2009, Groningen, The Netherlands

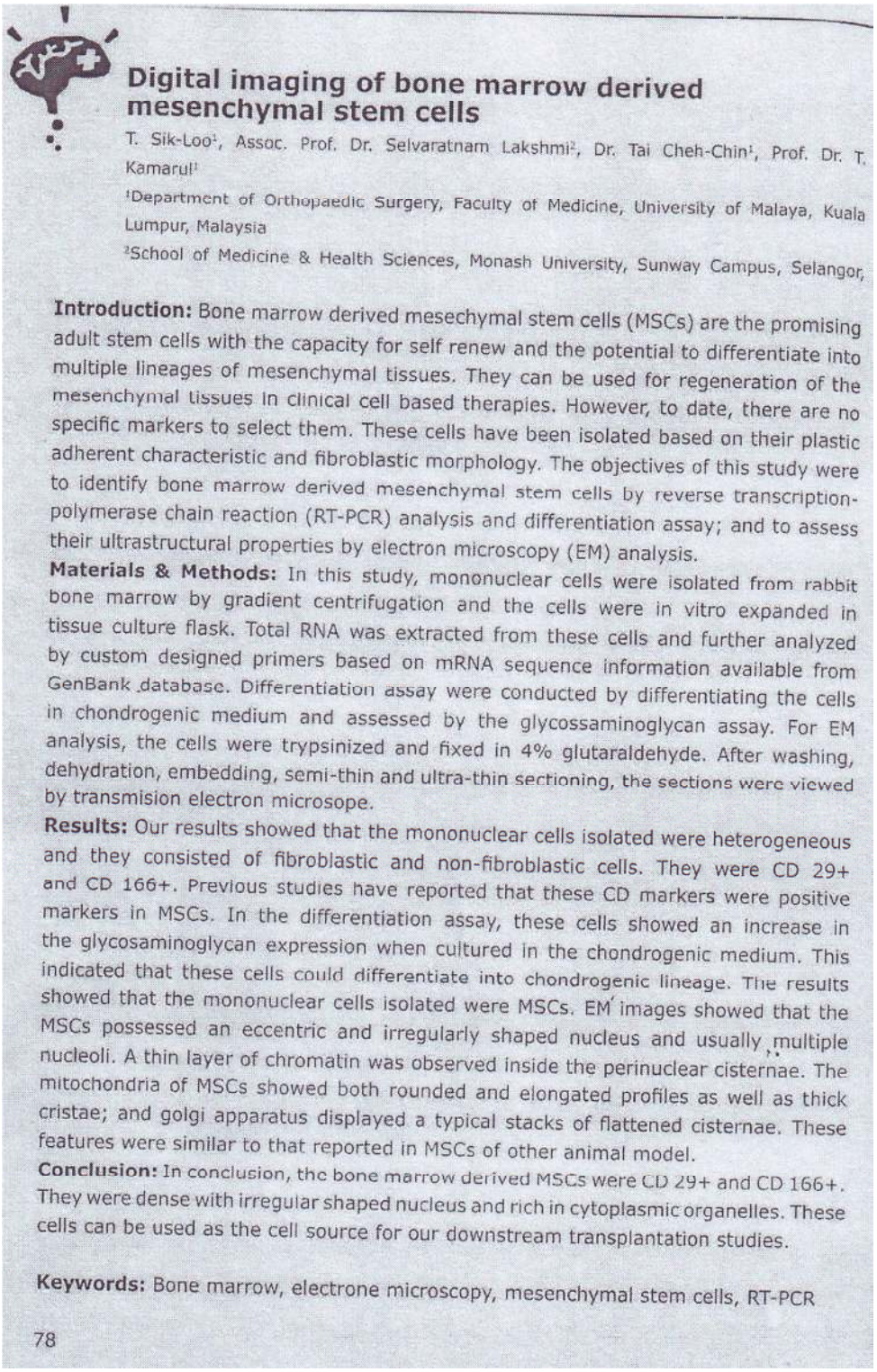

Digital imaging of bone marrow derived mesenchymal stem cells

T. Sik-Loo[1], Assoc. Prof. Dr. Selvaratnam Lakshmi[2], Dr. Tai Cheh-Chin[1], Prof. Dr. T. Kamarul[1]

[1]Department of Orthopaedic Surgery, Faculty of Medicine, University of Malaya, Kuala Lumpur, Malaysia

[2]School of Medicine & Health Sciences, Monash University, Sunway Campus, Selangor,

Introduction: Bone marrow derived mesechymal stem cells (MSCs) are the promising adult stem cells with the capacity for self renew and the potential to differentiate into multiple lineages of mesenchymal tissues. They can be used for regeneration of the mesenchymal tissues in clinical cell based therapies. However, to date, there are no specific markers to select them. These cells have been isolated based on their plastic adherent characteristic and fibroblastic morphology. The objectives of this study were to identify bone marrow derived mesenchymal stem cells by reverse transcription-polymerase chain reaction (RT-PCR) analysis and differentiation assay; and to assess their ultrastructural properties by electron microscopy (EM) analysis.

Materials & Methods: In this study, mononuclear cells were isolated from rabbit bone marrow by gradient centrifugation and the cells were in vitro expanded in tissue culture flask. Total RNA was extracted from these cells and further analyzed by custom designed primers based on mRNA sequence information available from GenBank database. Differentiation assay were conducted by differentiating the cells in chondrogenic medium and assessed by the glycossaminoglycan assay. For EM analysis, the cells were trypsinized and fixed in 4% glutaraldehyde. After washing, dehydration, embedding, semi-thin and ultra-thin sectioning, the sections were viewed by transmision electron microsope.

Results: Our results showed that the mononuclear cells isolated were heterogeneous and they consisted of fibroblastic and non-fibroblastic cells. They were CD 29+ and CD 166+. Previous studies have reported that these CD markers were positive markers in MSCs. In the differentiation assay, these cells showed an increase in the glycosaminoglycan expression when cultured in the chondrogenic medium. This indicated that these cells could differentiate into chondrogenic lineage. The results showed that the mononuclear cells isolated were MSCs. EM images showed that the MSCs possessed an eccentric and irregularly shaped nucleus and usually multiple nucleoli. A thin layer of chromatin was observed inside the perinuclear cisternae. The mitochondria of MSCs showed both rounded and elongated profiles as well as thick cristae; and golgi apparatus displayed a typical stacks of flattened cisternae. These features were similar to that reported in MSCs of other animal model.

Conclusion: In conclusion, the bone marrow derived MSCs were CD 29+ and CD 166+. They were dense with irregular shaped nucleus and rich in cytoplasmic organelles. These cells can be used as the cell source for our downstream transplantation studies.

Keywords: Bone marrow, electrone microscopy, mesenchymal stem cells, RT-PCR

78

APPENDIX Q

Poster Abstract for ISSCR 2009, Barcelona, Spain

BMSC-trasplantation combined to fasudil treated group (BMSC + fasudil group), then neurological function was serially evaluated after SCI, using Basso-Beattie-Bresnehan (BBB) score. An axonal tracer, Fluoro-ruby (FR), was injected into the dorsal CST 10 mm rostral to the injured site at 63 days after SCI. All animals were sacrificed at 68 days after SCI, and spinal cord section were immunostained. Result- Statistically significant improvements in motor function were observed in the BMSC + fasudil group, compared with vehicle-transplanted and fasudil-treated group. However, there was no significant improvement between the BMSC-transplanted group and the BMSC + fasudil group. The number of FR-positive axons was significantly larger at the dCST caudal to the injured site in the BMSC + fasudil group than in the BMSC-transplanted group. Conclusion- The findings strongly suggest that double therapy which is the BMSC transplantation combined to fasudil treatment further promotes axonal elongation of dCST on injured spinal cord in rat compared to the BMSC transplantation.

1397

ULTRASTRUCTURAL ANALYSIS AND IDENTIFICATION OF RABBIT BONE MARROW DERIVED MESENCHYMAL STEM CELLS

Sik Loo, Tan[1], Lakshmi, Selvaratnam[2], Cheh-Chin, Tai[1], T, Kamarul[1]
[1]*Department of Orthopaedic Surgery, University of Malaya, Kuala Lumpur, Malaysia,* [2]*School of Medicine & Health Sciences, Monash University, Sunway Campus,, Selangor, Malaysia*

Non-hematopoietic stem cells or mesenchymal stem cells (MSCs) are adult stem cells that are capable of differentiating into various mesenchymal lineages, and these including bone, cartilage, tendon, muscle, adipose and stromal. These cells have the therapeutic potential in cell based regenerative medicine because they can be used as an alternative cell sources for cell transplantations. Inspite of the advances in identifying MSCs, current methods for MSCs isolation have been relied on cells ability to adhere to plastic surfaces, fibroblastic appearance and expression of cell surface markers which are not absolute. Furthermore, there are no available surface proteins antibodies for various animals which are important considering that animal transplantation model are required for adaptation into clinical application. The ultra-architecture of MSCs has also not been described in detail. We therefore took upon ourselves to characterize bone marrow-derived MSCs from rabbits using reverse transcription-polymerase-chain reaction (RT-PCR) analysis; and to assess their ultra-structural properties to provide an improved assessment of MSCs. The objectives of this study were to isolate and characterize the rabbit bone marrow derived MSCs. In this study, plastic adherent mononuclear cells (MNCs) from the bone marrow were isolated by Ficoll-Paque gradient centrifugation. The morphology of the MNCs in *in vitro* culture was observed by phase contrast microscopy analysis. The characterizations of the MNCs were conducted by differentiation assay (chondrogenic differentiation), RT-PCR analysis and electron microscopy analysis. RT-PCR analysis were conducted by using our custom designed primers based on sequence information attained from NCBI GenBank database. Our results showed that the plastic adherent MNCs were heterogeneous and expressed the CD29 and CD166 surface marker genes. Chondrogenic differentiation assay showed that the MNCs were capable to differentiate into chondrogenic lineage. Ultrastructural analysis by electron microscopy showed that the MNC has an eccentric and irregular shaped nucleus. The entire peripheral of the cells were surrounded by many small pseudopodia. In conclusion, our custom designed primer appears to be suitable to identify rabbit MSCs (which have not been previously described). High resolution images have revealed cell structures which is useful for further understanding of MSC behaviour *in vitro*.

1399

IN VITRO DIFFERENTIATION OF BONE MARROW STEM CELLS TOWARD MICROGLIA AND FUNCTIONAL TESTING IN ADULT ORGANOTYPIC BRAIN SLICES

Stolzing, Alexandra, Hinze, Arnd
Institute for Cell Therapy and Immunology, Fraunhofer Gesellschaft, Leipzig, Germany

Systemic stem cells transplantation showed benefits in ischemic brain damage and reactivated endogenous stem cells. The mechanism of this benefit is not fully understood, but the interaction between adult stem cells and the microglial system might be involved. Microglia are part of the inflammatory system and known to influence neuronal stem cell behaviour. During aging and in neurodegenerative diseases microglia change from friend to foe, accompanied by a loss of function. Adult bone marrow derived stem cells from 3 month old mice were *in vitro* differentiated using astrocyte conditioned medium, Flt3, MG-CSF and other substances in different combinations. Cells were then tested for their surface antigen profile using flow cytometry (CD11b, F4/80, CD45). Phagocytotic activity, nitric oxide (NO) production and oxidative burst were tested using phorbol ester phorbol 12-myristate 13-acetate activation. Incorporation, survival and migration of the *in vitro* derived microglia were tested in adult organotypic brain slices. The expression profile of the cells after differentiation showed increased expression of macrophage/microglial marker and haematopoietic markers, including CD45, F4/80 and CD11b. The microglia-like cells showed phagocytotic activity and produced NO after stimulation with PMA. Invasion into adult mouse brain slice was observed between day 1-20. Only a few apoptotic cells were observed and microglia continued to proliferate in the slice. Exiting *in vitro* differentiation methods for microglia production could be improved and functional activity *in vitro* and in a slice model was shown. The *in vitro* production of microglia for replacement therapy might help in neurodegenerative diseases like Alzheimer or slow normal brain aging.

1401

ANGIOPOIETIN-LIKE-5 SECRETED BY MESENCHYMAL STEM CELLS SUPPORTS A LONG TERM *EX VIVO* EXPANSION OF HUMAN HEMATOPOIETIC STEM CELLS

Khoury, Maroun[1], Drake, Adam[2], Leskov, Ilya[2], Fragoso, Maria[2], Lodish, Harvey[3], Chen, Jianzhu[1]
[1]*Koch Institute for Integrative Cancer Research at MIT and SMART IRG Infectious Diseases, Massachussetts Institute of Technology and Singapore MIT Alliance for Research and Technology, Cambridge and Singapore, MA, USA,* [2]*Koch Institute for Integrative Cancer Research at MIT, Massachussetts Institute of Technology, Cambridge, MA, USA,* [3]*Whitehead Institute for Biomedical Research and Department of Biology, Massachusetts Institute of Technology, Cambridge, MA, USA*

Bone marrow transplantation, hematopoietic gene therapy approaches, as well as basic human hematopoiesis research are often limited by the numbers of available hematopoietic stem cells (HSC). Hence, robust methods for long term *ex vivo* expansion are required. Mesenchymal stem cells (MSC) play an important role in supporting HSC by producing cytokines, growth factors, and cell adhesion molecules involved in hematopoiesis. Angiopoietic-like-5 (Angptl5) is a recently identified factor that results in dramatic *ex vivo* expansion of human HSC. In this study, we evaluate the efficiency with which MSCs engineered to express Angptl5 can support *ex vivo* expansion of umbilical cord blood-derived HSCs. Methods: HSCs were cocultured with MSC-Angptl5 at a ratio of 1:5 in a serum free-media. Cultured cells were analyzed for the expression of stem cell markers (CD34 and CD133). After 10 days of culture, human stem/progenitor cells were injected into sublethally irradiated NOD/SCID/IL2Rgammanull newborn mice. Human cell engraftment

APPENDIX R

Poster Abstract for ORS 2010, New Orleans, LA

Tenogenic Expression of Differentiated Mesenchymal Stem Cells is Dependant on Growth and Differentiation Factor-5

+[1]Tan, S-L; [2]Selvaratnam, L; [1]Tai, C-C; [1]Kamarul, T
+[1]Tissue Engineering Group (TEG), Department of Orthopaedic Surgery, Faculty of Medicine, University of Malaya, Lembah Pantai, Kuala Lumpur, 50603, Malaysia, [2]School of Medicine & Health Sciences, Monash University, Sunway Campus, Selangor, Malaysia.
tansikloo@yahoo.com

INTRODUCTION:

Although the use of growth-differentiation factor-5 (GDF-5) and mesenchymal stem cells to repair damaged tendons has been previously described[1], the optimal amount of GDF-5 concentration required to elicit a favourable tenogenic response from mesenchymal stem cells (MSCs) has not been clearly established. To determine this relationship, a study was conducted to ascertain the amount of tenogenic expression of mesenchymal stem cells at different GDF-5 concentrations *in vitro* and to compare these changes to native tenocyte.

MATERIALS & METHODS:

Ethics approval for this study was granted by the Animal Care and Use Committee in University of Malaya (Reference number: PM/24/06/2008/TKZ). Rabbit tenocytes and bone marrow derived MSCs from New Zealand White rabbits were harvested, processed and expanded following methods previously established[2]. Characterization of the MSCs and tenocytes was performed to confirm the homogeneity and validity of the appropriate cell lineage utilized in the current study[3]. To determine the dose response between GDF-5 and the phenotypic expression as the result of MSC transformation, MSCs seeded in six-well culture plates were maintained in serum free culture medium supplemented with GDF-5 at different concentrations for 4 days. MSCs cultured in basal cell culture medium (supplemented with 10% FCS) and tenocytes cultured in serum free medium were used as controls. The total collagen expression of the MSCs was determined by using Sircol™ collagen assay. Four (n=4) samples were used in this experiment, each conducted in triplicates. Real-time PCR was also conducted to assess the gene expression profile of the tendon specific marker, Scleraxis (Scx) and type-I collagen (Col-I) in: (1) tenocytes, (2) MSCs cultured in growth medium supplemented with 10% FCS, and (3) MSCs treated with GDF-5. Data attained from the study was analyzed using SPSS statistical software package (ver. 13.0).

RESULTS:

Cells isolated and cultured from rabbit bone marrows exhibited mesenchymal stem cell characteristics[2]. Primary tenocytes attained from rabbits demonstrated increased expression of type I/III collagen and none to collagen type II[2]. Increasing GDF-5 concentrations in cell cultures increased collagen expression proportionately (Figure 1). Although there was a reduction in the total collagen expressed in cultures supplemented with low concentrations of GDF-5 (i.e. 5 and 25 ng/ml), these differences were not significant when compared to untreated MSCs, (Mann Whitney-U test: $p>0.05$). Total collagen expression was significantly higher in cell cultures treated at higher concentrations of GDF-5 (i.e. 100 and 500 ng/ml) than that at lower concentrations (i.e. 0, 5, 25 ng/ml). At high concentrations, total collagen was also comparable to that of tenocyte cultures.

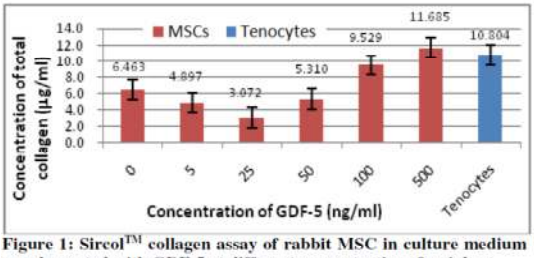

Figure 1: Sircol™ collagen assay of rabbit MSC in culture medium supplemented with GDF-5 at different concentrations for 4 days.

Tenogenic differentiation in MSCs treated with GDF-5 (T-MSC) was confirmed using immunohistological methods. T-MSCs had similar characteristics to native tenocytes, expressing Collagen types 1 and III, but not to type II.

Gene expression analyses demonstrated significant increase ($p<0.05$) in the tendons specific markers, Scleraxis (*SCX*) and Collagen-I (*Col-I*) genes, in MSCs treated with GDF-5 at 50 and 100ng/ml as compared to untreated MSCs (Figure 2). Although both genes in MSCs appear to be highest when treated with 50ng/ml of GDF-5, these were not significantly different to MSCs treated with 100ng/ml ($p>0.05$)

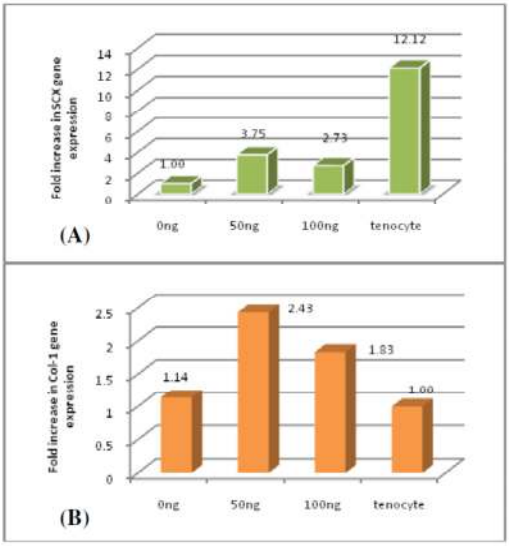

Figure 2: Gene expression analysis of (A) Scx gene and (B) Col-I gene in rabbit tenocytes and MSCs treated with GDF-5.

DISCUSSIONS:

This study demonstrated a correlation between total collagen expression and the increasing dose of GDF-5 in MSCs. Based on the dose response curve attained from this study, it appears that GDF-5 concentration between 100-500ng/ml produced comparable collagen expression to that of native tenocytes. However, tenogenic specific gene expressions appear to be highest when treated with 50ng/ml of GDF-5. While previous studies have demonstrated the importance of GDF-5 in MSCs transformation[3], our study contributes to further observation that a minimum amount of 100ng/ml of GDF-5 concentration is required to elicit optimal tenogenic differentiation in T-MSCs.

CONCLUSION:

The use of GDF-5 in the differentiation of MSCs to T-MSCs is dose dependant with an observed optimal GDF-5 concentration of 100-500ng/ml required to produce an appropriate tenogenic response. However, at the concentration of 50ng/ml of GDF-5, T-MSCs expressed tendon specific genes (*SCX* and *Col-I*) compatible or better than the native tenocytes.

References:

1. Dines et al., J Shoulder Elbow Surg 2007; 16: 215S-221S.
2. Tan et al., International Society for Stem Cell Research (ISSCR) 7th Annual Meeting 2009; Pg226.
3. Farng et al., Clin Orthop Relat Res 2008; 466: 1930-1937.

APPENDIX S

Poster Abstract for ORS 2011, Long Beach, CA

Optimizing Tenogenic Differentiation of Human Mesenchymal Stem Cells using Growth & Differentiation Factor-5

+[1]Tan, S-L; [1]Merican, AM; [1]Abas, AA; [1]Ng, W-M; Chan, [1]C-C; [1]Zyroul, R; Selvaratnam, L; [1]Tai, C-C; [1]R E Ahmad; [1]Sara, T; [1]Kamarul, T
+[1]Tissue Engineering Group (TEG), NOCERAL, Department of Orthopaedic Surgery, Faculty of Medicine, University of Malaya, Lembah Pantai, Kuala Lumpur, 50603, Malaysia, [2]School of Medicine & Health Sciences, Monash University, Sunway Campus, Selangor, Malaysia.
tansikloo@yahoo.com

INTRODUCTION:

Recent endeavors in tendon tissue engineering have exploited the potential application of cell-based therapy for tendon regeneration. More recently, the use of mesenchymal stem cells (MSCs) as an alternative source of tenocytes has been extensively studied. Various techniques have been explored to induce tenogenic differentiation of the MSCs, which include mechanotransduction, gene transfer and co-culture systems, however, there is no optimal method that have yet been established to provide best culture conditions which would induce the MSCs to differentiate into tenogenic lineage. An approach which has previously been utilized for MSCs differentiation is the use of growth factors such as growth and differentiation factor-5 (GDF-5)[1]. While this has been previously studied in relations to mechanotransduction of the MSCs, there is no previous report on direct supplementation of GDF-5 and its optimal concentration in providing the best culture environment to induce tenogenic differentiation of the MSCs. The objective of this study was therefore to determine the optimal condition for human MSCs tenogenic differentiation by GDF-5.

MATERIALS & METHODS:

Ethics approval for this study was granted by the UMMC Ethics Committee (Reference number: 602.22). Human MSC were isolated from bone marrow procured from the consented patients and expanded *in vitro* following methods previously established[2]. To induce the MSCs tenogenic differentiation, MSCs were maintained in serum free culture medium supplemented with GDF-5 at 0, 50 and 100ng/ml. MSCs cultured in basal cell culture medium (supplemented with 10% FCS) were used as controls (Untreated). On day-3 of the differentiation induction, the total collagen expression of the MSCs was determined by using Sircol™ collagen assay. Gene expression profile of type-I collagen (Col-*I*), type-III collagen (*Col-III*), scleraxis (*Scx*), decorin (*Dec*), nucleostemin (*Nst*) on day 0 and day 3 were analyzed by real-time PCR analysis. Data attained from the study was analyzed by using SPSS statistical software package (ver. 13.0). Three samples were used in this experiment, each conducted in triplicates.

RESULTS:

Cells isolated and cultured from human bone marrows exhibited mesenchymal stem cell characteristics which is described elsewhere[2]. Primary human MSCs culture showed fibroblastic morphology with a spindle-shaped appearance. When differentiated in culture medium supplemented with GDF-5, the cells showed a more elongated appearance when culture with higher concentration of GDF-5 than those with at lower concentrations (Figure 1). There was an increase in total collagen expression in the MSCs culture when the medium was supplemented with higher concentration of GDF-5 (Figure 2).

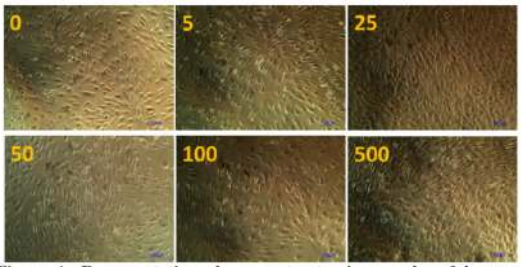

Figure 1: Representative phase contrast micrographs of human MSCs treated with GDF-5 at different concentrations (10X objective). The concentration of the GDF-5 used were denoted at the left corner of the image at ng/ml.

Gene expressions were found to be altered when different amount of GDF-5 were used to induce tenogenic differentiation in MSCs (Figure 3). At 100ng/ml of GDF-5, the genes related to tendon collagen fibers formation, *Col-I and Col-III*, and gene related to matrix assembly[3], *Dec*, were significantly increased ($p<0.05$) on day-3 of cell culture. The increase in *Col-I* expression (the most abundant collagen in tendon) was not observed for MSCs exposed to 0 and 50ng/ml of GDF-5. Tenogenic marker genes *Scx*, and the undifferentiated stem cells marker gene *Nst*, were also increased in MSCs cultured in 100ng/ml of GDF-5.

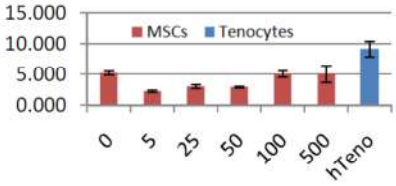

Figure 2: Sircol™ collagen assay of human MSC in culture medium supplemented with GDF-5 at different concentrations on day-3.

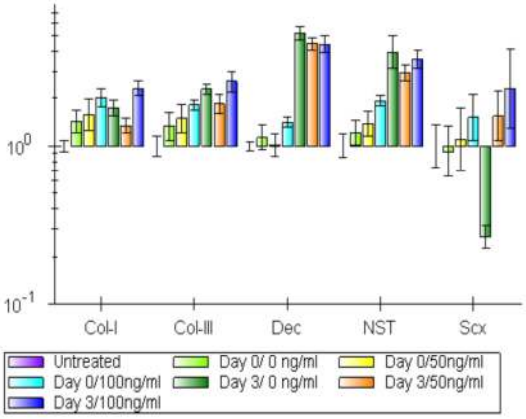

Figure 3: Gene expression analysis of *Col-I, Col-III, Dec, Nst* and *Scx* in human MSCs treated with GDF-5.

DISCUSSION:

This study demonstrated that the tenogenic specific genes expression (eg. *Col-I*, *Scx* and *Dec*) appears to be highest when treated with 100ng/ml of GDF-5. While previous studies have demonstrated the importance of GDF-5 in MSCs transformation[1], our study demonstrates that a minimum amount of 100ng/ml of GDF-5 concentration is required to elicit optimal tenogenic differentiation in human MSCs.

CONCLUSION:

The use of GDF-5 in the differentiation of human MSCs to tenogenic MSCs is dose dependant with an observed optimal GDF-5 concentration of 100ng/ml required to produce an appropriate tenogenic response.

REFERENCES:

1. Farng et al., Clin Orthop Relat Res 2008; 466: 1930-1937.
2. Chong et al., The 3rd Asian Federation of Laboratory Animal Science Association (AFLAS) Congress and The 8th Chinese Association for Laboratory Animal Sciences (CALAS) Annual Meeting (ISSCR) 7th Annual Meeting 2009; Pg31-32.
3. Sini et al., Glycoconj J 1997; 14:871-874.